


<b>Title</b>	Synthesis of iminophosphine and phosphinoiminol cyclometallated Pt (II) and Pt (IV) chloro complexes and studies into their biological and photophysical properties
<b>Author(s)</b>	O'Donoghue, John Daniel
<b>Publication date</b>	2013
<b>Original citation</b>	O'Donoghue, J. D. 2013. Synthesis of iminophosphine and phosphinoiminol cyclometallated Pt (II) and Pt (IV) chloro complexes and studies into their biological and photophysical properties. PhD Thesis, University College Cork.
<b>Type of publication</b>	Doctoral thesis
<b>Rights</b>	© 2013, John D. O'Donoghue. <a href="http://creativecommons.org/licenses/by-nc-nd/3.0/">http://creativecommons.org/licenses/by-nc-nd/3.0/</a> 
<b>Item downloaded from</b>	<a href="http://hdl.handle.net/10468/1298">http://hdl.handle.net/10468/1298</a>

Downloaded on 2017-02-12T08:32:12Z

**Synthesis of Iminophosphine and Phosphinoiminol  
Cyclometallated Pt (II) and Pt (IV) Chloro Complexes and  
Studies into their Biological and Photophysical Properties**



**John Daniel O'Donoghue, B. Sc**

A thesis presented for the degree of  
Doctor of Philosophy  
to  
The National University of Ireland, Cork  
University College Cork  
Department of Chemistry

*Under the Supervision of: Dr. Orla M. Ní Dhubhghaill  
Head of Department: Prof. Michael Morris*

*August 2013*

---



I hereby confirm that the body of work described within this thesis, for the degree of Doctor of Philosophy, is the result of research carried out by me, within University College Cork, under the supervision of Dr. Orla M. Ní Dhubhghaill, and that this thesis has not been previously reproduced elsewhere, to the best knowledge of this author, in whole or in part, prior to presentation for this degree.

Name:

Date:

---



# Contents

**Abstract**.....(vii)

**Acknowledgements**.....(ix)

**Abbreviations**.....(xv)

## **Chapter 1**

General Introduction.....1

## **Chapter 2**

Design and synthesis of platinum (II) cyclometallated iminophosphine and phosphinoiminol complexes via coordination to mixed donor ligands.....61

## **Chapter 3**

Design and synthesis of cationic platinum (II) PPh<sub>3</sub> complexes via substitution and platinum (IV) cyclometallated complexes via oxidation.....181

## **Chapter 4**

Studies into the reactivity of platinum (II) complexes towards biomolecules, *in-vitro* cancer cell testing and luminescence.....255

## **Chapter 5**

Final conclusions and future work .....317

## **Appendices**

Papers for publication



## **Abstract:**

This thesis focuses on the synthesis and analysis of novel chloride based platinum complexes derived from iminophosphine and phosphinoamide ligands, along with studies on their reactivity towards substitution and oxidation reactions. Also explored here are the potential applications of these complexes for biological and luminescent purposes.

Chapter one provides an extensive overview of platinum coordination chemistry with examples of various mixed donor ligands along with the history of platinum anticancer therapy. It also looks at metals in medicine, both for biological functions as well as for therapeutic purposes and gives a background to some other applications for platinum complexes.

Chapter two outlines the design and synthetic strategies employed for the development of novel platinum (II) chloride complexes from iminophosphine and phosphinoamide ligands. Also reported is the cyclometallation of these complexes to form stable tridentate mixed donor platinum (II) compounds. Crystal structures and a detailed analysis of the NMR spectroscopy for these complexes, as well as their ligands, are also included in this chapter.

In Chapter three the development of a direct method for displacing a chloride from a platinum metal centre with a desired phosphine is reported. Numerous methods for successful oxidation of the platinum (II) complexes will also be explored, leading to novel platinum (IV) complexes being reported here also. The importance of stabilisation of the displaced anion, chloride, by the solvent system will also be discussed in this chapter.

Chapter four investigates the reactivity of the platinum (II) complexes towards two different biomolecules to form novel platinum bio-adducts. The potential application of the platinum (II) cyclometallates as chemotherapeutics will also be explored here using *in-vitro* cancer cell testing. Finally, luminescence studies are also reported here for the ligands and platinum complexes reported in chapter two and three to investigate potential applications in this field also.

Chapter five provides a final conclusion and an overall summary of the entire project as well as identifying key areas for future work.





## **Acknowledgements:**

The completion of this thesis would not be possible without the help and support of a huge amount of people. First and foremost I would like to express my sincerest gratitude to my supervisor Dr. Orla Ní Dhubhghaill for her guidance, encouragement, time and above all else... her patience! And I also want to apologise for all the times I burst in your door unannounced with some random NMR spectra to look at! Thank you for affording me this amazing opportunity and for remaining enthusiastic throughout this project which really helped me overcome the various obstacles that arose during this work. I'd also like to thank Kerry County Council for the financing to complete this work.

In addition, I have been privileged to work with and collaborate with so many people in the Chemistry Department and in the Cork Cancer Research Centre in UCC. Firstly I want to thank everyone in the ONíD research group that have helped me at some stage over the years including Michelle, Terence and Páraic. And to everyone in the SEL research group I also want to sincerely thank for keeping me so grounded over the years from Lab G34 to Lab 4.27 including David (Duny), the fello Listowel man Stephen, the Corkman Kevin and the girl from Clare, Carla. There are also numerous other people in the Kane Building over the years who have always been so approachable at all times from synthesis to analysis and for that I sincerely thank you.

Also I want to thank everyone in the UCC CRAC lab, in particular Dr. Ruairi O'Concubhair and Dr. Dave O'Connor, along with Dr. Trevor Carey in the Phys. Chem. teaching labs for all their help with the luminescence studies within this project. I am also very grateful to Dr. Simon Lawrence and Dr. Kevin Eccles for obtaining the x-ray crystal structures of the complexes reported in this thesis and to Dr. Sharon McKenna and Dr. Tracy O'Donovan for their collaboration in conjunction with the *in-vitro* cell testing in the Cork Cancer Research Institute. Many thanks also go to Dr. Lorraine Bateman for her patience and effort in helping me obtain the NMR data presented in this work. Thanks also go to Terry Horgan and Dr. Florence McCarthy for the elemental analysis and mass spec analysis respectively.

I would also like to say a huge thank you to all of the technical and administrative staff who helped me in so many ways during my time in UCC, from demonstrating to MCQ exams to chemistry magic shows! To Chrissie, Donnacha, Noel, Pat, Rose, Terry, Johnny, Eileen, Christine, Debbie, Collette, Derry and Tina thank you so much for all your help and support. I also want to extend a huge thank you to Mathias for helping me keep my old laptop limping to all the way to the end.

I want to also thank all the people from the Cavanagh Pharmacy building who put up with me during my random "breaks" from research, especially during the summer months, including Naomi, Elaine, Linda, Catherine, Kate, Roisin, Dee and Brian. And a special thank you goes to Donal for keeping me motivated by distracting me; just keep all footballs away from him when he's indoors.

I also want to thank all my old classmates who stayed in UCC to do their PhD/Masters, in particular Ger for the bird watching and having fun on the radio, Nicola for listening to my ramblings, along with Eoin, John and Mark for the pool hall days. Having all of you around made it so much easier. I also want to thank everyone involved with me over the years in the UCC Chemical Society (in particular our staff rep Dr. Dave Otway), the UCC Postgrad Society, UCC Clubs and the UCC Societies Guild including Richard, Eoin, Kilian, Sara, Alicia, Tim, Shelly O’C, Niamh, Roisin and Prof. Alan Kelly along with Michelle Nelson in the UCC Graduate Studies Office. I also want to send a special thank you to all the staff, past and present, in the UCC Accommodation and Student Services Office, in particular Dave and Maura, for making life easier for me while I tried to balance my PhD with my extra-curricular activities.

There have also been a number of standout people that I met or lived with over the years and made my entire time in UCC one to remember. In terms of housemates I have to mention Eoghan, Stephen (the invisible sheep), Dave, the inglorious cousins Pa and Mark, Eric and everyone else (including Tony the Garda) who put up with me from Brookfield to Magazine Road to Clashduv over the years. Also to Grace, a thanks is extended for keeping my PhD on track and listening to my ramblings. And not to forget the man who ran away to Canada, Kieran; thanks for the beer garden afternoons when you came home. You have all been there with me through thick and thin so thank you for the spectacular distractions!

Finally, last but very much not least, a huge thank you goes to all my family. To my bothers Maurice, Gerard and Daniel and my amazing grandmother Nan who have been so supportive throughout years I’ve been in UCC. A thank you is also sent to all my aunts, uncles, cousins and extended family who are too numerous to mention. Thanks also go to my grandfather “Corkgrandad” for helping me in every way you could. A particular thank you also goes to my godmother Mai who put me up in her house so many times over the years for all the conferences and events I attended in the big smoke! Finally I owe the biggest thank you of all to my mother and father who have supported me every single step of the way, I hope I’ve made all of you proud.

*For Auntie Mai,  
Sister Máire McElligott*



*“For years I’ve been saying this is the first  
platinum-based drug we discovered”*

*“It can’t possibly be the best one.  
It’s disappointing that the scientific community  
has not been able to find better ones.”*

***Barnett (Barney) Rosenberg (1926-2009)***



## Abbreviations:

<b>DCM</b>	Dichloromethane	<b>CHCl<sub>3</sub></b>	Chloroform
<b>MeOH</b>	Methanol	<b>EtOH</b>	Ethanol
<b>MeCN/ACN</b>	Acetonitrile	<b>DMSO</b>	Dimethylsulfoxide
<b>DMF</b>	Dimethylformamide	<b>thf</b>	Tetrahydrofuran
<b>EtOAc</b>	Ethyl acetate	<b>Et<sub>2</sub>O</b>	Diethyl ether
<b>AcOH</b>	Acetic acid	<b>CDCl<sub>3</sub></b>	Chloroform- <i>d</i> <sub>3</sub>
<b>py</b>	Pyridine	<b>TEA</b>	Triethylamine
<b>NaOAc</b>	Sodium acetate	<b>cod</b>	1,5-cyclooctadiene
<b>Dabco<sup>TM</sup></b>	1,4-Diaza-bicyclo[2.2.2]octane	<b>CYS</b>	Cysteine
<b>PPh<sub>3</sub></b>	Triphenylphosphine	<b>GLU</b>	Glutamic acid
<b>P(tolyl)<sub>3</sub></b>	Tri- <i>para</i> -tolylphosphine	<b>R<sub>f</sub> value</b>	Retardation factor
<b>dppa</b>	<i>bis</i> -Diphenylphosphinoaniline	<b>IR</b>	Infra-red
<b>NMR</b>	Nuclear Magnetic Resonance		
<b>dppm</b>	<i>bis</i> -Diphenylphosphinomethane		
<b>dpe</b>	diphenylethyne		
<b>RSH</b>	<i>N</i> -acetyl- <i>L</i> -cysteine		
<b>GSH</b>	reduced glutathione ( $\gamma$ -GLU-CYS-GLY)		
<b>HSA</b>	Human serum albumin		
<b>DNA</b>	Deoxyribonucleic acid		
<b>NMR</b>	Nuclear magnetic resonance		
<b>HETCOR</b>	Heteronuclear Correlation		
<b>COSY</b>	Correlation Spectroscopy		
<b>HSQC</b>	Heteronuclear Single Quantum Correlation		
<b>TLC</b>	Thin layer chromatography		
<b>MLCT</b>	Metal-to-Ligand Charge Transfer		
<b>IC</b>	Inhibitory Concentration		
	e.g. IC <sub>50</sub> – dose at which 50% of cell growth is inhibited		
<b>EDG</b>	Electron Donating Group		
<b>EWG</b>	Electron Withdrawing Group		





# **Chapter 1:**

## **General Introduction**

## Contents

<b>1.1 Chapter 1 Background</b> .....	4
<b>1.2 The Biological Role of Metal Ions</b> .....	4
<b>1.3 Non Platinum Based Metallo Drugs</b> .....	4
1.3.1 Background.....	6
1.3.2 Gold Based Metallo Drugs .....	8
1.3.3 Vanadium Based Metallo Drugs .....	11
1.3.4 Ruthenium Based Metallo Drugs .....	12
1.3.5 Titanium and Gallium Based Metallo Drugs .....	13
<b>1.4 Platinum Based Metallo Drugs</b> .....	15
1.4.1 Background.....	15
1.4.2 Cisplatin Pharmacokinetics .....	16
1.4.3 Mechanism of Action of Cisplatin I (DNA Binding) .....	17
1.4.4 Mechanism of Action of Other Platinum Anti-cancer Agents (Intercalation and Non-DNA interactions).....	20
1.4.5 Second Generation Platinum Drugs .....	23
1.4.5.1 Carboplatin.....	23
1.4.5.2 Oxaliplatin .....	24
1.4.5.3 Other second Generation Pt Drugs.....	26
1.4.6 Third Generation Platinum Drugs.....	28
1.4.7 New Second and Third Generation Platinum Drug Design.....	31

---

<b>1.5 Hemilabile Mixed Donor ligands as Non-Leaving Groups</b> .....	33
1.5.1 Hemilability Overview.....	33
1.5.2 Types of Hemilability .....	35
1.5.2.1 Type I: Spontaneous Opening .....	36
1.5.2.2 Type II: Intramolecular competition .....	36
1.5.2.3 Type III: Coordination by an external reagent .....	37
1.5.3 Hemilabile Functional Phosphines and Their Complexes .....	38
<b>1.6 The Types of Platinum Complexes in this Work</b> .....	40
1.6.1 Platinum Complexes from Iminophosphines.....	40
1.6.2 Platinum Complexes from Phosphinoamines .....	41
1.6.3 Biologically Active Cyclometallated Complexes .....	42
<b>1.7 Photophysical Properties of Platinum Complexes</b> .....	44
1.7.1 Inorganic Complexes in Photodynamic Therapy (PDT) .....	44
1.7.2 Luminescence of Platinum Based Complexes .....	46
<b>1.8 Summary and Objectives</b> .....	48
<b>1.9 Bibliography</b> .....	51

## 1.1 Chapter 1 Background:

Since the discovery of the anti-cancer activity of Cisplatin  $cis\text{-}[\text{PtCl}_2(\text{NH}_3)_2]$  by Rosenberg *et al* in the 1960's the entire area of metallo-drugs has expanded rapidly.<sup>1</sup> This is especially true for complexes associated with the group 10 transition metals, particularly platinum. This chapter aims to explore the current progress of platinum based drugs and any future potential which they may hold and their relevance to this research project. The role of metals in biological organisms is also detailed here along with the success of other metals in medicine.

Emphasis is placed on the discovery of Cisplatin (and its analogues), which became the first and most successful platinum based anti-cancer drug and will be discussed in detail later in this chapter. Cisplatin works by binding to the DNA of fast developing cancer cells and suppresses the division of those cells.<sup>2</sup> This biological interaction has stimulated the development of a vast range of other biologically active metal complexes. Both the mechanism of these biological interactions as well as the structure of all biologically active metal complexes will be discussed in detail in this chapter.

This chapter also aims to introduce the concepts and principles of coordination chemistry that are utilised in the design, synthesis and applications of platinum complexes. The **Hard Soft Acid Base** (HSAB) theory and hemilability of various ligands will also be discussed along with the development of Cisplatin analogues.

## 1.2 The Biological Role of Metal Ions:

Living organisms do not employ the elements in accordance with their abundance in the Earth's crust. Elements such as aluminium and silicon, which are in high abundance, are rarely found in mammals. But elements such as copper, zinc and selenium, some of which are only present in trace amounts in the Earth's crust, play a crucial role in living organisms; such as cobalt in coenzyme B<sub>12</sub>.<sup>3</sup>

The vitamin coenzyme B<sub>12</sub>, which involves a cobalt-carbon bond, is the only known organometallic compound found in nature. Its structure incorporates a cobalt ion as Co(III) into a corrin ring structure, **101, Figure 1.1**. When the compound is isolated from natural sources the adenosine group is usually replaced by a cyanide group. It is in this form that the compound is used medicinally and is known as Vitamin B<sub>12</sub>. Coenzyme B<sub>12</sub> is known to prevent anaemia and it has also been found to have some catalytic properties.<sup>4</sup>

In this structure, **Figure 1.1**, the cobalt can be counted as Co (III), as stated by Miessler *et al*, where the four corrin nitrogens contribute two electrons each and a charge of -2 by delocalisation. The benzimidazole nitrogen contributes two electrons and the adenosine structure also contributes two electrons and a charge of -1. Therefore the octahedral complex contains six coordination bonds to cobalt which contribute 12 electrons in total, when added to the 6 valence electrons of Co (III) this gives a stable 18 electron complex.<sup>4</sup>

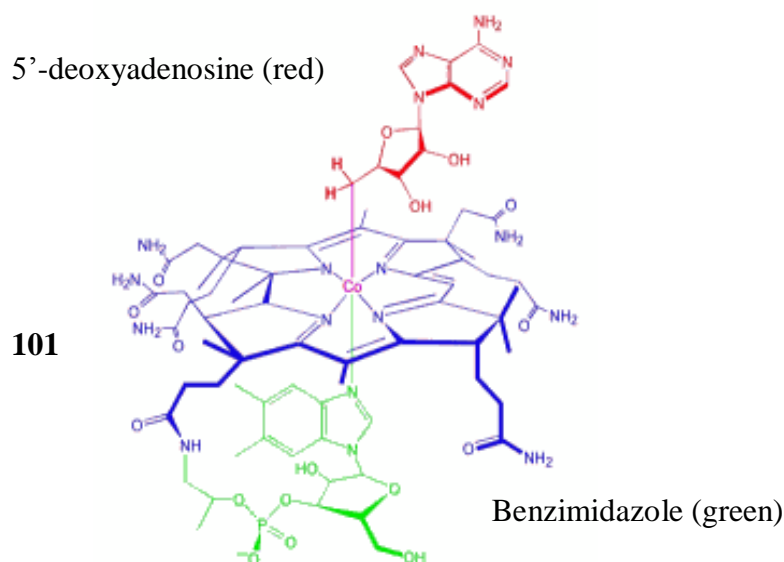


*Figure 1.1: The octahedral coenzyme B<sub>12</sub> 101 complex where the red section is 5'-Deoxyadenosine and the green section is Benzimidazole.*

Many catalytic proteins, known as *metallo-enzymes*, already have naturally occurring metals such as Zn (II) or Cu (I)/(II) in their active sites. Around thirty percent of enzymes have a metal atom at the active site and facilitate a variety of reactions such as acid-catalysed hydrolysis, redox reactions and the rearrangement of carbon-carbon bonds.<sup>5</sup>

Metal based proteins are also used in the binding and transport of oxygen, which is essential because of its role in respiration and its production in photosynthesis. They are commonly referred to as “oxygen carriers” and each of them make use of a metal atom or pair of metal atoms at an active site.<sup>3</sup>

Two such proteins used by vertebrates are haemoglobin, **102**, **Figure 1.2**, which is an oxygen carrier, and myoglobin, which is used for oxygen storage. A second type of oxygen carrier, hemocyanin, **103**, **Figure 1.2**, is found in snails and crabs while a third type, hemerythrin, **104**, **Figure 1.2**, is found in some sea worms. The O<sub>2</sub> binding site in haemoglobin consists of a single Fe (II) ion while hemocyanin uses a pair of Cu (I) ions and hemerythrin consists of a pair of Fe (II) ions.<sup>3</sup>

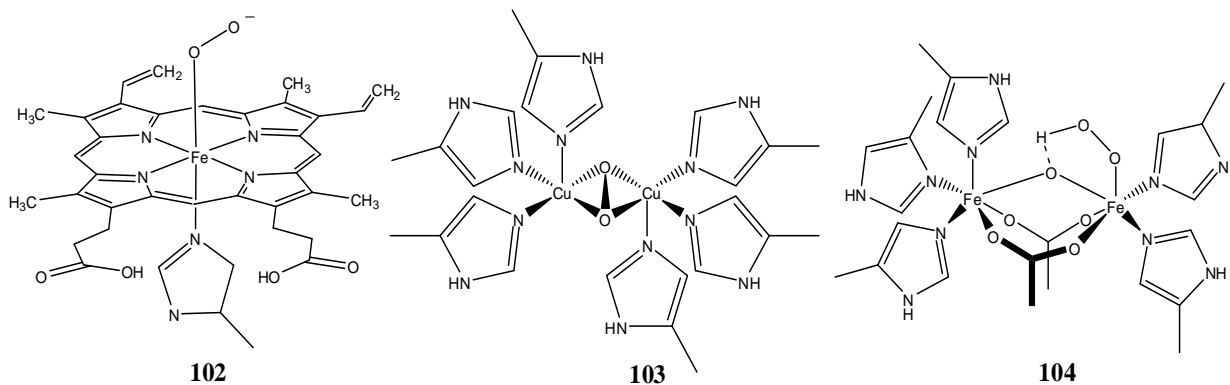


*Figure 1.2: Oxygen Carriers: A fragment of haemoglobin 102, hemocyanin 103 and hemerythrin 104 with an oxygen molecule bound to the active site.<sup>3</sup>*

As well as catalytic, transport and storage functions metal ions can play significant structural roles in biological systems, such as Ca (II) ions which are involved in protein folding. In general metal ion containing molecules serve important functions within biological systems. The manner in which they act is also highly varied where some metal ions can exert an inductive effect by coordination to the site of reaction. These can serve as redox sites that function by either electron or atom transfer. Selectivity can also be achieved by using ions of the appropriate size, stereochemical preference, hard-soft character, or reduction potential to perform a given task.<sup>3</sup>

### 1.3 Non Platinum-based Metallo-drugs:

#### 1.3.1 Background:

The human body has tens of thousands of different proteins, all of which have significant roles with specific functions such as catalysis, transport and providing structure. Metal ions in the form of a metallo-drug can attach themselves to a part of a protein that is critical for its function. The addition of a metallo-drug to a protein of this kind can result in displacement of the natural metal ion with that of the metallo-drug using the same ligands on the protein as donor atoms. This can then inhibit the protein from fulfilling its biological function which sometimes can be enough to kill the cell.<sup>5</sup>

As well as proteins, another important biomolecule that can be targeted by metallo-drugs is *deoxyribonucleic acid* or DNA. This polymeric molecule is critical for cell division and therefore any disruption in its function can have a disastrous effect on the cell. DNA

contains all the genetic information for all the cells that make up the body and found wrapped around proteins called *histones* which together form a particle known as a *nucleosome*.<sup>3,5</sup>

There are over ten million nucleosome particles in the human genome serving to organise the entire DNA into a relatively small nuclear space. The resulting protein-DNA complex is called *chromatin*. This complex is much less vulnerable to attack by metallo-drugs, in comparison to purified DNA, due to the blocking effects of the histones. But when a DNA sequence is being read to transcribe a gene, segments of the DNA are exposed and therefore susceptible to attack by drugs, **Figure 1.3**.<sup>5,6</sup>

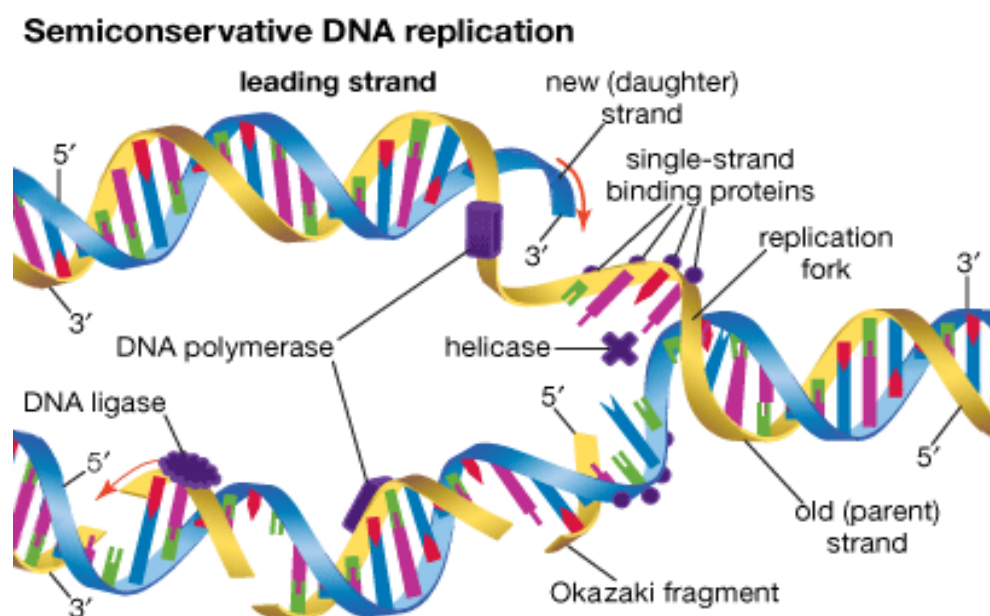


*Figure 1.3: DNA replication where segments of the strand are exposed to attack by various drugs.*<sup>6</sup>

DNA is made up of four different monomers called *nucleotides* which themselves consist of a heterocyclic base, a deoxyribose sugar and a phosphate group. There are donor groups on the DNA bases that can serve as nucleophiles towards metallo-drugs. They are also generally located on the exposed edges of the base pairs, making metal DNA binding easier. The most important metal binding sites that have been identified are N-7 positions of adenine and guanine, both of which are located in the major groove (elongated stretch) of double helical DNA.<sup>5</sup>

The lone pairs on the nitrogen atoms of these bases are only weakly basic towards a proton, so competition between a proton and a metal ion for these sites at neutral pH is not a factor. For these reasons metallo-drugs are often bound quite easily to these donor atoms and



since these atoms are considered intermediate bases on the Hard Soft Acid Base (HSAB) scale, **Table 1.1** and **Table 1.2**, they form the most favourable complexes with intermediate acids.<sup>7</sup>

<i>Hard Bases</i>	<i>Borderline Bases</i>	<i>Soft Bases</i>
		H <sup>-</sup>
F <sup>-</sup> , Cl <sup>-</sup>	Br <sup>-</sup>	I <sup>-</sup>
H <sub>2</sub> O, OH <sup>-</sup> , O <sup>2-</sup>		H <sub>2</sub> S, HS <sup>-</sup> , S <sup>2-</sup>
ROH, RO <sup>-</sup> , R <sub>2</sub> O, CH <sub>3</sub> COO <sup>-</sup>		RSH, RS <sup>-</sup> , R <sub>2</sub> S
NO <sub>3</sub> <sup>-</sup> , ClO <sub>4</sub> <sup>-</sup>	NO <sub>2</sub> <sup>-</sup> , N <sub>3</sub> <sup>-</sup>	SCN <sup>-</sup> , CN <sup>-</sup> , RNC, CO
CO <sub>3</sub> <sup>2-</sup> , SO <sub>4</sub> <sup>2-</sup> , PO <sub>4</sub> <sup>3-</sup>	SO <sub>3</sub> <sup>2-</sup>	S <sub>2</sub> O <sub>3</sub> <sup>2-</sup>
NH <sub>3</sub> , RNH <sub>2</sub> , N <sub>2</sub> H <sub>4</sub>	C <sub>6</sub> H <sub>5</sub> NH <sub>2</sub> , C <sub>5</sub> H <sub>5</sub> N, N <sub>2</sub>	R <sub>3</sub> P, (RO) <sub>3</sub> , R <sub>3</sub> AsC <sub>2</sub> H <sub>4</sub> , C <sub>6</sub> H <sub>6</sub>

*Table 1.1: Examples of “Hard and Soft Bases”, adapted from R.G. Pearson.<sup>7</sup>*

<i>Hard Acids</i>	<i>Borderline Acids</i>	<i>Soft Acids</i>
H <sup>+</sup> , Li <sup>+</sup> , Na <sup>+</sup> , K <sup>+</sup>		
Be <sup>2+</sup> , Mg <sup>2+</sup> , Ca <sup>2+</sup> , Sr <sup>2+</sup>		
BF <sub>3</sub> , CCl <sub>3</sub> , B(OR) <sub>3</sub>	B(CH <sub>3</sub> ) <sub>3</sub>	BH <sub>3</sub> , Tl <sup>+</sup> , Tl(CH <sub>3</sub> ) <sub>3</sub>
Al <sup>3+</sup> , Al(CH <sub>3</sub> ) <sub>3</sub> , AlCl <sub>3</sub> , AlH <sub>3</sub>		
Cr <sup>3+</sup> , Mn <sup>2+</sup> , Fe <sup>3+</sup> , Co <sup>3+</sup>	Fe <sup>2+</sup> , Co <sup>2+</sup> , Ni <sup>2+</sup> , Cu <sup>2+</sup> , Zn <sup>2+</sup> , Rh <sup>3+</sup> , Ir <sup>3+</sup> , Ru <sup>3+</sup> , Os <sup>2+</sup>	Cu <sup>+</sup> , Ag <sup>+</sup> , Au <sup>+</sup> , Cd <sup>2+</sup> , Hg <sub>2</sub> <sup>2+</sup> , Hg <sup>2+</sup> , CH <sub>3</sub> Hg <sup>+</sup> , Pd <sup>2+</sup> , Pt <sup>2+</sup> , Pt <sup>4+</sup>
Ions with oxidation states of 4 or higher	SO <sub>3</sub> <sup>2-</sup>	Br <sub>2</sub> , I <sub>2</sub>
Hydrogen-bonding molecules	C <sub>6</sub> H <sub>5</sub> NH <sub>2</sub> , C <sub>5</sub> H <sub>5</sub> N, N <sub>2</sub>	Metals(0), π-acceptors

*Table 1.2: Examples of “Hard and Soft Acids”, adapted from R.G. Pearson.<sup>7</sup>*

### 1.3.2 **Gold based Metallo-Drugs:**

Gold in its many forms has been used medicinally for hundreds of years for the treatment of various ailments, particularly arthritis. Elemental gold is relatively rare and chemically inert but can be easily extracted from the earth and shaped into a variety of forms. It has a long association with humans and found its way into nearly every culture in the form

of jewellery, ornaments and monetary exchange. Gold compounds on the other hand are much more chemically reactive and serve a variety of medicinal applications such as treating cancer, malaria and AIDS.<sup>8,9</sup>

Rheumatoid arthritis is a systemic disorder that causes the immune system to attack joints of the body which ultimately results in the loss of the lubricating fluid causing the joint to swell and deform.<sup>10</sup> The use of gold for treating rheumatoid arthritis was first described by Forestier in 1934 when he described the use of gold salts for the treatment of tuberculosis and arthritis.<sup>11</sup> Since then numerous studies of gold compounds in biological media have raised the issue of stability in low pH environments, such as the stomach. Unfortunately this property reduces the effectiveness of the drugs towards treatment of arthritis. It has been found by some investigators that auranofin in particular, a popular gold based rheumatoid arthritis treatment, degrades in stomach acid; leaving only 25% of the oral dose to be absorbed through the intestine.<sup>4,12</sup> Despite these stability problems, a wide range of gold compounds have approved for use for the treatment of rheumatoid arthritis, **Figure 1.4**.

Gold compounds have also been investigated in connection with their activity as anti-cancer agents.<sup>8</sup> Some early work on auranofin, **108**, **Figure 1.4** and its analogues revealed that Au (I) complexes which contained phosphine and thioglucose ligands were quite effective at killing melanoma and leukaemia cells *in-vitro*.<sup>13,14</sup>

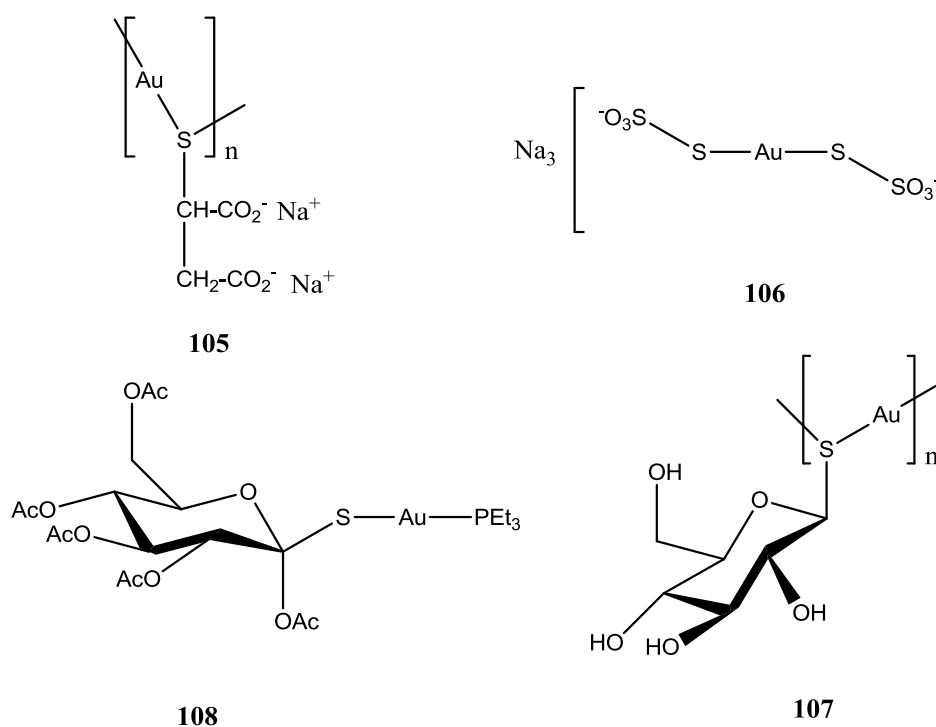


**Figure 1.4:** Structure of gold-based drugs used for the treatment of arthritis; sodium aurothiomalate **105**, aurothiosulphate **106**, aurothioglucose **107**, auranofin **108**.

Unlike other metal based anti-cancer agents, such as Pt (II); which are stable towards reduction, many Au (III) complexes were found to be easily reduced by thiol based biomolecules. There has been however some initial success with organometallic type compounds which contained Au (III)-carbon bonds, **112**, **Figure 1.5**, along with some compounds with bulky ligands. This bond strongly donates electrons to the metal ion via a  $\sigma$  bond, which makes the metal ion more difficult to reduce. Some of these complexes also contained two easily displaced ligands such as  $\text{Cl}^-$ ,  $\text{SCN}^-$  or  $\text{OAc}^-$  in *cis* configurations, which has been found to be very important for anti-cancer activity and will be discussed further in **Section 1.6**.<sup>15</sup>

Work by Berners-Price and Sadler also found that the presence of five-membered chelate rings and phosphorus atoms with bulky phenyl groups can block nucleophiles from attacking the central gold ion.<sup>16</sup> Further work by Che and co-workers resulted in the synthesis of the square planer  $\text{Au}(\text{TPP})\text{Cl}$  complex, **111**, **Figure 1.5**. This compound was designed with a tetraphenylporphyrin ligand bound to Au (III) giving a very stable complex in biological environments.<sup>17,18</sup> Further *in-vitro* screening of the compound resulted in high anti-cancer activity and good  $\text{IC}_{50}$  values against nasopharyngeal carcinoma.<sup>19</sup>

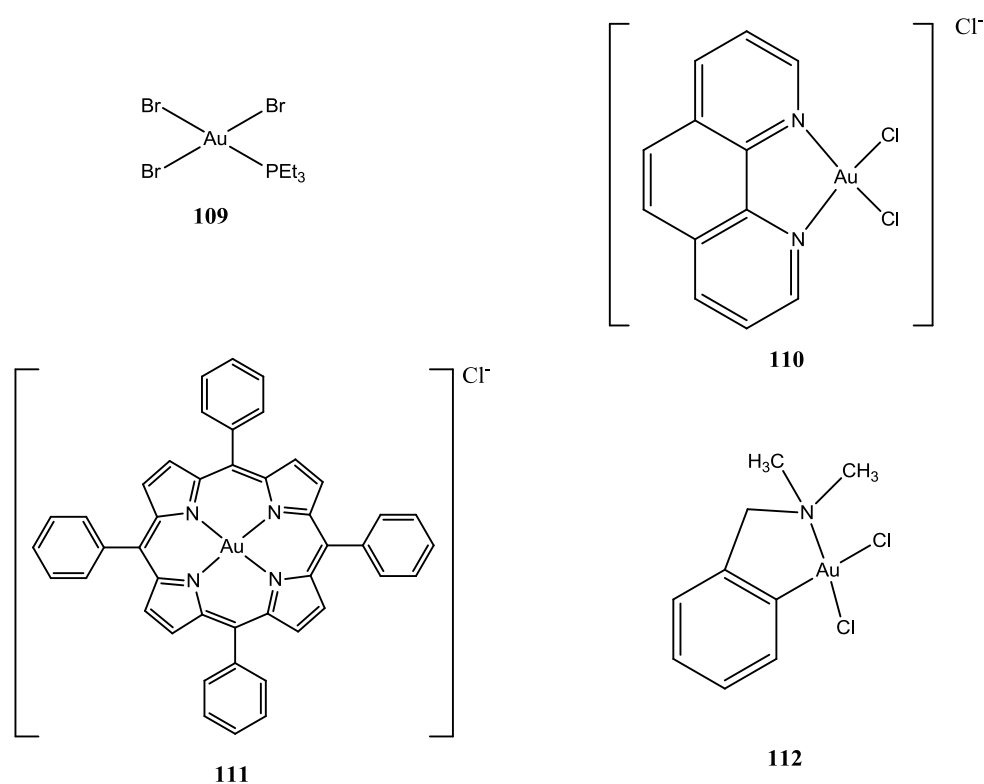


**Figure 1.5:** Structure of some gold-based anti-cancer drugs: sodium  $\text{AuBr}_3(\text{PEt}_3)$  **109**,  $\text{AuCl}_2(\text{phen})\text{Cl}$  **110**,  $\text{Au}(\text{TPP})\text{Cl}$  **111**,  $\text{AuCl}_2(\text{damp})$  **112**.

The organometallic gold anti-cancer compounds went on to show activity against bladder and ovarian cancer cell lines and some analogues even exhibited activity comparable to cisplatin.<sup>20</sup> The Au (III) ion in these and other compounds, **110**, **Figure 1.5**, is an intermediate acid on the HSAB scale, therefore allowing it to bind to the intermediate bases on DNA. Work by Mirabelli *et al* has demonstrated that these complexes can clearly change the degree of supercoiling of DNA.<sup>21</sup>

Currently specific cellular targets for the phosphine type compounds have not been identified, but some reports have shown the site of action to be the mitochondria within the cell.<sup>22,23</sup> Other investigations gave indications that the complex  $[\text{AuBr}_3(\text{PEt}_3)]$  **109**, **Figure 1.5** in particular binds to the N-7 position of guanine bases on double stranded DNA.<sup>24,25</sup> Also, more recent studies with triphenylphosphine type complexes have revealed inhibition of the enzyme lipoxygenase whose metabolites can regulate cellular proliferation or apoptosis.<sup>26</sup>

### 1.3.3 Vanadium based Metallo-Drugs:

Vanadium has been used as a treatment for diabetes for over a hundred years. In 1899 the French physician B. Lyonnet described the ability of sodium vanadate,  $\text{Na}_3\text{VO}_4$ , to lower the blood sugar levels of diabetic patients.<sup>27,28</sup>

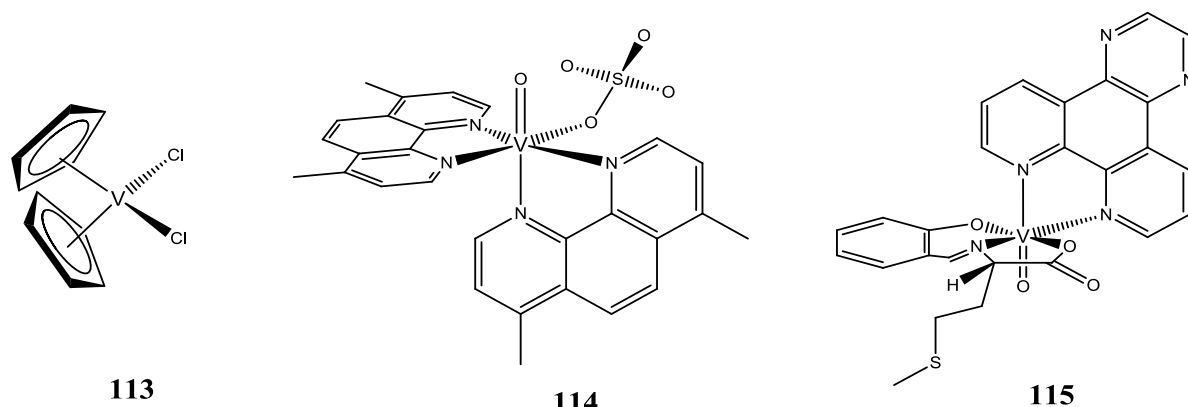


**Figure 1.6:** Structure of vanadocene dichloride **113**, bis(4,7 – dimethyl-1, 10-phenanthroline) sulfatooxovanadium (IV) [metvan] **114**, and VO[salmet](dpg) **115**, all of which have anti-tumour properties.

Modern vanadium complexes, such as those in **Figure 1.6**, are insulin mimics in the forms of vanadate (which contains V (V)) and vanadyl  $\text{VO}^{2+}$  (which contains V (IV)). The

vanadyl compounds currently exhibit very few side effects and certain complexes also help maintain proper glucose levels for individuals.<sup>27</sup>

As well as having anti-diabetic properties, some vanadium complexes also have anti-cancer effects, first reported by Kopf-Maier *et al.* During testing for anti-cancer activity, in particular for vanadocene dichloride **113**, **Figure 1.6**, these vanadium based metallo drugs exhibited less toxicity and fewer side effects than cisplatin (the benchmark metallo anti-cancer drug). Some of these complexes have also been found to bind to DNA and form similar adducts as those formed with cisplatin.<sup>29</sup>

The planar oxovanadium (IV) compound bis(4,7 – dimethyl-1, 10-phenanthroline) sulfatooxovanadium (IV), metvan **114**, **Figure 1.6** has shown huge potential as an anti-cancer agent by inducing cell apoptosis in human leukemia cells, some myelomas and solid tumour cell lines.<sup>30–32</sup> Other oxovanadium (IV) complexes such as VO[(salmet)(dpg)] **115**, **Figure 1.6** which contain Schiff base ligands, have also been investigated by Chakravarty and coworkers in connection with photodynamic therapy (PDT).<sup>33</sup> PDT is the use of light to destroy tumours in connection with a photosensitive anti-cancer drug and has been effective in connection with quite a few anti-cancer metallo drugs.<sup>34</sup> It will be discussed further in **Section 1.7**.

#### **1.3.4 Ruthenium based Metallo-Drugs:**

Although the use of metals in medicine is largely overshadowed by platinum, ruthenium is sometimes seen as a very attractive alternative due to its rich synthetic chemistry and range of oxidation states (Ru (II), Ru (III) and Ru (IV)). These features are quite significant since the activities of most metal-based anti-cancer drugs rely heavily on their oxidation state.<sup>35,36</sup>

For many years ruthenium complexes were used exclusively as metal catalysts for chemical transformations,<sup>37</sup> but since the late 1980's their anti-cancer activity has been the focus of considerable interest. Some of the anti-cancer active complexes kill the primary tumour cells while others prevent the tumour from spreading to other parts of the body.<sup>36</sup> Two compounds in particular, NAMI-A and KP1019 (both containing Ru (III)), are currently involved in clinical trials, **Figure 1.7**, as well as other complexes such as KP1339.<sup>38–40</sup>

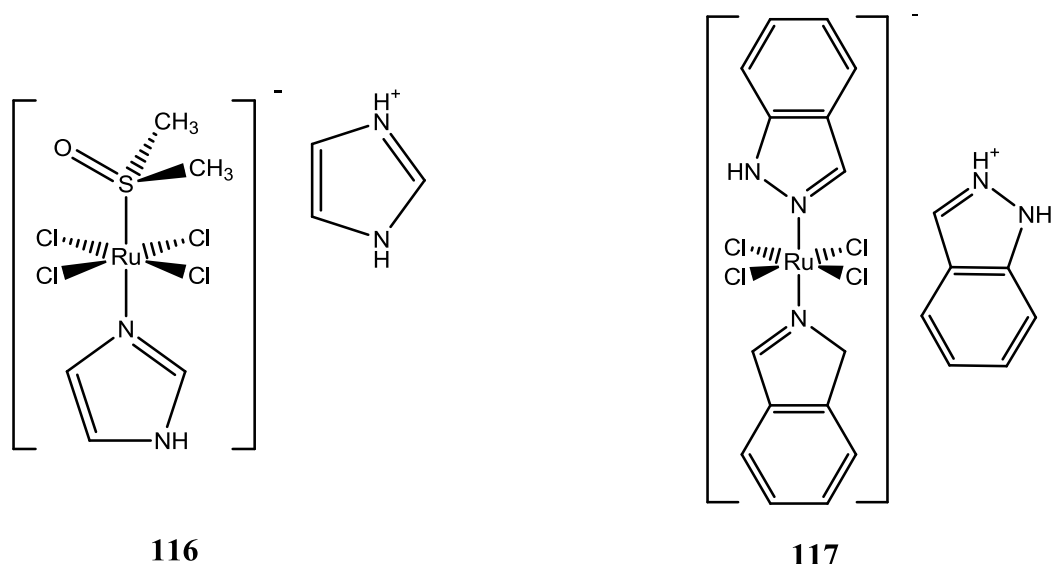


**Figure 1.7:** Structure of NAMI-A **116** and KP1019 (FFC14A) **117**, both of which contain Ru (III) and are currently undergoing clinical trials for anti-cancer activity.

As well as various oxidation states, ruthenium is also well suited to medical use due to its ability to exchange ligands rapidly and mimic iron in binding to certain biological molecules such as transferrin. In rapidly dividing cancer cells there is a greater demand for iron so the transferrin receptors are over-expressed, allowing ruthenium metallo-drugs to enter the cell with greater efficiency.<sup>36,41</sup>

More recent work on organometallic based ruthenium complexes has also shown promising results against some cisplatin-resistant human ovarian cell lines.<sup>42,43</sup> These complexes contain Ru (II) and represent an interesting class of mixed arene and phosphine based compounds with anti-cancer activity, **Figure 1.8**.<sup>44,45</sup> Similar to platinum based anti-cancer drugs, as part of their biological activity, these compounds have been reported to lose their bound ligands and react with target molecules in the cell.<sup>46</sup>

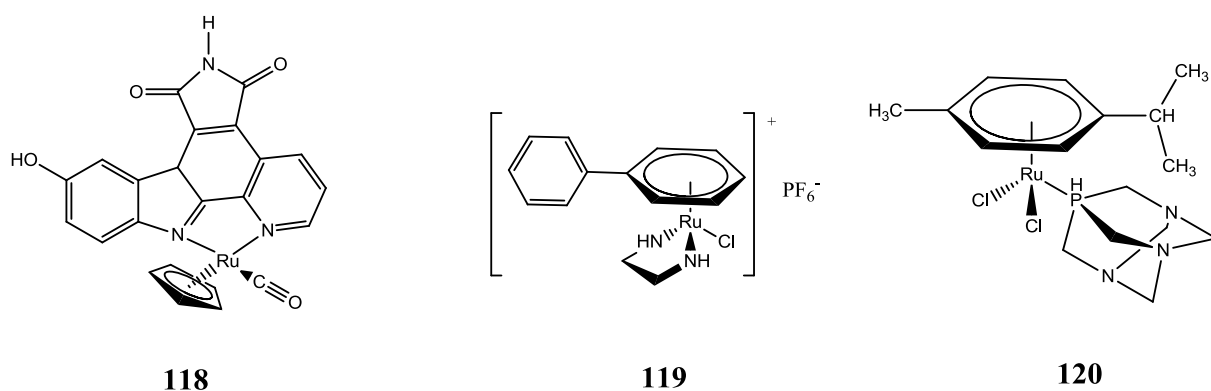


**Figure 1.8:** Structure of DW12 **118**,  $[(\eta^6\text{-biphenyl})\text{Ru}(\text{en})\text{Cl}]\text{PF}_6$  **119** and  $[(\eta^6\text{-}p\text{-cymene})\text{Ru}(\text{pta})\text{Cl}_2]$  **120**, all of which contain Ru (II) and have displayed significant anti-cancer potential.<sup>46</sup>

### 1.3.5 Titanium and Gallium based Metallo-Drugs:

In 1979, one year after cisplatin was approved for use as a drug, Kopf and Kopf-Maier reported a simple titanium based metallocene that exhibited potent antitumor properties, called titanocene dichloride.<sup>47</sup> Titanocene dichloride, **121**, **Figure 1.9**, was found to interact with DNA in a similar manner to cisplatin due to the two chloride leaving groups present. The compound was also found to accumulate in the nuclei of human tumours and bind to DNA in a similar manner to cisplatin.<sup>48</sup> As well as this it was also found to have less toxicity than cisplatin and displayed no nephro- or myelotoxicity (which are commonly associated with cisplatin).<sup>47</sup>

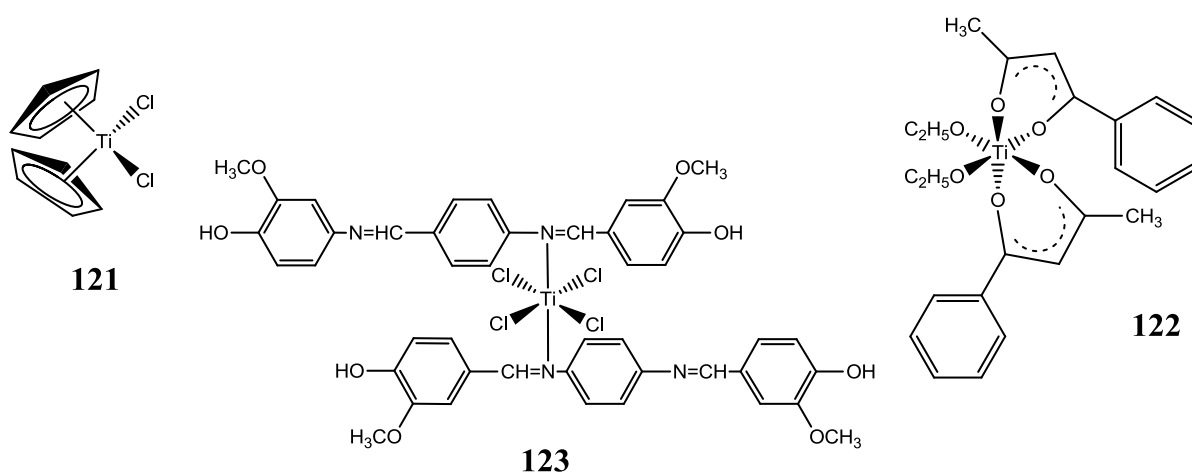


*Figure 1.9: Structures of titanocene dichloride **121**, budotitane **122** and a Schiff-base titanium complex **123**, all of which have been confirmed to have anti-cancer activity.<sup>49</sup>*

This discovery prompted other research groups to investigate a wide range of titanium based metallo-drugs including  $\beta$ -diketonate complexes consisting of a Ti (IV) metal centre **122**, **Figure 1.9**, called budotitane. Titanocene dichloride on the other hand went on to become the first non-platinum metal complex to enter clinical trials along with various other complexes synthesised by Keppler and coworkers.<sup>49</sup>

Studies with budotitane in particular reported that due to the presence of the phenyl groups on the  $\beta$ -diketonate ligands the compound may bind to DNA via intercalation; a method of biological interaction which has also become evident for some platinum complexes (further discussed in **Section 1.4**).<sup>50</sup> Further clinical trials were later discontinued however due to hydrolytic instability of the complexes at physiological pH and difficulty in formulating a solution that could be used in chemotherapy.<sup>51</sup>

Recently however there has been some interest in the more stable titanium Schiff-base coordination complexes featuring a mixture of chelating nitrogen and oxygen donor atoms. A report from Obeid *et al* in particular has seen *in-vitro* antibacterial and antitumor activity via DNA cleavage from some novel Schiff-base titanium complexes, **123**, **Figure 1.9**.<sup>52</sup>

Chelating nitrogen and sulphur based ligands have also been investigated in connection with both titanium and in particular gallium metallo-drugs as anti-cancer agents. Recently Kowol and co-workers have reported the anti-cancer properties of a Ga (III) compound containing a thiosemicarbazone ligand. This tri-dentate five-coordinate distorted square-pyramidal complex is isolated from the reaction of GaCl<sub>3</sub> with a pyridine-dimethylthio-semicarbazone ligand **124**, **Figure 1.10**. Through a proposed interaction with ribonucleotide reductase, it has exhibited potent toxicity towards human ovarian carcinoma (41M) and mammary carcinoma (SK-BR-3) cells *in-vivo*.<sup>53</sup>

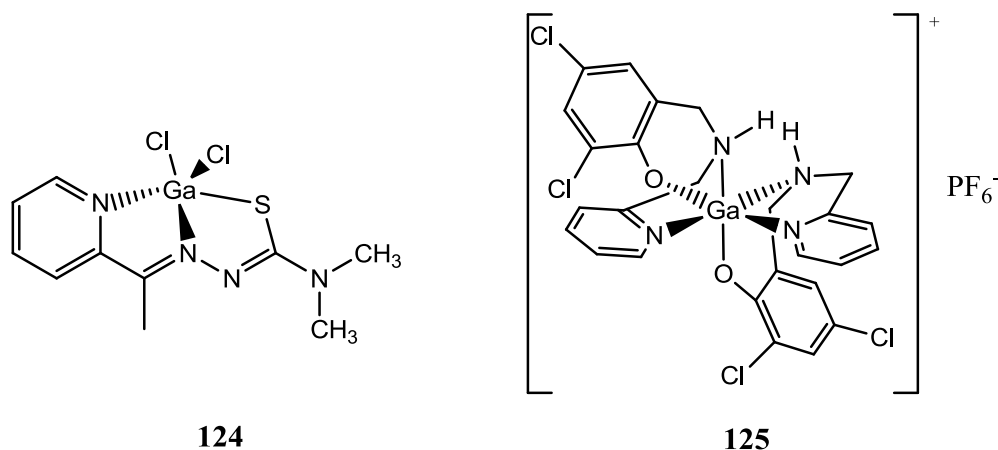


**Figure 1.10:** Structures of the anti-cancer active complex GaLCl<sub>2</sub> **124**, and the octahedral complex *cis, cis, cis*-[GaL<sub>2</sub>]ClO<sub>4</sub> **125**.

Further work by Veriani and co-workers have also revealed anti-cancer properties with octahedral Ga (III) complexes **125**, **Figure 1.10**. The cytotoxicity of these tridentate N<sub>2</sub>O complexes have revealed strong activity towards human neuroblastoma (SK-N-Be(2)) cells and the mechanism of action is thought to target the proteasome in prostate cancer cell lines.<sup>54</sup>



## 1.4 **Platinum-based Metallo-Drugs:**

### 1.4.1 **Background:**

Platinum and palladium have distinctly different properties than the 1<sup>st</sup> row group 10 transition element nickel. Although nickel does exist in Ni (III) and Ni (IV) oxidation states, the octahedral structures it forms tend to be distorted due to its small size so Ni (II) is the primary oxidation state. This is in contrast to palladium and platinum whose M (IV) oxidation states generally form regular octahedral complexes.<sup>55</sup>

Although four coordinate Ni (II) complexes can form both tetrahedral and square planar structures, Pt (II), which has the electronic configuration of 5d<sup>8</sup> and is diamagnetic (S=0), only forms square planar complexes. In these square planar structures the  $d_x^2 - y^2$  orbital is pushed higher in energy and the large energy difference between the  $d_x^2 - y^2$  and the  $d_{xy}$  orbitals results in only the  $d_{xy}$  orbital being occupied, therefore only square planar complexes are formed.

The common occurrence of square planar 4d<sup>8</sup> and 5d<sup>8</sup> complexes correlates with the high values of the ligand-field splitting parameter in these two series, which give rise to a high ligand-field stabilisation of the low-spin square-planar complexes. This is one of the primary distinguishing differences between nickel and the other group 10 metals in the d<sup>8</sup> configuration.<sup>56</sup>

Palladium, like platinum, also has a strong disposition to form coordination complexes. The distinguishing difference between palladium and platinum is that in the d<sup>8</sup> configuration Pd (II) complexes tend to be less stable (both kinetically and thermally) than their Pt (II) analogues.<sup>56</sup> This chapter will primarily focus on platinum in the (II) and (IV) oxidation states and complexes with square planar and octahedral geometry respectively.

### 1.4.2 **Cisplatin Pharmacokinetics:**

The bright yellow compound *cis*-diamminedichloroplatinum(II) was first reported by the Italian chemist Michele Peyrone in 1844 and was later named Peyrone's Salt.<sup>57</sup> The molecular structure of the compound, including its isomerism, was then determined by Alfred Werner as part of his 1913 Nobel Prize winning work.<sup>58</sup> But it was not until 1965 that the biological activity of Peyrone's Salt was discovered by Rosenberg, van Camp *et al* of

Michigan State University and the compound subsequently became known as *cisplatin*, **126**, **Figure 1.11**.

Rosenberg initially discovered that electrolysis of platinum electrodes generated a soluble complex which inhibited binary fission in *E. coli* bacteria. The bacterial growth actually continued but the cell division was stopped resulting in long filaments of bacterial growth. It was discovered that while the electric current was running it created a tiny concentration (~10 ppm) of the platinum complexes *cis*-dichlorodiammine-platinum (II) and *cis*-tetrachlorodiammine-platinum (IV).<sup>59</sup> These *cis* complexes inhibited the cell division in bacteria, however the *trans* analogues were not found to be active and will be discussed in more detail in **Section 1.3.2**.

When dissolved in water, cisplatin, *cis*-[PtCl<sub>2</sub>(NH<sub>3</sub>)<sub>2</sub>] slowly reacts losing its two chloride ligands to form the diaquated species, **128**, **Figure 1.11**.<sup>60</sup> When solvated, known as Platinol-AQ, it is stored in an aqueous solution containing sodium chloride at a pH that has been adjusted to between 3.5 and 4.5. The additional chloride ions push the equilibrium to the left in favour of the anti-cancer active dichloro form of the drug, **126**.<sup>61,60</sup>

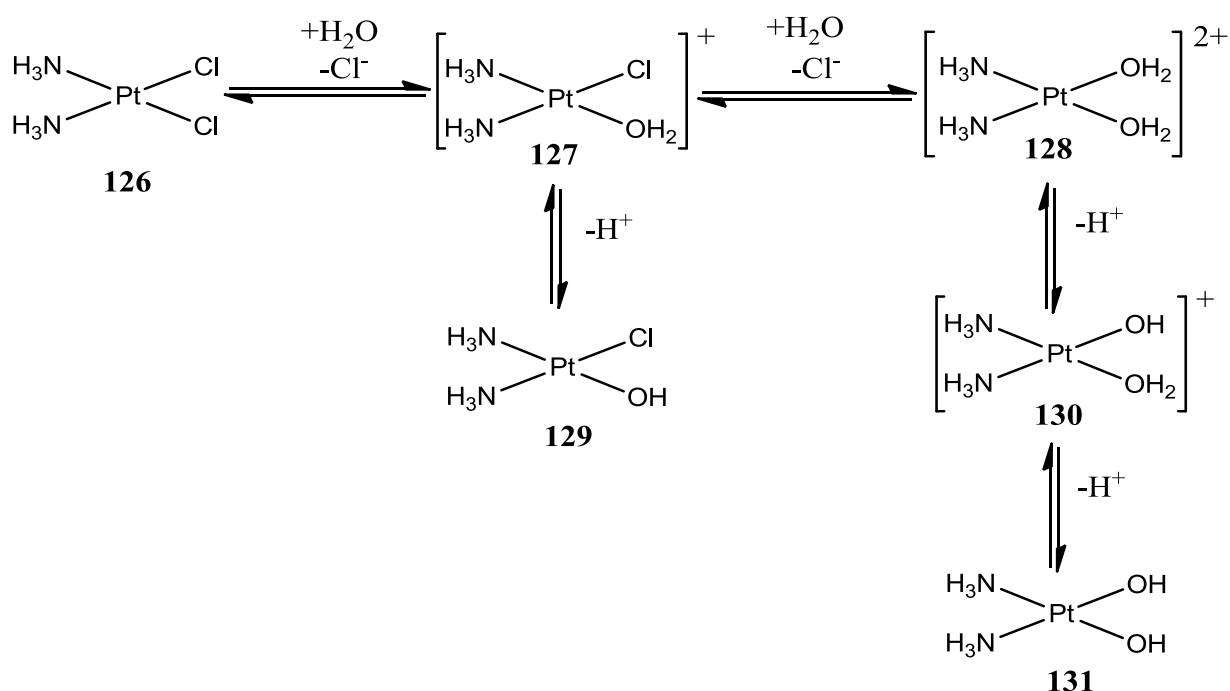


**Figure 1.11:** Speciation of cisplatin **126**, in aqueous solution where the chloride ligands are substituted by water to form the diaquated species **128**.<sup>60</sup>

The concentration of cisplatin in solution must be kept less than 105 mM in order to keep the concentration of chloride ions less than that found naturally in blood. This is to prevent

unwanted hydrolysis prior to entering the body which reduces the uptake of cisplatin into the cell. When added into blood, Le Chatelier's principle states that the system will move to the right in favour of the aquated species. Also the hydroxo form, **129**, **Figure 1.11**, has been found to predominate at 37°C (body temperature) which may have detrimental effects on the activity of cisplatin due to the hydroxide ion being a poorer leaving group than water.<sup>60,62</sup>

### 1.4.3 Mechanism of Action of Cisplatin (DNA Binding):

Shortly after the discovery of the anti-cancer activity of Cisplatin, Rosenberg and coworkers<sup>59</sup> along with Howle and Gale<sup>63</sup> suggested that its cellular target was DNA, **Figure 1.12**. Early research by Harder found that the platinum complexes were inhibiting the synthesis of DNA in cells. It was reported that although it prevented DNA replication it did not hinder RNA or protein synthesis. Evidence was also presented that the synthesis of precursors to DNA synthesis were not blocked. Therefore it was concluded that the platinum complex's mode of action was most likely due to a primary lesion in DNA itself.<sup>64</sup>

*Interstrand crosslinking* was initially ruled out since the distance between strands was greater than that which could be spanned by a single platinum metal complex ion (3.3 Å). Researchers therefore proposed that Cisplatin connected two adjacent purine bases on the same strand of DNA to form an *intrastrand purine dimer* (which are stacked 3.4 Å apart). Later studies supported this initial investigation and identified the major DNA adduct as Pt-GG along with lesser amounts of the DNA adduct Pt-AG, both of which were found to be *1,2 intrastrand crosslinks*.<sup>65,66</sup>

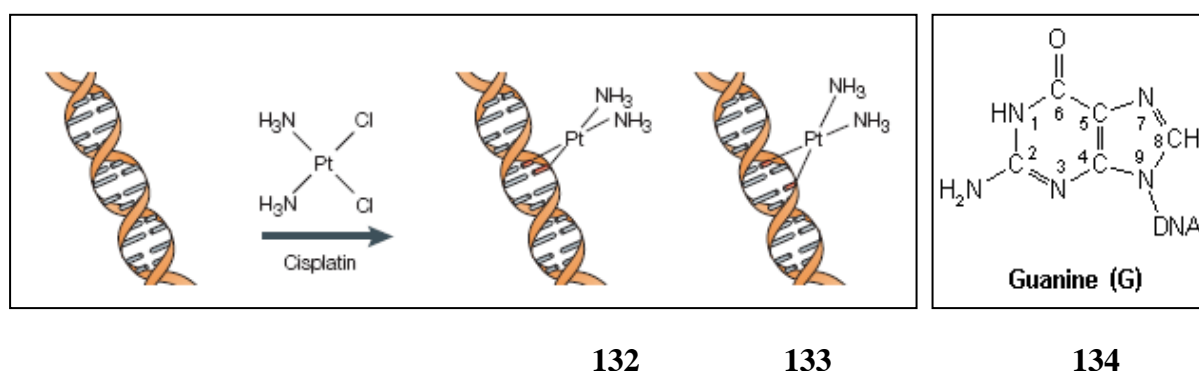


**Figure 1.12:** 1,2 intrastrand crosslinking **132**, and 1,3 intrastrand crosslinking **133**. Guanine with the N-7 position labelled **134**.<sup>2</sup>

From these early studies it was also determined that Cisplatin could form *1,3 intrastrand crosslinks* with guanine bases in trinucleotide sequences along with *interstrand crosslinks* between both DNA strands again using guanines. In all cases it was found that the primary donor atom used for binding to Pt (II) metal centres was the N-7 position of adenine or guanine, **134 Figure 1.12**. Once formed Cisplatin-DNA adducts induce a variety of cellular responses such as replication arrest, transcription inhibition, cell cycle arrest, induces necrosis and apoptosis.

Further studies by Hambley and co-workers determined the full mechanism of action for Cisplatin in the body, **Figure 1.13**. Once the Cisplatin complex enters the cell it is converted to the aqua form by losing its chloride *leaving groups* which can then displace its H<sub>2</sub>O ligands to coordinate to DNA easily. The aqua forms of the drug are in a proton equilibrium with their respective hydroxo (HO<sup>-</sup>) forms, but only the diaquated form can lose its ligands easily.<sup>67</sup>

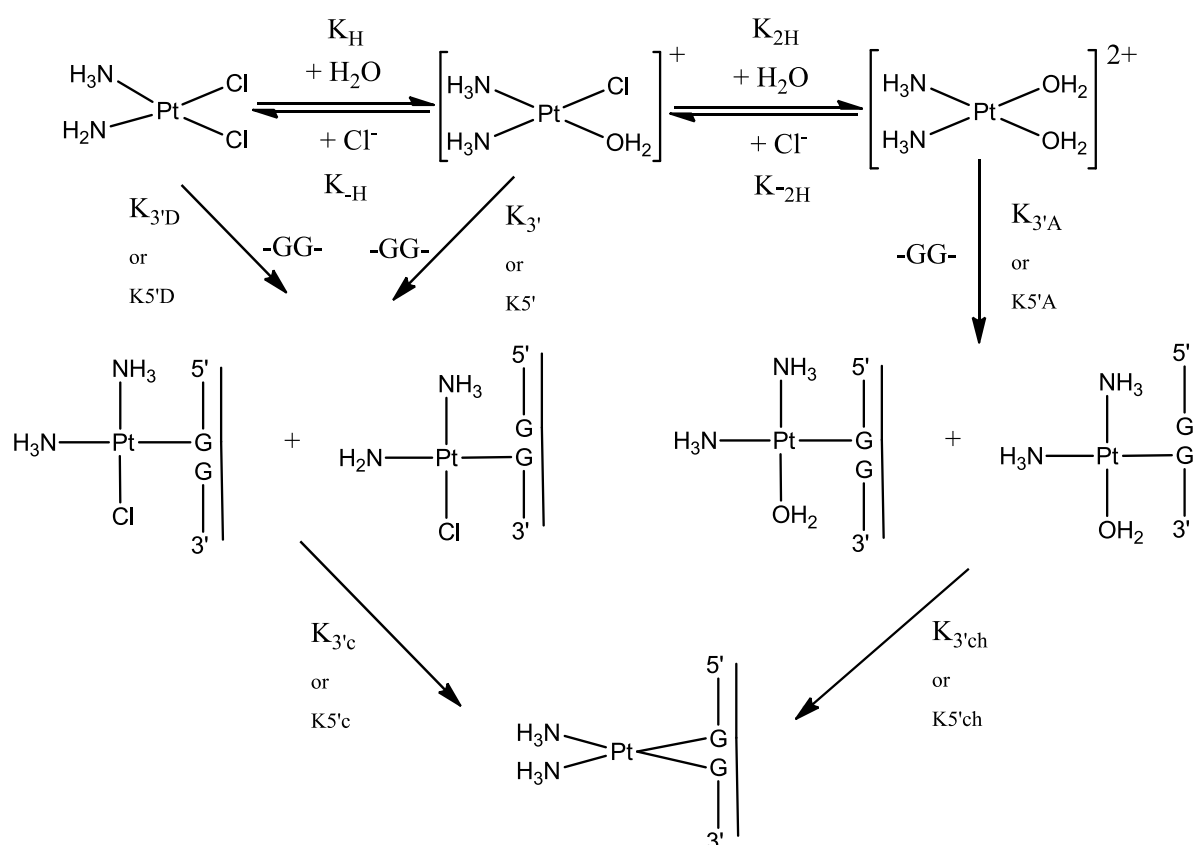


**Figure 1.13:** The reaction scheme for the binding of cisplatin to guanine base pairs on DNA strands (-GG-).<sup>67</sup>

The initial *in-vivo* trials with cisplatin saw 95% of the induced tumours in animals achieve complete regression. The complex even cured animals which were within a few days

of death. However drawbacks to this form of therapy were identified. The drugs also inhibit the cell-division in normal human tissue and somatic cells as well the ones present in the tumours, especially fast dividing cells such as the intestinal wall, causing severe internal damage.<sup>64,2</sup>

Although it is one of the world's foremost anti-cancer drugs, it still has some severe side effects including kidney damage and neurotoxicity along with nausea and vomiting.<sup>2</sup>

Its isomer, transplatin, on the other hand is not anti-cancer active due to its inability to form *intrastrand crosslinks*. Recent studies however has identified that isomers of *transplatin* are cytotoxic when photo-activated, using Photo Dynamic Therapy (PDT). By using lasers and fibre optics, site-specific activation of photo active chemotherapeutic agents is possible and will be discussed in more detail later in this chapter.<sup>68</sup>

#### **1.4.4 Mechanism of Action of Other Platinum Anti-cancer Agents (Intercalation and Non-DNA interactions):**

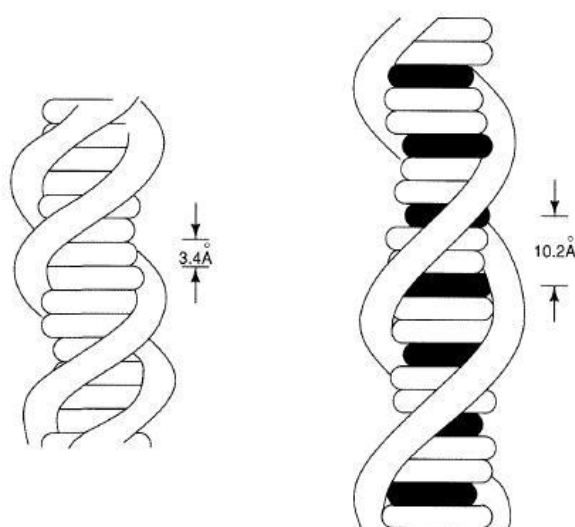


*Figure 1.14: Schematic representation of double stranded DNA without (left) and with (shaded area, right) a bound intercalator.<sup>69</sup>*

Another interesting feature of double-stranded DNA is that flat planar molecules (usually containing aromatic groups) that are hydrophobic, can insert themselves between the base pairs of DNA through a process known as intercalation. By doing this, the spacing between the base pairs of DNA must increase in order to accept the intercalating molecule, **Figure 1.14**. This also increases the length of the DNA helix, which will affect the template function of DNA in terms of replicating.<sup>5,69</sup>

Therefore, aside from simply binding a metal centre to a donor atom on a DNA strand, certain metal complexes that contain flat aromatic residues can also bind to DNA by intercalation. The driving force for this interaction is the association of the hydrophobic DNA base pairs with the hydrophobic region of the drug molecule.<sup>5,36</sup>

Some investigators have found that ruthenium compounds which contain an arene residue have the ability to intercalate between base pairs, as well as forming direct Ruthenium-DNA adducts to the N7 position of guanine (through mono-functional binding) such as those previously discussed in **Figure 1.8, Section 1.3.4.**<sup>70,71</sup> Further work by Nair *et al* on chromium (III) complexes has also shown bifunctional mechanisms with intercalation and binding in the major groove of a DNA double helix.<sup>72</sup>

As well as ruthenium and chromium complexes, bifunctional metallointercalator compounds have been identified for a variety of other metals but here the focus will be on platinum compounds.

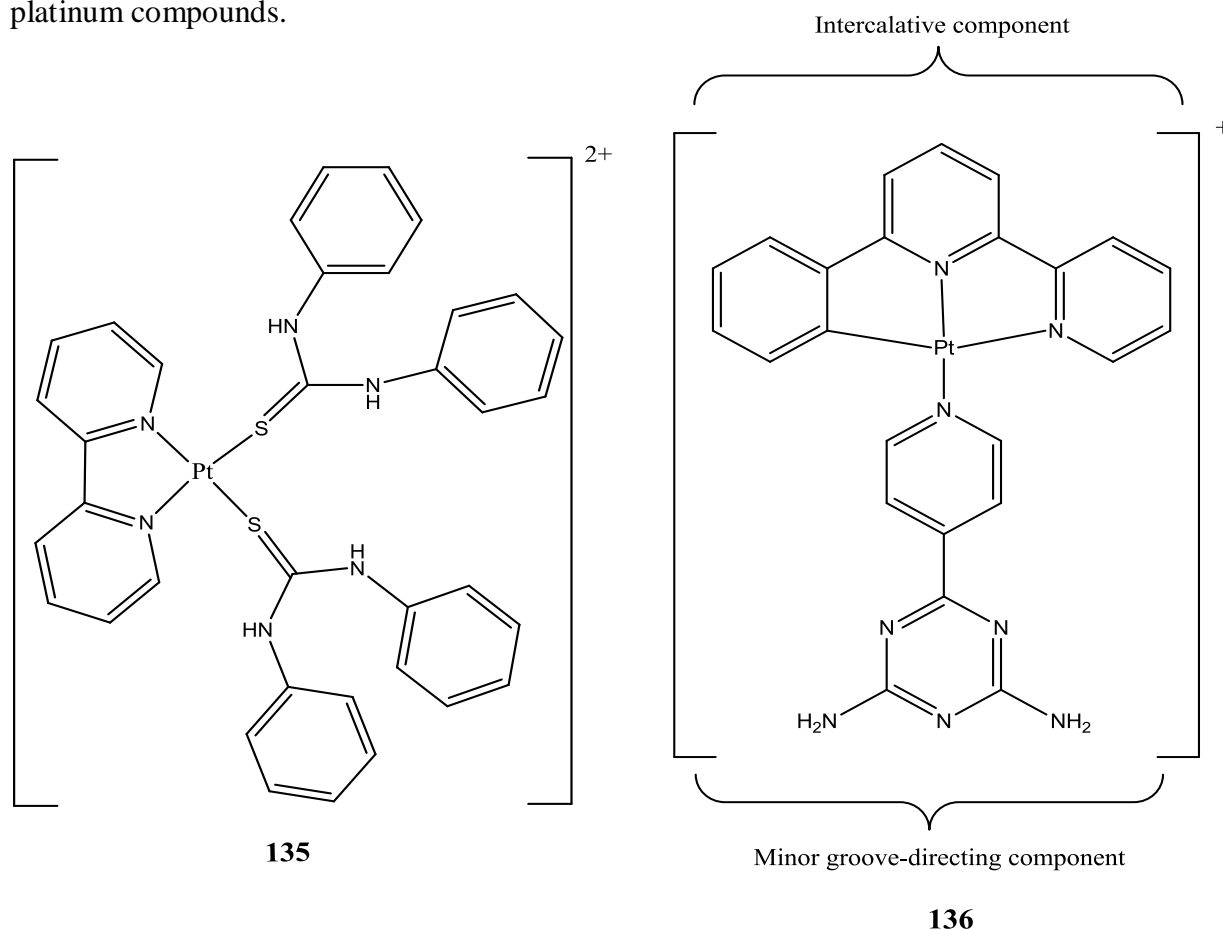


**Figure 1.15:** An intercalating Pt (II) bipyridyl complex with diphenylthiourea,  $[Pt(pipy)(ph2tu)_2]Cl_2$  **135**,<sup>73</sup> and the cyclometallated Pt (II) complex  $[Pt(CNN)(4-dpt)]PF_6$  **136** identifying the intercalating and non-intercalating portions of the complex.<sup>74</sup>

Lippard *et al* pioneered studies on DNA-metallointercalators using square-planar Pt (II) complexes with ligands containing aromatic groups,<sup>75</sup> while Barton *et al* subsequently extended the scope to various octahedral metal complexes with aromatic di-imine ligands.<sup>76</sup> As well as hydrophobic similarities, these metallointercalators also bind to DNA through  $\pi$ - $\pi$  and electrostatic interactions. Extensive reports by Mingos *et al* advocate design studies based on metal complexes with nitrogen-donor ligands that can participate in both hydrogen bonding and  $\pi$ - $\pi$  interactions.<sup>77</sup> Two such cationic platinum based complexes are presented in **Figure 1.15**.

Pt (II) square planar complexes containing aromatic ligands in particular are very suitable for intercalation with DNA, as they often possess the appropriate geometry for the interaction. It is also possible to tune to a large extent their electronic and steric properties by suitable choice of the ligands. As seen in work by Frassinetti *et al* on bifunctional platinum intercalating anti-cancer complexes, they have revealed that the bipyridyl complex with diphenylthiourea, [Pt(pipy)(ph2-tu)<sub>2</sub>]Cl<sub>2</sub> **135**, shown in **Figure 1.15** is active towards both cisplatin sensitive and resistant human ovarian cell lines.<sup>73</sup>

Also for the cyclometallated Pt (II) complex [Pt(CNN)(4-dpt)]PF<sub>6</sub> **136** in **Figure 1.15**, a mixed DNA binding mode is observed with the Pt(CNN) moiety intercalating into the helical stack and the 4-dpt ligand protruding into the minor groove of the double helix.<sup>74</sup>

New monobinding cyclometallated Pt (II) complexes have recently presented high cytotoxicity with only *one leaving group* present. This is in contrast to the traditional view of needing bifunctional lesions for good activity (double binding to DNA), like those present in cisplatin and most second generation platinum metallo-drugs, **Section 1.4.5**. However, many monobinding platinum complexes presented to date have been charged, like those in **Figure 1.15**. This raises other issues such as membrane permeability which may influence the biological activity of these complexes adversely.<sup>78</sup>

Extensive work by Edwards *et al*,<sup>79</sup> Kodaka *et al*<sup>80</sup> and Navarro-Ranninger *et al*<sup>81</sup> on the other hand has demonstrated a new range of highly cytotoxic neutral platinum anti-cancer drugs with new biological functionality in comparison to cisplatin and its analogues. As well as singly binding to DNA and intercalating, some charged platinum cyclometallated complexes have shown anti-cancer activity by preferentially accumulating in the cytoplasmic structures of the cells instead of covalently binding to nuclear DNA (**137**, **Figure 1.16**).<sup>82</sup>

The platinum carbon bond(s) have been reported as being quite strong, therefore rendering the Pt (II) cyclometallated complexes to display unique photophysical properties

(discussed further in **Section 1.7**) and enhanced stability against biological reduction and ligand exchange reactions.<sup>79</sup>

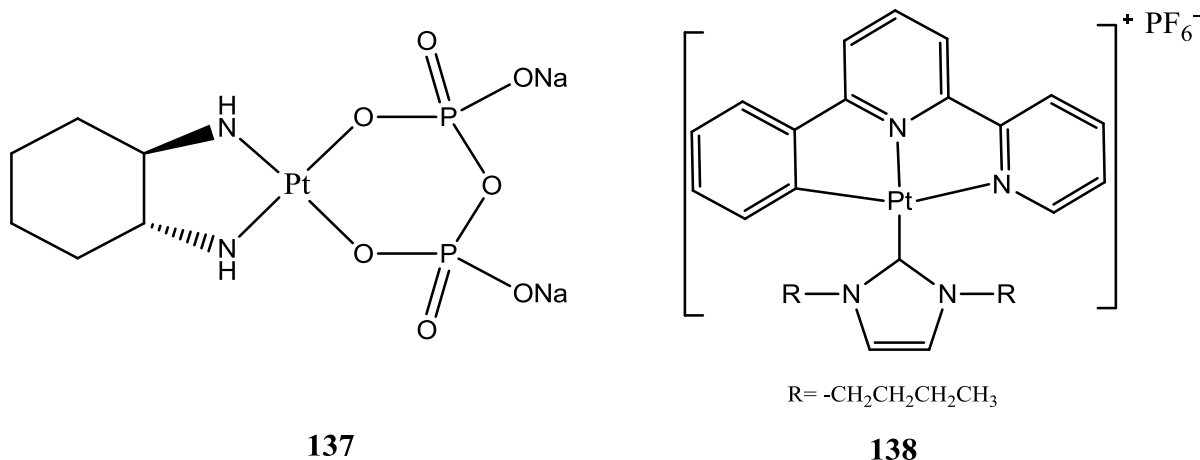


**Figure 1.16:** The structure of a pyrophosphate Pt (II) complex which is cytotoxic and doesn't bind to DNA **137**,<sup>83</sup> and a charged cyclometallated Pt (II) complex **138** which inhibits tumour growth by accumulating in cytoplasmic structures.<sup>82</sup>

Milton *et al* have also reported a class of Pt (II) and Pt (IV) pyrophosphato complexes (**138**, **Figure 1.16**) that exhibit cytotoxicity comparable with and, in some cases, better than cisplatin in some ovarian cell lines, yet no evidence of covalent binding to DNA was observed. They propose numerous alternative cytotoxic mechanisms for their mode of action including a pathway that involves an interaction with fas ligand proteins and two antiapoptotic genes.<sup>83</sup>

## 1.4.5 Second Generation Platinum Drugs:

### 1.4.5.1 Carboplatin:

Since 1971, second and third generation platinum analogues have been investigated in an attempt to broaden the spectrum of activity, fight rising resistance and overcome toxic side-effects. **Figure 1.17** shows the first analogue to obtain approval for clinical use by the US Food and Drug Administration (FDA) in the United States, called carboplatin.

Carboplatin was first reported by Cleare and Hoeschele in 1973 and later obtained approval by the FDA under the brand name Paraplatin in 1978.<sup>84</sup> As stated by Edwards *et al*, active platinum agents require two kinetically inert ligands to form the *non-leaving group*, for example primary amines or ammonia, and two labile anionic ligands in a *cis* configuration,



such as that seen in cisplatin with chlorides, to enable bifunctional binding to the heterocyclic bases of the target DNA (*the leaving group*).<sup>79</sup> Carboplatin does possess these structural features, but the key difference between the structures of carboplatin and cisplatin is that the former possess a six-membered dicarboxylate ring, which, because of the chelate effect, makes it much less chemically reactive than cisplatin.<sup>85</sup>

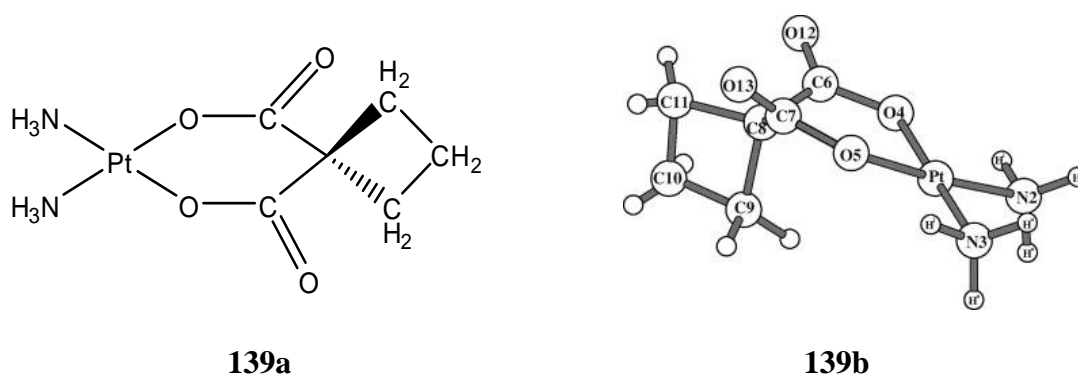


**Figure 1.17:** Carboplatin  $[Pt(cbdca-O,O')(NH_3)_2]$  **139a**, where *cbdca* is cyclobutane-1,1-dicarboxylate and *O* and *O'* are the ligand donor atoms. The single-crystal x-ray structure of carboplatin **139b**, where the *cbdca* ligand is orientated perpendicular to the plane.<sup>85</sup>

Although carboplatin is much less chemically reactive than cisplatin, it still possesses potent anti-cancer properties, which has prompted many investigators to focus on ways to enhance its activity. Studies on the bio-activity of carboplatin have shown that most of the drug is eliminated in the urine as the unreacted starting material, with the remainder bound to proteins and forming small-molecule biotransformation products. The free ligand, *cbdca*, is found in the urine of patients receiving the drug, indicating that biological nucleophiles may have attacked the metal centre and displaced the dicarboxylate ligand.<sup>86</sup>

Extensive work by Sadler and co-workers on carboplatin's activity towards various biomolecules (found naturally in the body) showed that the presence of the *cbdca* chelate ring makes a dramatic difference in the reactivity of platinum compounds towards thiols. *N*-acetyl-cysteine, *N*-acetyl-L-cysteine and the tripeptide, Glutathione, all displayed unusually low reactivity towards the drug despite the Pt (II) being a soft acid and the thiol a soft base.<sup>87</sup>

Further studies on carboplatin's interaction with cellular targets have revealed, like cisplatin, that DNA is the most important target.<sup>88,89</sup> It was determined that carboplatin, like cisplatin, forms intrastrand DNA crosslinks as a difunctional platinum-DNA adduct. However, since the concentration of carboplatin required to reach a DNA-unwinding state

comparable to that of cisplatin was 100 times greater, carboplatin is much less reactive toward DNA than cisplatin.<sup>90</sup>

Carboplatin by itself or in combination with other drugs is still in worldwide clinical uses today for the treatment of a variety of different cancers, including head and neck cancer, along with ovarian, breast, small cell lung, testicular, bladder and brain tumours. Although carboplatin is much less nephro- and ototoxic than cisplatin, it is myelosuppressive, which leads to a reduction in the white cell count in the blood, thus exposing the patient to infection by various organisms.<sup>91</sup>

#### 1.4.5.2 Oxaliplatin:

[Oxalate(2-)-*O,O'*][1*R,2R*-cyclohexanediamine-*N,N'*] platinum (II) (**Figure 1.18**) was the first platinum anti-cancer drug approved that was capable of overcoming cisplatin resistance. It was found to be especially effective when used in combination with 5-fluorouracil against colorectal cancer (the first anti-cancer drug to see effectiveness against this particular cancer). It was also found to be much less nephro- and ototoxic than cisplatin as well as being less myelosuppressive than cisplatin.<sup>92</sup>

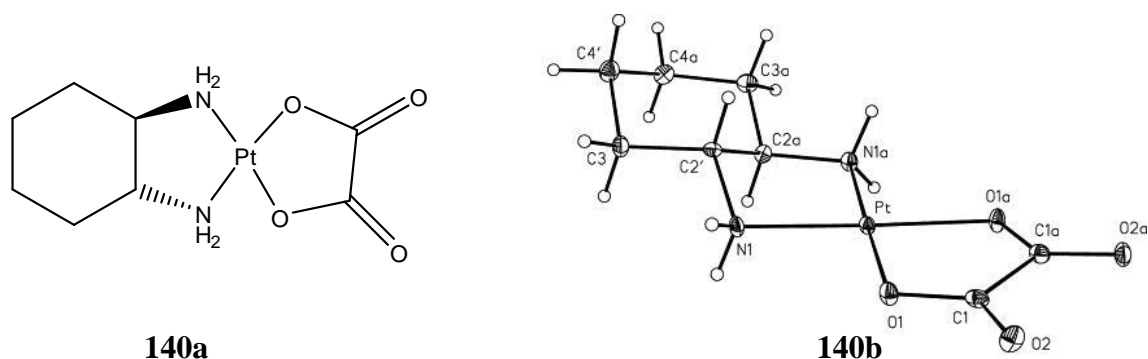


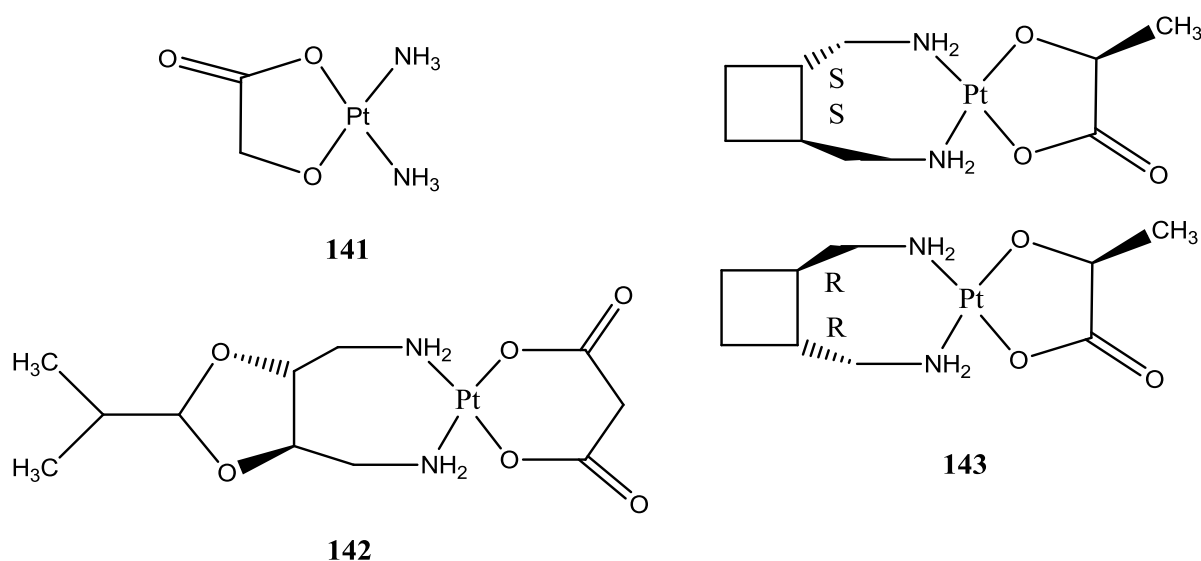
**Figure 1.18:** Oxaliplatin [Pt(1*R,2R*-dach-*N,N'*)oxalate] **140a**, where dach is cyclohexanediamine and *N, N'* are the ligand donor atoms. The single-crystal x-ray structure of oxaliplatin **140b**, where the dach ligand is in a chair-shaped confirmation.<sup>93</sup>

In oxaliplatin the two ammine ligands (present in both cisplatin and carboplatin) have been replaced by a single bidentate ligand, (1*R,2R*)-cyclohexane-1,2-diamine (*R,R*-dach) which act as the *non-leaving group*.<sup>93</sup> The synthesis of oxaliplatin and determination of its anti-cancer properties were first reported by Yoshinori Kidanin *et al* in 1976.<sup>94</sup> It gained approval for clinical use in the European Union in 1999 (France in 1996) and in the United States in 2002, followed by Japan in 2005.<sup>95,96</sup>

Similarly to the other clinically approved platinum based anti-cancer drugs, the major cellular target for oxaliplatin is DNA. Extensive work by Claneay and coworkers determined that the DNA adducts formed by oxaliplatin resemble those formed by cisplatin but with significant differences between the two structures.<sup>97</sup> Further work has revealed that the oxaliplatin-GG structure has a narrow minor groove and the adduct forces a bend in the helix that is around 30°, while the cisplatin-GG adduct produces a wide minor groove and a helix bend of 60-80°.<sup>98</sup> It is these differences in the structure of the DNA adducts that provide oxaliplatin with the ability to overcome cisplatin resistance by preventing the DNA damage repair proteins from doing their job.

### 1.4.5.3 Other Second Generation Platinum Drugs:

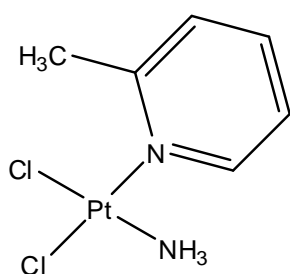
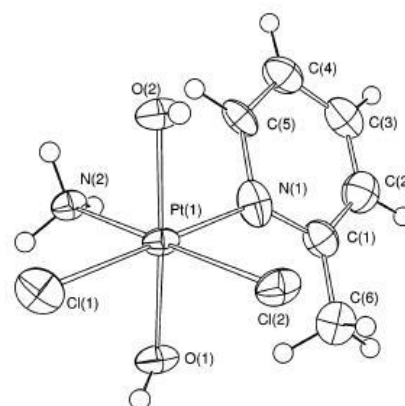
As well as cisplatin, carboplatin and oxaliplatin, there are numerous platinum based anti-cancer drugs currently approved for use in certain regions of the world. The structures of nedaplatin **141**, lobaplatin **142**, and heptaplatin **143** are given in **Figure 1.19**. Diammine[hydroxyacetato(2-)-O,O']platinum (II) or nedaplatin **141** is currently approved for clinical use in Japan for the treatment of ovarian and cervix carcinomas as well as head/neck tumours, oesophageal and bladder cancer.<sup>99</sup> It is structurally quite similar to carboplatin with the same *cis*-ammonia non-leaving groups, but contains a dianionic form of glycolic acid as its leaving group.<sup>100</sup>



**Figure 1.19:** Nedaplatin **141** (approved for use in Japan), lobaplatin **142** (approved for use in China) and heptaplatin **143** (approved for use in the Republic of Korea).<sup>99</sup>

The stability and low toxicity of the *leaving group* is quite often seen as integral to the ongoing success of new platinum anti-cancer compounds. [2-hydroxypropanoato(2-)-O1,O2][1, 2-cyclobutanedimethanamine-N,N']platinum (II) or lobaplatin **142** (Figure 1.19) has been approved for use as a drug in China and is generally found as a mixture of two diastereomeric compounds. Its *leaving group* takes the form of a naturally occurring optically-active form of lactic acid while its *non-leaving group* is a stable metal-nitrogen bound seven-membered chelate ring. Lobaplatin is used to treat non-small-cell-lung cancer, breast tumours, certain forms of leukaemia and more recently cholangiocarcinoma. Ongoing investigations and clinical trials have found it to be less nephro-, neuro- or ototoxic than cisplatin.<sup>101,102</sup>

In South Korea, heptaplatin **143** (Figure 1.19) has been approved for use as a drug to treat gastric cancer and, in combination with Paclitaxel, head and neck squamous cancers.<sup>103</sup> The *non-leaving group* is a chiral form of a seven-membered diamine with a fused five-membered diether, while the *leaving group* is a dianion of malonic acid.<sup>104</sup> The drug has, however, been found to cause mild hepatotoxicity and myelosuppression as well as nephrotoxicity. Recently, further investigations have reported a water soluble analogue of heptaplatin with more activity and less toxicity.<sup>105</sup>

**144****145**

**Figure 1.20:** Picoplatin **144** (currently in phase II clinical trials), an x-ray crystal structure of a Pt (IV) analogue of picoplatin **145**, showing the pyridine ring sitting nearly perpendicular to the metal centre.<sup>106</sup>

Further evolution of second-generation platinum anti-cancer complexes has led to new structural innovations to provide stability, increased activity and less toxicity. Picoplatin (*cis*-amminedichlorido(2-methylpyridine)platinum (II)) **Figure 1.20** for instance was designed primarily to circumvent glutathione-mediated drug resistance. The presence of a 2-methyl pyridine ligand perpendicular to the coordination plane of the metal ion reduces the

possibility of substitution reactions with biomolecules which require a five-coordinate transition state which is discussed in further detail in Chapter 3.<sup>107</sup>

The methyl group's position over the metal centre in both picoplatin and its Pt (IV) analogue (**Figure 1.20**) provides steric hindrance to the attack of the drug by nucleophiles, particularly thiols.<sup>108,106</sup> *In-vitro* studies of picoplatin have demonstrated that it has some ability to overcome some drug resistance, showing anti-cancer activity in cisplatin, carboplatin and oxaliplatin resistant cell lines. *In-vivo* studies have shown that it possesses little or no neuro- or nephro- toxicity and it is currently being investigated as an effective anti-cancer agent in combination with other drugs.<sup>109,110</sup>

#### 1.4.6 Third Generation Platinum Drugs:

As well as 16 electron square planar complexes, platinum can also form stable 18 electron octahedral compounds with a variety of ligands. These Pt (IV) complexes can be synthesised through two different routes, oxidation of a Pt (II) complex and direct synthesis. Both routes are explored in this project and are further discussed in **Chapter 3**.

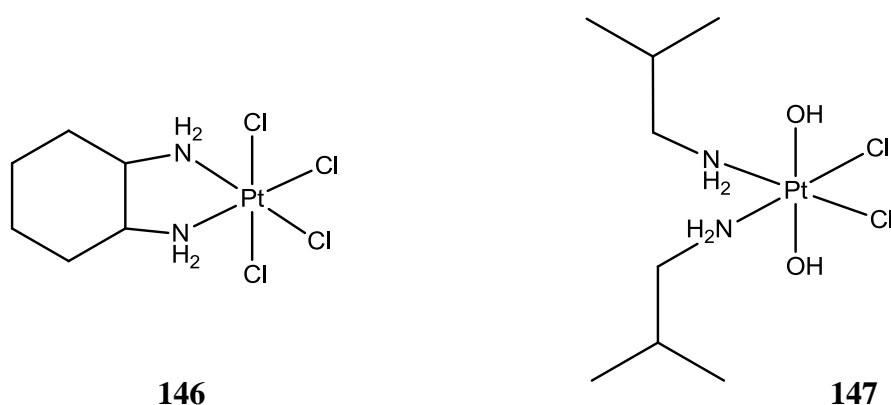


*Figure 1.21: Tetraplatin 146 and Iproplatin 147, both Pt (IV) octahedral complexes which reached Phase I clinical trials but later discontinued due to high toxicity.<sup>111</sup>*

As seen in **Figure 1.21**, the Pt (IV) complexes contain additional functional groups (compared to their Pt (II) analogues) above and below the plane of the traditional equatorial leaving and non-leaving groups. These additional functional groups are normally referred to as the “axial groups”. One of the primary advantages identified by Hall *et al* that Pt (IV) complexes present is the large number of chemical and biological variations that can be achieved by substituting different groups on the axial positions.<sup>112</sup>

The axial and equatorial ligands determine a large array of anti-tumour mechanisms, unfortunately the full extent of these mechanisms have yet to be studied in extensive detail. In studies carried out by Choi *et al* it was been found that Pt (IV) compounds are generally inert towards ligand substitution reactions relative to their Pt (II) analogues. In order to bind to DNA it has been proposed that they must first be reduced to their Pt (II) analogue. It was also found that they are reduced by both extracellular and intracellular agents such as ascorbate, glutathione and other protein sulfhydryls.<sup>113,114</sup> The proposed mechanism for the reduction of Pt (IV) complexes is illustrated in **Figure 1.22**.

**Figure 1.22** shows the fate of a typical Pt (IV) chloride complex *in-vivo*. The extracellular chloride concentration outside the cell (left hand side) (100 mM) is much higher than the concentration inside the cell, intracellular (4 mM). The molecule passes into the cell in response to the chloride concentration gradient through a process similar to osmosis.<sup>115</sup> Because the Pt (IV) drugs need to be reduced prior to binding to the target DNA, these complexes are therefore often called prodrugs.<sup>116</sup>

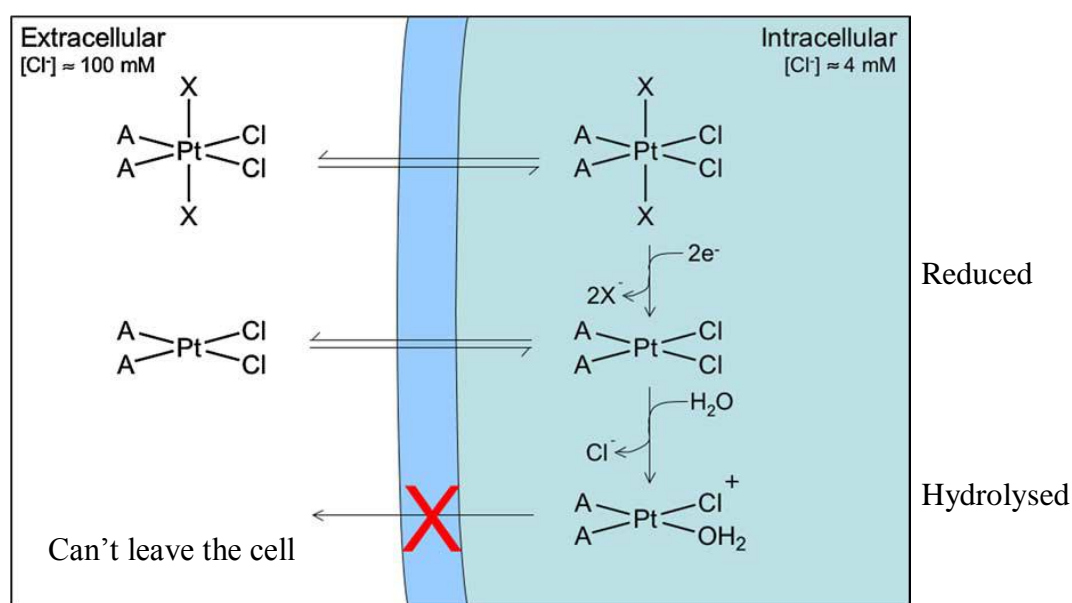


**Figure 1.22:** The mechanism of Pt (IV) reduction *in-vivo* of a typical chloride based octahedral complex, the cell membrane is shown in the middle in blue.<sup>115</sup>

Further work by Choi *et al* on cyclometallated Pt (IV) complexes has shown that the platinum complexes with hydroxo axial ligands reduced very slowly while those with chloro axial ligands reduced very fast. Acetate ligands generally show a moderate reduction rate, while certain complexes reported were not reduced under the conditions investigated.

It was also noted that reduction is favoured by the presence of electron withdrawing axial ligands and bulky axial ligands. Electronegative axial ligands, such as chlorides, increased the reduction rate by promoting destabilisation of the Pt (IV) state, due to electron-withdrawing effects. Complexes with bulky axial ligands also promote destabilisation of the Pt (IV) state, which results in a faster reduction to the more stable Pt (II) state.<sup>113</sup>

In the presence of reducing agents such as glutathione and ascorbate, Pt (IV) complexes generally show enhanced reactivity towards DNA. This supports the proposal that the Pt (IV) complexes need to be reduced to their active Pt (II) analogue in order to have anti-cancer activity.<sup>112</sup> However, in certain cases the parent Pt (IV) complex is actually more active than its analogous Pt (II) complex. Choi *et al* and Galanski *et al* have both reported some examples of Pt (IV) complexes which can bind to DNA and RNA fragments without being reduced (**Figure 1.23**).<sup>113,117</sup>

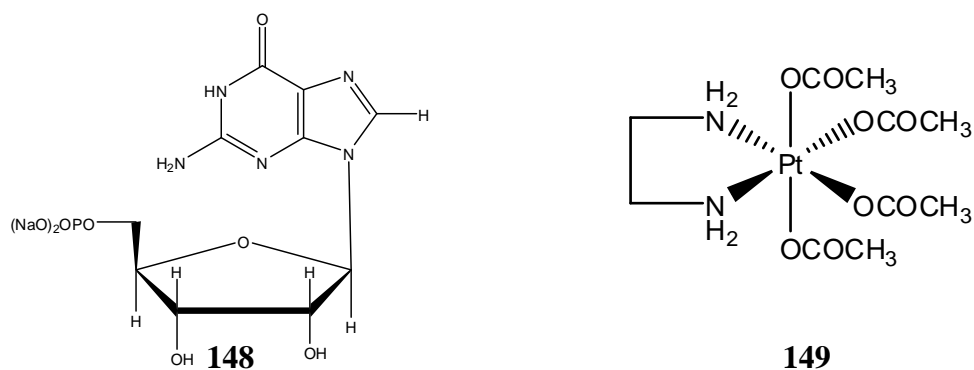


*Figure 1.23: The structure of the Pt (IV) complex [enPt(OCOCH<sub>3</sub>)<sub>4</sub>] 148 and the GMP disodium salt 149 used to form the platinum bio-adduct.<sup>117</sup>*

Galanski and Bernhard have created a Pt (IV)-5'-GMP bio-adduct species in their studies from the above salt **148** and Pt (IV) complex **149**, **Figure 1.23**. They have also confirmed the stability of the species over several weeks by (<sup>1</sup>H and <sup>15</sup>N) NMR spectroscopy. Interestingly, the analogous Pt (II) reduced species was not detected in the final products.<sup>117</sup>

One particular Pt (IV) complex which has attracted quite a lot of interest in the past number of years is “satraplatin” (bis-aceto-amine-dichloro-cyclohexylamine platinum (IV)) or JM-216, first reported by Kelland *et al* in 1993, **Figure 1.24**.<sup>118</sup> Initial *in-vitro* studies on Satraplatin found it to be around 3 fold more potent than cisplatin in some cell lines and it had 4.2 fold better intracellular accumulation compared to cisplatin.<sup>118</sup> Also, in Phase I and II clinical trials it was observed to have no cardiac, renal, hepatic, or neurologic toxicity.<sup>119</sup> More recently it has proceeded to Phase III trials in combination with other therapies such as Docetaxel where moderate success has been achieved.<sup>120</sup>

Although satraplatin is not vastly beneficial over existing treatments, in all the clinical trials one feature has made it very attractive; it is orally active.<sup>119,120</sup> The traditional platinum agents, cisplatin, carboplatin, and oxaliplatin are all administered intravenously and are associated in varying degrees with neurotoxicity, nephrotoxicity, myelosuppression, and ototoxicity. As an oral based drug, Satraplatin has convenient dosing and so far has not been associated with the same level of toxicity as the currently approved platinum based anti-cancer compounds. Currently it remains in clinical trials in the United States but given the lack of an overall survival benefit, satraplatin has not yet received approval by any regulatory authority.<sup>121</sup>

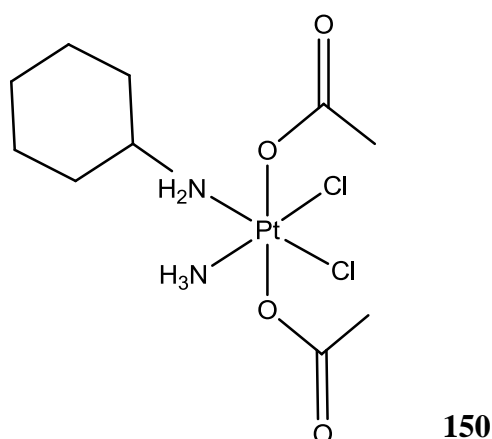


*Figure 1.24: The structure of Satraplatin 150, a Pt (IV) complex that has reached phase III clinical trials and will be discussed further in Chapter 3.*

#### **1.4.7 New Second and Third Generation Platinum Drug Design:**

Current investigations into drug design for second and third generation Pt (II) anti-cancer complexes are primarily concerned with providing structural stability for the non-leaving groups and reducing the toxicity of the leaving groups. An important feature of active Pt (II) complexes, which has been frequently identified, is the strong relationship between the halide leaving groups and the overall biological activity of the complex. Studies between Pt-Cl and Pt-Br complexes have concluded that the heavier bulkier halides lead to more active complexes - which is in accordance with the relative metal-halide bond strengths.<sup>79</sup>

Edwards *et al* have investigated the role of the non-leaving groups of platinum complexes. It was shown that these ligands were not involved in the biological action of the complex *per se*, however, the introduction of steric crowding around the metal centre leads to greatly increased biological activity. Edwards *et al* achieved this by the introduction of



successive  $\alpha$ -substituent's on the *non-leaving groups*. For good activity to be achieved, it was identified that these bulky ligands must remain coordinated to the metal centre while in the body. *In-vivo* testing has confirmed this through stability studies of certain complexes towards biomolecules which will be discussed further in **Chapter 4**.<sup>79</sup>

The potential of Pt (II) complexes still remains much higher than its Pd (II) analogues, even though the coordination chemistry of Pt (II) and Pd (II) are very similar. Edwards *et al* have confirmed that the anti-cancer activity of palladium complexes *in-vivo* was only moderate at best, while further studies of the newest analogues of the platinum complexes show continuing success. This was explained by way of the slightly nucleophilic behaviour of the platinum complexes in comparison to the purely electrophilic behaviour of palladium, along with solubility and stability issues within Pd (II) complexes. The palladium complexes also react too quickly to achieve their aim due to their high lability relative to platinum analogues.<sup>79</sup>

The use of hemilabile Schiff base bidentate and tridentate ligands as *non-leaving groups* has been investigated by Crouse *et al* (S-benzylthiocarbazates) and Smith *et al* (thiosemicarbazones) among others. Tridentate cycloplatinated thiosemicarbazone complexes, **151**, **Figure 1.25** were seen to have both antitumour and antiparasitic properties, while tridentate S-benzylthiocarbazates compounds, **152**, **Figure 1.25** were also reported to have strong cytotoxicity against human ovarian cancer cell lines.<sup>122,123</sup>

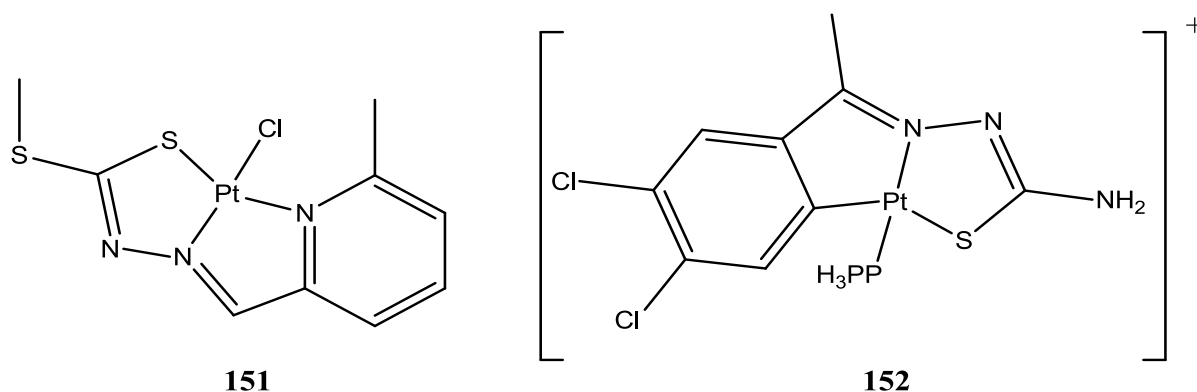


*Figure 1.25: The structure of the tridentate Pt (II) complex [Pt(mpasme)Cl] 151 and the thiosemicarbazone platinum complex 152.*<sup>117</sup>

Further work by Edwards *et al* on iminophosphine type ligands has also shown cytotoxic activity against cancer cell lines. It was seen that in general the compounds reported affect growth inhibition at low concentrations and form stable complexes where the ligands are not readily displaced.<sup>79</sup>

Edwards *et al* also reported that palladium complexes incorporating a phosphorus donor moiety have lower biological activity than analogous platinum complexes because of the greater lability of the palladium to phosphorus bond. This greater lability means that the phosphine based ligands are released too quickly from the complex and the metal centre reacts before reaching its intended target. In addition to this, this would also result in unwanted side effects from the palladium based drugs.<sup>79</sup>

## 1.5 Hemilabile Mixed Donor ligands as Non-Leaving Groups:

### 1.5.1 Hemilability Overview:

Coordination ligands which have the ability to both stabilise a metal centre and create an empty coordination site for further reaction, are becoming an increasingly studied area. Ligands which have this ability are termed as being “hemilabile”. This concept was introduced in terms of phosphine-amine and phosphine-ether bifunctional ligands in 1979 by Jeffrey and Rauchfuss.<sup>124</sup> Hemilability arises from the mixed bonding characteristics of hybrid ligands such as iminophosphines (further details in **Section 1.6.1**).<sup>125</sup>

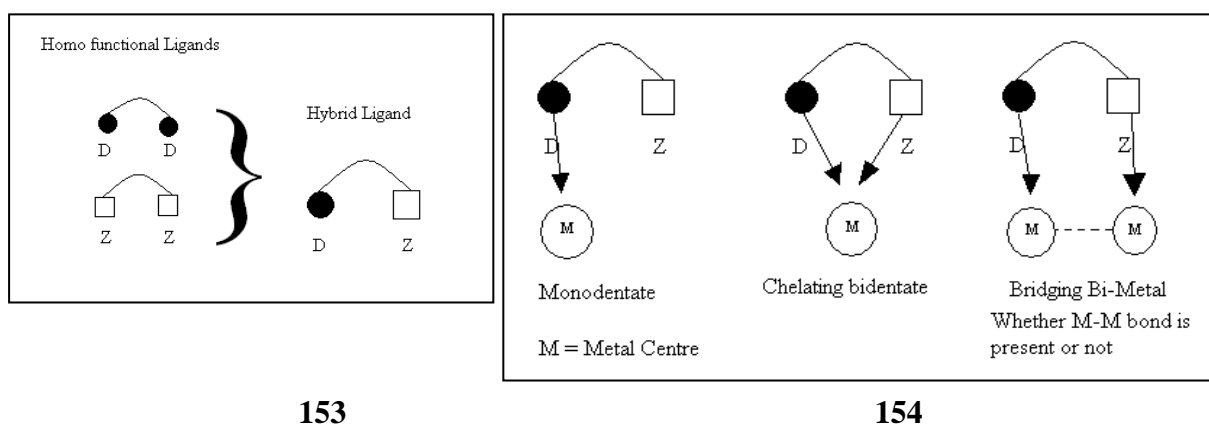


*Figure 1.26: Types of hemilabile ligands 153. Homo functional ligands can join to form mixed donor ligands 154.<sup>126</sup>*

Hemilabile ligands are usually found to be “polydentate” because they consist of mixed donor moieties (**153, Figure 1.26**). These type of ligands contain two or more different functional sites on the same ligand which are all capable of coordinating to the metal in their own specific way (**154, Figure 1.26**).

Specific functionalities of a donor moiety will influence the bonding and/or reactivity of other ligands or substrates to the metal in particular this is determined by whether the group is hard or soft as defined by the HSAB theory.<sup>126</sup> Hard Soft Acid Base theory (HSAB) plays an important role in the properties of these ligands. Acids and bases are defined as being hard or soft by the stability of the complexes they form (see **Table 1.1** and **1.2, Section 1.2**). As a general rule, “like binds like”. Pt (II) (a “soft” acid) binds to the phosphine (a “soft” base) of the ligand in **Figure 1.27** below, followed by subsequent binding to the “hard-soft” nitrogen.<sup>127</sup>

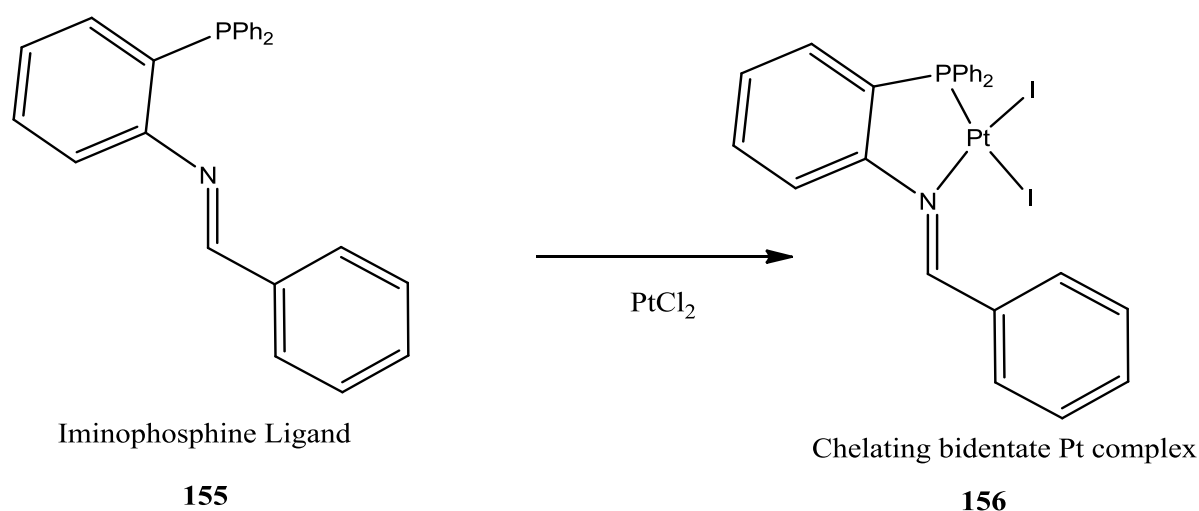


**Figure 1.27:** A mixed donor iminophosphine ligand **155**. Platinum bound chelating bidentate iminophosphine complex **156** (an example of the HSAB theory and hemilability).<sup>128</sup>

For a Lewis acid/base to be defined as being soft or hard, the concept depends on the size and electro-negativity of the atom. In this way oxygen is a small, highly electro-negative, donor base, so it is therefore defined as being “hard” in nature. Hard base components such as oxygen (nitrogen is defined as “borderline” meaning it is between soft and hard, **Table 1.1, Section 1.2**) do not bind as strongly to the “soft” platinum centre, hence the primary criteria for hemilabile behaviour is satisfied in the above structure because one of the defining features of a hemilabile ligand is to have at least one substitutionally labile donor functional group (also “Z” in **Figure 1.28**).<sup>126,127</sup>

The HSAB theory also explains the properties of the metal centre, since metals tend to get softer as they get heavier. This is one of the defining characteristics between analogous Pt (II) and Pd (II) complexes. For example, platinum is heavier than palladium and is therefore “softer” so it binds more strongly to “soft” bases such as phosphines. This also explains the previously discussed observation that similar palladium complexes are too labile for anti-

cancer activity because they react too fast *in-vivo* and subsequently decompose, **Section 1.4.7.**<sup>127</sup>

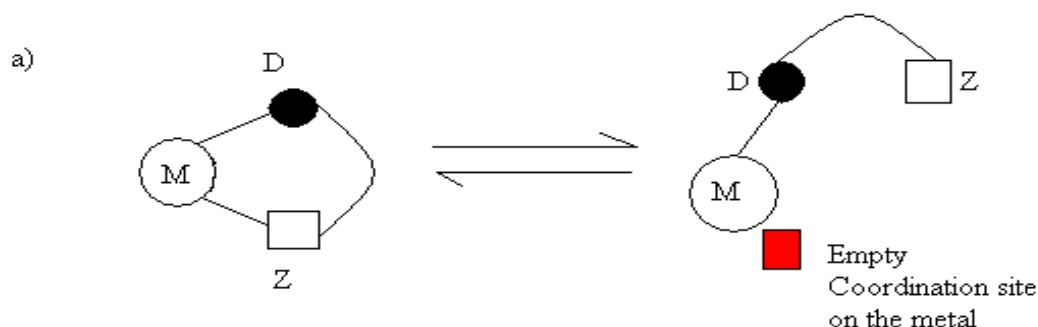


**Figure 1.28:** An example of mixed donor ligands and formation of coordination sites.<sup>126</sup>

In **Figure 1.28** the “D” functional group remains bound to the metal centre while the other functional group “Z” disconnects to leave a coordination site open. In this way the “Z” donor group “swings” away from the metal in a “wind-screen wiper” type analogy.<sup>126</sup> This process involves a dynamic equilibrium that can be observed at lower temperatures as in **Figure 1.29** where the metal centre is a copper atom and the exchanging group can be seen on the left of the complex.<sup>129</sup>

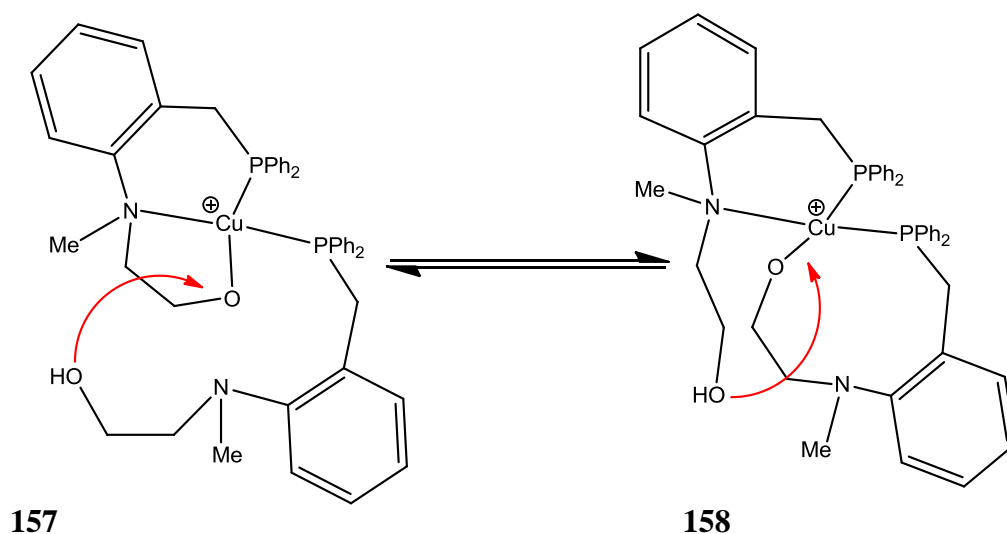


**Figure 1.29:** An example of dynamic equilibrium that can be observed at lower temperatures where the exchanging group is shown on the left of each structure.<sup>129</sup>

The most useful consequence of hemilabile ligands in a complex is that they significantly influence the coordination of incoming substrates, therefore allowing transformations in the complex that would not normally occur. This may also happen faster or slower depending on the nature of the coordination sphere.<sup>126</sup>

### 1.5.2 Types of Hemilability:

There are three specific types of hemilability characterised by the way in which the labile donor group coordinates i.e. whether it is easily displaced or not.

#### 1.5.2.1 Type I: Spontaneous opening:

This is observed by the DZ (**Figure 1.30**) chelate opening of its own accord without any external help. This may occur in both mononuclear and polynuclear (DZ bridge) systems. Type I is usually seen in metals which can easily vary their coordination numbers and more relevant to this research  $d^8$   $ML_4/ML_3$  ( $4 \rightleftharpoons 3$ ) and  $d^8$   $ML_5/ML_4$  ( $5 \rightleftharpoons 4$ ), where “M” is a Metal centre and “L” is a coordinating ligand.

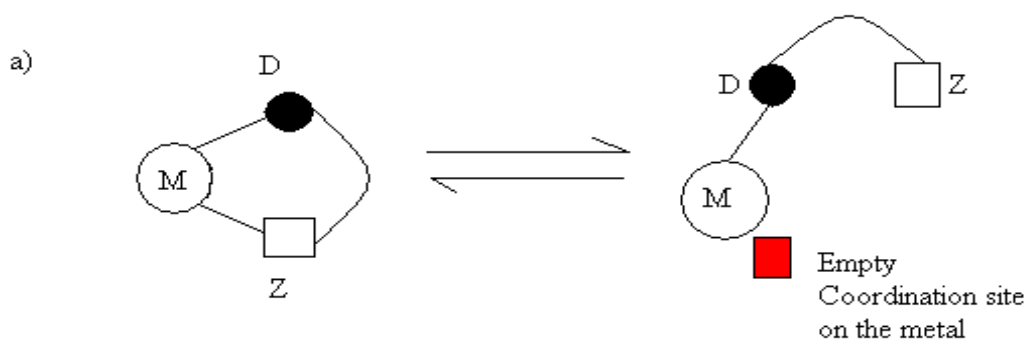


*Figure 1.30: A schematic of spontaneous opening, leaving an empty coordination site.<sup>126</sup>*

#### 1.5.2.2 Type II: Intramolecular competition:

This is characterised by competition within the same metal-ligand complex usually between two or more hybrid ligands. The competition between two donor functional groups causes a switching from one group to the other, which joins to the metal with loss of the first. There are two main types as illustrated in **Figure 1.31**; there are also many other examples of this but they are not relevant to this research and as a result will not be discussed here. Intramolecular competition will be explored further in **Chapter 2** where competition between the formation of a tridentate (P,N,O) complex and a tridentate (P,N,C) complex of the same ligand will be investigated. Examples of P,N,O complexes studied within this research group can be observed in **Figure 1.34**.

Another type of intramolecular competition within a single ligand is a fluxional “tick tock” process where the “D, Z” ligand can connect/disconnect frequently illustrated in **Figure 1.31**.

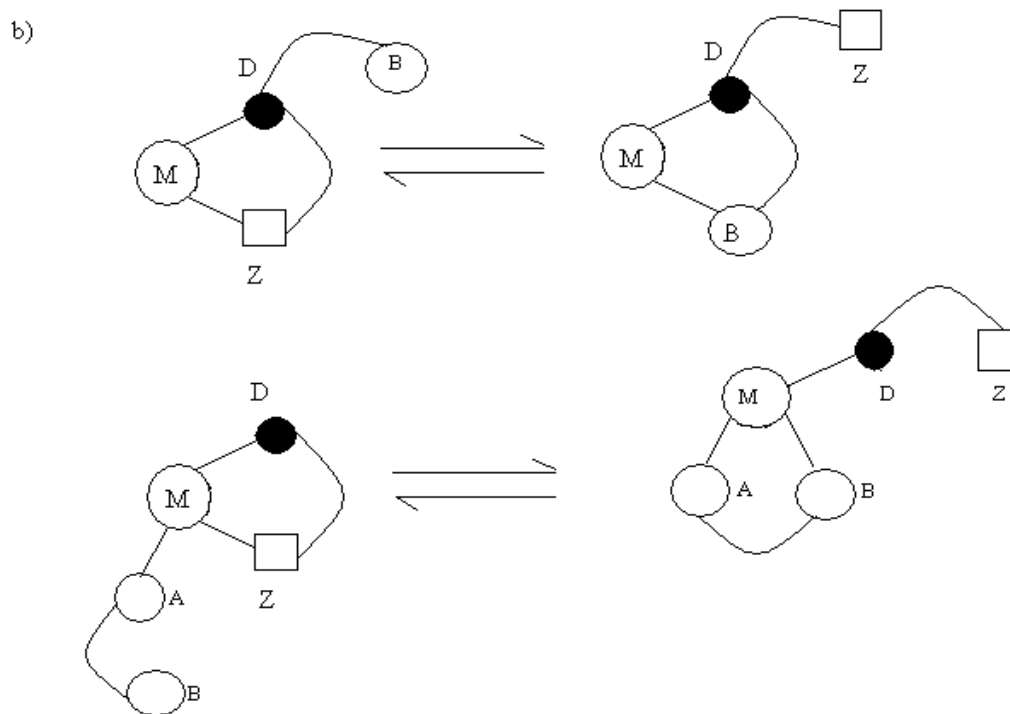


*Figure 1.31: A schematic of intramolecular fluxional competition.*<sup>126</sup>

### 1.5.2.3 Type III: Coordination by an external reagent:

In this type, the DZ hybrid ligand is attacked by an external substrate (B) which displaces the weakest donor group, “Z” in **Figure 1.32**. The new substrate will then coordinate to the metal, causing the hybrid ligand to swing away while still attached to the metal centre through the D donor group.<sup>126</sup>

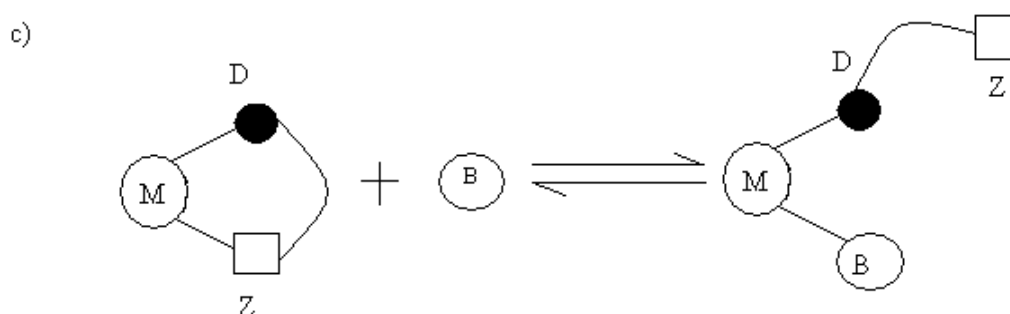


*Figure 1.32: A schematic of coordination by an external reagent.*<sup>126</sup>

This type of hemilability is an intermolecular process rather than an intramolecular process; which is prominent for Type I and Type II. The introduction of an external ligand results in displacement of one of the coordinated donor moieties of the hemilabile polydentate ligand in favour of coordinating the newly introduced external ligand in its place. Substitution reactions similar to this will be discussed further in **Chapter 3**, where displacement of a halide ligand from a metal centre by an external phosphine will be attempted.

### 1.4.3 Hemilabile Functional Phosphines and Their Complexes:

As we have already seen, early work on hemilability with Jeffrey and Rauchfuss involved phosphine based ligands. From their work, the P,O based ligands were found to function as asymmetric bidentate chelates with metal centres. Other research groups have also reported similar metal chelates with P,N and P,C based ligands, **Figure 1.33**.<sup>124,130,131</sup>

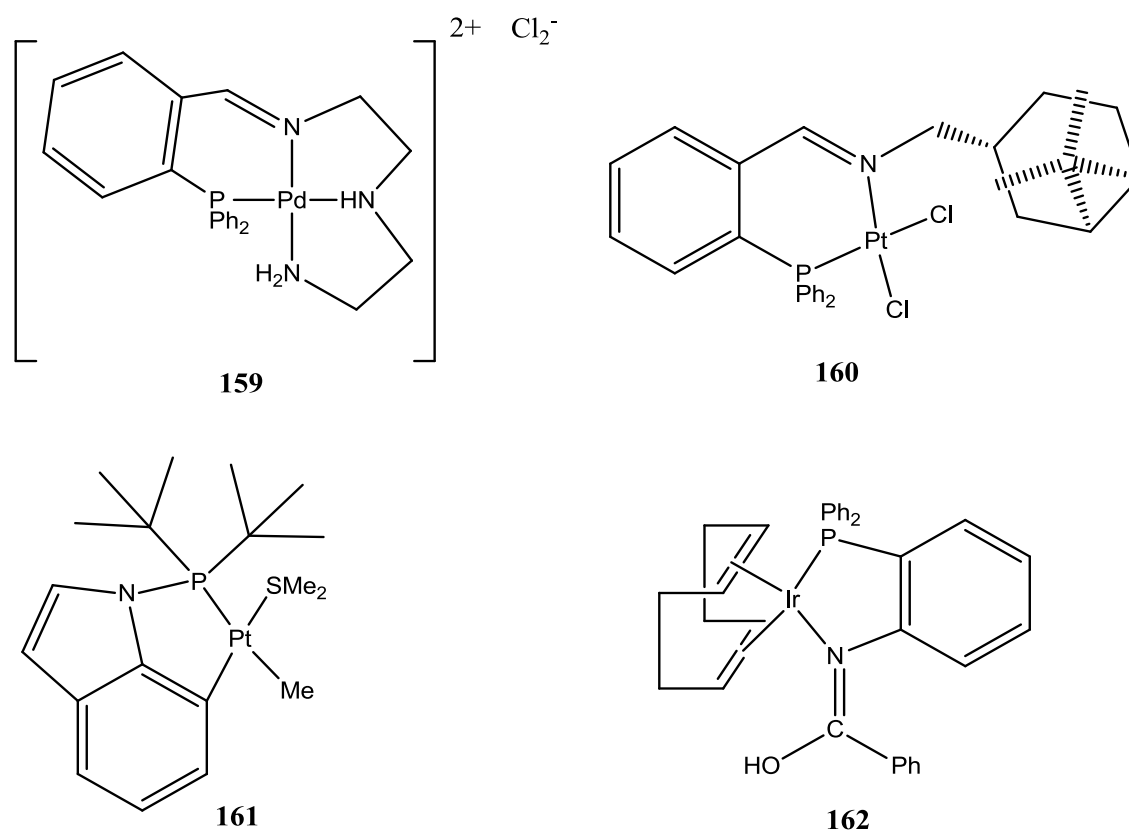


**Figure 1.33:** The structures of some P,N and P,C type metal complexes: A Pd (II) iminophosphine complex **159**,<sup>132</sup> a Pt (II) iminophosphine complex **160**,<sup>130</sup> a Pt (II) cyclometallated phosphine complex **161**,<sup>133</sup> and an iridium P,N complex **162**.<sup>134</sup>

Phosphorus-oxygen (P,O) and phosphorus-nitrogen (P,N) based hybrid ligands, have both “soft” (phosphine), “hard” (oxygen) donor groups or “hard/soft” (Nitrogen) donor groups. Again these characteristics are essential properties of a hemilabile ligand which are especially useful in the current research involving coordinating the ligand to the platinum centre (see **Table 1.1** and **1.2, Section 1.2**) for HSAB acids and bases.

These hybrid ligands are among the most widely used hemilabile ligands in coordination and organometallic chemistry. Their late transition metal complexes can adopt several coordination (P monodentate, N monodentate, P,N bridging and P,N chelate) depending on the ligand bite and the hardness of the metal atoms.<sup>130</sup>

Phosphorus based ligands have been described as being one of the most stabilising and common ligands towards a variety of transition metal centres. The bond strengths provided by the phosphorus and nitrogen/oxygen bonds are specific to the hard/soft nature of the metal centre involved. The phosphorus as previously explained will bind very well to Pt (II) metal centres as they are both “soft” in nature. But if say Fe (III) was the metal centre, this would produce a weak M-P bond due to the “hard” nature of Fe (III).<sup>127</sup>

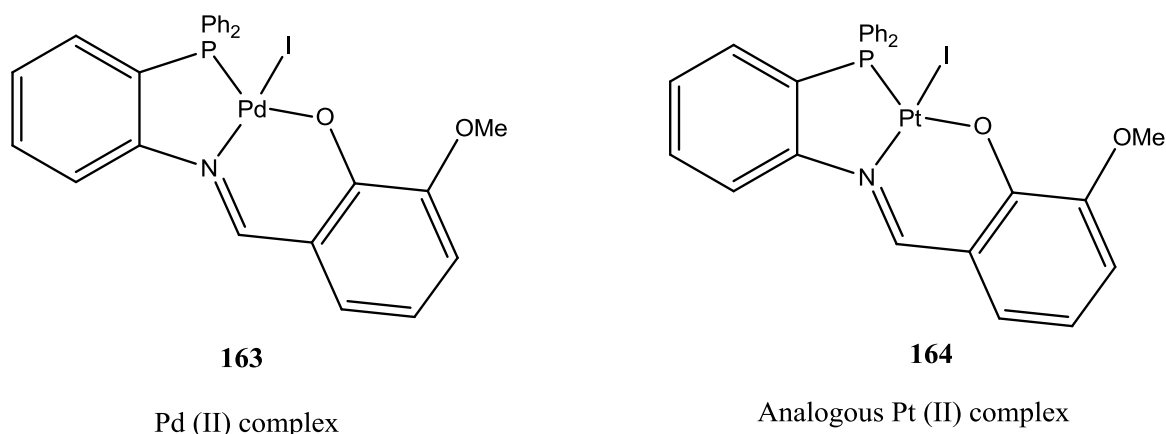


*Figure 1.34: The structures of a Pd (II) 163 and Pt (II) 164 P,N,O type complexes*

One of the well documented properties about analogous Pd (II) complexes is that the covalent Pd-O bond in the Pd (P,O ligand) complex does not display any lability, unlike the other donor ligands. This also appears in the chemistry of Pt-O in the same or similar complex (See **Figure 1.34** where both complexes have been made in our research group). The HSAB theory therefore does not apply here, as it does for other donor ligands, since oxygen uses its extra lone pair of electrons to donate into the metal centre which demonstrates the limitations of the HSAB theory. This makes the Pd/Pt-O bond very useful to stabilize the complex for oxidation and substitution reactions.<sup>135</sup>



## 1.6 The Types of Platinum Complexes in this Work:

### 1.6.1 Platinum Complexes From Iminophosphines:

As previously mentioned phosphine based ligands are favourable for platinum complex formation because of the stable complexes they form. Mixed donor ligands are also attractive, particularly iminophosphine P, N type ligands, due to the weak  $\pi$ -accepting nature of the imine C=N bond and the  $\sigma$ -donor ability of the phosphine. In comparison to analogous amines, imines are harder to displace/cleave under acidic conditions as they form stronger metal to nitrogen bonds which are less labile than equivalent metal to amine bonds. Furthermore, the lability of the imino-group can also be influenced by substituents present within the ligand.<sup>136</sup>

On coordination to transition metals the soft/hard nature of P,N ligands creates asymmetry in the metal orbitals, which then affects the reactivity of the complexes. This can be easily illustrated by the difference in the *trans* influence of the phosphorus donor atom compared to the nitrogen. In iminophosphine complexes the bond *trans* to the phosphorus is longer than that *trans* to the nitrogen, indicating the greater *trans* influence of phosphorus compared to the imine functionality.<sup>137,138</sup>

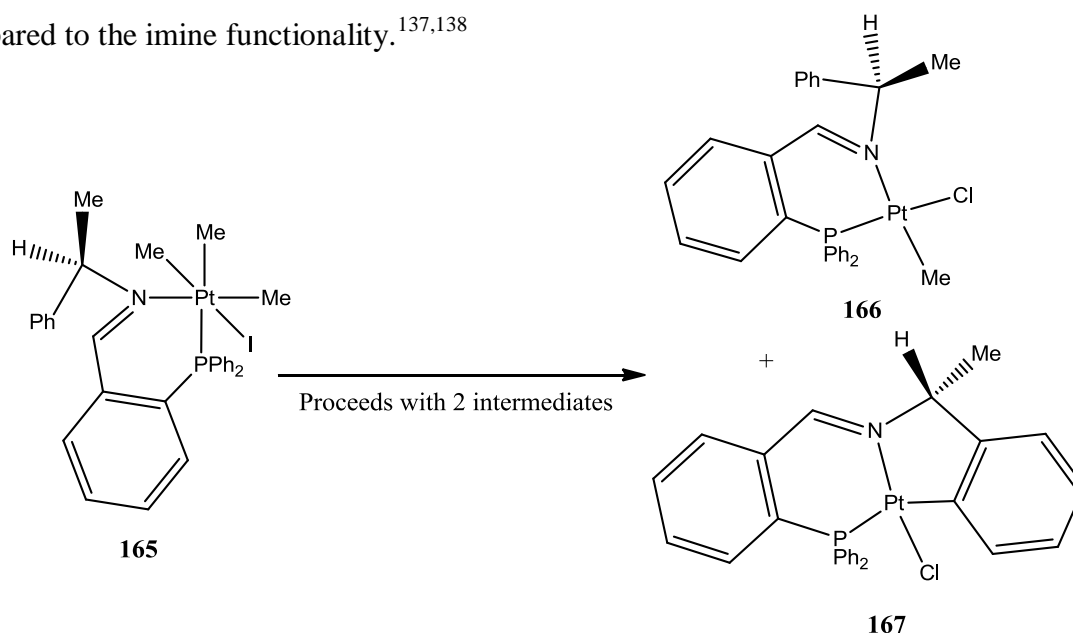


**Figure 1.35:** The structures of a tridentate iminophosphine P, N, C type Pt (II) complex **167** formed alongside its bidentate analogue **166**, both from a Pt (IV) iminophosphine complex **165**.

The vast majority of iminophosphine metal complexes reported to date are bidentate chelates between phosphorus and nitrogen donor moieties. Tridentate complexes of the form

P, N, C are not as common, particularly cyclometallated iminophosphine based complexes. Work by Balana *et al* on an iminophosphine Pt (IV) complexes have revealed the possibility of stabilising the platinum metal centre for C-H activation and subsequent cyclometallation to form a Pt (II) iminophosphine tridentate complex **167**, as well as a Pt (II) phosphinoamine bidentate complex, **166** **Figure 1.35**.<sup>139</sup>

### 1.6.2 Platinum Complexes From Phosphinoamines:

Chiral phosphinoamine and phosphinoamide ligands are generally used in conjunction with palladium or rhodium, as metal complexes, as catalysts for asymmetric allylic alkylation.<sup>140,141</sup> Phosphinoamide ligands can easily form chelate complexes with 5 or 6 membered rings. This is usually facilitated via hemilability with insertion of the metal centre into the N-H bond assisted by chelation to the phosphorus anchor.<sup>134</sup>

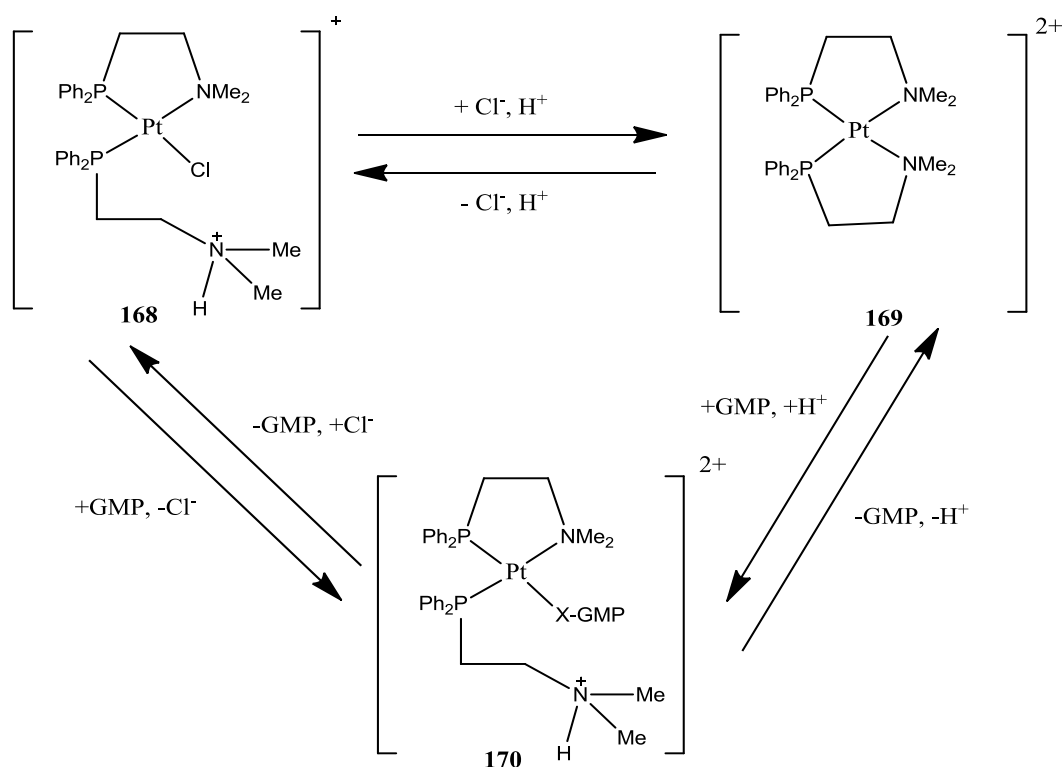


*Figure 1.36: Scheme of the platinum phosphinoamide complex **168**, ring opening **169** and coordination with guanine through the N1 or N7 position (X) **170**.*<sup>142</sup>

From a biological point of view, some phosphinoamide Pt (II) complexes have shown to be cytotoxic against cancer cells with potency close to that of cisplatin, while others have been reported as active against cisplatin resistant cell lines also.<sup>143,144</sup> The ability of Pt (II) phosphinoamine as well as phosphinoamide complexes to undergo reversible ring opening in

aqueous media (**Figure 1.36**) has also been reported by numerous research groups similar to the hemilabile example given in **Figure 1.27**.<sup>144,142</sup> These properties have made Pt (II) phosphinoamine and analogous phosphinoamide complexes a popular choice for ongoing anti-cancer drug design.

### 1.6.3 Biologically Active Cyclometallated Complexes:

Cyclometallated Pt (II) complexes have been studied extensively for activity against cancerous cells. The relatively strong Pt-C bond(s) means that many complexes display unique photophysical properties (more detail in **Section 1.7**) and enhanced stability in biological systems e.g. against reduction or ligand exchange.<sup>82</sup>

As previously mentioned in **Section 1.3.3**, work undertaken by Edwards *et al* has reported that tridentate cyclometallated Pt (II) complexes with only one labile ligand could act as monofunctional DNA binding agents. In the low chloride concentration of intracellular fluid, aquation would lead to a reactive cationic species which may bind directly to DNA as well as interacting via intercalation of the planar chromophore into the DNA double helix.<sup>79</sup>

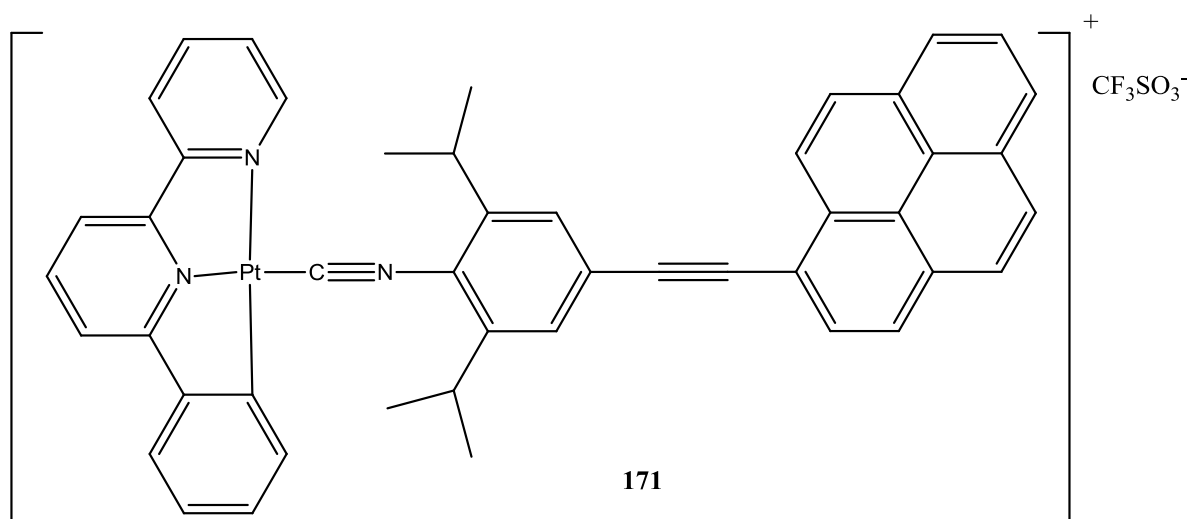


**Figure 1.37:** The structure of the biologically active cyclometallated N, N, C type Pt (II) complex **171** which intercalates with and binds to DNA.<sup>145</sup>

There has been some success for cyclometallated complexes in terms of biological activity. N, N, C type complexes reported by Che *et al* bind to the major groove of DNA along with behaving as DNA intercalators. One of their complexes **171**, **Figure 1.37** also suppressed the activity of CREB (a cAMP response element-binding protein) which normally regulates cell cycle regulatory genes such as cyclin A1 and cyclin D2. It did this by

selectively blocking the CREB/DNA interaction site by binding to the major groove of DNA.<sup>145</sup>

Other successful biologically active cyclometallates include those with Schiff base type ligands, particularly those of thiosemicarbazones. First described by Vázquez-García *et al.*,<sup>146</sup> these S, N, C type complexes, **Figure 1.38**, have shown good cytotoxicity in recent work carried out by Smith *et al.* Compound **172**, **Figure 1.38**, showed the highest activity out of all the compounds reported against cisplatin sensitive and cisplatin resistant ovarian cell lines. Interestingly the compounds with the single platinum metal centre did not show an overall advantage over the bimetallic species, **173**, **Figure 1.38**, which was also active against both cell types but only where the diphosphine bridge was bis(diphenylphosphino)ferrocene.<sup>123</sup>

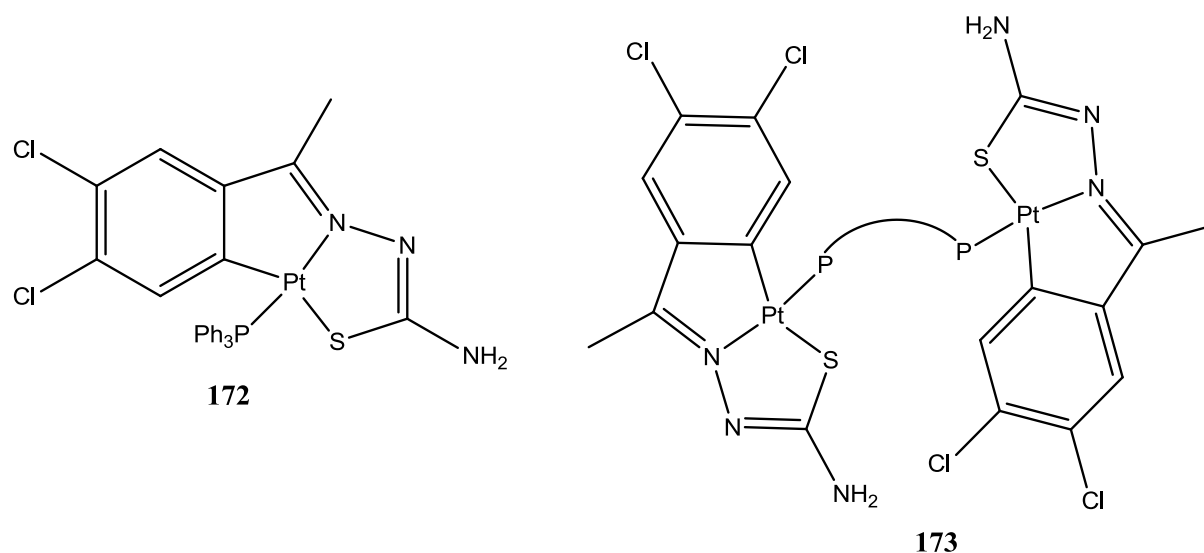


*Figure 1.38: The structure of two biologically active S, N, C type thiosemicarbazone complexes as a mono-platinum compound 172 and a bimetallic species 173.*<sup>123</sup>

Cyclometallated phosphine type complexes such as **161**, **Figure 1.33**, **Section 1.4.3**, are relatively common due to the stabilising ability of the strong Pt-P bond.<sup>133</sup> Tridentate cyclometallated complexes of the type P, N, C on the other hand are much less common with reports by Balana *et al* **167**, **Figure 1.35**, **Section 1.5.1** being the only available structures at the time of writing.<sup>139</sup> Other P, N bidentate structures like **166**, **Figure 1.35**, **Section 1.5.1** have the potential to form cyclometallated complexes of the type P, N, C, but there are no reports of this to date.<sup>130</sup>

## 1.7 Photophysical Properties of Platinum complexes

### 1.7.1 Inorganic Complexes in Photodynamic Therapy (PDT)

Photodynamic Therapy (PDT) is a clinically used cancer treatment that utilizes a sensitizing agent (an anti-cancer complex for instance), biological molecular oxygen and light to generate a reactive chemical species that kills cancer cells. Usually the anti-cancer complex is nontoxic and unreactive in its injected form. Once the patient is administered the drug it can be localised and activated to the site of the tumour due to pH variations and then irradiated using high intensity light on the cancerous area. For tumours on exposed portions of the body this irradiation of light can be done externally to the body but fibre optics can also be used to target internal tumours.<sup>147,148</sup>

Porphyrins have been identified as the most effective class of sensitizing agents for use in photodynamic therapy (PDT). These macrocyclic structures are naturally occurring, nontoxic and have relatively strong absorptions in the red and near-infrared region of the spectrum and can be stimulated by light (**Figure 1.39**).<sup>149</sup>

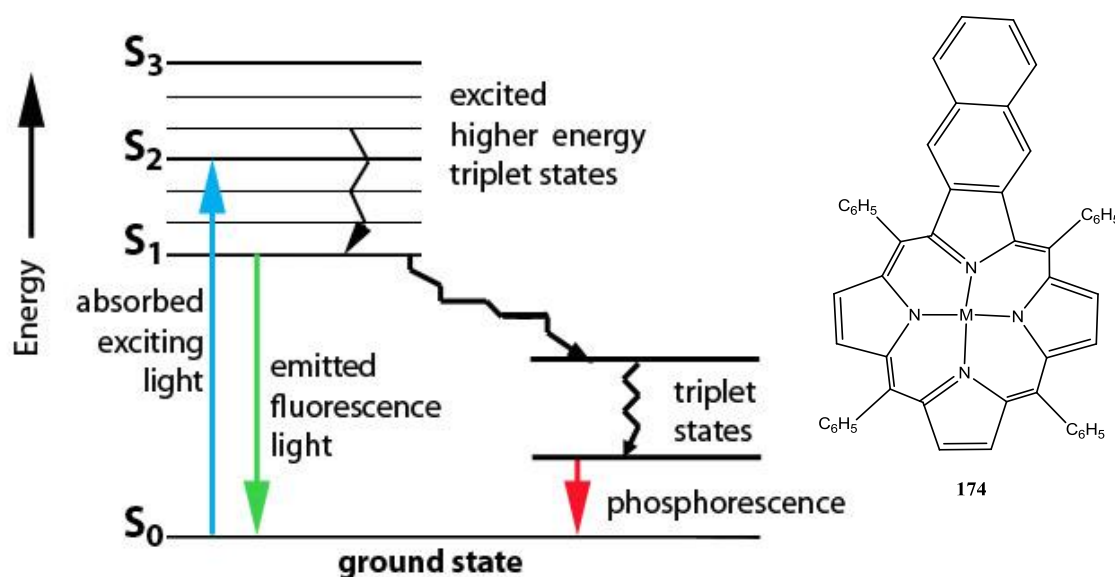


**Figure 1.39:** The structure of a porphyrin coordinated to a metal centre **174** and a Jablonski diagram to illustrate the photoactivation process.<sup>149</sup>

These photosensitizers use oxygen in their mechanism of action which can be explained by a “Jablonski diagram”, **Figure 1.39**. The compound (with or without a metal centre) absorbs light and is converted from its ground state,  $S_0$ , to a higher, excited singlet state,  $S_1$ . This process is very fast and promotes an electron from a bonding molecular orbital to a higher vibrational level.

Normally this excited state,  $S_1$ , is not stable very long and it decays very quickly back to the ground state,  $S_0$ , through a process called “fluorescence”. This process releases a photon ( $h\nu$ ) which is lower in energy than the excited photon. However, if oxygen is near the excited sensitizer the energy

in the excited  $S_1$  state can be transferred through a process known as an “intersystem crossing” to the oxygen molecule to form a “triplet state” T in the sensitizer molecule.<sup>150</sup>

Since the singlet state of oxygen is lower in energy than the triplet (T) state of the sensitizer molecule, the collision of an oxygen molecule with an excited sensitizer molecule can result in the transfer of energy from the triplet (T) state of the sensitizer to the singlet (S) state of oxygen. Singlet oxygen is quite reactive and can attack biological molecules near the sensitizer. This can then cause damage to certain biomolecules which can result in the cell entering apoptosis and dying. However, the requirement for oxygen is a major drawback as many malignant and aggressive cancer cells are hypoxic.<sup>150,151</sup>

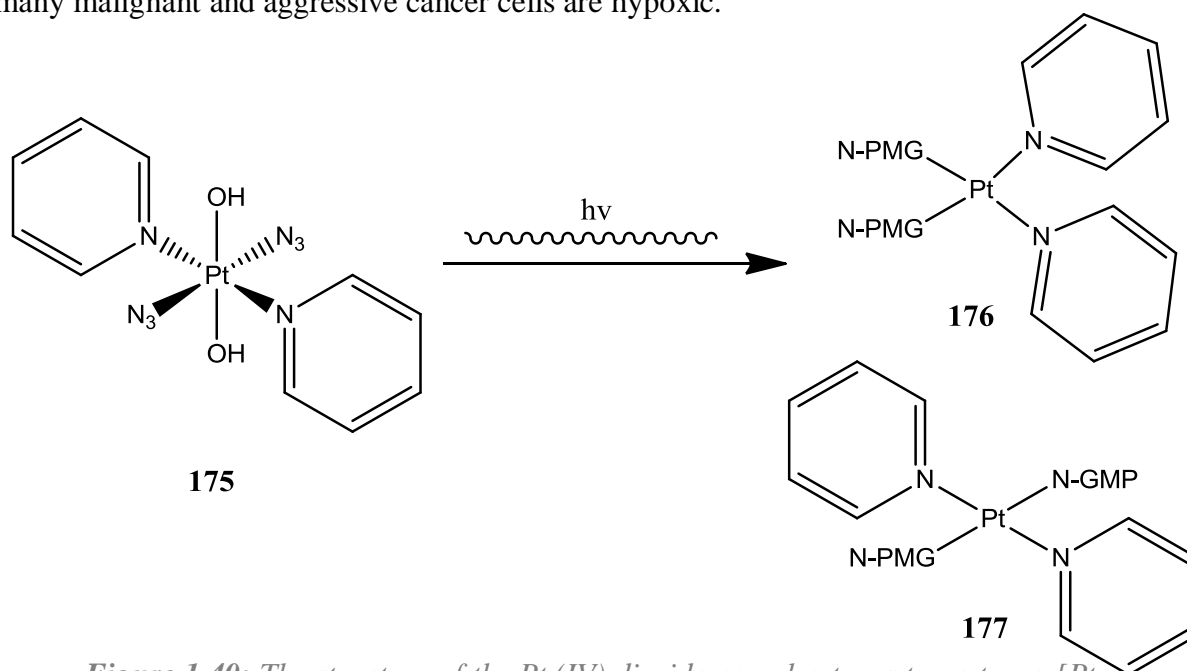


**Figure 1.40:** The structure of the Pt (IV) diazido complex *trans,trans,trans*-[Pt-( $N_3$ )<sub>2</sub>(OH)<sub>2</sub>(pyridine)<sub>2</sub>] **175**, which is unreactive in the dark but is cytotoxic when photoactivated by UVA and visible light ( $h\nu$ ) and binds strongly to guanine nucleotides (GMP) on DNA strands **176-177**.<sup>152</sup>

One of the primary advantages of PDT over conventional forms of therapy is that since light is the activation agent, the area of irradiation can be carefully controlled. This has resulted in the development of photoactivatable prodrugs of platinum-based antitumor agents aimed at increasing the selectivity and hence lowering the toxicity. These drugs could find use in treating localised tumours accessible to laser-based fibre-optic devices. So far Pt (IV) complexes have appeared the most attractive as candidates for PDT because they are usually substitution inert and require reduction to the Pt (II) species to become cytotoxic (as discussed in **Section 1.3.5**).<sup>151</sup>

Recently Pracharova *et al* have reported a Pt (IV) diazido complex that is stable and non-cytotoxic in the dark but can exhibit significant toxicity in cancer cells upon irradiation with short

wavelengths (365 nm) (**Figure 1.40**). Its activation with UVA irradiation to produce cytotoxic and reactive Pt (II) analogues does not require oxygen, which is a huge advantage over conventional photosensitizers currently in clinical use for PDT. It was also reported that the selective photoactivation of these Pt (IV) complexes in cancer cells may help overcome limitations normally connected with toxic side effects of antitumour platinum drugs.<sup>152</sup>

It was reported that this Pt (IV) diazido complex, upon irradiation, did bind to DNA in a number of human cancer cell lines. Importantly it was also noted that no platinum was found to be bound to DNA if the cells were treated with the Pt (IV) complex in the dark. Measurements of DNA-bound platinum after exposure to the photoactivatable platinum drug under irradiation revealed that the amount of platination by the Pt (IV) diazido complex was 16 fold higher compared to that determined after the treatment with the same dose of cisplatin in the dark for the same length of time.<sup>152</sup>

### 1.7.2 Luminescence of Platinum Based Complexes

Since the late 1980's square planar Pt (II) complexes have gained significant interest outside of biological applications because of their interesting excited state properties and their suitability for a number of advanced technological applications. The photochemical and photophysical properties of cyclometallated complexes in particular have received the majority of attention due to fact that many of these complexes have been successfully applied as phosphorescent dopants in the manufacture of highly efficient organic light-emitting devices (OLEDs).<sup>153,154</sup>

Various studies have revealed how the excited state energies and hence colour in several classes of Pt (II) complexes can be controlled through rational ligand design. Concepts such as rigidity of the complex and assessment of ligand-field strengths can provide a qualitative prediction of the extent of luminescence (via decay from an excited state). There are two types of decay from an excited state under which Pt (II) complexes may undergo; radiative and non-radiative.<sup>155</sup>

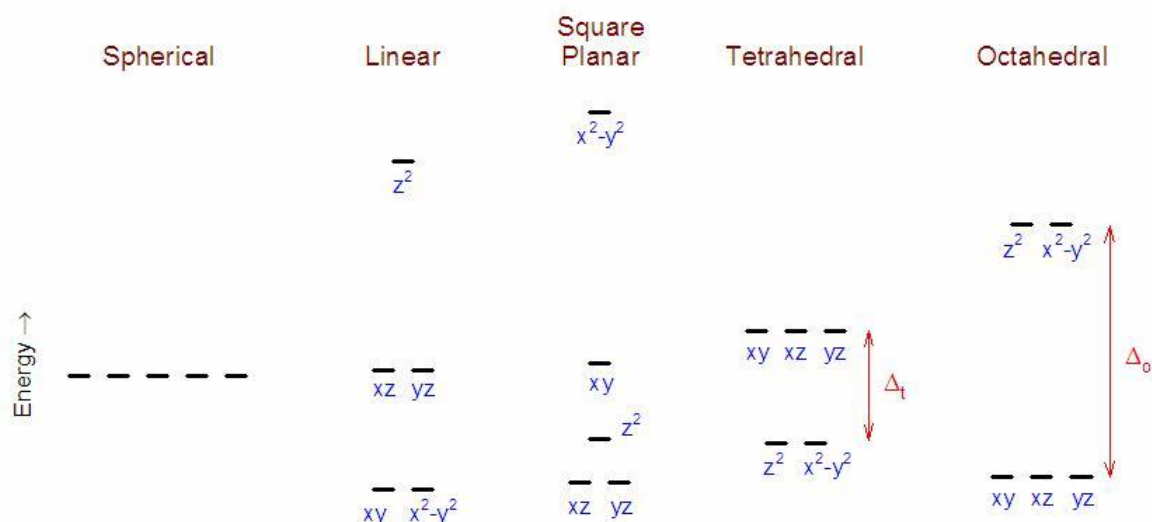


**Figure 1.41:** The Crystal field Ligand Splitting Energies of various geometries. The  $d_{x^2-y^2}$  orbital is the highest in energy for square planar complexes.

Radiative decay is the release of observable luminescence from an emission of a photon due to the decay of energy from an excited state to the ground state. The extent to which this occurs depends on the contribution of metal orbitals to the lowest energy triplet excited state. Non-radiative decay is also due to the decay of energy from an excited state to the ground state but with no emission of a photon and therefore no luminescence.<sup>156</sup>

The strong preference of Pt (II) complexes to be square planar owing to ligand field stabilisation, results in the unoccupied  $d_{x^2-y^2}$  orbital being strongly anti-bonding (**Figure 1.41**). Population of this orbital will be accompanied by elongation of Pt-L bonds and severe distortion which promotes non-radiative decay of metal centred excited states to the ground state (known as d-d states). In order to promote radiative decay over non-radiative decay it is necessary that the lowest lying excited state is not a metal centred one (d-d state).<sup>155</sup>

Ligand centred (LC) or charge-transfer (CT) states are much more favourable for radiative decay. A large energy gap is also desired, between the lowest lying excited state and the highest lying metal centred d-d state. By increasing the ligand field splitting energy for square planar complexes, the  $d_{x^2-y^2}$  orbital is also raised in energy, resulting in a larger energy gap. This can be achieved using strong-field ligands or co-ligands and/or substitution of weak field ligands such as halides with strong field ligands such as imines and phosphines.<sup>155</sup>



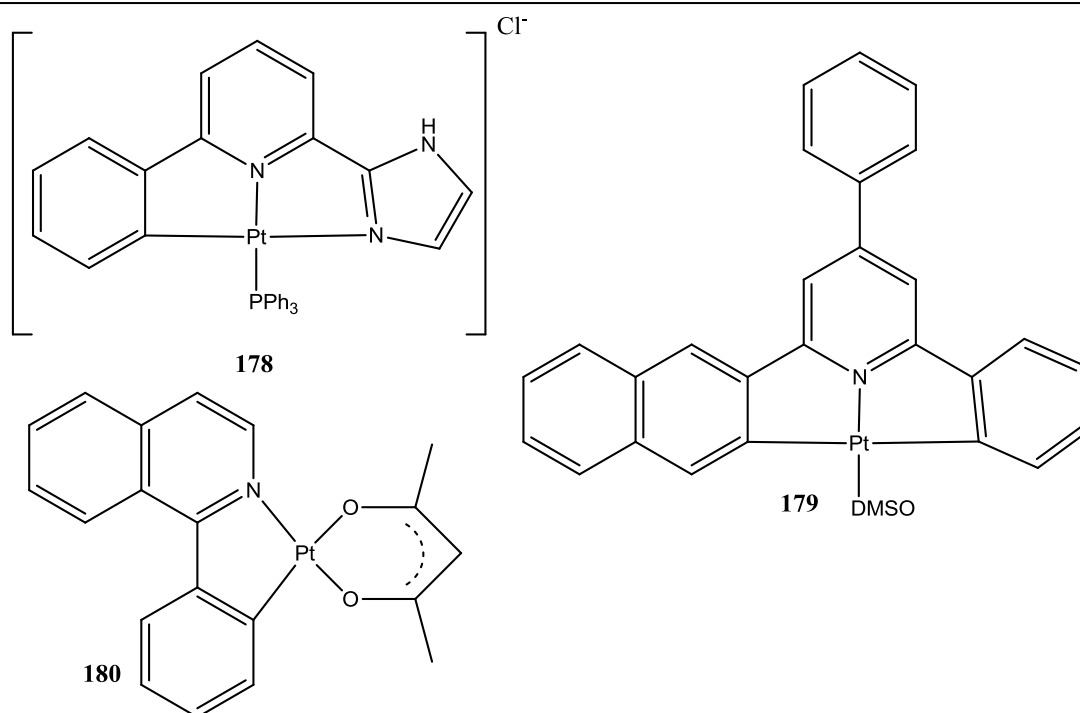


Figure 1.42: The structure of a CNN type complex **178**, a CNC type complex **179** and a CN bidentate complex **180**, all of which are luminescent.<sup>157–159</sup>

Cyclometallated tridentate ligands of the type NNC, NCN and CNC coordination types have all been explored extensively, as well as C, N bidentate complexes. Many of these compounds have been reported to produce very high luminescence along with providing the ability to tune the colours across the visible spectrum by making small changes to the ligands. However there have been no reports found at the time of writing of luminescent PNC type platinum complexes or mixed donor iminophosphine ligands.<sup>157–159</sup>

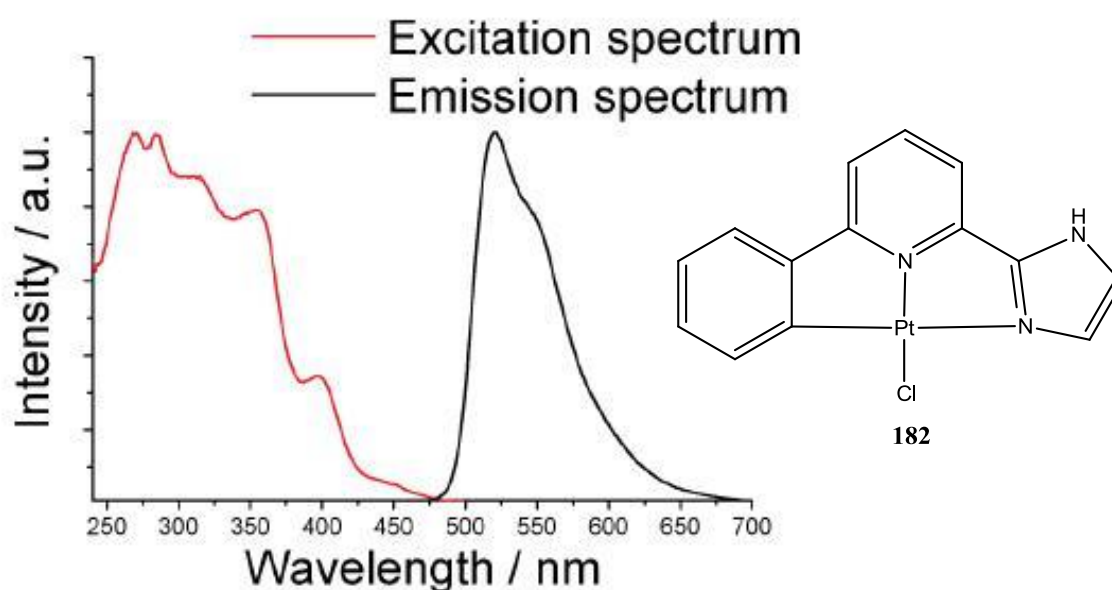


Figure 1.43: The normalised excitation and emission spectra of a cyclometallated CNN type complex, inset (concentration  $10^{-5}M$ ).<sup>157</sup>

## 1.8 Summary and Objectives

The uses of mixed-donor or hemilabile ligands to stabilise and generate complexes with potential medicinal applications, specifically with anti-cancer activity, are numerous and well studied. The interest in the medicinal applications of metal complexes stems from the success of the anti-cancer complex cisplatin. The use of mixed-donor, or hemilabile, ligands has been identified as an effective way of stabilising a metal centre and allowing substitution by another external ligand.

The nature of these coordination complexes is influenced primarily by the Hard Soft Acid Base theory (i.e. like binds to like). The most useful ligands have been identified to contain phosphorus and nitrogen donor moieties and demonstrate the potential to generate stable metal complexes with reversible binding in the presence of other donor substrates/ligands. Mixed donor hemilabile ligands have been reported to be very effective for platinum complexes designed for medicinal applications, such as iminophosphines.

The wide-scale use of cisplatin as an anti-cancer therapeutic drug has generated huge interest in developing other effective metal complexes with equal or increased potency as anti-cancer agents. Cisplatin, despite its continued use in the clinic, exhibits high toxicity and undesirable side effects as well as an acquired resistance by way of repair to damaged cancerous DNA caused by cisplatin. Second generation analogues were therefore developed in the hope of reducing side-effects and increasing resistance like that found for carboplatin and oxaliplatin, both of which are FDA approved and used in the clinic worldwide. Many of the other analogues developed were found to have greater toxicities than that of cisplatin and so further research into third generation platinum complexes are ongoing.

The third generation platinum drugs to be developed were Pt (IV) type complexes such as satraplatin, which is currently in phase III clinical trials as the first orally active platinum drug. These inorganic prodrugs, with reduced lability, can be reduced *in-vivo* to generate active Pt (II) complexes, which can then act as anti-cancer agents by binding to DNA. It has been postulated that the identity of the axial ligands (and their associated reduction potentials) correlates directly with their biological activity.

With the potential of complexes with mixed-donor (hemilabile) ligands to exhibit anti-tumour activity, it is the aim of this project to develop novel tridentate P,N,C and P,N,O ligands containing iminophosphine and phosphinoamide functional groups derived from 2-diphenylphosphinoaniline and to investigate the coordination behaviour and reactivity of these ligands towards a platinum metal centre in both +2 and +4 oxidation states in an

attempt to generate a novel series of Pt (II) and Pt (IV) cycloplatinated complexes which would potentially exhibit biological activity. The platinum complexes studied in this report will be of the chloro type, similar to already FDA approved platinum anti-cancer drugs, as opposed to the previously reported iodo-complexes from this research group.

The advantage of chlorides over iodides for platinum complexes, deemed potentially active for an anti-cancer drug, will also be explored. The reactivity of the chloro cycloplatinated species formed towards monophosphine substitutions will be investigated in an attempt to develop stable complexes with potential biological activity, and investigate the lability of the Pt-Cl bond which is reported as an important functionality for successful anti-cancer activity.

Further applications of iminophosphine and phosphinoamide platinum complexes will also be explored in the form of luminescence studies to investigate if the rigid cyclometallated compounds correlate in regards to intensity with already known Pt (II) cyclometallated luminescence complexes.

## 1.9 Bibliography

1. B. Rosenberg, L. Vancamp, and T. Krigas, *Nature*, 1965, **205**, 698–699.
2. D. Wang and S. J. Lippard, *Nature reviews. Drug discovery*, 2005, **4**, 307–320.
3. D. F. Shriver and P. W. Atkins, in *Inorganic Chemistry*, Oxford University Press, 3rd Ed., 1999, pp. 649–671.
4. G. L. Miessler and D. A. Tarr, in *Inorganic Chemistry*, Pearson Education Inc., 3rd Ed., 2004, pp. 594–635.
5. J. C. Dabrowiak, in *Metals in Medicine*, John Wiley & Sons, Ltd., 1st Ed., 2009, pp. 49–72.
6. E. Britannica, *Encyclopædia Britannica, Inc*, 2012, Webpage, Accessed July 2012.
7. R. G. Pearson, *Journal of Chemical Education*, 1968, **45**, 581–587.
8. J. C. Dabrowiak, in *Metals in Medicine*, 1st Ed., 2009, pp. 191–214.
9. S. P. Fricker, *Gold Bulletin*, 1996, **29**, 53–60.
10. V. Majithia and S. A. Geraci, *The American Journal of Medicine*, 2007, **120**, 936–939.
11. J. Forestier, *The Lancet*, 1934, **224**, 646–648.
12. C. Shaw, *Chemical Reviews*, 1999, 2589–2600.
13. M. Simon and H. Kunishima, *Cancer*, 1979, **44**, 1965–1975.
14. C. K. Mirabelli, R. K. Johnson, D. T. Hill, L. F. Faucette, G. R. Girard, G. Y. Kuo, C. M. Sung, and S. T. Crooke, *Journal of Medicinal Chemistry*, 1986, **29**, 218–23.
15. R. V. Parish, B. P. Howe, J. P. Wright, J. Mack, R. G. Pritchard, R. G. Buckley, A. M. Elsome, and S. P. Fricker, *Inorganic Chemistry*, 1996, **35**, 1659–1666.
16. S. J. Berners-Price and P. J. Sadler, *Inorganic Chemistry*, 1986, **25**, 3822–3827.
17. R. W.-Y. Sun, D.-L. Ma, E. L.-M. Wong, and C.-M. Che, *Dalton Transactions*, 2007, 4884–92.
18. C.-M. Che, R. W.-Y. Sun, W.-Y. Yu, C.-B. Ko, N. Zhu, and H. Sun, *Chemical Communications*, 2003, 1718–9.
19. Y. F. To, R. W.-Y. Sun, Y. Chen, V. S.-F. Chan, W.-Y. Yu, P. K.-H. Tam, C.-M. Che, and C.-L. S. Lin, *International Journal of Cancer*, 2009, **124**, 1971–1979.

20. R. G. Buckley, a M. Elsome, S. P. Fricker, G. R. Henderson, B. R. Theobald, R. V Parish, B. P. Howe, and L. R. Kelland, *Journal of Medicinal Chemistry*, 1996, **39**, 5208–14.
21. C. K. Mirabelli, C.-M. Sung, J. P. Zimmerman, D. T. Hill, S. Mong, and S. T. Crooke, *Biochemical Pharmacology*, 1986, **35**, 1427–1433.
22. S. J. Berners-Price, P. S. Jarrett, and P. J. Sadler, *Inorganic Chemistry*, 1987, **26**, 3074–3077.
23. S. J. Berners-Price, C. K. Mirabelli, R. K. Johnson, I. Chloride, M. R. Mattern, F. L. McCabe, L. F. Faucette, S. Mong, P. J. Sadler, and S. T. Crooke, *Cancer Research*, 1986, **46**, 5486–5493.
24. B. Ward and J. C. Dabrowiak, *Journal of the American Chemical Society*, 1987, **3**, 3810–3811.
25. L. Messori, P. Orioli, C. Tempi, and G. Marcon, *Biochemical and Biophysical Research Communications*, 2001, **281**, 352–60.
26. E. Georgiou, A. Metsios, N. Kourkoumelis, S. Karkabounas, K. Charalabopoulos, A. Badeka, and S. K. Hadjikakou, *Journal of Enzyme Inhibition and Medicinal Chemistry*, 2011, **26**, 592–7.
27. J. C. Dabrowiak, in *Metals in Medicine*, 1st Ed., 2009, pp. 219–242.
28. B. Lyonnet, M. Martz, and E. Martin, *La Presse Médicale*, 1899, **32**, 191–192.
29. P. Köpf-Maier and H. Köpf, *Chemical Reviews*, 1987, **1**, 1137–1152.
30. O. J. D’Cruz and F. M. Uckun, *Expert Opinion on Investigational Drugs*, 2002, **11**, 1829–36.
31. R. K. Narla, C. L. Chen, Y. Dong, and F. M. Uckun, *Clinical Cancer Research*, 2001, **7**, 2124–2133.
32. Y. Dong, R. K. Narla, E. Sudbeck, and F. M. Uckun, *Journal of Inorganic Biochemistry*, 2000, **78**, 321–30.
33. P. K. Sasmal, A. K. Patra, M. Nethaji, and A. R. Chakravarty, *Inorganic Chemistry*, 2007, **46**, 11112–21.
34. D. F. Zigler and K. J. Brewer, in *Metal Complex–DNA Interactions*, John Wiley & Sons, Ltd, 2009, pp. 235–272.
35. W. Han Ang and P. J. Dyson, *European Journal of Inorganic Chemistry*, 2006, **2006**, 4003–4018.
36. J. C. Dabrowiak, in *Metals in Medicine*, 1st Ed., 2009, pp. 149–184.

37. M. J. J. Kim, *Polyhedron*, 1996, **15**, 3787–3793.
38. C. G. Hartinger, S. Zorbas-Seifried, M. a Jakupec, B. Kynast, H. Zorbas, and B. K. Keppler, *Journal of Inorganic Biochemistry*, 2006, **100**, 891–904.
39. M. Vadori, S. Pacor, F. Vita, S. Zorzet, M. Cocchietto, and G. Sava, *Journal of Inorganic Biochemistry*, 2013, **118**, 21–7.
40. P. Heffeter, B. Atil, K. Kryeziu, D. Groza, G. Koellensperger, W. Körner, U. Jungwirth, T. Mohr, B. K. Keppler, and W. Berger, *European Journal of Cancer*, 2013, **In Press**.
41. C. Allardyce, *Platinum Metals Review*, 2001, 62–69.
42. Y. Han, Q. Luo, X. Hao, X. Li, F. Wang, W. Hu, K. Wu, S. Lü, and P. J. Sadler, *Dalton Transactions*, 2011, **40**, 11519–29.
43. K. Wu, Q. Luo, W. Hu, X. Li, F. Wang, S. Xiong, and P. J. Sadler, *Metallomics: Integrated Biometal Science*, 2012, **4**, 139–48.
44. J. Maksimoska, L. Feng, K. Harms, C. Yi, J. Kissil, R. Marmorstein, and E. Meggers, *Journal of the American Chemical Society*, 2008, **130**, 15764–5.
45. R. Aird, J. Cummings, A. Ritchie, and M. Muir, *British Journal of Cancer*, 2002, **86**, 1652–1657.
46. C. Scolaro, A. B. Chaplin, C. G. Hartinger, A. Bergamo, M. Cocchietto, B. K. Keppler, G. Sava, and P. J. Dyson, *Dalton Transactions*, 2007, **2**, 5065–72.
47. H. Köpf and P. Köpf-Maier, *Angewandte Chemie (International Ed. in English)*, 1979, **18**, 477–478.
48. P. Köpf-Maier, *Journal of Structural Biology*, 1990, **105**, 35–45.
49. B. K. Keppler, C. Friesen, H. G. Moritz, H. Vongerichten, and E. Vogel, *Structure and Bonding*, 1991, 97–127.
50. S. Frühauf and W. J. Zeller, *Cancer Research*, 1991, **51**, 2943–2948.
51. J. H. Toney and T. J. Marks, *Journal of the American Chemical Society*, 1985, **66**, 947–953.
52. A. Obeid, A. El-Shekeil, and S. Al-Aghbari, *Journal of Coordination Chemistry*, 2012, 37–41.
53. C. R. Kowol, R. Berger, R. Eichinger, A. Roller, M. a Jakupec, P. P. Schmidt, V. B. Arion, and B. K. Keppler, *Journal of Medicinal Chemistry*, 2007, **50**, 1254–65.
54. D. Chen, M. Frezza, R. Shakya, Q. C. Cui, V. Milacic, C. N. Verani, and Q. P. Dou, *Cancer Research*, 2007, **67**, 9258–65.

55. D. F. Shriver and P. W. Atkins, in *Inorganic Chemistry*, Oxford University Press, 3rd Ed., 1999, pp. 211–282.
56. F. A. Cotton and G. Wilkinson, in *Advanced Inorganic Chemistry*, John Wiley & Son, 6th Ed., 1999, pp. 1072–1073.
57. M. Peyrone, *Justus Liebigs Annalen der Chemie*, 1844, **51**, 1–29.
58. A. Werner, *Zeitschrift für Anorganische Chemie*, 1893, **3**, 267–330.
59. B. Rosenberg, *Platinum Metals Review*, 1971, **15**, 42–51.
60. S. J. Berners-Price, L. Ronconi, and P. J. Sadler, *Progress in Nuclear Magnetic Resonance Spectroscopy*, 2006, **49**, 65–98.
61. A. Eastman, in *Cisplatin*, Verlag Helvetica Chimica Acta, 1999, pp. 111–134.
62. J. L. Nitiss, *Proceedings of the National Academy of Sciences of the United States of America*, 2002, **99**, 13963–13965.
63. J. A. Howle and G. R. Gale, *Biochemical Pharmacology*, 1970, **19**, 2757–2762.
64. H. C. Harder and B. Rosenberg, *International Journal of Cancer*, 1970, **6**, 207–216.
65. a M. Fichtinger-Schepman, J. L. van der Veer, J. H. den Hartog, P. H. Lohman, and J. Reedijk, *Biochemistry*, 1985, **24**, 707–13.
66. F. a Blommaert, H. C. van Dijk-Knijnenburg, F. J. Dijt, L. den Engelse, R. a Baan, F. Berends, and a M. Fichtinger-Schepman, *Biochemistry*, 1995, **34**, 8474–80.
67. M. S. Davies, S. J. Berners-Price, and T. W. Hambley, *Inorganic Chemistry*, 2000, **39**, 5603–13.
68. P. Muller, B. Schroder, J. A. Parkinson, N. A. Kratochwil, R. A. Coxall, A. Parkin, S. Parsons, and P. J. Sadler, *Angewandte Chemie (International Ed. in English)*, 2003, **42**, 335–339.
69. J. K. Barton and S. J. Lippard, *Metal Ions in Biology*, 1980, **1**, 31–113.
70. M. Castellano-Castillo, H. Kostrhunova, V. Marini, J. Kasparkova, P. J. Sadler, J.-M. Malinge, and V. Brabec, *Journal of Biological Inorganic Chemistry*, 2008, **13**, 993–9.
71. M. Melchart, A. Habtemariam, O. Novakova, S. Moggach, F. P. Fabbiani, S. Parsons, V. Brabec, and P. J. Sadler, *Inorganic Chemistry*, 2007, **46**, 8950–62.
72. N. S. Raja and B. U. Nair, *Toxicology*, 2008, **251**, 61–5.
73. G. Marverti, A. Ligabue, M. Montanari, D. Guerrieri, M. Cusumano, M. L. Di Pietro, L. Troiano, E. Di Vono, S. Iotti, G. Farruggia, F. Wolf, M. G. Monti, and C. Frassinetti, *Investigational New Drugs*, 2011, **29**, 73–86.

74. D.-L. Ma and C.-M. Che, *Chemistry (Weinheim an der Bergstrasse, Germany)*, 2003, **9**, 6133–44.
75. M. Howe-Grant and S. J. Lippard, *Biochemistry*, 1979, **18**, 5762–9.
76. K. E. Erkkila, D. T. Odom, and J. K. Barton, *Chemical Reviews*, 1999, **99**, 2777–96.
77. A. D. Burrows, C. Chan, M. M. Chowdhry, J. E. Mcgrady, D. Michael, P. Mingos, J. Mccrady, and A. Burrows, *Chemical Society Reviews*, 1995, **24**, 329–339.
78. T. W. Hambley, *Coordination Chemistry Reviews*, 1997, **166**, 181–223.
79. G. L. Edwards, D. S. C. Black, G. B. Deacon, and L. P. G. Wakelin, *Canadian Journal of Chemistry*, 2005, **83**, 980–989.
80. I. M. El-Mehasseb, M. Kodaka, T. Okada, T. Tomohiro, K. Okamoto, and H. Okuno, *Journal of Inorganic Biochemistry*, 2001, **84**, 157–158.
81. S. Fernández, M. M. García, R. Navarro, and E. P. Urriolabritia, *Journal of Organometallic Chemistry*, 1998, **561**, 67–76.
82. R. Wai-Yin Sun, A. Lok-Fung Chow, X.-H. Li, J. J. Yan, S. Sin-Yin Chui, and C.-M. Che, *Chemical Science*, 2011, **2**, 728.
83. R. N. Bose, L. Maurmann, R. J. Mishur, L. Yasui, S. Gupta, W. S. Grayburn, H. Hofstetter, T. Salley, and T. Milton, *Proceedings of the National Academy of Sciences of the United States of America*, 2008, **105**, 18314–9.
84. M. J. Cleare and J. D. Hoeschele, *Platinum Metals Review*, 1973, **17**, 2–13.
85. S. Neidle, I. M. Ismail, and P. J. Sadler, *Journal of Inorganic Biochemistry*, 1980, **13**, 205–212.
86. J. D. Ranford, P. J. Sadler, K. Balmano, and D. R. Newell, *Magnetic Resonance in Chemistry*, 1991, **29**, S125–S129.
87. K. J. Barnham, M. I. Djuran, P. D. S. Murdoch, J. D. Ranford, and P. J. Sadler, *Inorganic Chemistry*, 1996, **35**, 1065–1072.
88. P. M. A. B. Terheggen, A. C. Begg, J. Y. Emond, R. Dubbelman, B. G. Froot, and L. den Engelse, *British Journal of Cancer*, 1991, **63**, 195–200.
89. R. J. Parker, I. Gill, R. Tarone, J. A. Vionnet, S. Grunberg, F. M. Muggia, and E. Reed, *Carcinogenesis*, 1991, **12**, 1253–1258.
90. R. J. Knox, F. Friedlos, D. A. Lydall, and J. J. Roberts, *Cancer Research*, 1986, **46**, 1972–1979.
91. T. Boulikas and M. Vougiouka, *Oncology Reports*, 2003, **10**, 1663–1682.



92. E. Raymond, S. G. Chaney, A. Taamma, and E. Cvitkovic, *Annals of Oncology*, 1998, **9**, 1053–71.
93. A. S. Abu-Surrah, T. A. . Al-Allaf, M. Klinga, and M. Ahlgren, *Polyhedron*, 2003, **22**, 1529–1534.
94. Y. Kidani, K. Inagaki, and S. Tsukagoshi, *Gann Japanese Journal of Cancer Research*, 1976, **67**, 921–922.
95. L. Kelland, *Nature reviews. Cancer*, 2007, **7**, 573–84.
96. J. Graham, M. Mushin, and P. Kirkpatrick, *Nature reviews. Drug discovery*, 2004, **3**, 11–2.
97. S. G. Chaney, S. L. Campbell, E. Bassett, and Y. Wu, *Critical Reviews in Oncology/Hematology*, 2005, **53**, 3–11.
98. L. G. Marzilli, J. S. Saad, Z. Kuklenyik, K. A. Keating, and Y. Xu, *Journal of the American Chemical Society*, 2001, **123**, 2764–70.
99. N. J. Wheate, S. Walker, G. E. Craig, and R. Oun, *Dalton Transactions*, 2010, **39**, 8113–8127.
100. M. Galanski, M. A. Jakupec, and B. K. Keppler, *Current Medicinal Chemistry*, 2005, **12**, 2075–2094.
101. Z. Wang, X. Tang, Y. Zhang, R. Qi, Z. Li, K. Zhang, Z. Liu, and X. Yang, *Biomédecine & Pharmacothérapie*, 2012, **66**, 161–6.
102. C.-Y. Xie, Y.-P. Xu, W. Jin, and L.-G. Lou, *Anti-Cancer Drugs*, 2012, **23**.
103. J.-W. Lee, J.-K. Park, S.-H. Lee, S.-Y. Kim, Y.-B. Cho, and H.-J. Kuh, *Anti-Cancer Drugs*, 2006, **17**.
104. M. A. Bruck, R. Bau, M. Noji, K. Inagaki, and Y. Kidani, *Inorganica Chimica Acta*, 1984, **92**, 279–284.
105. W. Liu, X. Chen, Q. Ye, Y. Xu, C. Xie, M. Xie, Q. Chang, and L. Lou, *Inorganic Chemistry*, 2011, **50**, 5324–6.
106. A. R. Battle, R. Choi, D. E. Hibbs, and T. W. Hambley, *Inorganic Chemistry*, 2006, **45**, 6317–6322.
107. J. Holford, F. Raynaud, B. A. Murrer, K. Grimaldi, J. A. Hartley, M. Abrams, and L. R. Kelland, *Anti-Cancer Drug Design*, 1998, **13**, 1–18.
108. Y. Chen, Z. Guo, S. Parsons, and P. J. Sadler, *Chemistry - A European Journal*, 1998, **4**, 672–676.

109. J. Holford, S. Y. Sharp, B. A. Murrer, M. Abrams, and L. R. Kelland, *British Journal of Cancer*, 1998, **77**, 366–373.
110. I. Zanellato, I. Bonarrigo, E. Gabano, M. Ravera, N. Margiotta, P.-G. Betta, and D. Osella, *Inorganica Chimica Acta*, 2012, **393**, 64–74.
111. T. Boulikas, A. Pantos, E. Bellis, and P. Christofis, *Cancer Therapy*, 2007, **5**, 537–583.
112. M. Hall, *Biochemical Pharmacology*, 2004, **67**, 17–30.
113. S. Choi, C. Filotto, S. D. Bisanzo, D. Lagasee, J. L. Whitworth, A. Jusko, C. Li, N. A. Wood, J. Willingham, A. Schwenker, and K. Spaulding, *Inorganic Chemistry*, 1998, **37**, 2500–2504.
114. E. L. Weaver and R. N. Bose, *Journal of Inorganic Biochemistry*, 2003, **95**, 231–239.
115. M. D. Hall, S. Amjadi, M. Zhang, P. J. Beale, and T. W. Hambley, *Journal of Inorganic Biochemistry*, 2004, **98**, 1614–1624.
116. T. W. Hambley, A. R. Battle, G. B. Deacon, E. T. Lawrenz, G. D. Fallon, B. M. Gatehouse, L. K. Webster, and S. Rainone, *Journal of Inorganic Biochemistry*, 1999, **77**, 3–12.
117. M. Galanski and B. Keppler, *Inorganica Chimica Acta*, 2000, **300**, 783–789.
118. L. R. Kelland, G. Abel, M. J. Mckeage, M. Jones, P. M. Goddard, M. Valenti, B. A. Murrer, and K. R. Harrap, *Cancer Research*, 1993, **53**, 2581–2586.
119. A. D. Ricart, J. Sarantopoulos, E. Calvo, Q. S. Chu, D. Greene, F. E. Nathan, M. E. Petrone, A. W. Tolcher, and K. P. Papadopoulos, *Clinical Cancer Research*, 2009, **15**, 3866–3871.
120. J. Cetnar, G. Wilding, D. McNeel, N. K. Loconte, T. A. McFarland, J. Eickhoff, and G. Liu, *Urologic Oncology*, 2011.
121. G. Doshi, G. Sonpavde, and C. N. Sternberg, *Expert Opinion on Drug Metabolism & Toxicology*, 2012, **8**, 103–11.
122. M. A. Ali, A. H. Mirza, R. J. Butcher, and K. A. Crouse, *Transition Metal Chemistry*, 2006, **31**, 79–87.
123. P. Chellan, K. M. Land, A. Shokar, A. Au, S. H. An, C. M. Clavel, P. J. Dyson, C. De Kock, P. J. Smith, K. Chibale, and G. S. Smith, *Organometallics*, 2012, **31**, 5791–5799.
124. J. C. Jeffrey and T. B. Rauchfuss, *Inorganic Chemistry*, 1979, **18**, 2658–2666.
125. M. Bassetti, *European Journal of Inorganic Chemistry*, 2006, **2006**, 4473–4482.

126. P. Braunstein and F. Naud, *Angewandte Chemie (International Ed. in English)*, 2001, **40**, 680–699.
127. D. F. Shriver and P. W. Atkins, in *Inorganic Chemistry*, Oxford University Press, 3rd Ed., 1999, pp. 211–247.
128. T. Maguire, *PhD Thesis*, 2009, UCC, 100–153.
129. P. Braunstein, M. Knorr, C. Stern, L. Pasteur, and B. Pascal, *Coordination Chemistry Reviews*, 1998, **180**, 903–965.
130. H.-B. Song, Z.-Z. Zhang, and T. C. W. Mak, *Polyhedron*, 2002, **21**, 1043–1050.
131. E. W. Ainscough, A. M. Brodie, A. K. Burrell, A. Derwahl, G. B. Jameson, and S. K. Taylor, *Polyhedron*, 2004, **23**, 1159–1168.
132. S. E. Watkins, D. C. Craig, and S. B. Colbran, *Inorganica Chimica Acta*, 2000, **307**, 134 – 138.
133. K. Grice, W. Kaminsky, and K. I. Goldberg, *Inorganica Chimica Acta*, 2011, **369**, 76–81.
134. D. Hedden, M. D. Roundhill, W. C. Fultz, and A. L. Rheingold, *Journal of the American Chemical Society*, 1984, **106**, 5014–5016.
135. M. Crespo, X. Solans, and M. Font-Bardia, *Journal of Organometallic Chemistry*, 1996, **518**, 105–113.
136. J. A. March and M. B. Smith, *Advanced Organic Chemistry*, Wiley, 6th Ed., 2007.
137. S. Dalili, A. Caiazzo, and A. K. Yudin, *Journal of Organometallic Chemistry*, 2004, **689**, 3604–3611.
138. K. S. Coleman, M. L. H. Green, S. I. Pascu, N. H. Rees, a. R. Cowley, and L. H. Rees, *Journal of the Chemical Society, Dalton Transactions*, 2001, 3384–3395.
139. P. Ramírez, R. Contreras, M. Valderrama, D. Carmona, F. J. Lahoz, and A. I. Balana, *Journal of Organometallic Chemistry*, 2008, **693**, 349–356.
140. G. Sánchez, J. García, D. Meseguer, J. L. Serrano, L. García, J. Pérez, and G. López, *Inorganica Chimica Acta*, 2006, **359**, 1650–1658.
141. T. Mino, Y. Tanaka, M. Sakamoto, and T. Fujita, *Tetrahedron: Asymmetry*, 2001, **12**, 2435–2440.
142. A. Habtemariam, J. A. Parkinson, N. Margiotta, T. W. Hambley, S. Parsons, and P. J. Sadler, *Journal of the Chemical Society, Dalton Transactions*, 2001, 362–372.
143. A. Habtemariam and P. J. Sadler, *Chemical Communications*, 1996, 1785.

144. K. Nepelchová, J. Kaspárková, O. Vrána, O. Nováková, A. Habtemariam, B. Watchman, P. J. Sadler, and V. Brabec, *Molecular Pharmacology*, 1999, **56**, 20–30.
145. P. Wang, C. H. Leung, D. L. Ma, R. W. Sun, S. C. Yan, Q. S. Chen, and C. M. Che, *Angewandte Chemie (International Ed. in English)*, 2011, **50**, 2554–2558.
146. D. Vázquez-García, A. Fernández, J. J. Fernández, M. López-Torres, A. Suárez, J. M. Ortigueira, J. M. Vila, and H. Adams, *Journal of Organometallic Chemistry*, 2000, **595**, 199–207.
147. T. J. Dougherty, C. J. Gomer, B. W. Henderson, G. Jori, D. Kessel, M. Korbelik, J. Moan, and Q. Peng, *Journal of the National Cancer Institute*, 1998, **90**, 889–905.
148. M. R. Detty, S. L. Gibson, and S. J. Wagner, *Journal of Medicinal Chemistry*, 2004, **47**, 3897–3915.
149. J. a. S. Cavaleiro, H. Görner, P. S. S. Lacerda, J. G. MacDonald, G. Mark, M. G. P. M. S. Neves, R. S. Nohr, H.-P. Schuchmann, C. von Sonntag, and A. C. Tomé, *Journal of Photochemistry and Photobiology A: Chemistry*, 2001, **144**, 131–140.
150. K. J. Laidler, J. H. Meiser, and B. C. Sanctuary, *Physical Chemistry*, Houghton Mifflin Company, 4th Ed., 2003.
151. P. J. Bednarski, F. S. Mackay, and P. J. Sadler, *Anti-cancer Agents in Medicinal Chemistry*, 2007, **7**, 75–93.
152. J. Pracharova, L. Zerzankova, J. Stepankova, O. Novakova, N. J. Farrer, P. J. Sadler, V. Brabec, and J. Kasparkova, *Chemical Research in Toxicology*, 2012, **25**, 1099–111.
153. B.-P. Yan, C. C. C. Cheung, S. C. F. Kui, H.-F. Xiang, V. a. L. Roy, S.-J. Xu, and C.-M. Che, *Advanced Materials*, 2007, **19**, 3599–3603.
154. V. Sicilia, J. Forniés, J. M. Casas, A. Martín, J. a López, C. Larraz, P. Borja, C. Ovejero, D. Tordera, and H. Bolink, *Inorganic Chemistry*, 2012, **51**, 3427–35.
155. L. Flamigni, A. Barbieri, C. Sabatini, B. Ventura, F. Barigelletti, and J. A. G. Williams, in *Photochemistry and Photophysics of Coordination Compounds*, eds. V. Balzani and S. Campagna, Springer Berlin Heidelberg, 2007, vol. 281, pp. 143–203.
156. J. a G. Williams, A. J. Wilkinson, and V. L. Whittle, *Dalton Transactions*, 2008, 2081–99.
157. Y.-M. Ho, C.-K. Koo, K.-L. Wong, H.-K. Kong, C. T.-L. Chan, W.-M. Kwok, C.-F. Chow, M. H.-W. Lam, and W.-Y. Wong, *Dalton Transactions*, 2012, **41**, 1792–800.
158. Z. Hu, Y. Wang, D. Shi, H. Tan, X. Li, L. Wang, W. Zhu, and Y. Cao, *Dyes and Pigments*, 2010, **86**, 166–173.

159. S. C. F. Kui, F.-F. Hung, S.-L. Lai, M.-Y. Yuen, C.-C. Kwok, K.-H. Low, S. S.-Y. Chui, and C.-M. Che, *Chemistry (Weinheim an der Bergstrasse, Germany)*, 2012, **18**, 96–109.

## **Chapter 2:**

# **Coordination and Cyclometallation**

## Contents

<b>2.1 Chapter 2 Background</b> .....	63
<b>2.2 Phosphorus and Nitrogen as Donor Ligands</b> .....	64
2.2.1 PN Complexes.....	64
2.2.2 Iminophosphine Ligands .....	67
2.2.3 Phosphinoamide Ligands .....	70
<b>2.3 Organometallic Compounds, C-H Activation, Cyclometallation</b> .....	71
2.3.1 Main-Group Organometallic Chemistry.....	71
2.3.2 Formation of Cyclometallated Complexes .....	72
2.3.3 Cyclometallated Complexes .....	77
2.3.4 Stabilisation of Liberated Chloride Anions .....	81
2.3.5 Influence of Ligand Substituents on Cyclometallation .....	85
<b>2.4 Conclusion</b> .....	88
<b>2.5 Syntheses</b> .....	89
2.5.1 Synthesis of the Iminophosphine Ligands $HL^{1-4}$ .....	89
2.5.2 Synthesis of the Phosphinoamide Ligands $HL^{5-7}$ .....	91
2.5.3 Synthesis of bidentate iminophosphine complexes with the general formula $[Pt(\eta^2-PN-L^{1-3})Cl]$ <b>271-273</b> METHOD A .....	92
2.5.4 Synthesis of platinum complexes of the $HL^4$ ( <b>264</b> ) ligand with the general formula $[Pt(\eta^3-PNO-L^4)Cl]$ <b>285</b> METHOD A.....	98
2.5.5 Synthesis of cyclometallated tridentate iminophosphine complexes with the general formula $[Pt(\eta^3-PNC-L^{1-3})Cl]$ <b>281-283</b> METHOD B.....	100
2.5.6 Synthesis of platinum complexes of the $HL^4$ ( <b>264</b> ) ligand with the general formula $[Pt(\eta^3-PNC-L^4)Cl]$ and $[Pt(\eta^3-PNO-L^4)Cl]$ <b>284-285</b> METHOD B.....	109
2.5.7 Synthesis of cyclometallated tridentate phosphinoiminol complexes with the general formula $[Pt(\eta^3-PNC-L^{5-7})Cl]$ and $[Pt(\eta^3-PNO-L^6)Cl]$ <b>286-289</b> .....	111

<b>2.6 Infra-Red Spectroscopic Studies</b> .....	118
2.6.1 Iminophosphine ligands HL1-4 ( <b>261-264</b> ) and their Pt (II) complexes [Pt( $\eta^2$ -PN-L <sup>1-3</sup> )Cl] ( <b>271-273</b> ), [Pt( $\eta^3$ -PNC-L <sup>1-4</sup> )Cl] ( <b>281-284</b> ) and [Pt( $\eta^3$ -PNO-L <sup>4</sup> )Cl] ( <b>285</b> )..	118
2.6.2 Phosphinoamide ligands HL <sup>5-7</sup> ( <b>265-267</b> ) and their Pt (II) iminol complexes [Pt( $\eta^3$ -PNC-L <sup>5-7</sup> )Cl] ( <b>286-288</b> ) .....	120
<b>2.7 NMR Spectroscopic Studies</b> .....	122
2.7.1 NMR data for the Iminophosphine ligands HL1 <sup>4</sup> ( <b>261-264</b> ):.....	122
2.7.2 NMR data for the Phosphinoamide ligands HL <sup>5-7</sup> ( <b>265-267</b> ) .....	126
2.7.3 NMR spectra for the tridentate Pt (II) iminophosphine complexes [Pt( $\eta^3$ -PNC-L <sup>1-4</sup> )Cl] <b>281-284</b> and [Pt( $\eta^3$ -PNO-L <sup>4</sup> )Cl] <b>285</b> .....	132
2.7.4 NMR spectroscopy for the tridentate Pt (II) phosphinoiminol complexes [Pt( $\eta^3$ -PNC-L <sup>5-7</sup> )Cl] <b>286-288</b> and [Pt( $\eta^3$ -PNO-L <sup>6</sup> )Cl] <b>289</b> .....	143
<b>2.8 X-ray crystallography</b> .....	151
2.8.1 Crystal and molecular structures of [Pt( $\eta^3$ -PNC-L <sup>2-3</sup> )Cl] <b>282</b> and <b>283</b> .....	151
<b>2.9 Summary and Conclusion</b> .....	154
<b>2.10 Chapter 2 Experimental</b> .....	158
2.10.1 Background.....	158
2.10.2 Preparation of the Iminophosphine ligands HL <sup>1-4</sup> <b>261-264</b> .....	159
2.10.3 Preparation of the Phosphinoamide ligands HL <sup>5-7</sup> <b>261-264</b> .....	161
2.10.4 Synthesis of Iminophosphine complexes [Pt( $\eta^2$ -PN-L <sup>1-3</sup> )Cl] <b>271-273</b> and [Pt( $\eta^3$ -PNO-L <sup>4</sup> )Cl] <b>285</b> (Method A): .....	163
2.10.5 Synthesis of the platinum iminophosphine complexes [Pt( $\eta^3$ -PNC-L <sup>1-3</sup> )Cl] <b>281- 283</b> and [Pt( $\eta^3$ -PNO-L <sup>4</sup> )Cl] <b>285</b> (Method B) .....	166
2.10.6 Synthesis of the platinum iminophosphine complexes [Pt( $\eta^3$ -PNC-L <sup>4</sup> )Cl] <b>284</b> and [Pt( $\eta^3$ -PNO-L <sup>4</sup> )Cl] <b>285</b> (Method B).....	169
2.10.7 Synthesis of the platinum phosphinoiminol cyclometallated complexes [Pt( $\eta^3$ -PNC-L <sup>5-7</sup> )Cl] <b>286-288</b> .....	171
<b>2.11 Bibliography</b> .....	173



## 2.1 Chapter 2 Background:

It is the intention of this chapter to extend the investigation of this research group into novel cyclometallated Pt (II) chloro complexes. The process of cyclometallation contained in this chapter involves the coordination of an organic ligand containing three potential coordination sites to a Pt (II) metal centre. The chelating organic iminophosphine and phosphinoamide ligands used in this chapter are derived from the reaction of the aminophosphine; 2-diphenylphosphinoaniline **201**, **Figure 2.1**, with the appropriate aldehyde **202** or acyl chloride **203**.

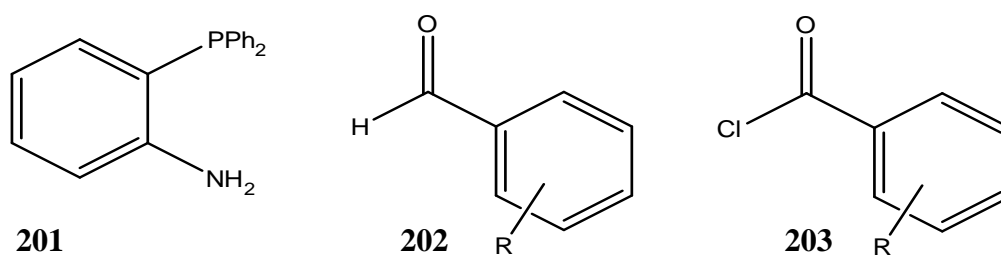


*Figure 2.1: The structure of 2-diphenylphosphinoaniline **201**, and the general structure of the aldehyde used to make the iminophosphine ligands, **202**, and the acyl chlorides used to make the phosphinoamides, **203**.*

Cyclometallation is the process where a metal centre can be cyclised by a ligand with the formation of a carbon-metal bond. The iminophosphine ligands used in this study are synthesised via a condensation reaction with an appropriate aldehyde (**202**, **Figure 2.1**). The phosphinoamide ligands are synthesised via loss of HCl by reacting 2-diphenylphosphinoaniline with the appropriate acyl chloride (**203**, **Figure 2.1**).

Both ligands undergo coordination to the Pt (II) metal centre in a variety of ways, which will be explored in this chapter. Previous work within this research group has investigated the effect of substituents on the ligand towards the cyclometallation of Pd (II) chloro and Pt (II) iodo complexes (as well as the formation of PNO type complexes).<sup>1,2</sup>

Focus for this current work is therefore the synthesis of a series of novel cyclometallated Pt (II) chloro complexes from iminophosphine and phosphinoamide ligands. Also investigated will be the factors affecting C-H bond activation as well as solvent effects. Subsequent oxidation and substitution type reactions will be explored in **Chapter 3**, while studies on the potential applications of these complexes will be discussed and reported in **Chapter 4**.

## 2.2 Phosphine and Nitrogen as Donor Ligands

### 2.2.1 PN Complexes:

Phosphines can be very effective coordination ligands, particularly for platinum metal complexes. The  $\sigma$ -donor ability and  $\pi$ -acceptor ability of phosphines can vary widely depending on the substituents present. In a comparison of IR (infra-red) stretching bands for a carbonyl group on a molybdenum complex, it can clearly be seen how the phosphine substituents can influence the other ligand on the complex (**Table 2.1**).  $\text{PF}_3$  for instance is the weakest  $\sigma$ -donor as a consequence of the highly electronegative fluorides, but is also the strongest  $\pi$ -acceptor.  $\text{PMe}_3$  on the other hand is the strongest  $\sigma$ -donor and weakest  $\pi$ -acceptor.<sup>3</sup>

Complex	$\nu(\text{CO}), \text{cm}^{-1}$
<i>Fac</i> - $\text{Mo}(\text{CO})_3(\text{PF}_3)_3$	2090, 2055
<i>Fac</i> - $\text{Mo}(\text{CO})_3(\text{PCl}_3)_3$	2040, 1991
<i>Fac</i> - $\text{Mo}(\text{CO})_3(\text{PClPh}_2)_3$	1977, 1885
<i>Fac</i> - $\text{Mo}(\text{CO})_3(\text{PMe}_3)_3$	1945, 1854

*Table 2.1: Examples of carbonyl IR stretching bands for a range of molybdenum complexes.*<sup>3</sup>

As a result, the molybdenum in  $\text{Mo}(\text{CO})_3(\text{PMe}_3)_3$  carries the greatest electron density and is therefore most able to donate electron density to the  $\pi^*$  orbitals of the CO ligands. This back bonding to CO lowers the energy of the carbonyl stretching vibrations. As a result of this, the CO ligands in  $\text{Mo}(\text{CO})_3(\text{PMe}_3)_3$  have the weakest C-O bonds of these set of complexes and the lowest energy stretching bands. Similar correlations between a metal environment and a variety of other ligands can be shown using IR spectroscopy and is therefore used throughout this work as a method of characterisation.<sup>3</sup>

Some types of phosphine ligands when coordinated to platinum metal centres promote C-H activation and hence favour the formation of cycloplatinated complexes, **Figure 2.2**. A large number of studies have indicated that to achieve C-H bond activation (and subsequent cyclometallation), a stable, soluble Pt (II) complex with a labile ligand is desirable. The labile ligand allows for a substitution reaction wherein the carbon can bind to the metal centre. C-H activation and cyclometallation will be further discussed in **Section 2.3**.

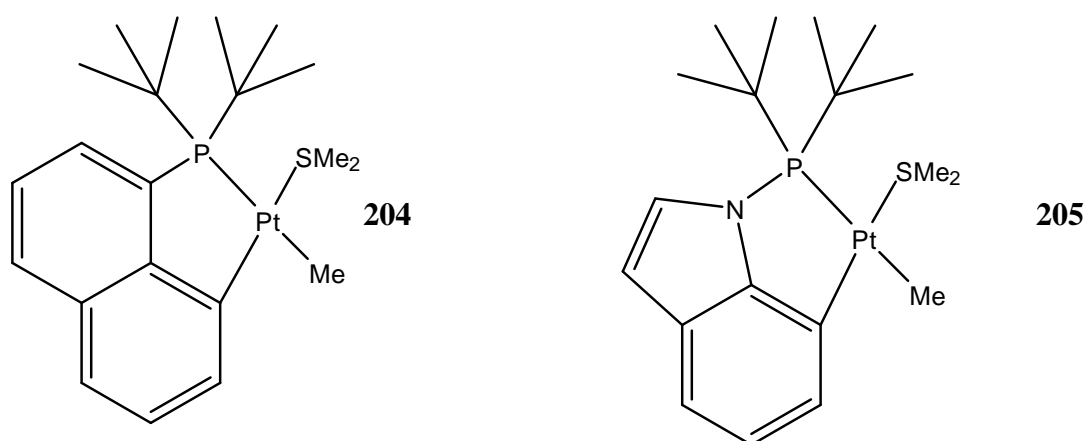


Figure 2.2: Examples of platinum phosphine cyclometallated complexes.<sup>4</sup>

Nitrogen has been used as a donor ligand for all of the currently approved platinum anti-cancer complexes including cisplatin, carboplatin and oxaliplatin. Nitrogen donor groups generally form part of the *non-leaving group* due to the stability of the complexes they form with platinum. But, all of the currently approved anti-cancer complexes are homo-donor chelate ligands. Hetero-donor ligands on the other hand (such as P, N donor chelates) have a distinct *trans* effect which can play an important role in controlling selectivity and activity of the complex.<sup>5,6</sup>

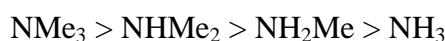
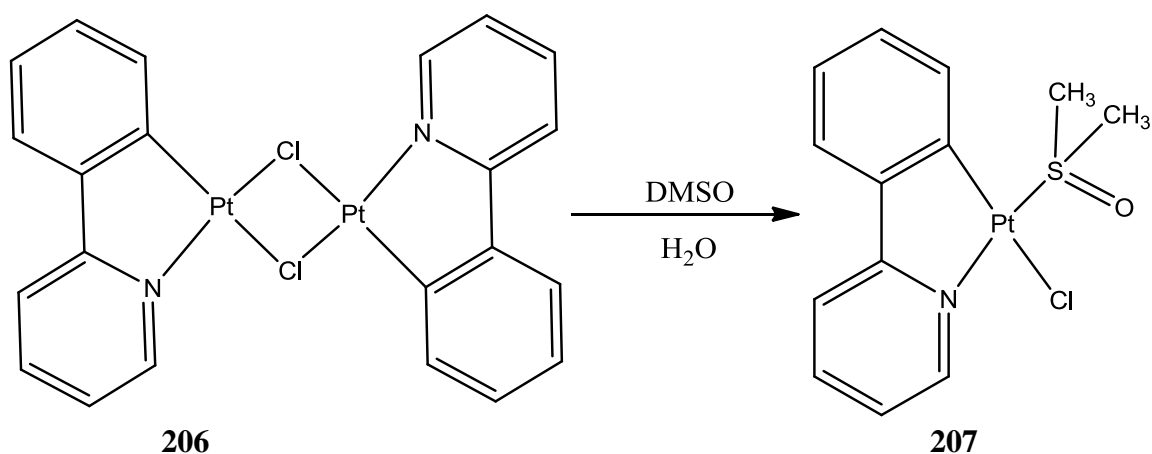


Figure 2.3: Some substitutions with alkyl groups instead of hydrogen on nitrogen based ligands can increase its donor ability by increasing its negative character, with the above giving us the order of base strength for difference nitrogen based substituents.<sup>7</sup>

As already seen for phosphines, the presence of electronegative substituents on a donor ligand can decrease the ability of the donor moiety to coordinate to the acid (metal centre). This also holds true for nitrogen based donor ligands also, but for imines in particular there is the added effect of increased electron density from the double bond which can actually contribute negative character to the nitrogen donor atom. Other methods for increasing the coordination ability of a nitrogen donor moiety include adding alkyl groups in the place of hydrogen which can actually increase its negative character making nitrogen a stronger donor moiety, **Figure 2.3**.<sup>7</sup>

Nitrogen is also a popular coordination ligand used for metal complex formation and C-H activation. Most C-H bond activation studies have involved chelating nitrogen donor ligands like those found in **Figure 2.4**. The stability provided by the strong phosphine-

platinum bond results in rapid C-H activation for the complexes shown in **Figure 2.2**. As previously discussed in **Chapter 1** and displayed in **Table 1.1, Section 1.3.1**, nitrogen type ligands are generally neither hard nor soft bases according to the HSAB theory (they are referred to as borderline). Imines, including Schiff bases in particular, which are employed for this project, are also very important intermediates in many metabolic pathways and organic synthetic routes.<sup>8</sup>



*Figure 2.4: The structure of two platinum complexes coordinated to an aromatic N-donor ligand, showing a chloro bridged dimer 206 and the DMSO substitute 207.<sup>9</sup>*

Aromatic N-donor ligands are also sometimes employed for coordination, particularly for platinum coordination, due to the possible anti-cancer activity they produce with platinum metal centres (**Figure 2.4**). These aromatic N-donor ligands can form very stable complexes due to the large electron density from the ring structure, which give the donor atom increased negative character.<sup>9</sup>

Successful platinum coordination to bulky di-imine ligands has also been reported, showing their success as coordinating ligands even under difficult sterically crowded conditions. The resulting complexes (**Figure 2.5**) can be subsequently cyclometallated in a variety of ways, forming mono-cyclometallated and doubly cyclometallated complexes. These will be discussed further under the context of cyclometallation in **Section 2.2**.<sup>10</sup>

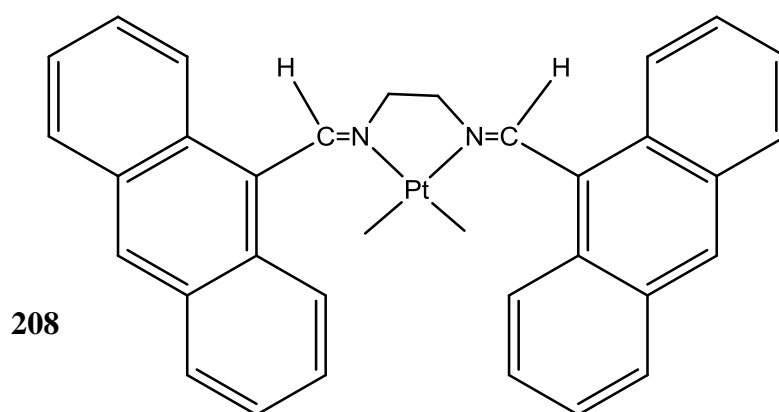


*Figure 2.5: The structure of a bidentate di-imine coordinated Pt (II) complex with a bulky ligand, prior to cyclometallation.<sup>10</sup>*

### 2.2.2 Iminophosphine Ligands:

A number of research groups have reported successful palladium and platinum coordination studies on a multitude of P, N mixed donor ligands. Early interest in these systems was driven by the possibilities of forming new catalysts (particularly with palladium) and generally focussed on bidentate ligands as seen in **Figure 2.6**.<sup>11–13</sup>

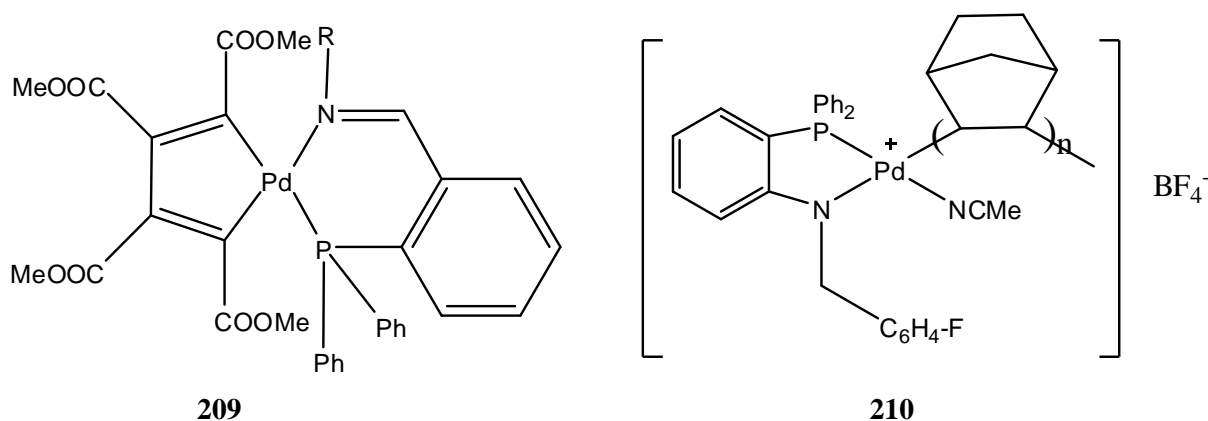


*Figure 2.6: The structure of two bidentate palladium complexes coordinated to a P, N mixed donor ligand. Both complex **209**<sup>11</sup> (iminophosphine) and **210**<sup>12</sup> are used as catalysts.*

On coordination to transition metals, the hard/soft combination of the P, N donor ligands creates asymmetry in the metal orbitals which then affects the reactivity of the complex. This property of palladium and platinum type complexes in particular has been widely reported with respect to other iminophosphine type ligands.<sup>5</sup>

Hetero-donor ligands like iminophosphines have a distinct *trans* effect which can play a role in controlling the selectivity/activity, particularly for catalytic processes. The *trans*

influence of the phosphorus donor moiety is significantly different to that of the nitrogen donor moiety. In an iminophosphine complex the bond *trans* to the phosphorus is longer than that *trans* to the nitrogen, indicating the greater *trans* influence of phosphorus compared to the imine donor functionality.<sup>14–16</sup>

This, as well as the hard/soft combination, lends itself to a versatile coordination behaviour with metal centres in different oxidation states and provides hemilabile functionality (as discussed in **Chapter 1, Section 1.5**). Moreover, these types of ligands allow modulation of the steric crowding around the metal centre through simple variation of the substituents on the imine and phosphine groups.<sup>17</sup>

Numerous transition metal complexes of iminophosphines have been reported (particularly palladium based), but only a limited amount of those containing platinum. Also most of the platinum complexes reported are designed for catalysis **Figure 2.7**.

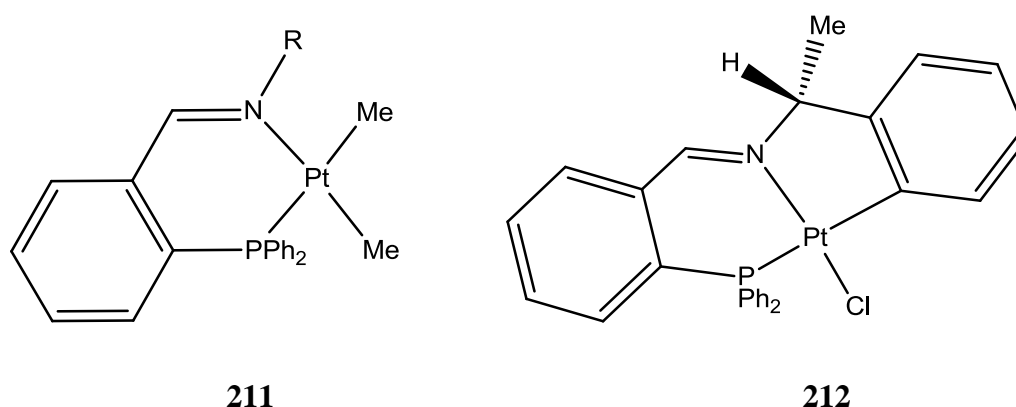


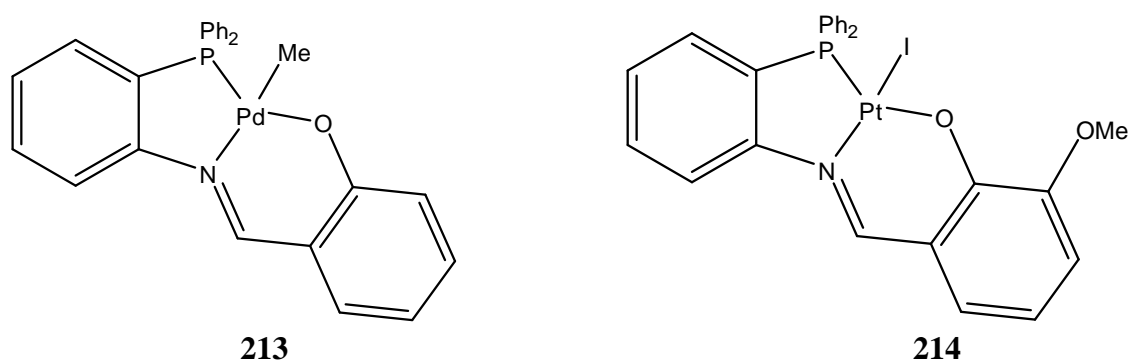
*Figure 2.7: The structure of two Pt (II) iminophosphine complexes. The bidentate complex 211 is used as a catalyst<sup>18</sup> while complex 212 is a rare example of a tridentate cyclometallated platinum P, N, C type iminophosphine complex.<sup>19</sup> (both feature an unusually large P, N bite angle).*

In terms of catalysis, an important property of these ligands is that they stabilise metal ions in a variety of oxidation states and geometries, which normally occur during a catalytic cycle. Similar ideas can be applied to anti-cancer activity where stability of the *non-leaving group* ligand is crucial to the development of new analogues of platinum based anti-cancer complexes.<sup>20</sup>

The  $\pi$ -acceptor ability of the phosphine, previously mentioned in **Section 2.1**, can also stabilise a metal centre, while the nitrogen  $\sigma$ -donor ability makes the metal centre more susceptible to oxidative addition reactions. For example, binding a phosphorus moiety directly to a more electronegative atom such as an oxygen or nitrogen will reduce its electron donating capability while also enhancing its  $\pi$ -acceptor capacity. On the other hand, the

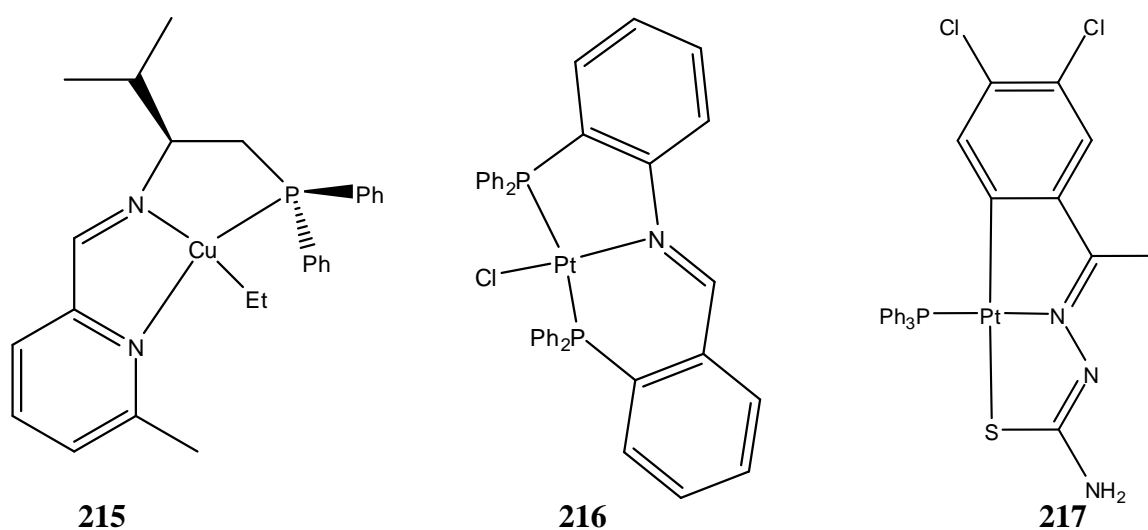
presence of an imino rather than an amino group will result in a nitrogen donor atom of greater  $\sigma$ -donating capabilities.<sup>21,6,22</sup>

As previously mentioned, studies which involve ligands containing mixed phosphorus and nitrogen atoms have generally focussed on bidentate type coordination. However, multidentate ligands such as that contained in complex **212**, **Figure 2.7** (P, N, C type) have recently become more popular due to their stability for catalysis and potential for anti-cancer activity.<sup>23</sup> Tridentate ligands involving platinum and palladium metal centres of the type “P, N, O” have been extensively studied by this research group and others, **Figure 2.8**.<sup>1,24</sup>



**Figure 2.8:** The structure of two tridentate P, N, O, type group 10 iminophosphine complexes. The palladium complex **213** is used as a catalyst<sup>24</sup> while complex **214** is a tridentate platinum iminophosphine complex previously reported by our research group.<sup>1</sup>

The reactivity of palladium versus platinum towards hemilabile P,N,O type tridentate ligands has also been reported with palladium coordinating to the hard oxygen ligand much more easily due to its higher reactivity over platinum.

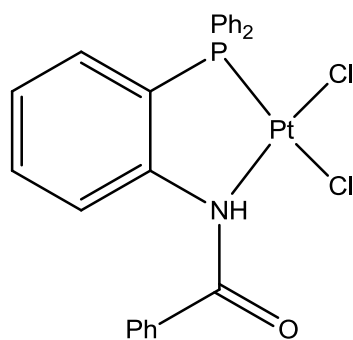
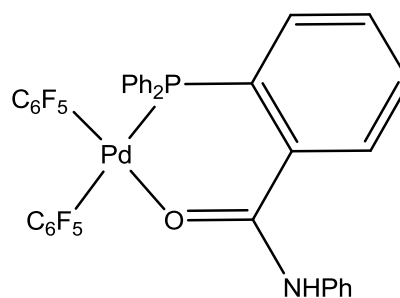


**Figure 2.9:** Examples of a P,N,N copper complex **215**,<sup>25</sup> a platinum based P,P, N iminophosphine type complex **216**,<sup>23</sup> and a P,N,S type complex, also with platinum as the metal centre **217**.<sup>26</sup>

The strong phosphorus-metal bond along with the phosphine ligands' strong *trans* influence and the chelate effect (discussed further in **Chapter 3**) also allow for P,N,O tridentate coordination in the above complexes.<sup>24</sup> Other tridentate iminophosphine complexes reported to date include P,N,N<sup>27</sup> types, P,P, N<sup>23</sup> types and C,N,S<sup>26</sup> types (with P outside of the chelate ring) as seen in **Figure 2.9**.

### 2.2.3 Phosphinoamide Ligands

Phosphinoamide type ligands have similar, but more versatile, coordination behaviour to iminophosphines with the same mixed donor atoms of phosphine and nitrogen as seen in **Figure 2.10**, however, the amide donor ligand has less donating ability (and hence negative character) than the equivalent imine ligand. This can lead to different hemilability and coordination behaviour towards certain metals. The coordination behaviour and hemilability of phosphinoamides has been exploited in several ways to bring about good stereoselectivity as catalytic complexes, like those featured in **Figure 2.10**.<sup>28</sup>

**218****219**

*Figure 2.10: Examples of a platinum phosphinoamide complex which has been reported as a very useful catalyst 218,<sup>29</sup> and a palladium phosphinoamide complex which interestingly coordinates to the harder oxygen ligand over the amide 219.<sup>30</sup>*

These functionalised phosphinoamides are generally used where it is desirable to have a hinging chelate arm ready for substitution as discussed in terms of hemilability in **Chapter 1, Section 1.5.2**. With this functionality in mind these ligands (coordinated to palladium in particular) have been reported to be efficient chirality sources for allylic alkylation as catalysts. As well as platinum and palladium other phosphinoamide complexes of rhodium (I) and iridium (I) have also been reported to be effective catalysts.<sup>28,29</sup>



## 2.3 Organometallic Compounds, C-H Bond Activation and Cyclometallation:

### 2.3.1 Main-Group Organometallic Chemistry:

Cyclometallation is core to the formation and development of the newest analogues of platinum anti-cancer complexes and the primary concept that will be explored over the course of the rest of this chapter. Cyclometallation involves surrounding a metal centre (platinum in the present case) with various ligands in a coordinated structure to produce at least one platinum-carbon bond via C-H bond activation.

For a long time it was assumed that transition metal-carbon bonds were too weak to yield stable metal alkyl complexes. Compounds such as  $\text{TiEt}_4$  are very reactive, decomposing at temperatures above minus  $50^\circ\text{C}$ . Main-group organometallic compounds on the other hand have long been reported and features such as the role of steric congestion around the central atom have been studied by various scientists as far back as the mid 19<sup>th</sup> century. One of the pioneers of main-group organometallic chemistry was the English chemist E.C. Frankland, who became the first person to synthesise dimethylzinc in 1848.<sup>31</sup>

In terms of stability, the trend for compounds of *p*-block elements is that methyl compounds of the light elements of groups 13 and 15 tend to react exothermically with this character decreasing down the group, and the compounds of the heaviest elements react endothermically. The relative instability of the heavy members of the group is a consequence of the decrease in metal-carbon bond strength where compounds such as  $\text{Pb}(\text{CH}_3)_4$  can undergo homolytic cleavage to produce  $\text{CH}_3$  radicals when heated in the gas phase. Similarly, dimethylcadmium can decompose explosively.<sup>31</sup>

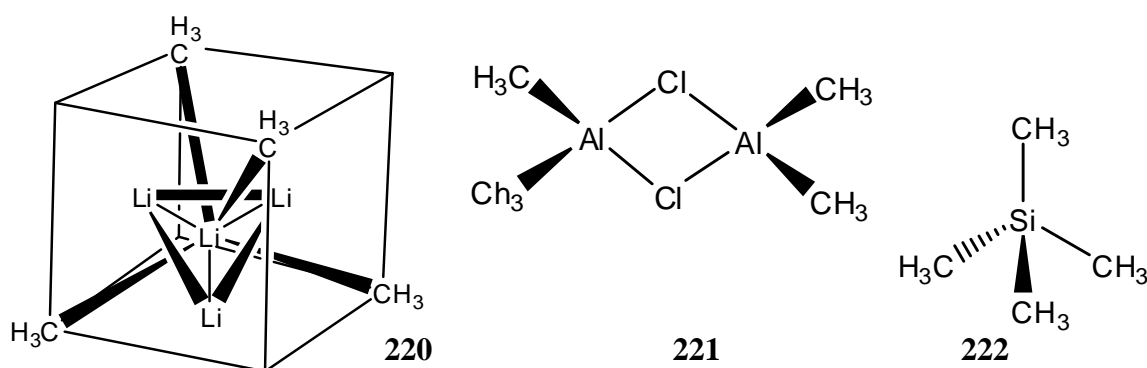


Figure 2.11: Examples of *s*-block 220 and *p*-block 221, 222 organometallic compounds.<sup>31</sup>

The alkyl compounds of *s*-block elements contain a highly polar Metal<sup>δ+</sup> - Carbon<sup>δ-</sup> bond. Some analyses of the bonding in these compounds indicate about 90% ionic character for the Li-CH<sub>3</sub> interaction, **220**, **Figure 2.11**. Methyl lithium is both strongly basic and highly nucleophilic due to the partial negative charge on carbon and is therefore particularly reactive towards electron acceptors and proton donors. Methyl lithium in non-polar solvents consists of a tetrahedron of Li atoms with each face bridged by a methyl group, **220**, **Figure 2.11**. Therefore operations involving methyl lithium require anhydrous conditions, because the compound is highly reactive toward water, oxygen and carbon dioxide.<sup>31,32</sup>

The first isolated organometallic compounds of any transition metal on the other hand were (CH<sub>3</sub>)<sub>3</sub>PtI, (CH<sub>3</sub>)<sub>3</sub>PtNO, (CH<sub>3</sub>)<sub>3</sub>PtOH and (CH<sub>3</sub>)<sub>3</sub>PtCl in 1907 by Pope and Peachy. It was noted at the 1907 proceedings of the Chemical Society of London that the authors of the report were congratulated on “having opened an entirely new branch of investigation which might indeed be said to be a wonderful find”. Since then there has been enormous interest in transition metal organometallic compounds, with particular interest given to platinum based ones due to their stability, their relative inertness to air and water along with the wide range of possible applications.<sup>33</sup>

### 2.3.2 Formation of Cyclometallated Complexes:

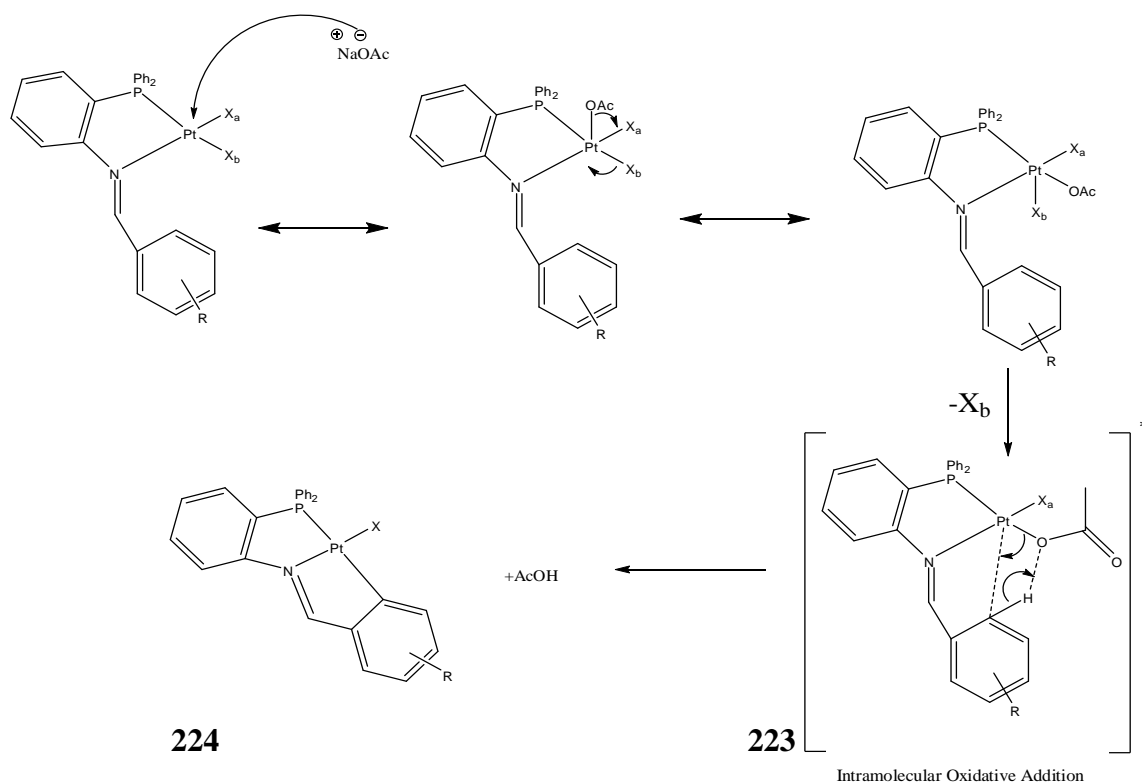
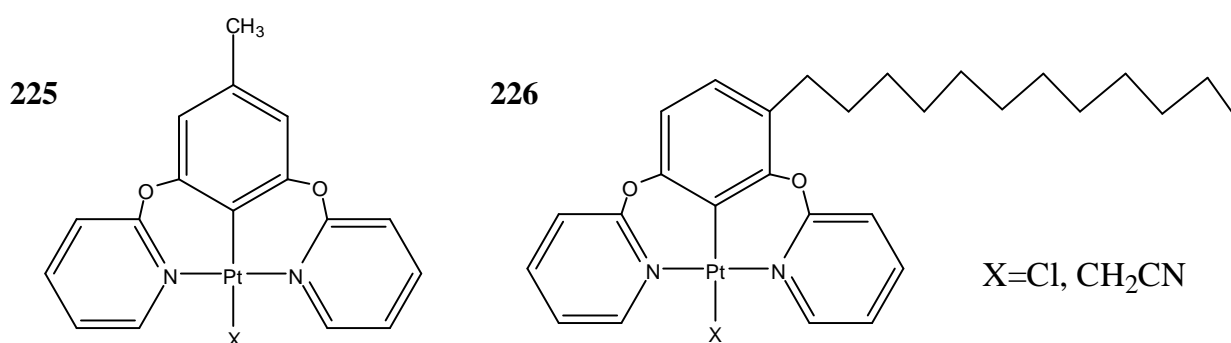


Figure 2.12: NaOAc assisted C-H bond activation and subsequent cyclometallation.<sup>2</sup>

Much of the basic organometallic chemistry of the *s*- and *p*-block metals was understood by the early part of the twentieth century, but that of the *d*- and *f*-blocks has only been developed more recently. Early methods of transition metal organometallic synthesis used thermal C-H activation to generate the metal-carbon bond. This involved using high temperature boiling point solvents (and more recently, solid state heating) to induce the C-H bond activation for subsequent binding to the metal centre.<sup>34,35</sup>

But it was soon discovered that thermolysis and low yields restricted the use of this method. Insolubility in high boiling point solvents such as toluene was also cited by Crespo *et al* as another possible reason for failure. However, in time, reagent assisted cyclometallation began to emerge as a creditable alternative to achieve metal-carbon bond formation, such as that displayed in **Figure 2.12**. This involves NaOAc acting as a nucleophile towards the metal centre followed by loss of one of the coordinated X ligands (where X = Cl, I, Br etc.). An intermediate of the type **223** shown in **Figure 2.12**, has been previously reported by Crespo *et al*.<sup>36–38</sup>

It has been well reported in the literature that C-H bonds are very strong and generally quite difficult to cleave, whether heterolytically or homolytically. Transition metal complexes on the other hand offer not only C-H bond activation, but also chemo- and regioselectivity for catalytic purposes by tweaking the properties of the complex through choice of metal and ligand design (as discussed in **Section 2.1**). Second and third row transition metals in particular offer relatively strong metal-carbon bonds. Pt (II) complexes have been reported to form the strongest metal-hydrogen bonds known as well as some of the strongest metal-carbon bonds for analogous systems.<sup>39,40</sup>



*Figure 2.13: Cyclometallated pincer-type N,N,C platinum complexes where C-H activation was achieved by thermal means.*<sup>41</sup>

Direct thermal C-H bond activation, though, remains the most desired approach to synthesising cyclometallates since it requires the least amount of substrates and synthetic steps to form the desired product i.e. C-H activation without the use of NaOAc in **Figure 2.12**. Limited success has been achieved within this area with various methods employed to achieve the desired result. Ka-Wen Chiu *et al* have achieved direct cyclometallation of “pincer”-type N,N,C Pt (II) chloride complexes interestingly using acetic acid as the solvent medium. Square planar geometry, as expected, was achieved for the complexes as identified by x-ray crystallographic studies. **Figure 2.13**.<sup>41</sup>

N,N,C platinum cyclometallates have also been studied by Vila *et al*, again synthesised by direct thermal cyclometallation but in this instance with toluene as the solvent, **227**, **Figure 2.14**. They also reported bi-metallic complexes (**228**, **Figure 2.14**) with each metal centre coordinated in a N,N,C type coordination, also achieved via thermal cyclometallation.<sup>42</sup>

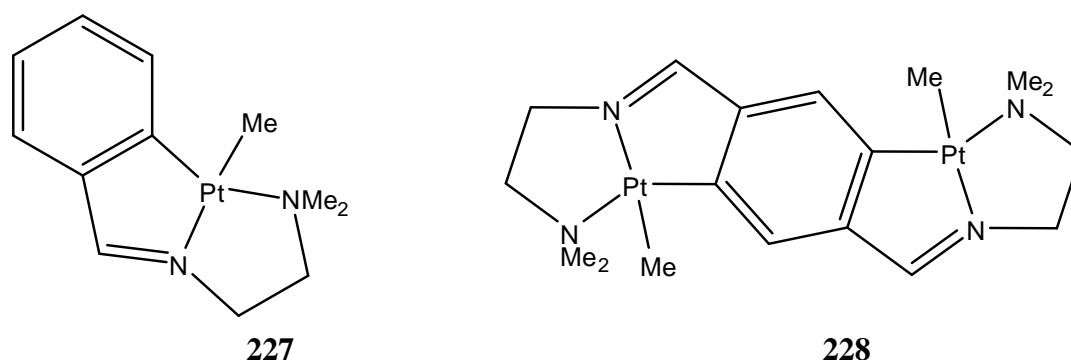


**Figure 2.14:** Cyclometallated Schiff-Base N,N,C type platinum complexes where C-H activation was achieved by thermal means using high boiling point solvents.<sup>42</sup>

The importance of solvent choice has been shown by Crespo *et al*, where they have discovered a protic solvent such as methanol assists cyclometallation. Although this method works well, it still requires the use of an external coordinating base such as NaOAc and a two step reaction mechanism. The role of solvent is highlighted further by Wong-Foy *et al* where they have proposed the inclusion of a solvent molecule in the C-H bond activation mechanism for the formation of cyclometallated complexes **Figure 2.15**.<sup>43,44</sup>

Wong-Foy *et al* have proposed two pathways for the cyclometallation described in **Figure 2.15**, either direct displacement or by a solvent-assisted pathway to give intermediate A. From intermediate A, the actual breaking of the C-H bond can proceed via an oxidative addition mechanism (Path I) to generate a Pt (IV) hydride which can then be deprotonated by a base in solution, or alternatively via direct deprotonation of the agostic complex (Path II).

The evidence they propose supports the formation of Pt(IV) hydrides as important intermediates in C-H bond activation and subsequent cyclometallation.<sup>44</sup>

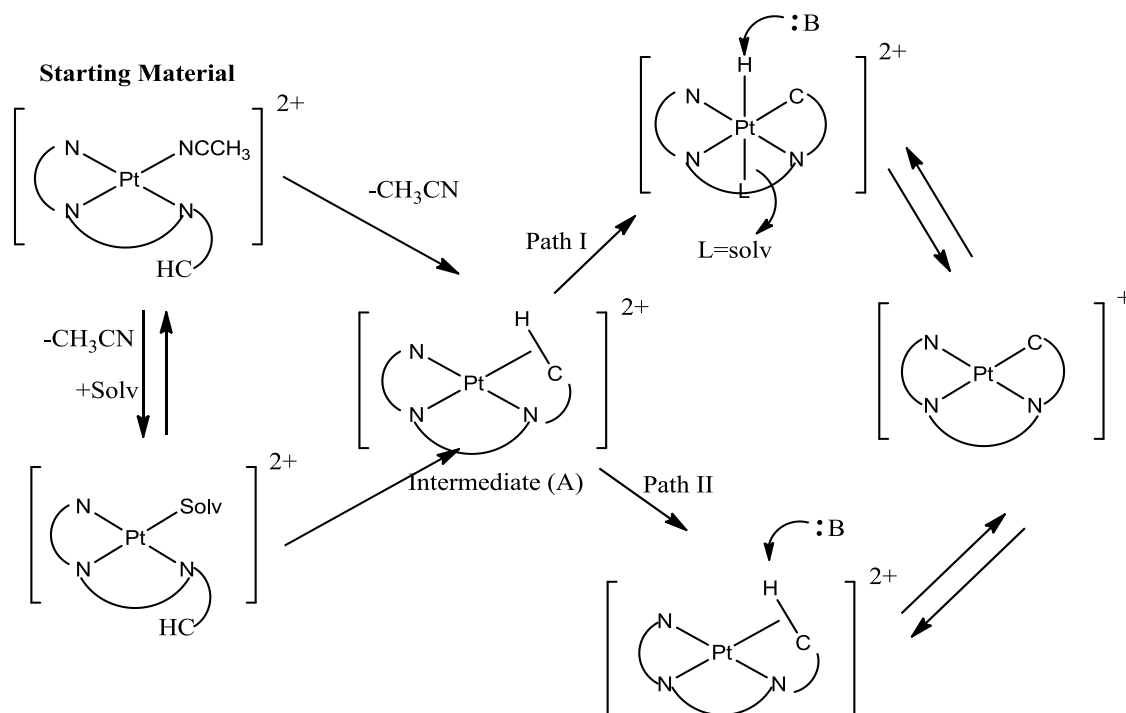


**Figure 2.15:** Solvent assisted cyclometallation of a tridentate  $N,N,N$  type platinum complex, where no external base was used (the reverse arrows are removed for clarity).<sup>44</sup>

Direct one-step cyclometallation of palladium complexes with no solvent or base assistance has been reported and discussed further in **Section 2.5.3**. The ability of the methoxy group to be ortho, para directing and delocalise its unshared electron pairs is crucial in stabilising the proposed arenium ion intermediate. NaOAc is not required for this palladium cyclometallation reaction but increased yields can be achieved using NaOAc in methanol. This type of C-H bond activation will be explored further in this current research using analogous chloro platinum complexes.<sup>45</sup>

Recently Crespo *et al* have also reported successful direct C-H bond activation (and subsequent cyclometallation) of platinum based bulky di-imine complexes. They report that compound **230**, **Figure 2.16** is very stable, but when refluxed in a high boiling point solvent (toluene) for about one hour, metallation of one of the anthryl substituents was achieved with loss of a single methane molecule (**231**, **Figure 2.16**). When the reaction time was increased to four hours, formation of compound **232**, **Figure 2.16** was also reported, in which both anthryl groups were metallated.<sup>10</sup>

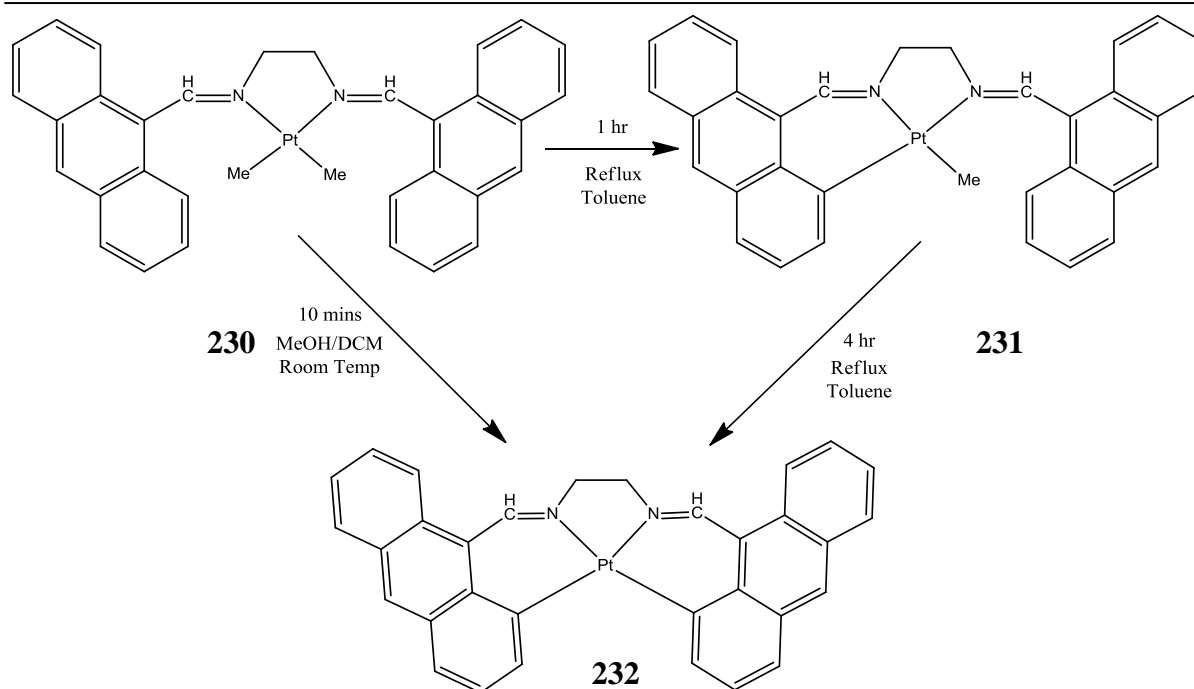


**Figure 2.16:** Direct cyclometallation of a bulky platinum diimine complex **230** using a variety of methods to form complex **231** and **232**.<sup>10</sup>

Double metallation of compound **230**, **Figure 2.16** was also achieved, unexpectedly, using acetyl chloride in a dichloromethane-methanol solution. The purpose of this reaction originally was to study the protonation of the compound using acetyl chloride as a source of anhydrous HCl. Crespo *et al* however found that it led to a good yield of **232**, **Figure 2.16** after ten minutes at room temperature. They propose that the acetyl chloride may be replacing the methyl groups on the platinum metal centre with chloride ligands, making it easier for metallation of the anthryl groups. Further work using a chloride analogue of **230**, **Figure 2.16**, displayed as **233**, **Figure 2.17**, resulted in metallation occurring at room temperature in dichloromethane.<sup>10</sup>

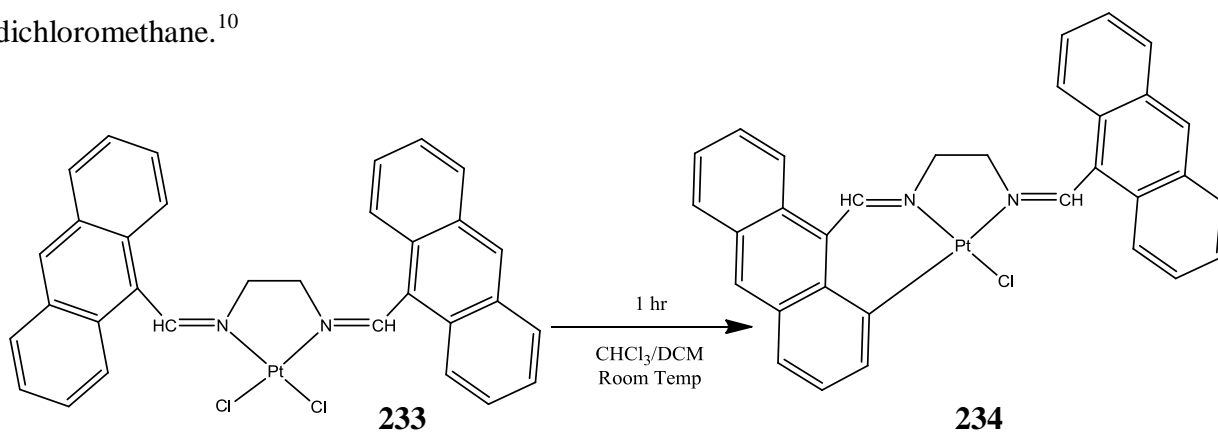


**Figure 2.17:** Direct cyclometallation of a platinum chloride diimine complex at room temperature in dichloromethane or chloroform.<sup>10</sup>

Crespo *et al* found that when compound **233**, **Figure 2.17** was left in dichloromethane or in deuterated chloroform for a few hours, a new compound, **234**, **Figure 2.17**, was formed. After 24 hours the major product was compound **234**, **Figure 2.17** where the release of HCl was noted from the reaction solution. Interestingly though, attempts to achieve complete transformation of compound **234** into the doubly metalated compound **232**, **Figure 2.16** using a variety of solvents and external reagents such as toluene and sodium acetate, proved to be unsuccessful.<sup>10</sup>

Crespo *et al* also report that the cyclometallation reaction is quite fast in chlorinated solvents, particularly for the chloride complexes, and view Z to E isomerisation as the cause for preventing conversion to compound **232**, **Figure 2.16**.<sup>10</sup>

Further work by Mamtora *et al* into the stabilisation of the liberated chloride ion by solvents, has reported that this may assist coordination of the platinum metal centre to the carbon of an aryl ring. In contrast to other solvents such as toluene, methanol or acetic acid previously reported by Crespo *et al* and Ka-Wen Chiu *et al*, Mamtora *et al* specifically cite the use of chlorinated solvents as having the ability to stabilise the liberated chloride ion via a hydrogen bond type of interaction. Chloroform in particular can allow direct cyclometallation without the use of NaOAc or other external reagents due to its stabilising effects.<sup>46</sup>

They propose that this stabilisation of the liberated chloride ion lowers the activation energy and hence increases the rate of reaction for a one step concerted cyclometallated mechanism. They therefore propose that the loss of the chloride is the rate determining step for the reaction. The stabilisation of chloride ions and solvent interactions into cyclometallation will be discussed further in **Section 2.2.4**.<sup>43,44,41</sup>

### **2.3.3 Cyclometallated Complexes:**

Cyclometallated complexes represent an important class of metal based compounds and are widely encountered in modern organometallic and coordination chemistry. Various examples of C-H activated ( $sp^2$  and  $sp^3$ ) achiral<sup>47</sup> or chiral<sup>48</sup> metal complexes have been reported and find numerous applications ranging from organic transformations, directed self-assembly, catalysis, chemical sensing and more recently as luminescent materials.<sup>49,50</sup>

The most common form of cyclometallation is “*ortho-metallation*”. This is an oxidative addition in which the *ortho* position of an aromatic ring becomes attached to the

metal (**235**, **Figure 2.18**). The other type of cyclometallation occurs by the process of reductive elimination, shown as **236** in **Figure 2.18**.<sup>51</sup>

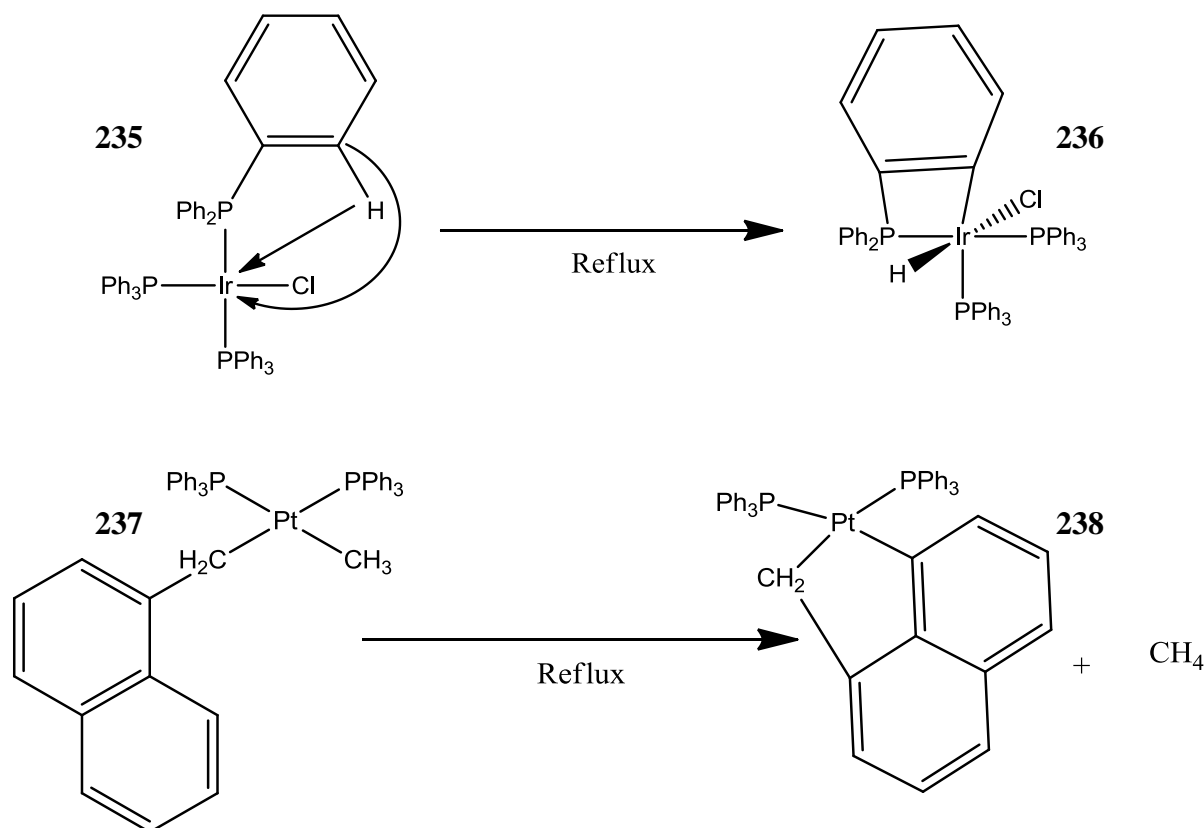


**Figure 2.18:** Cyclometallation reactions by oxidative addition **235** and by reductive elimination **237**, which is the opposite of an oxidative addition.<sup>51</sup>

Initial coordination of a metal to donor moieties, such as phosphorus or nitrogen as previously discussed in **Section 2.2**, stabilises the metal centre to allow C-H bond activation on the aryl ring of the ligand and hence cyclometallation of the complex with the formation of a metal-carbon bond as seen in **237**, **Figure 2.18**.<sup>37</sup>

Following on from previous work with cyclopalladation reactions, Crespo *et al* have completed further study on cycloplatinated species using N-benzylidenebenzylamines and the platinum substrate  $[\text{Pt}_2\text{Me}_4(\mu\text{-SMe}_2)_2]$ . The study identifies a possible nucleophilic behaviour in the platinum substrates not identified in the palladium complexes. In the palladium analogues the reaction occurs solely as an intramolecular electrophilic attack of the Pd at the carbon atom. However it has been proposed that the platinum centre possesses the ability to attack carbon as an electrophile or as a nucleophile. C-H bond activation allows intramolecular oxidative addition to take place, hence generating the cyclometallate.<sup>37,52</sup>

Another specific feature of these reactions identified by Crespo *et al* is that substituents bound to the carbon adjacent to the metallation position (i.e. the alpha position)



hinder the reaction. It was found that the reactivity of the carbon centre depends on the specific substituents attached to the alpha position for example chloride or methyl groups. One particular example of this interaction is shown in **Figure 2.19**.<sup>37</sup>

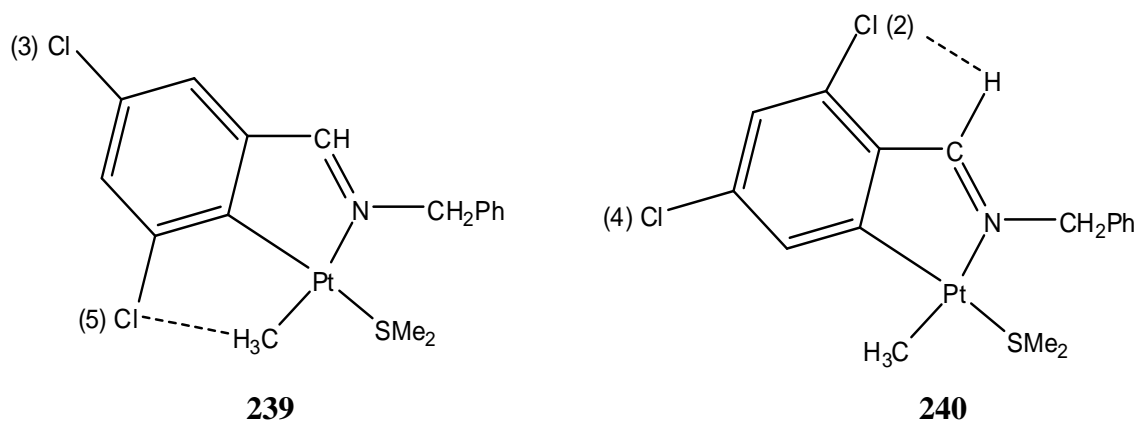


**Figure 2.19:** Example of an interaction within a molecule between a  $\text{CH}_3$  group and a Cl group, complex **239** and a H to a Cl group in complex **240**.<sup>37</sup>

In the case of compound **239**, cyclometallation was achieved due to the electron withdrawing ability of the chloride centre at the 5 position and its interaction with the methyl group coordinated to the metal centre, confirmed by  $^1\text{H}$  NMR studies. In compound **240**, the hydrogen interaction with the chloride on the aryl ring also influenced the cyclometallation outcome. NMR studies of compound **240** showed that the imine resonance was shifted slightly downfield in comparison to other analogous complexes. It was concluded that this was due to the interaction between the imine proton and the chloride centre at the 2 position in **240**. The effect of substituents on a ligand towards cyclometallation and C-H bond activation will be discussed further in **Section 2.2.5**.<sup>37</sup>

As mentioned previously, nitrogen donor groups on the ligand also play an important role as they enhance the nucleophilic nature of the platinum metal centre. Crespo *et al* have performed much of their studies on Pt (II) **241** and Pt (IV) **242** N,N,C type complexes, like those in **Figure 2.20**.<sup>52</sup>

In the cyclic voltammetry tests performed by Crespo *et al* some interesting properties about the reductive effects of the Pt (IV) aromatic complexes **242** were identified. It was confirmed that the reduction of Pt (IV) complexes is mainly centred on the aromatic ring system, like that present in **Figure 2.20**. From this evidence it was documented that one of the driving forces for the formation of a Pt (II) metallacycle involves the filled d-orbitals and the fused *endo* metallacycle with the aryl ring.<sup>52</sup>

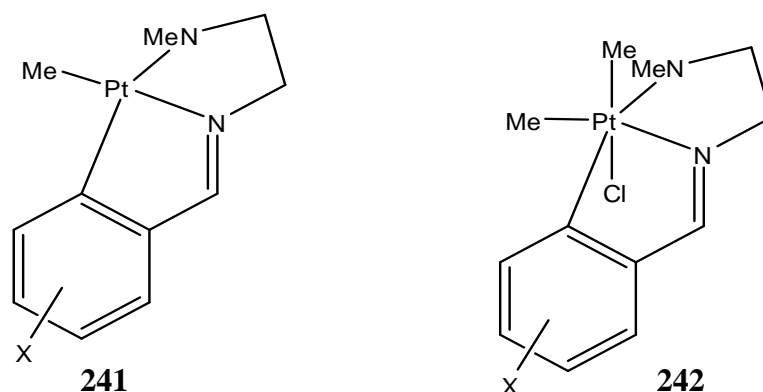


**Figure 2.20:** Example of two *N, N, C* cyclometallated platinum complexes studied by Crespo *et al*, a Pt (II) type **241** and a Pt (IV) type **242**.<sup>52</sup>

It was seen that during the cyclometallation of the Pt (II) complex **241**, **Figure 2.20**, not only does it lead to the formation of a Pt-C<sub>aryl</sub> bond, but it also leads to an extension of the  $\pi$  system to form a “platina-isoindole” system. This is proposed to be a major contributor to the stabilisation of the extra electron obtained from the electric current during the voltammetry experiment carried out by Crespo *et al*.<sup>52</sup>

The majority of platinum cyclometallates reported to date are from nitrogen based ligands, imines in particular. Phosphorus based compounds on the other hand such as tertiary phosphines, phosphinites, phosphites, iminophosphoranes and PCP-pincer ligands have not been as widely studied for their C-H activation processes, with only a few exceptions as seen in **Figure 2.21**.

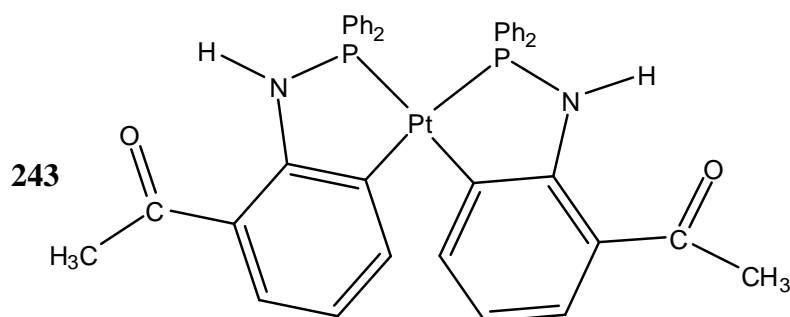


**Figure 2.21:** A doubly cyclometallated (phosphino)amine platinum complex with five membered metallacycles.<sup>53</sup>

It has been well reported however by Gaw *et al* and others that a general feature of phosphinoamine chemistry is the air/moisture sensitivity of these ligands due to the reactive nature of the heterolytic P-N bond.<sup>54,55</sup> However, phosphinoamines have been shown to undergo thermally induced orthometallation at Pt (II) and Rh (III) metal centres giving rare

examples of thermally stable metal-P-N-C<sub>arene</sub>-C<sub>arene</sub> five-membered metallacycles, **243**, **Figure 2.21**.<sup>53</sup>

Very recently successful thermal cyclometallation was also achieved for another phosphinoamine type ligand, again *trans* to a phosphine moiety, using a protic solvent (methanol) for the reaction at room temperature, **Figure 2.22**. For this complex a rare thermally stable metal-P-N-C<sub>arene</sub>-C<sub>arene</sub> five-membered metallacycle is also formed.<sup>54</sup>

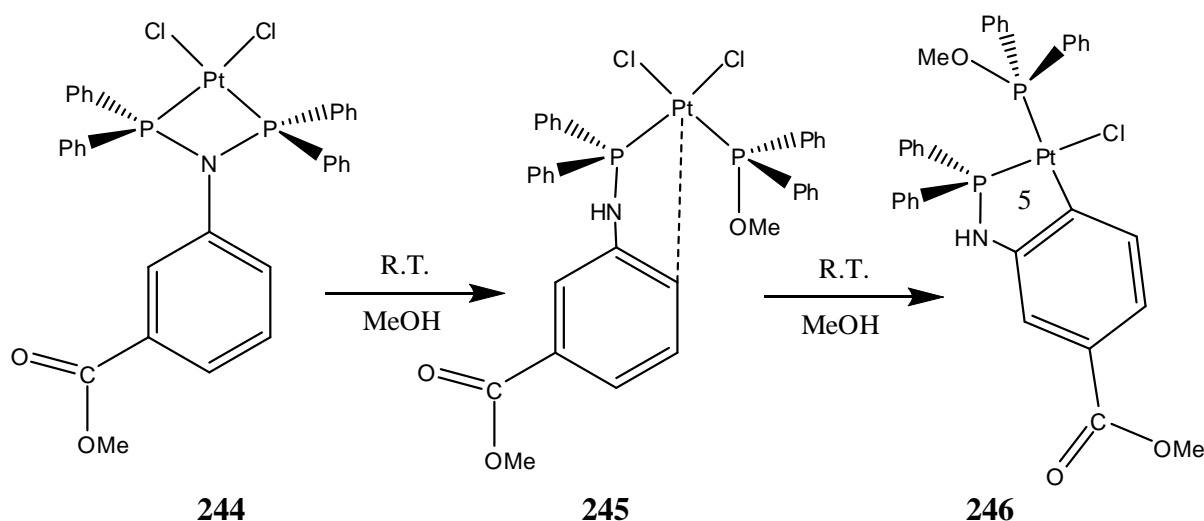


*Figure 2.22: Cyclometallation of a (Phosphino)amine complex in a protic solvent at room temperature, with C-H activation *para* to an electron donating group.*<sup>54</sup>

Interestingly, the C-H activation for this complex is also *para* to an electron-donating substituent on the aryl ring (-H and -COOMe). The influence of electron donating and electron withdrawing substituents on C-H activation will be discussed further in **Section 2.3.5**.

### 2.3.4 Stabilisation of Liberated Chloride Anions:

To understand how stabilisation of the chloride ion can assist in facilitating cyclometallation, we must first look at hydrogen bonding interactions of the free chloride anion and how different solvents influence the overall reaction. Recently, in a comparison of solvents by López *et al* and Narayan Biswas *et al* for platinum and palladium cyclometallation reactions, the polarity and nature of the solvent was cited as playing a key role in the stabilisation of C-H activation and subsequent cyclometallation reactions.<sup>56,57</sup>

Pedzisa and Hay have recently completed extensive studies using electronic structure calculations, MP2/aug-cc-pVDZ, into energies of hydrogen bonds with chloride anions (C-H-

· · Cl) for a series of X-CH<sub>3</sub> donor groups and common organic solvents in which the electron-withdrawing ability of X is varied over a wide range of values **Figure 2.23**.<sup>58</sup>

Worth noting about this study is the difference between chloroform and methanol in binding energies (-19.6 vs -16.6 kcal/mol). Chloroform has a stronger affinity for the liberated chloride ion in comparison to methanol (a protic solvent), which has been used extensively to facilitate C-H bond activation by a variety of research groups.<sup>58</sup>

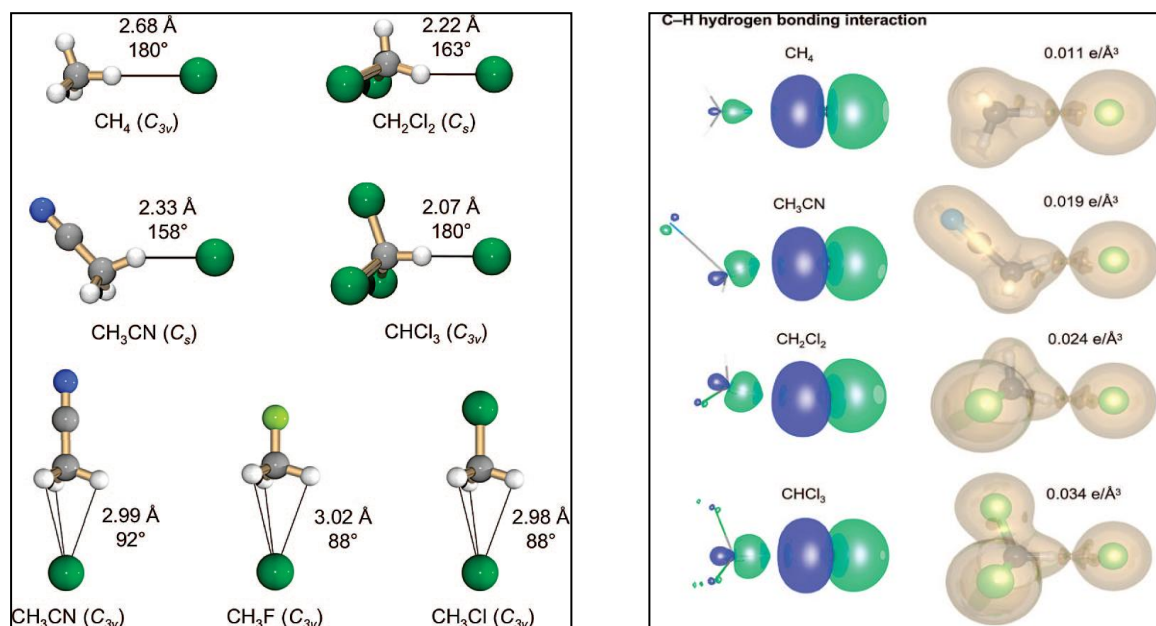


**Figure 2.23:** All stable geometries located, at the computational method MP2/aug-cc-pVDZ level of theory, for Cl<sup>-</sup> interactions to common organic solvents. Note chloroform CHCl<sub>3</sub> has the shortest bond length with the chloride anion at 2.07 Å.<sup>58</sup>

The three chlorides in the chloroform molecule cause an electron withdrawing effect leaving a δ-positive charge on the hydrogen of the solvent molecule. This results in a stronger hydrogen bond with the free chloride anion, than that of any other solvent listed above, even the O-H donor solvents such as methanol. Chloroform is therefore ideal for stabilising the liberated chloride ion from a platinum cyclometallation reaction.

The results obtained by Pedizsa and Hay are supported by a study conducted by Kryacho *et al* where chloroform was also found to have the strongest interaction with free chloride ions. **Figure 2.24** shows anion binding abilities of chloroform in comparison to other solvents.<sup>59</sup>

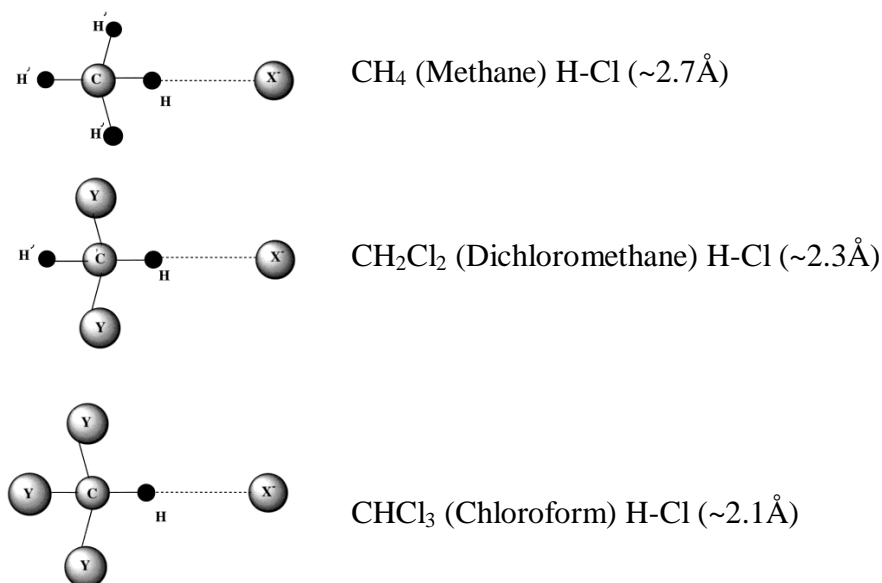


*Figure 2.24: Comparison of withdrawing groups on different solvents and their influence on anion binding.<sup>59</sup>*

Work by Mamtora *et al* has shown rapid oxidations and C-H activation at low temperatures for Pt (II) complexes in chlorinated solvents (chloroform in particular) as discussed previously in **Section 2.3.2**. Reaction of compound **247**, **Figure 2.25** with PhICl<sub>2</sub> in chloroform gives a clean and rapid conversion to the Pt (IV) species **248** through a C-H activation and oxidation with the addition of a chloride ligand. Further details on oxidation reactions and Pt (IV) complexes will be discussed in **Chapter 3**.<sup>46</sup>

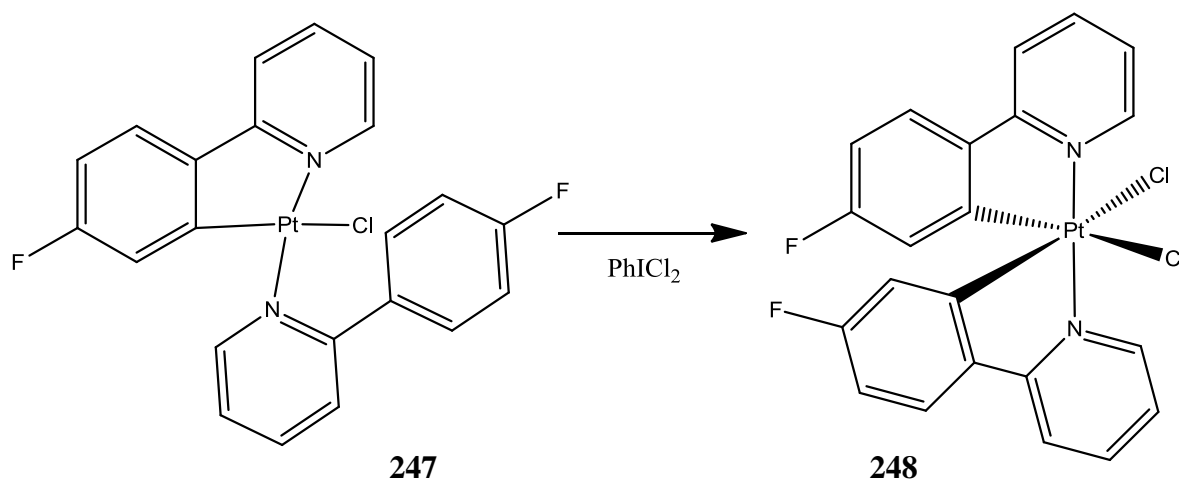


*Figure 2.25: Oxidation and C-H activation at low temperatures for a nitrogen based heterocyclic complex in chloroform.<sup>46</sup>*

During the oxidation of compound **245**, **Figure 2.25**, C-H activation was also observed to form a cyclometallated Pt (IV) complex **248**. The oxidation reactions in chloroform were complete in 5 mins, whereas comparable reactions in acetone did not go to

completion, even after an hour and increased temperature. Interestingly, in the oxidation of a second complex, compound **249**, **Figure 2.26**, the researchers also got an isomeric by-product (**250**, **Figure 2.26**) when the reaction was completed in acetone. However, only one product (compound **251**, **Figure 2.26**) is observed when compound **249** is reacted under the same conditions in chloroform.<sup>46</sup>

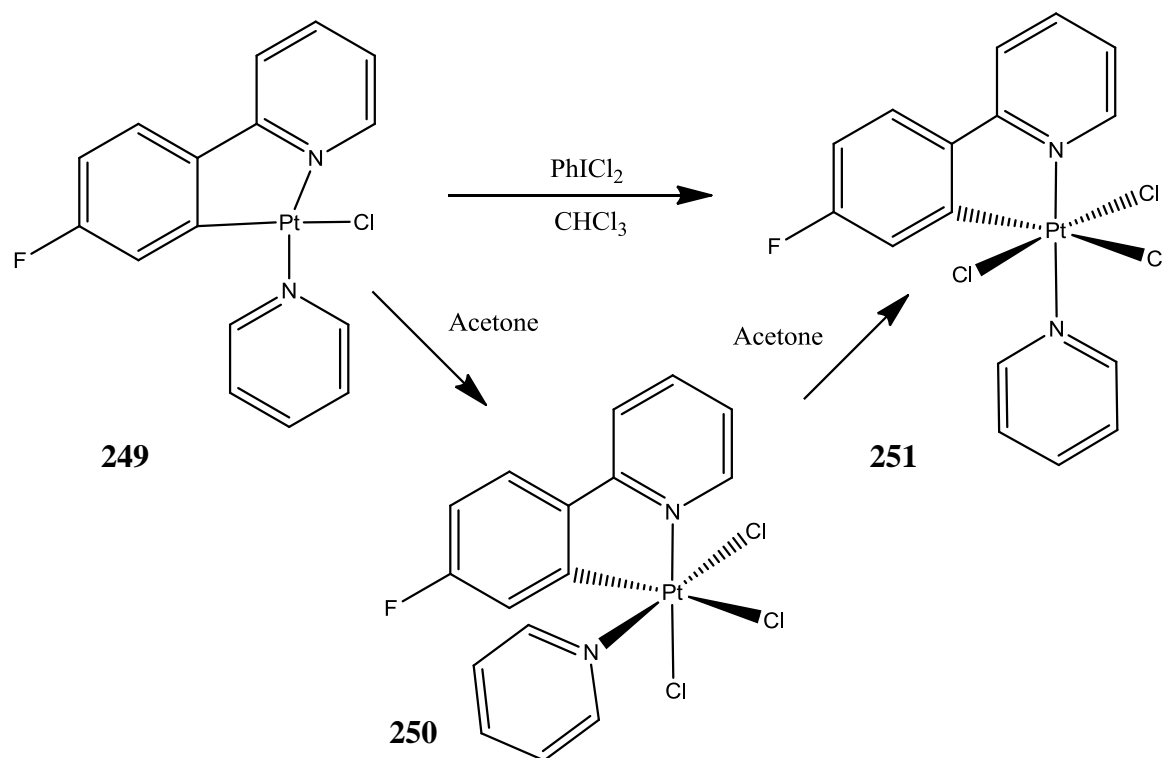


**Figure 2.26:** Oxidation of a nitrogen based heterocyclic complex in chloroform and acetone. A secondary by-product was formed in acetone, but not chloroform.<sup>46</sup>

Based on previous work by Kryacho *et al* and Slater *et al* they report that chloroform's ability to solubilise chloride anions through hydrogen bonding would allow the liberated chloride from PhICl<sub>2</sub> to move more freely in solution. Therefore only the thermodynamic product **251** is formed when chloroform is used as a solvent. This hydrogen-bonding type of stabilisation of the chloride ion is also used to explain the more rapid reaction in chloroform compared to acetone for these complexes.<sup>46,59,60</sup>

It is also worth noting that they suggest an S<sub>N</sub>2 type attack on the PhICl<sub>3</sub>, giving a five-coordinate cationic intermediate during the oxidation reaction. This intermediate would exist as a tight ion-pair in acetone, resulting in two products formed.<sup>46</sup> The hydrogen bonding interactions between a chloroform molecule and the chlorides on the platinum metal centre of compound **251** are shown in **Figure 2.27**.

251

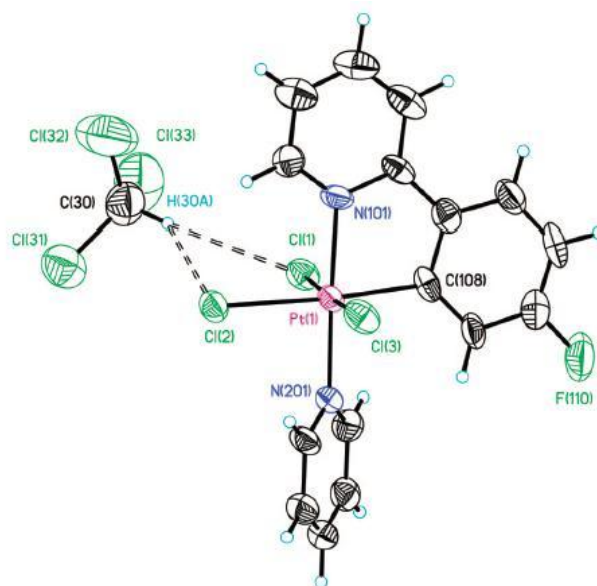


*Figure 2.27: H-bonding interactions between the chloroform solvate and the platinum chlorides in the X-ray crystal structure of 251, Figure 2.25.<sup>46</sup>*

### 2.3.5 Influence of the Ligand Substituents on Cyclometallation:

As previously mentioned, P,N-Donor bidentate ligands are among the most used hemilabile ligands in coordination and organometallic chemistry. In general, the rigid and short-bite P,N-ligands coordinate to metal atoms in the bridging mode, whereas a non-rigid ligand can easily form a five- or six-membered chelate ring as previously seen within this research group and others.<sup>61,2,45</sup>

The ligand substituents at or near the cyclometallation site (or C-H activation site) can also influence the outcome of the reaction, as seen in **Figure 2.22** earlier. These substituent effects have been studied by a variety of research groups, including ours. As discussed earlier in **Section 2.2.4**, the presence of an aromatic ring at the C-H activation position allows for resonance delocalisation, stabilising the possible arenium ion intermediate via electron donation from the substituent *para* to the activation position.<sup>61</sup>

As previously seen, Vila *et al* and Crespo *et al* have both used methoxy and methyl-substituted aryl groups in tridentate and tetradentate type ligands to form cyclometallated complexes using high boiling point solvents such as toluene. It was found that C<sub>aryl</sub>-H bond activation was achievable under relatively mild conditions for C-3 methyl and methoxy group substituted rings, **Figure 2.28**.<sup>42,62</sup>

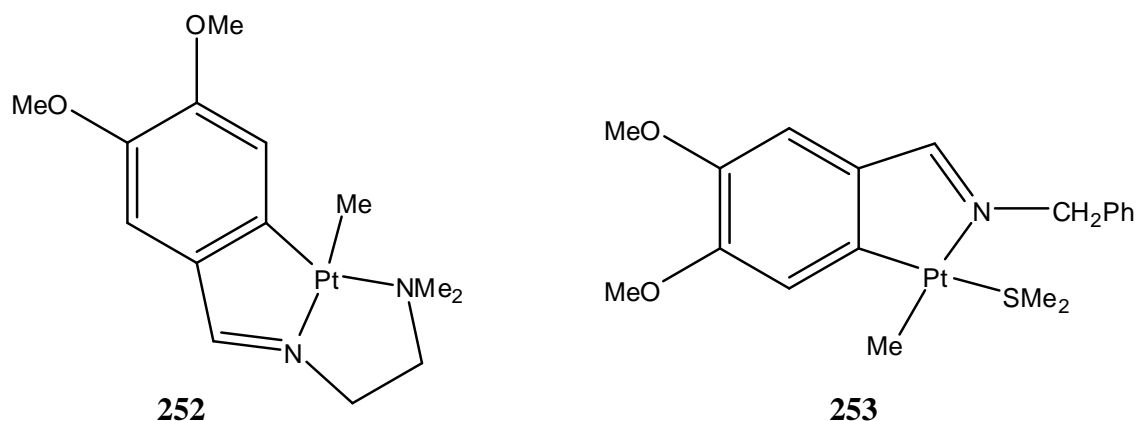


**Figure 2.28:** Examples of cyclometallated aryl substituted platinum complexes. **252** is a C, N, N type complex<sup>42</sup> and **253** is a benzylidenebenzylamine type complex.<sup>37</sup>

The effect of electron withdrawing groups such as chlorides and bromides on the other hand can vary depending on their position on the aryl ring. Some reports suggest that the presence of chloro substituents adjacent to the activated *ortho* position does not affect the formation of cycloplatinates. On the other hand, other studies suggest that the presence of a chloro substituent adjacent to the site of cycloplatination does influence the ability, and hence regioselectivity, of cycloplatination.<sup>63,62</sup>

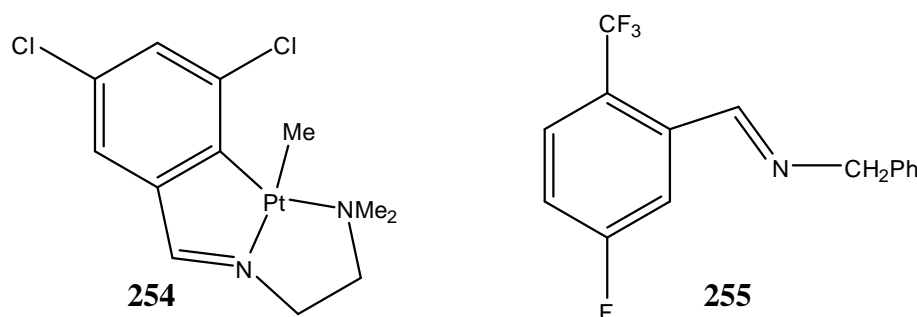


**Figure 2.29:** Examples of electron withdrawing aryl substituted compounds. Compound **254** is a C, N, N type complex cyclometallated under severe conditions<sup>42</sup> and **255** is a benzylidenebenzylamine type ligand that does not allow cyclometallation even under severe conditions.<sup>63</sup>

Compound **254**, **Figure 2.29** is formed after the reagents have been heated to reflux for 16 hours at reflux in toluene. This is in contrast to the reactivity of ligands with electron donating substituents like those shown in **Figure 2.28**, which can achieve cyclometallation under mild conditions at room temperature. Sometimes chloro substituents adjacent to the C-H bond to be activated can inhibit cyclometallation of the complex. Compound **255**, **Figure 2.29** on the other hand does not allow cyclometallation with platinum due to the unfavourable electronic effects present within the ligand.<sup>63,62</sup>



Heterocyclic ligands have also been shown to influence the formation of cyclometallated metal complexes. Work by Anderson *et al* has focused on complexes with multi ring systems and the behaviour of thienyl imines towards metal centres in particular. It was reported that C-H bond activation is achieved exclusively at the carbon alpha ( $\alpha$ ) to the sulphur moiety. It was also noted that after 15 minutes only the nitrogen coordinated complex existed (**257**, **Figure 2.30**) while further stirring at room temperature for 16 hours resulted in the formation of the cyclometallated product **258** without the need for heat or an external reagent.<sup>64</sup>

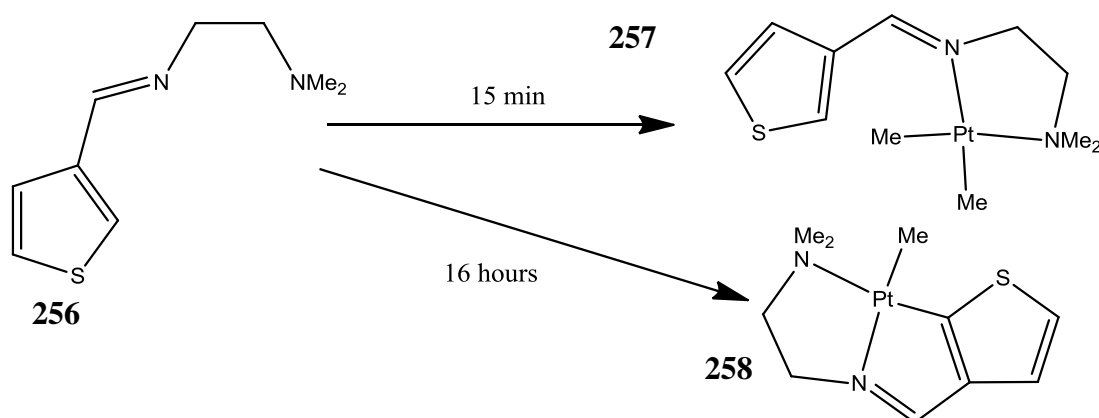


**Figure 2.30:** Direct cyclometallation of a thienyl imine **256**, is achieved by stirring at room temperature for 16 hours in acetone to form compound **258** from **257**.<sup>64</sup>

The proximity of the metal centre to the C-H bond to be activated is also an important consideration in terms of ligand design. Song *et al* have used tridentate P,N,C type ligands with a large P,N, bite angle for this purpose, **Figure 2.31**. The advantage of these type of ligands is their hemilability as discussed in **Section 2.1**. For Pd (II) and Pt (II) complexes the soft phosphorus moiety binds strongly to the metal centre followed by the harder (borderline) nitrogen donor moiety which binds more weakly to Pt (II) and Pd (II) metal centres. This sets up the metal centre into a bidentate chelating environment such as that seen for compound **260**, **Figure 2.31**. The proximity of a carbon near the metal centre then allows cyclometallation to subsequently occur.<sup>61</sup>

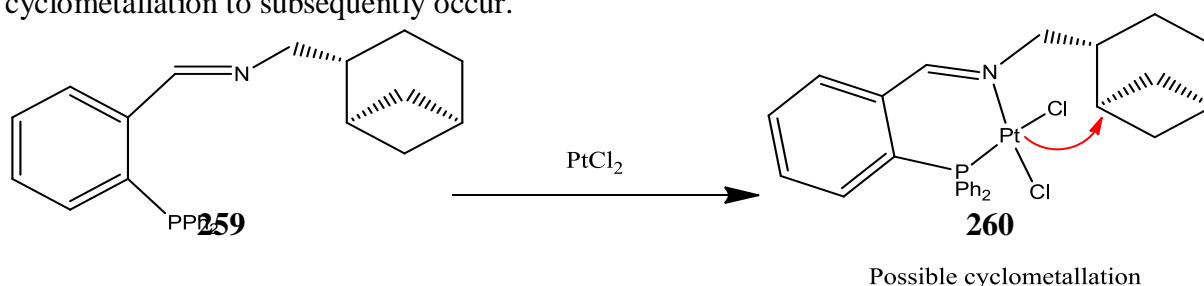


**Figure 2.31:** Example of a P,N ligand **259** and bidentate platinum compound **260**, with a C-H bond in close proximity for activation and subsequent cyclometallation.<sup>61</sup>

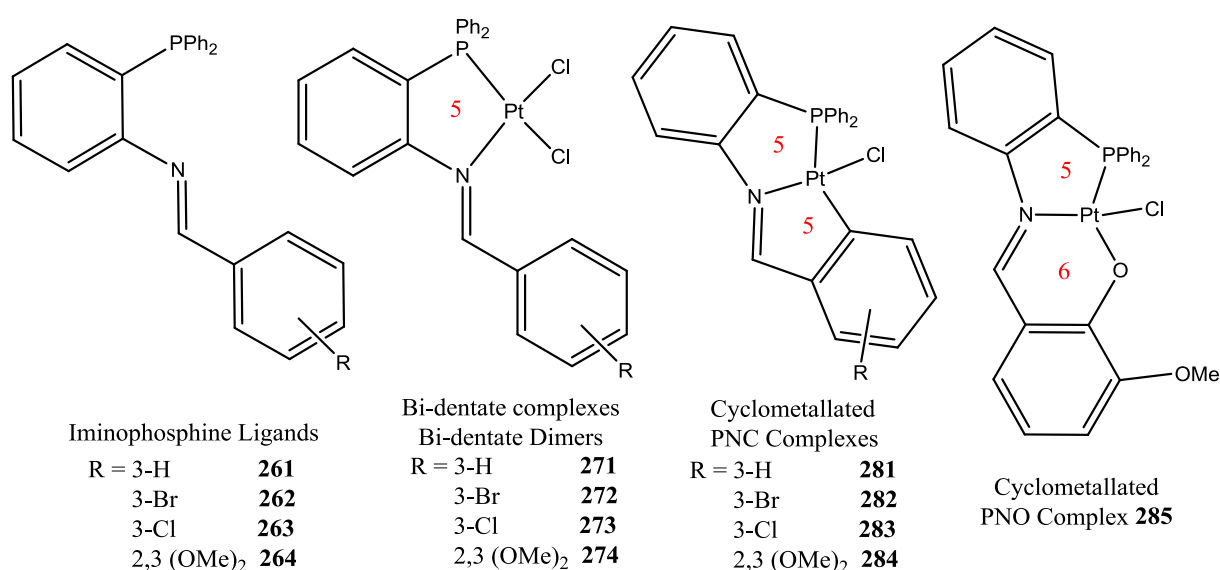
## 2.4 Conclusions:

In conclusion, it can be seen that the solvent used along with the nature of the coordinating ligand can influence whether or not the cycloplatinated species are formed. The location of the substituent can also facilitate activation of the desired C-H bond or the presence of a heterocyclic system can assist in achieving one-step cyclometallation under mild conditions.

In order to achieve one-step cyclometallation, the solvent used must not only facilitate C-H activation but also stabilise the liberated chloride anion. Chloroform is ideally suited to this task, rather than methanol which was previously used along with NaOAc by both this research group and others, thus it will be the solvent of choice for this current work.

Studies into the influence of electron donating substituents, like methyl and methoxy groups, will also be undertaken as well as the effects of electron withdrawing substituents. However, these factors alone will not ensure the successful synthesis of a cycloplatinated species. Other factors investigated will include the influence of the steric bulk of a ligand as well as the reaction conditions.

In contrast to the previously studied iodo platinum complexes, the smaller chloride ligands attached to the platinum metal centre should allow the halide to move closer to the metal and metal to be in closer proximity to the C-H bond to be activated. The thermodynamically stable side product which will be formed from the cyclometallation reaction, HCl, may also drive the reaction i.e. increasing entropy.



*For clarity: A summary of all the complexes and ligands discussed in the results and discussion section of this chapter.*



starting materials that may be present. After separation, the organic layer was then dried over  $\text{MgSO}_4$ , filtered and reduced to dryness *in vacuo*. The resulting oil was then crystallised from hot distilled methanol yielding the crystallised product. The physical appearances and yields of the ligands are shown in **Table 2.2**.

Attempts were made to synthesise other novel imine ligands using other aldehydes. Both 3-(diethoxymethyl)-benzaldehyde and 3-(4-methoxyphenoxy)-benzaldehyde were used with variations of previously reported methods, but only trace amounts of the desired imine were detected by NMR and IR characterisation possibly due to hydrolysis. It was therefore decided that they were not viable as ligands for further study in this project at this time.

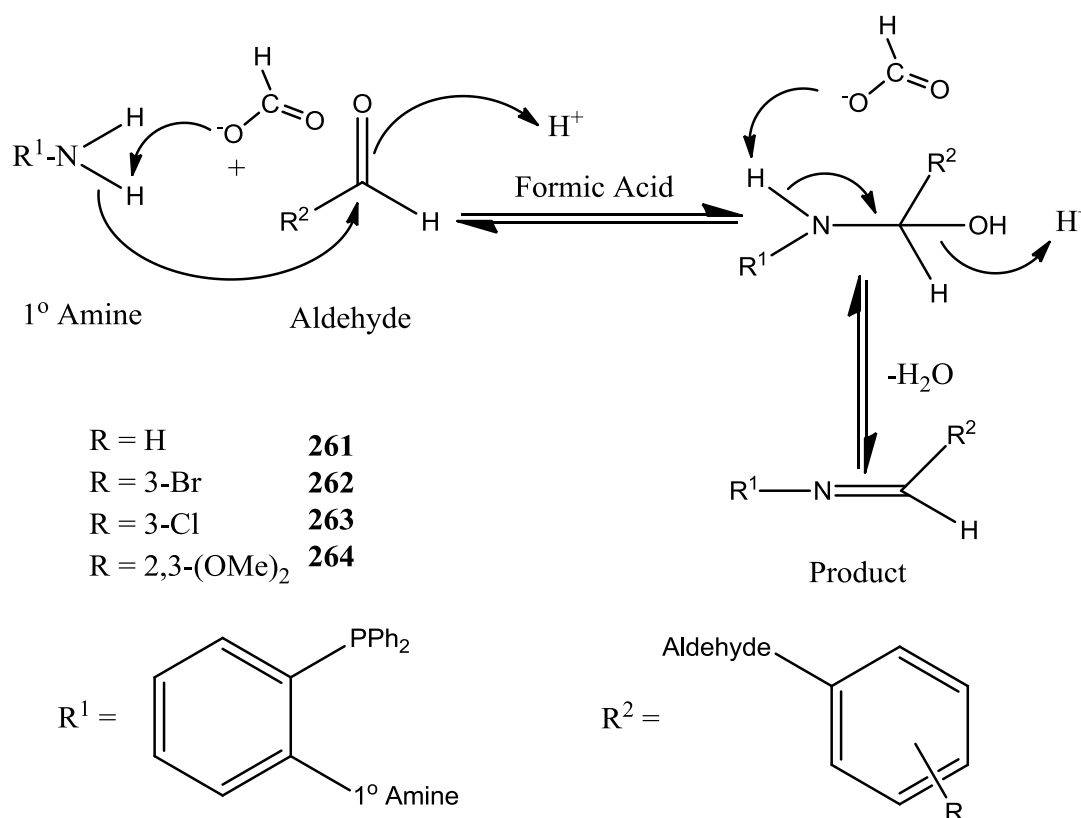


**Figure 2.33:** Acid catalysed formation of the imine functional group.<sup>67</sup>

Ligand	R	Physical appearance	Yield
HL <sup>1</sup> <b>261</b>	H	White powder	56%
HL <sup>2</sup> <b>262</b>	3-Br	Yellow needles	54%
HL <sup>3</sup> <b>263</b>	3-Cl	White needles	61%
HL <sup>4</sup> <b>264</b>	2,3-(OMe) <sub>2</sub>	Yellow powder	88%

**Table 2.2:** Physical appearances and yields for the successfully formed iminophosphine ligands **261**, **262**, **263** and **264**

### 2.5.2 Synthesis of the phosphinoamide ligands HL<sup>5-7</sup>

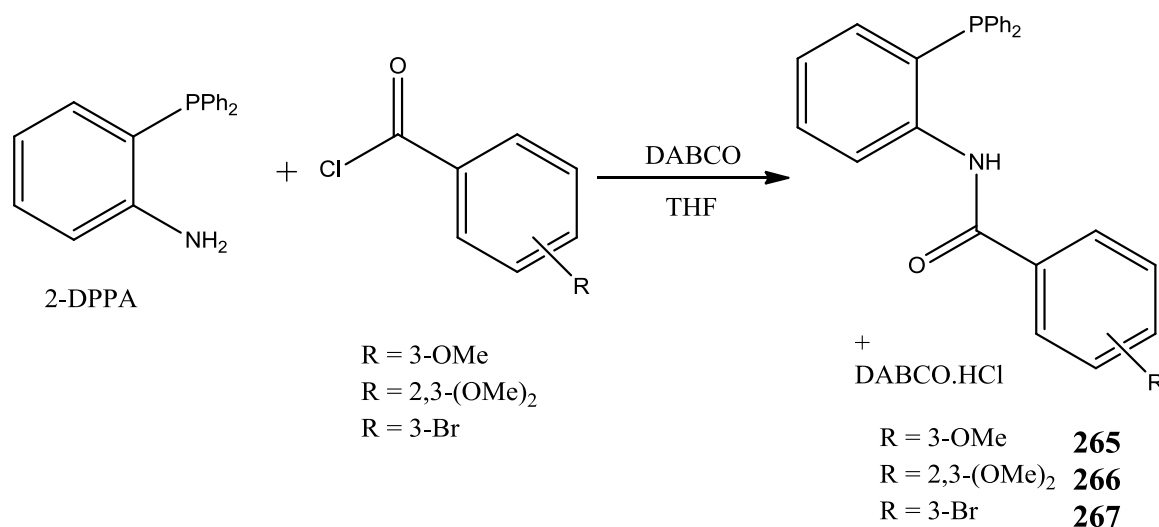


**Figure 2.34:** A condensation reaction based on a variation of previously reported methods to generate the phosphinoamide ligands with the loss of a HCl molecule as a salt.

As previously mentioned for the iminophosphine ligands in **Section 2.4.1**, the *o*-diphenylphosphinoaniline (2-DPPA) starting material was synthesised using a variation of a literature method.<sup>65</sup>

Synthesis of the phosphinoamide ligands HL<sup>5-7</sup> **265**, **266**, **267** was achieved by a variation of a previously reported method.<sup>29,68</sup> This involved the condensation of *o*-diphenylphosphinoaniline (2-DPPA) with one equivalent of the appropriate acyl chloride (3-OMe, 2,4-(OMe)<sub>2</sub>, 3-Br) in a minimum amount of THF, **Figure 2.35**. Two equivalents of DABCO (1,4-diazabicyclo[2.2.2]octane) were also added to the reaction mixture to neutralise the unwanted HCl formed during the reaction.

After stirring the mixture for 5 hours at room temperature, a white precipitate of DABCO.HCl was formed from the reaction of DABCO with the HCl formed. This was filtered to leave a light yellow solution which was then reduced to dryness *in vacuo* and the residue taken up in dichloromethane. The organic solution was then washed three times with distilled water to remove any traces of HCl or DABCO.HCl along with any remaining starting materials that may be present also.

After separation, the organic layer was dried over MgSO<sub>4</sub>, filtered and reduced to dryness *in vacuo*. The resulting oil was then crystallised from distilled dichloromethane-hexane yielding the crystallised product. The physical appearances and yields of the ligands are shown in **Table 2.3**.

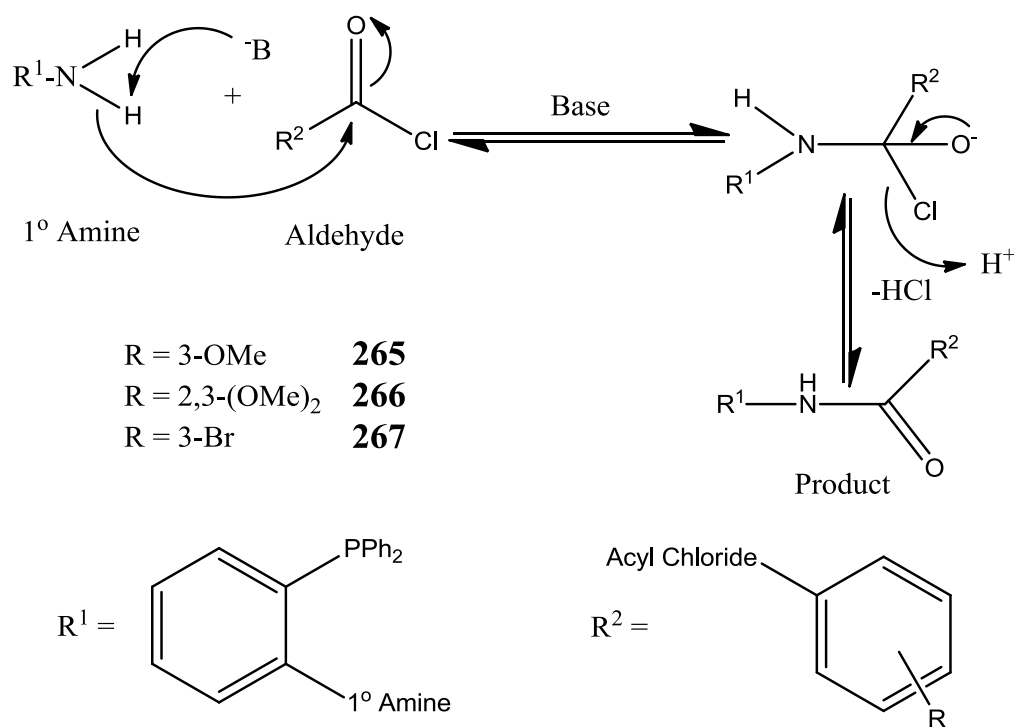


*Figure 2.35: The formation of the phosphinoamide ligands from a primary amine and an acyl chloride with the loss of a HCl molecule using an external base.*

Ligand	R	Physical appearance	Yield
HL <sup>5</sup> <b>265</b>	3-OMe	White powder	75%
HL <sup>6</sup> <b>266</b>	2,4-(OMe) <sub>2</sub>	White needles	61%
HL <sup>7</sup> <b>267</b>	3-Br	White needles	58%

*Table 2.3: Physical appearances and yields for the successfully formed phosphinoamide ligands 265, 266, and 267*

### 2.5.3 Synthesis of the bidentate iminophosphine complexes with the general formula [Pt( $\eta^3$ -PN-L<sup>1-3</sup>) Cl] 271-273 METHOD A:

As seen in **Section 2.2.5** the formation of cyclopalladated and cycloplatinated complexes is affected by substituents on the aryl ring of the ligand which contains the C-H bond to be activated. Previous work with iminophosphine ligands in our research group has found that one-step cyclopalladation did not occur when electron withdrawing substituents (such as chloride or bromide) were present in *meta* positions on the aryl ring (i.e. C2 and C4). Neither did it occur if the aryl ring was unsubstituted. In both cases, a  $\eta^2$ -P, N bidentate complex was formed rather than the  $\eta^3$ -P, N, C tridentate complex i.e. there was no C-H activation.<sup>45</sup>

In further work carried out by our research group into analogous iodo platinum iminophosphine complexes, similar results were seen to occur for both chloride and iodo based metal centres. Cycloplatination of the initially formed  $\eta^2$ -P, N bidentate iodo complexes was only achieved by using an external coordinating base, sodium acetate, in a protic solvent such as methanol in a variation of a method described by Crespo *et al.*<sup>37,2</sup>

However when an electron donating substituent such as a methoxy group was present in the C3 position on the aryl ring, both Lennon and Maguire identified that cyclometallated complexes were formed in a single step, regardless of solvent choice. The proposed mechanism of this cyclometallation involves resonance delocalisation, generating a highly reactive arenium ion intermediate, **Figure 2.36**. It was proposed that in order to generate this intermediate, an electron donating group must be present at the 3-position of the aryl ring. The arenium ion is then formed by resonance delocalisation at the C-6 position of the aryl ring as seen in **Figure 2.36**.<sup>2,45</sup>

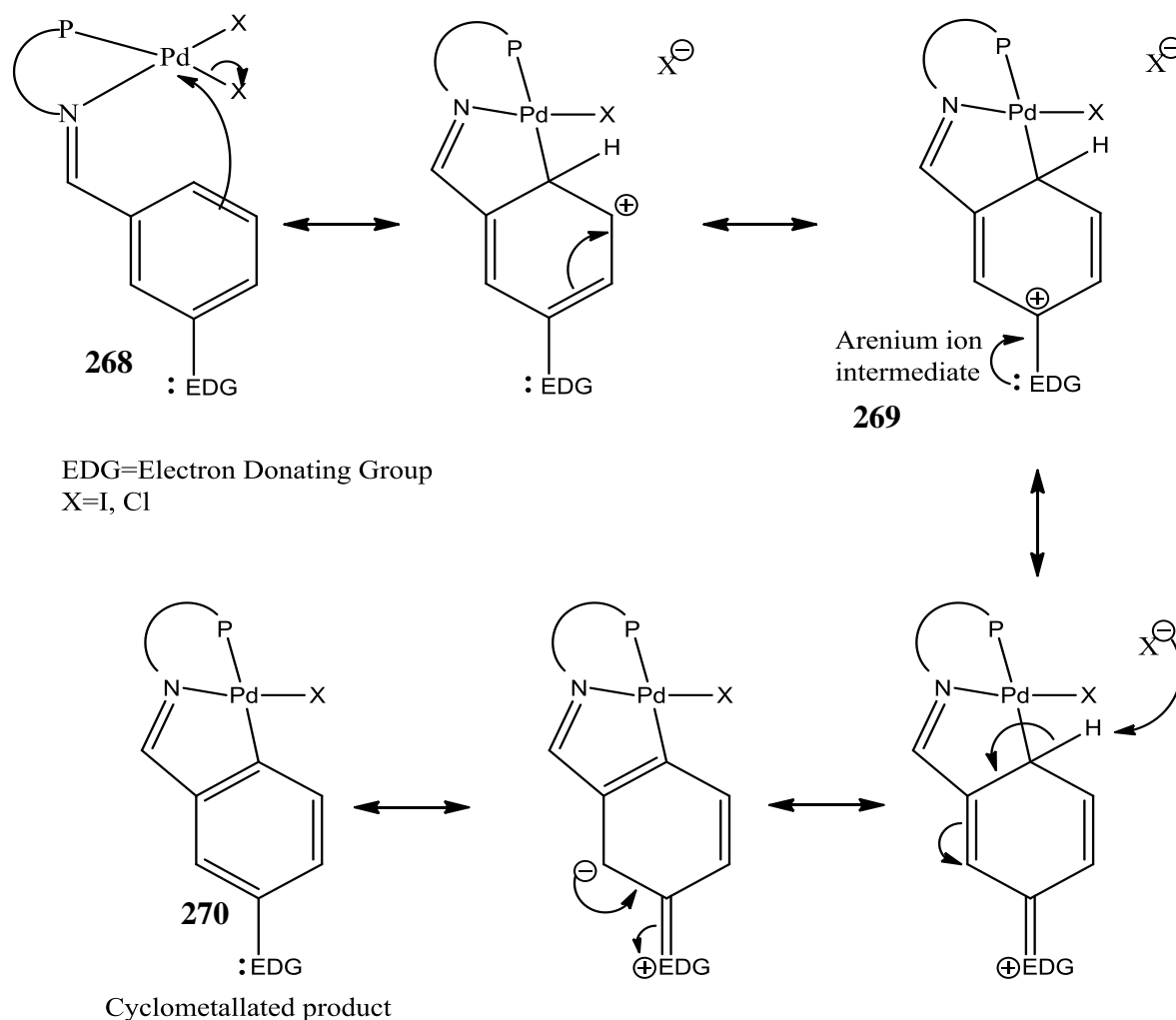


**Figure 2.36:** Mechanism of cyclometallation via generation of an arenium ion intermediate with the loss of a HCl molecule, proposed by Lennon.<sup>45</sup>

It is the intention of this section to investigate whether analogous chloro platinum complexes will produce similar results to iodo cycloplatinated complexes previously synthesised by our research group and whether direct cyclometallation is possible with electron withdrawing substituents on the aryl ring. To this end a slight excess of the appropriate iminophosphine ligand HL<sup>1-3</sup> **261**, **262** and **263** was reacted with one equivalent of platinum chloride [PtCl<sub>2</sub>], **Figure 2.37**.

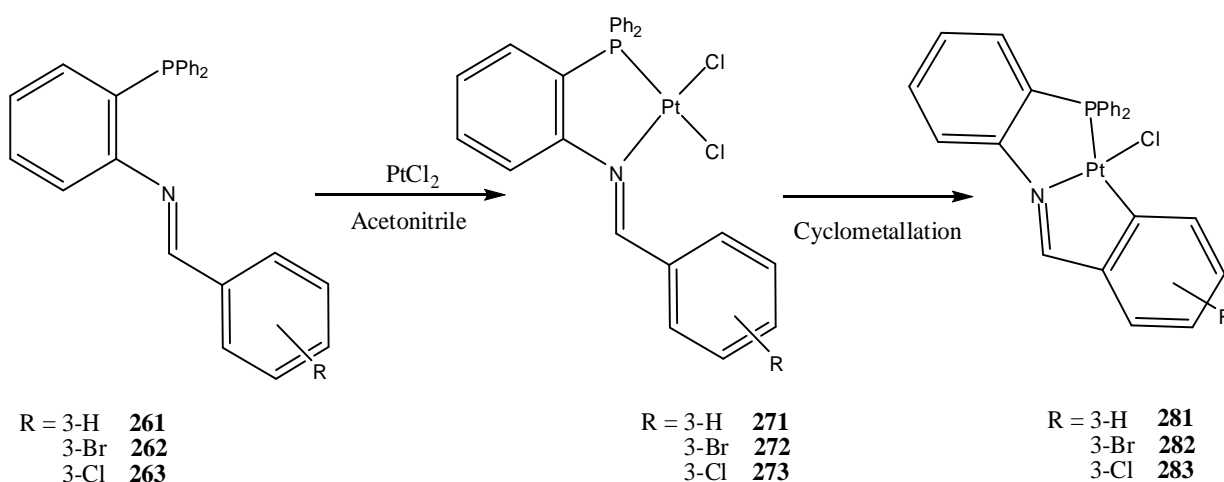


**Figure 2.37:** Reaction of PtCl<sub>2</sub> with the iminophosphine ligands HL<sup>1-3</sup> **261**, **262** and **263** using a variety of solvents including acetonitrile, dichloromethane, chloroform, methanol, tetrahydrofuran and toluene.

To a heated and stirred solution of PtCl<sub>2</sub> in acetonitrile a 1.1 equivalent of the appropriate ligand HL<sup>1-3</sup> **261**, **262** or **263** was added as a solid. Previously in our research group, acetonitrile was used when working with PtCl<sub>2</sub> due to its limited solubility in other solvents. The solubility of PtCl<sub>2</sub> is primarily limited to acetonitrile with only trace amounts being soluble in chlorinated and protic solvents. Acetonitrile on the other hand does have a high boiling point however, allowing for possible thermal cyclometallation.

Getting the platinum chloride into solution, prior to adding the ligand, proved to be crucial for coordination and cyclometallation. The PtCl<sub>2</sub> was therefore refluxed in acetonitrile for 30mins prior to the addition of the ligand. After the ligand was added slowly over an hour the resulting mixture was heated at reflux for up to 10 hours. Incompletion was noted at shorter reaction times where traces of a brown solid, proposed to be platinum chloride – PtCl<sub>2</sub>, was found in the final product.

As the reaction proceeded, HCl gas was noted from the reaction mixture using a pH probe and litmus paper. After refluxing for 10 hours a cloudy yellow/orange precipitate was formed with some black material evident at the bottom of the flask. The solution was filtered



and the filtrate was found to be a mixture of insoluble materials later identified as the bidentate complexes **271-273** using dichloromethane in place of acetonitrile.

The mother liquor was reduced down to dryness *in vacuo* and the residue was then taken up in dichloromethane and washed with 2 portions of de-ionised water before being dried over  $\text{MgSO}_4$ . The solution was then reduced to dryness again *in vacuo* and crystallised from dichloromethane-hexane to produce the cyclometallated complexes **281**, **282** and **283** in very low yields, **Table 2.4**.

Compound	Coordination	Physical appearance	Yield
<b>281</b>	$\eta^3\text{-PNC-L}^1$	Yellow powder	8%
<b>282</b>	$\eta^3\text{-PNC-L}^2$	Dark Yellow powder	1%
<b>283</b>	$\eta^3\text{-PNC-L}^3$	Orange powder	5%

*Table 2.4: Physical appearances and yields for the successfully formed cyclometallated complexes **281**, **282**, and **283** from  $\text{PtCl}_2$  in  $\text{CH}_3\text{CN}$*

The reactions were repeated with the same quantities in dichloromethane which has a lower boiling point in comparison to acetonitrile in order to prevent formation of the insoluble black material. The  $\text{PtCl}_2$  was refluxed in a large excess of dichloromethane for an hour in order to achieve solubility.  $\text{HCl}$  gas was not evident for the reaction of  $\text{PtCl}_2$  with the iminophosphine ligands **261-264** and there was no evidence of cyclometallation by NMR or IR spectroscopy even after 48 hours at reflux. There was also no evidence of the black material found previously but instead a large amount insoluble yellow powder was isolated.

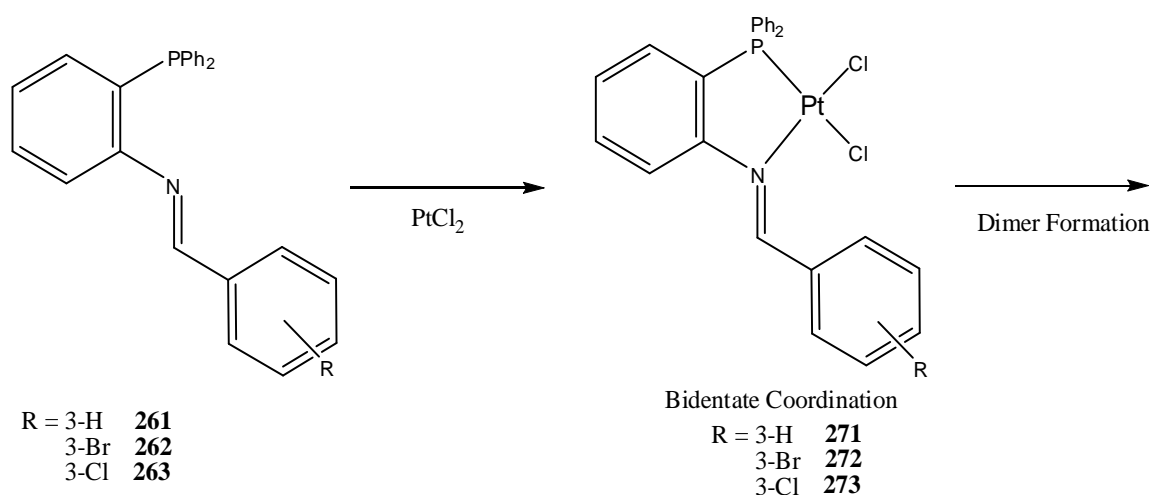


*Figure 2.38: Bidentate complexes are formed in low boiling point solvents which are also intermediates in the overall cyclometallation reaction and susceptible to dimerisation.*

Identification of the yellow powders (**271-273**) proved to be especially difficult due to their insolubility in all available deuterated NMR solvents. Accurate yields were also difficult to access due to uncertainty about the purity of the products. However, IR spectroscopy identified a shift in the imine stretching frequency in comparison to the uncoordinated ligands suggesting coordination with the metal centre (discussed further in **Section 2.6.1**). Also, elemental analysis confirmed the presence of a bidentate Pt (II) complex with a small amount of solvent of crystallisation present. It is therefore proposed that these compounds are bidentate complexes which have formed insoluble dimers due to the chlorides bring very good bridging ligands, **Figure 2.39**.<sup>69</sup>

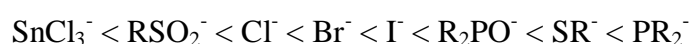


*Figure 2.39: The bridge tendencies for ligands associated with Pt (II) complexes.*<sup>70</sup>

Bidentate halo-bridging platinum dimers have also been reported by numerous research groups<sup>69,71,72</sup> and most of which have been found to be quite insoluble in all common solvents.<sup>42,58,41</sup> The first halo-bridged binuclear compound was first isolated as far back as 1870; the platinum carbonyl compound  $[\text{Pt}_2\text{Cl}_2(\mu\text{-Cl}_2)\text{CO}_2]$ ,<sup>73</sup> but more recently halo-bridged derivatives have been identified as key intermediates in platinum coordination and cyclometallation chemistry. They have also become especially useful in allowing preparation of complexes containing two different types of neutral ligands.<sup>69</sup>

Cotton and Wilkinson have identified three types of bridged  $d^8$  complexes, **Figure 2.40**. The structure of the first two types (a) and (b) are most often found when the bridging ligand ( $\mu\text{-X}$ ) is a halogen, an  $\text{S}^{2-}$  or an SR type ligand. The type (c) shown in **Figure 2.40** on the other hand is usually confined to  $\text{PR}_2$  and has shorter metal to metal distances in comparison to type (a) and (b). The  $\pi$ -donor ability of the bridging ligand can also be influential in the adoption of a particular geometry.<sup>70</sup>

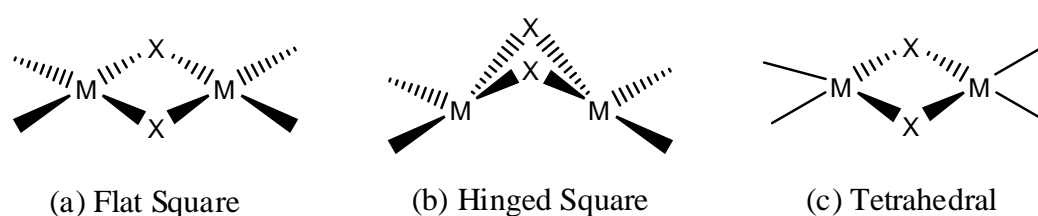


*Figure 2.40: The three types of bridged complexes formed with  $d^8$  metal complexes.*<sup>70</sup>

Platinum and palladium bridged complexes have been studied extensively but other  $d^8$  metal complexes can also adopt similar structures, for example  $\text{Rh}_2\text{Cl}_2(\text{CO})_4$  is an (a) type, **Figure 2.40** and  $\text{Ir}_2(\mu\text{-PPh}_2)_2(\text{CO})_2(\text{PMe}_3)_2$  forms a (c) type dimer, **Figure 2.40**. For Pt (II) complexes the bridge tendencies are in the order shown in **Figure 2.39**, where chloride can be seen as having the highest tendency to form bridged structures of all the halides.<sup>70</sup>

Based on previous work in our research group by Maguire it is proposed that the cyclometallated complexes, **281-283**, occur with the initial formation of a bidentate species, **Figure 2.38**. But there is also a competing dimerisation reaction occurring also which then prevents cyclometallation due to the high tendency for chloride ligands to form bridges.<sup>2</sup>

Analogous di-iodo bidentate complexes, synthesised by Maguire, were isolated and characterised by IR and elemental analysis but direct cyclometallation was not seen to occur with these complexes. In Maguire's research, sodium acetate was used to break the bridged ligands and induce cyclometallation. The chloride ligands however, as can be seen in **Figure 2.39**, are two orders of magnitude higher in tendency to form bridges than iodide and all attempts to use sodium acetate in the present work failed to produce cyclometallates.<sup>2</sup>

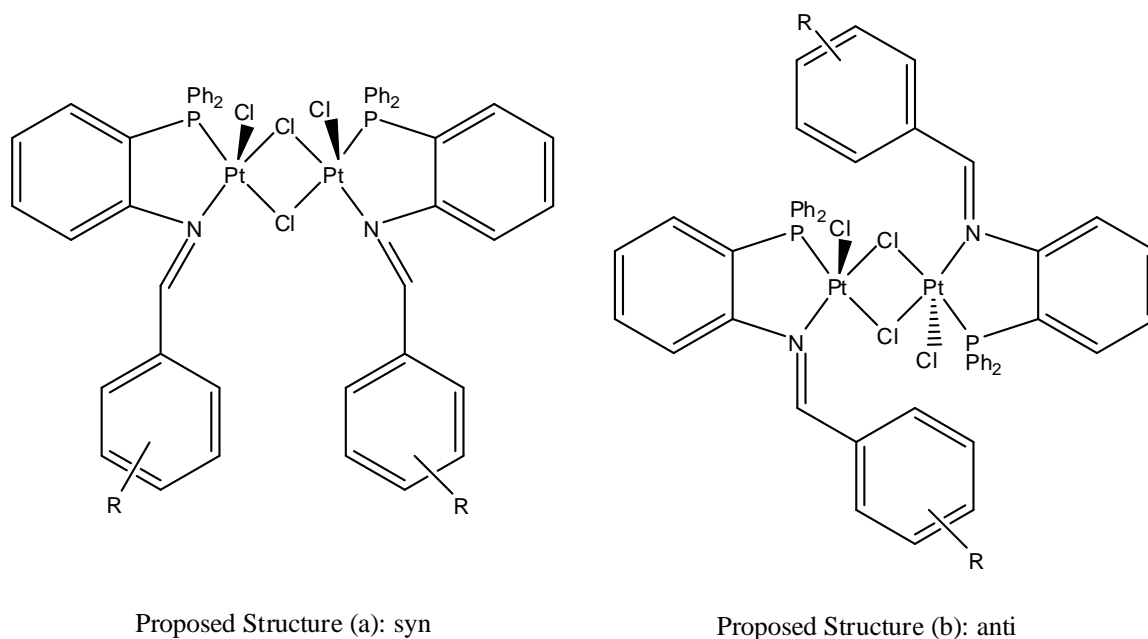


**Figure 2.41:** The proposed possible structures of the bridged bidentate platinum iminophosphine complexes by Maguire.<sup>2</sup>

These dimeric complexes are proposed to contain a penta-coordinate Pt (II) metal centre, **Figure 2.41**, similar to the previously proposed structures of the iodo platinum dimers reported by Maguire and type (a) as described by Cotton and Wilkinson in **Figure 2.40**. Further to the proposed structures in **Figure 2.41**, it can be seen that the steric and energetic constraints of a syn structure (a) would favour the formation of an anti structure (b). However

without further characterisation, the complete structure of these complexes cannot be confirmed. Attempts to break these dimers by solid state and solvent mediated thermal reactions failed along with additions of pyridine which was found to form further unidentifiable insoluble complexes at this time.

#### 2.5.4 Synthesis of platinum complexes of the HL<sup>4</sup> (264) ligand with the general formula [Pt(η<sup>3</sup>-PNO-L<sup>4</sup>)Cl] 285 METHOD A:

Reaction of the HL<sup>4</sup> **264** ligand with PtCl<sub>2</sub> under identical conditions used for the synthesis of [Pt(η<sup>3</sup>-PNC-L<sup>1-3</sup>)Cl] **281-283** reported for method A described in **section 2.4.3** initially produced only one identifiable product, a PNO type complex **285**, **Figure 2.42**. Also an insoluble yellow bidentate dimer, similar to those found for [Pt(η<sup>3</sup>-PNC-L<sup>1-3</sup>)Cl] **271-273**, was again found for this reaction which reduced the yields for the formation of a tridentate product due to the high tendency for chlorides to form bridges as discussed earlier.

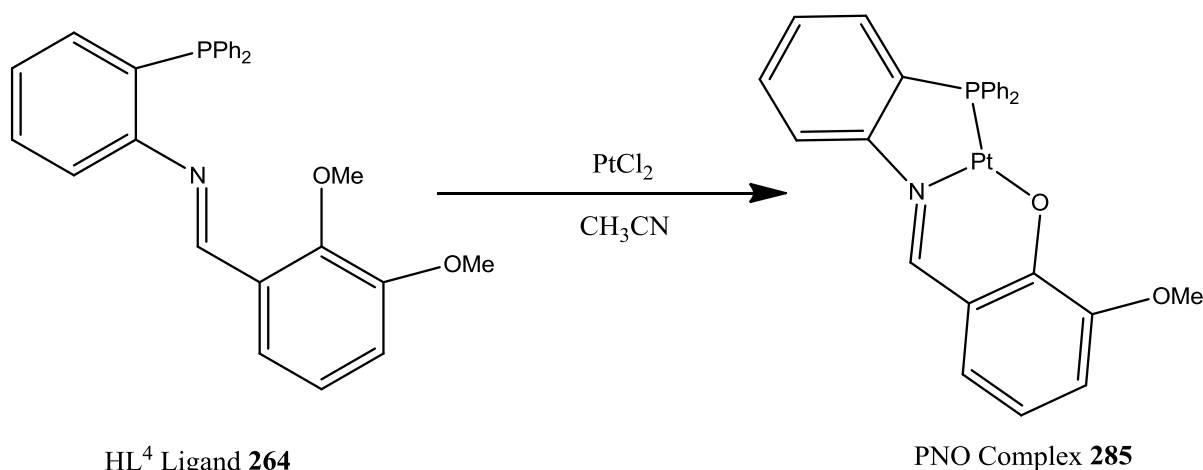


*Figure 2.42: The PNO complex formed from the HL<sup>4</sup> ligand with the loss of a MeCl.*

A cyclometallated product was not observed for this reaction, despite the presence of an electron donating group at the para position to the C-H bond to be activated. Interestingly the reaction prefers to form the PNO product **285** over the cyclometallated product even though the oxygen ligand is defined as hard by the HSAB theory and platinum is defined as soft as discussed in **Chapter 1**. Also, diluting the solution by adding more acetonitrile to reduce the possibility of bidentate dimer formation increased the yields by about 10% to 43%.

Attempts to form a cyclometallated product using polar protic solvents such as methanol and increasing the refluxing time were not successful. The use of an external coordinating base such as NaOAc as previously employed by our research group, Maguire, to

achieve cyclometallation also failed.<sup>2</sup> Reactions of the HL<sup>4</sup> ligand **264** with alternative platinum starting materials such as K<sub>2</sub>[PtCl<sub>4</sub>] and PtCl<sub>2</sub>(dms<sub>2</sub>)<sub>2</sub> also produced the PNO complex **285**, but in vastly reduced yields of 10 to 15 % in comparison to the reaction with PtCl<sub>2</sub> and also gave no evidence of the cyclometallated product **284** even in chlorinated solvents.

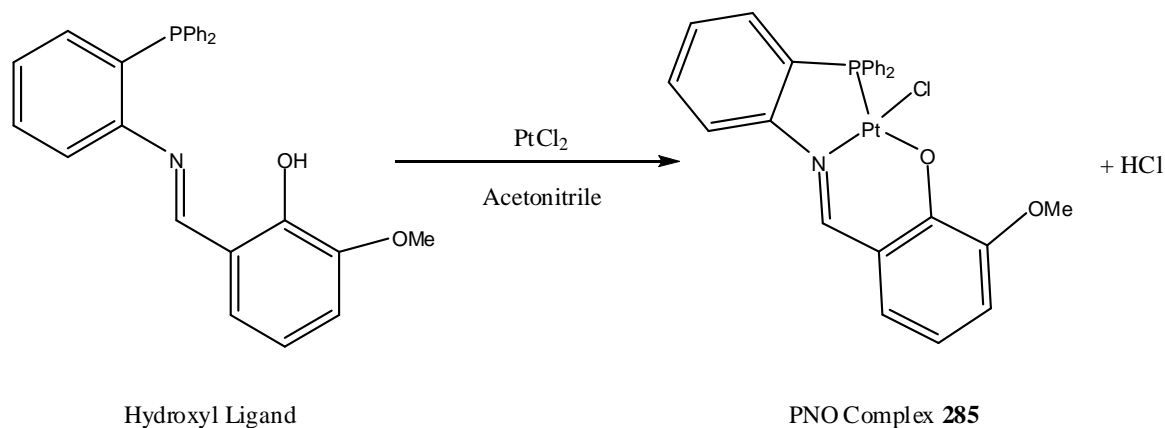


*Figure 2.43: The PNO complex formed from a hydroxyl ligand in yields of 77% by Lennon.<sup>45</sup>*

This PNO complex, **285**, **Figure 2.42**, has been previously reported by this research group but synthesised from an alternative ligand, **Figure 2.43**.<sup>45</sup> Work by Maguire also previously reported an analogous iodo PNO complex with the same ligand using in this research, HL<sup>4</sup> **264**, but also reported equal amounts of the PNC cyclometallated complex without the use of an external coordinating base, NaOAc.<sup>2</sup>

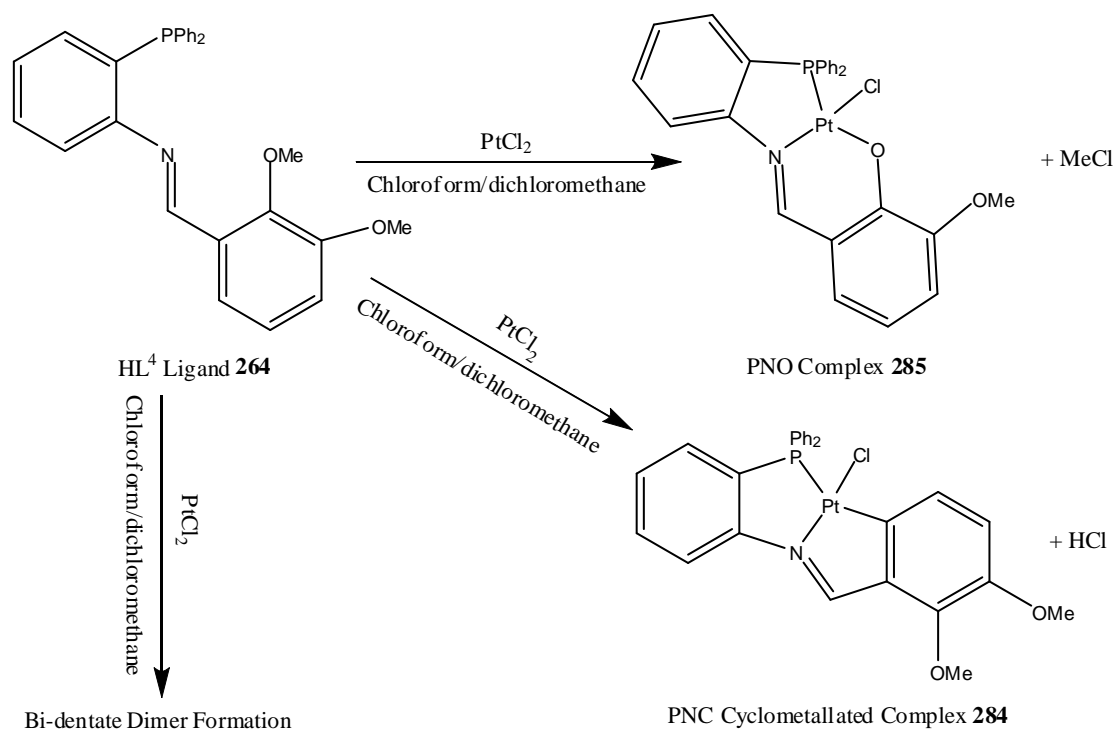


*Figure 2.44: The overall reaction of the HL<sup>4</sup> ligand with PtCl<sub>2</sub> in chlorinated solvents.*

When the reaction in **Figure 2.42** was repeated again under the same conditions as for the  $[\text{Pt}(\eta^3\text{-PNC-L}^{1-3})\text{Cl}]$  **271-273** complexes but with a chlorinated solvent instead of acetonitrile, trace amounts of a cyclometallated product, complex **284**, was identified by NMR and IR spectroscopy, **Figure 2.44**. The interesting coordination behaviour of the  $\text{HL}^4$  ligand **264** with platinum chloride reagents will be discussed further in **Section 2.5.6**.

### 2.5.5 Synthesis of cyclometallated tridentate iminophosphine complexes with the general formula $[\text{Pt}(\eta^3\text{-PNC-L}^{1-3})\text{Cl}]$ **281-283** METHOD B:

Due to the insolubility of  $\text{PtCl}_2$  in polar protic and chlorinated solvents, both of which (as previously discussed) have been identified as important for successful cyclometallation, alternative platinum starting materials were investigated. Initial work centred on  $\text{K}_2[\text{PtCl}_4]$  (potassium tetrachloroplatinate) and  $\text{PtCl}_2(\text{dmsO})_2$  (dimethyl sulfoxide dichloroplatinate) which have been used by other research groups as starting materials for coordination and cyclometallation.<sup>34,74,75,10</sup>

$\text{K}_2[\text{PtCl}_4]$  has a similar solubility profile to  $\text{PtCl}_2$  except that it is also soluble in water so unfortunately it is of no benefit to this research. It also is readily reduced to platinum metal in the presence of alcohols and bases. It was therefore decided not to proceed any further with it and instead it was used to synthesise  $\text{PtCl}_2(\text{dmsO})_2$  by reacting with dimethyl sulfoxide (dmsO) in a minimum amount of water giving a 90% yield of the desired product.

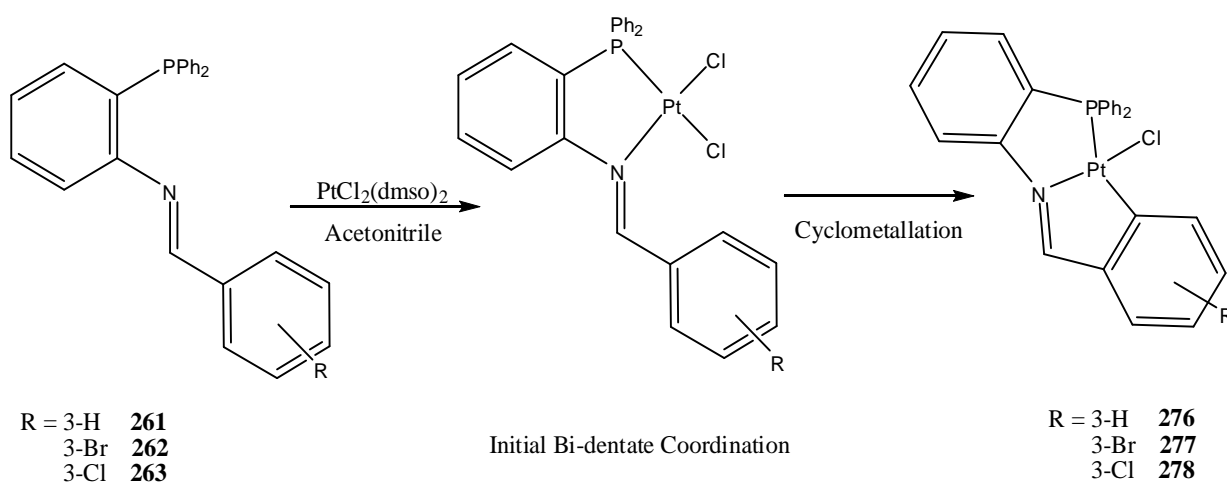


*Figure 2.45: Attempted reactions of the  $\text{HL}^{1-3}$  ligands with  $\text{PtCl}_2(\text{dmsO})_2$  produced the desired cyclometallated complexes but again, like  $\text{PtCl}_2$ , in very low yields.*

Reactions with ligands HL<sup>1-3</sup> **261**, **262**, and **263** in acetonitrile were attempted with PtCl<sub>2</sub>(dms<sub>o</sub>)<sub>2</sub>, **Figure 2.45**, but yields and results were almost identical to those reactions completed with PtCl<sub>2</sub> and reported in **Section 2.5.3** (Method A).

Previous work carried out by our research group into cyclometallated iodo complexes used [PtI<sub>2</sub>(cod)] ((1,5-cyclooctadiene)di-iodoplatinum) as a starting material for coordination to the iminophosphine ligands.<sup>2</sup> It was noted that its solubility in a large amount of solvents, particularly methanol and dichloromethane, was beneficial for coordination and increased yields. Other research groups have also found success with (1,5-cyclooctadiene) dichloroplatinum (II) [PtCl<sub>2</sub>(cod)] as their starting material for platinum chloride complex formation.<sup>76,22</sup>

[PtCl<sub>2</sub>(cod)] was therefore synthesised using a variation of two literature methods.<sup>77,78</sup> The starting material used was PtCl<sub>2</sub> instead of the more usual K<sub>2</sub>[PtCl<sub>4</sub>], Na<sub>2</sub>[PtCl<sub>4</sub>] or platinum. The product was isolated in average yields of 50-60% as a white crystalline powder. It was characterised by NMR, IR and elemental analysis.

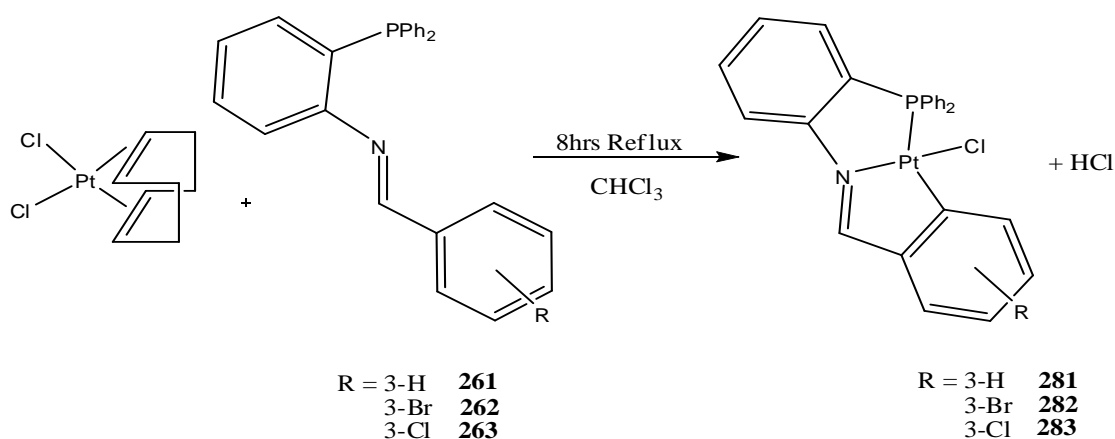


**Figure 2.46:** Direct cyclometallation of the iminophosphine ligands HL<sup>1-3</sup> **261**, **262** and **263** using PtCl<sub>2</sub>(cod) in chloroform.

A stirred solution of (1,5-cyclooctadiene) dichloroplatinum (II) [PtCl<sub>2</sub>(cod)] dissolved in chloroform (20ml) was reacted with 1.1 equivalents of the appropriate ligand **261-263**, which was also dissolved in chloroform (10ml). The ligand was added dropwise from an addition funnel over 4 hours to the solution, after which the reaction mixture was heated at reflux for an additional 4 hours. After 2 hours of reflux the solution changed colour from a pale yellow to dark orange with TLC analysis noting the formation of the desired cyclometallate with an R<sub>f</sub> value of 0.83, while the previously identified bidentate intermediates **271-273** displayed an R<sub>f</sub> value of 0.08, primarily due to insolubility.

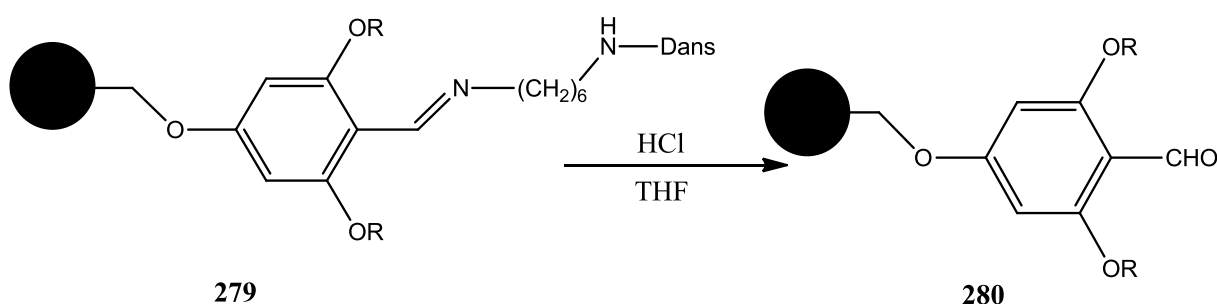
After 8 hours at reflux, the orange/yellow solution was reduced to dryness *in vacuo* and the residue was taken up in 20ml of singly distilled dichloromethane to which silica gel was added. This is similar to an analogous literature procedure and is employed here to remove any unwanted bidentate material and hydrolysed products.<sup>79,70</sup> Celite was also attempted initially but proved to be unsuccessful for achieving a high yield of the cyclometallate from the separation.

The silica gel was then filtered off and washed with two portions of dichloromethane. The yellow filtrate was again reduced to dryness *in vacuo* and crystallised from doubly distilled dichloromethane-hexane to yield cyclometallates **281-283**, Table 2.5.

Compound	Coordination	Physical appearance	Yield
<b>281</b>	$\eta^3$ -PNC-L <sup>1</sup>	Yellow, metallic powder	73%
<b>282</b>	$\eta^3$ -PNC-L <sup>2</sup>	Yellow, crystalline powder	7%
<b>283</b>	$\eta^3$ -PNC-L <sup>3</sup>	Orange, metallic powder	45%

*Table 2.5: The physical appearances and yields obtained for the PNC cyclometallated complexes 281-283 synthesised from PtCl<sub>2</sub>(cod), Method B.*

Shorter reaction times resulted in a reduced yield; longer reaction times also saw a slightly reduced yield primarily due to hydrolysis of the iminophosphine ligand by the HCl side product which is formed from the cyclometallation step. Acid catalysed hydrolysis of imines have been reported by a wide range of research groups and studied in depth by Madrigal *et al* in particular, **Figure 2.47**.<sup>80</sup>



Dansyl Chloride = (5-(dimethylamino)naphthalene-1-sulfonyl chloride)

*Figure 2.47: The hydrolysis of sasrin-like resin bound imines 279, as monitored by fluorescence spectroscopy, reforms the aldehyde starting material 280 which was used to synthesis the imines initially.<sup>80</sup>*

Hydrolysis was confirmed by the appearance of an aldehyde peak in <sup>1</sup>H NMR spectra in reactions that were refluxed for more than 10 hours. This corresponded to the aldehyde that



was used to synthesis the iminophosphine ligands as seen in **Figure 2.32** previously discussed in **Section 2.5.1**. In tests carried out on the isolated cyclometallated products **281-283** with HCl, hydrolysis was not observed to occur indicating that the cyclometallates are stable towards hydrolysis. However, in tests carried out with HCl on the free iminophosphine ligands HL<sup>1-4</sup> **261-264**, hydrolysis was observed to occur and the appearance of an aldehyde peak was also observed in the <sup>1</sup>H NMR

The hydrolysis indicates that the reaction did not go to completion as there are also indications of other platinum coordinated complexes, which could be the non dimerised bidentate intermediates. The extensive NMR studies on all the reactions will be discussed further in **Section 2.7**.

Microanalytical data obtained agreed with the proposed empirical formula (within experimental error). Most of the complexes were isolated with the presence of crystallisation solvent (CH<sub>2</sub>Cl<sub>2</sub>) which was also identified in the <sup>1</sup>H NMR spectra of these complexes.

As previously discussed in **Section 2.5.3** we propose that the cyclometallated complexes, **281-283**, occur via the initial formation of a bidentate species (which are not isolated here) which then have three possible routes within the reaction, **Figure 2.48**.

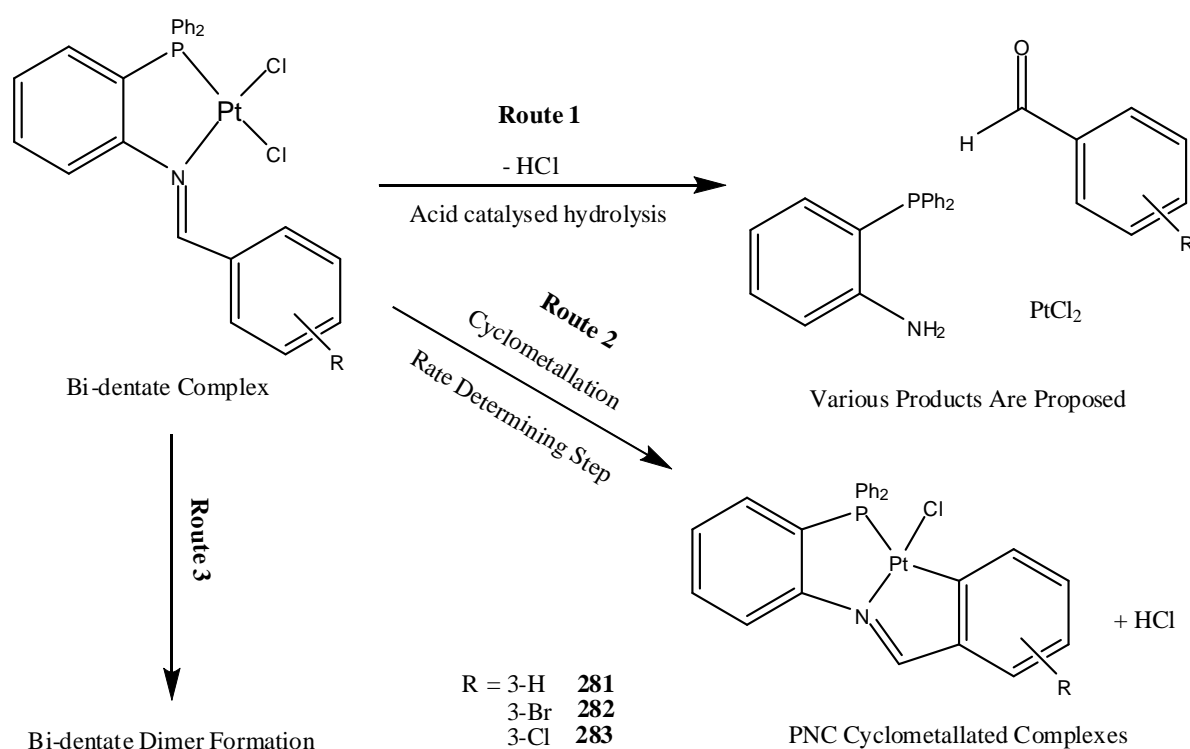


**Figure 2.48:** The various routes that the bidentate complex could take after formation. The possibility of **Route 1** and **3** can be reduced though, resulting in the formation of the desired cyclometallate via **Route 2**.

In order to increase the possibility of **Route 2** occurring in **Figure 2.48**, the possibility of the other two routes occurring must be reduced. The use of molecular sieves can reduce **Route 1** quite effectively and adding the ligands  $HL^{1-3}$  drop wise as a solution over 4 hours reduces the possibility of **Route 3** occurring. By adding the ligands slowly to a dilute solution of  $PtCl_2(cod)$  it allows the intra-molecular oxidative addition of the bidentate intermediate to occur in order to form the cyclometallates **281-283** which we propose is the rate determining step, **Figure 2.49**.

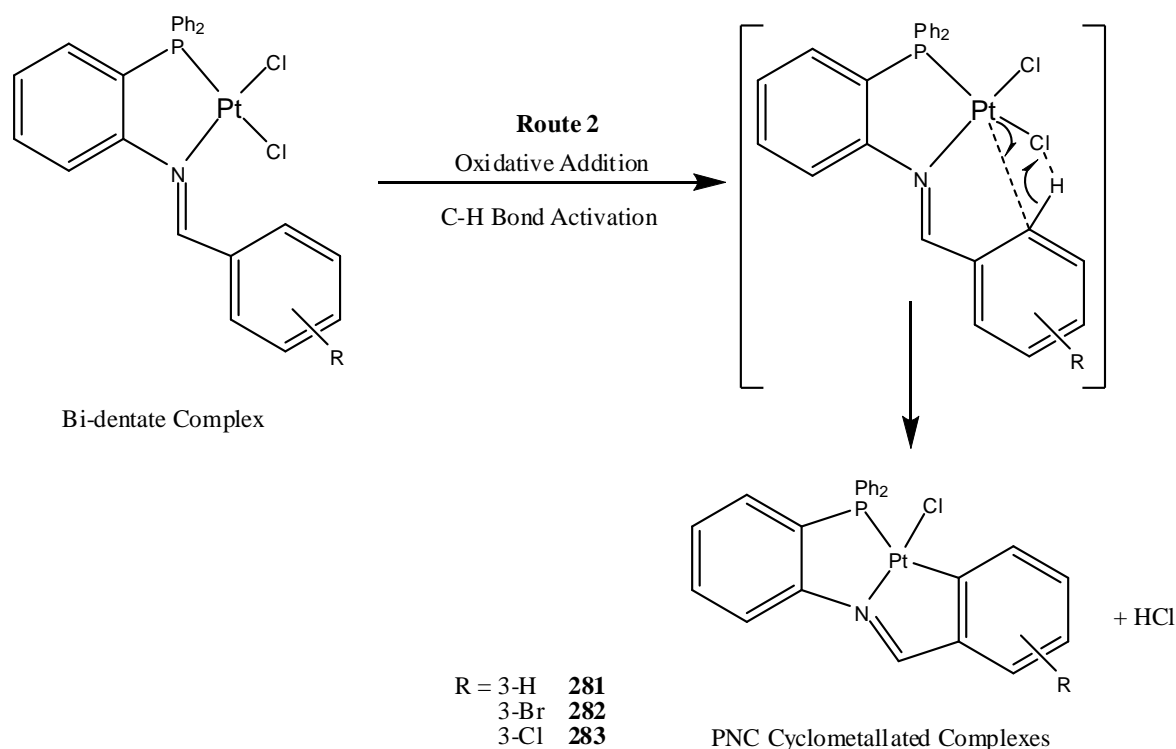


**Figure 2.49:** The intramolecular oxidative addition of the bidentate complexes to generate the cycloplatinated  $C_{aryl}-Pt$  bond, which is also the rate determining step of the overall reaction.

As discussed in the introduction to this chapter, early methods of achieving platinum cyclometallation used thermal activation to generate the metal-carbon bond and it was seen that higher boiling point solvents would assist in increasing the yields of these cyclometallates.

Synthesis of the cyclometallates **281-283** in dichloromethane with  $PtCl_2(cod)$  gave average yields but even better yields were achieved in the higher boiling point solvent chloroform ( $61^\circ C$ ). It is proposed that chlorinated solvents assist in the cyclometallation procedure and C-H bond activation, the higher boiling point of chloroform in comparison to dichloromethane also assists with thermal cyclometallation.

However, attempts to improve the yields of the cyclometallated complexes further by refluxing the HL<sup>1-4</sup> ligands **261-263** with PtCl<sub>2</sub>(Cod) in toluene (110°C) for 4 hours produced a black precipitate which may be platinum metal. <sup>1</sup>H NMR studies on the black precipitate showed the presence of an aldehyde peak indicating that hydrolysis of the ligand had again occurred.

Work by Crespo *et al* and others have also found that the use of toluene gave no reaction at all for Pt (II) cyclometallation. They cited extreme insolubility as a possible cause for failure, which is what is also proposed for this work along with thermal decomposition of the ligands, intermediates and starting materials at high temperatures.<sup>43,44</sup>

Other solvents were also studied in this work, however, as previously seen in **Section 2.5.3** high-boiling point solvents such as acetonitrile (81°C) only produced the cyclometallates in very small quantities. Protic solvents such as methanol gave reduced yields, in contrast to work by Crespo *et al* where they have identified the usefulness for a protic solvent in order to facilitate activation of the C<sub>aryl</sub>-H bond.<sup>43</sup>

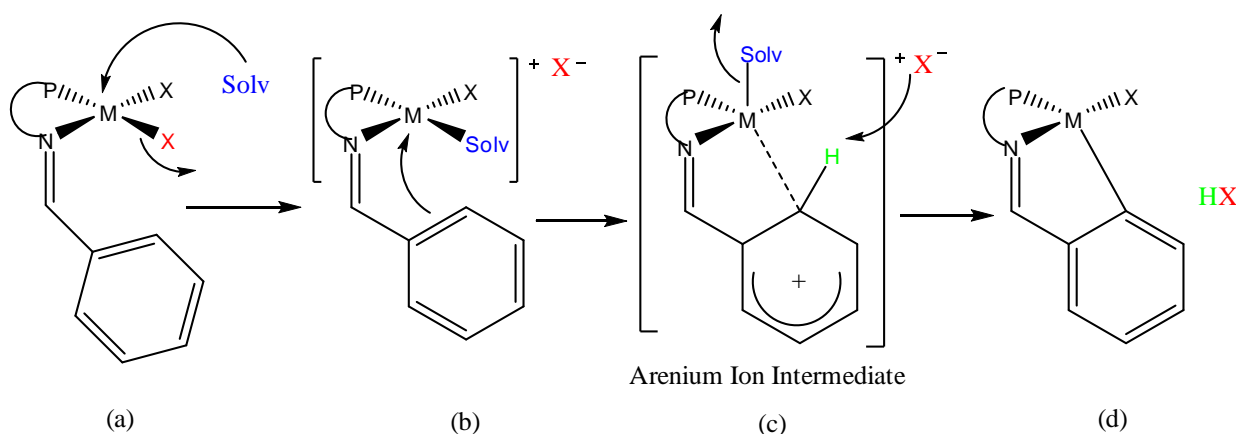


**Figure 2.50:** Solvent assisted cyclometallation with an aryl ring adapted from a proposed mechanism by Wong-Foy *et al* and previous work completed by Crespo *et al*.<sup>43,44</sup>

Therefore from these studies it can be seen that cyclometallation is not solely dependent on thermal conditions. Solvent dependent direct cyclometallation has been identified by Wong-Foy *et al*, where they have proposed the inclusion of the solvent in the mechanism for C-H activation, **Figure 2.50**. The displaced halide acts as a nucleophile to remove the aryl hydrogen in a concerted mechanism. The mechanism in **Figure 2.50** closely follows that proposed by Lennon in **Figure 2.36** for direct cyclometallation using palladium where a highly reactive arenium ion intermediate is formed by resonance delocalisation at the C-6 position of the aryl ring, **Step (c), Figure 2.50**.

As is apparent for **Step (c)**, **Figure 2.50**, the platinum metal centre becomes five-coordinate. Further mechanistic investigations have been reported in the literature where C-H activation and subsequent cyclometallation has been identified to proceed in two steps. Therefore it seems quite likely that the reactions reported here follow a similar mechanism. **Figure 2.51** gives a more detailed look at **Step (a)** to **Step (b)** from **Figure 2.50** where a five-coordinate intermediate is also formed.

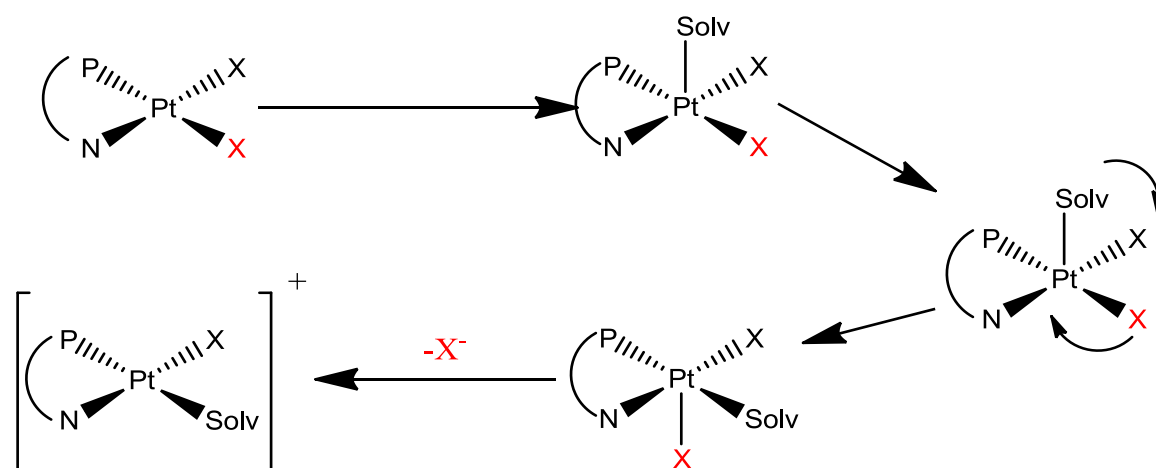


**Figure 2.51:** Proposed mechanism of *trans* effect substitution of the bidentate complexes adapted from a proposed mechanism by Wong-Foy *et al* and previous work completed by Crespo *et al*.<sup>43,44</sup>

The proposed mechanism in **Figure 2.51** involves coordination of a solvent molecule to the metal centre perpendicular to the square planar complex. The solvent molecule acts as a nucleophile towards the soft, electron poor metal centre. This generates a five coordinate intermediate as noted in the mechanism which follows the well established associative substitution mechanism which square planar complexes have been shown to follow.<sup>74</sup>

The substituents then rotate around the metal centre, resulting in incorporation of the solvent molecule *trans* to the strongest *trans*-effect ligand, the diphenylphosphino group in the present case. This then results in the substituent **X** being projected perpendicular to the square planar complex. **X** is then lost generating the four-coordinate complex (b) allowing the **X** to act as a nucleophile and cause C-H bond activation, resulting in metal-carbon bond formation.

The subsequent proposed reductive elimination generates hydrochloric acid which has been identified during the reaction using universal indicator paper. The result is the formation of the cyclometallated, square planar (four coordinate) tri-dentate complexes **281**, **282** and

**283.** Evidence for the generation of a five-coordinate intermediate has been reported by Crespo *et al* where an acetate group was present instead of a solvent molecule.<sup>43</sup>

As previously discussed in **Section 2.2.4**, Mamtora *et al* have completed extensive studies into C-H activation in chlorinated solvents and have found that chloroform was able to solubilise chloride anions via a hydrogen bond type of interaction, **Figure 2.27**, thus stabilising the liberated chloride anion in solution. This results in it being able to remove the hydrogen from the aryl ring as proposed in **Figure 2.50** and **2.51**.<sup>46</sup> This hydrogen-bonding type of stabilisation of the chloride anion in chloroform can be invoked to explain the more efficient reaction compared with similar reactions in acetonitrile or toluene studied over the course of this research.<sup>46</sup>

Attempted solid state reactions with the bidentate dimer complexes using heat over a number of hours initially found that HCl gas was being released from the solid sample. After approximately half an hour however it was no longer observed and upon analysis no cyclometallated complexes were found. This would imply also that the cyclometallation of these bidentate complexes is in fact solvent dependent, **Figure 2.51**, but further work is required to confirm this.

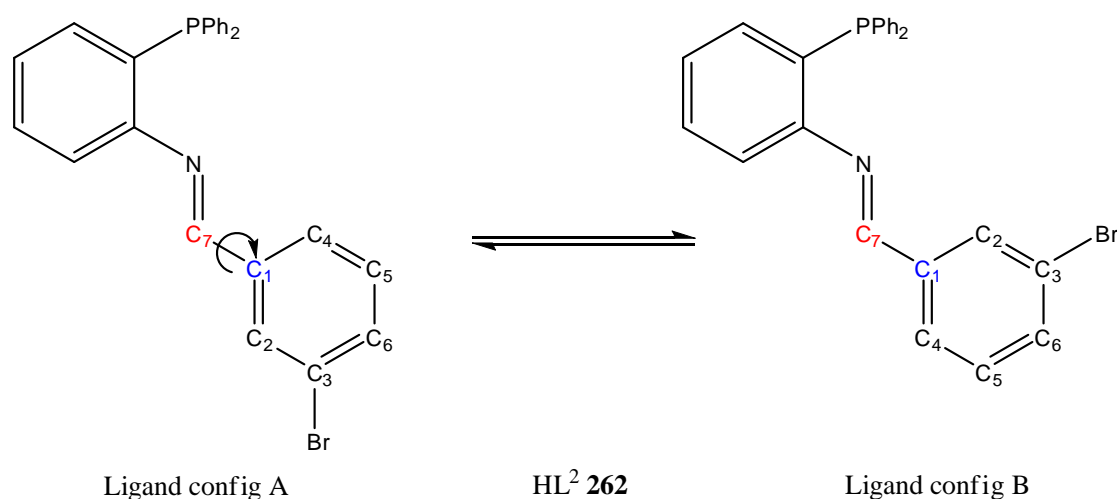


**Figure 2.52:** Showing the free rotation around the labelled C1 and C7 bond with the large bromine substituent causing steric crowding at a potential C-H activation site (in comparison to chloride and hydrogen for HL<sup>1</sup> and HL<sup>3</sup>).

The yields produced from the direct cyclometallation during the course of this research, 7% for the 3-Br complex **282**, 43% for the 3-Cl complex **283** and 73% for the unsubstituted 3-H complex **281**, identify a trend associated with the substituents present at the C3 position of the ligands. Physical properties such as steric factors due to the free rotation of

the C7-C2 bond in the ligand, indicated in **Figure 2.52**, significantly influence the yield of the reaction depending on the substitute present at the C3 position.

The unsubstituted HL<sup>1</sup> ligand **261** gives a much higher yield for cyclometallation since the bond rotation results in the same structure for both configurations opening up two possible sites for C-H activation. This means there are two sites (C2 and C4) at which the chloride anion can remove a hydrogen. This supports the proposed solvent assisted pathway shown in **Figure 2.50** and **2.51**. If the solvent displaces the chloride from the metal centre it would require a less sterically hindered environment, especially if ligand configuration B is taken into account **Figure 2.53**.

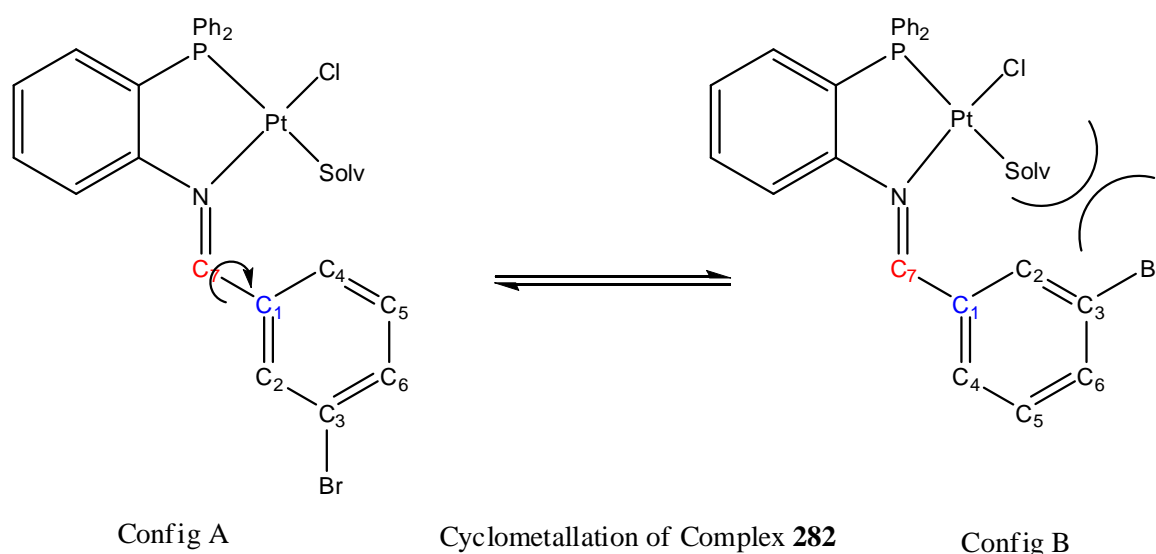


**Figure 2.53:** Cyclometallation in **Config B** is more difficult so only **Config A** reacts to form the desired product which results in a reduced yield for complex **282**. For the unsubstituted complex **281** despite the same rotation, only one configuration exists, which results in a much higher yield.

The substituents present at the C3 position of the ligand can also affect the stability of the arenium ion intermediate, proposed in **Figure 2.50**. Electron withdrawing substitutions such as chloride and bromide in ligands HL<sup>2</sup> and HL<sup>3</sup> (**262** and **263**) pull electron density away from the aryl ring, resulting in a less stable arenium ion intermediate. Electron donating groups such as methoxy groups can have the opposite effect where the electron donating ability of the substituents can in fact stabilise the arenium ion intermediate which will be discussed further in the next section, **Section 2.5.6**.<sup>45</sup>

### 2.5.6 Synthesis of platinum complexes of the HL<sup>4</sup> (264) ligand with the general formula [Pt( $\eta^3$ -PNC-L<sup>4</sup>)Cl] and [Pt( $\eta^3$ -PNO-L<sup>4</sup>)Cl] 284-285 METHOD B:

Reaction of the HL<sup>4</sup> ligand **264** with [PtCl<sub>2</sub>(cod)] under the same conditions used for the synthesis of [Pt( $\eta^3$ -PNC-L<sup>1-3</sup>)Cl] **281-283** discussed in **Section 2.5.5** produced two products. Crystallisation of the residue from dichloromethane-hexane yielded orange-red crystals. These crystals were identified to be a mixture of two products by TLC, firstly the cyclometallate [Pt( $\eta^3$ -PNC-L<sup>4</sup>)Cl] **284** and the tridentate [P, N, O] complex [Pt( $\eta^3$ -PNO-L<sup>4</sup>)Cl] **285** as confirmed by IR and NMR analysis (see **Sections 2.6** and **2.7**). As previously mentioned in **Section 2.5.4** the chloro P,N,O complex was synthesised previously by this research group using an alternative method and ligand, **Figure 2.43**.

TLC analysis gave three spots from the solution where one was at R<sub>f</sub>=0.83 (Fraction A), another at R<sub>f</sub>=0.33 (Fraction B) and one which stayed on the line with an R<sub>f</sub>=0 (Fraction C), **Figure 2.54**. The two complexes (Fraction A and B) were separated using wet-flash chromatography on silica gel, eluting from chloroform:methanol (98:2) which gave the best separation as noted by TLC. The third fraction (Fraction C) stayed on the column despite various attempts with a number of solvents to remove it.

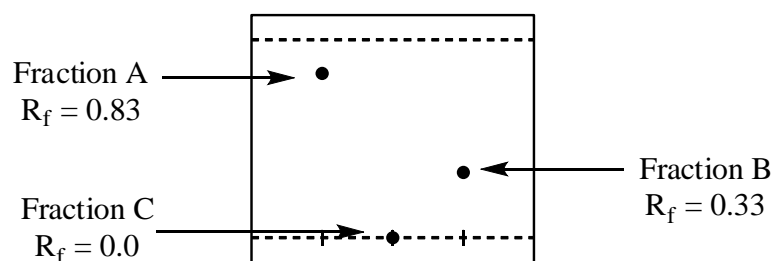


*Figure 2.54: Illustration of a TLC with the two primary products of the reaction (Fraction A and B) eluting from 98:2 CHCl<sub>3</sub>:MeOH while Fraction C remains on the column.*

Both products (Fraction A and B) were separated from 15 fractions and crystallised individually from dichloromethane-hexane. **Product A**, eluting first, was identified as the cyclometallated species [Pt( $\eta^3$ -PNC-L<sup>4</sup>)Cl] **284** while **Product B**, eluting second, was identified as the previously reported tridentate chloro PNO complex [Pt( $\eta^3$ -PNO-L<sup>4</sup>)Cl] **285**.

The material which stayed on the column (Fraction C) was found to be very insoluble and is again proposed to be a mixture of the bichloro bidentate complex and its proposed dimer. The yields and physical appearances of both products can be found in **Table 2.6**.

Compound	Coordination	Physical appearance	Yield
<b>284</b>	$\eta^3$ -PNC-L <sup>4</sup>	Orange, metallic powder	62%
<b>285</b>	$\eta^3$ -PNO-L <sup>4</sup>	Orange, crystalline powder	12%

*Table 2.6: The yields and physical appearances of the complexes 284 and 285*

Unlike the reactions with PtCl<sub>2</sub>, Method A as reported in **Section 2.5.4**, the cyclometallated complex [Pt( $\eta^3$ -PNC-L<sup>4</sup>)Cl] **284** formed in good yields here as well as the previously reported PNO complex [Pt( $\eta^3$ -PNO-L<sup>4</sup>)Cl] **285**. Similar to the reactions discussed in **Section 2.5.5** for the cyclometallated complexes **281-283**, the cyclometallated complex [Pt( $\eta^3$ -PNC-L<sup>4</sup>)Cl] **284** is formed here via the same proposed mechanisms by analogy with the use of the HL<sup>4</sup> ligand **264** via the bidentate intermediate, **Figure 2.55**.

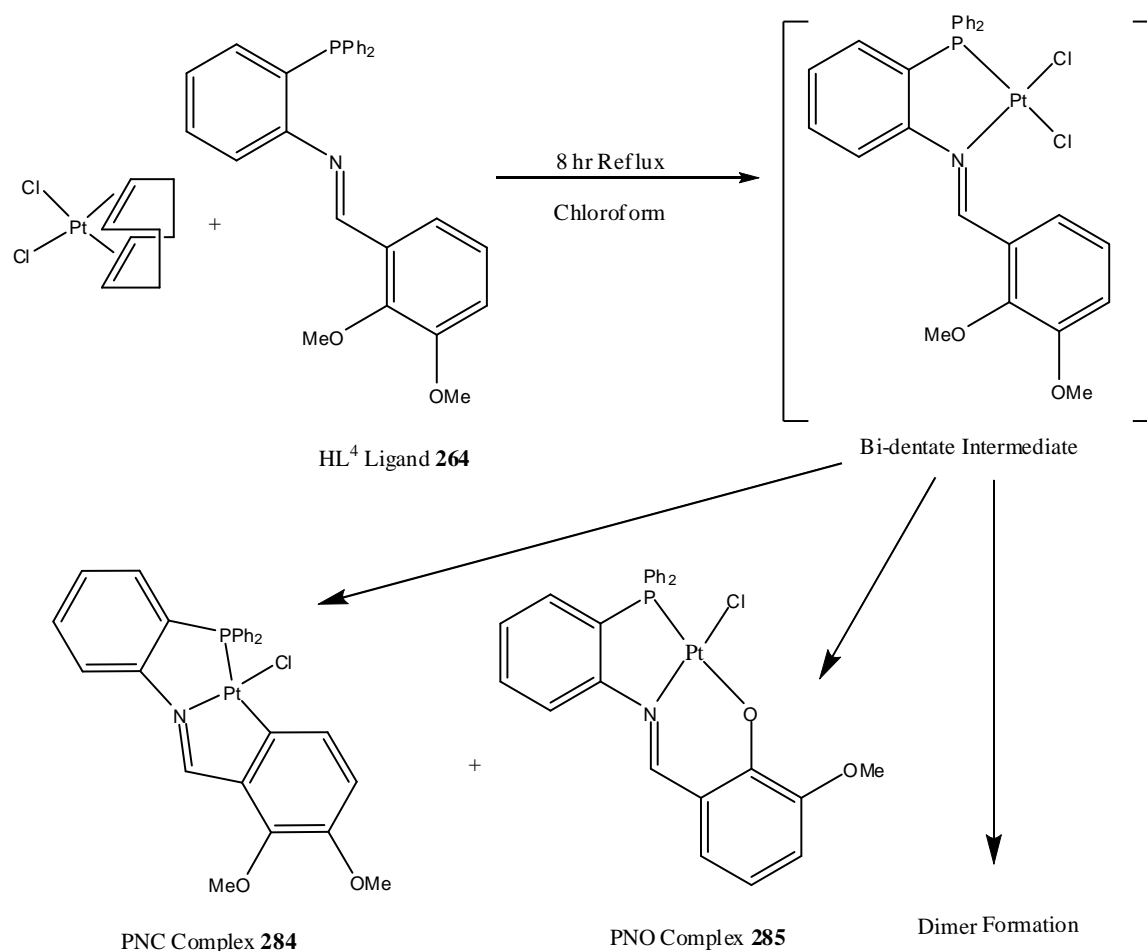


*Figure 2.55: The two tridentate products formed from the HL<sup>4</sup> ligand 264 formed via the bi-dentate intermediate in chloroform.*

The ability to form two products from the HL<sup>4</sup> ligand **264** stems from the fact discussed in **Section 2.4.5** with the bond rotation around C7-C2 as seen in **Figure 2.52**. But instead of the methoxy group preventing coordination like that seen for the HL<sup>2</sup> and HL<sup>3</sup>



ligands, a methyl group is displaced in order to coordinate to the oxygen heteroatom directly forming the PNO product **285**. Also the electron donating ability of the methoxy group para to the C-H bond to be activated helps to stabilise the arenium ion intermediate from the proposed cyclometallation mechanism in **Figure 2.50**.

In order to investigate the role of the solvent in the reaction of HL<sup>4</sup> **264** with PtCl<sub>2</sub>(cod) was repeated using acetonitrile rather than chloroform. The largest product from this reaction was the tridentate PNO complex **285** with only a trace amount of the cyclometallated Pt (II) PNC complex **284** formed. This is in contrast to the results from the reaction in chloroform where the cyclometallated complex **284** is the major product. These observations provide additional evidence for a solvent assisted pathway in cyclometallate formation.

It is also worth noting that unlike work completed with the analogous iodo complexes reported previously by our research group, an external base (NaOAc) was not required to form the cyclometallated complex **284**. Instead a one step solvent assisted cyclometallation was seen via the mechanisms discussed in **Section 2.5.5**.

### **2.5.7 Synthesis of cyclometallated tridentate phosphinoiminol complexes with the general formula [Pt ( $\eta^3$ -PNC-L<sup>5-7</sup>) Cl] and [Pt ( $\eta^3$ -PNO-L<sup>6</sup>) Cl] 286-289:**

As discussed in **Section 2.1.2** phosphinoamide type ligands have similar coordination behaviour to iminophosphines with the same mixed donor atoms of phosphine and nitrogen. However, the nitrogen group of the amide donor ligand has less donating ability (and hence negative character) than the equivalent imine ligand described already which can lead to different hemilability and coordination behaviour.

Previous work in this research group on phosphinoamide ligands with platinum iodo starting materials [PtI<sub>2</sub>(cod)] reported extensive difficulties attempting to form tridentate complexes. Initial work resulted in the formation of insoluble monodentate iodide bridged dimers ( $\mu$ -I) with coordination taking place solely through the diphenylphosphine group. This is due to the amide/nitrogen group having less donating ability in comparison to the analogous imine group on the iminophosphine ligands.

Additional refluxing for a number of days and the addition of a large excess of sodium acetate was required to form the bidentate complexes with coordination through both the phosphine and iminol. It was found by NMR spectroscopy that although the iminol group

possess similar coordination properties to imines described earlier, due to the presence of the hydroxyl moiety the ligands are more susceptible to hydrolysis.<sup>81</sup>

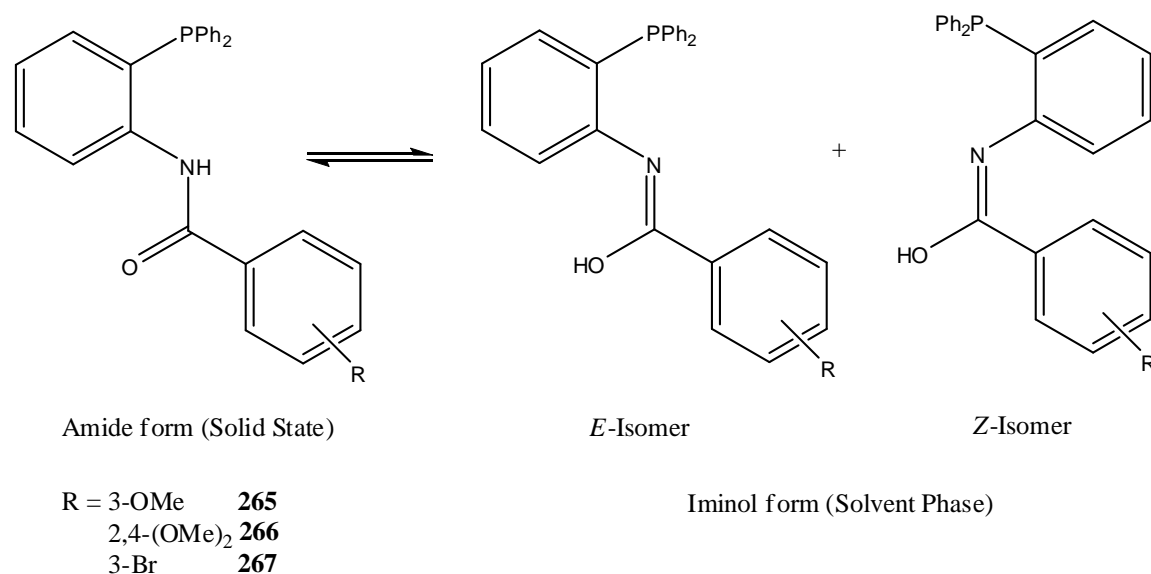


**Figure 2.56:** The phosphinoamide ligands exist as two forms. In the solid state they take the amide form while in solvents they tautomerise to form an iminol giving two possible isomers.

In order to achieve cyclometallation of the phosphinoamide complexes, an external base to induce tautomerism and assist in cyclometallation was required. The base-induced tautomerism of phosphine amides has also been reported by other research groups as well as their complexation to metal centres.<sup>29,68,82</sup>

The methodology for the synthesis of the platinum chloride cyclometallated complexes **286-288** is based on a combination of previously reported methods<sup>29,2</sup> and that which was successful for the iminophosphine complexes in **Section 2.4.5**. Initially the reactions with PtCl<sub>2</sub>(cod) and the HL<sup>5-7</sup> ligands **265-267** were attempted in chloroform using the same conditions as that found to be successful the iminophosphine complexes, **Section 2.5.5**. HCl was again generated (as detected by litmus paper and a pH meter), suggesting that cyclometallation had occurred. However yields of the products remained very low and NMR studies suggested extensive hydrolysis has taken place.

The reactions were therefore repeated using an external base to remove the HCl. Initially triethylamine was used to form Et<sub>3</sub>N.HCl, however multiple products were found upon completion of the reaction which suggested possible coordination between the metal centre and the external base. Therefore DABCO was used instead as its bulky molecular nature reduces any potential coordination with Pt (II) metal centres, **Figure 2.57**.

To a stirred refluxing dilute solution of  $\text{PtCl}_2(\text{cod})$  in chloroform with an excess of sodium carbonate (to maintain basic conditions) and DABCO added, the  $\text{HL}^{5-7}$  ligands **265**, **266** and **267** were added as a solution of chloroform from a drop-funnel over four hours. The solution was then refluxed for a further two hours to assist thermal cyclometallation. Immediately after adding the ligand the reaction became cloudy white with the formation of the  $\text{DABCO.HCl}$ .

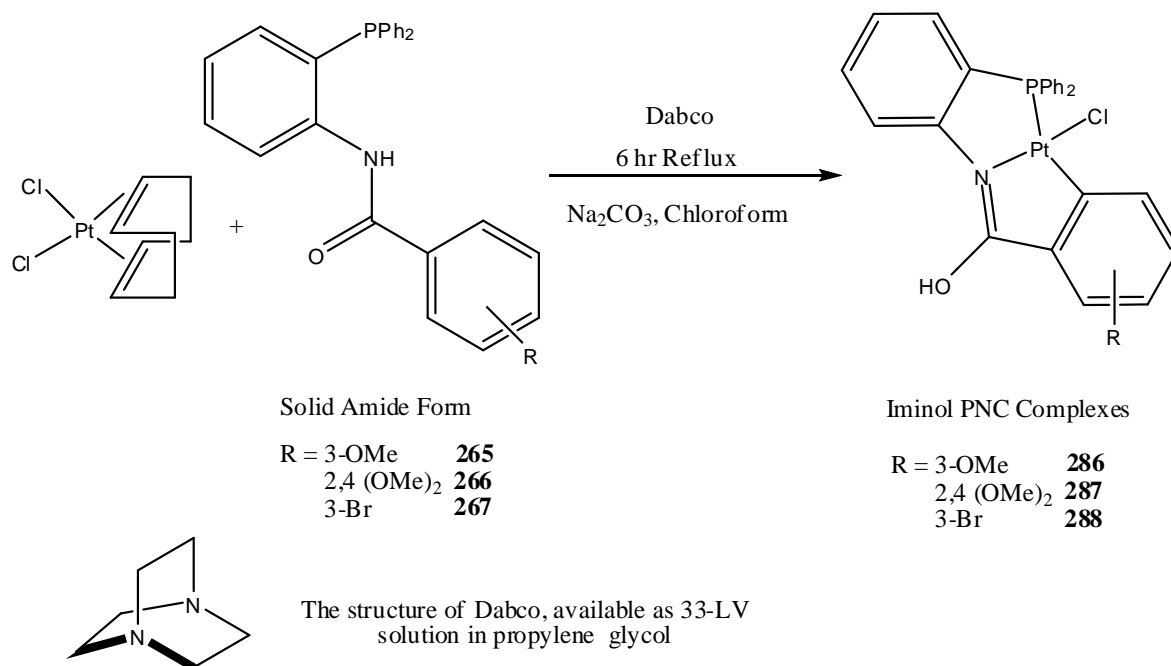


**Figure 2.57:** Synthesis of the cyclometallated platinum iminol complexes from the *E*-isomer of the tautomerised phosphinoamide ligands  $\text{HL}^{5-7}$  **265**, **266** and **267**. The *Z*-isomer of the iminol version of the ligand cannot form cyclometallated products.

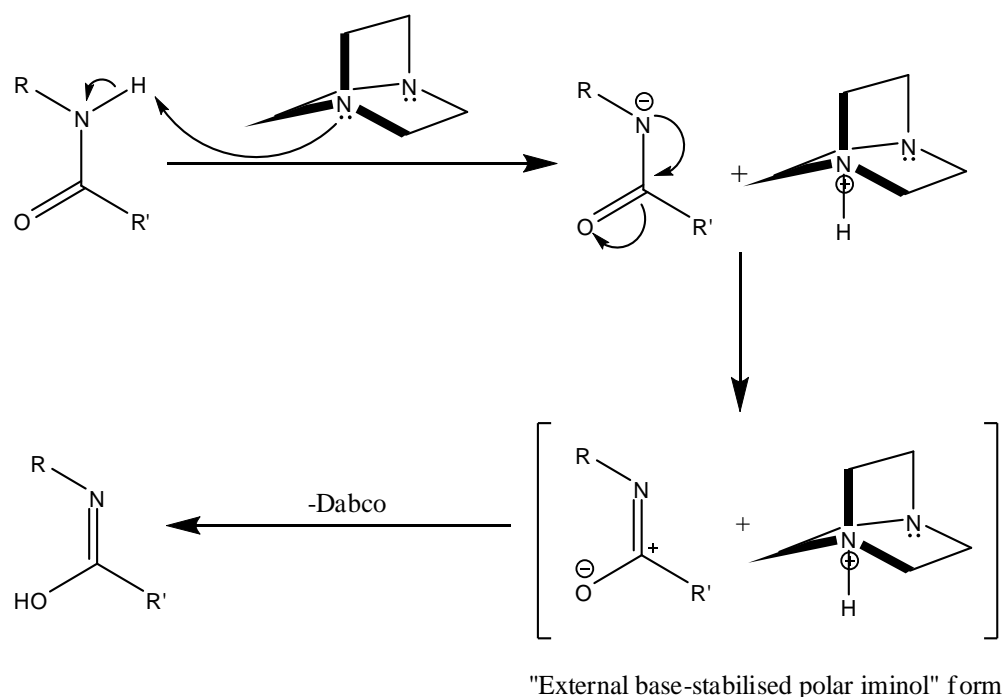
Compound	Coordination	Physical appearance	Yield
<b>286</b>	$\eta^3\text{-PNC-L}^5$	Pale yellow, metallic powder	42%
<b>287</b>	$\eta^3\text{-PNC-L}^6$	Yellow, crystalline powder	51%
<b>288</b>	$\eta^3\text{-PNC-L}^7$	Yellow, crystalline powder	12%

**Table 2.7:** The physical properties and yields for the cyclometallated platinum iminol complexes **286**, **287** and **288**

After six hours the bright yellow cloudy solution was filtered to remove the  $\text{DABCO.HCl}$  formed. The filtrate was then reduced to dryness *in vacuo*, taken up in dichloromethane, washed three times with de-ionised water and dried over  $\text{MgSO}_4$ . The

solution was then reduced to dryness again *in vacuo* and crystallised from dichloromethane-hexane to produce the cyclometallated complexes **286**, **287** and **288** in average yields, **Table 2.7**. Each complex was identified by elemental analysis, IR and NMR spectroscopy, **Section 2.6** and **2.7**.

The DABCO serves three possible roles in this reaction in order to achieve coordination and subsequently cyclometallation of the complexes **286-288** in good yields. Role A, **Figure 2.58**; Role B, **Figure 2.59** and Role C, **Figure 2.60**.<sup>2,43</sup> Firstly, the DABCO can assist in the formation of the iminol by forming an “external base-stabilised polar iminol form” which then allows the nitrogen donor moiety to increase its negative character, **Figure 2.58**.



R = PPh<sub>2</sub> aryl ring system  
R' = Substituent aryl ring system

**Figure 2.58: Role A: Base induced tautomerism of the amide ligands into their iminol form in solution, adapted from Crespo *et al.***<sup>43</sup>

In **Figure 2.58** the tautomerisation step is achieved by deprotonation of the amide N-H bond which results in resonance delocalisation and formation of the iminol. This polar form, as illustrated in **Figure 2.58**, has been identified as stabilised by external bases by Crespo *et al* where triethylamine was used as the external base.<sup>43</sup> From this step, reaction of PtCl<sub>2</sub>(cod) with the HL<sup>5-7</sup> ligands resulted in the formation of the bidentate intermediate through coordination through the phosphorus and nitrogen donor moieties, previously seen for complexes **281-285**.

The second role for DABCO is to form an ion-pair with the HCl formed from the cyclometallation procedure. The phosphinoamide ligands, particularly in the iminol form, are more sensitive to hydrolysis over the analogous iminophosphines and so an ion-pair base is necessary; Role B, **Figure 2.59**.

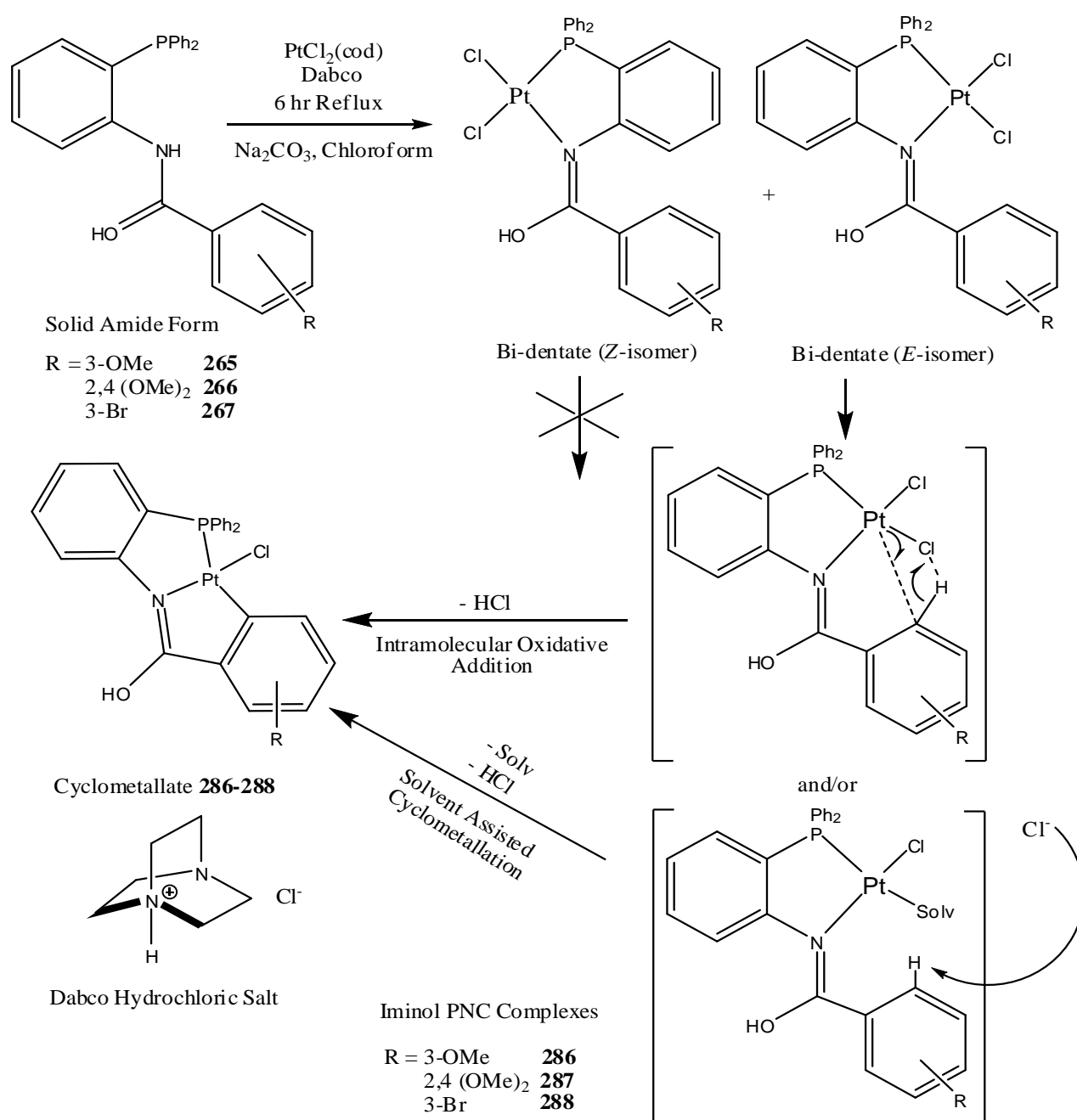


**Figure 2.59: Role B:** Cyclometallation of the *E*-isomer iminol Pt (II) complexes by removing the HCl formed from the reaction.

In Role B, **Figure 2.59**, the cyclometallate is formed from the *E*-isomer of the bidentate intermediate via intramolecular oxidative addition and by a solvent assisted mechanism as previously discussed in the context of the iminophosphine complexes in

**Section 2.4.5.** The Z-isomer cannot form cyclometallates and both bidentate intermediates form dimers with each other and themselves.

Finally, work by Crespo *et al* has reported a third role for DABCO (and other external bases such as triethylamine) which is that it can also assist in cyclometallation, Role C, **Figure 2.60**. In their work they also report that the process is solvent dependent and in order to facilitate the formation of a metal-C<sub>aryl</sub> bond, a carbanion is generated by transfer of a proton to the external base.<sup>43</sup>

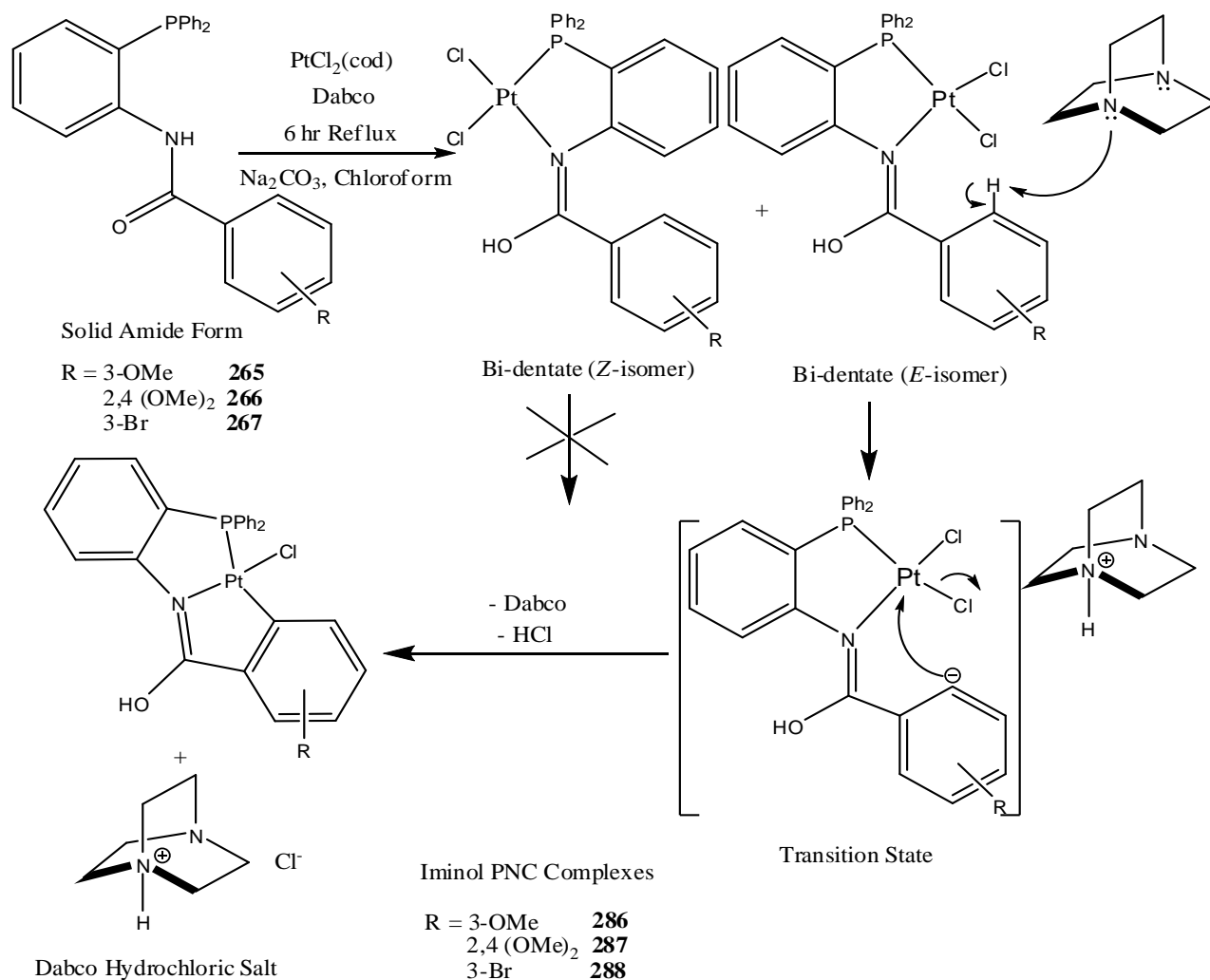


**Figure 2.60: Role C:** The proposed ion-pair cyclometallation of the (E-isomer) iminol platinum complexes via assistance by an external base, DABCO.<sup>43</sup>

The anionic carbon attacks the electrophilic Pt (II) metal centre with simultaneous elimination of a chloride, thus generating an ion-pair with the protonated external base (DABCO hydrochloric acid), **Figure 2.60**. Work by Crespo *et al* has found that this mechanism is most prominent in polar, non-protic solvents such as chloroform as used here. This further facilitates the transition state, **Figure 2.60**, which results in formation of the Pt-

$C_{aryl}$  bond formation. In the presence of solvents such as methanol, ion-pairs do not significantly influence the cyclometallation process due to the solvents' own participation in the cyclometallation process.

Attempts were made to increase the yields by refluxing for longer periods of time (up to 72 hours). However, the reactions involving ligands  $HL^5$  **265** and  $HL^7$  **267** in particular resulted in extensive hydrolysis of the complexes, ligands and intermediates which as a result produced lower yields of the cyclometallates.

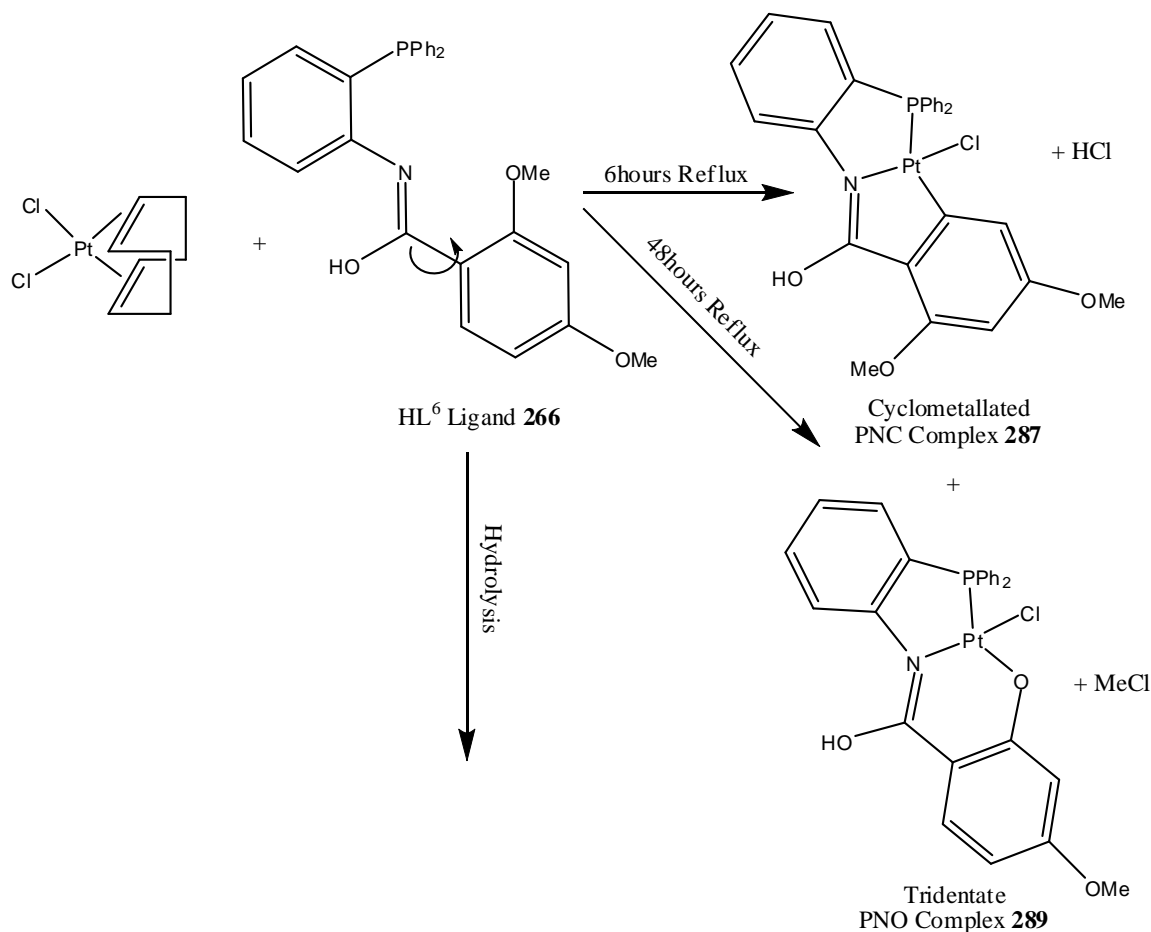


**Figure 2.61:** The formation of a secondary PNO product **289** from the *E*-isomer of the  $HL^6$  ligand as well as the cyclometallated PNC complex **287** in a similar manner to that which was seen for the iminophosphine ligand  $HL^4$  and its multiple products.

For the dimethoxy ligand  $HL^6$  **266** after 48 hours reflux the yield of the previously identified cyclometallate  $[Pt(\eta^3\text{-PNC-L}^6)\text{Cl}]$  **287** was reduced like that found for the other two ligands  $HL^5$  and  $HL^7$ . However, a secondary tridentate PNO type product  $[Pt(\eta^3\text{-PNO-L}^6)\text{Cl}]$  was identified in very low yields, **Figure 2.61**. Efforts to increase the yield of this PNO complex **289** were unsuccessful despite using different solvents (such as acetonitrile) and increasing the reflux time. Isolation of this compound from the cyclometallated product

**287** was also very difficult as it was found to be sensitive to the slight acidic nature of silica gel, which caused hydrolysis.

Using a variety of solvent systems and a more neutral alumina column also failed but recrystallisation techniques with dichloromethane and hexane did reduce the amount of the cyclometallated complex **287**. This left the PNO product as the majority compound which was then identified by IR and NMR spectroscopy. The product is proposed to be formed in a similar way to the iminophosphine PNO complex identified earlier in Sections 2.5.4 and 2.5.6 with ligand bond rotation bringing the methoxy group nearer to the metal centre, **Figure 2.61**.

The reaction mechanism for all the phosphinoiminol complexes is proposed to take place via numerous intermediates previously isolated for the analogous iodo complexes but not characterised here due to insolubility. The bidentate intermediate is again proposed as seen for the iminophosphine complexes along with a monodentate intermediate with coordination solely through the phosphine.

## 2.6 Infra-red spectroscopic studies

### 2.6.1 Iminophosphine ligands HL<sup>1-4</sup> (261-264) and their Pt (II) complexes [Pt( $\eta^2$ -PN-L<sup>1-3</sup>)Cl] (271-273), [Pt( $\eta^3$ -PNC-L<sup>1-4</sup>)Cl] (281-284) and [Pt( $\eta^3$ -PNO-L<sup>4</sup>)Cl] (285):

In the iminophosphine ligands and their complexes the most informative peak given by IR spectroscopy is the stretching band of the imine bond,  $\nu(\text{C}=\text{N})$ . The uncoordinated ligands typically exhibit a strong stretching band at *ca.* 1600  $\text{cm}^{-1}$  for this bond. The  $\nu(\text{C}=\text{N})$  values for ligands HL<sup>1-4</sup> **261-264** along with their corresponding bidentate and tridentate iminophosphine chloride complexes as synthesised from PtCl<sub>2</sub> (Method A) or PtCl<sub>2</sub>(cod) (Method B) are displayed in **Table 2.8** and **Table 2.9**.

Ligand HL <sup>1-3</sup>	$\nu(\text{C}=\text{N})$ $\text{cm}^{-1}$	[Pt( $\eta^2$ -PN-L <sup>1-4</sup> )Cl <sub>2</sub> ]	$\nu(\text{C}=\text{N})$ $\text{cm}^{-1}$	[Pt( $\eta^3$ -PNC-L <sup>1-3</sup> )Cl]	$\nu(\text{C}=\text{N})$ $\text{cm}^{-1}$
HL <sup>1</sup> <b>261</b>	1626	<b>271</b>	1595	<b>281</b>	1585
HL <sup>2</sup> <b>262</b>	1621	<b>272</b>	1591	<b>282</b>	1587
HL <sup>3</sup> <b>263</b>	1622	<b>273</b>	1584	<b>283</b>	1575

*Table 2.8: The  $\nu(\text{C}=\text{N})$  values for ligands HL<sup>1-3</sup> along with their analogous bidentate and tridentate complexes from the PtCl<sub>2</sub> starting material (METHOD A).*



Ligand HL <sup>4</sup>	$\nu(\text{C}=\text{N})$ cm <sup>-1</sup>	[Pt( $\eta^2$ -PN-L <sup>4</sup> )Cl <sub>2</sub> ]	$\nu(\text{C}=\text{N})$ cm <sup>-1</sup>	[Pt( $\eta^3$ -PNC-L <sup>4</sup> )Cl] [Pt( $\eta^3$ -PNO-L <sup>4</sup> )Cl]	$\nu(\text{C}=\text{N})$ cm <sup>-1</sup>
HL <sup>4</sup> <b>264</b>	1615	<b>274</b>	1589	<b>284</b>	1578
HL <sup>4</sup> <b>264</b>	1615	<b>274</b>	1589	<b>285</b>	1606

*Table 2.9: The  $\nu(\text{C}=\text{N})$  values for the ligand HL<sup>4</sup> along its analogous bidentate and tridentate PNO complex from the PtCl<sub>2</sub>(cod) starting material (METHOD B).*

Successful coordination of the imino-nitrogen to the platinum metal centre results in a reduction in the stretching frequency of the imine functionality from *ca.* 1620cm<sup>-1</sup> for the free ligands to *ca.* 1590cm<sup>-1</sup> for the bidentate intermediates, **271-274**, **Figure 2.62**. There is then a further reduction upon cyclometallation to the tridentate species to *ca.* 1580cm<sup>-1</sup> for complexes **281-283**, **Figure 2.62**. This confirms the presence of an imine-Pt bond in all of these complexes. Multiple aromatic stretching bands were also observed for the free ligands and the complexes at *ca.* 1450cm<sup>-1</sup> corresponding to aromatic carbon stretches.

The reduction in stretching frequency of the C=N bond in the complexes is due to the weakening and stretching of the C=N imine bond as a result of Pt-N bond formation which pulls electron density from the nitrogen interaction into the empty d-orbitals of the Pt (II) metal centre.<sup>83,84</sup> The large reduction in the stretching frequency for the tridentate cyclometallates, **281-284**, compared to that for the bidentate complexes, can be attributed to the formation of a sterically rigid, fixed geometry composed of two five-membered rings, around the electrophilic Pt(II) metal centre resulting in additional lengthening, and hence weakening, of the imine bond **Figure 2.62**.

The 2,3-(OMe)<sub>2</sub> iminophosphine complexes **274**, **284** and **285** also display the same trend of reduction in stretching frequency of the imine functionality in comparison with the free ligand HL<sup>4</sup> **264**, **Table 2.9**. However, there is significant difference in the imine stretching frequencies between the cyclometallated complex **284** and the PNO complex **285** which are both formed from the same ligand.

In the case of the PNO type complex [Pt( $\eta^3$ -PNO-L<sup>4</sup>)Cl] **285**, we see a higher  $\nu(\text{C}=\text{N})$  than that of the cyclometallated PNC complex [Pt( $\eta^3$ -PNC-L<sup>4</sup>)Cl] **284**. This would indicate that the imine bond of the PNO complex **285** is stronger than that of the cyclometallated complex **284**. For the PNO tridentate complex **285** a mixture of a five-membered ring and a six-membered ring are formed instead upon cycloplatination, **Figure 2.62**, resulting in a less sterically rigid complex and therefore causing less weakening of the imine bond which can be seen in **Table 2.9**.

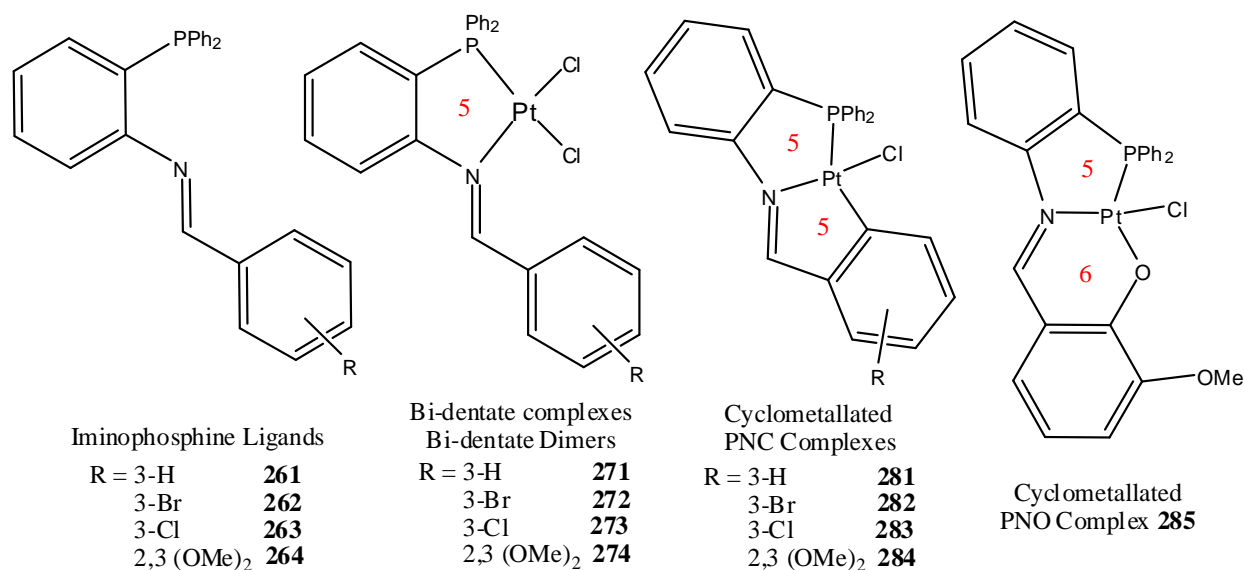


*Figure 2.62: The range of complexes described in this section with the types of rings formed upon coordination and cyclometallation highlighted.*

This concept will be discussed further on in this chapter and it is also worth noting that the stretching frequency of the C=N bond for the PNO complex [Pt( $\eta^3$ -PNO-L<sup>4</sup>)Cl] **285** matches that obtained previously by this research group in the alternative synthesis of this compound.<sup>1,45</sup> However, the stretching frequencies for the cyclometallated complexes of this research are significantly higher than that previously reported for similar iodo cyclometallated Pt (II) complexes which would suggest that the C=N imine bond in the chloro cyclometallates is stronger than that found in the iodo counterparts, implying increased stability.<sup>2</sup>

### **2.6.2 Phosphinoamide ligands HL<sup>5-7</sup> (265-267) and their Pt (II) iminol complexes [Pt( $\eta^3$ -PNC-L<sup>5-7</sup>)Cl] (286-288):**

As previously discussed in **Section 2.4.7**, the phosphinoamide ligands HL<sup>5-7</sup> **265**, **266** and **267** tautomerise in solution to the iminol form. This makes a direct comparison between the solid amide ligands and the Pt (II) iminol complexes **286-288** impossible using IR spectroscopy.

IR data for the phosphinoamide ligands HL<sup>5-7</sup> and the cyclometallated Pt (II) iminol complexes are given in **Table 2.10**. The amide ligands show the presence of  $\nu$ (C=O) and  $\nu$ (N-H) stretching bands and N-H bending frequencies along with various  $\nu$ (C=C) bands confirming that they exist as the amide tautomer in the solid state.

The platinum iminol cyclometallates **286-288** on the other hand show the presence of  $\nu(\text{C}=\text{N})$  and broad  $\nu(\text{O}-\text{H})$  stretches along with various  $\nu(\text{C}=\text{C})$  bands as well confirming that coordination of the iminol tautomer has occurred. Multiple aromatic stretching bands were also observed for the free ligands and the complexes at *ca.*  $1450\text{cm}^{-1}$  corresponding to aromatic carbon stretches.

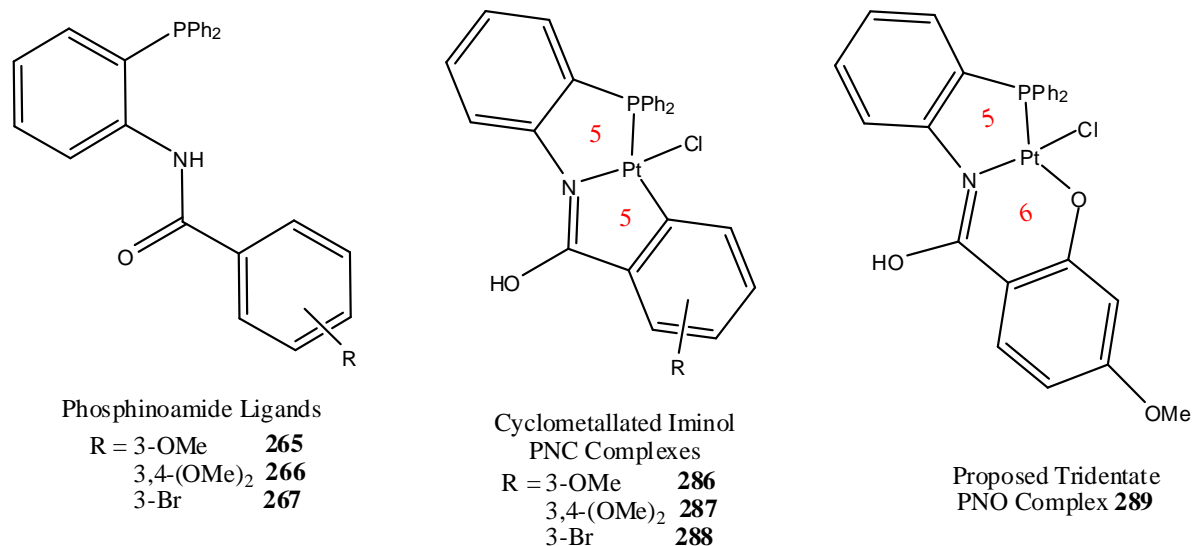


**Figure 2.64:** The range of compounds described in this section with the types of rings formed upon coordination highlighted. The notable stretching bands for each structure are given in **Table 2.10** and **Table 2.11**.

Ligand HL <sup>5-7</sup>	$\nu(\text{C}=\text{O})$ $\text{cm}^{-1}$	$\nu(\text{N}-\text{H})$ $\text{cm}^{-1}$	[Pt( $\eta^3$ -PNC-L <sup>5-7</sup> )Cl]	$\nu(\text{C}=\text{N})$ $\text{cm}^{-1}$	$\nu(\text{O}-\text{H})$ $\text{cm}^{-1}$
HL <sup>5</sup> <b>265</b>	1678	3362	<b>286</b>	1582	3330
HL <sup>6</sup> <b>266</b>	1649	3275	<b>287</b>	1575	3323
HL <sup>7</sup> <b>267</b>	1675	3366	<b>288</b>	1579	3328

**Table 2.10:** The  $\nu(\text{C}=\text{O})$  and  $\nu(\text{N}-\text{H})$  values for ligands HL<sup>5-7</sup> along with the  $\nu(\text{C}=\text{N})$  and  $\nu(\text{O}-\text{H})$  values for their analogous cyclometallated complexes **286-288**.

Ligand HL <sup>6</sup>	$\nu(\text{C}=\text{O})$ $\text{cm}^{-1}$	$\nu(\text{N}-\text{H})$ $\text{cm}^{-1}$	[Pt( $\eta^3$ -PNO-L <sup>5-7</sup> )Cl]	$\nu(\text{C}=\text{N})$ $\text{cm}^{-1}$	$\nu(\text{O}-\text{H})$ $\text{cm}^{-1}$
HL <sup>6</sup> <b>266</b>	1678	3362	<b>289</b>	1606	3331

**Table 2.11:** The  $\nu(\text{C}=\text{O})$  and  $\nu(\text{N}-\text{H})$  values for the ligand HL<sup>6</sup> **266** along with the  $\nu(\text{C}=\text{N})$  and  $\nu(\text{O}-\text{H})$  values for the PNO minor product **289**.

There is a significant difference in the imine stretching frequencies between the cyclometallated complex **287** and the PNO complex **289**, both of which are formed from the same ligand and bidentate intermediate. This is similar to the 2,3-(OMe)<sub>2</sub> iminophosphine ligand, HL<sup>4</sup> **264**, where the HL<sup>6</sup> ligand **266** is also seen to act in the same way with a PNC complex **287** forming as well as a PNO complex **289**, **Figure 2.61**.

In the case of [Pt(η<sup>3</sup>-PNO-L<sup>6</sup>)Cl] **289**, we see a higher ν(C=N) and ν(O-H) than that of the cyclometallate [Pt(η<sup>3</sup>-PNC-L<sup>6</sup>)Cl] **287** which would again indicate that the imine bond of the PNO complex **289** is also stronger than that of its analogous cyclometallated complex **287** like that seen for the iminophosphine complexes in **Section 2.6.1**. The difference in the rings formed during coordination can influence the imine stretching frequencies as highlighted in **Figure 2.64**.

## 2.7 NMR spectroscopic studies

### 2.7.1 NMR data for the Iminophosphine ligands HL<sup>1-4</sup> (261-264):

<sup>1</sup>H and <sup>31</sup>P{<sup>1</sup>H} spectroscopic data was obtained for all the iminophosphine ligands **261-264**. <sup>13</sup>C, [<sup>1</sup>H-<sup>1</sup>H] COSY plots and [<sup>13</sup>C DEPT 45-<sup>1</sup>H] HETCOR plots were carried out on the HL<sup>4</sup> ligand as a comparison for the cyclometallated complex **284** which is the most soluble of all the complexes reported and thus the only one for which it was possible to obtain <sup>13</sup>C NMR spectra.

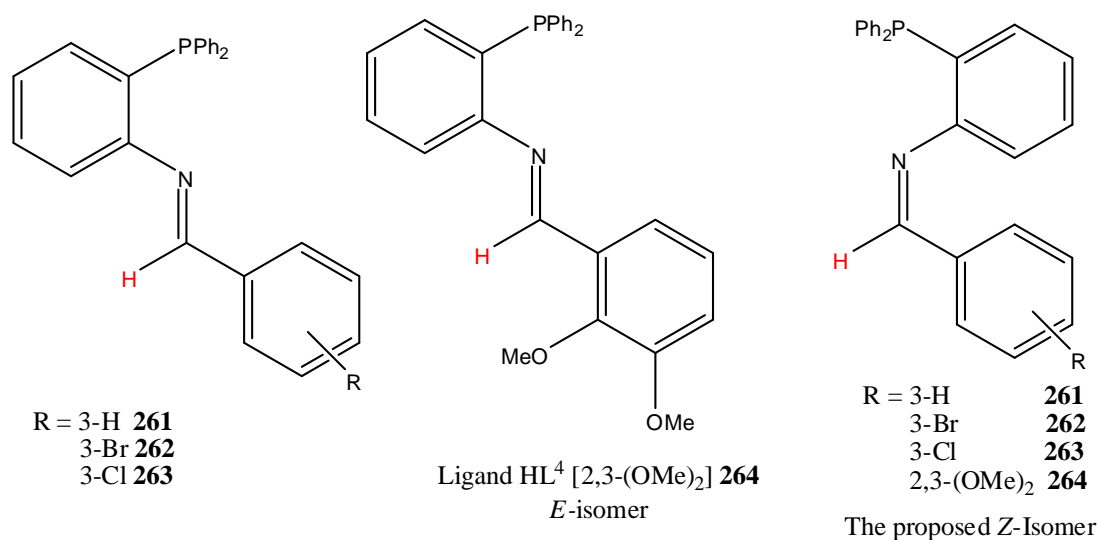


**Figure 2.64:** The iminophosphine ligands with a comparison of the *E* and *Z* possible isomers and the HL<sup>4</sup> ligand which has electron donating substituents unlike the other iminophosphine ligands.

The  $^1\text{H}$  NMR and  $^{31}\text{P}\{^1\text{H}\}$  data of the iminophosphine ligands are summarised in **Table 2.12**. All the spectra exhibit a singlet, integrating for one proton, in the range of  $\delta$  8.07-8.61 ppm which corresponds to the azomethine signal,  $\text{H-C=N}$ , **Figure 2.65**.

For the ligands **261** (3-H), **262** (3-Br) and **263** (3-Cl), a higher field azomethine signal is observed in comparison with the ligand **264** (2,3-(OMe)<sub>2</sub>) which contains two electron donating groups. The presence of the methoxy groups results in a significant deshielding effect and hence causes a further downfield shift of the azomethine signal. From this, it can be concluded that an inductive effect must enhance the strength of the imine C=N bond in the case of **264** in **Figure 2.54**, resulting in a further downfield shift of the azomethine signal.

Ligand	$\delta$ (H-C=N)	$\delta$ (H-Ar)	$\delta$ (R=OCH <sub>3</sub> )	$\delta$ ( $^{31}\text{P}\{^1\text{H}\}$ )
HL <sup>1</sup> <b>261</b>	8.14 (1H, s)	7.00-7.50 (19H, t,q,m,dd,m)	–	-14.2 (s)
HL <sup>2</sup> <b>262</b>	8.07 (1H, s)	6.62-7.75 (18H, t,q,m,dd,d)	–	-13.7 (s)
HL <sup>3</sup> <b>263</b>	8.08 (1H, s)	6.83-7.86 (18H, dd,t,m,q,d)	–	-13.8 (s)
HL <sup>4</sup> <b>264</b>	8.54 (1H, s)	6.52-7.86 (17, dd,t,m,t,q,m)	3.70 (3H, s) 3.85 (3H, s)	-14.5 (s)

1. Chemical shift values ( $\delta$ ) are expressed in ppm relative to the TMS standard for  $^1\text{H}$  and  $\text{H}_3\text{PO}_4$  for  $^{31}\text{P}$ .
2. s, singlet; d, doublet; dd, doublet of doublets; t, triplet; q, quartet; m, multiplet.
3. Coupling constants (J) are measured in Hz

**Table 2.12:**  $^1\text{H}$  and  $^{31}\text{P}\{^1\text{H}\}$  NMR data<sup>1,2,3</sup> for the iminophosphine ligands HL<sup>1-4</sup> **261-264** in  $\text{CDCl}_3$  at 300 MHz and 121.5 MHz respectively.

The  $^1\text{H}$  NMR spectra of the HL<sup>4</sup> ligand **264** also displays two singlet resonances at  $\delta$  3.70 and  $\delta$  3.85 ppm respectively. These correspond to the two methoxy (-OCH<sub>3</sub>) substituents present at the C-3 and C-2 position of the lower aryl ring and integrate for 3 hydrogens each. The aromatic signals for the iminophosphine ligands HL<sup>1-4</sup> are found with significant overlapping in the range of  $\delta$  6.45-7.81 ppm. [ $^1\text{H}$ - $^1\text{H}$ ] COSY plots, **Figure 2.65**, along with [ $^{13}\text{C}$  DEPT 45- $^1\text{H}$ ] HETCOR plots, **Figure 2.66**, were required to fully characterise the relative positions of the aromatic protons on the ligand.

The integrations of these aromatic protons were 19H (**261**), 18H (**262** and **263**) and 17H (**264**) respectively as expected. It was found to be very difficult to fully assign these signals for all the iminophosphine ligands due to signal overlaps. Only the HL<sup>4</sup> ligand gave

observable differences between the aromatic signals with only some overlapping signals observed. This allowed for a full characterisation of the individual aromatic proton signals.

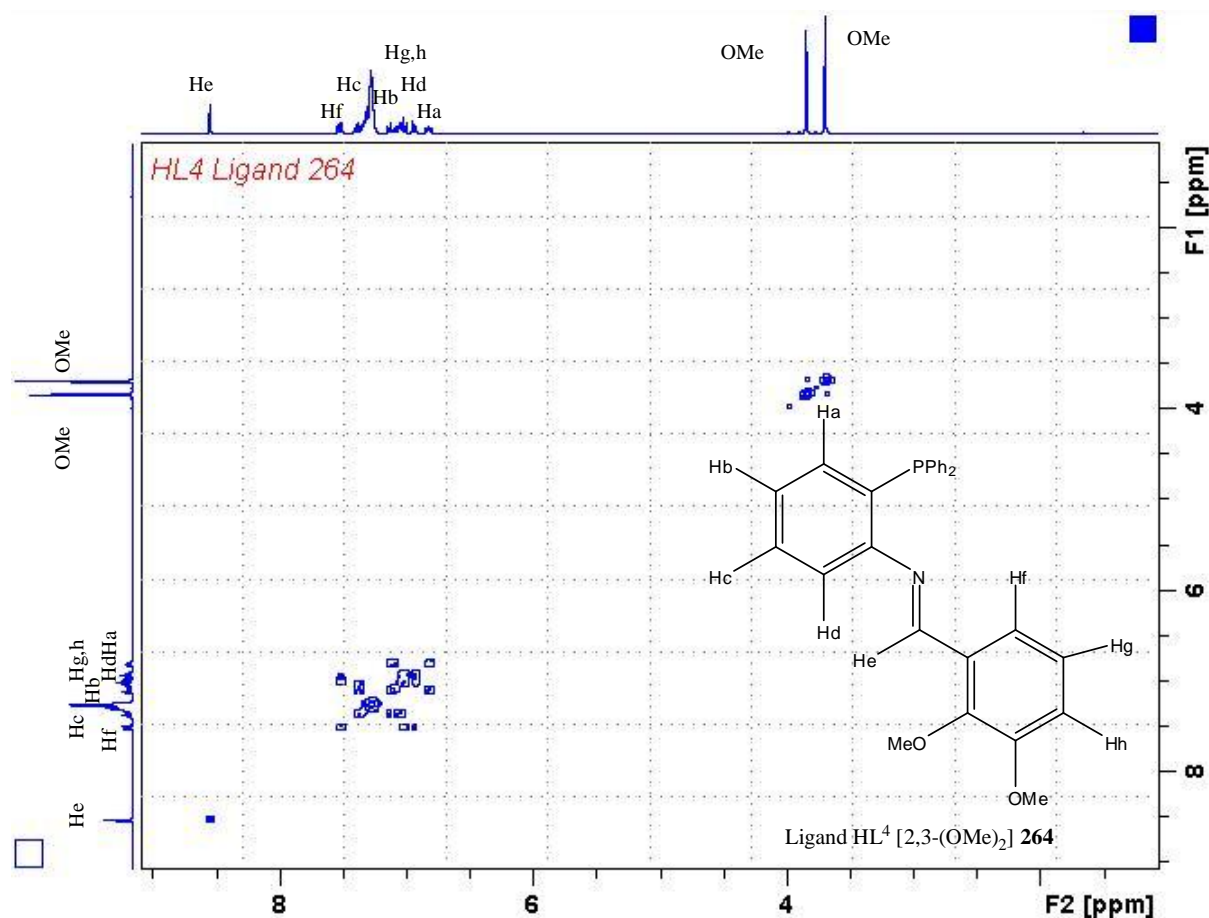


Figure 2.65: The [ $^1\text{H}$ - $^1\text{H}$ ] COSY NMR plot of the  $\text{HL}^4$  ligand 264 showing the interactions between the aromatic hydrogens as well as the position of the methoxy groups  $\text{OCH}_3$  and azomethine group  $\text{H}_e\text{-C}=\text{N}$  run at 300 MHz.

$\delta(^1\text{H})$ ppm	Peak Assignment	Observed Correlations
6.88 m	(Ha)	(Hb, Hc)
6.92 dd	(Hh)	(Hg, Hf)
7.05 d,q	(Hd, Hg)	(Hc, Hh)
7.14 t	(Hb)	(Ha, Hc, Hd)
7.20-7.35 m	Phosphinophenyl	Phosphinophenyl
7.37, t	(Hc)	(Ha, Hb, Hd)
7.53, dd	(Hf)	(Hg, Hh)

Table 2.13: Measured [ $^1\text{H}$ - $^1\text{H}$ ] COSY NMR correlations for the  $\text{HL}^4$  ligand 264.

From the [ $^1\text{H}$ - $^1\text{H}$ ] COSY plot in **Figure 2.65** of the  $\text{HL}^4$  ligand **264**, the aromatic protons in the region of 7.24-7.35 ppm can be assigned to the aromatic protons (10H) on the  $\text{PPh}_3$  group which only couple to each other. The other aromatic protons (7H) along with the azomethine and methoxy signals are assigned individually in **Figure 2.65**. The signal that resonated as a series of four doublets in the region 6.88 ppm with a coupling value ( $J$ ) of 7.62 Hz is due to the coupling to the phosphorus atom as well as the neighbouring aryl protons on the upper aryl ring.

For the corresponding (3-Br)  $\text{HL}^2$  **262** and (3-Cl)  $\text{HL}^3$  **263** ligands, the aromatic regions also showed three sets of signals in the range of 7.87-7.45 ppm corresponding to the protons on the aryl ring (4H) where the  $\text{PPh}_2$  substituent is attached. More aromatic signals at 7.45-7.10 ppm correspond to the  $\text{PPh}_2$  protons (10H) and finally at 6.85-7.20 ppm which correspond to the aryl protons of the salicyladimine (4H) ring. The multiplet signals for the aromatic region of these ligands though were much more complicated in comparison to the  $\text{HL}^4$  ligand **264** which meant it was impossible to assign the individual aromatic hydrogens with certainty for **261-263**.

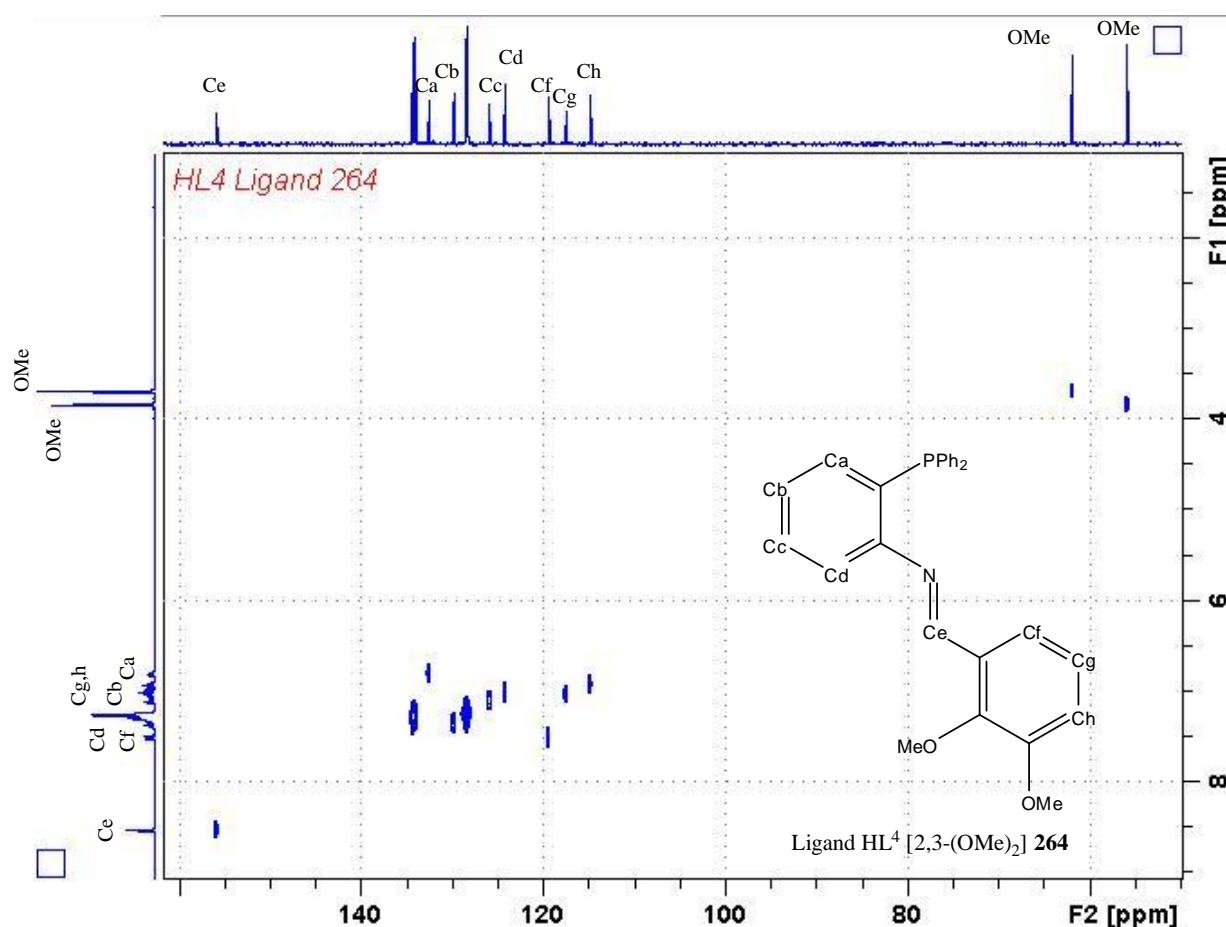


**Figure 2.66:** The [ $^{13}\text{C}$  DEPT 45 - $^1\text{H}$ ] HETCOR NMR plot of the  $\text{HL}^4$  ligand **264** showing the relationship between the carbons and protons present in the compound run at 300 MHz.

$^{13}\text{C}$  NMR data was also obtained for the  $\text{HL}^4$  ligand in order to compare the spectra with its coordinated platinum cyclometallated complex **284**, **Section 2.6.3**. In addition to various  $^{13}\text{C}$  and DEPT NMR experiments, a [ $^{13}\text{C}$  DEPT 45- $^1\text{H}$ ] HETCOR plot, **Figure 2.66**, was also obtained in order to better associate the individual aromatic CH signals with the  $^1\text{H}$  NMR spectra obtained for the  $\text{HL}^4$  ligand **264**.

In the  $^{13}\text{C}$  NMR spectra the doublet signal at 155.88 ppm was attributed to the carbon atom of the imine bond ( $\text{HC}=\text{N}$ ) which was also supported by the [ $^{13}\text{C}$  DEPT 45- $^1\text{H}$ ] HETCOR plot, **Figure 2.66**. It appears as a doublet due to  $^4\text{J}$  (1.51 Hz) coupling to the phosphorus donor moiety. The signals at 61.93 and 55.85 ppm were assigned to each carbon atom of the two methoxy substituent groups  $-\text{OCH}_3$ . Interestingly, the methoxy signals were found to be doublets, which may be tentative evidence for the existence of *E/Z* isomers in the iminophosphine ligands, similar to that found for the phosphinoamide ligands  $\text{HL}^{5-7}$  **265-267**, which is discussed in detail in **Section 2.7.2**. However, this is the only spectroscopic evidence for the iminophosphine *Z*-isomer at this time and will be discussed further in **Section 2.7.3**.

Strong multiple overlapping signals at 134.05-134.32 ppm and 128.28-128.50 ppm were assigned to the phosphinophenyl carbons as per the [ $^{13}\text{C}$  DEPT 45- $^1\text{H}$ ] HETCOR plot. Individual signals found from 114.80 ppm to 124.18 ppm were assigned to the salicyladimine ring while the remaining signals at 128.37-132.55 ppm were assigned to the aromatic hydrogens on the aryl ring with the  $\text{PPh}_2$  substituent using the results from the [ $^1\text{H}$ - $^1\text{H}$ ] COSY plot as a reference, **Figure 2.65**.

The phosphorus NMR spectra,  $^{31}\text{P}$  { $^1\text{H}$ }, of each ligand  $\text{HL}^{1-4}$ , displays a singlet resonance in the range of  $\delta$  -12.6 to -14.0 ppm which corresponds to the single phosphorus environment in the ligand. The starting material (2-diphenylphosphinoaniline) displays a peak at  $\delta$  -21 ppm not present in the final spectra of the ligand, indicating a shift of  $\delta$  6 – 8 ppm upon formation of the ligand. Also no evidence of the aldehyde was seen in the  $^1\text{H}$  NMR where a peak at *ca.* 10ppm would normally occur, indicating successful formation of the imine ligand.

### **2.7.2 NMR data for the Phosphinoamide ligands $\text{HL}^{5-7}$ (265-267)**

$^1\text{H}$  and  $^{31}\text{P}$ { $^1\text{H}$ } spectroscopic data was obtained for the phosphinoamide ligands **265-267**.  $^{13}\text{C}$ , [ $^1\text{H}$ - $^1\text{H}$ ] COSY plots and [ $^{13}\text{C}$  DEPT 45- $^1\text{H}$ ] HETCOR plots were also undertaken on the  $\text{HL}^6$  ligand as a comparison for its analogous cyclometallated complex **288** which is the most soluble of all the phosphinoamide complexes reported and thus the only one for





The integrations of these aromatic hydrogens were 18H (**265** and **267**) and 17H (**264**) respectively as expected for the proposed structure for the ligands in solution. It was found to be very difficult to fully resolve these signals for all the phosphinoamide ligands because of the overlapping signals. For the HL<sup>5</sup> **265** and HL<sup>7</sup> **267** ligands, the aromatic regions showed three sets of signals in the range of 8.43-7.48 ppm corresponding to the hydrogens on the phosphine and nitrogen substituted aryl ring (4H), 7.48-7.20 ppm corresponding to the phosphinophenyl protons (10H) and finally 7.20-6.95 ppm which correspond to the aryl protons of the salicyladimine (4H) roughly.

The multiple overlapping signals for these ligands meant it was impossible to assign the individual aromatic hydrogens with certainty. Only the HL<sup>6</sup> ligand **266** gave identifiable differences between the aromatic signals with just some overlapping observed in the spectra. This allowed for a full characterisation of the individual aromatic hydrogen signals using a [<sup>1</sup>H-<sup>1</sup>H] COSY plot, **Figure 2.68**, along with a [<sup>13</sup>C DEPT 45-<sup>1</sup>H] HETCOR plot, **Figure 2.69**, and identified the different isomers present as seen in **Figure 2.67**.

Ligand	$\delta$ (HO-C=N)	$\delta$ (H-Ar)	$\delta$ (R=OCH <sub>3</sub> )	$\delta$ ( <sup>31</sup> P{ <sup>1</sup> H})
HL <sup>5</sup> <b>265</b>	8.84 (1H, d) <sup>6</sup> J <sub>P-H</sub> =8	6.96-8.43 (18H, t,q,m,dd,m)	3.81 (3H, s)	-19.8 (s)
HL <sup>6</sup> <b>265</b>	10.50 (1H, d) <sup>6</sup> J <sub>P-H</sub> =6	6.43-8.47 (17H, dd,t,m,t,m)	3.86 (3H, s) 3.79 (3H, s)	-17.7 (s)
HL <sup>7</sup> <b>267</b>	8.60 (1H, d) <sup>6</sup> J <sub>P-H</sub> =8	6.95-8.34 (18H, dd,t,m,q,d)	–	-18.7 (s)

1. Chemical shift values ( $\delta$ ) are expressed in ppm relative to the TMS standard for <sup>1</sup>H and H<sub>3</sub>PO<sub>4</sub> for <sup>31</sup>P.
2. s, singlet; d, doublet; dd, doublet of doublets; t, triplet; q, quartet; m, multiplet.
3. Coupling constants (J) are measured in Hz

**Table 2.14:** The <sup>1</sup>H and <sup>31</sup>P{<sup>1</sup>H} NMR spectra<sup>1, 2, 3</sup> recorded for the phosphinoamide ligands HL<sup>5-7</sup> **265-267** in CDCl<sub>3</sub> at 300 MHz and 121.5 MHz respectively.

The <sup>1</sup>H NMR spectra of the HL<sup>6</sup> ligand **266** also displays two singlet resonances at  $\delta$  3.84 and  $\delta$  3.79 ppm respectively corresponding to the major *E*-isomer (due to the relative intensities of the signals and thermodynamically favourable structure). The spectra of the HL<sup>5</sup> ligand **265** on the other hand display a single resonance at  $\delta$  3.81 ppm, also corresponding to the *E*-isomer. These are assigned to the electron donating methoxy (-OCH<sub>3</sub>) substituents

present at the C-2 and C-4 position of the aryl ring system for the HL<sup>6</sup> ligand and at the C-3 position for the HL<sup>5</sup> ligand, all of which integrate for 3 hydrogens each. For the HL<sup>6</sup> ligand there are also a second set of methoxy signals at  $\delta$  3.68 and 3.71 ppm corresponding to the methoxy groups on the Z-isomer.

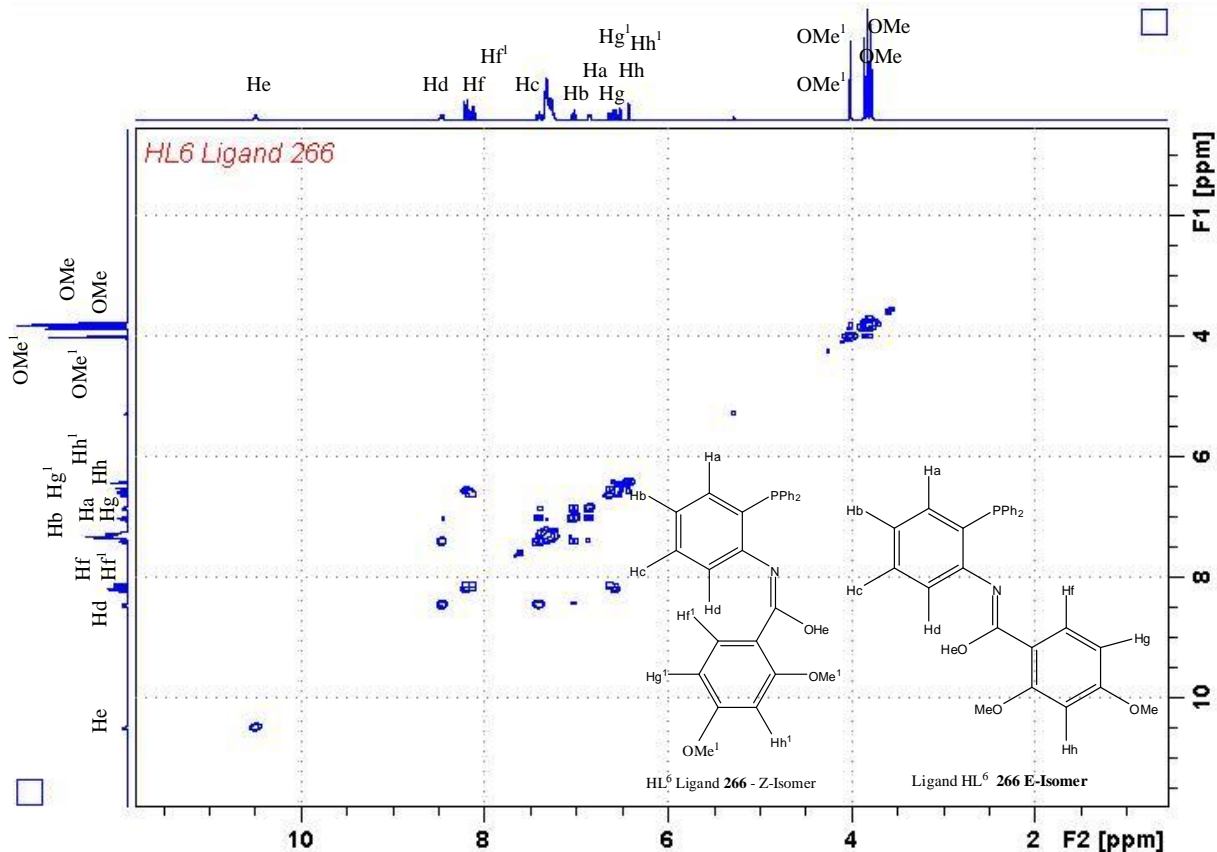


Figure 2.68: The [<sup>1</sup>H-<sup>1</sup>H] COSY NMR plot of the HL<sup>6</sup> ligand 266 showing the interactions between the aromatic hydrogens as well as the position of the methoxy groups OCH<sub>3</sub> and hydroxyl group HO-C=N run at 300 Mhz.

$\delta(^1\text{H})$ ppm	Peak Assignment	Observed Correlations
6.42 dd	(Hf)	(Hg)
6.42-6.51 m	(Hg)	(Hf, Hh)
7.85 q	(Ha)	(Hb,Hc)
7.19 t	(Hb)	(Ha, Hc, Hd)
7.24-7.38 m	Phosphinophenyl	Phosphinophenyl
7.43, t	(Hc)	(Ha, Hb, Hd)
8.21, dd	(Hf)	(Hg)
8.47, m	(Hd)	(Hc, Hb)

**Table 2.15:** Measured [ $^1\text{H}$ - $^1\text{H}$ ] COSY NMR correlations for the  $\text{HL}^6$  ligand **266**.

The aromatic protons in the region of 7.24-7.38 ppm are attributed to the phosphinophenyl protons (10H) which only couple to each other. The rest of the aromatic hydrogens (7H) along with the hydroxyl and methoxy signals are assigned individually in **Figure 2.68** as per their correlations outlined in **Table 2.17**.

$^{13}\text{C}$  NMR data was also collected for the  $\text{HL}^6$  ligand in order to compare the spectra with its coordinated platinum cyclometallated complex **288**, **Section 2.7.4**. The cyclometallated 2,4-(OMe) $_2$  complex **288** was the only phosphinoamide complex sufficiently soluble to enable  $^{13}\text{C}$  spectra to be obtained.

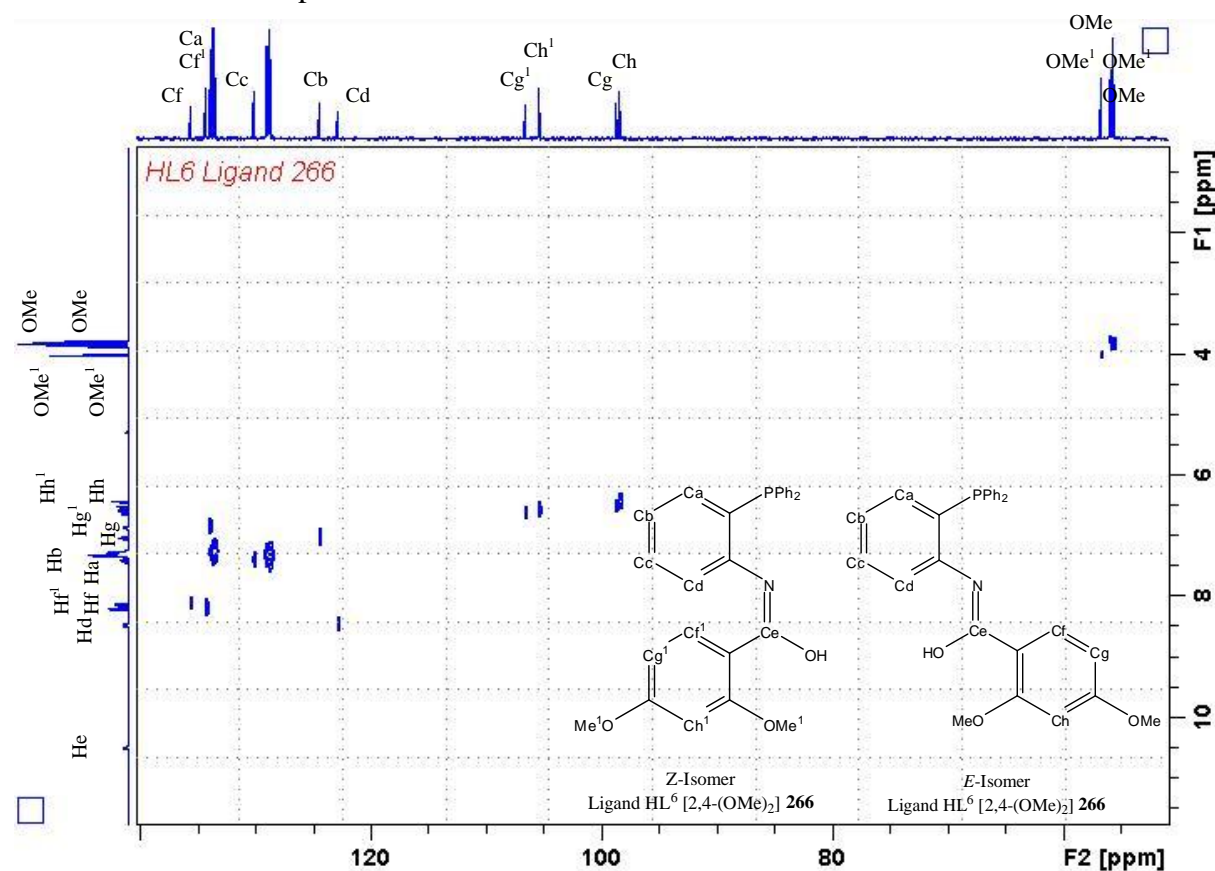


**Figure 2.69:** The [ $^{13}\text{C}$  DEPT 45- $^1\text{H}$ ] HETCOR NMR plot of the  $\text{HL}^6$  ligand **266** showing the relationship between the carbons and protons present in the compound run at 300 MHz/75.5MHz.

In addition to various  $^{13}\text{C}$  and DEPT NMR data, a [ $^{13}\text{C}$  DEPT 45- $^1\text{H}$ ] HETCOR plot, **Figure 2.69**, was also obtained in order to better associate the individual aromatic CH signals with the  $^1\text{H}$  NMR spectra obtained for the  $\text{HL}^6$  ligand **266**. This was also completed in order to later compare it to the analogous spectra obtained for the platinum coordinated complex **288** which is synthesised from the  $\text{HL}^6$  ligand in **Section 2.6.3**.

From the [ $^{13}\text{C}$  DEPT 45- $^1\text{H}$ ] HETCOR plot, strong multiple overlapping signals at 135.23-133.48 ppm and 128.95-128.67 ppm were assigned to the phosphinophenyl carbons. Individual signals found from 98.65 ppm to 124.40 ppm were assigned to the salicyladimine ring of each isomer while the remaining signals at 128.37-135.58 ppm were assigned to the aromatic hydrogens on the phosphino-imine aryl ring using the results from the [ $^1\text{H}$ - $^1\text{H}$ ] COSY plot as a further reference, **Figure 2.68**.

Interestingly, there were two carbon signals corresponding to some aromatic hydrogens according to the [ $^{13}\text{C}$  DEPT 45- $^1\text{H}$ ] HETCOR plot, **Figure 2.69**. The signals at 55.56, 55.80, 55.85 and 56.63 ppm were assigned to each carbon atom of two sets of the two methoxy substituent groups  $-\text{OCH}_3$ . There were also two carbon signals for each aromatic hydrogen on the salicyladimine ring (Hf, Hg and Hh, **Figure 2.69**), but not for the phosphine and nitrogen substituted ring. It is therefore proposed that there are two different salicyladimine ring environments present which would indicate the presence of the *E/Z* isomers.

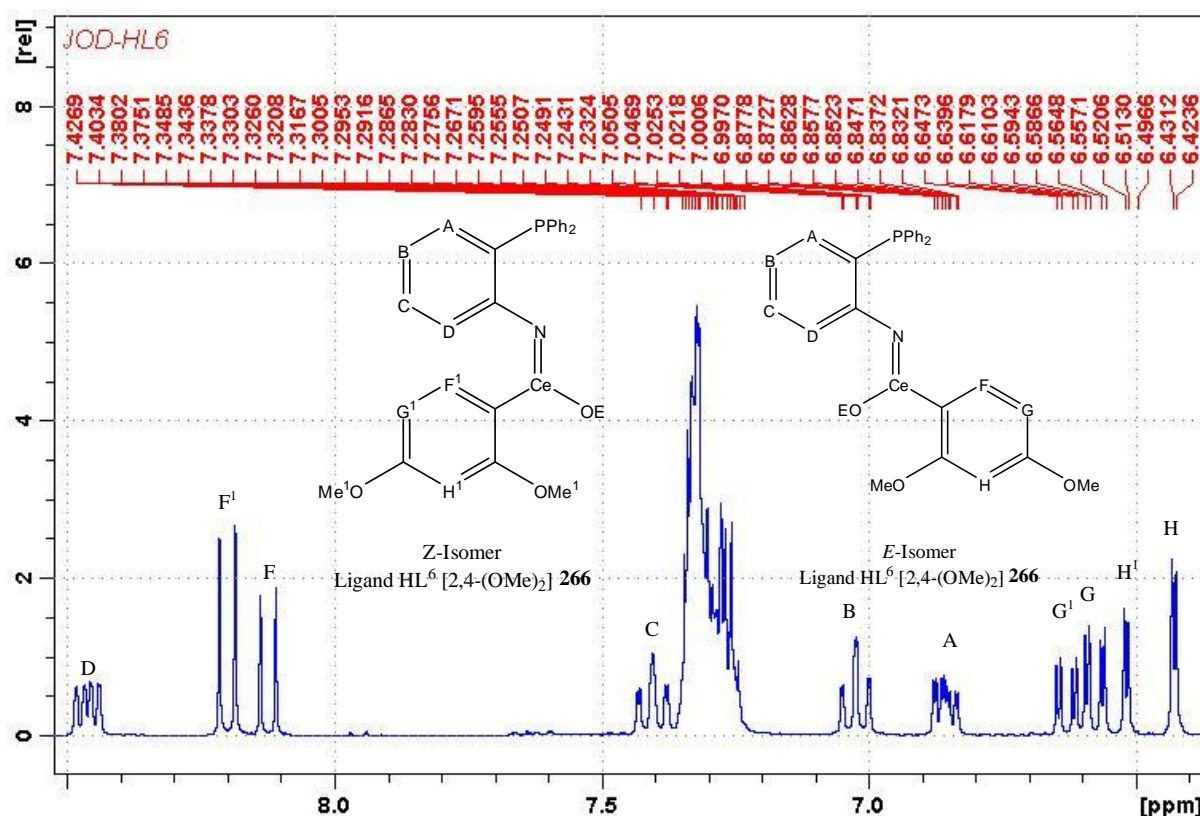


**Figure 2.70:** An expansion of the  $^1\text{H}$  NMR spectra of the  $\text{HL}^6$  ligand **266** showing the aromatic signals and inset: the structures of the isomers with the hydrogens removed for clarity, run at 300 MHz.

Further NMR studies run at 600 MHz to confirm the existence of the two isomers include a DEPTQ (a comparison of  $^{13}\text{C}$  quaternary signals with CH,  $\text{CH}_2$  and  $\text{CH}_3$  signals), a HSQC (similar to a HETCOR plot except for neighbouring carbons), a HMBC (a 2D plot showing the relationship between the  $^{13}\text{C}$  DEPTQ spectra and  $^1\text{H}$  NMR up to 2-3 bonds away) and a NOESY plot (showing protons that have a relationship through space up to  $5\text{\AA}$ ). From these studies and the  $^1\text{H}$  NMR it was determined that the isomers are in a 3:1 ratio with the preferred *E*-isomer in the majority as determined by the relative intensities of the signals and taking the *E*-isomer as the more thermodynamically stable structure.

In the *Z*-isomer no relationship between the Hf and Hd aromatic hydrogens was identified by the NOESY plot, indicating that the salicyladimine ring is in fact twisted where the Hd proton is pointing into the centre of the salicyladimine ring. Efforts to separate the isomers by various chromatographic methods were unsuccessful at the present time.

The phosphorus NMR spectra,  $^{31}\text{P}\{^1\text{H}\}$ , of each ligand  $\text{HL}^{1-4}$ , displays a singlet resonance in the range of  $\delta$  -17.7 to -18.8 which corresponds to the single phosphine present in the ligand. Interestingly only one signal was seen for both isomers, further proving that the change in the salicyladimine environment is the only observable spectrographic difference between the two isomers.

The starting material (2-diphenylphosphinoaniline) displays a peak at -21ppm, which is not present in the spectra of the ligand, indicating that the reaction of the starting materials has gone to completion. Also no evidence of the acyl chloride was seen in the  $^1\text{H}$  NMR where a peak at *ca.* 10ppm would normally occur, again indicating completion of the ligand reactions.

### **2.7.3 NMR spectra for the tridentate Pt(II) iminophosphine complexes $[\text{Pt}(\eta^3\text{-PNC-L}^{1-4})\text{Cl}]$ **281-284** and $[\text{Pt}(\eta^3\text{-PNO-L}^4)\text{Cl}]$ **285**:**

$^1\text{H}$  and  $^{31}\text{P}\{^1\text{H}\}$  spectroscopic data was obtained for all the cyclometallated complexes  $[\text{Pt}(\eta^3\text{-PNC-L}^{1-4})\text{Cl}]$  **281-284** and the PNO complex  $[\text{Pt}(\eta^3\text{-PNO-L}^4)\text{Cl}]$  **285**.  $^{13}\text{C}$ ,  $[\text{H}-^1\text{H}]$  COSY plots and  $[\text{C DEPT } 45\text{-}^1\text{H}]$  HETCOR plots were also completed for the dimethoxy cyclometallated complex **284** which is the most soluble of all the platinum complexes reported. A downfield shift in the  $^1\text{H}$  NMR spectra of the azomethine resonance frequency from *ca.* 8.20 ppm for the free ligands  $\text{HL}^{1-4}$  **261-264** to *ca.* 9.40ppm for the cyclometallated complexes **281-284**. The downfield shift observed indicates successful coordination of the imino-nitrogen to the Pt (II) metal centre.

Coordination of the imino-nitrogen to the metal centre, electron density is pulled towards the coordination bond (Pt-N), weakening the H-C bonds. This observed trend correlates also with a similar trend seen in the IR data for these complexes, **Section 2.6.1**. The  $^1\text{H}$  NMR and  $^{31}\text{P}\{^1\text{H}\}$  data of all the iminophosphine complexes (PNC and PNO) are summarised in **Table 2.16**.

Complex	$\delta$ (H-C=N)	$\delta$ (H-Ar)	$\delta$ (R=OCH <sub>3</sub> )	$\delta$ ( $^{31}\text{P}\{^1\text{H}\}$ )
3-H <b>281</b>	9.40 (1H, s) $J_{\text{Pt-H}} = 123$ Hz	7.41-8.21 (18H, q,dd,d,m)	-	25.3 $J_{\text{Pt-P}} = 2083$ Hz
3-Br <b>282</b>	9.40 (1H, s) $J_{\text{Pt-H}} = 123$ Hz	7.40-8.13 (17H, q,m)	-	25.6 $J_{\text{Pt-P}} = 2100$ Hz
3-Cl <b>283</b>	9.41 (1H, s) $J_{\text{Pt-H}} = 123$ Hz	7.34-8.15 (17H, m,m)	-	25.5 $J_{\text{Pt-P}} = 2123$ Hz
2,3-(OMe) <sub>2</sub> <b>284</b>	9.72 (1H, s) $J_{\text{Pt-H}} = 126$ Hz	7.27-8.17 (16H, dd,q,m)	3.88 (3H, s) 4.02 (3H, s)	25.2 $J_{\text{Pt-P}} = 2102$ Hz
PNO 3-OMe <b>285</b>	9.15 (1H, s) $J_{\text{Pt-H}} = 76$ Hz	6.59-7.90 (16H, d,q,m)	3.89 (3H, s)	13.1 $J_{\text{Pt-P}} = 3816$ Hz

- Chemical shift values ( $\delta$ ) are expressed in ppm relative to the TMS standard for  $^1\text{H}$  and  $\text{H}_3\text{PO}_4$  for  $^{31}\text{P}$ .
- s, singlet; d, doublet; dd, doublet of doublets; t, triplet; q, quartet; m, multiplet.
- Coupling constants (J) are measured in Hz

**Table 2.16:** The  $^1\text{H}$  and  $^{31}\text{P}\{^1\text{H}\}$  NMR spectra<sup>1,2,3</sup> recorded for the iminophosphine tridentate complexes **281-285**, all ran in  $\text{CDCl}_3$  at 300 MHz and 121.5 MHz respectively.

It is also worth noting that the downfield shift of the azomethine signals for the chloro cycloplatinated complexes are *ca.* 0.1 ppm less than the analogous iodo complexes previously reported by this research group, indicating a slightly stronger azomethine bond for the chloride complexes.<sup>2</sup> The smaller, more electronegative chloride in comparison with the larger, less electronegative, iodide (electronegativity values: 3.16 for chloride, 2.66 for iodide) pulls electron density away from the platinum metal centre and creates a stronger Pt-Cl bond than the analogous Pt-I bond.

It is proposed that this induces a  $\delta$  positive charge on the metal centre, inducing a  $\delta$  negative charge on the imino nitrogen increasing the electron density in the H-C=N system relative to that seen in the analogous iodo complexes previously reported. This trend is also

noticed in the IR spectroscopy of these same complexes where the stretching frequency of the C=N bonds are also higher than their iodo counterparts **section 2.5.1**. A summary of this change in the azomethine chemical shift for each of the iminophosphine tridentate complexes **281-285** compared with their free ligands are displayed in **Table 2.17**.

Ligand	$\delta(H-C=N)$ ppm	$[Pt(\eta^3-PNC-L^{1-4})Cl]$ $[Pt(\eta^3-PNO-L^4)Cl]$	$\delta(H-C=N)$ ppm	$\Delta\delta$ ppm
HL <sup>1</sup> <b>261</b>	8.14	3-H <b>281</b>	9.40	1.26
HL <sup>2</sup> <b>262</b>	8.07	3-Br <b>282</b>	9.40	1.33
HL <sup>3</sup> <b>263</b>	8.11	3-Cl <b>283</b>	9.41	1.30
HL <sup>4</sup> <b>264</b>	8.54	2,3-(OMe) <sub>2</sub> <b>284</b>	9.72	1.18
HL <sup>4</sup> <b>264</b>	8.54	PNO 3-OMe <b>285</b>	9.15	0.61

**Table 2.17:** A comparison of the azomethine signal between the free ligands **261-264** and their analogous tridentate complexes **281-285** from the <sup>1</sup>H NMR spectra.

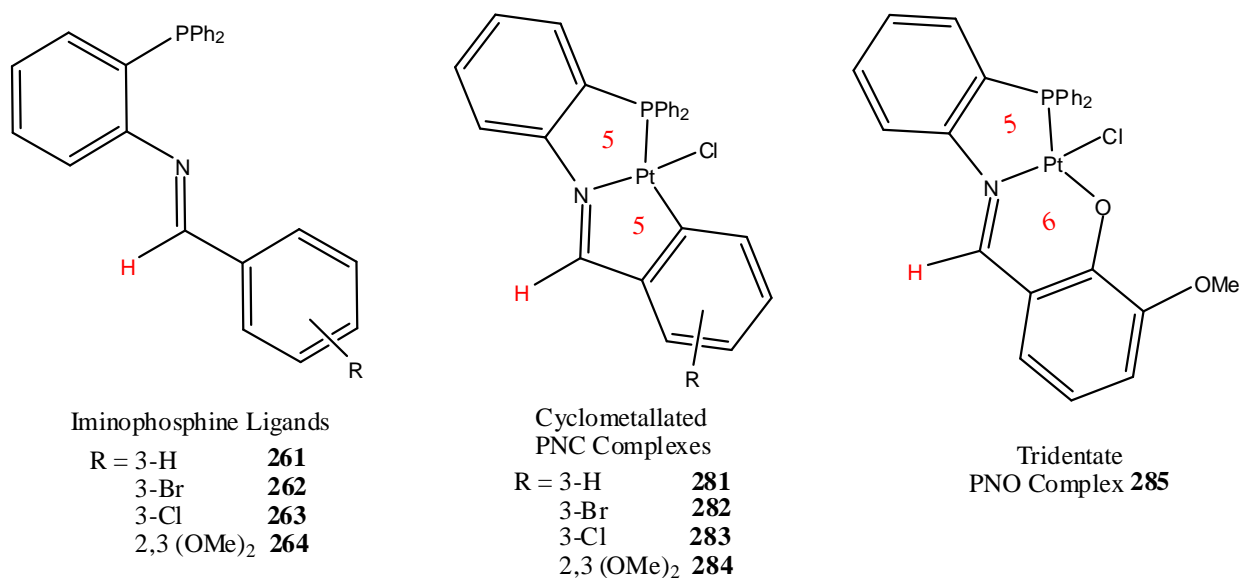


**Figure 2.71:** The range of complexes described in this section with the types of rings formed upon coordination and cyclometallation highlighted along with the azomethine hydrogen indicated in red for the ligands **261-264** and complexes **281-285**.

Platinum satellites are also observed for the H-C=N azomethine signals of all the tridentate complexes shown in **Figure 2.71**. This further confirms the successful coordination of the imino-nitrogen moiety to the Pt (II) metal centre. The <sup>3</sup>J<sub>H-Pt</sub> coupling constants for all the iminophosphine Pt (II) complexes are given in **Table 2.16**.



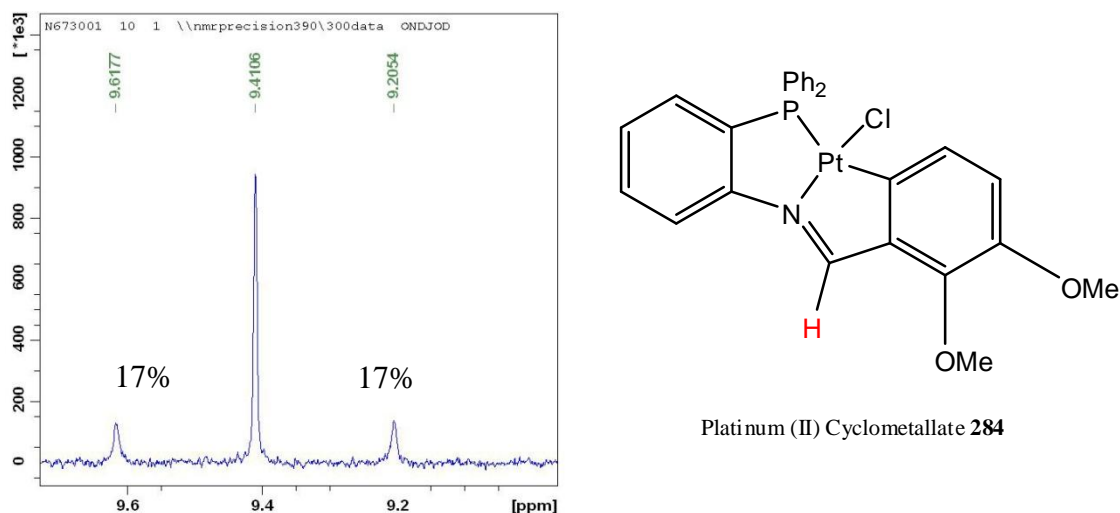


**Figure 2.72:** The azomethine peak with  $^{195}\text{Pt}$  satellite peaks corresponding to the relative abundances of the NMR active  $^{195}\text{Pt}$  isotope (34% abundant) in the cyclometallated complex **284** run at 300 MHz.

In the case of the PNO complex **285**, we see a smaller downfield shift of the azomethine signal to that of the cyclometallated complexes on comparison to the free ligands HL<sup>1-4</sup>. However, there is a much smaller  $^3J_{\text{H-Pt}}$  coupling constant (76 Hz) in comparison with that seen for the cyclometallated complexes (123 Hz), **Table 2.16**. We can therefore propose that the PNO complex **285** has a stronger imine-Pt bond than that of the cyclometallated complexes **281-284** which is also supported by the IR data obtained and reported in **Section 2.6.1**. This also correlates with the data previously obtained for this complex (from an alternative synthesis method) by our research group.<sup>1</sup>

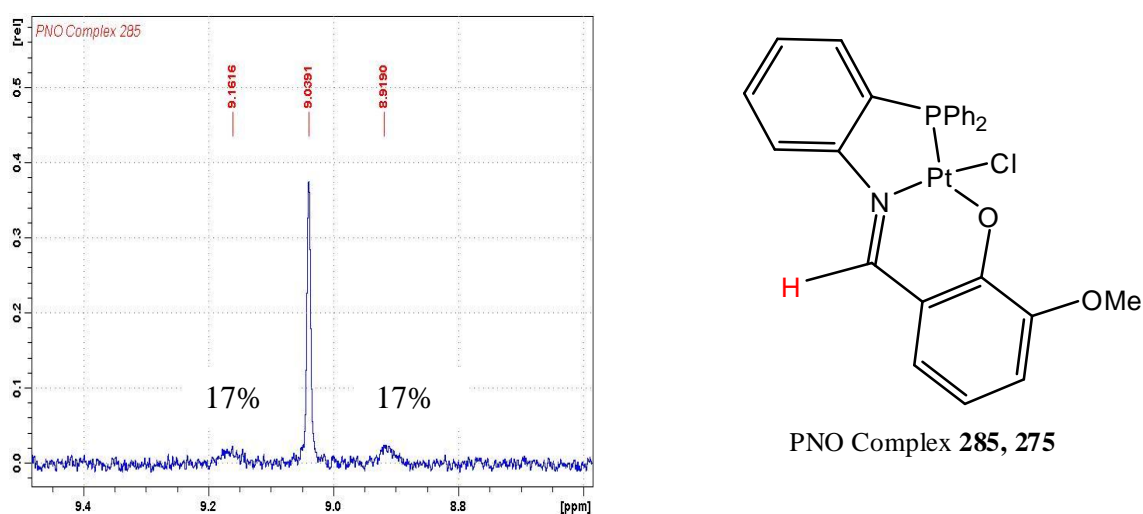


**Figure 2.73:** The azomethine peak with  $^{195}\text{Pt}$  satellite peaks corresponding to the relative abundances of the NMR active  $^{195}\text{Pt}$  isotope (34% abundant) in the PNO complex **285** run at 300 MHz.

This difference in chemical shift and coupling constant on formation of the cyclometallated complexes **281-284** is due to the 5-5 fused ring system of these PNC complexes which would be more sterically restricted and strained in comparison to the 5-6 fused ring system of the PNO complex **285**. This in turn could result in subsequent weakening of the C=N bond for the cyclometallated complexes **281-284** which is reflected in the  $^1\text{H}$  NMR data, **Table 2.18**.

The aromatic region for the cyclometallated complexes **281-284** show multiple overlapping signals making it very difficult to fully resolve these signals for all the complexes. However the signals integrate as expected for 18H (**281**), 17H (**282** and **283**) and 16H (**284** and **285**). There is also a noticeable downfield shift of the aromatic signals on comparison with the free ligands.

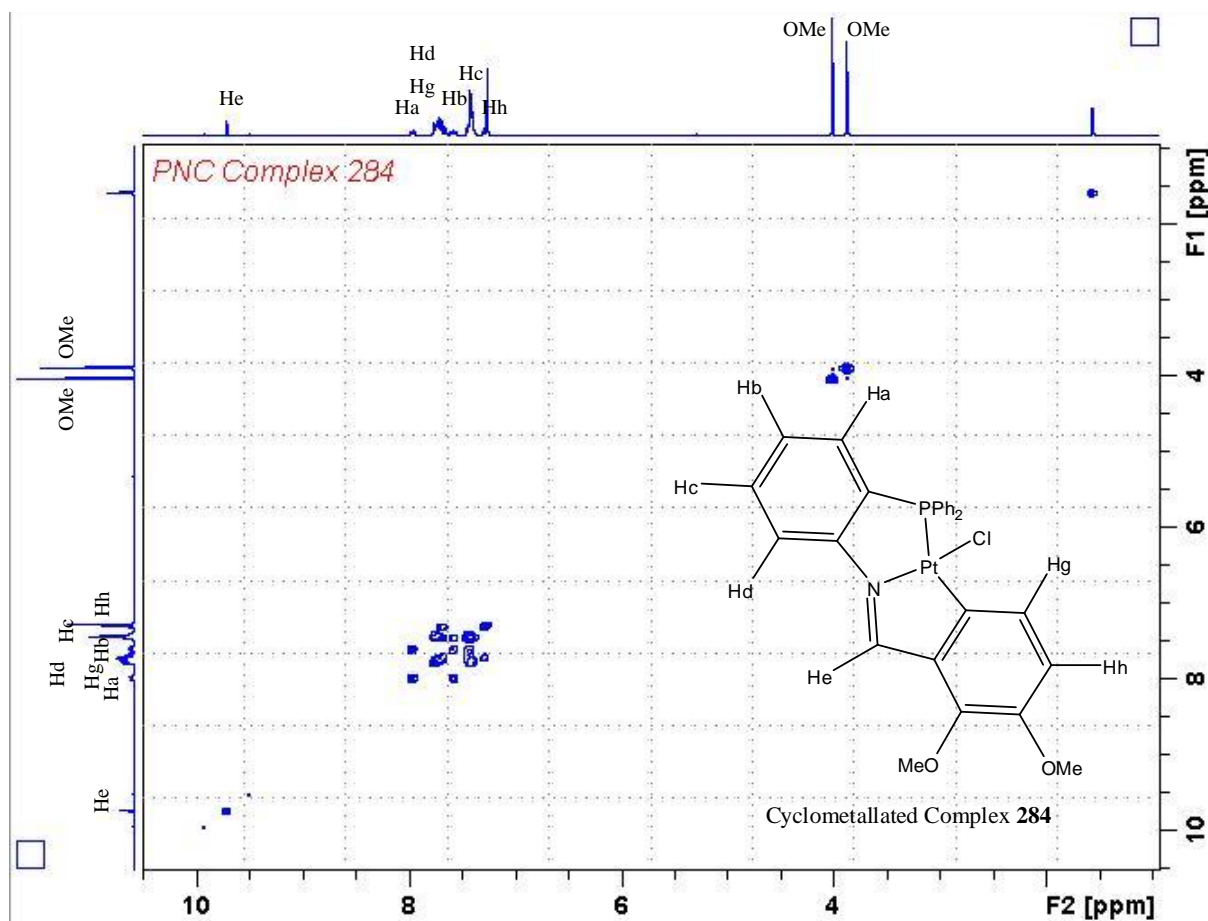


**Figure 2.74:** The  $[\text{}^1\text{H}-\text{}^1\text{H}]$  COSY NMR plot of the cyclometallated complex **284** showing the interactions between the aromatic hydrogens as well as the position of the methoxy groups ( $\text{OCH}_3$ ) and azomethine group  $\text{H}-\text{C}=\text{N}$  run at 300 MHz.

To more fully assign the aromatic region, a  $[\text{}^1\text{H}-\text{}^1\text{H}]$  COSY plot, **Figure 2.74**, of the 2,3-(OMe) $_2$  cyclometallated complex **284** was obtained. The aromatic protons in the region of 7.35-7.28 ppm and 7.68-7.77 ppm can be attributable to the phosphinophenyl protons ( $\text{PPh}_2$ )

(10H) which only couple to each other. The rest of the aromatic hydrogens (6H) are assigned based on their [ $^1\text{H}$ - $^1\text{H}$ ] COSY plot correlations in **Table 2.18**. The cyclometallated complex **284** has the least overlapping aromatic signals of the iminophosphine complexes reported, allowing for successful assignment but it can be used as a model for the other cyclometallated complexes also **281-283**. However, there are still some overlapping signals which make this a tentative assignment. The azomethine signal (He) and the two methoxy signals are easily assigned and reported previously in **Table 2.16**.

Unfortunately, due to the large shift in the signals for all the aromatic hydrogens, making a direct comparison with the free ligand HL<sup>4</sup> **264** is difficult. However, the most significant difference is the absence of any signal for Hf which previously corresponded to the aromatic proton of the carbon  $\alpha$  to the imine substituent on the free ligand HL<sup>4</sup> **264**. This is further evidence for the presence of a Pt-C bond formed due to cyclometallation.

$\delta(^1\text{H})$ ppm	Peak Assignment	Observed Correlations
7.25 d	(Hh)	(Hg)
7.38 m	(Hc), Phosphinophenyl	(Hb, Hd)
7.57 t	(Hb)	(Hc,Ha)
7.65-7.79 m	(Hd), (Hg), Phosphinophenyl	(Hc), (Hh), Phosphinophenyl
7.94, q of d	(Ha)	(Hb, Hc)

*Table 2.18: Measured [ $^1\text{H}$ - $^1\text{H}$ ] COSY NMR correlations for the 2,3-(OMe)<sub>2</sub> cyclometallated complex **284**.*

At  $\delta$  7.94 ppm a signal resonates as a quartet of doublets due to coupling to the phosphorus donor moiety as well as the neighbouring aryl protons on the phosphorus and nitrogen containing aryl ring. It is proposed to be the proton  $\alpha$  to the phosphorus donor moiety (Ha, **Figure 2.74**). This signal has shifted dramatically downfield with respect to the corresponding signal observed for the proton  $\alpha$  to the phosphorus group in the free ligand HL<sup>4</sup> **264** ( $\delta$  6.88 ppm). This is due to donation of electron density into the metal centre from the phosphorus donor moiety and gives further evidence for coordination of the metal centre to the phosphine group.

For the corresponding unsubstituted complex **281** and the halide substituted ligands complexes **282** and **263**, the aromatic regions show complicated overlapping sets of signals in the range of  $\delta$  7.45-7.56 ppm and  $\delta$  7.62-7.77 ppm corresponding to the phosphinophenyl

protons (10H) ( $\text{PPh}_2$ ). In addition there are some signals in the range  $\delta$  7.45-7.92 ppm corresponding to the remaining aromatic hydrogens. Because of significant signal overlap for some of these signals, it is not possible to assign these any further at this time.

The  $^1\text{H}$  NMR spectra of  $[\text{Pt}(\eta^3\text{-PNC-L}^4)\text{Cl}]$  **284** and  $[\text{Pt}(\eta^3\text{-PNO-L}^4)\text{Cl}]$  **285** display resonances for the methoxy groups present, as seen in **Table 2.16**. The cyclometallated complex **284** displays two singlet resonances at  $\delta$  3.88 and  $\delta$  4.02 ppm while the PNO complex **285** displays a singlet resonance at  $\delta$  3.89 ppm. These correspond to the two electron donating methoxy ( $-\text{OCH}_3$ ) substituents present at the C-3 and C-2 position of the lower aryl ring and integrate for 3 hydrogens each for the PNC complex **284**.

For the PNO complex **285** only one methoxy signal indicates the loss of one of the methoxy groups in comparison to the free ligand  $\text{HL}^4$  **264**, further confirming coordination of the platinum to the oxygen heteroatom. Along with the presence of the two methoxy groups in the cycloplatinate PNC complex **284**, this helps to distinguish between the two different tridentate complexes from the  $\text{HL}^4$  ligand **264** spectroscopically.

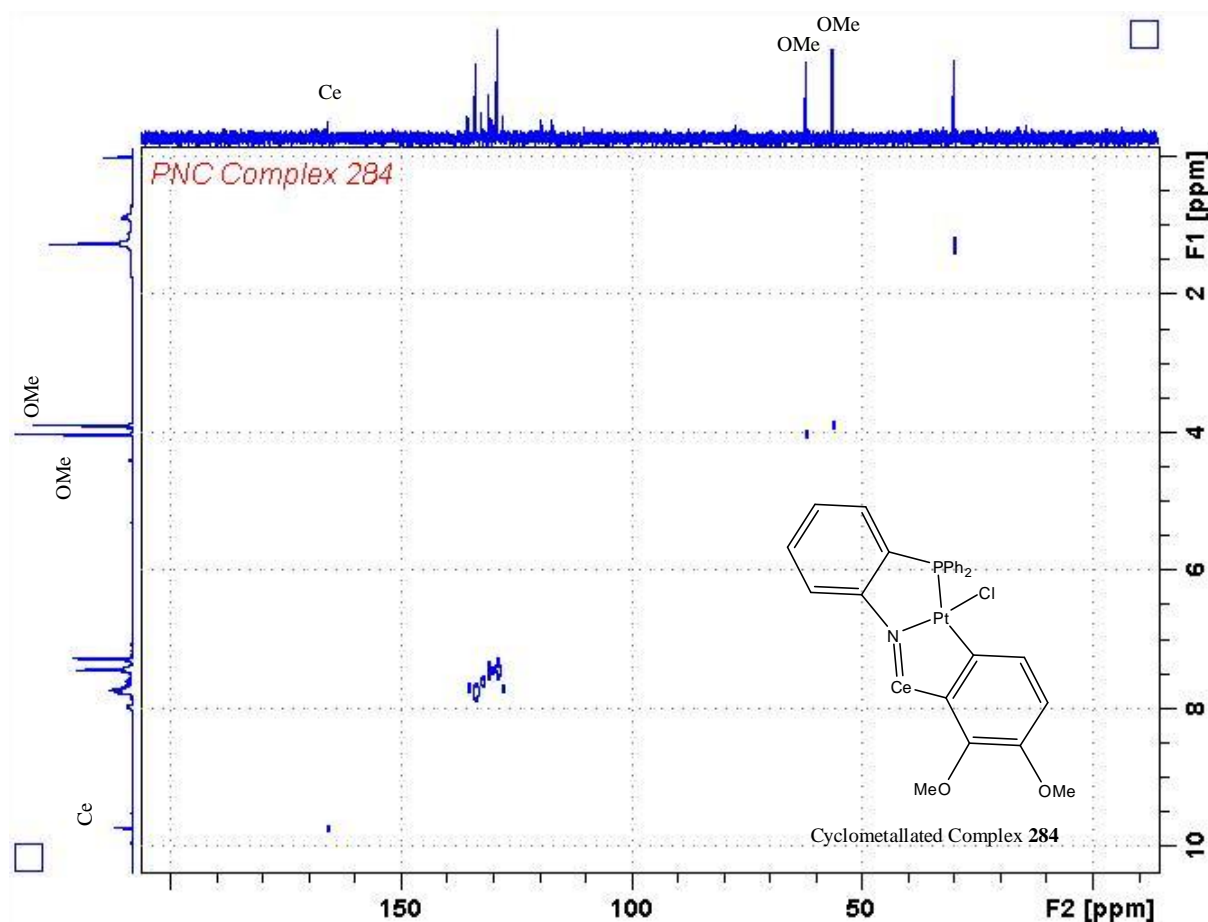


*Figure 2.75: The  $[\text{C}^{13}\text{DEPT } 45 \text{ } ^1\text{H}]$  HETCOR NMR plot of the 2,3-(OMe) $_2$  complex **284** showing the relationship between the carbons and protons present in the compound run at 300 MHz/75.5 MHz.*

It was hoped to obtain  $^{13}\text{C}$  NMR data for all the Pt (II) cyclometallated complexes in order to confirm that a Pt-C bond has indeed formed. However only the 2,3-(OMe)<sub>2</sub> cyclometallated complex [Pt( $\eta^3$ -PNC-L<sup>4</sup>)Cl] **284** was soluble enough to enable  $^{13}\text{C}$  spectra to be obtained. In addition to obtaining various  $^{13}\text{C}$  and DEPT NMR spectra, a [ $^{13}\text{C}$  DEPT 45- $^1\text{H}$ ] HETCOR plot, **Figure 2.75**, was also obtained in order to better associate the individual aromatic CH signals with the  $^1\text{H}$  NMR spectra obtained for the 2,3-(OMe)<sub>2</sub> complex **284**.

In the  $^{13}\text{C}$  NMR spectra the doublet signal at 165.78 ppm was attributed to the carbon atom of the imine bond (HC=N) which was also supported by the [ $^{13}\text{C}$  DEPT 45- $^1\text{H}$ ] HETCOR plot, **Figure 2.75**. This represents a 10 ppm shift downfield in comparison to the free ligand HL<sup>4</sup> **264**, due to coordination of the platinum metal centre to the nitrogen donor moiety on the imine bond. This also indicates weakening of the C=N bond since the electron density is being donated into the metal centre which was also reported for the  $^1\text{H}$  NMR and IR spectra. Like the free ligand HL<sup>4</sup> the iminic carbon is also coupling to the phosphorus donor moiety giving a coupling value of  $^4J = 6$  Hz which is an increase of 4.5 Hz over the free ligand due to the rigidity of the complex formed.

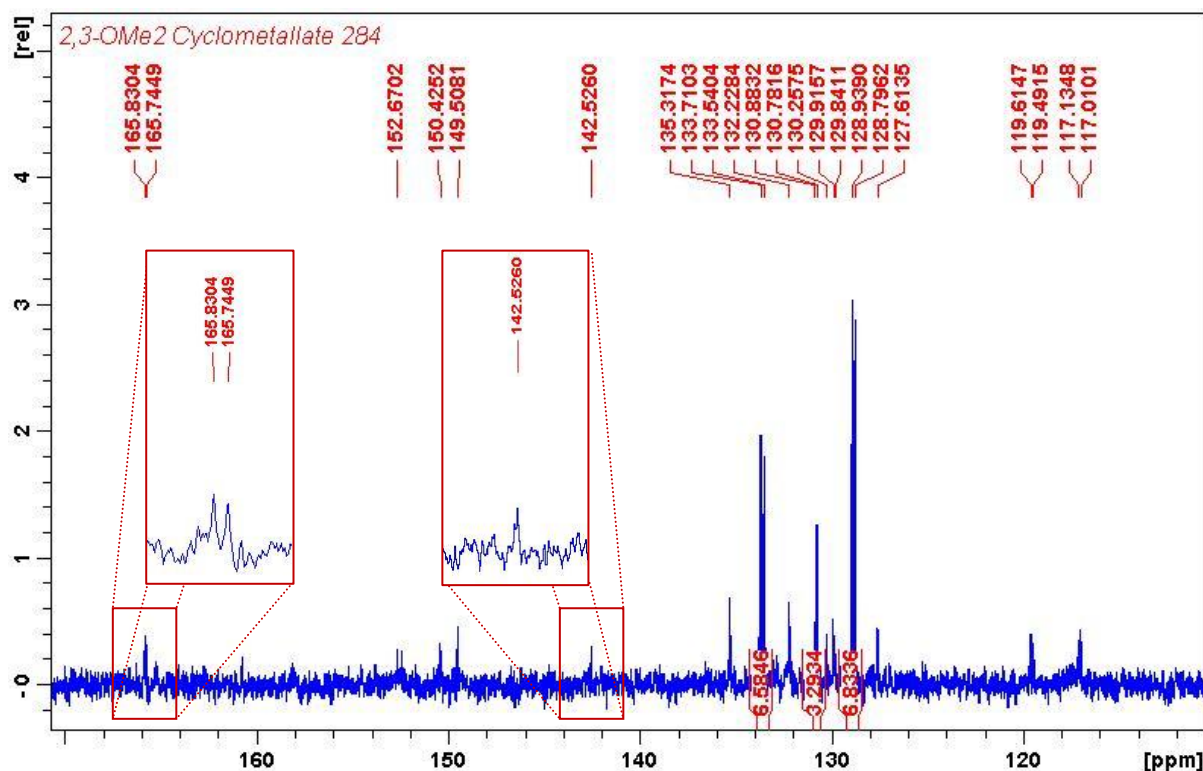


**Figure 2.76:** The  $^{13}\text{C}$  NMR spectra of the 2,3-(OMe)<sub>2</sub> complex **284** showing the iminic carbon at 164.78 ppm as a doublet due to coupling to the phosphorus moiety and the new quaternary metallic carbon at 142.53 ppm, run at 75.5 MHz.

For the cyclometallated complex, the signals for the aromatic carbons have also shifted by circa 12 ppm with respect to the free ligand HL<sup>4</sup> integrating for 16H in comparison to 17H for the ligand. Unfortunately these signals could not be assigned individually using the [<sup>13</sup>C DEPT 45-<sup>1</sup>H] HETCOR plot because of the limited solubility of the 2,3-(OMe)<sub>2</sub> complex **284**. It was however possible to assign the other aromatic carbon signals with strong overlapping signals at 133.71-133.54 ppm and 128.94-128.80 ppm assigned to the phosphinophenyl (PPh<sub>2</sub>) carbons. The individual signals that remained in the <sup>13</sup>C DEPT 45 NMR spectra belong to the 6 aromatic hydrogens on the rest of the complex.

A new signal for a quaternary carbon was found in the <sup>13</sup>C NMR spectra at 142.53 ppm which was not present in the spectra for the free HL<sup>4</sup> ligand **264**, **Figure 2.76**. It was assigned as the carbon of the Pt-C bond formed as a result of cyclometallation. The position of this signal also corresponds well with previous <sup>13</sup>C NMR studies on other platinum and palladium cyclometallates by our research group, as well as others.<sup>45,85</sup>

The signals at 61.93 and 55.85 ppm seen in both the <sup>13</sup>C NMR and the <sup>13</sup>C DEPT 45 NMR spectra were assigned to each carbon atom of the two methoxy substituent groups – OCH<sub>3</sub> and represent almost no shift in comparison to the free ligand HL<sup>4</sup> **264** which also had methoxy signals at 61.92 and 55.85 ppm.

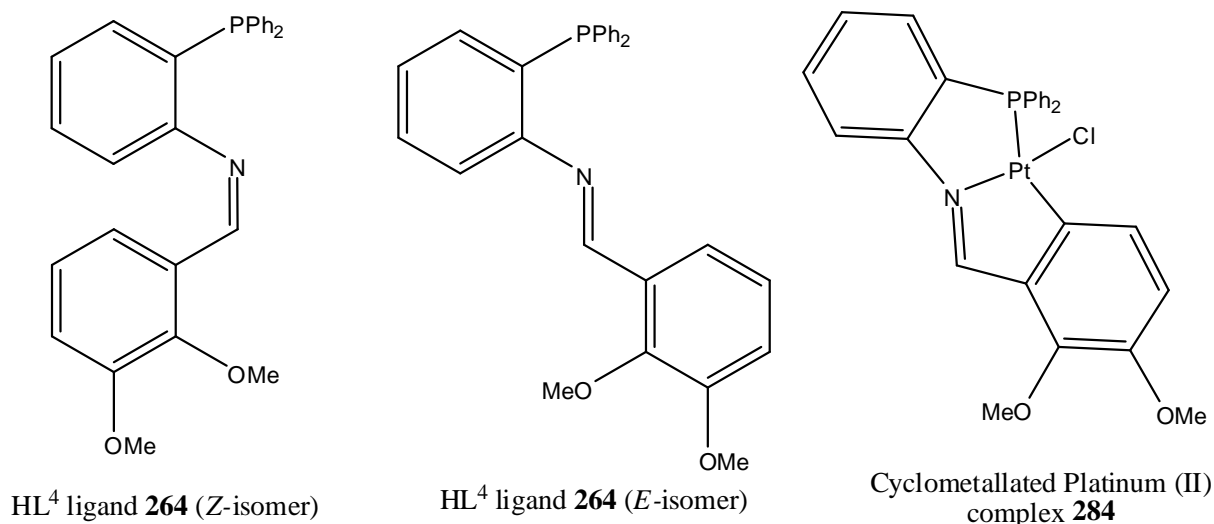


**Figure 2.77:** The <sup>13</sup>C NMR spectra of the free ligand HL<sup>4</sup> **264** has a doublet for the methoxy versus a singlet for the methoxy signals in the complex due to only one isomer present.

However, the methoxy signals found for the free ligand HL<sup>4</sup> **264**, as discussed in **Section 2.7.1** were found to be doublets, unlike the cyclometallated complex [Pt(η<sup>3</sup>-PNC-L<sup>4</sup>)Cl] **284** which are observed to be singlets. This is proposed to be further evidence for the

existence of *E/Z* isomers in the iminophosphine ligands, similar to that seen for the phosphinoamide ligands HL<sup>5-7</sup> **265-267**. But again the spectroscopic evidence for confirming the iminophosphine *Z*-isomer at this time is still too limited to confirm, **Figure 2.77**.

<sup>31</sup>P{<sup>1</sup>H} NMR spectroscopy of the complexes show a singlet resonance for each of the cyclometallated complexes **281-284** in the range of δ 25.1-25.3 ppm. On comparison with the free ligands, this represents a large downfield shift of around δ 40 ppm compared to the coordinated platinum complexes. For the PNO complex **285** on the other hand a singlet is observed at δ 13.1 ppm which represents a significantly different downfield shift, δ 28 ppm, in comparison with the cyclometallated complex **284** which is also formed from the same ligand HL<sup>4</sup> **264**. The <sup>31</sup>P{<sup>1</sup>H} NMR data are given in **Table 2.16**.

This dramatic downfield shift found in the phosphorus NMR also confirms coordination of the phosphine donor moiety to the Pt (II) centre for all the complexes and a comparison with the free ligands is given in **Table 2.19**.

Ligand	δ <sup>31</sup> P{ <sup>1</sup> H} ppm	[Pt(η <sup>3</sup> -PNC-L <sup>1-4</sup> )Cl] [Pt(η <sup>3</sup> -PNO-L <sup>4</sup> )Cl]	δ <sup>31</sup> P{ <sup>1</sup> H} ppm	Δδ ppm
HL <sup>1</sup> <b>261</b>	-14.2	3-H <b>281</b>	25.3	39.5
HL <sup>2</sup> <b>262</b>	-13.7	3-Br <b>282</b>	25.6	39.3
HL <sup>3</sup> <b>263</b>	-13.8	3-Cl <b>283</b>	25.5	40.0
HL <sup>4</sup> <b>264</b>	-14.5	2,3-(OMe) <sub>2</sub> <b>284</b>	25.2	39.7
HL <sup>4</sup> <b>264</b>	-14.5	PNO 3-OMe <b>285</b>	13.1	27.6

**Table 2.19:** Comparison of the <sup>31</sup>P{<sup>1</sup>H} signals between the free iminophosphine ligands **261-264** with the tridentate platinum complexes **281-285**.

The phosphorus NMR data for all the complexes also show <sup>195</sup>Pt satellites, **Figure 2.78**. The <sup>1</sup>J coupling constants for all the cyclometallated complexes **281-284** are in the range of 2080-2183 Hz, **Table 2.18**. These values are slightly higher than the analogous platinum iodo complexes previously reported by this research group but are still consistent with that expected for a P-Pt coupling *trans* to an aryl carbon group. The coupling is slightly smaller for the unsubstituted complex **281** at 2080 Hz, than the 3-Br/Cl **282/283** complexes (2099 Hz and 2123 Hz respectively) which may be influenced by the presence of an electron-withdrawing substituent in the C3 position of the aryl ring (*para* to the Pt-C bond).

The PNO complex **285** on the other hand gives a significantly different coupling constant of 3816 Hz as seen in **Table 2.18**. The data for the PNO complex **285** is also identical to that previously reported by our research group for this complex and is typical of a P-Pt coupling interaction *trans* to an O-Pt bond. From these J-values we can state that the Pt-O bond is stronger than that of the Pt-C<sub>aryl</sub> bond, due to the two different bonding heteroatom's (O and C<sub>aryl</sub>), coordinative (availability of free lone pairs) ability and the subsequent fused ring size produced on successful coordination.

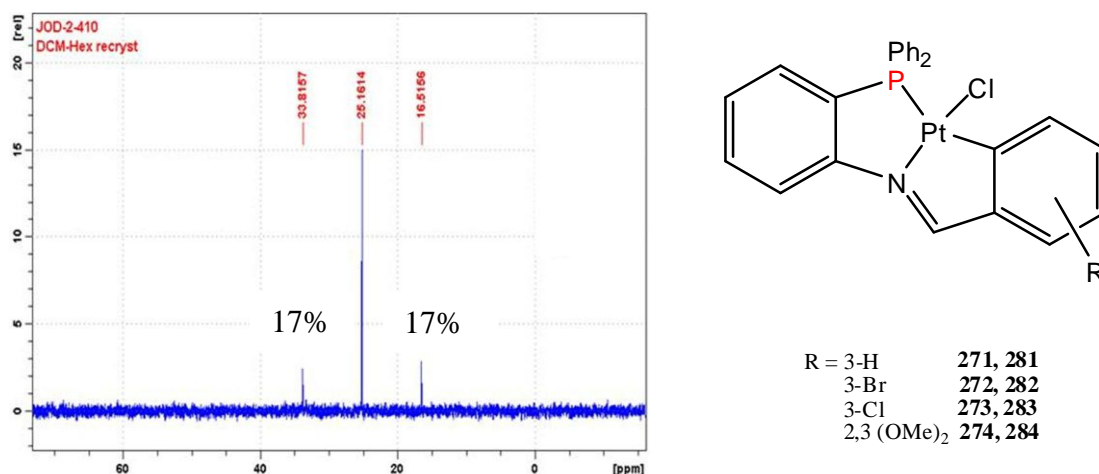


**Figure 2.78:** The single phosphorus peak with Pt<sup>195</sup> satellite peaks corresponding to the relative abundances of the NMR active Pt<sup>195</sup> isotope (34% abundant) in the cyclometallated complexes **281-284** run at 300 Mhz

As discussed in **Section 2.5.3**, owing to extensive solubility problems with the proposed bidentate intermediate complexes, NMR spectra could not be obtained. However in some <sup>1</sup>H NMR spectra of the unsubstituted platinum cyclometallated complex **281**, prior to filtration through silica gel, multiple possible azomethine signals were observed as well as evidence of hydrolysis, **Figure 2.79**.

Crude <sup>1</sup>H NMR data for [Pt(η<sup>3</sup>-PNC-L<sup>1</sup>)Cl] **281** show 4 signals in the region 9.12 to 10.03 ppm. One of the peaks, 9.42 ppm, corresponds to the azomethine signal for the tridentate cyclometallated complex **281**, while the other two peaks have not been reported previously for these complexes. The broad peak at 9.69 ppm displays <sup>195</sup>Pt satellite peaks indicates coordination to the metal centre with a coupling of 39 Hz. The peak at 10.03 ppm represents hydrolysis of the ligand reforming the free benzaldehyde used to synthesis the ligand, **Section 2.5.1**.



The final peak observed at 9.12 ppm may be proposed to be the bidentate unsubstituted complex **271** that has not undergone dimerisation. Unfortunately again due to the poor solubility of this complex, it cannot be confirmed.

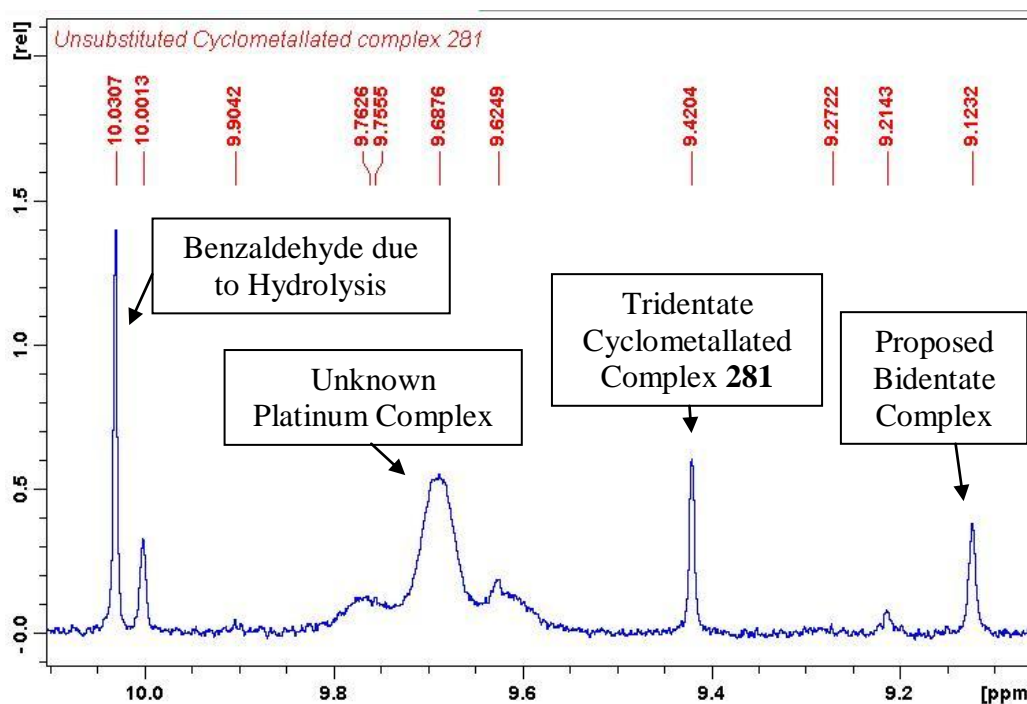


Figure 2.79: Multiple azomethine peaks found when the reaction was taken off after 2 hours for the unsubstituted complex **284**, run at 300 Mhz

#### 2.7.4 NMR spectroscopy for the tridentate Pt (II) phosphinoiminol complexes [Pt( $\eta^3$ -PNC-L<sup>5-7</sup>)]Cl **286-288** and [Pt( $\eta^3$ -PNO-L<sup>6</sup>)]Cl **289**:

<sup>1</sup>H and <sup>31</sup>P{<sup>1</sup>H} spectroscopic data were obtained for the phosphinoiminol complexes **286-289**. <sup>13</sup>C, [<sup>1</sup>H-<sup>1</sup>H] COSY plots and [<sup>13</sup>C DEPT 45-<sup>1</sup>H] HETCOR plots were also attempted for the 2,4-(OMe)<sub>2</sub> cyclometallated complex [Pt( $\eta^3$ -PNC-L<sup>6</sup>)]Cl **287** which is the most soluble of all the phosphinoiminol complexes reported.

All the cyclometallated phosphinoiminol complexes show a signal at circa  $\delta$  9.50 ppm corresponding to the iminol proton on the ligand. For complexes [Pt( $\eta^3$ -PNC-L<sup>5</sup>)]Cl **286** and [Pt( $\eta^3$ -PNC-L<sup>7</sup>)]Cl **288**, this signal is shifted downfield from that of the corresponding ligands HL<sup>5</sup> **265** and HL<sup>7</sup> **267** (circa  $\delta$  8.50 ppm). The iminol signal for the HL<sup>6</sup> ligand is further downfield than that of the other ligands at circa  $\delta$  10.50 ppm, perhaps due to the presence of the methoxy substituents. These do not appear to affect the relative position of

the iminol signal in the coordinated Pt (II) complex **287** in comparison to the other complexes formed.

The iminol resonance for the PNO complex **289**, [Pt( $\eta^3$ -PNO-L<sup>6</sup>)Cl], is further upfield than that of the cyclometallated complexes at  $\delta$  8.50 ppm, perhaps due to the nature of the structure sterically rigid structure that is formed, **Figure 2.80**. Also, in comparison with the free ligands HL<sup>5-7</sup>, where the iminol signal appear as a doublet (**Section 2.7.2**), the cyclometallated PNC and PNO complexes display a doublet of doublets. The observed shift in the signal and the formation of a doublet of doublets indicate successful coordination of the imino-nitrogen to the Pt (II) metal centre.

Complex	$\delta$ (H-C=N)	$\delta$ (H-Ar)	$\delta$ (R-OCH <sub>3</sub> )	$\delta$ ( <sup>31</sup> P{ <sup>1</sup> H})
3-OMe <b>286</b>	9.45 (1H, dd) J <sub>H-P</sub> = 12 Hz J <sub>H-H</sub> = 3 Hz	6.92-7.95 (17H, m,t,t,m)	3.87 (3H, s)	24.3 J <sub>Pt-P</sub> = 1928 Hz
2,4-(OMe) <sub>2</sub> <b>287</b>	9.49 (1H, dd) J <sub>H-P</sub> = 12 Hz J <sub>H-H</sub> = 3 Hz	6.10-7.86 (16H, m, q,m)	3.89 (3H, s) 3.74 (3H, s)	22.9 J <sub>Pt-P</sub> = 1928 Hz
3-Br <b>288</b>	9.45 (1H, dd) J <sub>H-P</sub> = 12 Hz J <sub>H-H</sub> = 3 Hz	6.77-8.10 (17H, m,m)	-	25.1 J <sub>Pt-P</sub> = 2041 Hz
PNO 4-OMe <b>289</b>	8.01 (1H, dd) J <sub>H-P</sub> = 15 Hz J <sub>H-H</sub> = 6 Hz	6.59-7.87 (16H, d,q,m)	3.46 (3H, s)	7.9 J <sub>Pt-P</sub> = 3340 Hz

1. Chemical shift values ( $\delta$ ) are expressed in ppm relative to the TMS standard for <sup>1</sup>H and H<sub>3</sub>PO<sub>4</sub> for <sup>31</sup>P.
2. s, singlet; d, doublet; dd, doublet of doublets; t, triplet; q, quartet; m, multiplet.
3. Coupling constants (J) are measured in Hz

*Table 2.20: The <sup>1</sup>H and <sup>31</sup>P{<sup>1</sup>H} NMR spectra<sup>1,2,3</sup> recorded for the phosphinoiminol tridentate complexes **286-289**. All ran in CDCl<sub>3</sub> at 300MHz and 121.5 MHz respectively.*

On donation of the lone pair of electrons on the imino-nitrogen into the metal centre, electron density is pulled towards the coordination bond (Pt-N), weakening the HO-C=N bonds. The observed shift in the NMR spectra correlates with this reduction in bond strength

also seen in the IR data for these complexes, **Section 2.5.2**. The  $^1\text{H}$  NMR and  $^{31}\text{P}\{^1\text{H}\}$  data of all the phosphinoiminol complexes are summarised in **Table 2.22**.

In the case of the PNO complex **289**, we see a larger shift of the iminol signal than that seen for the cyclometallated complex **287** on comparison with their free ligand HL<sup>6</sup> **266**, as well as a larger  $^6J_{\text{H-H}}$  and  $^6J_{\text{H-P}}$  coupling constant, **Table 2.20**. We can therefore propose that the PNO complex **289** has a stronger imine-Pt bond than that of the cyclometallated complexes **286-288** formed from the phosphinoiminol ligands which is also supported by the IR data obtained and reported in **Section 2.6.2**.

This difference in chemical shift and coupling constant on formation of the cyclometallated complexes **287-288** is due to the 5-5 fused ring system of these PNC complexes which would be more sterically restricted and strained in comparison to the 5-6 fused ring system of the PNO complex **289**, similar to that which was reported for the iminophosphine complexes in **Section 2.7.3**. This in turn could result in subsequent weakening of the C=N bond for the cyclometallated complexes **286-288** which is reflected in the  $^1\text{H}$  NMR data, **Table 2.20**.

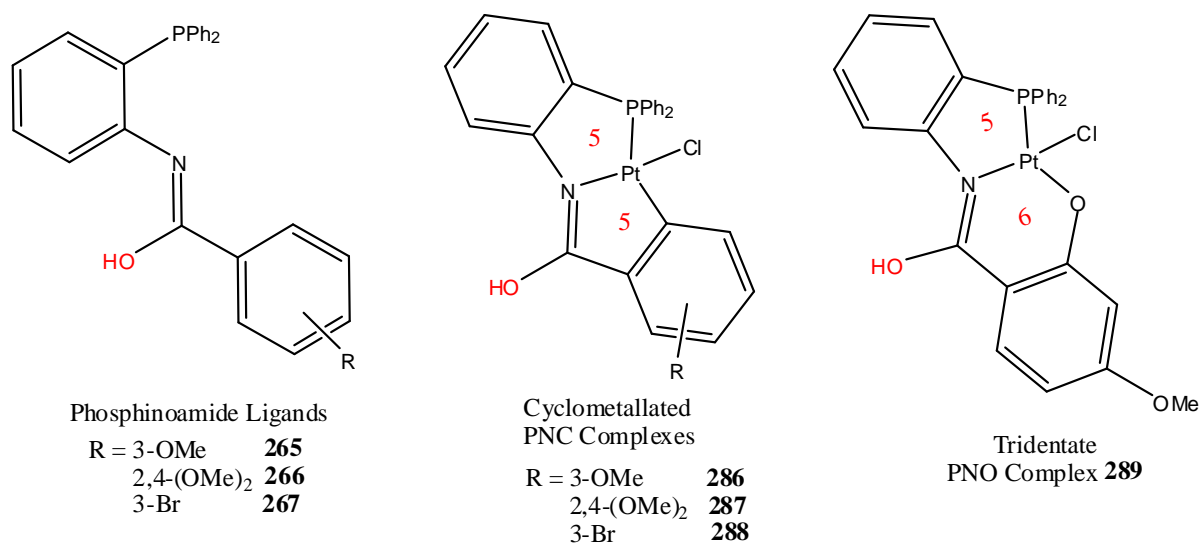


*Figure 2.80: The range of complexes described in this section with the types of rings formed upon coordination and cyclometallation highlighted along with the iminol hydrogen indicated in red with, complexes **286-289**.*

In comparison to the free ligands HL<sup>5-7</sup> **265-267**, the tridentate phosphinoiminol complexes are also more sterically rigid in a fixed position, thus long-range coupling is possible. The observed doublet of doublets signal can be attributed to coupling to an aryl proton and the phosphorus donor moiety of the coordinating phosphine, **Figure 2.81**,

incomparison to the doublet observed for the free ligands HL<sup>5-7</sup> **265-267** which corresponds to the *E/Z*-isomers present.

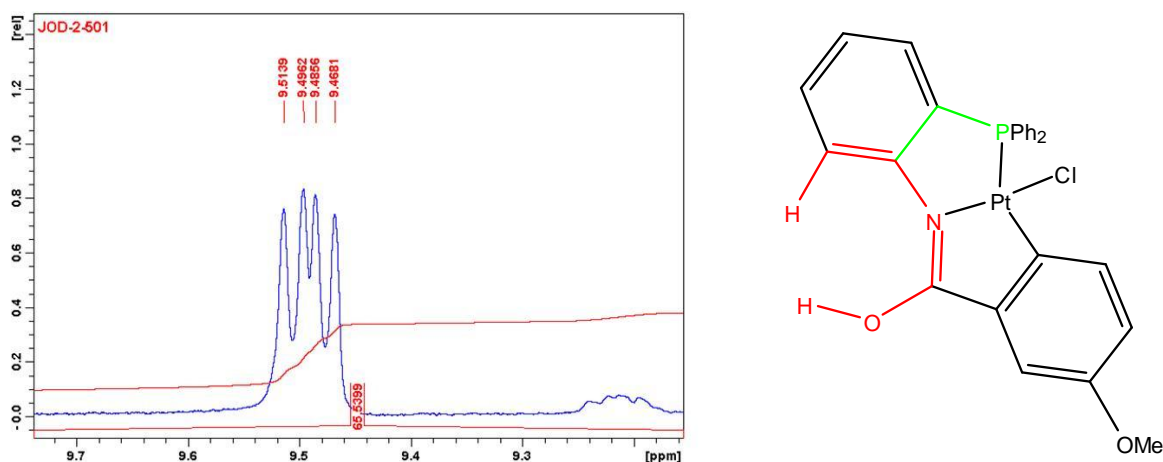


**Figure 2.81:** An example of the doublet of doublets for the iminol signal in the <sup>1</sup>H NMR spectra for the cyclometallated complex **286**. The <sup>6</sup>J ω-coupling responsible is highlighted in the structure of the rigid conjugated complex.

A summary of shift in the iminol signal for each of the phosphinoiminol tridentate complexes **286-289** compared with their free ligands HL<sup>5-7</sup> **265-267** are given in **Table 2.21**.

Ligand	$\delta(H-C=N)$ ppm	[Pt( $\eta^3$ -PNC-L <sup>5-7</sup> )Cl] [Pt( $\eta^3$ -PNO-L <sup>6</sup> )Cl]	$\delta(H-C=N)$ ppm	$\Delta\delta$ ppm
HL <sup>5</sup> <b>261</b>	8.84 (1H, d) <sup>6</sup> J <sub>P-H</sub> =8	3-OMe <b>286</b>	9.45 (1H, dd) <sup>6</sup> J <sub>H-P</sub> = 12 Hz <sup>6</sup> J <sub>H-H</sub> = 3 Hz	0.61
HL <sup>6</sup> <b>264</b>	10.50 (1H, d) <sup>6</sup> J <sub>P-H</sub> =6	2,4-(OMe) <sub>2</sub> <b>287</b>	9.49 (1H, dd) <sup>6</sup> J <sub>H-P</sub> = 12 Hz <sup>6</sup> J <sub>H-H</sub> = 3 Hz	1.01
HL <sup>7</sup> <b>262</b>	8.60 (1H, d) <sup>6</sup> J <sub>P-H</sub> =8	3-Br <b>288</b>	9.45 (1H, dd) <sup>6</sup> J <sub>H-P</sub> = 12 Hz <sup>6</sup> J <sub>H-H</sub> = 3 Hz	0.85
HL <sup>6</sup> <b>264</b>	10.50 (1H, d) <sup>6</sup> J <sub>P-H</sub> =6	PNO 3-OMe <b>289</b>	8.01 (1H, dd) <sup>6</sup> J <sub>H-P</sub> = 15 Hz <sup>6</sup> J <sub>H-H</sub> = 6 Hz	2.49

**Table 2.21:** A comparison of the iminol signal between the free ligands **265-267** and their analogous tridentate complexes **286-289** from the <sup>1</sup>H NMR spectra.

Generally coupling is found to occur up to a maximum of 4 bonds,  $^4J$ . However, long-range coupling has been reported for “zig-zag” type, highly conjugated systems.<sup>86</sup> It is described as omega ( $\omega$ ) coupling where the “zig-zag” structure can allow  $^6J$  coupling to occur. Because of this, the iminol proton has the ability to couple to distant NMR active nuclei via resonance, **Figure 2.82**. Because of the structure of the phosphinoiminol complexes, the result is two  $^6J$  coupling interactions that give a doublet of doublets in the  $^1H$  NMR spectra, **Figure 2.81**. We attribute the lower J-values (**Table 2.20**) to the iminol proton-aromatic proton interaction, (red path, **Figure 2.82**) and the greater J-value to the iminol proton-phosphorus coupling (green path, **Figure 2.82**).

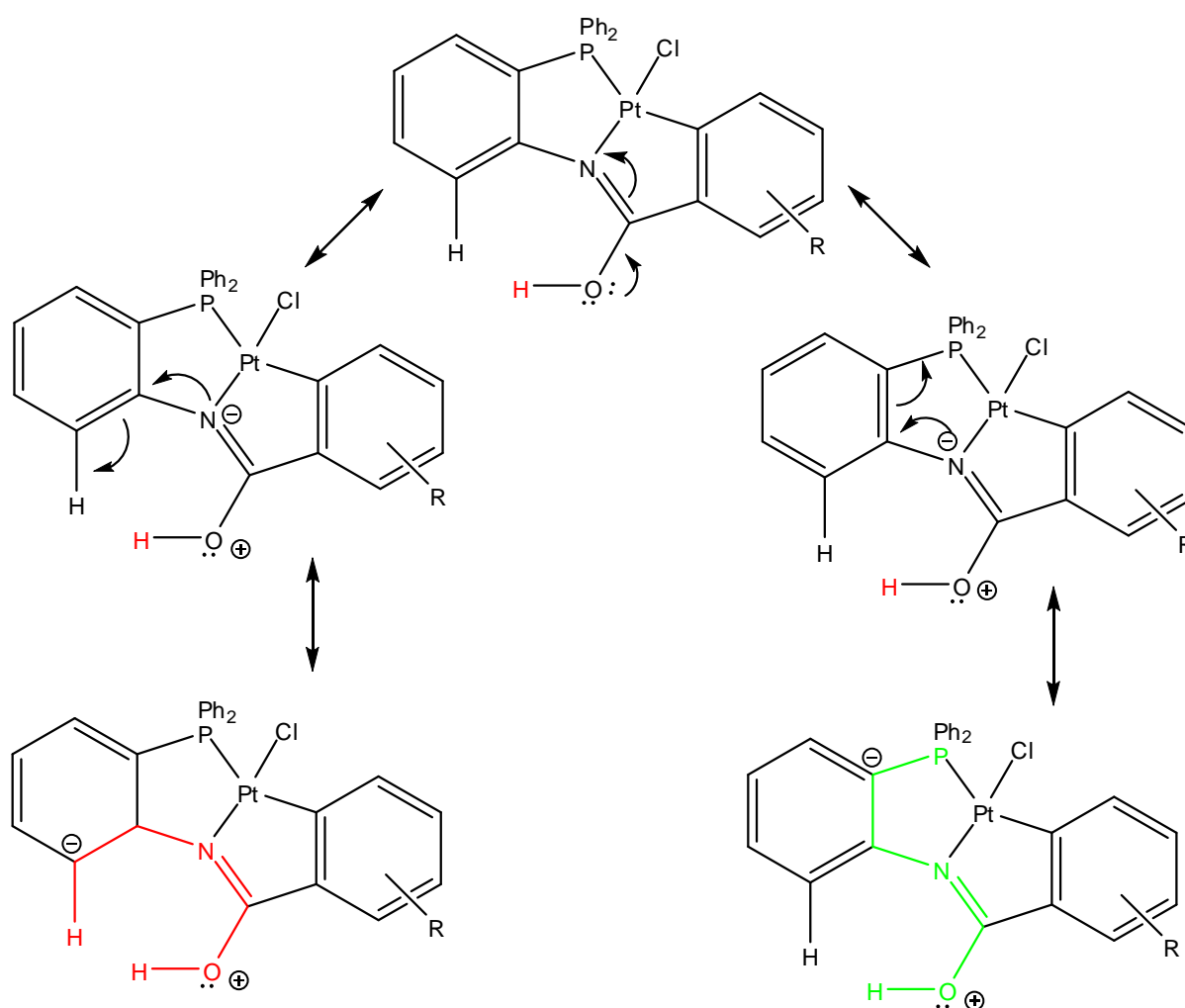


**Figure 2.82:** The  $^6J$   $\omega$ -coupling between the iminol proton ( $H$ ) and the two other NMR active nuclei in the rigid cyclometallated complexes. The resonance structure paths are illustrated in **Red** and **Green**.

Unfortunately because of extensive overlapping of the aromatic signals in the spectra of the platinum phosphinoiminol complexes, complete assignment of each aromatic signal is

impossible. However the aromatic signals integrate for the expected number of protons for each complex i.e. 17H for **286**, 16H for **287** and **289**, and 17H for **288**. The cyclometallated complex **287** is the only complex with minimal overlapping aromatic signals, allowing for some assignment but it can be also used as a model for the other phosphinoiminol complexes **286-289**.

A large shift in the equivalent signals for all the aromatic protons was also found in comparison to the free ligands, making a direct comparison with HL<sup>5-7</sup> **265-267** difficult, **Table 2.20**. However, there is no equivalent signal for Hf which was found for the free ligand HL<sup>6</sup> due to the platinum carbon bond formation in complex **287**. The C-H activation of Hf is further evidence of the successful cyclometallation of the 2,3-(OMe)<sub>2</sub> platinum complex. Only a limited number of other comparisons can be made at this time for the aromatic signals due to overlapping.

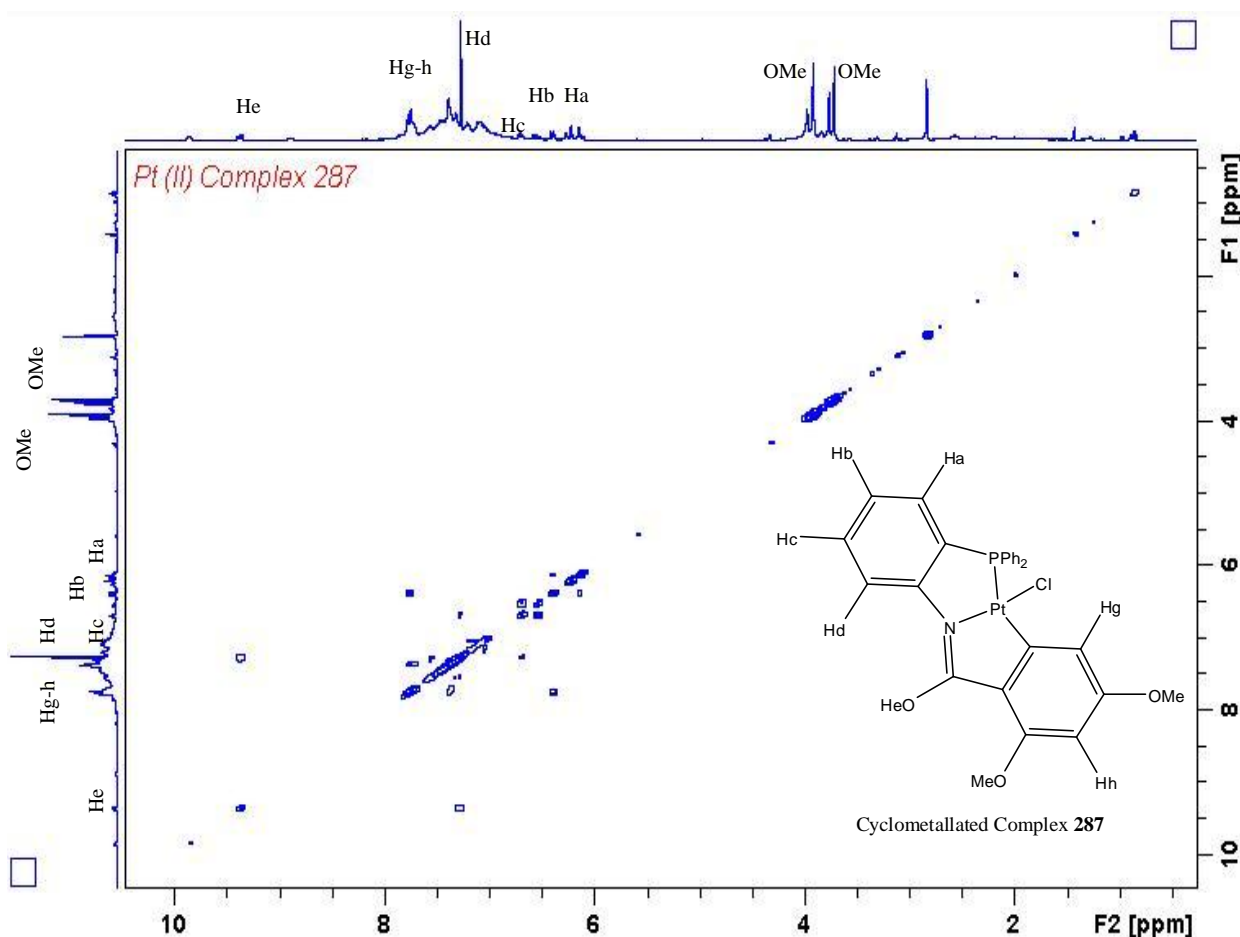


**Figure 2.83:** The [<sup>1</sup>H-<sup>1</sup>H] COSY NMR plot of the cyclometallated phosphinoiminol complex **287** showing the interactions between the aromatic hydrogens as well as the position of the methoxy groups (OCH<sub>3</sub>) and iminol group HO-C=N run at 300 MHz.

As per the [<sup>1</sup>H-<sup>1</sup>H] COSY plot in **Figure 2.83** of the 2,3-(OMe)<sub>2</sub> cyclometallated complex **287**, the aromatic protons in the region of 7.23-7.48 ppm and 7.62-7.79 ppm can be

attributable to the phosphinophenyl protons (10H) which only couple to themselves. The rest of the aromatic hydrogens (6H) are overlapping significantly. The azomethine signal (He) and the two methoxy signals are easily assigned and reported previously in **Table 2.20**. Further evidence for omega ( $\omega$ ) coupling can also be found in the [ $^1\text{H}$ - $^1\text{H}$ ] COSY plot where interaction between the iminol proton and an aromatic proton on the phosphine/imine ring system is immediately evident, **Figure 2.83**.

For the other phosphinoiminol tridentate complexes **286**, **288** and **289** the aromatic regions show complicated overlapping sets of signals in the range of 6.81-7.79 ppm corresponding to the phosphinophenyl protons (10H) and some signals overlapping between 6.11 ppm and 7.98 ppm corresponding to the remaining aromatic hydrogens. The multiplet signals for the aromatic region of these complexes though were much more complicated, with overlapping spectra structures, than the 2,4-(OMe)<sub>2</sub> complex **287** which meant it was impossible to assign the individual aromatic hydrogens with any certainty.

The  $^1\text{H}$  NMR data for the 3-OMe cyclometallated complex [Pt( $\eta^3$ -PNC-L<sup>5</sup>)Cl] **286** also displays a singlet at  $\delta$  3.87 ppm integrating for 3 protons, corresponding to the methoxy substituent present. The cyclometallated complex [Pt( $\eta^3$ -PNC-L<sup>6</sup>)Cl] **287** on the other hand displays two singlet resonances at  $\delta$  3.89 and  $\delta$  3.74 ppm while the PNO complex [Pt( $\eta^3$ -PNO-L<sup>6</sup>)Cl] **289** from the same ligand (HL<sup>6</sup> ligand **266**) also displays a singlet resonance at  $\delta$  3.46 ppm, integrating for 3 protons.

For the PNO complex [Pt( $\eta^3$ -PNO-L<sup>6</sup>)Cl] **289** only one methoxy signal indicates the loss of one of the methoxy groups to form a PNO complex, further confirming coordination to the oxygen heteroatom. Along with the presence of the two methoxy groups in the cycloplatinate PNC complex **287**, this helps to distinguish between the two different tridentate complexes from the HL<sup>6</sup> ligand **266** spectroscopically.

It was desirable to get  $^{13}\text{C}$  NMR data for the phosphinoiminol platinum complexes **286-289**, with the goal being a comparison with the free ligands **265-267**. However, the tridentate phosphinoiminol complexes have very limited solubility so only tentative  $^{13}\text{C}$  data was found for the 2,4-(OMe)<sub>2</sub> cyclometallated complex [Pt( $\eta^3$ -PNC-L<sup>6</sup>)Cl] **287**, which was the most soluble phosphinoiminol complex.

In the  $^{13}\text{C}$  NMR spectra of **287**, the singlet at 165.73 ppm was attributed to the carbon atom of the iminol bond (HO-C=N) following on from previous work with the iminophosphine complexes **281-285**. This represents a 2 ppm shift downfield in comparison to the free ligand HL<sup>6</sup> **266**, due to coordination of the platinum metal centre to the nitrogen

donor moiety on the imine bond. Unfortunately the aromatic carbon signals could not be assigned individually using the [ $^{13}\text{C}$  DEPT 45- $^1\text{H}$ ] HETCOR plot as the correlations are incomplete due to the limited solubility of the 2,4-(OMe) $_2$  complex **287**.

However, strong multiple overlapping signals at 133.71-133.37 ppm and 128.68-128.25 ppm were assigned to the phosphinophenyl carbons and signals at 56.07 and 54.68 ppm seen in both the  $^{13}\text{C}$  NMR and the  $^{13}\text{C}$  DEPT 45 NMR spectra were assigned to each carbon atom of the two methoxy substituent groups (OCH $_3$ ). There were no isomers found for the platinum cyclometallated complex as only the *E*-isomer of the ligand can form the cyclometallated complex as discussed earlier.

$^{31}\text{P}\{^1\text{H}\}$  NMR spectroscopy of the complexes show a singlet resonance for each of the cyclometallated complexes **287-289** in the range of  $\delta$  22.9-25.1 ppm. On comparison with the free ligands, this represents a large downfield shift of around  $\delta$  42 ppm. For the PNO complex **289** on the other hand a singlet is observed at  $\delta$  7.9 ppm which represents a significantly different downfield shift,  $\delta$  25.6 ppm, in comparison with the cyclometallated complex **287** which is also formed from the same ligand HL $^6$  **266**.

The full list of the  $^{31}\text{P}\{^1\text{H}\}$  NMR signals along with their platinum coupling frequencies for each complex are given in **Table 2.20**. This dramatic downfield shift found in the phosphorus NMR also confirms coordination of the phosphine donor moiety to the Pt (II) centre for all the complexes and a comparison with the free ligands is given in **Table 2.22**.

Ligand	$\delta$ $^{31}\text{P}\{^1\text{H}\}$ ppm	[Pt( $\eta^3$ -PNC-L $^{5-7}$ )Cl] [Pt( $\eta^3$ -PNO-L $^6$ )Cl]	$\delta$ $^{31}\text{P}\{^1\text{H}\}$ ppm	$\Delta\delta$ ppm
HL $^5$ <b>265</b>	-19.8	3-OMe <b>286</b>	24.3	44.1
HL $^6$ <b>266</b>	-17.7	2,4-(OMe) $_2$ <b>287</b>	22.9	40.6
HL $^7$ <b>267</b>	-18.7	3-Br <b>288</b>	25.1	43.8
HL $^6$ <b>266</b>	-17.7	PNO 4-OMe <b>289</b>	7.9	25.6

*Table 2.22: Comparison of the  $^{31}\text{P}\{^1\text{H}\}$  signals between the free phosphinoamide ligands 265-267 with the tridentate phosphinoiminol complexes 286-289.*

The phosphorus NMR data for all the complexes also show  $^{195}\text{Pt}$  satellites like that seen for the iminophosphine complexes. The  $^1\text{J}$  coupling constants for all the cyclometallated complexes **286-288** are in the range of 1928-2041 Hz, **Table 2.22**. These values are slightly



lower than the iminophosphine complexes **281-284** but are still consistent with that expected for a P-Pt coupling *trans* to an aryl carbon group.

The PNO complex **289** on the other hand gives a significantly different coupling frequency of 3340 Hz as seen in **Table 2.22**. The data for this PNO complex is also quite similar to the previously reported iminophosphine complex **285** and is typical of a P-Pt coupling interaction *trans* to an O-Pt bond. From these J-values we can state that the Pt-O bond is stronger than that of the Pt-C<sub>aryl</sub> bond, due to the two different bonding heteroatom's (O and C<sub>aryl</sub>), coordinative (availability of free lone pairs) ability and the subsequent fused ring size produced on successful coordination.

## 2.8 X-Ray Crystallography:

### 2.8.1 Crystal and molecular structures of [Pt( $\eta^3$ -PNC-L<sup>2-3</sup>)Cl] **282** and **283**:

Suitable crystals for X-ray analysis were grown by a slow evaporation of a CHCl<sub>3</sub> solution of **282** and **283** respectively. The single crystal analyses of these complexes were carried out by Dr. Curtis J. Elcoate and Dr. Simon E. Lawrence. Crystal data and relevant structure solution data for these complexes are given in the experimental **Section 2.10**.

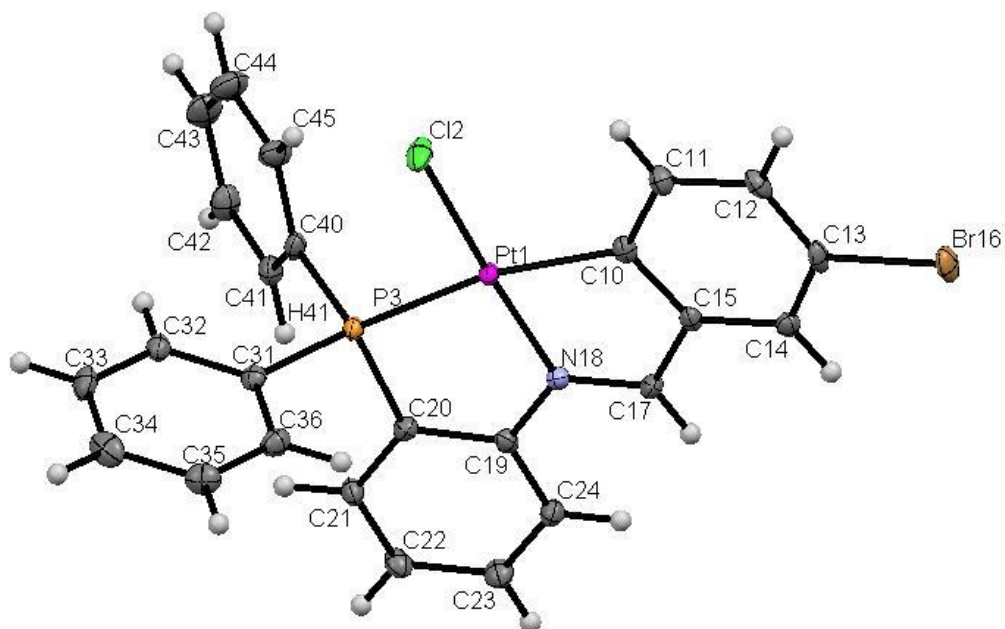


**Figure 2.84:** A view of [Pt( $\eta^3$ -PNC-L<sup>2</sup>)Cl] **282**, showing the structure and stereochemistry of the solid state compound. Ellipsoids are shown with 50% probability.

The X-ray structures of both complexes **282** and **283** are illustrated in **Figures 2.84** and **2.85** respectively. Both complexes contain central platinum atoms which are in a four coordinate distorted square planar environment. In compound **282**, the platinum metal centre coordinates to the **P3**, **N18** and **C10** moieties of the tridentate ligand and to the chloro ligand (**Cl2**), which is located *trans* to the nitrogen (**N18**) moiety in compound **282**, **Figure 2.84**. The bonding environment is mirrored in the analogous complex **283**, **Figure 2.85** and the C-Pt and the N-Pt bond distances established for both complexes were found to be consistent with each other.

The distortions from the idealised square-planar geometry about the metal centre may be due to the bulk of the phosphine group and to the bite angle of the P, N chelate as well as the 5-membered ring formed on cyclometallation. Similar distorted square-planar geometry about the metal centre was also observed by our research group previously for PNO type platinum and palladium complexes as well as iodo platinum cyclometallates.<sup>1,2</sup> Other research groups have also reported distorted square planar geometry for palladium PNO complexes of the type  $[\text{Pd}(\eta^3\text{-PNO-L})\text{Cl}]$ .<sup>87</sup>

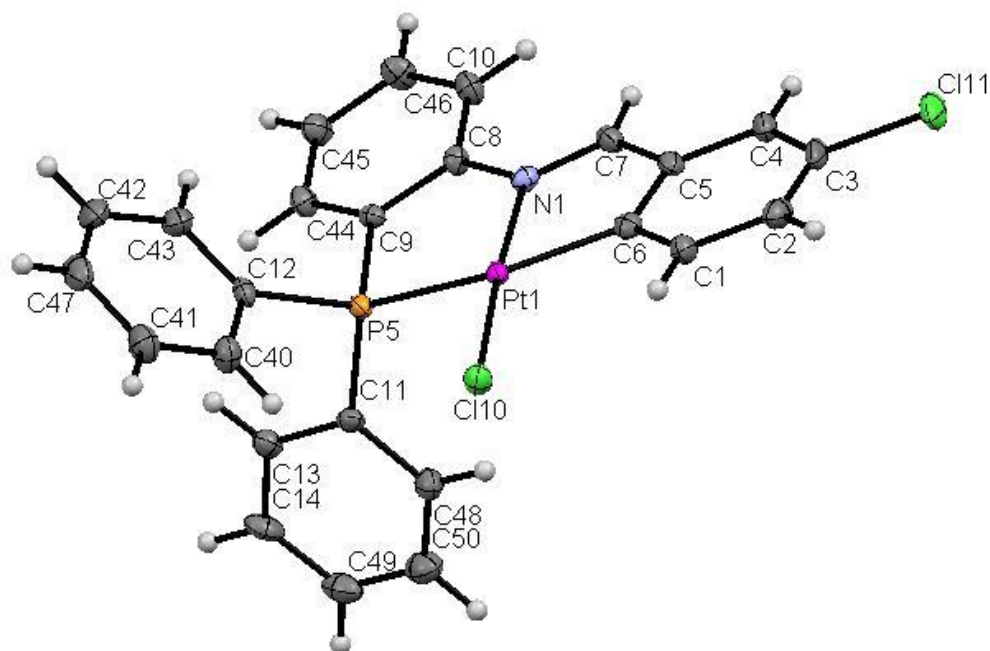


**Figure 2.85:** A view of  $[\text{Pt}(\eta^3\text{-PNC-L}^3)\text{Cl}]$  **283**, showing the structure and stereochemistry of the solid state compound. Ellipsoids are shown with 50% probability.

The bond angles around the platinum centre deviate from the expected  $90^\circ$  angle within a perfect square planar geometry, **Table 2.23**. The *trans* P-Pt-C [ $166.74(7)$ - $165.76(9)^\circ$ ] and *trans* N-Pt-Cl [ $175.47(6)$ - $175.36(7)^\circ$ ] axes are found to be less than  $180^\circ$  for both

complexes, **Table 2.23**. The *cis* P-Pt-N and *cis* N-Pt-C angles are also dependant upon the sizes of the P,N and N,C rings, which in for these complexes are both 5-membered. Previous work in our research group into PNO type palladium and platinum iminophosphine complexes have found that systems with mixed 5 and 6 membered fused ring systems give different bond angles for each ring.

Although the ring sizes are the same here, we also observed that the bond angles in each of the rings are different. The P-Pt-N angles for the P,N chelate ring are 85.46(6)° for **282** and 85.12(7)° for **283**, while the N-Pt-C angles for the N,C chelate ring are 81.27(10)° for **282** and 80.89(11)° for **283**. The bite angle of the platinum metal centre is therefore less for the N-Pt-C chelate ring primarily due to the P-Pt bond being stretched to accommodate the cyclometallation.

There is also large difference in the angles between the platinum metal centre and the tridentate ligand (P,N,C) and the angles between the Pt-P, Pt-Cl and Pt-C bonds (P-Pt-Cl and Cl-Pt-C), **Figure 2.86**. This is again due to the presence of the two 5-membered fused ring system.

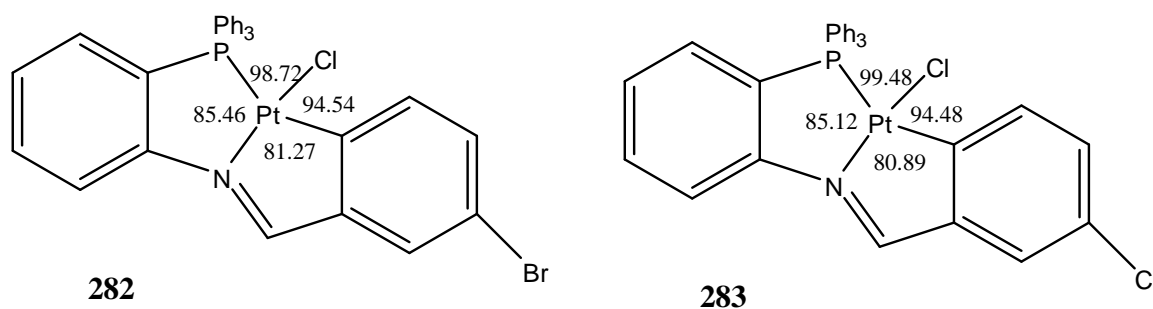


**Figure 2.85:** Complexes  $[Pt(\eta^3\text{-PNC-L}^2)\text{Cl}]$  **282** and  $[Pt(\eta^3\text{-PNC-L}^3)\text{Cl}]$  **283**, showing the angles around the metal centre.

$[Pt(\eta^3\text{-PNC-L}^2)\text{Cl}]$ <b>282</b>		$[Pt(\eta^3\text{-PNC-L}^3)\text{Cl}]$ <b>283</b>	
Angle	Degree (°)	Angle	Degree (°)
C(10)-Pt(1)-Cl(2)	94.54(7)	C(12)-Pt(1)-Cl(1)	94.48(9)
P(3)-Pt(1)-Cl(2)	98.72(2)	P(1)-Pt(1)-Cl(1)	99.48(3)
N(18)-Pt(1)-Cl(2)	175.47(6)	N(1)-Pt(1)-Cl(1)	175.36(7)
N(18)-Pt(1)-C(10)	81.27(10)	N(1)-Pt(1)-C(12)	80.89(11)
N(18)-Pt(1)-P(3)	85.46(6)	N(1)-Pt(1)-P(1)	85.12(7)
C(10)-Pt(1)-P(3)	166.74(7)	C(12)-Pt(1)-P(1)	165.76(9)

**Table 2.23:** A comparison of the inter-atomic bond angles around the metal centre for both complexes **282** and **283**.

All the metal-ligand bond distances around the platinum metal centre are within expected ranges. The observed similarities between the bond lengths of the two complexes (**282** and **283**) would suggest as expected that the substitution of a chloride for a bromide on the salicylic ring has little overall effect on the observed bond lengths around the metal centre.

**Table 2.24** compares all the bond distances around the metal centre are compared for each complex as well as the previously reported analogous iodo complex [Pt( $\eta^3$ -PNC-L<sup>1</sup>)I] **220**, **Table 2.24**. It can be seen that the Pt-nitrogen and Pt-phosphorus bonds for both the chloro complexes and the analogous iodo complex are quite similar. However the platinum-carbon bonds are shorter in the chloro complexes than the iodo one, indicating increased bond strength for both **282** and **283** when compared with the iodo complex **220**.

<b>Bond</b>	<b>282</b> <b>Distance (Å)</b>	<b>283</b> <b>Distance (Å)</b>	<b>224</b> <b>Distance (Å)</b>
Pt-Nitrogen	1.997(2)	2.002(3)	2.018(5)
Pt-Phosphorus	2.271(7)	2.289(7)	2.280(16)
Pt-Carbon	2.026(2)	2.031(8)	2.050(6)
Pt-X(Halide)	2.296(9)	2.305(3)	2.5826(5)

*Table 2.24: A comparison of the inter-atomic bond distances (Å) around the distorted square metal centre for both chloro complexes **282** and **283** and the previously reported analogous iodo complex **224***

## 2.9 Summary and Conclusion

The iminophosphine ligands HL<sup>1-4</sup>, **261-264**, were also prepared by an alternative method to that which was reported previously and characterised using NMR, 2D NMR plots, IR and elemental analysis. The preparation of the iminophosphine ligands HL<sup>1-4</sup> **261-264** involved the reaction of a methanolic solution of 2-diphenylphosphinoaniline with one equivalent of the appropriate benzaldehyde with a drop of formic acid to catalyse the Schiff base condensation producing the iminophosphine ligands HL<sup>1-4</sup> **261-264** in good yields.

The complexation of all four iminophosphine ligands HL<sup>1-4</sup> **261-264** towards a Pt (II) metal centre was investigated with PtCl<sub>2</sub> and PtCl<sub>2</sub>(cod) as starting materials. PtCl<sub>2</sub> proved to be insoluble in most common solvents, reducing the possibility of successful coordination and cyclometallation (Method A). It did however establish the methods and products that

could be formed from the iminophosphine ligands  $HL^{1-4}$ . The more versatile  $PtCl_2(cod)$  was found to be much more successful for coordination and cyclometallation to form the Pt (II) tridentate cyclometallates **281-284** in good yields (Method B).

In method A, the reaction of  $PtCl_2$  for up to 48 hours with the iminophosphine ligands  $HL^{1-4}$  yielded an insoluble yellow powder and some of the cyclometallated complexes **281-284** in very low yields. The insoluble complexes are proposed to be dimers of the bidentate intermediates **271-274** formed prior to cyclometallation and could only be characterised effectively by IR spectroscopy and elemental analysis. Also a refluxing acetonitrile solution of  $PtCl_2$  and the  $HL^4$  ligand **264** gave primarily the previously reported tridentate P,N,O complex **285**.

Several novel Pt (II) Schiff base complexes of the general formula  $[Pt(\eta^3-PNC-L^{1-4})Cl]$  ( $L = 3-H L^1$  **281**,  $3-Br L^2$  **282**,  $3-Cl L^3$  **283**,  $2,3-(OMe)_2 L^4$  **284**) were synthesised from  $PtCl_2(cod)$  and characterised by IR, NMR, elemental and X-ray crystallography (in selected cases). The previously reported PNO complex  $[Pt(\eta^3-PNO-L^4)Cl]$  **285** was also prepared from  $PtCl_2(cod)$  in chloroform.

The method to synthesis the cyclometallated complexes  $[Pt(\eta^3-PNC-L^{1-4})Cl]$  **281-284** involved a slow addition of the appropriate iminophosphine ligand ( $HL^{1-4}$  **261-264**) in chloroform over 6 hours to a refluxing chloroform solution of  $PtCl_2(cod)$ . Yields of the cyclometallated complexes from this method (Method B) improved significantly over those found for Method A with  $PtCl_2$ .

The coordination behaviour of the  $HL^4$  ligand **264** towards  $PtCl_2(cod)$  was found to be different to that established for its coordination to Pd (II), but analogous to its coordination to the previously reported iodo-platinum complexes.<sup>2</sup> Reaction of the  $HL^4$  ligand **264** with  $PtCl_2$  in acetonitrile (Method A) generated primarily the tridentate PNO complex  $[Pt(\eta^3-PNO-L^4)Cl]$  **274**, whereas the same reaction with ligand  $HL^4$  **264** with  $PtCl_2(cod)$  formed primarily the novel  $2,3-(OMe)_2$  cyclometallated complex  $[Pt(\eta^3-PNC-L^4)Cl]$  **284** in chloroform, via stabilisation of the liberated chloride anion.

The previously reported phosphinoamide ligands, **265-267**, were synthesised by an alternative method and fully characterised using NMR, 2D NMR plots, IR and elemental analysis. The preparation of the phosphinoamide ligands  $HL^{5-7}$  **265-267** involved the reaction of a thf solution of 2-diphenylphosphinoaniline with one equivalent of the appropriate benzoyl chloride with an excess of DABCO to prevent build up the HCl by-product. This was

then stirred at room temperature to produce the phosphinoamide ligands HL<sup>5-7</sup> **265-267** in very good yields.

Characterisation of the phosphinoamide ligands HL<sup>5-7</sup> **265-267** by IR spectroscopy identified the presence of the N-H signal, however in solution the ligands were found to tautomerise into an iminol form, as identified by <sup>1</sup>H NMR. Further characterisation with <sup>13</sup>C and 2D NMR plots also found that due to the tautomerisation in solution, two inseparable isomers are formed (*E* and *Z*). The desired *E*-isomer is in a 3:1 majority ratio to the *Z*-isomer but the presence of the other isomer reduces the chances of cyclometallation of the platinum complexes from the insoluble bidentate dimer intermediates.

Several novel Pt (II) phosphinoiminol complexes of the general formula [Pt( $\eta^3$ -PNC-L<sup>5-7</sup>)Cl] (L = 3-OMe L<sup>5</sup> **286**, 2,4-(OMe)<sub>2</sub> L<sup>6</sup> **287**, 3-Br L<sup>7</sup> **288**) were also synthesised from PtCl<sub>2</sub>(cod) and the phosphinoamide ligands HL<sup>5-7</sup>. A novel PNO complex [Pt( $\eta^3$ -PNO-L<sup>6</sup>)Cl] **289** was also prepared and characterised from the HL<sup>6</sup> ligand **266**, but it was not possible to fully characterise it at this time.

Synthesis of cyclometallated platinum phosphinoamide complexes **286-289** involved adding the ligands dropwise to a refluxing solution of PtCl<sub>2</sub>(cod) in chloroform with DABCO and sodium carbonate for up to 8 hours. A white precipitate was formed from the reaction of DABCO with the HCl formed from the cyclometallation reaction. Similar to the iminophosphine platinum complexes, insoluble compounds were also formed and are proposed to be dimers of bidentate complexes. Also a second novel tridentate P,N,O complex **289** was formed from the reaction of PtCl<sub>2</sub>(cod) and the HL<sup>6</sup> **266** ligand but it proved to be very sensitive to hydrolysis.

In the IR spectra of all the prepared ligands HL<sup>1-7</sup> the characteristic C=N imine/ HO-C=N iminol stretch was observed in the region of 1615-1678 cm<sup>-1</sup>. For all of the platinum complexes **271-274** and **281-289** however there was a distinct shift of this stretch to lower wavenumbers of between 9 and 48 cm<sup>-1</sup>, which is typical for Schiff base transition metal complexes in which the nitrogen of the imine is involved in coordination to the metal centre.<sup>87,88</sup> Other major peaks observed in the IR spectra of these complexes included aromatic C-H stretching in the 3000-3100 cm<sup>-1</sup> region, C=C ring stretching in the 1400-1500 cm<sup>-1</sup> region and in the case of the phosphinoiminol complexes **286-289**, broad O-H stretching in the 3100-3300 cm<sup>-1</sup> region.

<sup>1</sup>H NMR data for the azomethine proton for all the iminophosphine complexes **281-285** showed the typical downfield shift in the spectra relative to that of the free ligands HL<sup>1-4</sup> **261-264** confirming coordination of the platinum to the nitrogen donor moiety. <sup>195</sup>Pt satellite

signals were also observed for all the complexes with coupling frequencies of 123-126 Hz for the cyclometallates **281-284** and 76 Hz for the PNO complex **285**.

In the tridentate phosphinoiminol platinum complexes  $[\text{Pt}(\eta^3\text{-PNC-L}^{5-7})\text{Cl}]$  and  $[\text{Pt}(\eta^3\text{-PNO-L}^6)\text{Cl}]$  **286-289**, the iminol signal becomes a doublet of doublets in comparison to a doublet found for the free ligands HL<sup>5-7</sup> **265-267**. This is observed because of the rigidity of the platinum phosphinoiminols. Omega coupling also appears to be occurring between one of the aromatic hydrogens on the P,N aryl ring and the iminol proton as indicated by a [<sup>1</sup>H-<sup>1</sup>H] COSY NMR plot where a correlation is observed.

<sup>13</sup>C NMR data and a [<sup>1</sup>H-<sup>13</sup>C DEPT 45] HETCOR plot confirmed the shift in the equivalent azomethine signal of the iminophosphine platinum complex  $[\text{Pt}(\eta^3\text{-PNC-L}^4)\text{Cl}]$  **284** relative to its free ligand HL<sup>4</sup> **264**. The new platinum-carbon bond formed as a result of cyclometallation was also identified as a new quaternary carbon not present in the free ligand. Also the Pt (II) complex **284** was found to have one less aromatic signal in comparison to the free ligand HL<sup>4</sup> **264**, giving further evidence for the formation of a platinum-carbon bond.

The <sup>31</sup>P NMR data for all the complexes **281-289** showed a significant downfield shift of between 27.6 and 40.0 ppm on complexation of the ligands to the platinum metal centre as expected, indicating that the phosphorus donor moiety is coordinated to the metal.<sup>88</sup> The presence of platinum satellites with coupling frequencies of 1950 – 2100 Hz for the cyclometallated complexes and 3140-3380 Hz for the PNO complexes is further evidence of successful coordination of the phosphorus donor moiety to the metal centre.

X-ray crystal structures were obtained for complexes **282** and **283**, confirming their structures as deduced from IR, NMR and elemental evidence. Both of these cycloplatinated complexes show the ligand coordinated in a tridentate manner to the platinum metal centre and both structures identify the complexes to have a distorted, square planar geometry, identical to previously reported iodo-platinum complexes.

## 2.10 Chapter 2 Experimental:

### 2.10.1 Background:

All reaction solvents were distilled prior to use, unless purchased as analytical grade (all from Sigma Aldrich Chemical Co. Ltd.). Toluene and thf were distilled directly before use from sodium-benzophenone. Methanol was distilled over magnesium/iodine according to Armarego *et al.*<sup>89</sup> and hexane was distilled over phosphorus pentoxide. *O*-diphenylphosphinoaniline was synthesized according to a variation of a method by M. K. Cooper *et al.*<sup>65</sup>

The following reagents were used as supplied; 2,3-dimethoxybenzaldehyde, benzaldehyde, 3-bromobenzaldehyde, 3-chlorobenzaldehyde, formic acid (all Aldrich Chemical Co. Ltd). Elemental analyses (Perkin-Elmer 2400 CHN elemental analyser) were performed by the microanalytical laboratory, University College Cork.

The <sup>1</sup>H and <sup>31</sup>P{<sup>1</sup>H} NMR spectra were recorded on a Bruker Advance 300 MHz, 400 MHz or 600 MHz NMR spectrometer (where specified). Chemical shifts (δ) are expressed in parts per million (ppm) and referenced to external tetramethylsilane (δ0) for <sup>1</sup>H and 85% phosphoric acid (δ0) for <sup>31</sup>P{<sup>1</sup>H} NMR using the high frequency positive convention.

Infrared spectra were recorded as KBr disks on a Perkin-Elmer Paragon 1000 FT spectrometer. Relative intensities are designated (s), strong; (m), medium; (w), weak; (b), broad. Mass Spectra were recorded on a Waters/Micromass LCT Premier time of flight spectrometer (ESI). Single crystal X-ray diffraction studies of compounds **282** and **283** were performed by Dr. Curtis Elcoate, Dr Kevin Eccles and Dr Simon Lawrence, Department of Chemistry, UCC. Data was measured with Mo K $\alpha$  radiation on a Bruker APEX DUO diffractometer as described previously.<sup>90</sup> All calculations and refinements were made using the APEX software,<sup>91,92</sup> and the diagrams prepared using Mercury.<sup>93</sup>



### 2.10.2 Preparation of the Iminophosphine ligands HL<sup>1-4</sup> 261-264:

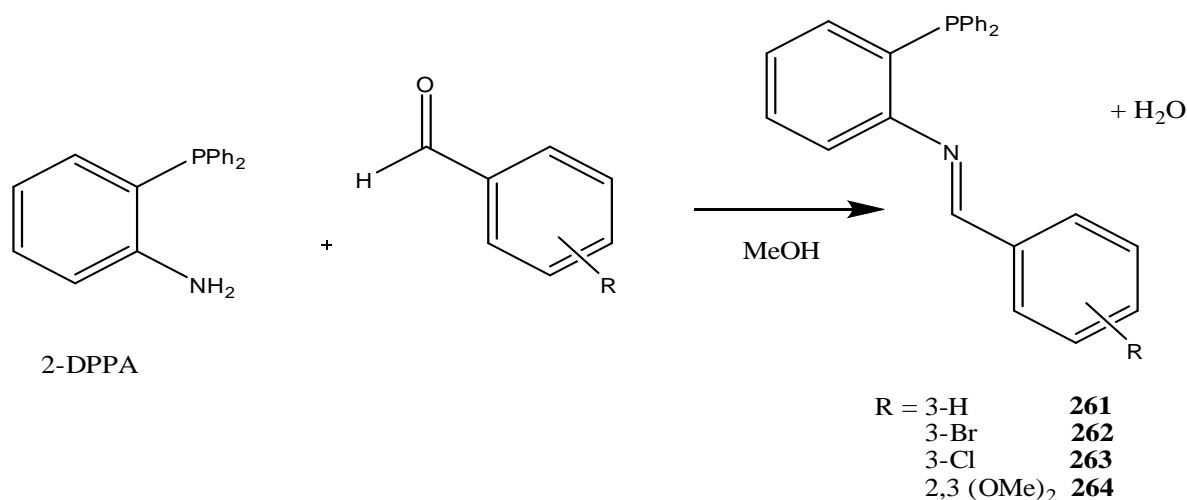
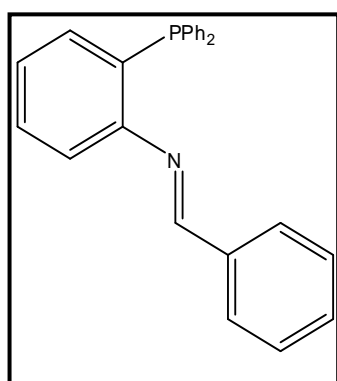


*Figure 2.86: Synthesis of the iminophosphine ligands HL<sup>1-4</sup> 261-264 from 2-diphenylphosphinoaniline and substituted benzaldehydes.*

2-(diphenylphosphino)-aniline (2-DPPA) was dissolved with one equivalent of the required benzaldehyde in 20 ml of methanol along with one drop of formic acid and stirred for 20 hours at 50°C under N<sub>2</sub>. The resulting yellow solution was then reduced to dryness *in vacuo* and the residue taken up in 20 ml of dichloromethane.

It was then washed with distilled water three times to remove any excess acid and any remaining starting materials that may be present. After separation, the organic layer was then dried over MgSO<sub>4</sub>, filtered and reduced to dryness *in vacuo*. The resulting oil was then crystallised from hot distilled methanol yielding the finely divided products HL<sup>1-4</sup> 261-264.



**HL<sup>1</sup> 261:** Benzaldehyde (0.37 ml, 3.60 mmol) and 2-(diphenylphosphino) aniline (1.000 g, 3.60 mmol) gave HL<sup>1</sup> 261 as a pale yellow crystalline solid. Yield: 0.609 g (46.3 %)

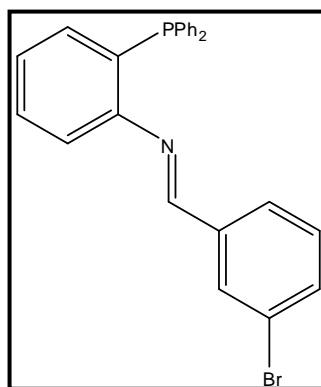
Found (required for C<sub>25</sub>H<sub>20</sub>NP): C, 81.88 (82.17); H, 5.40 (5.52); N, 3.88 (3.83).

IR  $\nu_{\max}$  (KBr): 3054 (H<sub>2</sub>O)(w), 3012 (s), 3027 (s), 2886 (s), 1626 (C=N)(s), 1574 (m), 1560 (w), 1492 (m), 1475 (Ar C=C)(s), 1460

(Ar C=C)(s), 1433 (Ar C=C)(s), 1369 (m), 1305 (m), 1268 (m), 1194 (w), 1166 (w), 1116 (s), 1090 (w), 1069 (m), 1025 (w), 995 (w), 999 (w), 981 (w), 974 (w), 885 (w), 859 (w), 828 (w), 766 (s), 694 (s), 687 (s), 506 (s).

<sup>1</sup>H NMR  $\delta$  ppm: 8.14 (1H, s), 7.00-7.50 (19H, m). <sup>31</sup>P NMR  $\delta$  ppm: -14.2 (s)

*m/z* (ESI) [(M+H)<sup>+</sup>]: 366.20



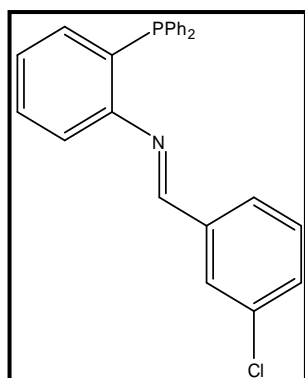
**HL<sup>2</sup> 262:** 3-Bromobenzaldehyde (0.420 ml, 3.60 mmol) and 2-(diphenylphosphino) aniline (1.000 g, 3.60 mmol) gave HL<sup>2</sup> **262** as a yellow crystalline solid. Yield: 0.854 g (53.4 %)

Found (required for C<sub>25</sub>H<sub>19</sub>BrNP): C, 67.53 (67.58); H, 4.39 (4.31); Br, 17.66 (17.98); N, 3.24 (3.15).

IR  $\nu_{\max}$  (KBr): 3649 (H<sub>2</sub>O)(w), 3250 (s), 3055 (s), 2362 (s), 1621 (C=N)(s), 1592 (Ar C-C)(s), 1560 (Ar)(s), 1507 (Ar)(m), 1474 (Ar C=C)(s), 1448 (Ar C=C)(s), 1434 (Ar C=C)(s), 1356 (m), 1305 (m), 1268 (m), 1174 (s), 1138 (m), 1116 (s), 1068 (m), 995 (w), 915 (w).

<sup>1</sup>H NMR  $\delta$  ppm: 8.07 (1H, s), 6.62-7.50 (18H, m). <sup>31</sup>P NMR  $\delta$  ppm: -13.7 (s)

*m/z* (ESI) [(M+H)<sup>+</sup>]: 446.10



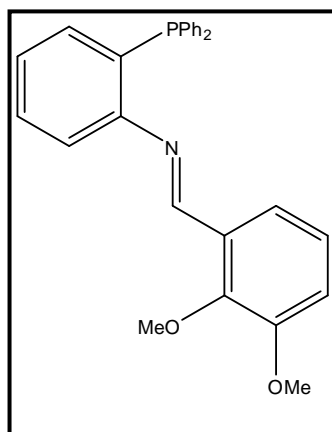
**HL<sup>3</sup> 263:** 3-Chlorobenzaldehyde (0.410 ml, 3.60 mmol) and 2-(diphenylphosphino) aniline (1.000 g, 3.60 mmol) gave HL<sup>3</sup> **263** as a yellow crystalline solid. Yield: 0.957 g (61.4 %)

Found (required for C<sub>25</sub>H<sub>19</sub>ClNP): C, 75.00 (75.09); H, 4.72 (4.79); N, 3.07 (3.50).

IR  $\nu_{\max}$  (KBr): 3700 (b), 3056 (m), 2925 (m), 2855 (m), 1622 (C=N)(s), 1563 (m), 1476 (Ar C=C)(s), 1434 (Ar C=C)(s), 1369 (w), 1307 (w), 1270 (w), 1239 (w), 1193 (m), 1093 (w), 1076 (m), 1027 (w), 999 (w), 981 (w), 889 (w), 843 (w), 791 (w), 749 (s), 696 (s), 681 (m), 544 (w), 528 (w), 505 (m), 470 (w)

<sup>1</sup>H NMR  $\delta$  ppm: 8.11 (1H, s), 6.83-7.86 (18H, m). <sup>31</sup>P NMR  $\delta$  ppm: -13.8 (s)

*m/z* (ESI) [(M+H)<sup>+</sup>]: 400.20



**HL<sup>4</sup> 264:** 2,3-dimethoxybenzaldehyde (0.604 g, 3.60 mmol) and 2-(diphenylphosphino) aniline (1.000 g, 3.60 mmol) gave HL<sup>4</sup> **264** as a fluffy yellow crystalline solid. Yield: 1.343 g (87.7 %)

Found (required for C<sub>27</sub>H<sub>24</sub>NO<sub>2</sub>P): C, 76.10 (76.22); H, 5.80 (5.69); N, 3.55 (3.29).

IR  $\nu_{\max}$  (KBr): 4244 (w), 3901 (w), 3056 (m), 2936 (C-H)(m), 1616(C=N)(s), 1576(s), 1561(s), 1477(Ar C-C)(s), 1430(s), 1356 (m), 1308 (m), 1270 (s), 1228 (m), 1207 (m), 1168 (m), 1072 (s),

996 (s), 930 (w), 864 (w), 790 (s), 764 (m), 742 (s), 697 (s), 591 (w), 547 (m), 506 (s).

$^1\text{H}$  NMR  $\delta$  ppm: 8.54 (1H, s), 6.52-7.86 (18H, m), 3.70 (3H, s), 3.85 (3H, s).

$^{31}\text{P}$  NMR  $\delta$  ppm: -14.5 (s)

$m/z$  (ESI)  $[(\text{M}+\text{H})^+]$ : 426.20

### 2.10.3 Preparation of the Phosphinoamide ligands HL<sup>5-7</sup> 261-264:

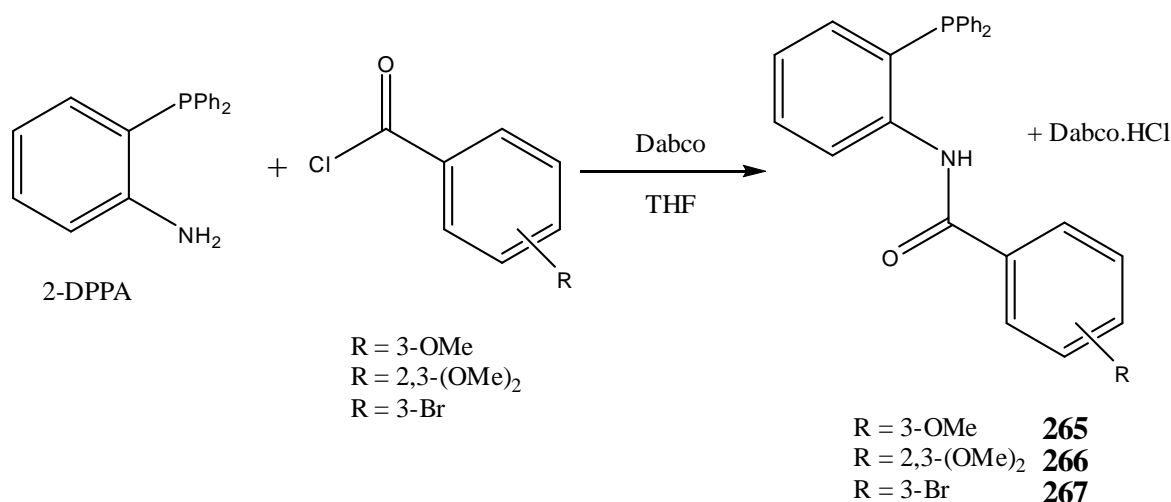
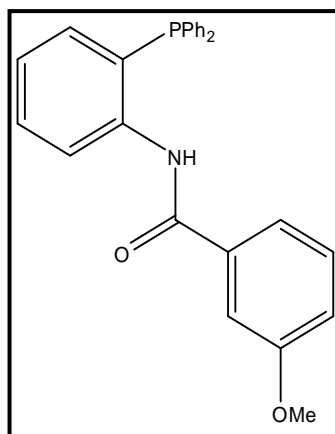


**Figure 2.86:** Synthesis of the phosphinoamide ligands HL<sup>5-7</sup> 265-267 from 2-diphenylphosphinoaniline and substituted benzoyl chlorides.

To a solution of 2-diphenylphosphinoaniline (2-DPPA) in THF, one equivalent of the appropriate acyl chloride (3-OMe HL<sup>5</sup> 265, 2,4-(OMe)<sub>2</sub> HL<sup>6</sup> 266, 3-Br HL<sup>7</sup> 267) and 2 equivalents of DABCO (1,4-diazabicyclo[2.2.2]octane) were added and stirred for 5 hours at room temperature.

A white precipitate of DABCO.HCl was formed which was filtered off to leave a light yellow solution. This was then reduced to dryness *in vacuo* and taken up in 20ml of dichloromethane. This organic solution was then washed three times with distilled water to remove any excess acid or salts along with any remaining starting materials.

After separation, the organic layer was then dried over MgSO<sub>4</sub>, filtered and reduced to dryness *in vacuo*. The resulting oil was then crystallised from distilled dichloromethane-hexane yielding the finely separated products, ligands HL<sup>5-7</sup> 265-267.



**HL<sup>5</sup> 265:** Anisoyl Chloride (0.49 ml, 3.60 mmol) and 2-(diphenylphosphino) aniline (1.000 g, 3.60 mmol) gave HL<sup>5</sup> **265** as a white crystalline solid. Yield: 1.112 g (75.1 %)

Found (required for C<sub>26</sub>H<sub>22</sub>NO<sub>2</sub>P.(CH<sub>2</sub>)<sub>4</sub>O): C, 74.41 (74.52); H, 5.40 (6.20); N, 2.90 (2.69).

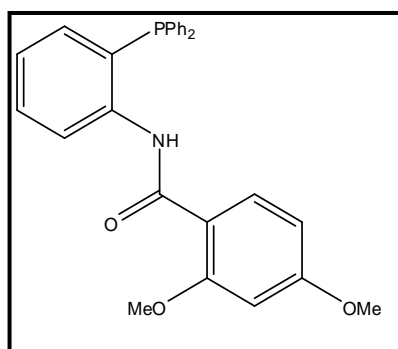
IR  $\nu_{\max}$  (KBr): 3362 (N-H)(s), 3054 (s), 3007 (w), 2956 (m), 2934 (w), 2833 (w), 1783 (w), 1677 (C=O)(s), 1600 (w), 1572 (m), 1511 (m), 1487 (Ar C=C)(s), 1433 (Ar C=C)(s), 1306 (s), 1290

(s), 1275 (s), 1260 (s), 1217 (m), 1180 (w), 1132 (m), 1120 (w), 1096 (m), 1069 (w), 1042 (m), 991 (w), 945 (w), 919 (w), 870 (w), 857 (w), 870 (w), 799 (w), 787 (s), 751 (s), 713 (w), 696 (s) 683 (s), 596 (s), 569 (m), 506 (m).

<sup>1</sup>H NMR  $\delta$  ppm: 8.84 (1H, d), 6.96-8.43 (18H, t,q,m,dd,m), 3.81 (3H, s).

<sup>31</sup>P NMR  $\delta$  ppm: -19.8 (s)

$m/z$  (ESI) [(M+H)<sup>+</sup>]: 412.20



**HL<sup>6</sup> 266:** 2,4-dimethoxybenzoyl chloride (0.72 g, 3.60 mmol) and 2-(diphenylphosphino) aniline (1.000 g, 3.60 mmol) gave HL<sup>6</sup> **266** as a white crystalline solid. Yield: 0.964 g (60.6 %)

Found (required for C<sub>27</sub>H<sub>24</sub>BrO<sub>3</sub>P): C, 73.65 (73.76), H, 5.41 (5.48), N, 3.10 (3.17).

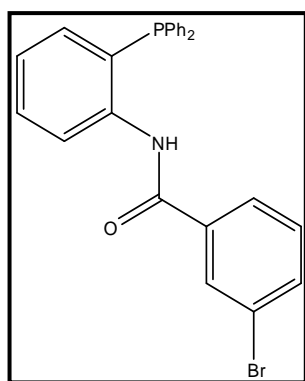
IR  $\nu_{\max}$  (KBr): 3275 (N-H)(w), 2936 (s), 2835 (s), 2362 (s),

1720 (s), 1649 (C=N)(s), 1610, (s) 1573 (Ar C=C)(s), 1531 (Ar)(s), 1501 (Ar)(m), 1453 (Ar C=C)(s), 1433 (Ar C=C)(s), 1329 (m), 1305 (w), 1299 (m), 1260 (m), 1241 (m), 1212 (s), 1164 (s), 1117 (m), 1086 (m), 1033 (m), 945 (w), 829 (w), 812 (w), 766 (m), 746 (m), 699 (m), 671 (m), 546 (w), 512 (m), 473 (m).

<sup>1</sup>H NMR  $\delta$  ppm: 10.50 (1H, d), 6.43-8.47 (17H, dd, t, m, t, m), 3.86 (3H, s), 3.79 (3H, s).

<sup>31</sup>P NMR  $\delta$  ppm: -17.7 (s)

$m/z$  (ESI) [(M+H)<sup>+</sup>]: 442.30



**HL<sup>7</sup> 267:** 3-Bromobenzoyl chloride (0.48 ml, 3.60 mmol) and 2-(diphenylphosphino) aniline (1.000 g, 3.60 mmol) gave HL<sup>7</sup> **267** as a yellow crystalline solid. Yield: 0.957 g (57.8 %)

Found (required for C<sub>25</sub>H<sub>19</sub>ClNP): C, 65.10 (65.23), H, 3.95 (4.16), N, 2.94 (3.04).

IR  $\nu_{\max}$  (KBr): 3366 (N-H)(s), 3057 (m), 1964 (w), 1923 (w), 1785 (w), 1721 (w), 1675 (C=O)(s), 1576 (m), 1522 (m), 1473 (Ar C=C)(s), 1433 (Ar C=C)(s), 1305 (m), 1242 (m), 1174 (m), 1090 (w), 1068 (m), 1024 (w), 997 (w), 942 (w), 921 (w), 903 (w), 892 (w), 852 (w), 864 (w), 794 (w), 752 (s), 732 (s), 697 (s), 669 (s), 590 (w), 565 (w), 548 (m), 503 (m), 470 (w).

<sup>1</sup>H NMR  $\delta$  ppm: 8.60 (1H, d), 6.95-8.34 (18H, dd, t, m, q, d). <sup>31</sup>P NMR  $\delta$  ppm: -18.7 (s)

*m/z* (ESI) [(M+H)<sup>+</sup>]: 462.10

#### 2.10.4 Synthesis of Iminophosphine complexes [Pt( $\eta^2$ -PN-L<sup>1-3</sup>)Cl] **271-273** and [Pt( $\eta^3$ -PNO-L<sup>4</sup>)Cl] **285** (Method A):

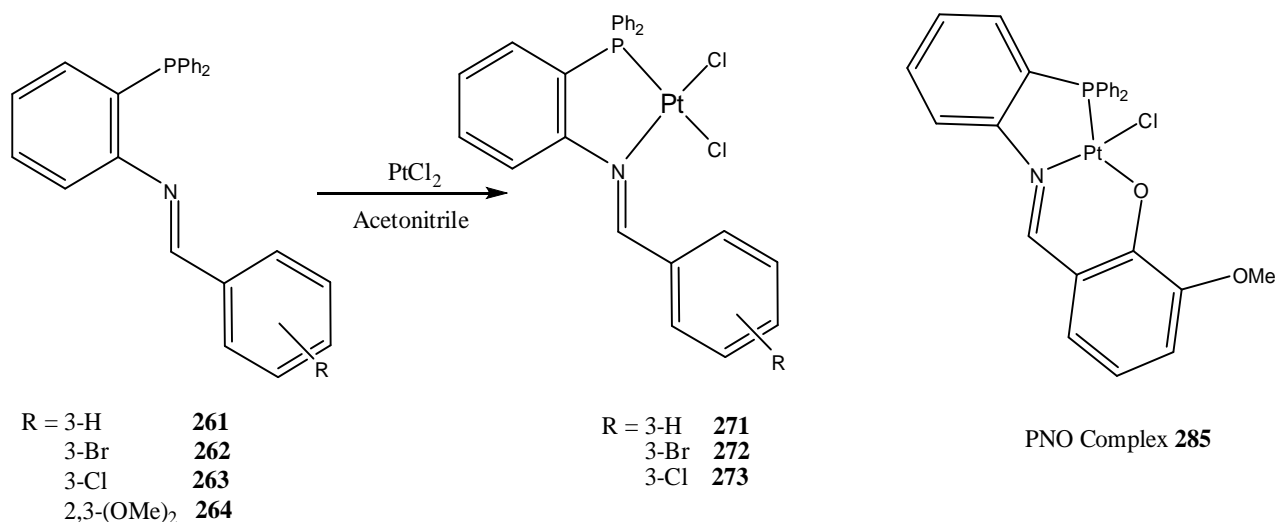
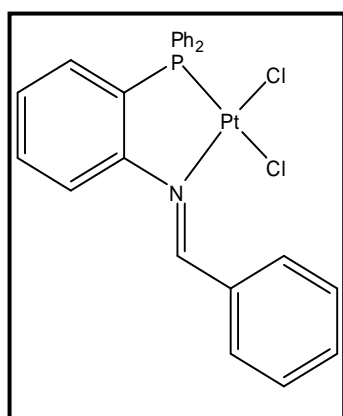


**Figure 2.87: METHOD A:** Synthesis of the platinum iminophosphine bidentate complexes **271-273** (as dimers) and the PNO tridentate complex **285**.

PtCl<sub>2</sub> was first refluxed in acetonitrile for 30mins prior to the addition of the ligand in order to ensure it was in solution. To the refluxing solution of PtCl<sub>2</sub> in acetonitrile a 1.1 equivalent of the appropriate ligand HL<sup>1-4</sup> **261-264** was added as a solid over an hour. The resulting mixture was then heated at reflux for 10 hours. A cloudy yellow/orange solution was produced and filtered to give a yellow solid which was washed with dichloromethane to produce the bidentate products **271-273**.

The bidentate complexes **271-273** proved to be too insoluble for NMR analysis so only IR spectroscopy and elemental analysis is presented here.

For the PNO complex **285**, the solution turned bright orange after reflux which was reduced to dryness *in vacuo*. The residue was then taken up in dichloromethane and washed with 2 portions of distilled water before being dried over MgSO<sub>4</sub>. The solution was then reduced to dryness again *in vacuo* and crystallised from dichloromethane-hexane to produce the PNO complex **285**.

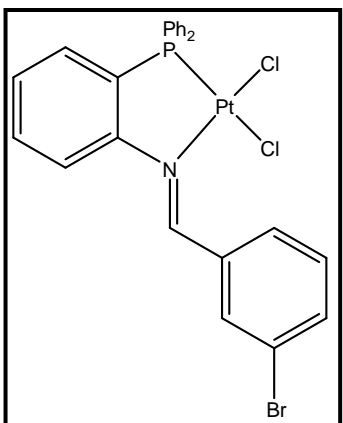


**271:** HL<sup>1</sup> (0.088 g, 0.24 mmol) **261** and PtCl<sub>2</sub> (0.059 g, 0.22 mmol) gave [Pt(η<sup>2</sup>-PN-L<sup>1</sup>)Cl]**271** as a yellow powder.

Yield: 0.119 g (85.7%)

Found (required for C<sub>25</sub>H<sub>20</sub>Cl<sub>2</sub>NPt.0.5CH<sub>2</sub>Cl<sub>2</sub>): C, 45.90 (45.85); H, 3.20 (3.15); N, 2.44 (2.21)

IR  $\nu_{\max}$  (KBr): 3430 (w), 3058 (w), 2924 (w), 1595 (C=N)(s), 1566 (m), 14.81 (Ar C=C)(s), 1437 (Ar C=C)(m), 1303 (w), 1274 (w), 1227 (m), 1187 (m), 1175 (w), 1104 (m), 1066 (m), 1028 (w), 998 (w), 972 (w), 924 (w) 828 (s), 783 (s), 768 (s), 756 (m), 720 (m), 692 (s), 592 (s), 567 (s), 549 (m), 542 (m), 512 (s), 499 (m), 458 (w).

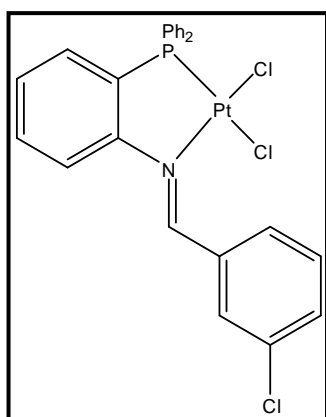


**272:** HL<sup>2</sup> (0.107 g, 0.24 mmol) **262** and PtCl<sub>2</sub> (0.059 g, 0.22 mmol) gave [Pt(η<sup>2</sup>-PNC-L<sup>1</sup>)Cl]**292** as a yellow powder.

Yield: 0.098 g (62.7%)

Found (required for C<sub>25</sub>H<sub>19</sub>BrCl<sub>2</sub>NPt.2.5CH<sub>2</sub>Cl<sub>2</sub>): C, 36.53 (36.77); H, 3.89 (3.82); N, 3.30 (3.21)

IR  $\nu_{\max}$  (KBr): 3329 (w), 2969 (w), 2920 (w), 2334 (m), 1683 (w), 1591 (C=N)(s), 1519 (m), 1480 (Ar C=C)(m), 1436 (Ar C=C)(m), 1319 (w), 1158 (w), 1118 (s), 1098 (m), 1069 (s), 1026 (w), 996 (w), 823 (w), 751 (m), 734 (s), 709 (s), 667 (s), 573 (s), 520 (m).



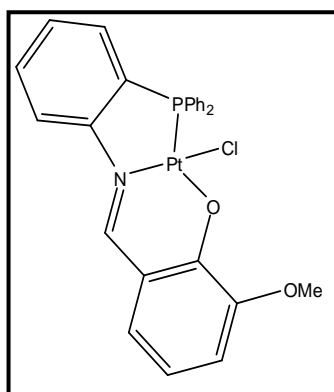
**273:** HL<sup>3</sup> (0.088 g, 0.24 mmol) **263** and PtCl<sub>2</sub> (0.059 g, 0.22 mmol) gave [Pt(η<sup>2</sup>-PN-L<sup>3</sup>)Cl]**293** as a yellow powder.

Yield: 0.087 g (59.4 %)

Found (required for C<sub>25</sub>H<sub>19</sub>Cl<sub>3</sub>NPPt): C, 43.85 (43.96); H, 2.75 (2.86); N 1.94, (2.03).

IR  $\nu_{\max}$  (KBr): 3432 (H<sub>2</sub>O)(br)(m), 3171 (w), 2924 (w), 2851 (w), 2353 (w), 2008 (w), 1703 (w), 1584 (C=N)(s), 1557 (m), 1475 (s), 1436 (Ar C=C)(m), 1336 (s), 1287 (w), 1230 (w), 1181 (m), 1101

(s), 1078 (m), 1068 (w), 1028 (w), 998 (w), 877 (m), 826 (s), 779 (s), 751 (m), 742 (m), 733 (m), 715 (m), 692 (s), 625 (w), 572 (m), 527 (s), 500 (s), 456 (w).



**285:** HL<sup>4</sup> (0.102 g, 0.24 mmol) **264** and PtCl<sub>2</sub> (0.059 g, 0.22 mmol) gave [Pt(η<sup>3</sup>-PNO-L<sup>4</sup>)Cl]**275** as an orange crystalline powder.

Yield PNO: 0.006g (4.9%)

Found (required for C<sub>26</sub>H<sub>21</sub>ClNO<sub>2</sub>PPt.0.2CH<sub>2</sub>Cl<sub>2</sub>): C, 47.56 (47.83); H, 3.14 (3.28); N, 2.12 (2.13); Cl, 7.23 (7.54).

IR  $\nu_{\max}$  (KBr): 3854(w), 3806(w), 3751(w), 3427(m,b), 1654(w),

1607 (C=N)(s), 1590(s), 1570(s), 1540(s), 1478(w), 1458(w), 1436(s), 1387(m), 1333(m), 1249(s), 1231(s), 1174(s), 1101(m), 986(w), 876(w), 741(s), 714(m), 691(s), 564(s), 509(s), 476(w), 467(w), 458(w).

<sup>1</sup>H NMR  $\delta$  ppm: 9.15 (1H, s) (<sup>3</sup>J<sub>Pt-H</sub> 76 Hz), 6.59-7.90 (16H, d, q, d, m), 3.89 (3H, s).

<sup>31</sup>P NMR  $\delta$  ppm: 13.1 (s) (<sup>1</sup>J<sub>Pt-P</sub> 3816 Hz)

### 2.10.5 Synthesis of the platinum iminophosphine complexes $[\text{Pt}(\eta^3\text{-PNC-L}^{1-3})\text{Cl}]$ **281-283** and $[\text{Pt}(\eta^3\text{-PNO-L}^4)\text{Cl}]$ **285** (Method B):

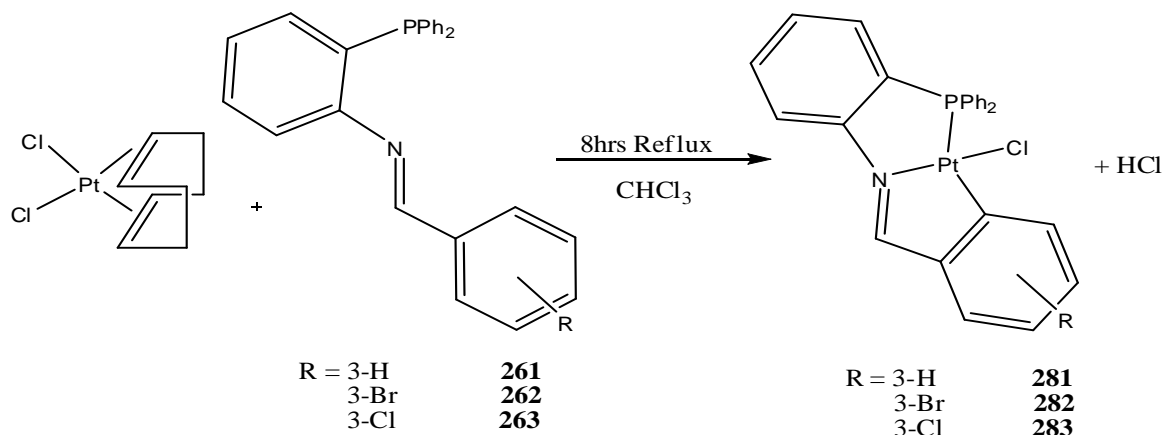
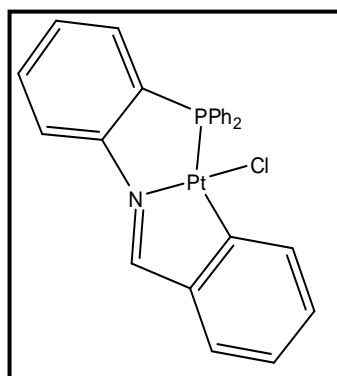


**Figure 2.88: METHOD B:** Synthesis of the platinum iminophosphine cyclometallated complexes **281-283** via thermal and solvent assisted C-H activation.

A stirred solution of (1,5-cyclooctadiene) dichloroplatinum (II)  $[\text{PtCl}_2(\text{cod})]$  in chloroform (20ml) was reacted with 1.1 equivalents of the appropriate ligand **261-263**, which was also dissolved in chloroform (10ml). 4Å molecular sieves were added to the solution to ensure the absence of moisture. The ligand was added drop wise from an addition funnel over 4 hours, after which the reaction mixture was heated at reflux for an additional 4 hours.

The resulting orange/yellow solution was then reduced to dryness *in vacuo*. The residue was taken up in 20ml of singly distilled dichloromethane to which silica gel was added to remove unwanted bidentate dimer complexes and hydrolysed ligand material. The silica gel was then filtered off and washed with two portions of dichloromethane. The filtrate was reduced to dryness *in vacuo* and crystallised from doubly distilled dichloromethane-hexane to yield cyclometallates **281-283**.



**281:** HL<sup>1</sup> (0.080 g, 0.22 mmol) **261** and  $\text{PtCl}_2(\text{cod})$  (0.076 g, 0.20 mmol) gave  $[\text{Pt}(\eta^3\text{-PNC-L}^1)\text{Cl}]$  **281** as a yellow metallic crystalline powder. Yield: 0.088 g (73.9 %)

Found (required for  $\text{C}_{25}\text{H}_{19}\text{ClNPPt} \cdot 0.1\text{CH}_2\text{Cl}_2$ ): C, 49.92 (49.96); H, 3.17 (3.21); N, 2.68 (2.32); Cl, 6.75 (7.05).

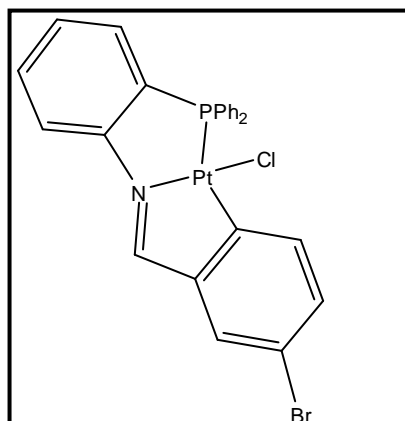
IR  $\nu_{\text{max}}$  (KBr): 3434 (w), 3047 (w), 3031 (w), 1585 (C=N)(s), 1560 (m), 1527 (s), 1478 (Ar C=C)(m), 1467 (Ar C=C)(m), 1438



(Ar C=C)(s), 1301 (w), 1269 (w), 1238 (m), 1186 (m), 1098 (s), 997 (w), 948 (w), 768 (s), 751 (s), 719 (s), 692 (s), 572 (s), 526 (s), 506 (s), 498 (s).

$^1\text{H}$  NMR  $\delta$  ppm: 9.40 (1H, s) ( $^3J_{\text{Pt-H}}$  123 Hz), 7.41-8.21 (18H, q, dd, d, m).

$^{31}\text{P}$  NMR  $\delta$  ppm: 25.3 (s) ( $^1J_{\text{Pt-P}}$  2083 Hz)



**282:** HL<sup>2</sup> (0.097 g, 0.22 mmol) **262** and PtCl<sub>2</sub>(cod) (0.076 g, 0.20 mmol) gave [Pt(η<sup>3</sup>-PNC-L<sup>1</sup>)Cl] **282** as a metallic yellow crystalline powder. Yield: 0.009g (6.7%)

Found (required for C<sub>25</sub>H<sub>18</sub>BrClNPPt): C, 44.45 (44.56); H, 2.65 (2.69); N, 1.92 (2.08).

IR  $\nu_{\text{max}}$  (KBr): 3422 (b), 3048 (w), 1587 (C=N)(s), 1556 (m), 1518 (s), 1479 (Ar C=C)(m), 1471 (Ar C=C)(m), 1435 (Ar C=C)(s), 1335 (w), 1287 (w), 1229 (m), 1180 (m), 1100

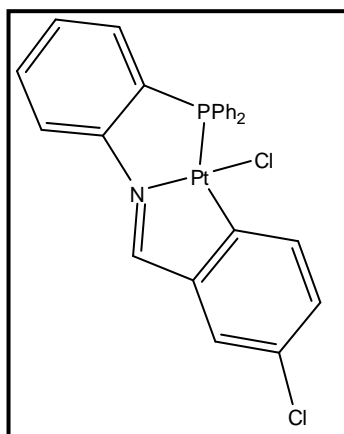
(s), 998 (w), 922 (w), 823 (m), 766 (m), 743 (s), 691 (s), 572 (s), 527 (m), 499 (s).

$^1\text{H}$  NMR  $\delta$  ppm: 9.40 (1H, s) ( $^3J_{\text{Pt-H}}$  123 Hz), 7.40-8.13 (17H, q, m).

$^{31}\text{P}$  NMR  $\delta$  ppm: 25.6 (s) ( $^1J_{\text{Pt-P}}$  2100 Hz)

X-Ray: Crystals of [Pt(η<sup>3</sup>-PNC-L<sup>2</sup>)Cl] **282**, suitable for X-ray analysis, were grown from the slow evaporation of a CHCl<sub>3</sub> solution:

<b>Formula:</b>	[Pt <sup>II</sup> (η <sup>3</sup> -PNC-L <sup>2</sup> )Cl]	<b>Volume (Å<sup>3</sup>)</b>	2162.7(7)
<b>Empirical Formula:</b>	C <sub>25</sub> H <sub>18</sub> BrClNPPt	<b>Z</b>	Z=4, Z'=0
<b>Weight:</b>	629.36	<b>Abs. coeff., <math>\mu</math></b>	8.545
<b>Space Group</b>	P 2 <sub>1</sub> /n	<b>Reflections Total</b>	5417
<b>Crystal System</b>	Monoclinic	<b>Radiation Type</b>	MoK $\alpha$ (0.71073cm <sup>-1</sup> )
<b>a (Å)</b>	9.5692(18)	<b>Reflections unique</b>	5028
<b>b (Å)</b>	12.410(3)	<b>Parameters</b>	271
<b>c (Å)</b>	18.326(4)	<b>R factor</b>	1.68%
<b><math>\alpha</math> (°)</b>	90	<b>R<sub>1</sub></b>	>2 $\sigma$ I
<b><math>\beta</math> (°)</b>	96.394(4)	<b>Crystal Colour</b>	Brown-yellow
<b><math>\gamma</math> (°)</b>	90		
<b>Crystal Description</b>	pyramid		



**283:** HL<sup>3</sup> (0.088 g, 0.22 mmol) **263** and PtCl<sub>2</sub>(cod) (0.076 g, 0.20 mmol) gave [Pt(η<sup>3</sup>-PNC-L<sup>3</sup>)Cl] **283** as an orange metallic crystalline powder. Yield: 0.047g (37.1%)

Found (required for C<sub>25</sub>H<sub>18</sub>Cl<sub>2</sub>NPPt): C, 47.31 (47.71); H, 2.85 (2.88); N, 1.89 (2.23); Cl, 11.38 (11.27).

IR  $\nu_{\max}$  (KBr): 3479 (w), 3185 (w), 3050 (w), 2921 (w), 2851 (w), 1742 (w), 1576 (C=N)(s), 1557 (m), 1523 (s), 1474 (Ar C=C)(m), 1436 (Ar C=C)(m), 1384 (s), 1336 (w), 1287 (w),

1230 (m), 1181 (m), 1101 (s), 1078 (m), 1068 (w), 1029 (w), 927 (w), 877 (m), 826 (s), 779 (s), 693 (s), 625 (w), 572 (m), 527 (s), 499 (s).

<sup>1</sup>H NMR  $\delta$  ppm: 9.40 (1H, s) (<sup>3</sup>J<sub>Pt-H</sub> 123 Hz), 7.34-8.15 (17H, m, m).

<sup>31</sup>P NMR  $\delta$  ppm: 25.5 (s) (<sup>1</sup>J<sub>Pt-P</sub> 2123 Hz)

X-Ray: Crystals of [Pt<sup>II</sup>(η<sup>3</sup>-PNC-L<sup>3</sup>)Cl] **283**, suitable for X-ray analysis, were grown from the slow evaporation of a CHCl<sub>3</sub> solution:

<b>Formula:</b>	[Pt <sup>II</sup> (η <sup>3</sup> -PNC-L <sup>3</sup> )Cl]	<b>Volume (Å<sup>3</sup>)</b>	2178.84
<b>Empirical Formula:</b>	C <sub>25</sub> H <sub>18</sub> Cl <sub>2</sub> NPPt	<b>Z</b>	Z=4, Z'=0
<b>Weight:</b>	629.36	<b>Abs. coeff., <math>\mu</math></b>	6.771
<b>Space Group</b>	P 2 <sub>1</sub> /n	<b>Reflections Total</b>	5295
<b>Crystal System</b>	Monoclinic	<b>Radiation Type</b>	MoK $\alpha$ (0.71073cm <sup>-1</sup> )
<b>a (Å)</b>	10.1435(11)	<b>Reflections unique</b>	4620
<b>b (Å)</b>	17.491(2)	<b>Parameters</b>	271
<b>c (Å)</b>	12.2865(14)	<b>R factor</b>	1.97%
<b><math>\alpha</math> (°)</b>	90	<b>R<sub>1</sub></b>	>2 $\sigma$ I
<b><math>\beta</math> (°)</b>	91.725(2)		
<b><math>\gamma</math> (°)</b>	90		

### 2.10.6 Synthesis of the platinum iminophosphine complexes $[\text{Pt}(\eta^3\text{-PNC-L}^4)\text{Cl}]$ **284** and $[\text{Pt}(\eta^3\text{-PNO-L}^4)\text{Cl}]$ **285** (Method B):

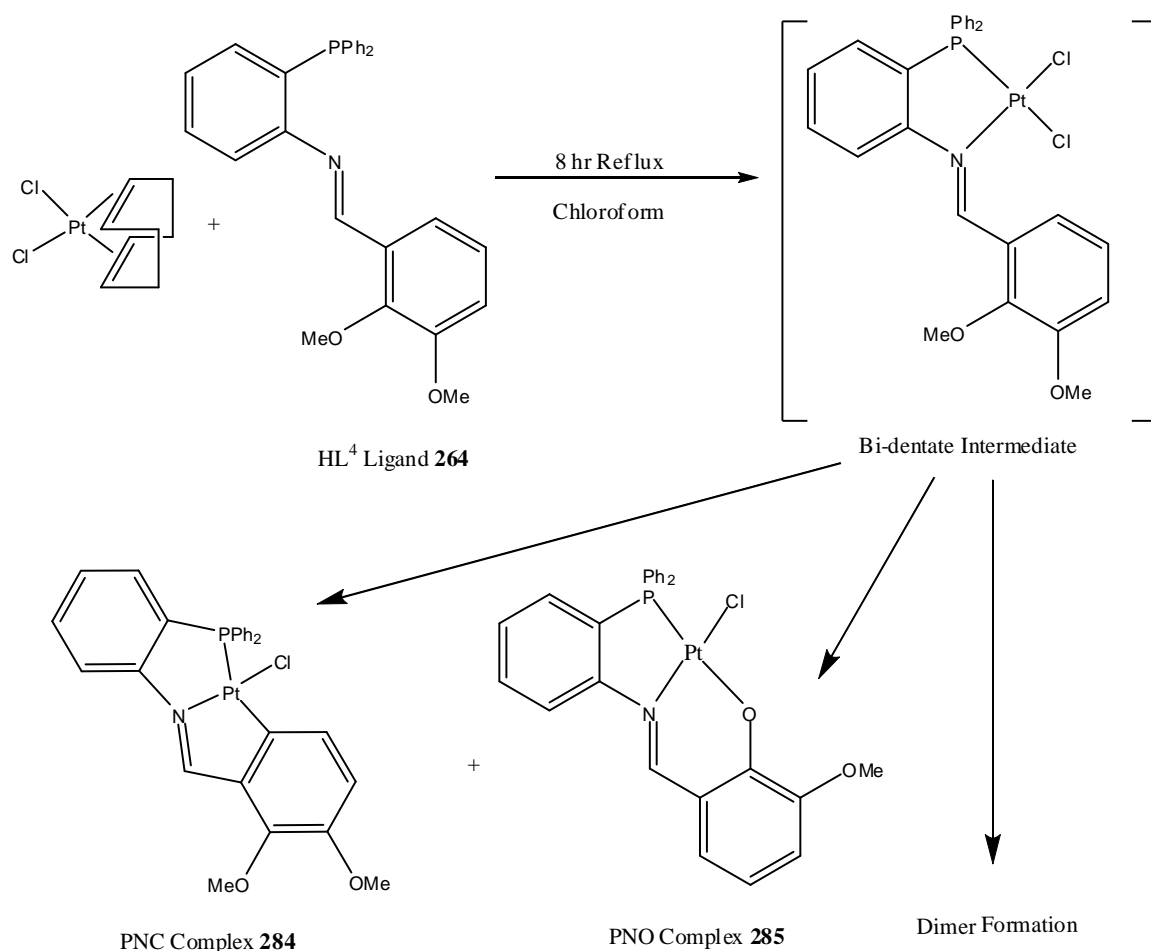
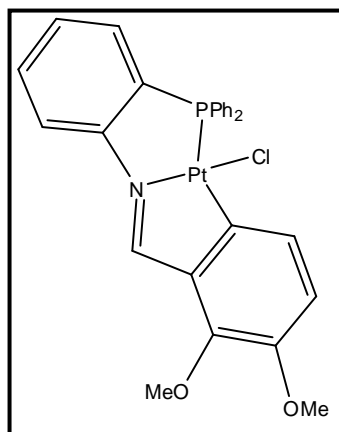


**Figure 2.89: METHOD B:** Synthesis of the platinum iminophosphine cyclometallated complex **284** as well as the previously reported PNO complex **285**.

A stirred solution of (1,5-cyclooctadiene) dichloroplatinum (II)  $[\text{PtCl}_2(\text{cod})]$  in chloroform (20ml) was reacted with 1.1 equivalents of the HL<sup>4</sup> ligand **264**, which was also dissolved in chloroform (10ml). 4Å molecular sieves were added to the solution to ensure the absence of moisture. The ligand was added dropwise from an addition funnel over 4 hours, after which the reaction mixture was heated at reflux for an additional 4 hours.

The resulting orange/yellow solution was found to be a mixture of products identified by TLC and was then reduced to dryness *in vacuo*. The two tridentate complexes were separated using wet-flash chromatography on silica gel, eluting from chloroform:methanol (98:2). Visualisation under UV light using TLC gave 3 spots from the column where one was at  $R_f=0.83$ , another at  $R_f=0.33$  and one which stayed on the line with an  $R_f=0$ .

The 2 soluble products were crystallised from dichloromethane-hexane to give the cyclometallated complex  $[\text{Pt}(\eta^3\text{-PNC-L}^4)\text{Cl}]$  **284** and the previously reported PNO complex  $[\text{Pt}(\eta^3\text{-PNO-L}^4)\text{Cl}]$  **285**. The insoluble material that stayed on the silica column is tentatively proposed to be the proposed bidentate complex **274**.



**284:** HL<sup>4</sup> (0.095 g, 0.22 mmol) **264** and PtCl<sub>2</sub>(cod) (0.076 g, 0.20 mmol) gave  $[\text{Pt}(\eta^3\text{-PNC-L}^4)\text{Cl}]$  **284** as a metallic orange crystalline powder. Yield PNC: 0.083 g (63.1 %)

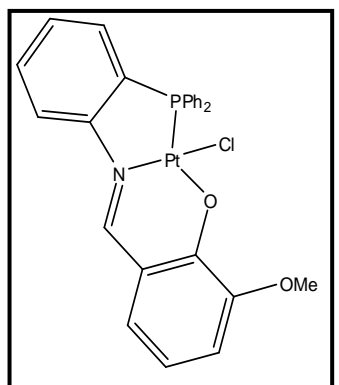
Found (required for C<sub>27</sub>H<sub>23</sub>ClINO<sub>2</sub>PPt.0.2CH<sub>2</sub>Cl<sub>2</sub>): C, 48.27 (48.62); H, 3.46 (3.51); N, 1.79 (2.08); Cl, 7.41 (7.39).

IR  $\nu_{\text{max}}$  (KBr): 3379 (w), 3053 (w), 2924 (m), 2853 (w), 1658 (w), 1578 (C=N)(s), 1529 (m), 1474 (Ar C=C )(m), 1462 (s), 1436 (Ar C=C)(m), 1424 (s), 1330 (w), 1264 (s), 1242 (m), 1203

(m), 1183 (s), 1130 (m), 1099 (w), 1076 (w), 1013 (m), 955 (m), 824 (s), 755 (s), 694 (s), 662 (w), 588 (m), 565 (s), 525 (s).

<sup>1</sup>H NMR  $\delta$  ppm: 9.72 (1H, s) (<sup>3</sup>J<sub>Pt-H</sub> 126 Hz), 7.27-8.17 (17H, m), 3.88 (3H, s), 4.02 (3H, s).

<sup>31</sup>P NMR  $\delta$  ppm: 25.2 (s) (<sup>1</sup>J<sub>Pt-P</sub> 2102 Hz)



**285:** HL<sup>4</sup> (0.095 g, 0.22 mmol) **264** and PtCl<sub>2</sub>(cod) (0.076 g, 0.20 mmol) gave  $[\text{Pt}(\eta^3\text{-PNO-L}^4)\text{Cl}]$  **285** as a orange crystalline powder. Yield PNO: 0.015 g (12 %)

Found (required for C<sub>26</sub>H<sub>21</sub>ClINO<sub>2</sub>PPt.0.4CHCl<sub>3</sub>): C, 45.85 (46.04); H, 3.27 (3.13); N, 2.20 (2.03).

IR  $\nu_{\text{max}}$  (KBr): 3443 (w), 3051 (w), 1607 (C=N)(s), 1590 (s), 1540(s), 1477 (w), 1437 (w), 1395 (m), 1331 (m), 1279 (s), 1251

(s), 1231 (m), 1178 (s), 1158 (m), 1102 (s), 1066 (m), 986 (w), 879 (w), 856 (w), 742 (s), 716 (m), 691 (s), 583 (w), 566 (s), 583 (m), 509 (s), 459 (w).

<sup>1</sup>H NMR  $\delta$  ppm: 9.15 (1H, s) (<sup>3</sup>J<sub>Pt-H</sub> 76 Hz), 6.59-7.90 (16H, d, q, d, m), 3.89 (3H, s).

<sup>31</sup>P NMR  $\delta$  ppm: 13.1 (s) (<sup>1</sup>J<sub>Pt-P</sub> 3816 Hz)

### 2.10.7 Synthesis of the platinum phosphinoiminol cyclometallated complexes $[\text{Pt}(\eta^3\text{-PNC-L}^{5-7})\text{Cl}]$ **286-288**:

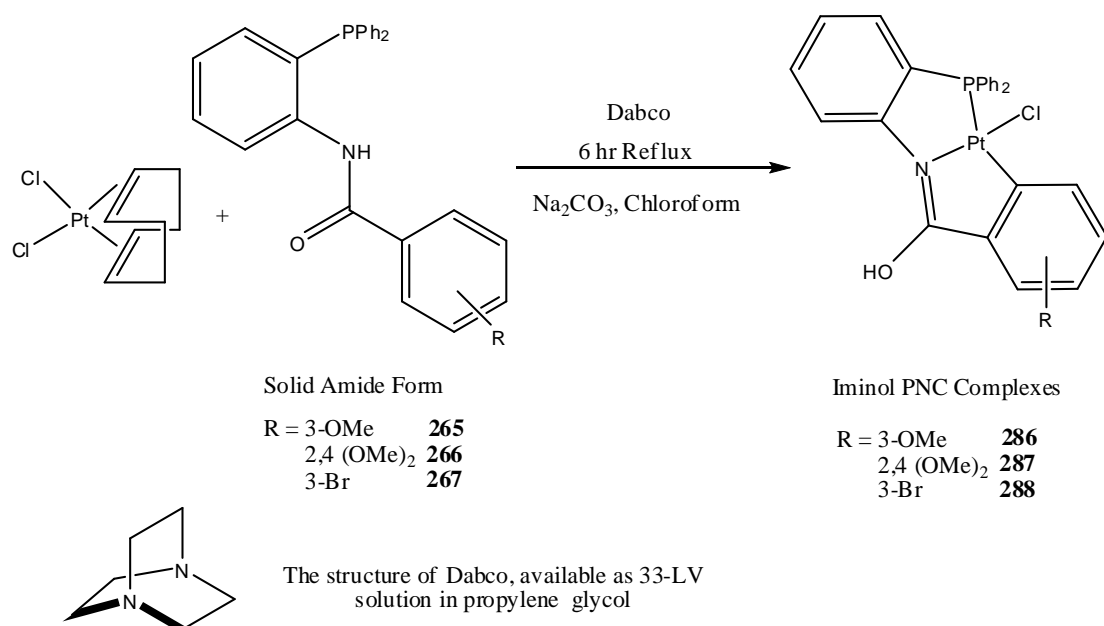
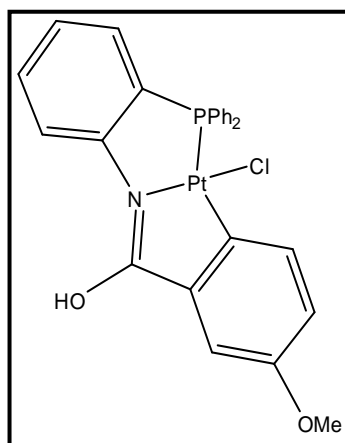


**Figure 2.90:** Synthesis of the platinum phosphinoiminol cyclometallated complex **286-288**.

To a stirred refluxing solution of  $\text{PtCl}_2(\text{cod})$  in 30ml of chloroform with an excess of sodium carbonate (0.04 g) and DABCO (0.05 ml) added, the  $\text{HL}^{5-7}$  ligands **265-267** were added as a solution of chloroform from a drop funnel over four hours. The solution was then refluxed for a further two hours to assist thermal cyclometallation. Immediately after adding the ligand the reaction became cloudy white with the formation of the DABCO hydrochloric salt. After six hours the bright yellow cloudy solution was reduced to dryness *in vacuo*, taken up in dichloromethane, washed three times with de-ionised water and dried over  $\text{MgSO}_4$ . The solution was then reduced to dryness again *in vacuo* and crystallised from dichloromethane-hexane to produce the cyclometallated complexes **286**, **287** and **288**.



**286:**  $\text{HL}^5$  (0.091 g, 0.22 mmol) **265** and  $\text{PtCl}_2(\text{cod})$  (0.076 g, 0.20 mmol) gave  $[\text{Pt}(\eta^3\text{-PNC-L}^5)\text{Cl}]$  **286** as a pale yellow crystalline powder. Yield: 0.054 g (42.2 %)

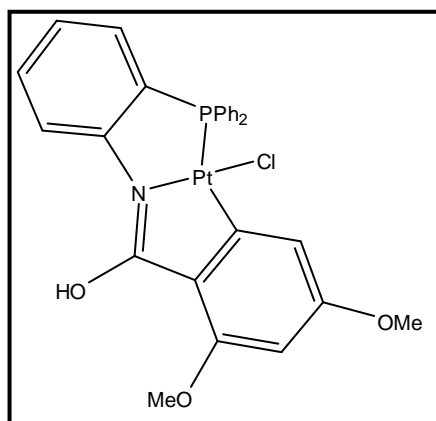
Found (required for  $\text{C}_{26}\text{H}_{21}\text{ClNO}_2\text{PPt}\cdot\text{CH}_2\text{Cl}_2$ ): C, 44.83 (44.67); H, 3.27 (3.19); N, 2.10 (1.93).

IR  $\nu_{\text{max}}$  (KBr): 3329 (w), 3053 (w), 2932 (w), 1678 (w), 1582 (C=N)(s), 1503 (m), 1484 (s) (Ar C=C)(s), 1458 (Ar C=C)(m),

1437 (Ar C=C)(m), 1321 (w), 1296 (m), 1264 (m), 1211 (m), 1181 (w), 1160 (w), 1098 (w), 1039 (w), 998 (w), 870 (w), 796 (s), 780 (s), 748 (s), 694 (s), 533 (s), 492 (s), 508 (s).

$^1\text{H}$  NMR  $\delta$  ppm: 9.45 (1H, dd) ( $^6J_{\text{H-P}}$  12 Hz,  $^6J_{\text{H-H}}$  3 Hz), 7.92-7.95 (17H, m), 3.87 (3H, s).

$^{31}\text{P}$  NMR  $\delta$  ppm: 24.3 (s) ( $^1J_{\text{Pt-P}}$  1928 Hz)



**287**: HL<sup>6</sup> (0.097 g, 0.22 mmol) **266** and PtCl<sub>2</sub>(cod) (0.076 g, 0.20 mmol) gave [Pt( $\eta^3$ -PNC-L<sup>6</sup>)Cl] **287** as a dark yellow crystalline powder. Yield: 0.068 g (51 %)

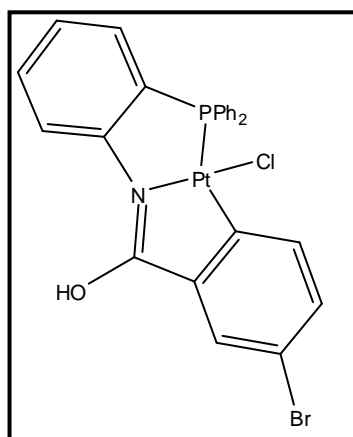
Found (required for C<sub>27</sub>H<sub>23</sub>ClINO<sub>3</sub>PPt.0.5CH<sub>2</sub>Cl<sub>2</sub>): C, 46.15 (46.30); H, 3.38 (3.39); N, 2.07 (1.96).

IR  $\nu_{\text{max}}$  (KBr): 3052 (w), 2929 (w), 1575 (C=N)(s), 1482 (Ar C=C)(m), 1457 (Ar C=C)(m), 1436 (Ar C=C)(s), 1260 (s), 1209 (w), 1157 (m), 1137 (m), 1099 (s), 1062

(w), 1037 (m), 999 (w), 943 (w), 833 (m), 748 (m), 694 (s), 656 (s), 536 (m), 505 (s).

$^1\text{H}$  NMR  $\delta$  ppm: 9.49 (1H, dd) ( $^6J_{\text{H-P}}$  12 Hz,  $^6J_{\text{H-H}}$  3 Hz), 6.10-7.86 (16H, m), 3.89 (3H, s), 3.74 (3H, s).

$^{31}\text{P}$  NMR  $\delta$  ppm: 22.9 (s) ( $^1J_{\text{Pt-P}}$  1928 Hz)



**288**: HL<sup>7</sup> (0.101 g, 0.22 mmol) **267** and PtCl<sub>2</sub>(cod) (0.076 g, 0.20 mmol) gave [Pt( $\eta^3$ -PNC-L<sup>3</sup>)Cl] **288** as a pale yellow crystalline powder. Yield: 0.017 g (11.9 %)

Found (required for C<sub>25</sub>H<sub>18</sub>BrCINOPPt.CH<sub>2</sub>Cl<sub>2</sub>) C, 42.36 (42.15); H, 3.72 (3.62); N, 2.05 (1.94).

IR  $\nu_{\text{max}}$  (KBr): 3328 (w), 3052 (w), 2920 (m), 1677 (m), 1615 (m), 1579 (C=N)(s), 1501 (m), 1457 (Ar C=C)(m), 1436 (Ar C=C)(m), 1392 (s), 1313 (w), 1261 (w), 1183 (m), 1159 (s),

1100 (m), 1063 (s), 998 (m), 940 (w), 863 (w), 795 (w), 777 (s), 745 (s), 693 (s), 608 (w), 534 (m), 505 (s).

$^1\text{H}$  NMR  $\delta$  ppm: 9.45 (1H, dd) ( $^6J_{\text{H-P}}$  12 Hz,  $^6J_{\text{H-H}}$  3 Hz), 6.77-8.10 (17H, m).

$^{31}\text{P}$  NMR  $\delta$  ppm: 25.1 (s) ( $^1J_{\text{Pt-P}}$  2041 Hz)

**2.11 Bibliography:**

1. O. M. Ni Dhubhghaill, J. Lennon, and M. G. Drew, *Dalton Transactions*, 2005, 3213–3220.
2. T. Maguire, *PhD Thesis*, 2009, UCC, 100–153.
3. G. L. Miessler and D. A. Tarr, in *Inorganic Chemistry*, Pearson Education Inc., 3rd Ed., 2004, pp. 505–507.
4. K. Grice, W. Kaminsky, and K. I. Goldberg, *Inorganica Chimica Acta*, 2011, **369**, 76–81.
5. P. J. Guiry and C. P. Saunders, *Advanced Synthesis & Catalysis*, 2004, **346**, 497–537.
6. T. Mahamo, M. M. Mogorosi, J. R. Moss, S. F. Mapolie, J. C. Sloopweg, K. Lammertsma, G. S. Smith, and J. Chris Sloopweg, *Journal of Organometallic Chemistry*, 2012, **703**, 34–42.
7. G. L. Miessler and D. A. Tarr, in *Inorganic Chemistry*, Pearson Education Inc., 3rd Ed., 2004, pp. 195–197.
8. J. McMurry, in *Organic Chemistry*, Brooks/Cole-Thompson Learning, 6th Ed., 2004, pp. 1095–1127.
9. A. Esmailbeig, H. Samouei, S. Abedanzadeh, and Z. Amirghofran, *Journal of Organometallic Chemistry*, 2011, **696**, 3135–3142.
10. C. M. Anderson, M. Crespo, and J. M. Tanski, *Organometallics*, 2010, **29**, 2676–2684.
11. G. Sánchez, J. Vives, J. L. Serrano, J. Pe'rez, and G. Lo'pez, *Inorganica Chimica Acta*, 2002, **328**, 74–80.
12. Y. Chen, C. Chen, J. Chen, and S. Liu, *Organometallics*, 2001, **20**, 1285–1286.
13. H. Yoshida, Y. Honda, T. Hiyama, and E. Shirakawa, *Chemical Communications*, 2001, **2**, 1880–1881.
14. S. Dalili, A. Caiazza, and A. K. Yudin, *Journal of Organometallic Chemistry*, 2004, **689**, 3604–3611.
15. M. L. Clarke, A. M. Z. Slawin, M. V Wheatley, and J. D. Woollins, *Journal of the Chemical Society, Dalton Transactions*, 2001, 3421–3429.
16. K. S. Coleman, M. L. H. Green, S. I. Pascu, N. H. Rees, a. R. Cowley, and L. H. Rees, *Journal of the Chemical Society, Dalton Transactions*, 2001, 3384–3395.
17. C. A. Ghilardi, S. Midollini, S. Moneti, and A. Orlandini, *Journal of the Chemical Society, Dalton Transactions*, 1992, 3371–3376.

18. T. F. Vaughan, D. J. Koedyk, and J. L. Spencer, *Organometallics*, 2011, **30**, 5170–5180.
19. P. Ramírez, R. Contreras, M. Valderrama, D. Carmona, F. J. Lahoz, and A. I. Balana, *Journal of Organometallic Chemistry*, 2008, **693**, 349–356.
20. S. Antonaroli and B. Crociani, *Journal of Organometallic Chemistry*, 1998, **560**, 137–146.
21. L. Crociani, F. Tisato, F. Refosco, G. Bandoli, B. Corain, and M. Avanzati, *European Journal of Inorganic Chemistry*, 1998, 1689–1697.
22. M.-H. Thibault, B. E. G. Lucier, R. W. Schurko, and F.-G. Fontaine, *Dalton Transactions*, 2009, 7701–16.
23. E. W. Ainscough, A. M. Brodie, A. K. Burrell, A. Derwahl, G. B. Jameson, and S. K. Taylor, *Polyhedron*, 2004, **23**, 1159–1168.
24. P.-Y. Shi, Y.-H. Liu, S.-M. Peng, and S.-T. Liu, *Organometallics*, 2002, **21**, 3203–3207.
25. T. Morimoto, Y. Yamaguchi, M. Suzuki, and A. Saitoh, *Tetrahedron Letters*, 2000, **41**, 10025–10029.
26. P. Chellan, K. M. Land, A. Shokar, A. Au, S. H. An, C. M. Clavel, P. J. Dyson, C. De Kock, P. J. Smith, K. Chibale, and G. S. Smith, *Organometallics*, 2012, **31**, 5791–5799.
27. S.-M. Kuang, L.-M. Zhang, Z.-Z. Zhang, B.-M. Wu, and T. C. W. Mak, *Inorganica Chimica Acta*, 1999, **284**, 278–283.
28. T. Mino, Y. Tanaka, M. Sakamoto, and T. Fujita, *Tetrahedron: Asymmetry*, 2001, **12**, 2435–2440.
29. D. Hedden and M. D. Roundhill, *Inorganic Chemistry*, 1985, **24**, 4152–4158.
30. G. Sánchez, J. García, D. Meseguer, J. L. Serrano, L. García, J. Pérez, and G. López, *Inorganica Chimica Acta*, 2006, **359**, 1650–1658.
31. D. F. Shriver and P. W. Atkins, in *Inorganic Chemistry*, Oxford University Press, 3rd Ed., 1999, pp. 499–535.
32. J. F. Beck and J. A. R. Schmidt, *Dalton Transactions*, 2012, **41**, 860–70.
33. W. J. Pope and S. J. Peachy, *Proceedings of The Chemical Society*, 1907, **23**, 86–87.
34. Y. Scaffidi-Domianello, A. . Nazarov, M. Haukka, M. Galanski, B. K. Keppler, J. Schneider, P. Du, R. Eisenberg, and V. Y. Kukushkin, *Inorganic Chemistry*, 2007, **46**, 4469–4482.



35. D. F. Shriver and P. W. Atkins, in *Inorganic Chemistry*, Oxford University Press, 3rd Ed., 1999, pp. 538–580.
36. M. Crespo, M. Martinez, and J. Sales, *Organometallics*, 1992, **11**, 1288–1295.
37. M. Crespo, X. Solans, and M. Font-Bardia, *Journal of Organometallic Chemistry*, 1996, **518**, 105–113.
38. M. Crespo, X. Solans, and M. Font-Bardía, *Journal of Organometallic Chemistry*, 1996, **509**, 29–36.
39. G. Al Takhin, H. A. Skinner, and A. Zaki, *Journal of the Chemical Society, Dalton Transactions*, 1984, 371.
40. A. Miedaner, J. W. Raebiger, C. J. Curtis, S. M. Miller, and D. L. Dubois, *Organometallics*, 2004, **23**, 2670–2679.
41. B. K.-W. Chiu, M. H.-W. Lam, D. Y.-K. Lee, and W.-Y. Wong, *Journal of Organometallic Chemistry*, 2004, **689**, 2888–2899.
42. J. M. Vila, M. T. Pereira, J. M. Ortigueira, D. Lata, M. Lopez-Torres, J. J. Fernández, A. Fernández, and H. Adams, *Journal of Organometallic Chemistry*, 1998, **566**, 93–101.
43. M. Crespo, M. Font-Bardía, J. Granell, M. Martinez, X. Solans, and M. Martínez, *Dalton Transactions*, 2003, 3763–3769.
44. A. Wong-Foy, L. M. Henling, M. Day, J. A. Labinger, and J. E. Bercaw, *Journal of Molecular Catalysis A*, 2002, **189**, 3–16.
45. J. Lennon, *PhD Thesis*, 2005, UCC, 184–290.
46. J. Mamtora, S. H. Crosby, C. P. Newman, G. J. Clarkson, and J. P. Rourke, *Organometallics*, 2008, **27**, 5559–5565.
47. D. Aguilar, R. Bielsa, T. Soler, and E. P. Urriolabeitia, *Organometallics*, 2011, **30**, 642–648.
48. L. Barloy, J.-T. Issenhuth, M. G. Weaver, N. Pannetier, C. Sirlin, and M. Pfeffer, *Organometallics*, 2011, **30**, 1168–1174.
49. Y.-F. Han, H. Li, L.-H. Weng, and G.-X. Jin, *Chemical Communications*, 2010, **46**, 3556–8.
50. L. Murphy, A. Congreve, L.-O. Pålsson, and J. a G. Williams, *Chemical Communications*, 2010, **46**, 8743–5.
51. G. L. Miessler and D. A. Tarr, in *Inorganic Chemistry*, Pearson Education Inc., 3rd Ed., 2004, pp. 524–528.

52. M. Crespo, C. Grande, and A. Klein, *Journal of the Chemical Society, Dalton Transactions*, 1999, 1629–1637.
53. K. G. Gaw, A. M. Z. Slawin, and M. B. Smith, *Organometallics*, 1999, **18**, 3255–3257.
54. K. G. Gaw, M. B. Smith, J. B. Wright, A. M. Z. Slawin, S. J. Coles, M. B. Hursthouse, and G. J. Tizzard, *Journal of Organometallic Chemistry*, 2012, **699**, 39–47.
55. P. W. Dyer, J. Fawcett, M. J. Hanton, R. D. W. Kemmitt, R. Padda, and N. Singh, *Dalton Transactions*, 2003, 104–113.
56. C. López, A. González, R. Bosque, P. K. Basu, M. Font-Bardía, and T. Calvet, *RSC Advances*, 2012, **2**, 1986.
57. A. N. Biswas, P. Das, V. Bagchi, A. Choudhury, and P. Bandyopadhyay, *European Journal of Inorganic Chemistry*, 2011, 3739–3748.
58. L. Pedzisa and B. P. Hay, *Journal of Organic Chemistry*, 2009, **74**, 2554–2560.
59. E. S. Kryachko and T. Zeegers-Huyskens, *The Journal of Physical Chemistry A*, 2002, **106**, 6832–6838.
60. J. W. Slater, D. P. Lydon, N. W. Alcock, and J. P. Rourke, *Organometallics*, 2001, **20**, 4418–4423.
61. H.-B. Song, Z.-Z. Zhang, and T. C. W. Mak, *Polyhedron*, 2002, **21**, 1043–1050.
62. M. Crespo, C. Grande, A. Klein, M. Font-Bardía, and X. Solans, *Journal of Organometallic Chemistry*, 1998, **563**, 179–190.
63. M. Crespo, X. Solans, and M. Font-Bardía, *Polyhedron*, 1998, **17**, 1651–1657.
64. C. Anderson, M. Crespo, J. Morris, and J. M. Tanski, *Journal of Organometallic Chemistry*, 2006, **691**, 5635–5641.
65. M. K. Cooper, J. M. Downes, P. A. Duckworth, M. C. Kerby, R. J. Powell, and M. D. Soucek, in *Inorganic Syntheses*, John Wiley & Sons, Inc., 1989, pp. 129–133.
66. S. Doherty, J. G. Knight, T. H. Scanlan, M. R. J. Elsegood, and W. Clegg, *Journal of Organometallic Chemistry*, 2002, **650**, 231–248.
67. J. A. March and M. B. Smith, *Advanced Organic Chemistry*, Wiley, 6th Ed., 2007.
68. D. Hedden, M. D. Roundhill, W. C. Fultz, and A. L. Rheingold, *Journal of the American Chemical Society*, 1984, **106**, 5014–5016.
69. D. B. Dell’Amico, L. Labella, F. Marchetti, and S. Samaritani, *Dalton Transactions*, 2012, **41**, 1389.

70. F. A. Cotton and G. Wilkinson, in *Advanced Inorganic Chemistry*, John Wiley & Son, 6th Ed., 1999, pp. 1072–1073.
71. C. Navarro Ranninger, I. López-Solera, V. M. González, J. M. Pérez, A. Alvarez-Valdés, A. Martín, P. R. Raithby, J. R. Masaguer, and C. Alonso, *Inorganic Chemistry*, 1996, **35**, 5181–5187.
72. C. Navarro Ranninger, I. Lopez-Solera, J. M. Pérez, J. Rodríguez, J. L. García-Ruano, P. R. Raithby, J. R. Masaguer, and C. Alonso, *Journal of Medicinal Chemistry*, 1993, **36**, 3795–3801.
73. R. Schutzenberger, *Bulletin de la Societe Chimique de France*, 1870, **14**, 17.
74. M. Lersch and M. Tilset, *Chemical Reviews*, 2005, **105**, 2471–526.
75. S. van Zutphen, E. Pantoja, R. Soriano, C. Soro, D. M. Tooke, A. L. Spek, H. den Dulk, J. Brouwer, and J. Reedijk, *Dalton Transactions*, 2006, 1020–1023.
76. A. Habtemariam and P. J. Sadler, *Chemical Communications*, 1996, 1785.
77. D. C. Giedt, C. J. Nyman, J. Young, and R. K. Murmann, in *Inorganic Syntheses Volume 8*, John Wiley & Sons, Inc., 1966, pp. 239–241.
78. D. Drew, J. R. Doyle, and A. G. Shaver, in *Inorganic Syntheses Volume 28*, John Wiley & Sons, Inc., 1990, pp. 346–349.
79. M. S. Kharasch and T. A. Ashford, *Journal of the American Chemical Society*, 1936, **58**, 1733–1738.
80. D. Madrigal, I. A. Rivero, and G. Pina-Luis, *Journal of the Mexican Chemical Society*, 2006, **50**, 175–179.
81. J. Andrieu, B. R. Steele, C. G. Screttas, C. J. Cardin, and J. Fornies, *Organometallics*, 1998, **17**, 839–845.
82. M. Benedetti, J. Malina, J. Kasparikova, V. Brabec, and G. Natile, *Environmental Health Perspectives*, 2002, **110**, 779–782.
83. D. F. Shriver and P. W. Atkins, in *Inorganic Chemistry*, Oxford University Press, 3rd Ed., 1999, pp. 211–282.
84. G. Sánchez, J. L. Serrano, M. A. Moral, J. M. Pérez, E. Molins, and G. López, *Polyhedron*, 1999, **18**, 3057–3064.
85. S. D. Perera and B. L. Shaw, *Journal of the Chemical Society, Dalton Transactions*, 1995, 641–647.
86. L. M. Harwood and T. D. W. Claridge, *Introduction to Organic Spectroscopy*, Oxford University Press, 4th Ed., 1997.

- 
87. P. Bhattacharyya, M. L. Loza, J. Parr, and A. M. Z. Slawin, *Journal of the Chemical Society, Dalton Transactions*, 1999, 2917–2921.
  88. J. Parr, *Inorganica Chimica Acta*, 2000, **303**, 116–120.
  89. W. L. F. Armarego and C. Li Lin Chai, in *Purification of Laboratory Materials*, Elsevier Inc., 6th Ed., 2009, pp. 88–444.
  90. K. S. Eccles, S. P. Stokes, C. A. Daly, N. M. Barry, S. P. McSweeney, D. J. O’Neill, D. M. Kelly, W. B. Jennings, O. M. Ní Dhubhghaill, H. a Moynihan, A. R. Maguire, and S. E. Lawrence, *Journal of Applied Crystallography*, 2011, **44**, 213–215.
  91. Madison and B. AXS, in *APEX2 v2009.3-0*, WI, 2009.
  92. G. M. Sheldrick, *Acta Cryst.*, 2008, **A64**, 112–122.
  93. C. F. Macrae, I. J. Bruno, J. A. . Chrisholm, P. R. . Edgington, P. McCabe, E. . Pidcock, L. . Rodriguez-Monge, R. Taylor, J. . Van Streek, and P. A. Wood, *Journal of Applied Crystallography*, 2008, **41**, 466–470.



**Chapter 3:**  
**Substitutions and Oxidations**

## Contents

<b>3.1 Chapter 3 Background</b> .....	182
<b>3.2 Substitution Reactions of Platinum Complexes</b> .....	183
3.2.1 The <i>Trans</i> -Effect in Platinum Chemistry.....	183
3.2.2 The Pt-X Bond; Sigma and Pi Bonding Effects .....	185
3.2.3 Nucleophilic Ligand Replacements (The 5-Coordinate Intermediate) .....	186
<b>3.3 Phosphine Substitutions of Pt-Halide Bonds</b> .....	188
3.3.1 Phosphine Substitutions Involving Halide Scavengers.....	188
3.3.2 One-Step Phosphine Substitutions.....	192
<b>3.4 Platinum (V) Anti Cancer Drugs</b> .....	194
3.4.1 The Current Clinical Status of Pt (IV) Anti-cancer Drugs.....	194
3.4.2 Stability and the Chelate Effect .....	196
3.4.3 Oxidation of Pt (II) Complexes Using Hydrogen Peroxide .....	197
3.4.4 Oxidation of Pt (II) Complexes Using Group 17 Elements .....	201
3.4.5 Other Methods for Oxidising Pt (II) Complexes .....	203
<b>3.5 Conclusion</b> .....	205
<b>3.6 Syntheses</b> .....	207
3.6.1 Synthesis of cationic triphenylphosphine (PPh <sub>3</sub> ) substituted Pt (II) complexes of the general formula [Pt( $\eta^3$ -PNC/PNO-L <sup>1-4</sup> )PPh <sub>3</sub> ]Cl <b>371-375</b> .....	207
3.6.2 Discussion of Factors Influencing the Substitution Reactions .....	210
3.6.3 Attempted oxidation of Pt (II) complexes Using H <sub>2</sub> O <sub>2</sub> and NaOCl.....	212
3.6.4 Synthesis of Pt (IV) chloro complexes of the general formula [Pt( $\eta^3$ -PNC-L <sup>1-4</sup> )Cl <sub>3</sub> ] <b>381-384</b> .....	214

<b>3.7 Infra-Red Spectroscopic Studies</b> .....	220
3.7.1 Cationic triphenylphosphine (PPh <sub>3</sub> ) substituted Pt (II) complexes of the general formula [Pt( $\eta^3$ -PNC/PNO-L <sup>1-4</sup> )PPh <sub>3</sub> Cl] <b>371-375</b> .....	220
3.7.2 Infra-red spectra of Pt (IV) chloro complexes of the general formula [Pt( $\eta^3$ -PNC-L <sup>1-4</sup> )Cl <sub>3</sub> ] <b>381-384</b> .....	221
<b>3.8 NMR Spectroscopic Studies</b> .....	223
3.8.1 NMR spectroscopy of the ionic, cyclometallated and PNO triphenylphosphine substituted complexes of the general formula [Pt( $\eta^3$ -PNC-L <sup>1-4</sup> )PPh <sub>3</sub> Cl] <b>371-375</b> ...	223
3.8.2 NMR spectra of tridentate, cycloplatinated Pt (IV) chloro iminophosphine complexes [Pt( $\eta^3$ -PNC-L <sup>1-4</sup> )Cl <sub>3</sub> ] <b>381-384</b> .....	230
3.8.3 NMR studies of the proposed mixed axial Pt (IV) intermediates, <b>386</b> and the PNO type Pt (IV) complex <b>385</b> .....	236
<b>3.9 Summary and Conclusion</b> .....	239
3.9.1 The Triphenylphosphine Substituted Pt (II) Complexes.....	239
3.9.2 Synthesis of the Pt (IV) Complexes.....	241
3.9.3 Overall Summary and Conclusion.....	242
<b>3.10 Chapter 3 Experimental</b> .....	243
3.10.1 Background.....	243
3.10.2 Synthesis of the substituted Pt (II) complexes [Pt( $\eta^3$ -PNC-L <sup>1-4</sup> )PPh <sub>3</sub> Cl] <b>371-375</b> .....	244
3.10.3 Synthesis of the Pt (IV) complexes [Pt( $\eta^3$ -PNC-L <sup>1-4</sup> )Cl <sub>3</sub> ] <b>381-384</b> .....	247
<b>3.11 Bibliography</b> .....	249



### 3.1 Chapter 3 Background:

The influence of phosphines as part of the tridentate iminophosphine ligand of the Pt (II) complexes and their properties have been highlighted extensively in **Chapter 1** and **Chapter 2**. This chapter on the other hand aims to focus on synthetic routes to generate phosphine substitutions of the tridentate Pt (II) complexes **281-289** reported in **Chapter 2**, specifically via displacement of halide group.

Phosphine substitutions can be of two different types, monophosphine substitution and polyphosphine substitution. The reactivity of multi-dentate platinum complexes with tertiary monodentate phosphines, such as triphenylphosphine, will be explored in this chapter as will the paths towards successful coordination of the phosphines with the platinum by displacement of a halide from the metal centre.

The HSAB theory and the *trans*-effect will be employed throughout this chapter by way of explaining the results obtained. The soft-acid/soft-base interaction proposed by the HSAB theory is classed as a favourable process i.e. “soft base” phosphine – “soft acid” Pt (II). Phosphine moieties are also known to be strong *trans*-effect ligands, as a result we see an effect on the already coordinated tridentate iminophosphine ligand of the complex on introduction of new phosphine moieties *trans* across the metal centre which will be an important consequence for analysis and identification of these complexes by IR and NMR techniques.<sup>1</sup>

This chapter also intends to discuss and compare synthetic routes and practical aspects encountered in the preparation of Pt (IV) chloro iminophosphine complexes. The biological implications and uses of these platinum complexes were discussed in detail in **Chapter 1**. Previously within this research group, preparation of Pt (IV) complexes of analogous iodo complexes were seen to be quite cumbersome and their reaction products difficult to predict; most of the time producing mixtures of products along with unreacted starting materials.

The work undertaken in this chapter reports the substitution and oxidation of both the tridentate cycloplatinated species  $[\text{Pt}(\eta^3\text{-PNC-L}^{1-7})\text{Cl}]$  **281-284**, **286-288** and the previously reported tridentate P,N,O complex  $[\text{Pt}(\eta^3\text{-PNO-L}^4)\text{Cl}]$  **285**. Their reactivity towards tertiary, monophosphine substitution and chloride based oxidising agents to produce two series of novel platinum complexes will be investigated.

### 3.2 Substitution Reactions of Platinum Complexes:

#### 3.2.1 The *Trans*-Effect in Platinum Complexes:

Chernyaev introduced the concept of the *trans*-effect in 1926 for platinum chemistry. He discovered that after synthesising many square planar Pt (II) complexes that the presence of certain ligands attached to the metal ion had the ability to cause the loss of the group that was in the position directly *trans* to it.<sup>2</sup>

In reactions of square planar Pt (II) compounds, ligands *trans* to chloride in particular are more easily replaced than those *trans* to ligands such as ammonia.<sup>3</sup> Therefore the chloride ligand is said to have a stronger *trans*-effect than ammonia. In the simplest terms, Dabrowiak describes the *trans*-effect as the following: *the trans-effect pertains to the ability of a ligand in a complex to direct substitution opposite, or trans, to itself.*<sup>4</sup>

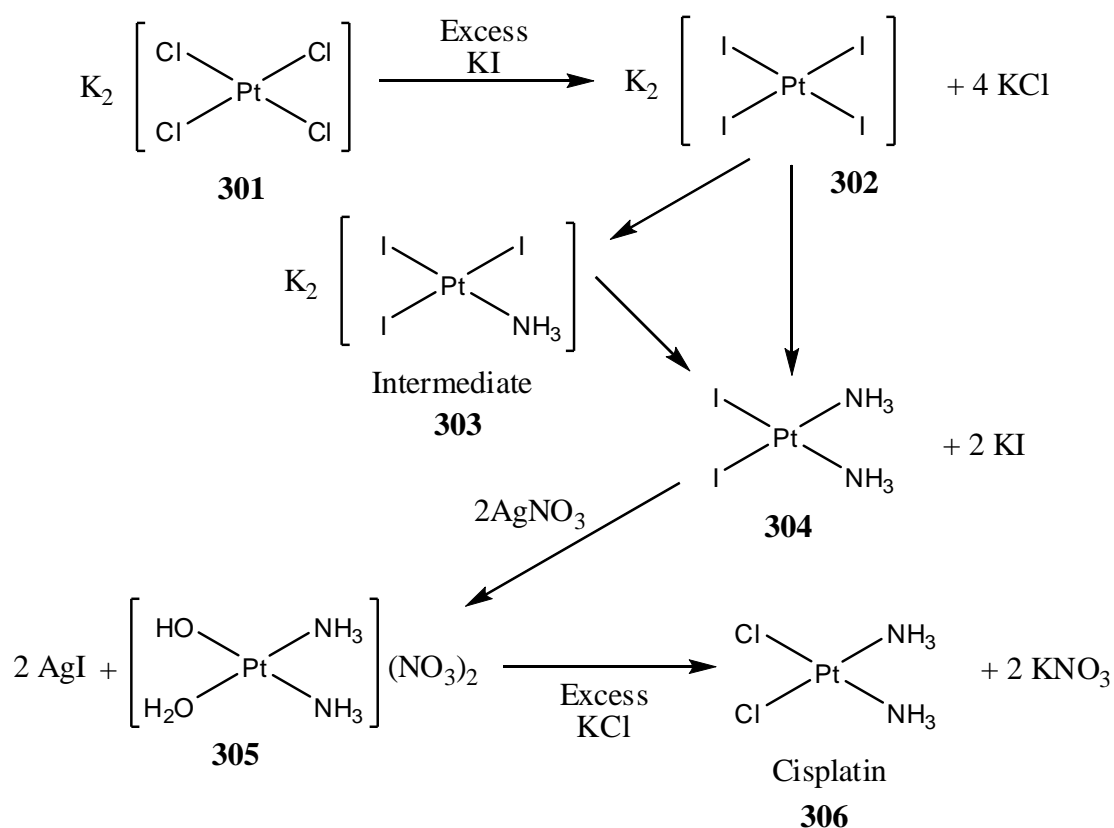


*Figure 3.1: The commercial synthesis of cisplatin 306 via the Dhara Synthesis, which demonstrates the trans-effect with the formation of the intermediate 303.*

The synthesis of the world's number one platinum based anti-cancer drug, cisplatin, which forms two isomers (transplatin and cisplatin), is a great illustration of how the *trans*-

effect works. Known as the “Dhara Synthesis”, potassium tetrachloroplatinate,  $K_2[PtCl_4]$  **301**, is reacted with excess potassium iodide in an associative mechanism, **Figure 3.1**, until all the chloride ligands are replaced by iodides **302**.

$[PtI_4]$  is reacted with two equivalents of ammonia but only substitutes the iodides in a *cis*-manner due to the *trans*-effect of the iodide ligands **304**. This is the most interesting feature of this synthesis since two geometric isomers are possible, *cis* and *trans*, and the *cis* would be less thermodynamically stable than the *trans*, but only the *cis* isomer is formed in the reaction.

When a second equivalent of ammonia is added to the key intermediate, indicated in **Figure 3.1**, it only substitutes the iodide *trans* to another iodide rather than *trans* to the amine group already present. In this synthesis only the *cis* product is isolated, showing the ability of iodide to direct substitution *trans* to itself being greater than that of ammonia to direct substitution *trans* to itself.<sup>5</sup>

Also of interest is the last part of the “Dhara Synthesis”, **Figure 3.1**, which involves the replacement of both iodides with two water molecules using two equivalents of  $AgNO_3$ . This results in the formation of the insoluble salt  $AgI$ , with the metal complex staying as an equilibrium in the aqueous solution **305**. This phenomenon is called a phase change, which involves the formation of insoluble  $AgI$  and  $NO_3^-$  acting as a spectator ion due to the large concentration of water molecules.  $KCl$  is then used in excess to displace the water molecules and drive the equilibrium to the formation of cisplatin which precipitates from solution. This method of substitution has been used by our research group in the past as the primary method for substituting the Pt-X bond in platinum iminophosphine complexes.<sup>6-8</sup>

Not all ligands however share the same strength in what has been called the “*trans* directing ability” and as a result a series was created to rank the most common ligands by their ability to direct an incoming nucleophile to the coordination site *trans* to themselves, **Figure 3.2**.

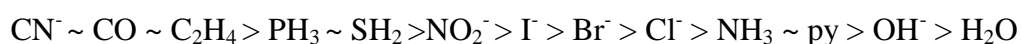


*Figure 3.2: The “Tran-Effect Series” which orders common ligands in relation to their trans directing ability. As can be seen, CN is the strongest trans directing ligand and water is the weakest.*

A number of models have been proposed to explain the *trans*-effect and why a given ligand is where it is in the series as described in **Figure 3.2**. Early models focussed on the

structure of the reactants along with thermodynamic arguments which assumed that if a bond was slightly longer in the starting complex then it would be the bond broken in the substitution reaction.<sup>4</sup>

Other models, based on transition state theory, addressed the structure of the transition state or activated complex in the reaction thus providing a kinetic focus to the theory. While these models address the *trans*-effect from a kinetic perspective, difficulties in estimating the electronegativities of some groups and a lack of knowledge of the structure of the transition state make it difficult to use. Some of this model will be discussed in **Section 3.1.1**.<sup>4</sup>

Recently however, two factors have been put forward to explain the *trans*-effect; weakening of the Pt-X bond and stabilisation of the five-coordinate intermediate (which was previously encountered as part of the mechanism proposed for cyclometallation in **Chapter 2**). Both of these concepts will be discussed separately and in more detail in the following **Sections 3.2.1** and **3.2.2** respectively.

### 3.2.2 The Pt-X Bond; Sigma and Pi Bonding Effects:

The Pt-X bond is influenced by the Pt-T bond in **307**, **Figure 3.3**, because both use the  $p_x$  and  $d_{x^2-y^2}$  orbitals on the platinum metal centre. When the Pt-T bond is strong, it uses a larger part of these orbitals and therefore leaves less for the Pt-X bond. As a result, the Pt-X bond is weaker and its ground state (sigma-bonding orbital) is higher in energy, leading to a small activation energy required for the breaking of this bond.

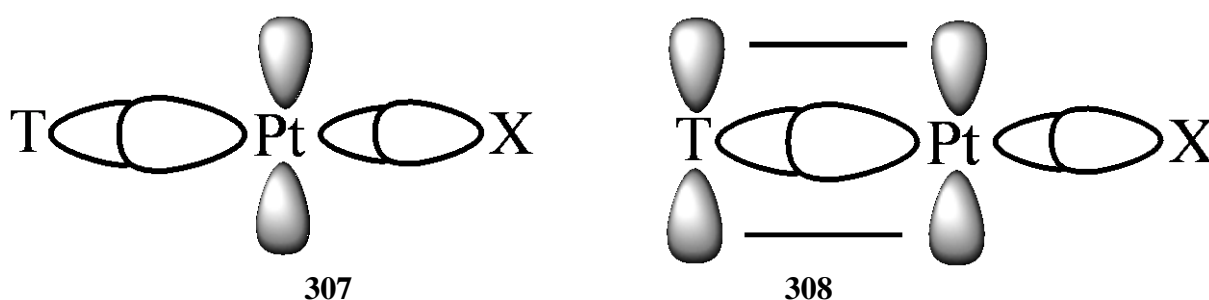


*Figure 3.3: Sigma-bonding effects, 1 and Pi-bonding effects in the Pt-T bond, 2. A strong  $\sigma$  bond between the Pt and T weakens the Pt-X bond, leading to a small activation energy for this bond. Further orbital structures are omitted for clarity.*

This ground state effect is sometimes called the *trans*-influence and primarily applies to the leaving group. It is a thermodynamic effect and can partly predict the order for the *trans*-effect series based on the relative  $\sigma$ -donor properties of the ligands. However an

additional factor is needed to fully explain the order of the *trans*-effect series in **Figure 3.2**;  $\pi$ -bonding.<sup>3</sup>

The formation of a strong  $\pi$ -bond in the Pt-T bond, **308**, **Figure 3.3**, results in charge being removed from the platinum metal centre and the entrance of another ligand to form a 5-coordinate intermediate is more likely. In addition to the charge effect, the  $d_{x^2-y^2}$  orbital, which as previously mentioned is also involved in  $\sigma$ -bonding for square planar geometry, and both the  $d_{xz}$  and  $d_{yz}$  orbitals can contribute to  $\pi$ -bonding in the trigonal-bipyramidal 5-coordinate transition state (discussed further in **Section 3.1.2**).<sup>9</sup>

The full *trans*-effect series, **Figure 3.2**, is therefore as a result of the combination of the two effects where ligands highest in the series are strong  $\pi$ -acceptors, followed by strong  $\sigma$ -donors. Ligands at the low end of the series therefore have neither strong  $\sigma$ -donor nor  $\pi$ -acceptor abilities.<sup>9</sup>

### 3.2.3 Nucleophilic Ligand Replacements (The 5-Coordinate Intermediate):

It is generally accepted that substitution reactions of square-planar compounds are associative where an incoming ligand (Y, **Figure 3.4**) approaches along the z-axis. There is also a general agreement that the reactions involve nucleophilic attack of the entering ligand (Y) at the metal centre, with the resulting 5-coordinate intermediate passing through a square pyramidal and trigonal-bipyramidal stages, **Figure 3.4**.

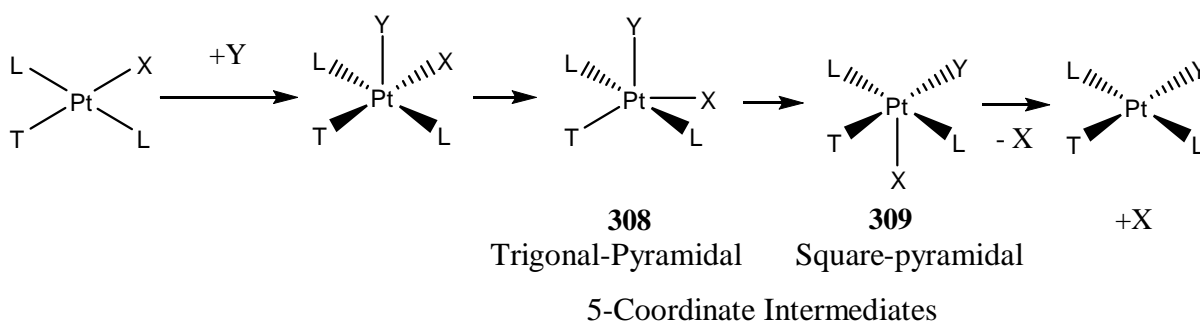


*Figure 3.4: Direct substitution of the platinum square-planar complex by the Y ligand, resulting in the loss of the X ligand.<sup>9</sup>*

As the X leaves, **Figure 3.4**, the new Y ligand moves down into the plane of T, Pt, and the two L ligands to form the trigonal-bipyramidal structure **308**. The evidence for the 5-coordinate intermediate (**308**, **309** **Figure 3.4**) is very strong with numerous reports detailing its existence. Several 5-coordinate complexes with trigonal-bipyramidal geometry, **308** such as  $[\text{Pt}(\text{SnCl}_3)_5]^{3-}$  have been isolated as discussed in **Chapter 2, Section 2.3.2**.

A second argument has also been put forward proposing the existence of a 6-coordinate intermediate, with assistance from a solvent molecule, but the subsequent replacement of the co-ordinated solvent molecule (S) by the entering ligand (Y) is fast, making it difficult to isolate and confirm so a 5-coordinate mechanism is used, **Figure 3.5**.<sup>10,11</sup>

The trigonal-bipyramidal complex of **Figure 3.4** and **3.5** has been regarded as a reaction intermediate by both this research group and others, with the two square-pyramidal species (with the X ligand on the top or bottom of the plane) as transition states **309**.

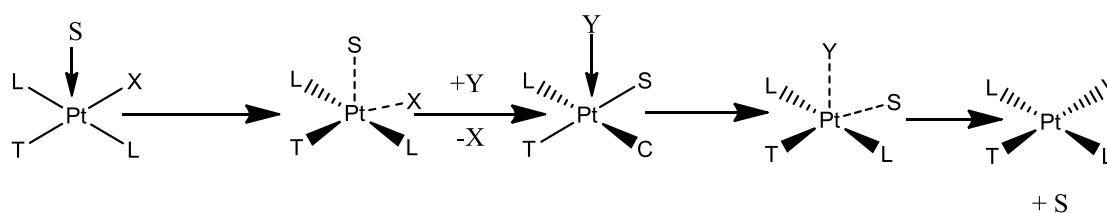


*Figure 3.5: Solvent-assisted substitution of the platinum square-planar complex by the Y ligand, resulting in the loss of the X ligand.*<sup>9</sup>

This mechanism explains the effect of the incoming ligand in both cases. A strong Lewis base is likely to react readily, but the hard-soft nature of the base (the incoming ligand) has an even larger effect. Pt (II) is generally regarded as a soft acid, so soft ligands react more readily with it but it also depends on the *trans*-effect.

For substitution reactions involving Pt-Cl bonds in a methanolic solution, a relationship has been found for certain ligands (excluding the influence of the *trans*-effect), **Figure 3.6**. Soft Lewis bases such as phosphine ligands (PR<sub>3</sub>) are the highest on the list while hard ligands such as Cl<sup>-</sup> are the most difficult to use a substituting ligand.

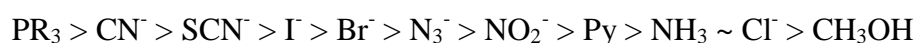


*Figure 3.6: The order of ligand reactivity for substituting a platinum metal centre.*<sup>9</sup>

By the same argument, the leaving group (X, **Figure 3.4** and **3.5**), should also have a significant influence on the rate, and it does. The order of good leaving groups from a platinum metal centre is nearly the reverse of the list given in **Figure 3.6**, with hard ligands such as Cl<sup>-</sup>, NH<sub>3</sub> and NO<sub>3</sub><sup>-</sup> leaving quickly. Soft ligands such as CN<sup>-</sup>, I<sup>-</sup> and NO<sub>2</sub><sup>-</sup> are very reluctant to leave which is what was observed for the previously reported iodo platinum complexes reported by our research group.<sup>6</sup>

### 3.3 Phosphine Substitutions of Pt-Halide Bonds:

#### 3.3.1 Phosphine Substitutions Involving Halide Scavengers:

Previous reports by our research group undertaken by Maguire and Lennon have revealed the difference in lability of a Pt-Cl bond in contrast to a Pt-I bond.<sup>6,8</sup> In similar investigations by Capape *et al*, phosphine substitutions were reported, interestingly, to displace nitrogen moieties and sulphur moieties in preference to chlorides (**Figure 3.7**).<sup>11</sup>

These investigations further indicate the greater importance of the *trans*-effect and the strength of the platinum chloride bond, compared with the HSAB theory described in **Section 3.2.2**. In **Figure 3.7**, the sulphur donor moiety on compounds **310** is substituted rather than the chloride because of the weak *trans*-effect found for imines relative to the carbon on the aryl ring. However, HSAB theory and the *trans*-effect are not the only concepts that are important here; relative bond strengths also play a significant role.

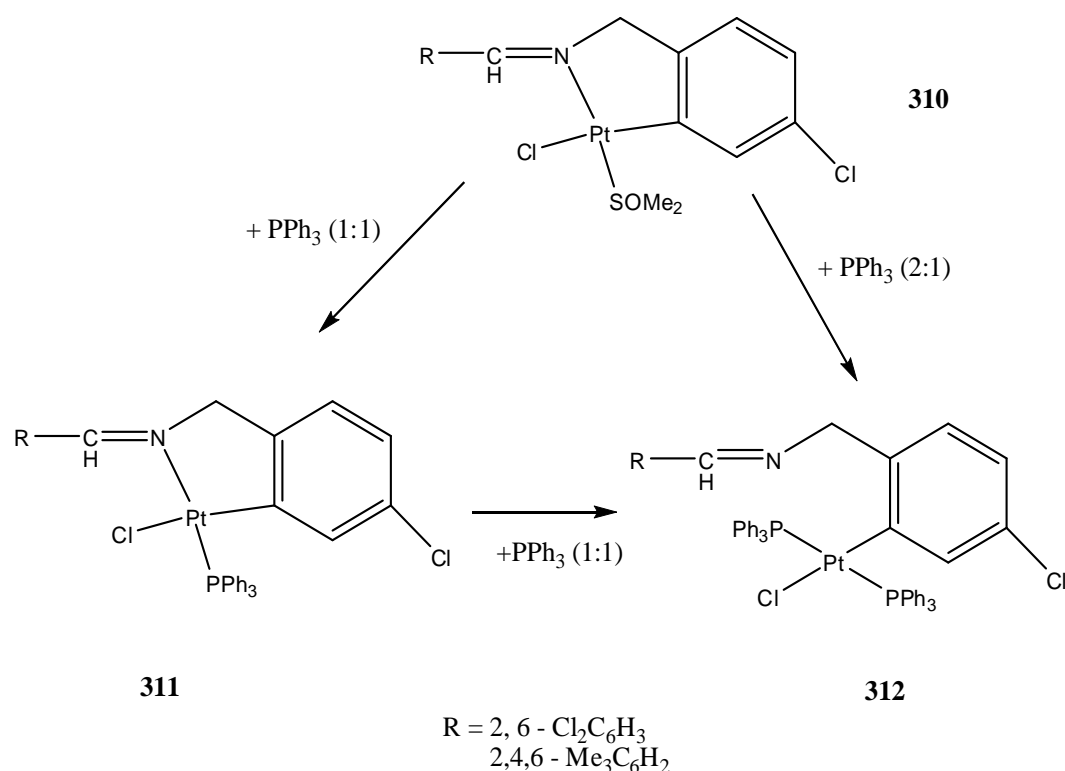


**Figure 3.7:** Reaction of triphenylphosphine with a cyclometallated Pt (II) complex where the nitrogen and sulphur moieties are substituted over chloride.<sup>11</sup>

According to the theories put forward in the last part of **Section 3.2.2**, the chloride (being a hard Lewis base and platinum being a soft acid) should be substituted by a phosphine without any difficulty. Instead the chlorine (*trans* to a Pt-C bond to a phenyl

group) remains intact, even with two equivalents of triphenylphosphine present (**312**, **Figure 3.7**).

Also worthy of note in **Figure 3.7** is the apparent strength of the organometallic bond of the platinum metal centre and the carbon of the aromatic ring system where a monodentate complex is the result of substitution with the introduction of two phosphine moieties.

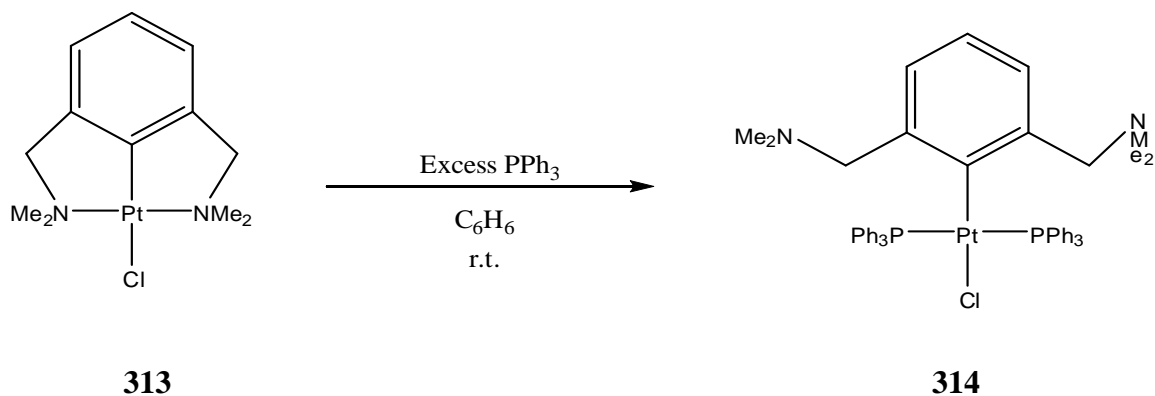


*Figure 3.8: Direct substitution of Pt-N bonds resulting in ring opening of the 5-membered chelate structure. Again the Pt-Cl bond remains unsubstituted in contrast to the theories proposed by the HSAB theory.*

These types of unusual substitutions have also been reported by Albrecht *et al* for  $\eta^3$ -C,N,N pincer type complexes where again the nitrogen moieties were displaced over the chloride ligand even though the iminic nitrogen would be considered borderline (1:1 soft:hard base) according to the hard-soft acid base theory (HSAB), unlike the significantly harder chloride base, **Figure 3.8**. In the case of these  $\eta^3$ -C,N,N systems, opening of the chelate ring is also observed on introduction of the new phosphine moiety like that seen for the complex in **Figure 3.7**.<sup>12</sup>

Investigations undertaken by our research group have also revealed the increased lability of the platinum iodide bond over the platinum chloride bond of analogous complexes by way of achieving direct substitution for the metal-halide bond in the iodo complexes but not the previously reported PNO chloride complexes reported in **Chapter 2**.<sup>7,6</sup>

In work reported by Fernandez *et al*, cyclometallated palladium complexes of the [C,N,O] and [C,N,N] type were initially treated with a silver(I) salt to remove the chloride ligand from the metal centre as silver chloride, resulting in the vacant co-ordination site being later occupied by the desired phosphine donor moiety, **Figure 3.9**. This is similar to the mechanism employed by the last part of the Dhara synthesis of cisplatin in **305**, **Figure 3.1**.<sup>13</sup>



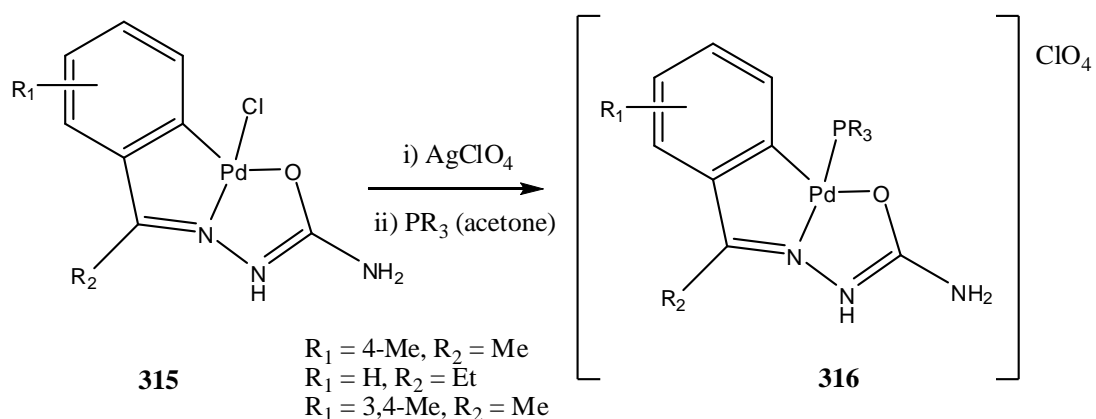


**Figure 3.9:** The use of silver (I) perchlorate to achieve substitution of a series of cyclometallated palladium CNN type complexes (**315**) to form the substituted complexes as perchlorate salts (**316**).<sup>13</sup>

Interestingly, unlike previous examples in **Figure 3.7** and **3.8**, the cyclopalladated complex in **Figure 3.9** reacts with numerous monophosphines,  $\text{PR}_3$  (including  $\text{PPh}_3$ ), to form the desired phosphine substituted complex by substitution of the Pd-Cl bond. Of particular interest in this reaction is the resulting geometry. The introduced monophosphine is located *trans* to the imino-nitrogen; the position occupied by the halide ligand in the starting material. Interestingly however, unlike that seen for the Pt-N bonds in **Figure 3.8**, the Pd-O bond is not broken here despite the oxygen being a hard base according to the HSAB theory. This is similar to previous work completed within our research group on PNO type complexes, **Figure 3.10**.<sup>6</sup>

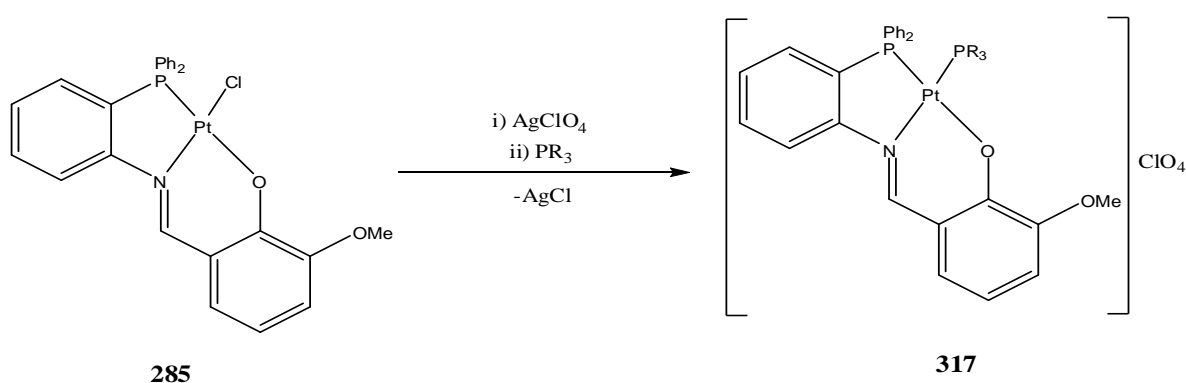


**Figure 3.10:** The use of silver (I) perchlorate to achieve substitution of the PNO complex 275/285, previously reported by this research group and again in the current studies in **Chapter 2** from a different synthesis method.<sup>7</sup>

It can be seen therefore that the Pt (II) chloro complexes require the use of halide scavenger to achieve chloride abstraction, like  $\text{AgCF}_3\text{SO}_3$  or  $\text{AgClO}_4$ , in order to remove the

halide from the platinum centre. Direct substitution, like that observed for the previously reported iodo complexes, has proven very difficult to achieve for platinum-chloride bonds without the use of these perchlorate salt to initially remove the halide from the metal centre. Extensive work within our research group on platinum chloride iminophosphines of the  $\eta^3$ -P,N,O type has only yielded substitution with phosphines in the presence of silver perchlorate, **Figure 3.10**.<sup>7</sup>

This method has been established to allow phosphine substitution without the loss of the tridentate ligand coordination or undesired displacement of a donor moiety from the metal centre, as reported by other research groups in **Figure 3.8** and **Figure 3.9**. However, the properties of the phosphine were also found to be particularly significant when substituting with Pt (II) complexes. In particular reduced reactivity was found for the Pt (II) complexes in comparison to the analogous Pd (II) complexes due to the proposed reduced lability of the Pt-Cl bond in comparison to the Pd-Cl bond. Also no reaction was observed for some of the platinum iodo complexes reported with certain phosphines.

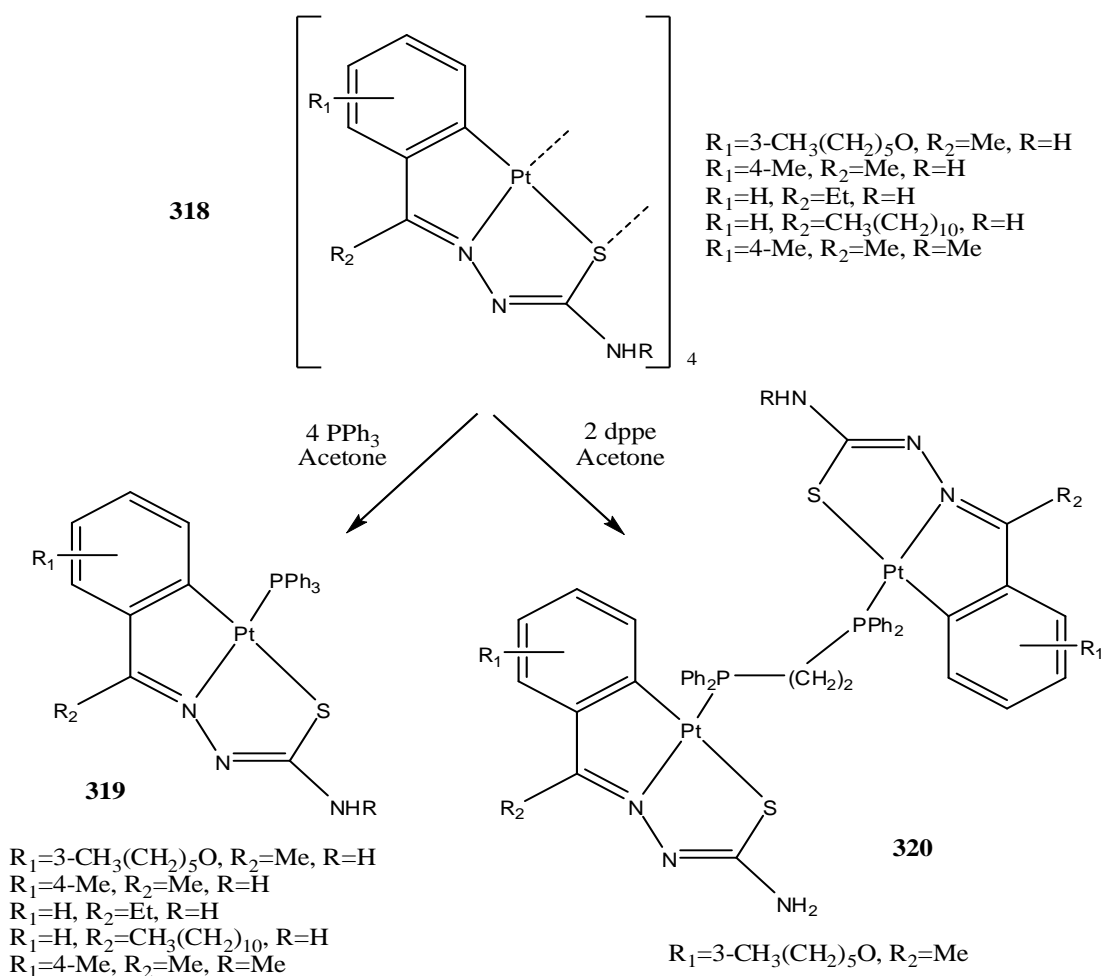


**Figure 3.11:** Direct phosphine substitution of tridentate CNS type platinum chloro complexes with mono and di-phosphine ligands.<sup>14</sup>

Reactions of reduced cone angle phosphines like tris(2-cyanoethyl)phosphine were found to be successful over sterically bulky phosphines such as triphenylphosphine in spite of the higher acidity of these ligands. Previous studies within our research group indicated that the use of a more labile halide group, such as iodide, within these complexes results in successful direct phosphine substitution however, direct substitution for chlorides did not occur.<sup>6</sup>

Also worthy of note is the extensive work completed by Vila *et al* into substitutions of  $\eta^3$ -C,N,S complexes derived from thiosemicarbazones, **Figure 3.11**.<sup>14</sup> For these complexes diphosphine substitution was achieved using diphenylphosphinoethane (dppe) in acetone as well as direct substitution (without a halide scavenger) using monophosphine ligands. These phosphine-bidentates, **320**, **Figure 3.11**, have also been a subject of interest in our research group but have not yielded any significant success due to the insolubility of the products.<sup>15</sup>

### 3.3.2 One-Step Phosphine Substitutions:

Within our research group direct phosphine substitution, i.e. without the use of a halide scavenger, has been achieved with moderate success primarily with iodo platinum PNC and PNO complexes **224** and **258** respectively, **Figure 3.12**.

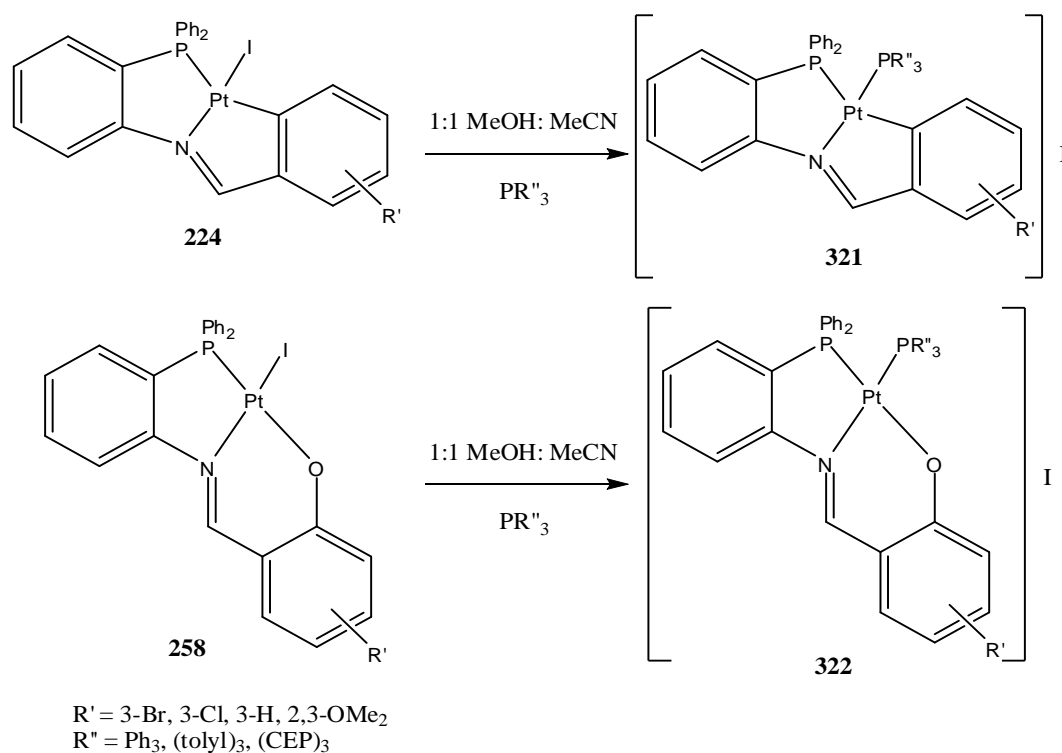


*Figure 3.12: Direct phosphine substitution of tridentate PNC and PNO type platinum iodo complexes with mono phosphine ligands previously reported by our research group.<sup>6</sup>*

The success of these reactions has been attributed to the increased lability of the platinum iodide bond over the platinum chloride bond. The use of the above indicated mixed solvent system also plays a part in achieving direct substitution. The importance of solvent choice has been discussed in the previous section. From previous reports and from work in our research group, it was found that direct substitution of platinum chloride bonds without displacing the coordination of the tridentate iminophosphine ligand from the metal centre is very difficult to achieve without the use of a halide scavenger.<sup>6,7</sup>

However, extensive work completed by Anderson *et al* and work reported in **Chapter 2**, has highlighted the importance of chlorinated solvents for chloride ion stabilisation. Anderson *et al* have reported that the presence of a silver (I) salt (or other halide scavengers) is not necessary for the formation of phosphine substituted complexes from chloro Pt (II) precursors **Figure 3.13**.<sup>16</sup>

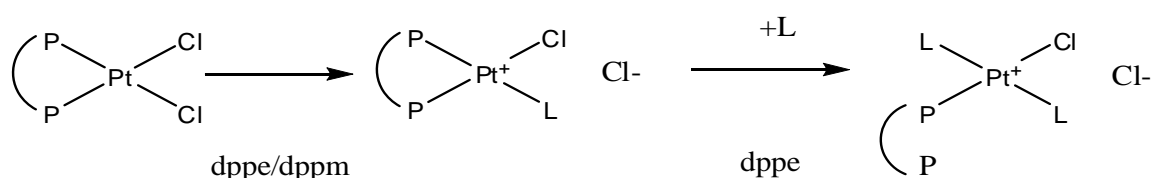


*Figure 3.13: Direct phosphine substitution of platinum chloro complexes with di-phosphine ligands with the loss of a chloride from the metal centre completed in chloroform.*<sup>16</sup>

Following on from **Figure 3.13**, both chlorides by way of an associative mechanism, can be displaced by dppe again in the absence of a silver (I) salt. Anderson *et al* have also completed work in comparing perchlorate cationic platinum salts and cationic platinum complexes where the displaced chloride acts as the counter-ion instead of the perchlorate anion.<sup>16</sup>

Interestingly, when the cationic platinum complex is not isolated as its perchlorate salt, that is when the counter-ion is chloride, the  $^{31}\text{P}\{\text{H}\}$  NMR spectra are somewhat broad at ambient temperature, but when the sample is cooled to  $-40^\circ\text{C}$  the spectra become sharp. They propose that this observation is due to the interaction of the highly electronegative chloride ion with the metal complex through ligand exchange or ion-pair formation.<sup>16</sup>

Another point of interest in the work by Anderson *et al*, is that when the platinum-dmpe complex was treated with  $\text{PPh}_3$ , the triphenylphosphine displaces the other previously introduced phosphine ligands, **Figure 3.13**. It is generally considered that the  $\text{PMePh}_2$  (dmpe) is a better donor ligand than  $\text{PPh}_3$  because of the electron-donating methyl group present over

the electron-withdrawing phenyl group. However when  $[\text{PtCl}_2(\text{dmpe})]$  is treated with triphenylphosphine, displacement is seen to occur for the dmpe group.<sup>16</sup>

### 3.4 Pt (IV) Anti-cancer Drugs:

#### 3.4.1 The Current Clinical Status of Pt (IV) Anti-cancer Drugs:

A large amount of Pt (II) and Pt (IV) anti-cancer drugs approved for clinical use around the world, including those in advanced clinical trials, have chloride ligands as part of their structure (see **Chapter 1**). Cisplatin, the first generation platinum anticancer drug, has chloride ligands as do some of the second and third generation platinum anti-cancer drugs such as Picoplatin, JM 11 and NSC 170898.<sup>17</sup>

This is primarily due to the fact that it has been widely reported that chloro platinum complexes remain intact in the bloodstream due to the relatively high concentration of chloride ions present (~100 mM). They readily dissociate their chloride ligands when they enter a cell (due to the lower chloride concentration) to form reactive hydroxyl analogues ready for DNA binding.<sup>18</sup>

Tetraplatin (also known as Ornaplatin) was the first Pt (IV) drug developed for anti-cancer activity and its structure is mostly composed of chloride ligands, **Figure 3.14**. The method of action of these Pt (IV) pro-drugs has been covered in detail in **Chapter 1, Section 1.4.6** so instead here we will discuss their synthesis, stability and reactivity, along with their current progress within clinical trials.

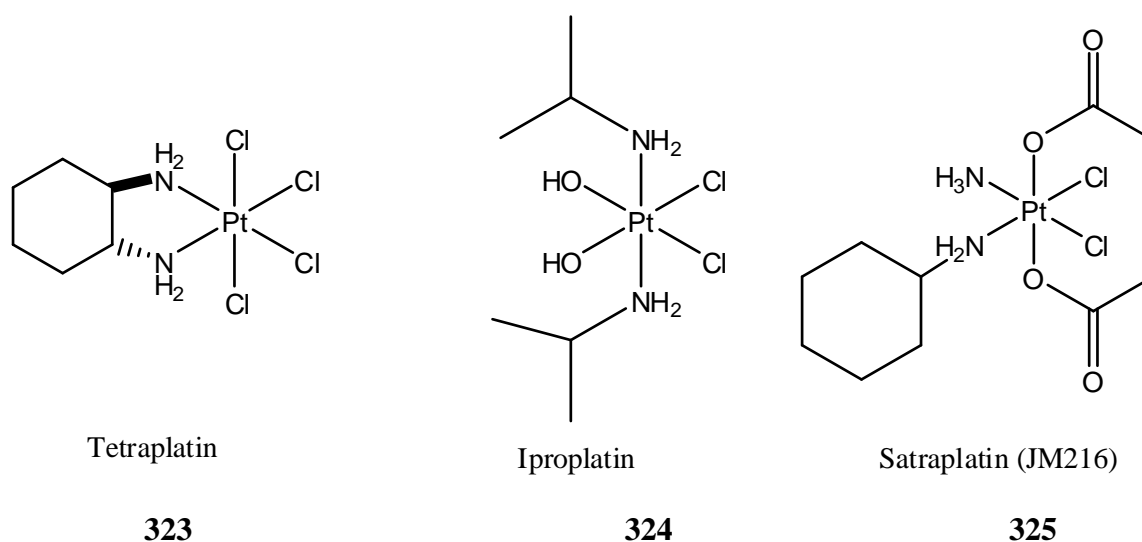


*Figure 3.14: The three Pt (IV) anti-cancer drugs that have reached advanced clinical trials.*

Tetrachloro (1,2-cyclohexanediamine-N,N') Pt (IV) or Tetraplatin, **323**, is a pro-drug that undergoes reduction by proteins in tissue and blood plasma to its active Pt (II) analogue. Multiple Phase I clinical trials were conducted but severe neurotoxicity was observed at high doses and to date no Phase II trials have been reported in the literature.<sup>19</sup>

*cis, trans, cis*-Dichlorodihydroxidobis (isopylamine) Pt (IV) or Iproplatin, **324**, on the other hand has been extensively studied with multiple Phase I, Phase II and Phase III clinical trials. Its activity was examined for a variety of cancer types including ovarian, urothelial, malignant pleural mesothelioma, breast, squamous cell carcinoma and cervical cancer to name only a few. However, advancement of the drug was hindered by some toxic related deaths, dose reductions due to cumulative effects and its response rate being no different to cisplatin.<sup>19</sup>

Developed over 16 years ago, bis(acetato-O)amminedichloro(cyclohexylamine) Pt (IV) or satraplatin (JM216), **325**, was found to have the lowest IC<sub>50</sub> value to date of any platinum anticancer drug (Pt (II) or Pt (IV)) coupled with dramatically decreased cytotoxicity. Recently, it was also found to be 2.8 times more effective against human ovarian carcinoma cell lines than cisplatin. Also, further studies by Ricart *et al* have laid the foundation for the drug to progress into phase III of clinical trials.<sup>20-22</sup>

Satraplatin is the first orally administered platinum anti-cancer drug where the patients can self administer the tablet over a five day basis. The advantages of this method of delivery are immense; including self administration for the patients in their own homes which is cost-effective over making frequent trips to a clinic. It was also reported again by Ricart *et al* that there was no cardiac, renal, hepatic or neurologic toxicity associated with this Pt (IV) chloride drug. It has reported to be very effective in particular against non-small cell lung cancer (NSCLC) and Hormone Refractory Prostate Cancer (HRPC).<sup>20,23</sup>

Current studies involving satraplatin are concerned with the dosage limits and response time for the drug by oral administration, along with the effect of food on diffusion of the drug from the stomach. Other studies include further *in-vitro* testing of satraplatin on new types of cancers along with extensive investigations into the pharmacokinetics of the drug after administration. In light of the ongoing research into this new generation of platinum anti-cancer drugs and the advanced stage of clinical trials at which satraplatin is currently in, it is hoped that further analogous Pt (IV) chloride complexes can be synthesised and brought to clinical trials.<sup>21,23-25</sup>

### 3.4.2 Stability and the Chelate Effect:

Unfortunately there are some reports of Pt (IV) complexes that suffer from greatly reduced stability over their Pt (II) analogues.<sup>26</sup> However, it has been recognised for many years that ligands which form a ring structure that includes the metal ion, called a chelate ring, have exceptional thermodynamic stability. This increased stability, beyond which could be achieved with a similar non-chelate system, is called The Chelate Effect.<sup>5,9</sup>

Like the complexes reported in **Chapter 2 (281-289)**, chelate rings that have a total of five or six atoms in the ring (including the metal ion) are more stable than rings with four or seven members. While the arrangement of chelate rings, the nature of the donor atoms and their charge, and the size of the rings all affect the stability of the complex, in general ligands which have multiple points of attachment to the metal ion produce the most stable complexes.<sup>5</sup>

Therefore, it can be extrapolated that tridentate chelate platinum complexes would have increased stability over analogous bidentate chelate platinum complexes such as Tetraplatin, **323**, **Figure 3.14**. Previous work by our research group on analogous iodo platinum complexes utilized this increased stability to isolate stable Pt (IV) iodo complexes, **Figure 3.15**.

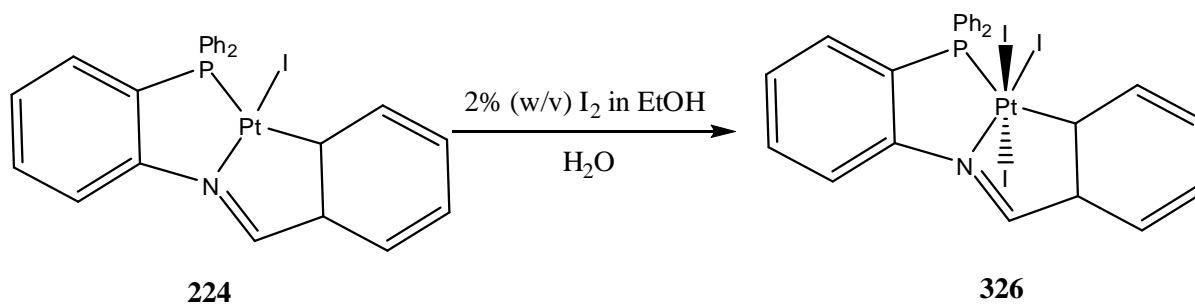


*Figure 3.15: The previously reported oxidation of iodo Pt (II) complexes by our research group to form stable Pt (IV) complexes.*

The exceptional stability of the metal chelate ring, which will also be explored in this chapter for the complexes **281-289**, implies that the binding constant of the ligand toward the metal ion is large. Also the increase in entropy going from left to right (with the loss of HCl from the complex because of cyclometallation as seen in **Chapter 2**) is often cited as the thermodynamic basis for the chelate effect.<sup>5,3</sup>

Although the Chelate Effect does enhance the stability of metal complexes, reductive elimination of the newly introduced axial ligands on some Pt (IV) complexes to produce the Pt (II) precursor have been reported, **Figure 3.16**. However, isolation and characterisation of the Pt (IV) complex **328** was achieved with the crystal structure showing a distorted octahedral geometry. For both complexes displayed in **Figure 3.16**; the interaction of the carbene ligands (neutral carbon with a valance of 2 and 2 unshared valence electrons) with the platinum metal centre *trans* to each other is considered a coordination bond, as confirmed by x-ray crystallography.<sup>26</sup>

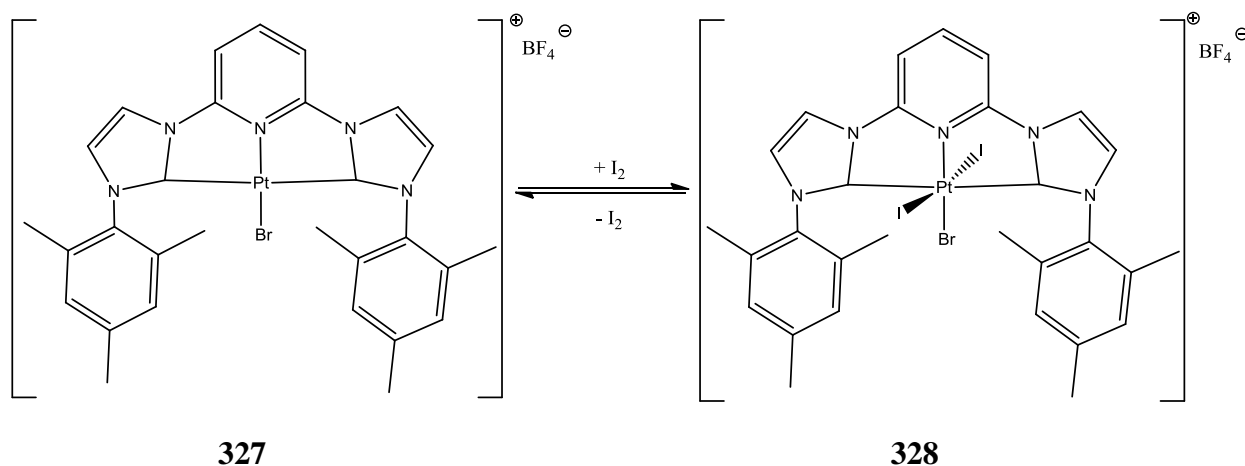


**Figure 3.16:** The oxidation of the CNC type chelate platinum complex **327** and the reductive elimination of the resulting Pt (IV) complex **328** due to instability.<sup>26</sup>

### 3.4.3 Oxidation of Pt (II) Complexes Using Hydrogen Peroxide:

The most common oxidation reagent used in the synthesis of Pt (IV) complexes is hydrogen peroxide, H<sub>2</sub>O<sub>2</sub>. In general reactions with Pt (II) complexes involving hydrogen peroxide results in the *trans* oxidative addition of the HO-OH bond across the Pt (II) metal centre to form octahedral structures. To achieve oxidations of this type, aqueous solutions of 30% (w/v) H<sub>2</sub>O<sub>2</sub> have been added to varying solutions of the Pt (II) complex at room temperature primarily for short periods of time.

Numerous examples of this method have been reported in the literature<sup>27-29</sup> and moderate success has been achieved previously within our research group using peroxide on bidentate iodo iminophosphine Pt (II) complexes shown in **Figure 3.17**. These complexes were synthesised by stirring a dichloromethane solution of **329** with 30% H<sub>2</sub>O<sub>2</sub> at room temperature for 16h to form the *trans*-dichloromethane Pt (IV) analogue **334** by picking up two solvent molecules during the oxidation process.<sup>6</sup>



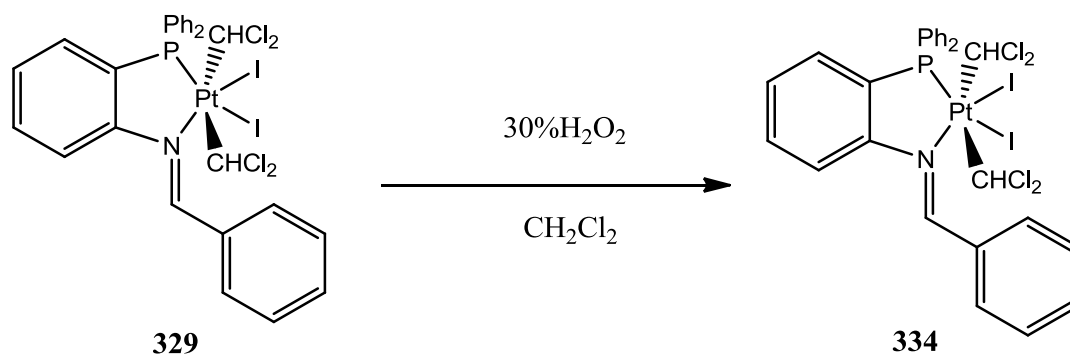


*Figure 3.17: The oxidation of the bidentate Pt (II) iminophosphine complex 329 using hydrogen peroxide to form the stable Pt (IV) complex 334.<sup>6</sup>*

The proposed mechanism of the interaction occurring in **Figure 3.17** involves oxidative addition of hydrogen peroxide (HO-OH) to the Pt (II) initially generating the Pt (IV) species HO-Pt<sup>IV</sup>-OH (**332**), **Figure 3.18**. The solvent, dichloromethane, is partially polar due to the electronegative atoms present within the molecule (Cl) (as previously discussed in detail in **Chapter 1** and **2**).

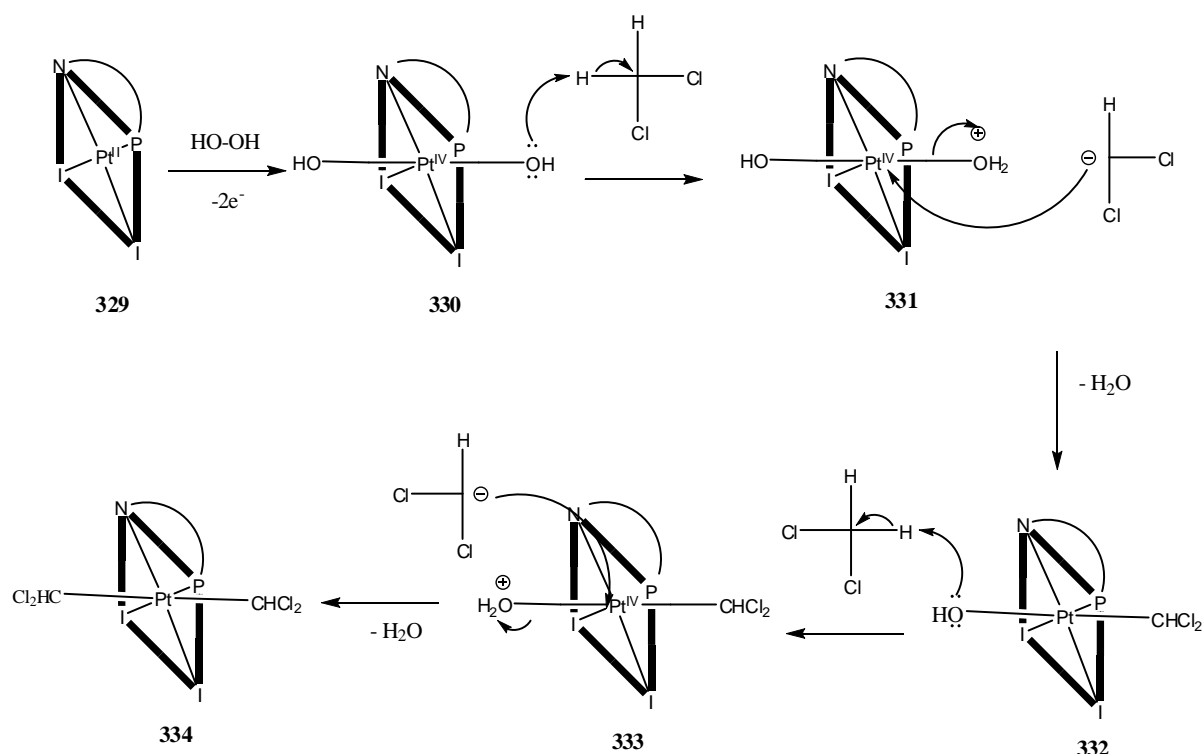


*Figure 3.18: The proposed solvent mediated mechanism to generate the Pt (IV) species via an  $S_N2$  mechanism.<sup>6</sup>*

The ionic species generated,  $[\text{CHCl}_2]^-$ , due to abstraction of one of the  $\delta^+$  hydrogens from the dichloromethane, attacks the Pt (IV) centre, thereby displacing water (an excellent

leaving group) to generate **332**, **Figure 3.18**. This intermediate, **332**, then reacts with another dichloromethane molecule to generate an ionic Pt (IV) species, **334**, and another water anion. Subsequent attack by the  $[\text{CHCl}_2]^-$  anion on the Pt (IV) centre liberates another water molecule and generates the final complex **334**, **Figure 3.18**.

An alternative mechanism can be proposed for this reaction which involves the presence of free radicals. Two hydroxyl radicals are generated by irradiation of light, which then react with dichloromethane to yield water and the radical  $\bullet\text{CHCl}_2$ . The subsequent interaction of the dichloro radical with the bidentate Pt (II) complex may form a highly reactive Pt (III) intermediate, which is similar to by-products found for other Pt (IV) forming reactions reported by Whitfield *et al.*<sup>30</sup>

Further reports into methods to generate Pt (IV) complexes have shown hydrogen peroxide to be a very versatile oxidising agent. Ellis *et al* have demonstrated oxidative addition of various anhydrides to a Pt (IV) metal centre to generate a wide variety of analogues in addition to a *trans* axial chloro Pt (IV) complex **337**, **Figure 3.19**.<sup>31</sup>

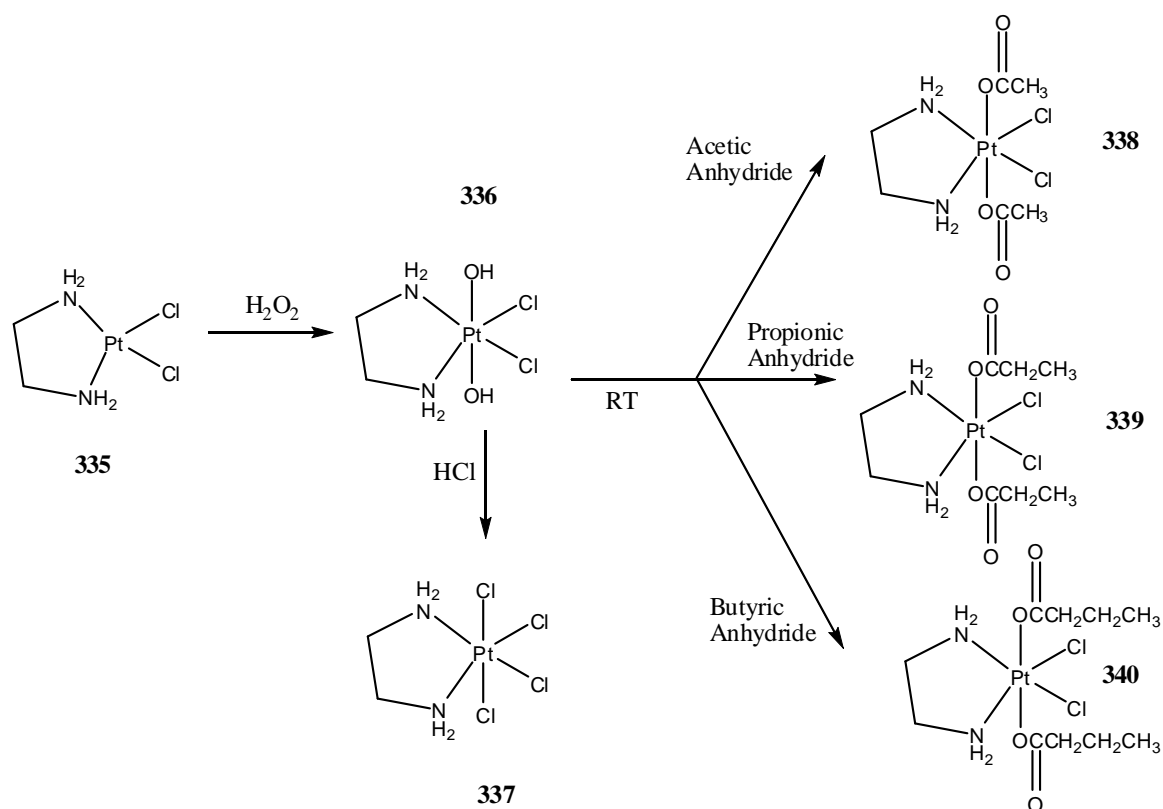


**Figure 3.19:** The oxidation of the Pt (II) complex **335** by hydrogen peroxide, followed by a reaction of anhydrides to form a range of products **338-340**. Of interest also is the formation of a chloro Pt (IV) complex using  $\text{HCl}$ , **337**.<sup>31</sup>

In **Figure 3.19**, the reaction of the Pt (II) complex **335** with hydrogen peroxide generates the Pt (IV) hydroxo analogue **336** via *trans* oxidative addition, which is consistent with the previously discussed oxidation in **Figure 3.18**. Further reaction of **336** with the appropriate anhydride generates the three Pt (IV) complexes **338-340**. But of particular interest to this project, the reaction of the Pt (IV) hydroxo complex **336** with HCl generates the Pt(IV) tetrachloride complex **337** in good yields (circa 82%).

In the literature there are few reports involving the oxidation of cyclometallated Pt (II) species using hydrogen peroxide, primarily because of the difficulties in obtaining pure Pt (IV) products. However, recent work by Newman *et al* reports the successful oxidation of phenylpyridine Pt (II) type complexes **341**, **Figure 3.20**.<sup>27</sup>

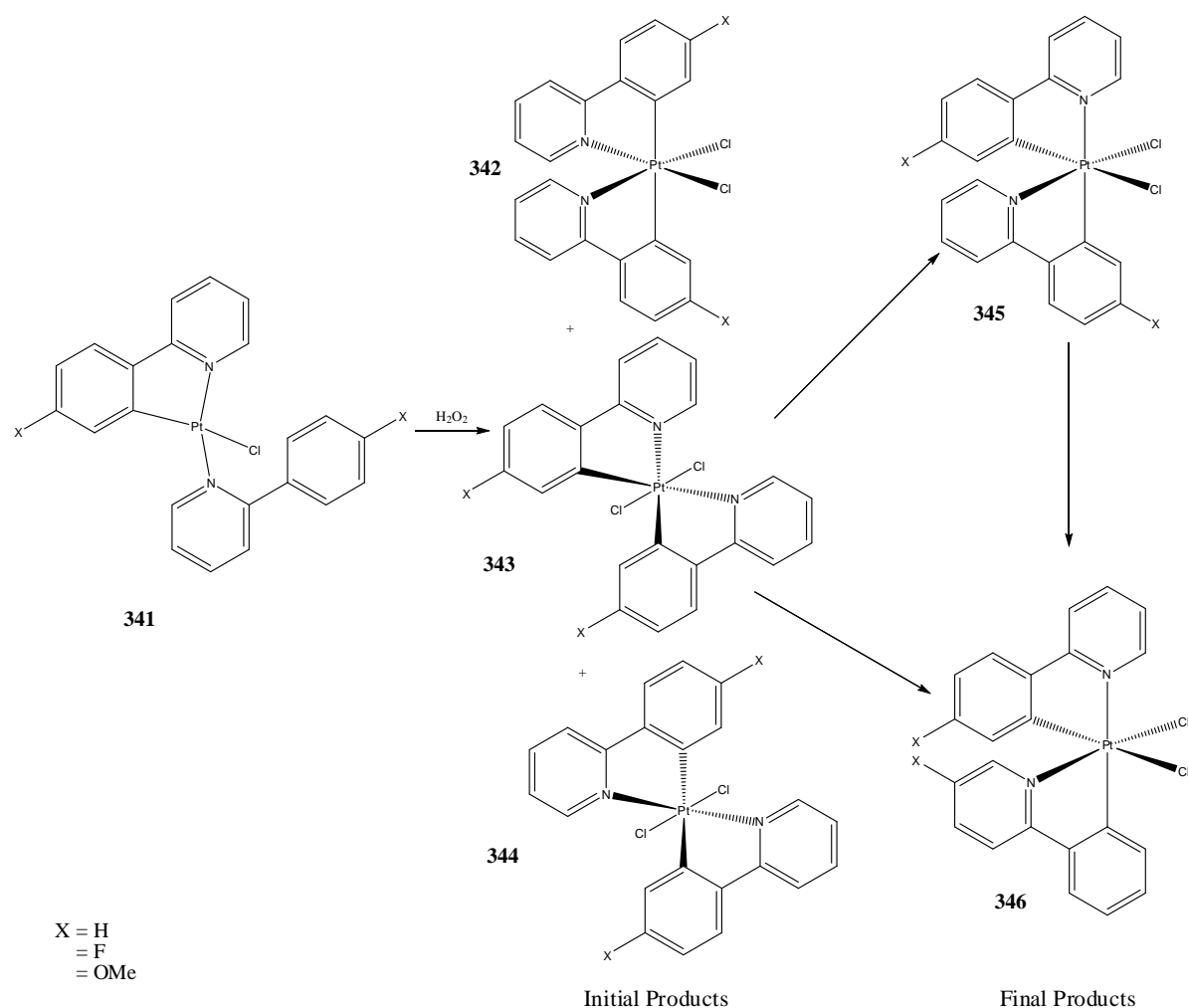


**Figure 3.20:** The oxidation of the Pt (II) complex **341** to form the isomeric products **342-346** using hydrogen peroxide.

The use of hydrogen peroxide as an oxidising agent had two effects in **Figure 3.20**; firstly, as expected, it resulted in the oxidation of the Pt (II) complex to its Pt (IV) analogue

and secondly, interestingly, it induced activation of a C-H bond to generate the bis-cyclometallated species **342-346**, which have the potential to exist in five isomeric forms.<sup>30</sup>

Two possible reaction mechanisms are proposed: (i) oxidation to Pt (IV) followed by cyclometallation or (ii) cyclometallation followed by oxidation. As covered in detail in **Chapter 2** of this report, cyclometallation is defined as primarily an electrophilic attack of the metal centre by a carbon centre. As Pt (IV) is more electrophilic than Pt (II), owing to its higher oxidation state, cyclometallation would be a more efficient and favourable process if oxidation to Pt (IV) occurred first, thus mechanism (i) is considered more probable.<sup>30</sup>

### 3.4.4 Oxidation of Pt (II) Complexes Using Group 17 Elements:

The oxidation of Pt (II) complexes to produce chlorinated Pt (IV) products has been explored in detail in the inorganic literature, traditionally using  $\text{Cl}_2$  as the oxidant. One of the earliest examples was provided by Rund *et al*, studying the oxidative addition of chlorine to dihalo (1,10-phenanthroline) Pt (II) **346**, **Figure 3.21**. Chlorine oxidation of this Pt (II) complex produced a new Pt (IV) species **347**, with the chloride ligands in a *cis* orientation to one another at the axial positions of an octahedral structure.<sup>32</sup>

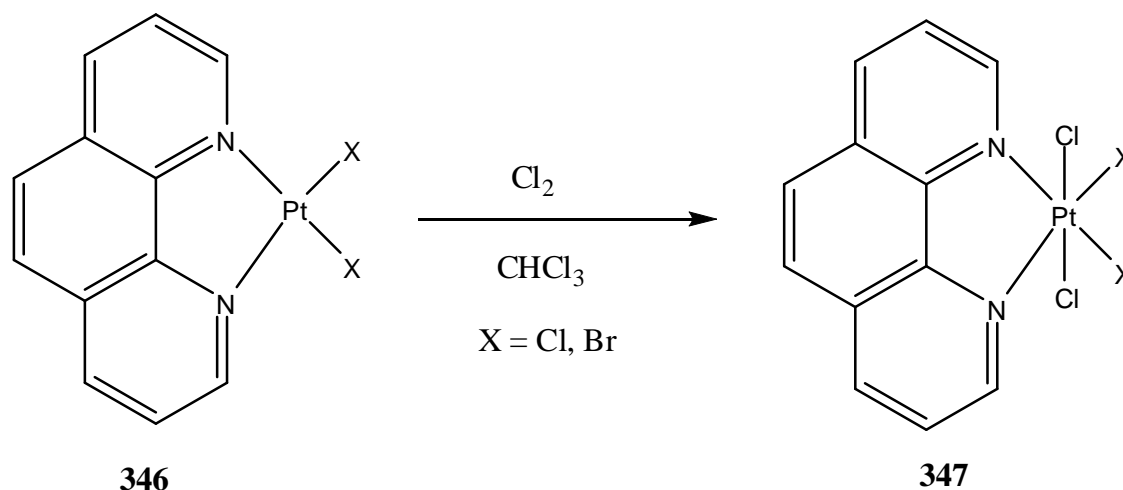


*Figure 3.21: The oxidation of the Pt (II) complex 349 using molecular chlorine gas,  $\text{Cl}_2$ .*

The proposed mechanism for these transformations is an ionic pathway involving nucleophilic attack on the Pt (II) metal centre to generate a cationic five-coordinate Pt (IV) intermediate **349**, **Figure 3.22**. This is similar to the associative mechanism proposed for the substitution reactions in **Section 3.2.3**.

The five-coordinate intermediate, **349**, is then followed by coordination of an  $X^-$  (halide anion) to produce the neutral Pt (IV) chloride product **351**. This mechanism was first proposed by Skinner *et al* (specifically using bromine).<sup>33</sup> Other investigations using  $Cl_2$  and  $I_2$  have also confirmed a similar mechanism.<sup>34–36</sup>

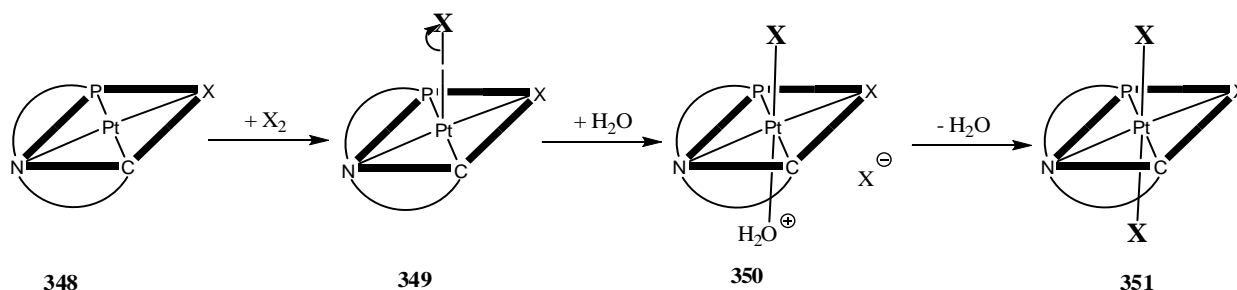


*Figure 3.22: The oxidation of the Pt (II) complex 351 via oxidative addition of a halide to a Pt (II) metal centre with assistance from a donor solvent  $H_2O$ .*<sup>33</sup>

In previous work by our research group, Pt (IV) complexes were formed from reacting an excess of molecular iodine with the relevant Pt (II) complexes in an ethanolic solution over the course of five days at room temperature giving yields ranging from 30 % to 60%. However, the crude products almost always contained some Pt (II) starting material.<sup>6</sup>

Using molecular iodine is convenient due to the fact that it is a solid at room temperature, but in order to oxidise Pt (II) complexes using  $Cl_2$ , a gas system is required in order to bubble the chlorine through the solution. This inconvenient set-up can be very hazardous so alternative methods to chlorinate these complexes have been developed by Liu *et al* and others and discussed further in the next section.<sup>30,37</sup>

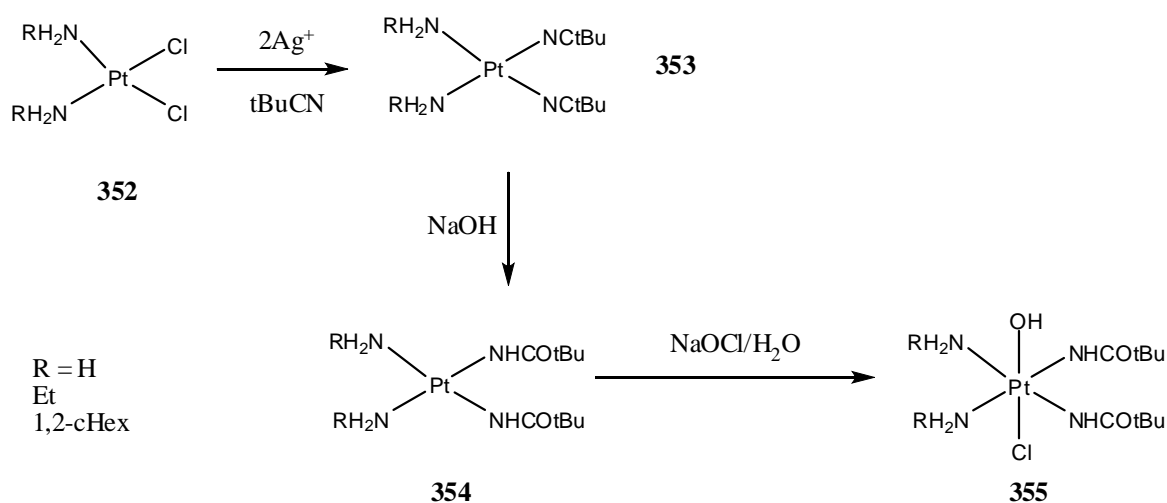


*Figure 3.23: Oxidation of a Pt (II) complex using an aqueous solution of sodium hypochlorite.*<sup>37</sup>



been used in limited instances for the oxidation of  $\text{Pt}^{\text{II}}$  species. For example,  $[\text{Pt}^{\text{II}}\text{Me}_2(\alpha\text{-diimine})]$  **359** and  $[\text{Pt}^{\text{II}}\text{Me}_2(\text{DPK})]$  **362** have been shown to react with NCS in MeOH to afford  $\text{Pt}^{\text{IV}}$  products that incorporate 1 equiv of chloride and an OMe group from the solvent, **Figure 3.25**.<sup>40</sup>

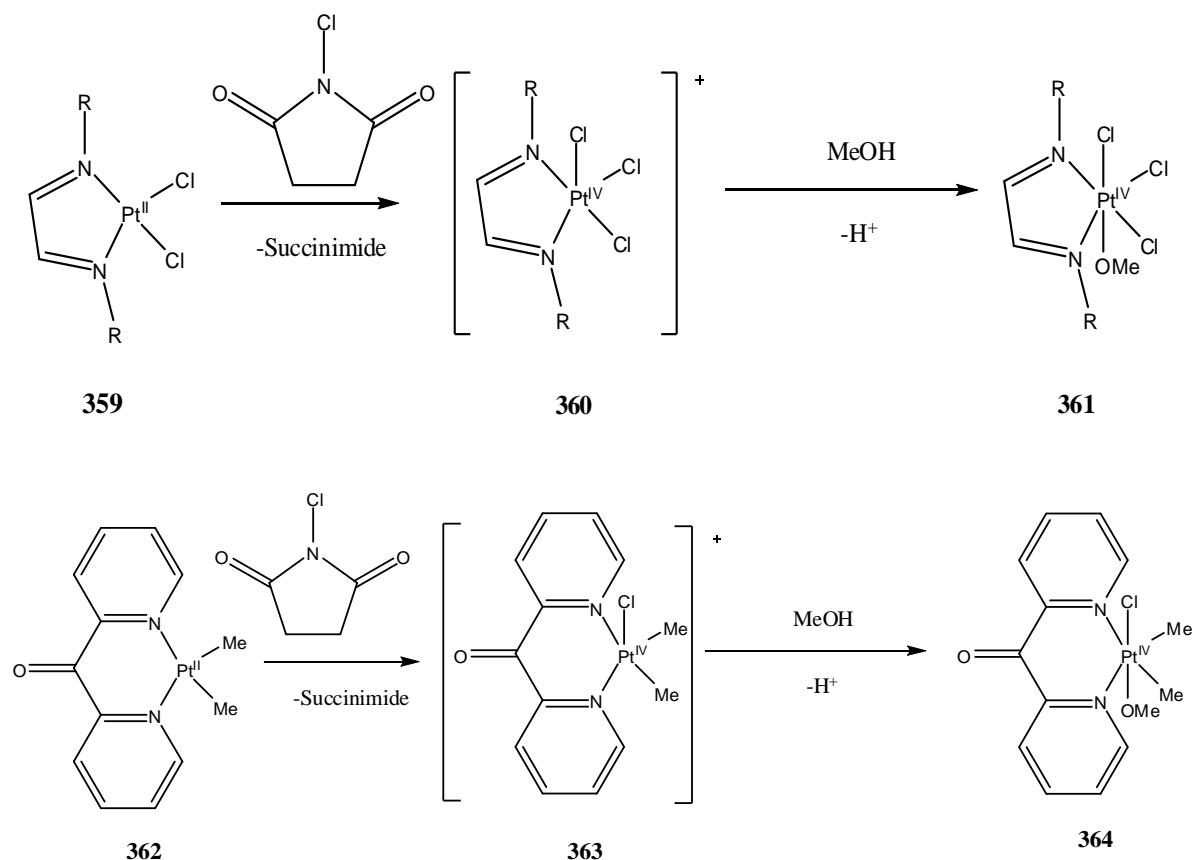


**Figure 3.25:** Formation of  $\text{Pt}^{\text{IV}}$  products, **361** and **364** due to the oxidation of  $[\text{Pt}^{\text{II}}\text{Me}_2(\alpha\text{-diamine})]$  **359** and  $[\text{Pt}^{\text{II}}\text{Me}_2(\text{DPK})]$  **362** respectively with *N*-chlorosuccinimide (NCS) in methanol.

As shown in **Figure 3.25**, the mechanism of these transformations are presumed to involve initial, two electron oxidation of the  $\text{Pt}^{\text{II}}$  complexes in order to form a cationic  $\text{Pt}^{\text{IV}}$  intermediate, **360** and **363**, which is then followed by trapping of the intermediate with the solvent to form the stable  $\text{Pt}^{\text{IV}}$  complexes **361** and **364**.<sup>40</sup>

Sanford *et al* have also produced similar results using NCS as an oxidant involving the phenylpyridine  $\text{Pt}^{\text{II}}$  complex **365**, **Figure 3.26**. Also of significance in this work is the  $\text{Pt}^{\text{III}}$  intermediate, **366**, which for the first time was observed and isolated with NCS as an oxidant. Interestingly they have also reported similar palladium oxidations to form stable  $\text{Pd}^{\text{IV}}$  chloride complexes with the same phenylpyridine ligands.<sup>30</sup>

Also worth noting for these series of reactions was the role of light in the reaction mechanism and the photophysical properties the complexes were seen to have. The Pt (IV) complexes (**367** and **368**) increased in yield while the oxidation reaction was carried out under intense light and as a result the yield of the Pt (III) complex **366** decreased. This was explained by way of photoexcitation of the Pt (II) starting material **365**, followed by  $\text{Cl}^\bullet$  radical abstraction from the solvent to form the Pt (III) radical and finally radical cage recombination to afford the Pt (IV) complexes, **367** and **368**.

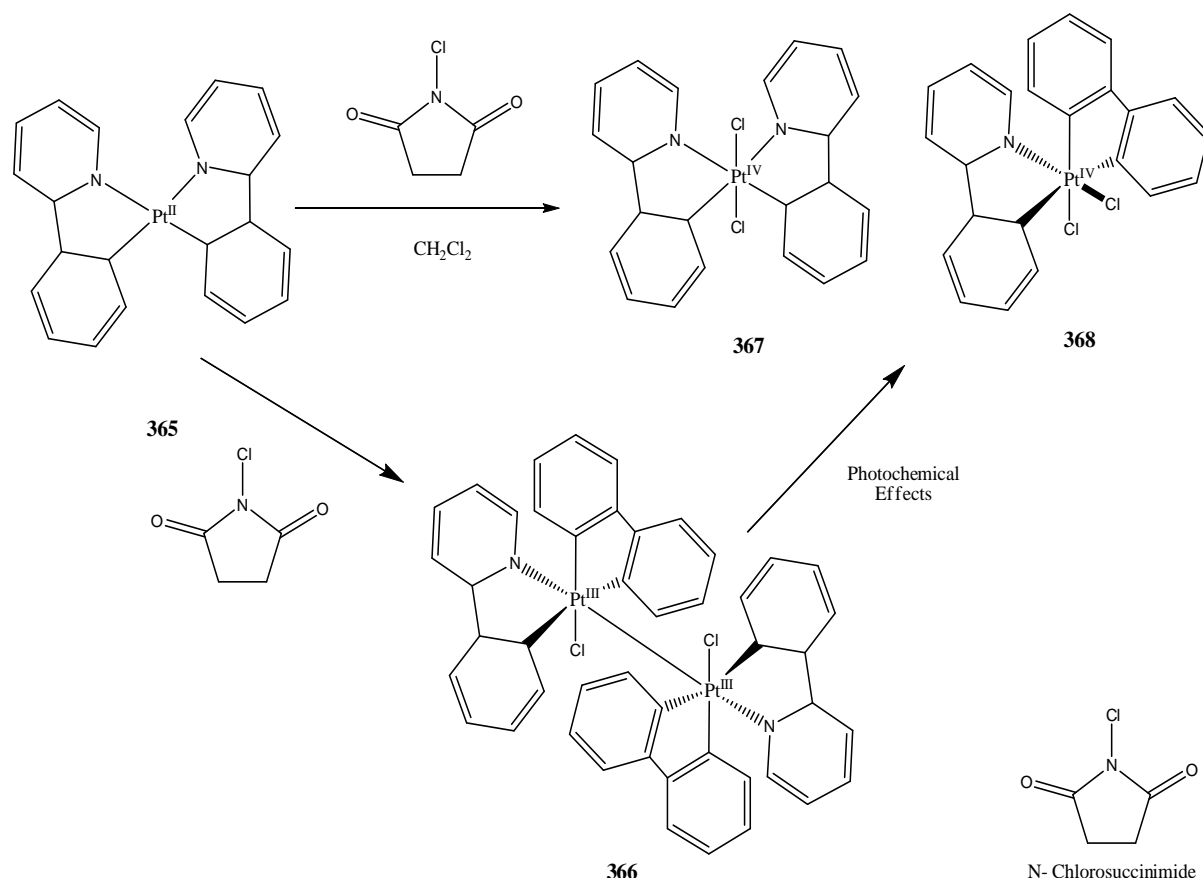


*Figure 3.26: Formation of Pt (IV) products, **367** and **368** due to the oxidation of phenylpyridine Pt (II) complex **365** with N-chlorosuccinimide (NCS) in dichloromethane. Also of note is the formation of the Pt (III) complex **366** which under intense light also undergoes oxidation.<sup>30</sup>*

### 3.5 Summary and Conclusions:

From the literature reviewed it is apparent that, although difficult, it is possible to achieve one-step substitution of platinum chloride bonds and the methods used have been seen to be dependent on solvent-ion stabilisation previously discussed in reference to chloroform in **Chapter 2**. From work completed previously by our research group,



particularly in the case of group 10 metal-halide bonds, the lability of these bonds have been reported to increase down the group (F > Cl > Br > I). Generally, on substituting chloro ligands in tridentate complexes, if no chloride scavenger is present either no reaction occurs or displacement of one of the tridentate ligand donor moieties has been observed.

Following on from work completed within our research group into iodo platinum substitutions, it is therefore the aim of the first part of this chapter to investigate the possibility of achieving direct substitution of chloride platinum iminophosphines using methods employed by Anderson *et al* which involves using mixed chlorinated solvent systems such as chloroform:methanol. Chlorinated solvent systems have already shown to be successful in this project as reported in **Chapter 2** by stabilisation of the chloride anion to allow cyclometallation.

Pt (IV) chloride complexes on the other hand can be synthesised using a variety of means, affording varying stable and unstable products. Previous work in our research group and others has achieved stable Pt (IV) iodo complexes using molecular iodine as the oxidising agent. Molecular chlorine is a possibility towards oxidising the Pt (II) chloride analogues, but from the literature reviewed oxidising platinum complexes using various cheap alternative and less hazardous methods are a more desirable route. Oxidising agents such as sodium hypochlorite and electrophilic oxidising agents such as *N*-chlorosuccinimide have shown some success in recent studies by Sanford *et al* and others.

With these reagents in mind oxidations of all the Pt (II) complexes reported in **Chapter 2** will be attempted and reported in the second part of this chapter. It is also hoped that eventually these proposed Pt (IV) chloride complexes may also have the potential to be precursors for the preparation of other Pt (IV) complexes via displacement of chloride ligands using the methods developed in the first part of this chapter. It is also hoped that these proposed Pt (IV) chloride complexes may hold potential anti-cancer activity as pro-drugs, as discussed in **Chapter 1**.

### 3.6 Syntheses:

All the starting materials used in this chapter are prepared as per the procedures outlined in **Chapter 2** for the synthesis of the cyclometallated Pt (II) complexes consisting of the cyclometallated iminophosphines **281-285** and the cyclometallated phosphinoamides **286-288**. All were characterised by NMR spectroscopy, X-Ray crystallography (in selected cases), IR spectroscopy and elemental analysis prior to being used in this chapter.

Substitution and oxidation reactions of the insoluble proposed bidentate complexes **271-273** were also attempted. It was hoped that the resulting products would be more soluble and agreeable to further characterisation. However all the products formed were also insoluble and therefore difficult to characterise. No further substitution or oxidation reactions were therefore attempted with these complexes and all further work was concentrated on the cyclometallated complexes **281-288**.

#### 3.6.1 Synthesis of cationic triphenylphosphine (PPh<sub>3</sub>) substituted Pt (II) complexes of the general formula [Pt( $\eta^3$ -PNC/PNO-L<sup>1-4</sup>)PPh<sub>3</sub>]Cl 371-375:

The synthesis utilised for the substitution reactions is a variation of a literature procedure previously utilised for iodo complexes both by this research group and others.<sup>41</sup> Previous reports by this research group into both chloro and iodo platinum substitution required a halide scavenger (silver perchlorate) to initially remove the halide from the metal centre before substitution with the required phosphine was undertaken.<sup>8,6</sup>

Direct substitution (without the use of a halide scavenger) was, however, seen to occur for the iodo cyclometallates using a mixed solvent system of acetonitrile:methanol but it was never successfully applied to the analogous chloro palladium or platinum complexes. This may be due to the relative reactivity of the platinum iodide bond compared with the platinum chloride bond, discussed previously in **Figure 3.6**.

The iminophosphine cycloplatinated PNC or PNO complexes **281-285** were stirred with 1.1 equivalents of triphenylphosphine (PPh<sub>3</sub>) at room temperature for 6 hours in a 1:1 methanol:chloroform mixed solvent system.

The solution immediately changed from orange to a pale straw yellow colour on addition of the phosphine. After 6 hours it was then reduced to dryness *in vacuo*, and recrystallised from doubly distilled dichloromethane layered with diethyl ether, **Figure 3.27**.

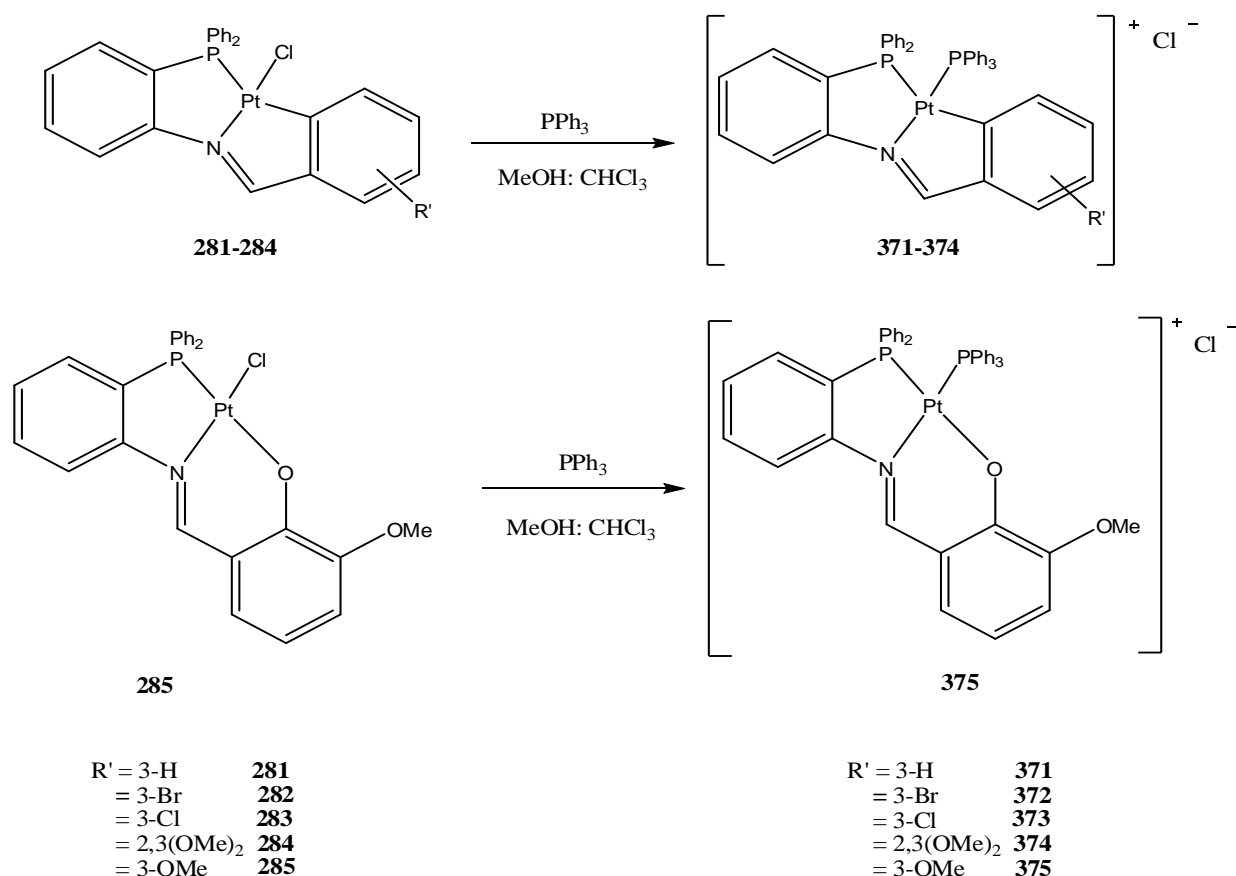


*Figure 3.27: Direct substitution of the cyclometallated platinum iminophosphine complexes, 281-285, with triphenylphosphine (PPh<sub>3</sub>).*

This procedure involves the direct displacement of the chloride moiety owing to the stronger Pt-P (soft acid-soft base) interaction from the introduced phosphine over that of the weaker Pt-Cl (soft acid-hard base) bond, coupled with stabilisation of the liberated chloride anion. A summary of the complexes synthesised, their yields and physical appearances, are displayed in **Table 3.1**.

Substituted Complex	Precursor	Physical appearance	% Yield
<b>371</b>	281	Pale yellow metallic crystalline powder	88
<b>372</b>	282	Dark yellow metallic crystals	71
<b>373</b>	283	Pale yellow metallic crystals	69
<b>374</b>	284	Orange metallic crystalline powder	89
<b>375</b>	285	Yellow metallic crystalline powder	68

*Table 3.1: Yields and appearances for the cationic chloro Pt (II) phosphine substituted products, obtained by novel direct substitution methods.*

Non-mixed solvent systems consisting of just chloroform or just methanol proved to be unsuccessful in the case of methanol and gave reduced yields of up to 30% in the case of chloroform. It was also hoped that refluxing would increase the yield but in fact it reduced the yield due to decomposition identified by the appearance of an insoluble black material in the reaction vessel. Longer reaction times (i.e. greater than 6 hours) also did not increase the yield as the reaction itself was primarily quantitative with no starting material identified after 5 hours stirring at room temperature.

Previously our research group used a methanol:acetonitrile solution to achieve one-step substitutions, but this was unsuccessful here as it only gave the starting material as the majority product even after 24 hours stirring at room temperature. Instead it was found that a 1:1 mixture of dry methanol:chloroform gave much better yields of the desired phosphine substituted product. The importance of stabilisation of the displaced anion, chloride, by the solvent system (like that reported previously in **Chapter 2**) was again identified here by using chloroform. Therefore in order for direct substitution to occur, it is proposed that the liberated anion must be stabilised allowing for substitution of the metal centre by the bulky incoming triphenylphosphine ( $\text{PPh}_3$ ) ligand.

These complexes were characterised and confirmed by IR and NMR spectroscopy as well as elemental analysis which are all consistent with the proposed structure of these compounds and compares well with previously reported analogous complexes.<sup>8</sup>

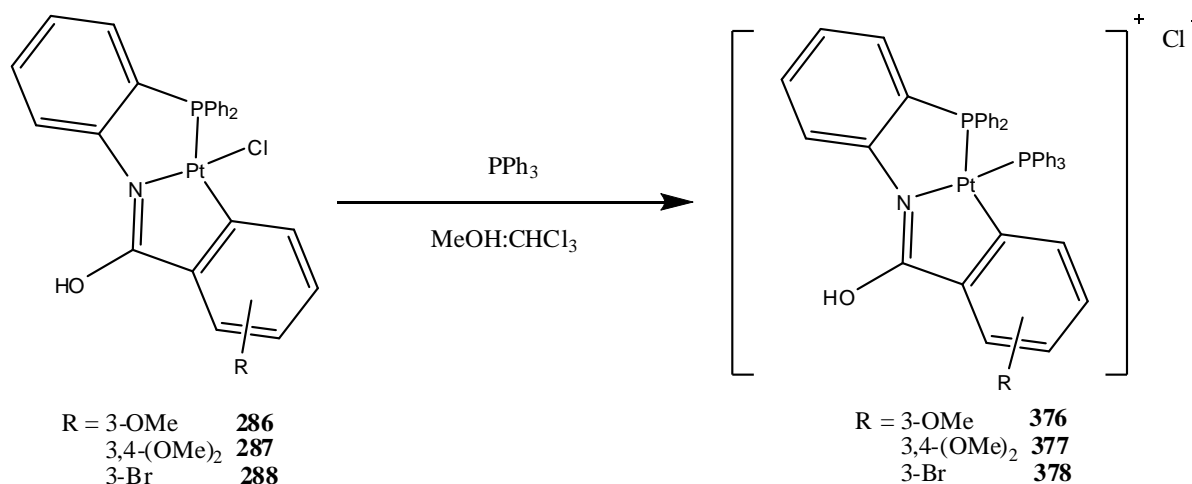


*Figure 3.28: Proposed direct substitution of the cyclometallated platinum phosphinoamide complexes, 286-288, with triphenylphosphine ( $\text{PPh}_3$ ).*

Substitution of the cyclometallated phosphinoamide complexes **286-288** using the same method employed for the iminophosphine Pt (II) complexes **281-285** proved to give

multiple unidentifiable products, **Figure 3.28**. TLC analysis of the solution after 6 hours stirring at room temperature in a 1:1 methanol:chloroform system gave circa 5 products, all of which were very insoluble in all common solvents making characterisation unachievable at this time. Separation of the products also proved unsuccessful using a variety of chromatographic eluents and methods including silica gel, alumina and celite.

It is proposed that substitution of the phosphinoamide complexes is occurring at not only the platinum chloride bond, but also at the platinum carbon and platinum nitrogen bond due to the previously identified unstable nature of these complexes in the presence of reagents.<sup>7</sup>

### 3.6.2 Discussion of Factors Influencing the Substitution Reactions:

Previous work within this research group with substitution reactions involving phosphines encountered various difficulties with and without the use of a silver perchlorate salt to remove the halide from the metal centre.<sup>8,6,7</sup> Triphenylphosphine (PPh<sub>3</sub>) was reported to be one of the most difficult to achieve one-step substitution of platinum metal centres due to its steric bulk, while tris-cyanoethylphosphine was found to be one of the easiest. Because of this it was proposed that the potential influences that determine platinum halide substitution by monophosphines were the basicity of the phosphine being used and the space occupied or cone-angle of the phosphine ligands.

Previously it was proposed by our research group that the greater lability of the iodo-Pt (II) bond should allow direct substitution of the tridentate PNO and PNC complexes over any equivalent chloro complexes. However, here we find using an appropriate solvent to stabilise the smaller chloride ion can achieve one-step substitution. Also the chloride ligand, being less bulky compared to the iodide, allows the sterically bulky phosphine to get closer to the metal centre, allowing for substitution to occur. This is proposed to assist displacement in a concerted mechanism involving stabilisation by the solvent as described in **Chapter 2, Figure 3.29**.

As discussed previously in **Chapter 2**, chloroform has the unique ability to stabilise liberated chloride anions. We have already seen how important this was to the cyclometallation mechanism for the parent Pt (II) complexes **281-284** but we can also see its influence here.

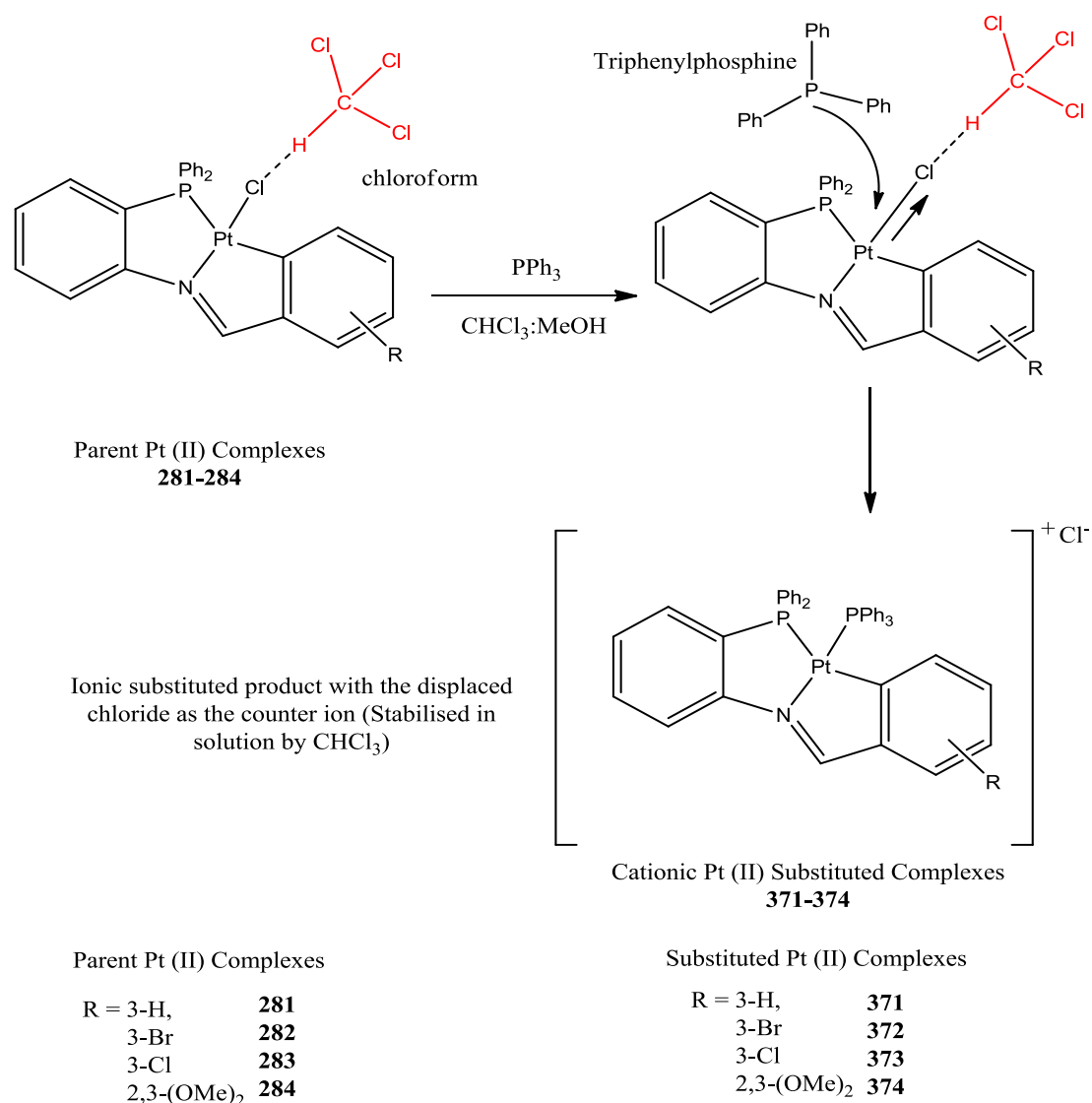


*Figure 3.29: Proposed mechanism for direct substitution of the cyclometallated Pt (II) iminophosphine complexes, 281-284, with triphenylphosphine (PPh<sub>3</sub>).*

Chloroform, possessing three electron withdrawing groups in the form of chlorides, has a dipole. This allows the  $\delta^+$  H to interact quite strongly with the halide on the platinum metal centre. This interaction between the hydrogen of the solvent molecule and the chloride of the complex weakens the platinum chloride bond. This elongates it, as the highly electronegative chloride on the metal centre and hydrogen of the chloroform molecule bond gets shorter. This would then make it easier for triphenylphosphine to cause direct displacement of the chloride moiety from the metal centre, **Figure 3.29**.

It was found previously that the influence of basicity and steric factors was also particularly relevant to the substitution of Pt (II) tridentate PNO complexes. Previous work by our research group, which focussed on the substitution of Pt (II) PNO chloro-complexes,

found that triphenylphosphine substitution of the chloride ligand could not be achieved and that substitution using tri-*p*-tolylphosphine (which is more basic but has the same steric parameters) was achieved, but only with certain substituents.<sup>8</sup>

However, the experimental evidence obtained in this study for the previously reported PNO complex  $[\text{Pt}(\eta^3\text{-PNO-L}^4)\text{Cl}]$  **285** has shown that stabilising the liberated anion facilitates an important requirement in the reaction mechanism causing it to overcome one of the primary reasons stopping one-step substitution of chloro complexes. Phosphine substitution of  $[\text{Pt}(\eta^3\text{-PNO-L}^4)\text{Cl}]$  **285**, which was previously reported by our research group as described in **Chapter 2**, was never successfully reported with or without the use of a silver perchlorate salt. Here it is reported via direct substitution with triphenylphosphine forming the cationic Pt (II) PNO complex **375**, **Figure 3.27**.

### 3.6.3 Attempted oxidation of Pt (II) complexes Using $\text{H}_2\text{O}_2$ and NaOCl:

Initial attempts to form Pt (IV) analogues of the iminophosphine complexes reported in **Chapter 2** involved the use of  $\text{H}_2\text{O}_2$ , **Figure 3.30** (all proposed Pt (IV) products are based on previous reports). This procedure involved an adaptation of a previously reported method that was found to be very successful for both our research group and others.<sup>27,6</sup> The Pt (II) complexes reported in **Chapter 2** (**271-273**, **281-285** and **286-288**) were suspended in a dichloromethane solution to which 30% (w/v) aqueous hydrogen peroxide was added slowly over one hour.

The biphasic solution was stirred vigorously for 16 hours but no observable difference was noticed for the solution in terms of colour or consistency. The solution was transferred to a separating funnel where the organic layer was washed with de-ionised water, dried over  $\text{MgSO}_4$  and reduced to dryness *in vacuo*. In the case of the tridentate iminophosphine complexes **281-285**, only the Pt (II) starting materials were recovered with yields of greater than 90%, indicating little or no reaction with the peroxide.

The insoluble bidentate iminophosphine complexes **271-273** were also found to have no reaction with peroxide as their IR spectra after the reaction was identical to what was obtained prior to the reaction. In contrast a reaction did take place between  $\text{H}_2\text{O}_2$  and the tridentate phosphinoamide cyclometallated complexes **286-288**. TLC showed several products had formed, however spectroscopic analysis showed that there were no longer any evidence of the starting materials or any Pt (IV) complexes. This indicated that, like that

found for the triphenylphosphine ( $\text{PPh}_3$ ) substitution reactions earlier, **Section 3.6.1**, decomposition of the complexes had again occurred.

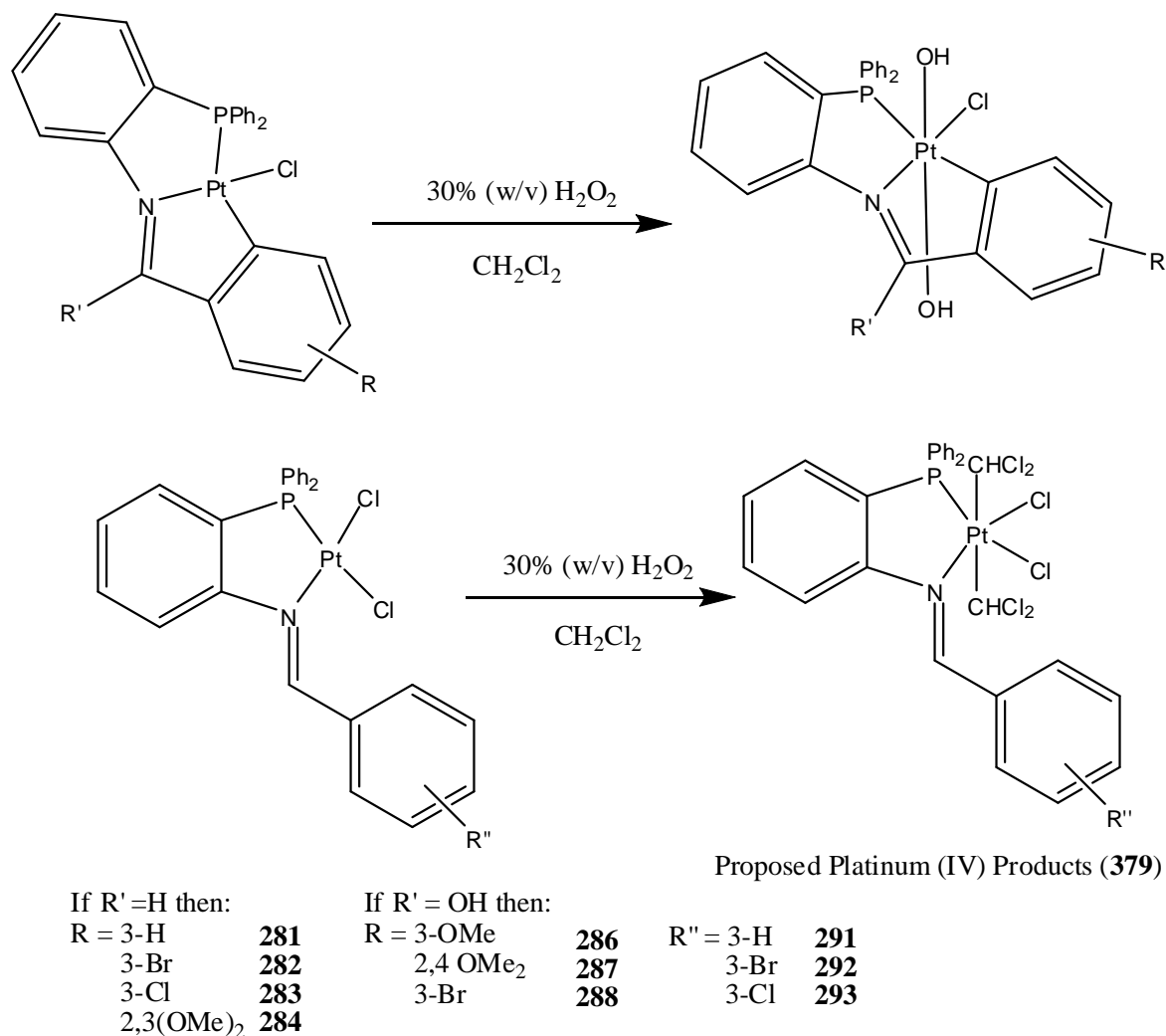


**Figure 3.30:** Proposed oxidation reaction of the Pt (II) iminophosphine and phosphinoamide complexes with hydrogen peroxide.

Variations of the procedure with different solvents, refluxing and longer/shorter reaction times were also unsuccessful for the formation of Pt (IV) complexes, despite previous success by our research group and others with this method.<sup>6,29</sup>

Further reports in the literature also cite sodium hypochlorite ( $\text{NaOCl}$ ) as a potential oxidising agent for Pt (II) complexes giving mixed axial ligands of chloride and hydroxyl groups. The most stable Pt (II) complexes (**Chapter 2**), the cyclometallated iminophosphines **281-284**, were attempted initially with this method due to the higher chances of achieving characterisation upon completion, **Figure 3.31**.



The Pt (II) complexes were dissolved in chloroform and NaOCl was added slowly over one hour. The biphasic solution was then stirred at room temperature for a further 2 hours after which the solution turned a very dark red. TLC analysis of the solution gave 4-5 products and NMR spectra also displayed multiple imino-hydrogen signals and multiple phosphorus signals, indicating a mixture of products. Interestingly there was no evidence of the Pt (II) starting material present in the solution and separation of the products has proved impossible to date.

Further work with the phosphinoamide complexes, **286-288**, involving NaOCl, again only gave decomposition products for the reaction which further emphasised the difference in stability between the Pt (II) iminophosphine complexes **281-285**, in comparison to the Pt (II) phosphinoamide complexes **286-288**.

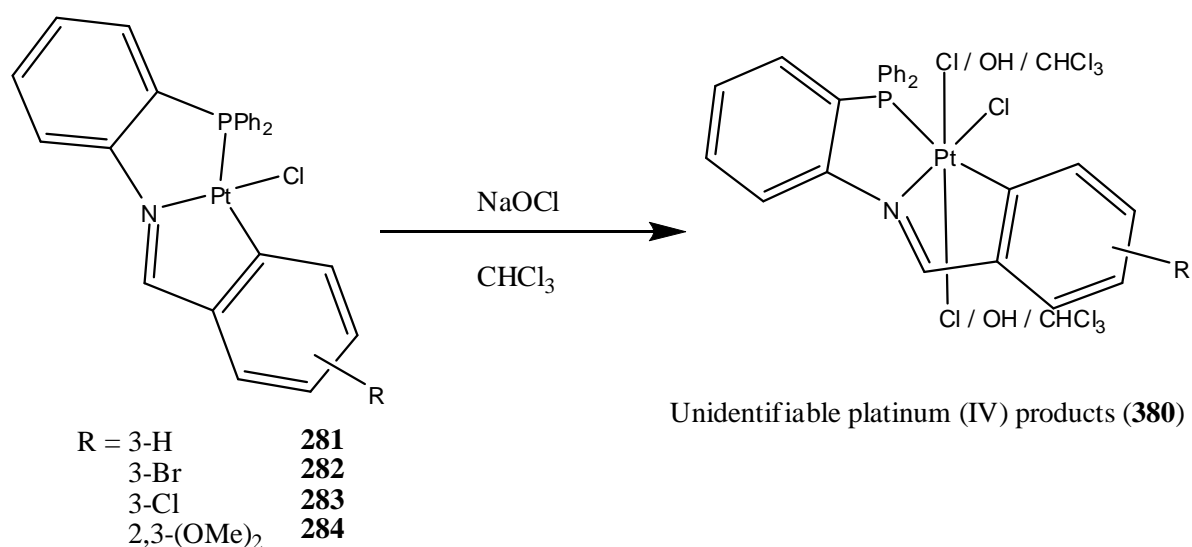


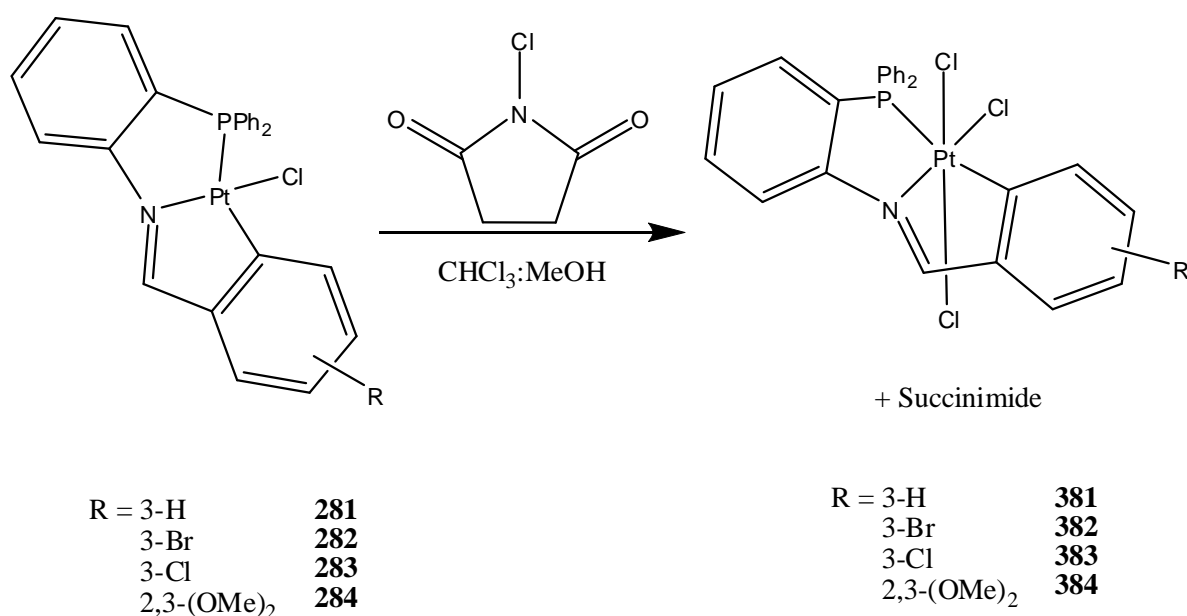
*Figure 3.31: Proposed oxidation reaction of the Pt (II) iminophosphine and phosphinoamide complexes with NaOCl was somewhat successful for the iminophosphine complexes, however the products could not be characterised at this time.*

#### 3.6.4 Synthesis of Pt (IV) chloro complexes of the general formula $[\text{Pt}(\eta^3\text{-PNC-L}^{-1}\text{-}^4\text{Cl}_3)]$ **381-384**:

Synthesis of the chloro iminophosphine Pt (IV) complexes **381-384**, via oxidative addition of chloride using *N*-chlorosuccinimide, was successful using a variation of a previously reported method, **Figure 3.32**.<sup>30</sup> To a mixed solvent solution (1:1 chloroform:methanol) of the appropriate Pt (II) iminophosphine complex (**281-284**), an excess of *N*-chlorosuccinimide was added as a solid.

The solution immediately changed from a bright orange colour to a dark orange/red upon addition of NCS. It was then left to stir at room temperature for 16 hours, after which the resulting orange solution was transferred to a separation funnel and washed with water 3 times to remove the remaining *N*-chlorosuccinimide and the succinimide product, **Figure 3.33**.

The organic phase was then dried over magnesium sulphate and reduced to dryness *in vacuo*. The resulting red oil was crystallised from dichloromethane-hexane to give moderate yields of the Pt (IV) cyclometallates. Any residual starting material (i.e. the Pt (II) complex **281-284**) remained in the mother liquor after crystallisation. This was confirmed by TLC of the solution with a 98:2 CHCl<sub>3</sub>:MeOH elution. The R<sub>f</sub> value obtained was identical to that established for the Pt (II) complexes (as previously identified in **Chapter 2**). Interestingly, in the case of [Pt(η<sup>3</sup>-PNC-L<sup>4</sup>)Cl<sub>3</sub>] **384**, no residual Pt (II) complex was identified even though the yield was still significantly low. A summary of the yields and physical appearances of the Pt (IV) complexes **381-384** are summarised in **Table 3.2**.



NCS = N-Chlorosuccinimide

**Figure 3.32:** Successful oxidative addition of two equivalents of chlorine to the iminophosphine Pt (II) complexes, **281-284** using *N*-chlorosuccinimide was successful in creating novel Pt (IV) complexes.

Elemental analysis data agrees, within experimental error, with the proposed empirical formula for the complexes where solvent of crystallisation is included; this solvent is also apparent in the <sup>1</sup>H NMR spectra. The mechanism of oxidative addition of Br<sub>2</sub> has been previously investigated and identified in 1969 by Skinner and Jones, **Figure 3.33**.<sup>33</sup> By

analogy with the results we propose a similar mechanism for oxidation of the Pt (II) iminophosphine cyclometallates **281-284** and is backed-up by a similarly proposed NCS oxidation mechanism reported by Sanford *et al*, **Figure 3.33**.<sup>30</sup>

Pt (IV) complex	Pt (II) Precursor	Physical appearance	Yield (%)
<b>381</b>	<b>281</b>	Black-red crystalline solid	30
<b>382</b>	<b>282</b>	Brown crystalline solid	11
<b>383</b>	<b>283</b>	Brown crystalline solid	25
<b>384</b>	<b>284</b>	Red crystalline solid	36

*Table 3.2: Physical appearances and yields obtained for the Pt (IV) iminophosphine complexes 481-484.*

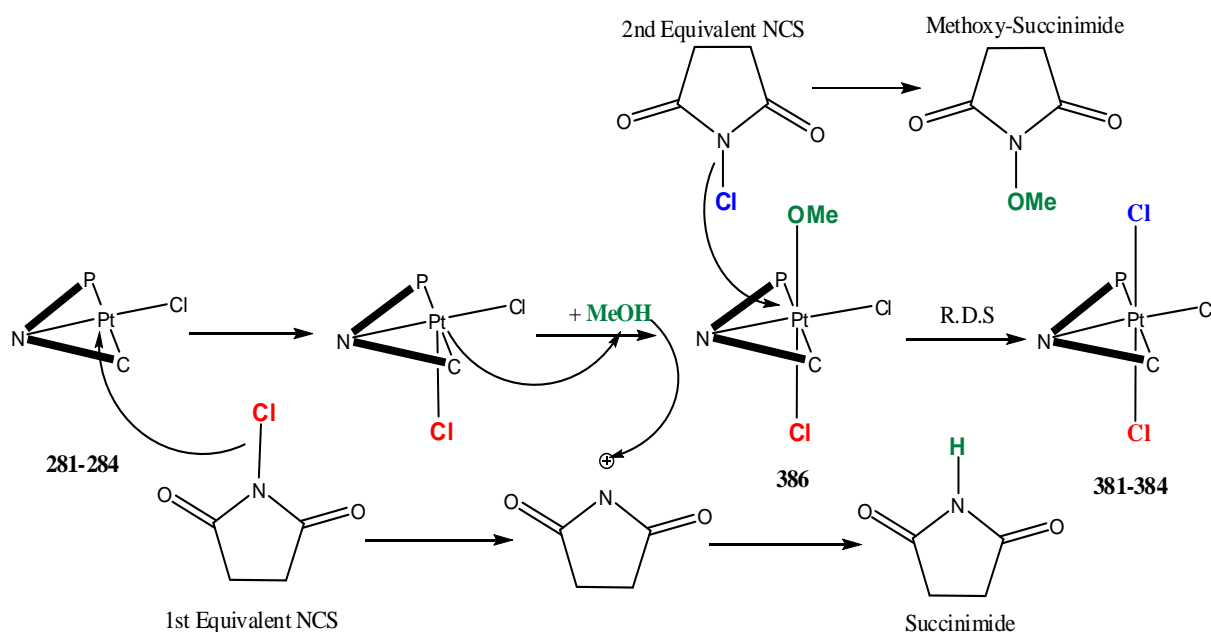


*Figure 3.33: The mechanism for oxidative addition of two equivalents of chlorine to the iminophosphine Pt (II) complexes, **281-284** using N-chlorosuccinimide in the presence of a protic solvent – methanol (MeOH).*

The mechanism proposed in **Figure 3.33** uses two equivalents of N-chlorosuccinimide and a protic solvent in order to form the stable Pt (IV) iminophosphine complexes with two chloro axial ligands (given as **Blue** and **Red** in **Figure 3.33**). The last step of the mechanism is the rate determining step as the methoxy-chloro mixed axial intermediate, **386**, has been isolated during shorter reaction times. Evidence for this mechanism in this work has also been identified with the isolation of the mixed axial

intermediate **386**, **Figure 3.34** at shorter reaction times. This suggests that the reaction of the Pt (II) iminophosphines proceed via this mechanism to form the final Pt (IV) complexes **381-384**.

Based on the work of Sanford *et al*, reactions of the Pt (II) complexes with NCS were initially undertaken in dichloromethane. Reaction times shorter than 1 hour did not go to completion and a significant amount of the parent Pt (II) starting materials were recovered. However, reaction times longer than 1 hour resulted in the solution turning green and the presence of no identifiable products due to proposed decomposition.<sup>30</sup>

A protic solvent, methanol (MeOH), was found to be crucial for formation of stable Pt (IV) complexes with NCS, which has also been reported by Sanford *et al* as an important factor in the mechanism for oxidative addition, **Figure 3.32**.<sup>30</sup> Reaction times of 16 hours were found to be ideal, as shorter reaction times resulted in the isolation of the photo-sensitive Pt (IV) intermediate **386** with mixed chloro/methoxy axial ligands, **Figure 3.34**. These type of complexes have also been reported by Sanford *et al* and identified here by <sup>1</sup>H NMR studies, **Figure 3.34**.<sup>30</sup>

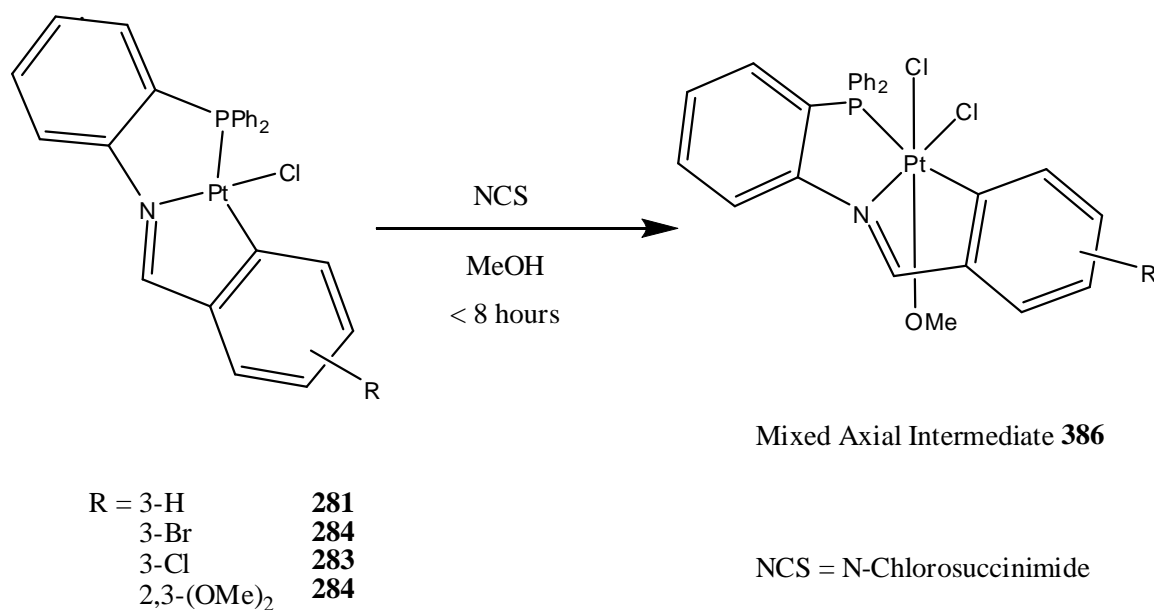


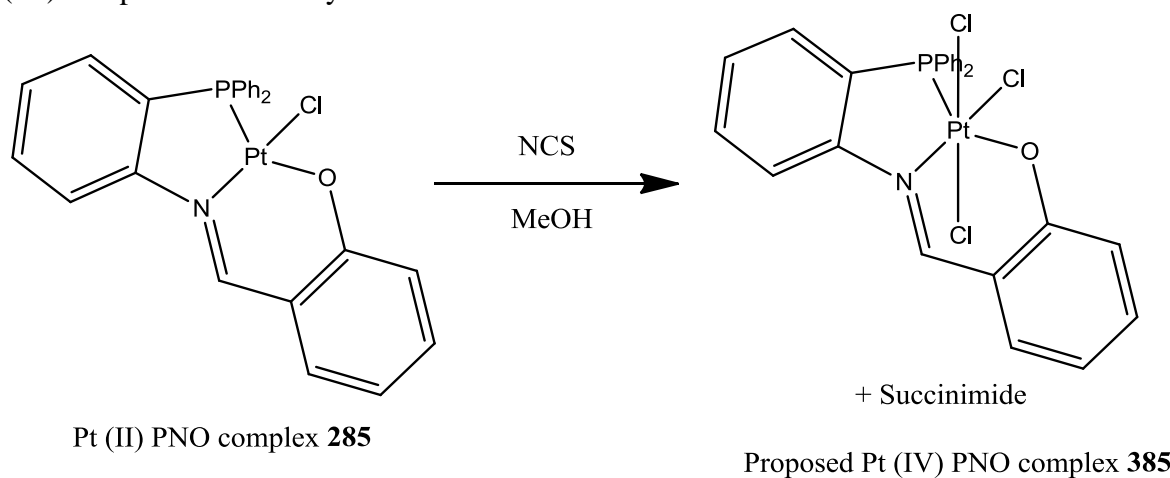
**Figure 3.34:** Shorter reaction times gave mixed axial ligands of methoxy and chloride, but these Pt (IV) complexes proved to be unstable in light and serve as an intermediate to the reaction mechanism described in **Figure 3.32**.

It was therefore decided, in order to stabilise the intermediate **386** and ensure formation of the final chloride Pt (IV) product, a mixed solvent system was required. A mixed solvent system of chloroform and methanol, like that employed for the substitution reactions **Section 3.5.1**, gave the best yields. The methanol was required as per the

mechanism described in **Figure 3.33** and the chloroform, as detailed previously in **Chapter 2**, has the unique ability of stabilising chloride anions necessary to increase the yield of the desired Pt (IV) complexes.

The reaction products were also found to contain some Pt (II) starting material for the **382** and **283** complexes as identified by TLC and NMR analysis. Attempts to force the reactions to completion by heating the reaction mixtures resulted in the formation of a black insoluble product. Identification of this material has at this time failed, but it is proposed to be platinum metal resulting from thermal decomposition.<sup>6</sup> Hydrolysis of the ligands was also seen to occur on occasion when the reaction solution was stirred for longer than 24 hours. This was identified by the appearance of an aldehyde peak in the <sup>1</sup>H NMR spectra.

Having developed a successful route to cycloplatinated Pt (IV) chloride iminophosphine complexes for **381-384**, attempts were then made to apply these methodologies to achieve oxidation of the tridentate P,N,O Pt (II) chloride complex **285**, **Figure 3.35**. However, although some oxidation is thought to have occurred, the reactions did not go to completion and attempts to separate the Pt (II) starting material and proposed Pt (IV) complex via a variety of means has failed to date.



NCS = N-Chlorosuccinimide

*Figure 3.35: Proposed oxidation of the PNO complex **285** to its analogous Pt (IV) complex **385** via the same mechanism and intermediate described in **Figure 3.32**.*

Analogous to work previously reported by our research group, despite using a range of solvent systems, the Pt (II) and Pt (IV) PNO species had such similar R<sub>f</sub> values that it was not possible to separate them by conventional means. The best separation at this time was found with 98:2 CHCl<sub>3</sub>:MeOH as the eluent where R<sub>f</sub> of the Pt (II) complex = 0.78 (from **Chapter 2**) and R<sub>f</sub> of the Pt (IV) = 0.81, **Figure 3.36**.

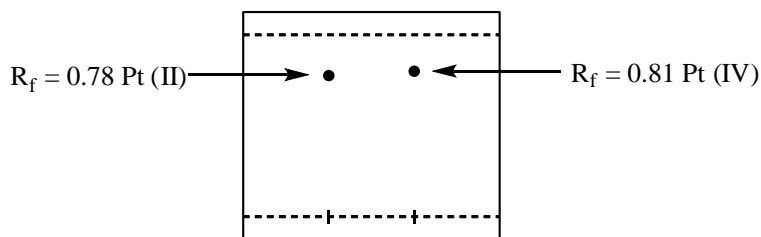


**Figure 3.36:** Illustration of a TLC separation of the PNO Pt (II) and PT (IV) complexes

The products from attempted oxidations of the tridentate phosphinoamide cyclometallated complexes **286-288** with N-chlorosuccinimide, **Figure 3.37**, on the other hand did not provide any evidence indicating successful oxidation. There was also no longer evidence of the Pt (II) starting material in the solution but there was also no evidence to suggest Pt (IV) complexes had formed either. TLC and NMR analysis on the resulting green solution indicated that multiple complexes and decomposition products existed.

This indicated that, like that found for the triphenylphosphine ( $\text{PPh}_3$ ) substitution reactions earlier and attempted oxidation with peroxide and sodium hypochlorite, decomposition of the complexes had once again occurred.

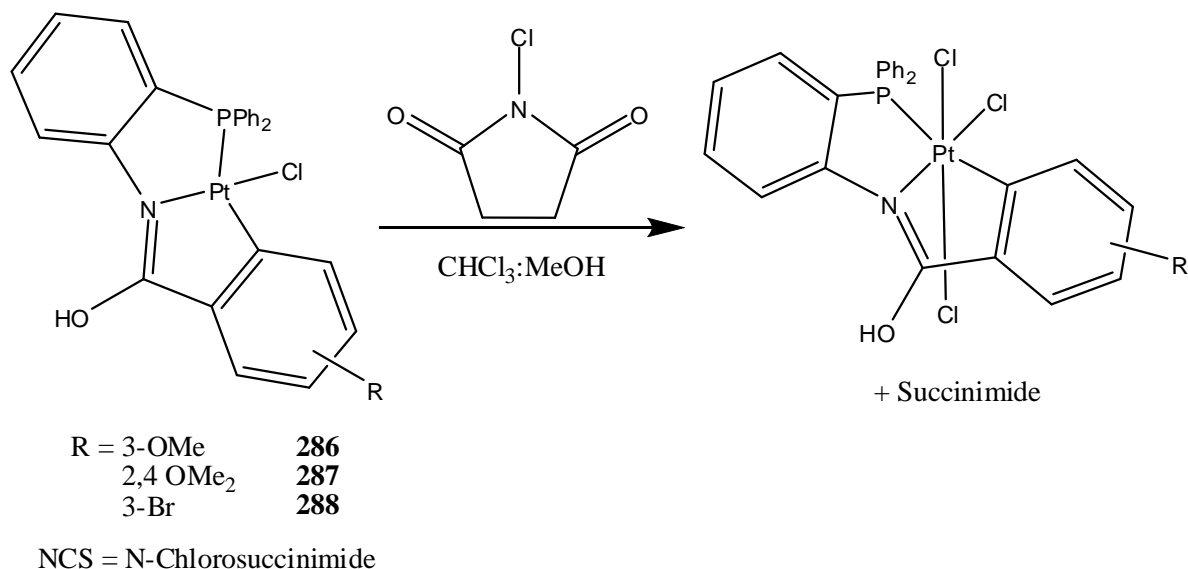


**Figure 3.37:** Unsuccessful oxidation of the phosphinoamide Pt (II) complexes **286-288** to their analogous Pt (IV) complexes with N-chlorosuccinimide via the same mechanism and intermediates described in **Figure 3.32**.

### 3.7 Infra-red spectroscopic studies:

#### 3.7.1 Cationic triphenylphosphine (PPh<sub>3</sub>) substituted Pt (II) complexes of the general formula [Pt( $\eta^3$ -PNC/PNO-L<sup>1-4</sup>)PPh<sub>3</sub>]Cl 371-375:

Like that seen for the parent Pt (II) chloro iminophosphine complexes **281-285** in **Chapter 2**, the most informative peak in the IR spectra of the triphenylphosphine substituted complexes is the imine stretching band,  $\nu(\text{C}=\text{N})$  at approx  $1600\text{cm}^{-1}$ . A comparison of the stretching frequencies of the parent complexes **281-285** with their analogous triphenylphosphine substituted complexes **371-375** are contained in **Table 3.3**, along with the stretching frequencies of the free iminophosphine ligands **HL<sup>1-4</sup> 261-264**.

Free Ligands	$\nu(\text{C}=\text{N})$ $\text{cm}^{-1}$	Parent complex	$\nu(\text{C}=\text{N})$ $\text{cm}^{-1}$	Phosphine complex	$\nu(\text{C}=\text{N})$ $\text{cm}^{-1}$
<b>HL<sup>1</sup> 261</b>	1626	<b>281</b>	1585	<b>371</b>	1590
<b>HL<sup>2</sup> 262</b>	1621	<b>282</b>	1587	<b>372</b>	1591
<b>HL<sup>3</sup> 263</b>	1622	<b>283</b>	1576	<b>373</b>	1590
<b>HL<sup>4</sup> 264</b>	1615	<b>284</b>	1578	<b>374</b>	1587
<b>HL<sup>4</sup> 265</b>	1615	<b>285</b>	1607	<b>375</b>	1589

*Table 3.3: IR data comparing the  $\nu(\text{C}=\text{N})$  of the triphenylphosphine substituted cyclometallated platinum complexes **371-375** with their parent complexes **281-285** and their free ligands **261-264**.*

On substitution of these iminophosphine chloro complexes by triphenylphosphine, we see an increased  $\nu(\text{C}=\text{N})$  stretching frequency for the substituted cyclometallates **371-374** and a reduction for the PNO complex **375**. In the case of the cyclometallated substituted products, this indicates a strengthening of, and hence shortening of, the imine C=N bond. This bond strengthening can be attributed to the weakening of the imino-nitrogen-platinum coordination bond. This is due to the strong *trans effect* exerted by the new phosphine donor ligand introduced *trans* to this coordination bond. These trends mirror those obtained previously by our research group for the analogous iodo cyclometallated phosphine substituted complexes.

The PNO tridentate complex **285** on the other hand gave a reduced stretching frequency when substituted by triphenylphosphine, complex **375**, indicating a weakening, and hence lengthening, of the imine C=N.

This trend has also been reported previously by our research and is in direct contrast to that observed for the tridentate cyclometallated triphenylphosphine substitutions **381-384**. It has been proposed that this apparent weakening could be attributed to the steric strain on the six-membered fused ring system of the PNO complex interacting with the introduced triphenylphosphine moiety, causing repulsion and lengthening of the ligand bonds to accommodate the extra steric bulkiness.<sup>7</sup>

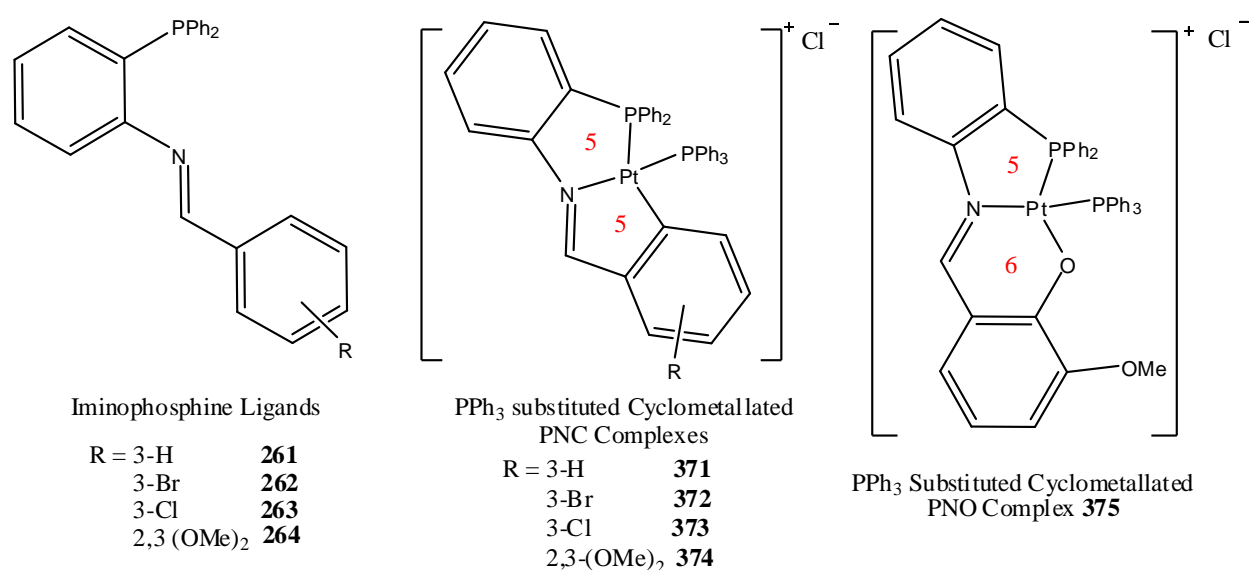


*Figure 3.38: The range of complexes described in this section with the types of rings involved in the structure of each complex as discussed previously in Chapter 2.*

### 3.7.1 Infra-red spectra of Pt (IV) chloro complexes of the general formula [Pt( $\eta^3$ -PNC- $L^{1-4}$ )Cl<sub>3</sub>] **381-384**:

Chlorination of the Pt (II) cyclometallated complexes **281-284** yielded the corresponding Pt (IV) cycloplatinate complexes **381-384**. Like that seen for the parent Pt (II) chloro iminophosphine complexes **281-285** in Chapter 2 and the PPh<sub>3</sub> substituted complexes in Section 3.6.1, the most informative peak in the IR spectra of the Pt (IV) chloro iminophosphine complexes is the imine stretching band,  $\nu(\text{C}=\text{N})$  at approx  $1600\text{cm}^{-1}$ . A comparison of the stretching frequencies of the parent complexes **281-285** with their Pt (IV) analogous complexes **381-384** are contained in Table 3.4, along with the stretching frequencies of the free iminophosphine ligands **HL<sup>1-4</sup>** **261-264**.



Free Ligand	$\nu(\text{C}=\text{N})$ $\text{cm}^{-1}$	Pt (II) $\eta^3$ -chloro complex	$\nu(\text{C}=\text{N})$ $\text{cm}^{-1}$	Pt (IV) $\eta^3$ -chloro complex	$\nu(\text{C}=\text{N})$ $\text{cm}^{-1}$
<b>HL<sup>1</sup> 261</b>	1626	<b>281</b>	1585	<b>381</b>	1591
<b>HL<sup>2</sup> 262</b>	1621	<b>282</b>	1587	<b>382</b>	1595
<b>HL<sup>3</sup> 263</b>	1622	<b>283</b>	1576	<b>383</b>	1596
<b>HL<sup>4</sup> 264</b>	1615	<b>284</b>	1578	<b>484</b>	1586

*Table 3.4: IR data comparing the  $\nu(\text{C}=\text{N})$  of the cyclometallated Pt (IV) chloro complexes 381-384 with their parent complexes 281-285 and their free ligands 261-264.*

We again see the expected trend of lower stretching frequencies for the  $\nu(\text{C}=\text{N})$  bond on comparison of the Pt (IV) cycloplatinated complexes **381-384** with the free ligands **261-264** due to continued successful coordination of the C=N group to the Pt (IV) metal centre. However, on comparison of the Pt (II) complexes **281-284** with their Pt (IV) cycloplatinated analogues **381-384** we see an increase in the imine stretching frequency representing an increase in imine bond strength for the Pt (IV) complex.

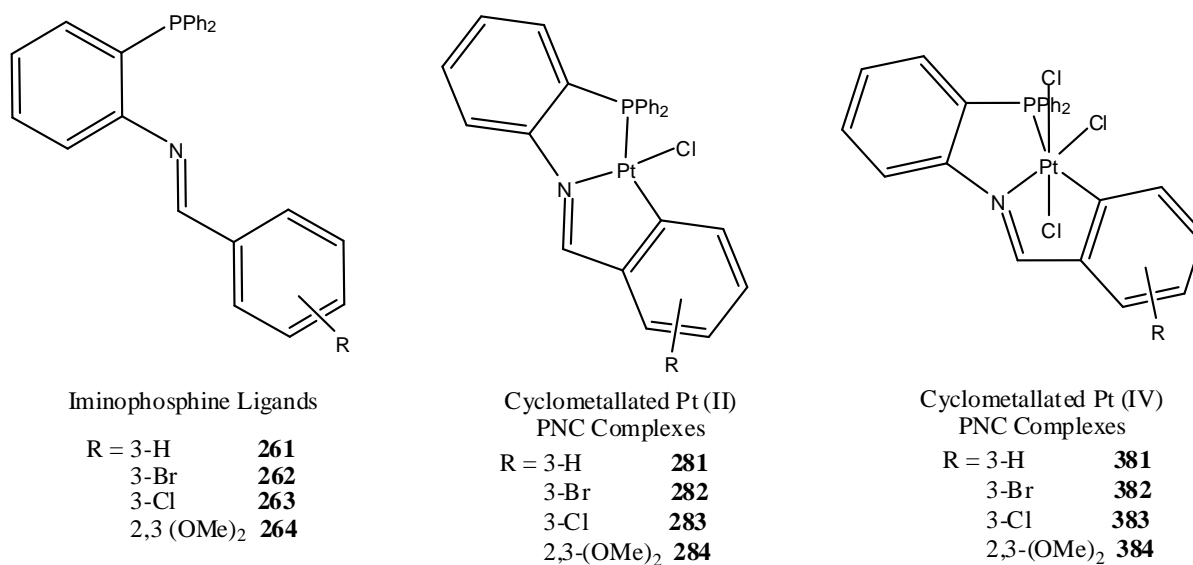


*Figure 3.39: The range of Pt (IV) complexes described in this section including the free ligands and Pt (II) complexes discussed previously in Chapter 2.*

This is due to the increased electrophilicity of the Pt (IV) metal centre. The increased electrophilicity arises because of the increased charge on the Pt (IV) centre relative to the Pt (II) centre due to the addition of electron withdrawing groups in the form of chlorides. This pulling of electron density away from the metal centre weakens the platinum-nitrogen bond

but strengthens the imine bond resulting in an increase in stretching frequencies. This is also similar to the analogous iodo Pt (IV) complexes previously reported by our research group.<sup>6</sup>

### 3.8 NMR spectroscopic studies:

#### 3.8.1 NMR spectroscopy of the ionic, cyclometallated and PNO triphenylphosphine substituted complexes of the general formula $Pt[\eta^3\text{-PNC-L}^{1-4}]\text{PPh}_3(\text{Cl})$ 371-375:

Complex	$\delta$ (H-C=N)	$\delta$ (H-Ar)	$\delta$ (R=OCH <sub>3</sub> )	$\delta$ ( <sup>31</sup> P{ <sup>1</sup> H})	$\delta$ ( <sup>31</sup> P{ <sup>1</sup> H})
3-H <b>371</b>	11.02 (1H, d) J <sub>Pt-H</sub> = 87 Hz J <sub>Pt-Pb</sub> = 10Hz	6.50-7.80 (33H, m)	-	33.3 (d) <sup>2</sup> J <sub>Pa-Pb</sub> = 15 J <sub>Pt-Pa</sub> = 1911 Hz	18.4 (d) <sup>2</sup> J <sub>Pa-Pb</sub> = 16 J <sub>Pt-Pb</sub> = 3794 Hz
3-Br <b>372</b>	11.36 (1 H, d) J <sub>Pt-H</sub> = 88 Hz J <sub>Pt-Pb</sub> = 9Hz	6.40-7.75 (32 H, m)	-	33.4 (d) <sup>2</sup> J <sub>Pa-Pb</sub> = 16 J <sub>Pt-Pa</sub> = 1945 Hz	17.8 (d) <sup>2</sup> J <sub>Pa-Pb</sub> = 16 J <sub>Pt-Pb</sub> = 3732 Hz
3-Cl <b>373</b>	11.31 (1 H, d) J <sub>Pt-H</sub> = 87 Hz J <sub>Pt-Pb</sub> = 9Hz	6.40-8.20 (32 H, m)	-	33.4 (d) <sup>2</sup> J <sub>Pa-Pb</sub> = 16 J <sub>Pt-Pa</sub> = 1949 Hz	17.9 (d) <sup>2</sup> J <sub>Pa-Pb</sub> = 16 J <sub>Pt-Pb</sub> = 3737 Hz
2,3- (OMe) <sub>2</sub> <b>374</b>	9.91 (1 H, d) J <sub>Pt-H</sub> = 86 Hz J <sub>Pt-Pb</sub> = 9Hz	6.17-8.27 (31 H, m)	3.60 (3 H, s) 4.14 (3 H, s)	33.4 (d) <sup>2</sup> J <sub>Pa-Pb</sub> = 16 J <sub>Pt-Pa</sub> = 1956 Hz	17.5 (d) <sup>2</sup> J <sub>Pa-Pb</sub> = 16 J <sub>Pt-Pb</sub> = 3815 Hz
PNO 3-OMe <b>375</b>	10.06 (1 H, d) J <sub>Pt-H</sub> = 61 Hz J <sub>Pt-Pb</sub> = 14Hz	6.59-7.90 (31 H, m)	3.20 (3 H, s)	19.0 (d) <sup>2</sup> J <sub>Pa-Pb</sub> = 22 J <sub>Pt-Pa</sub> = 3607 Hz	9.1 (d) <sup>2</sup> J <sub>Pa-Pb</sub> = 22 J <sub>Pt-Pb</sub> = 3434 Hz

7. Chemical shift values ( $\delta$ ) are expressed in ppm relative to the TMS standard for <sup>1</sup>H and H<sub>3</sub>PO<sub>4</sub> for <sup>31</sup>P.

8. s, singlet; d, doublet; dd, doublet of doublets; t, triplet; q, quartet; m, multiplet.

9. Coupling constants (J) are measured in Hz

*Table 3.5: <sup>1</sup>H and <sup>31</sup>P{<sup>1</sup>H} NMR data<sup>1,2,3</sup> for the PPh<sub>3</sub> substituted iminophosphine Pt (II) complexes 371-375. All ran in CDCl<sub>3</sub> at 300MHz and 121.5 Hz respectively.*

The <sup>1</sup>H and <sup>31</sup>P{<sup>1</sup>H} NMR data of all the PPh<sub>3</sub> substituted complexes **371-375** are summarised in **Table 3.5**. All of the complexes display doublet signals, integrating for 1H, in

the azomethine region of the  $^1\text{H}$  NMR spectra. The doublet arises from coupling between the newly introduced phosphine and the azomethine signal with  $^4J_{\text{H-P}}$  of 9-10 Hz.

As previously discussed in **Chapter 2**, the azomethine resonances of the parent cycloplatinated species appear as singlets, thus the appearance of a doublet here coupling to a second phosphorus signal supports the presence of the new phosphine ligand.

The observed downfield shift in the NMR spectra correlates with this reduction in bond strength also seen in the IR data for these complexes, **Section 3.7.1**. The shifts for these complexes are also consistent with previously obtained results by our research group and others for analogous complexes.<sup>42,6,8</sup> A comparison of the azomethine shifts for the  $\text{PPh}_3$  substituted iminophosphine complexes and their respective parent Pt (II) chloro complexes is shown below in **Table 3.6**.

Pt (II) parent complex	$\delta(\text{H-C=N})$ ppm	$\text{PPh}_3$ Substituted Complex	$\delta(\text{H-C=N})$ ppm	$\Delta\delta$ ppm
3-H <b>281</b>	9.40 (1H, s)	<b>371</b>	11.02 (1 H, d)	1.26
3-Br <b>282</b>	9.40 (1H, s)	<b>372</b>	11.36 (1 H, d)	1.33
3-Cl <b>283</b>	9.41 (1H, s)	<b>373</b>	11.31 (1 H, d)	1.30
2,3-(OMe) <sub>2</sub> <b>284</b>	9.72 (1H, s)	<b>374</b>	9.91 (1 H, d)	1.18
PNO 3-OMe <b>285</b>	9.15 (1h, s)	<b>375</b>	10.06 (1 H, d)	0.61

*Table 3.6: Comparison of the  $^1\text{H}$  azomethine signals between the parent complexes 281-285 and that recorded for the  $\text{PPh}_3$  substituted iminophosphine Pt (II) complexes 371-375. All ran in  $\text{CDCl}_3$  at 300MHz.*

There is a downfield shift of the azomethine signal on coordination of the introduced phosphine moiety *trans* to the nitrogen of between 0.20 and 1.6 ppm. These shifts are in general larger than the analogous iodo complexes, possibly due to the parent chloro complexes having a further upfield signal than the iodo complexes to begin with (**Chapter 2**). Like that found for the parent Pt (II) complexes on donation of the lone pair of electrons on the imino-nitrogen into the metal centre, electron density is pulled towards the coordination bond (Pt-N), weakening the  $\text{H-C=N}$  bonds.

Like the previously reported iodo complexes, the largest shift is noticed for the HL<sup>1</sup> ligand complexes **281/371** and the smallest shift is observed for substitution of **284** (complex **374**). We propose that this is attributed to the presence of electron-donating substituents

within the ligand affecting the electronic properties of the molecule in the complexes **284/374**.

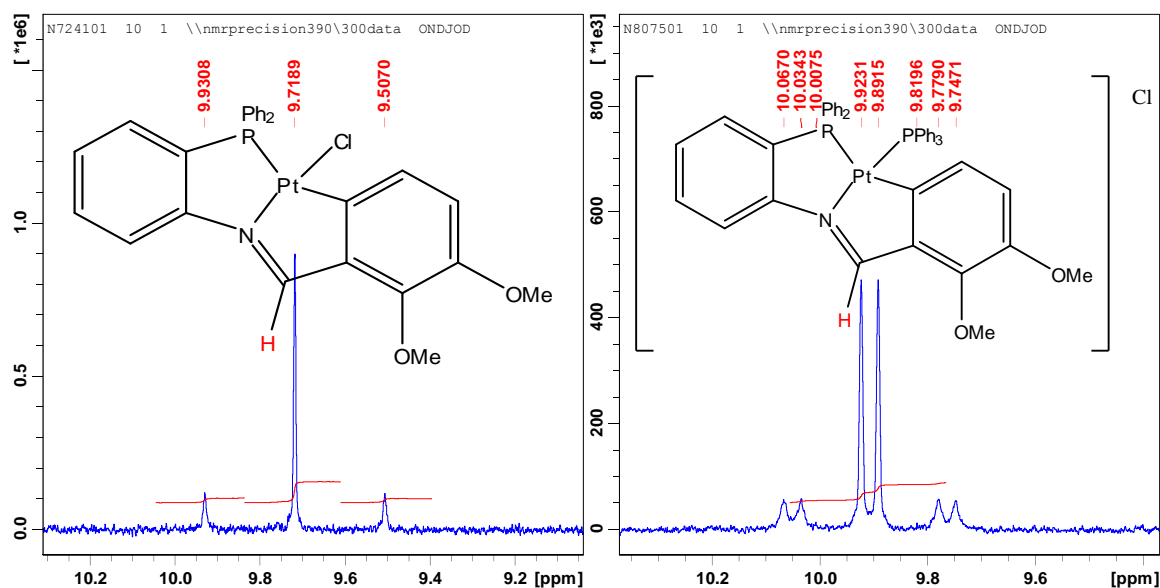


**Figure 3.40:** Comparison of the <sup>1</sup>H azomethine signal spectra for the parent cyclometallated Pt (II) complex **284** (left) and the analogous phosphine substituted complex **374** (right).

As previously mentioned the azomethine signal is now displayed as a doublet complete with <sup>195</sup>Pt satellites with a <sup>3</sup>J<sub>H-Pt</sub> coupling of ca. 83-86 Hz, **Figure 3.40**. These Pt-H coupling constants are around 40 Hz less than that of the parent complexes. This reduction can be attributed to the decreased electrophilicity of the Pt (II) metal centre on successful coordination of the electron-rich triphenylphosphine moiety.

In the case of the PNO complex **375**, we see a significantly smaller downfield shift to that of the cyclometallated complexes on comparison to the parent Pt (II) complexes as well as a smaller <sup>3</sup>J<sub>H-Pt</sub> coupling constant (61Hz) which is compared in **Table 3.5** and **3.6**. We can propose therefore, like that discussed in **Chapter 2**, that the PNO complex **375** has a stronger imine bond (C=N) than that of the cyclometallated complexes **271-274** which is also supported by the IR data obtained and reported in **Section 2.6.1**.

The <sup>1</sup>H NMR spectra of the dimethoxy cyclometallated complex **374** also displays two singlet resonances at δ 3.60 and δ 4.14 ppm respectively. These again correspond to the two electron donating methoxy (-OCH<sub>3</sub>) substituents present at the C-3 and C-2 position of the lower aryl ring and integrate for 3 hydrogens each. This also represents a slight shift downfield in comparison with the parent Pt (II) complex **284** and is due to the addition of the new electron-donating triphenylphosphine ligand, **Table 3.5**. For the PNO complex **375** only one methoxy signal is again present at δ 3.20 ppm and integrates for 3H.

Aromatic signals appear as very complex multiplets with considerable overlap of signals in the range of  $\delta$  6.27 – 9.14 ppm, more so than that seen for the parent complexes **281-285**. However, the integration of these aromatic signals are as expected for each complex, detailed in **Table 3.5**.

$[^1\text{H}-^1\text{H}]$  COSY plots, **Figure 3.41**, unfortunately did not allow for full aromatic characterisation due to the large overlapping signals caused by the extra phenyl groups on the newly introduced triphenylphosphine ligand. Attempted  $[^{13}\text{C}$  DEPT 45- $^1\text{H}]$  HETCOR plots are inconclusive at this time for further characterisation due to solubility issues for all the substituted complexes, but did provide some information on the azomethine signal and methoxy signals in the case of **374** and **375**.

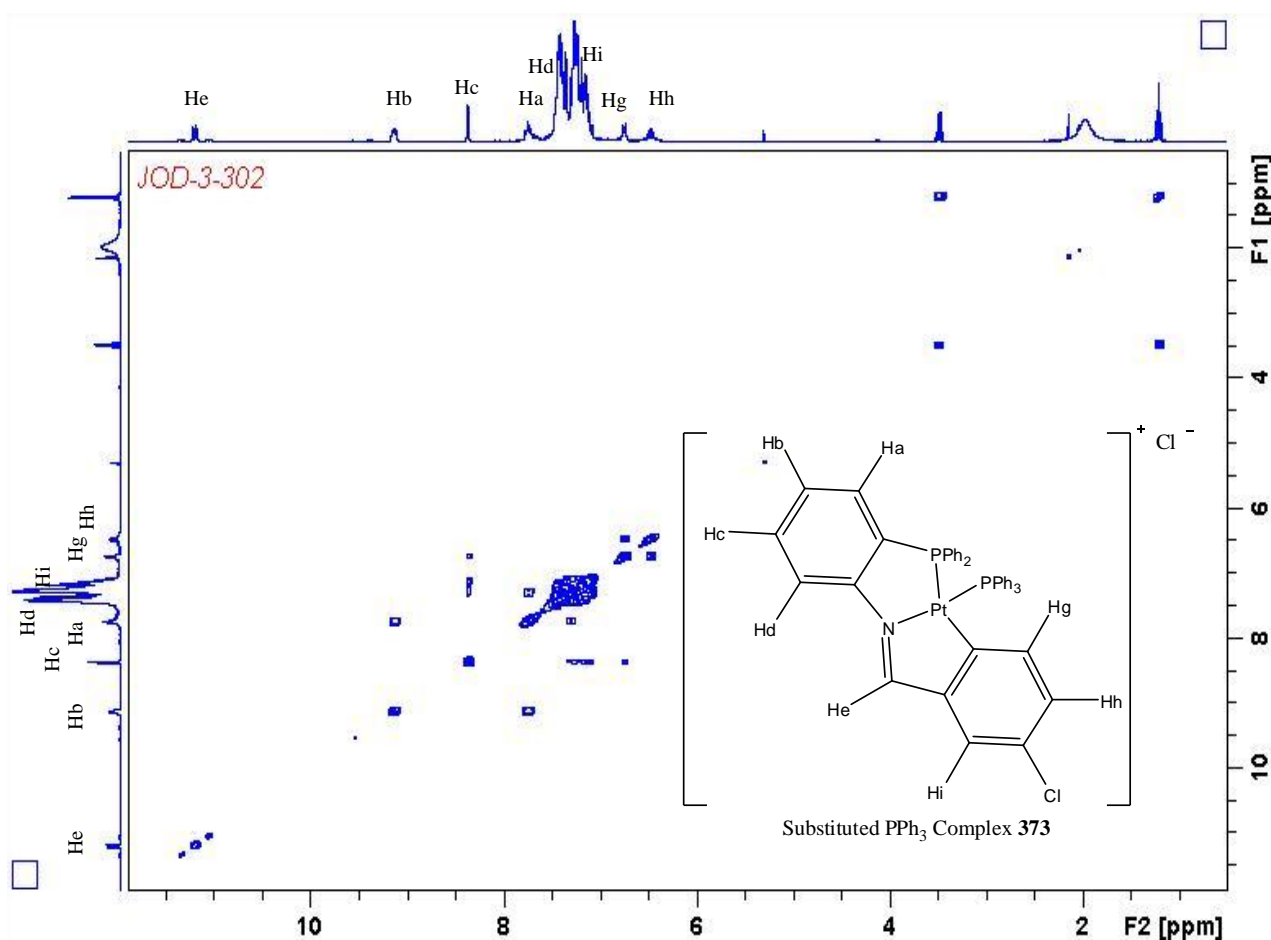


*Figure 3.41: The  $[^1\text{H}-^1\text{H}]$  COSY NMR plot of the 3-Cl triphenylphosphine substituted cyclometallated complex **373** tentatively showing the interactions between some aromatic hydrogens as well as the position of the azomethine group (He) H-C=N run at 300 Mhz.*

Unfortunately due to the large shift in the signals of all the aromatic hydrogens, making a direct comparison with the parent complex **283** is difficult. The coupling frequencies and spectral structure of some signals however do allow for some comparisons to be made. As can be seen from the  $[^1\text{H}-^1\text{H}]$  COSY plot, there are now more aromatic

hydrogens in the phosphinophenyl region ( $\delta$  6.80 – 7.61 ppm) than the parent complex, as expected with the introduction of the triphenylphosphine ligand.

$\delta(^1\text{H})$ ppm	Peak Assignment	Observed Correlations
6.52 m	(Hh)	(Hg)
6.76 t	(Hg)	(Hh, Hi)
6.80-7.63 m	(Hd), (Hi), Phosphinophenyl	(Hc), (Hg), Phosphinophenyl
7.77, q	(Ha)	(Hb, Hc)
8.36 m	(Hc)	(Hb, Hd)
9.14 q	(Hb)	(Hc, Ha)

*Table 3.7: Measured [ $^1\text{H}$ - $^1\text{H}$ ] COSY NMR correlations for the triphenylphosphine substituted 3-Cl cyclometallated complex **373**, Figure 3.41.*

As per the [ $^1\text{H}$ - $^1\text{H}$ ] COSY plot in **Figure 2.74** of the substituted 3-Cl cyclometallated complex **373**, the aromatic protons in the region of 6.80-7.63 ppm can be attributable to the phosphinophenyl protons from the complex (10 H) and the newly introduced triphenylphosphine ligand (15 H), which only couple to themselves.

The rest of the aromatic hydrogens (7 H) are assigned from their [ $^1\text{H}$ - $^1\text{H}$ ] COSY plot correlations in **Table 3.7**, but the extensive overlaps make this a very tentative assignment. The azomethine signal (He) is easily assigned and reported previously in **Table 3.5**, and as is seen in the [ $^1\text{H}$ - $^1\text{H}$ ] COSY plot only couples to itself. The substituted 3-Cl cyclometallated complex **373** is the only complex with minimal overlapping aromatic signals, allowing for some assignment but its limited solubility prevents further detailed studies at this time.

Unfortunately various attempts to collect useful  $^{13}\text{C}$ , DEPT NMR and [ $^{13}\text{C}$  DEPT 45- $^1\text{H}$ ] HETCOR plots were unsuccessful at this time due to the limited solubility of the complexes.  $^{13}\text{C}$  NMR data was also difficult to get for these complexes, with the goal being a comparison between the parent complexes **281-285** and the substituted complexes **371-375** to demonstrate any changes in the metallic Pt-C bond. In the  $^{13}\text{C}$  NMR spectra only strong multiple overlapping signals at 128.56-135.04 ppm were found and assigned to the phosphinophenyl carbons as per the spectra obtained for the parent complexes in outlined in **Chapter 2**.

The  $^{31}\text{P}\{^1\text{H}\}$  NMR data obtained for the triphenylphosphine substituted complexes **371-375** display two sets of doublet signals. Each phosphorus signal represents one of the

two phosphorus environments now present due to the two phosphines (**Pa** and **Pb**) and doublet signals are observed due to *cis*  $^2J_{P-P}$  coupling.

Pt (II) parent complex	$\delta^{31}\text{P}\{\text{H}\}$ ppm	Pt (II) $\text{PPh}_3$ Complex	$\delta^{31}\text{P}\{\text{H}\}$ ppm ( <b>Pa</b> )	$\delta^{31}\text{P}\{\text{H}\}$ ppm ( <b>Pb</b> )	$\Delta\delta$ ppm ( <b>Pa</b> )
3-H <b>281</b>	25.3 (s)	<b>371</b>	33.3 (d)	18.4 (d)	8.0
3-Br <b>282</b>	25.4 (s)	<b>372</b>	33.4 (d)	18.0 (d)	8.0
3-Cl <b>283</b>	25.5 (s)	<b>373</b>	33.4 (d)	17.9 (d)	7.9
2,3-(OMe) $_2$ <b>284</b>	25.2 (s)	<b>374</b>	33.4 (d)	17.5 (d)	8.2
PNO 3-OMe <b>285</b>	13.1 (s)	<b>375</b>	19.0 (d)	9.1 (d)	5.9

*Table 3.8: Comparison of the  $^{31}\text{P}\{\text{H}\}$  signals between the parent Pt (II) complexes 281-285 with the triphenylphosphine substituted Pt (II) complexes 271-275.*

The signal at circa  $\delta$  34 ppm seen for the substituted complexes (**Pa**, **Figure 3.42** and **3.43**) is assigned to the phosphine group of the tridentate ligand i.e. for the cyclometallated complexes this is *trans* to the  $\sigma$  Pt-C<sub>aryl</sub> bond. This represents a shift downfield of circa  $\delta$  8 ppm in comparison to the parent Pt (II) complexes which had a phosphine signal at circa  $\delta$  25ppm, **Table 3.8**.

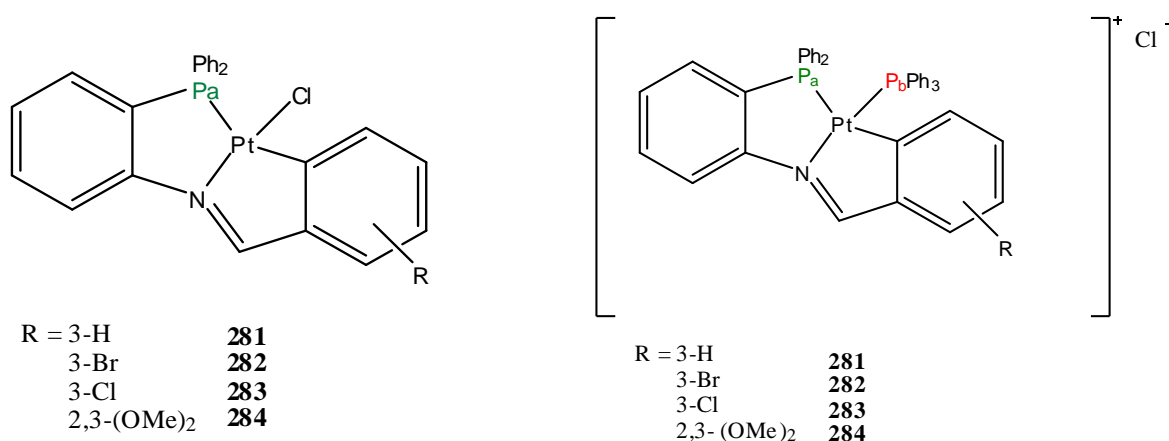


*Figure 3.42: A comparison of the single phosphine on the parent complexes 281-284 (left) with the two phosphine ligands on the substituted complexes 371-374 (right).*

In a similar fashion, two phosphine environments are also observed for the substituted PNO type complex **375** with the signal at  $\delta$  19.0 ppm assigned to the phosphine of the tridentate ligand **Pa** (P-Pt-O) and representing a shift of  $\delta$  5.9 ppm in comparison to its parent

complex, while the signal at  $\delta$  9.1 ppm is assigned to the newly introduced phosphine **Pb** (P-Pt-N).

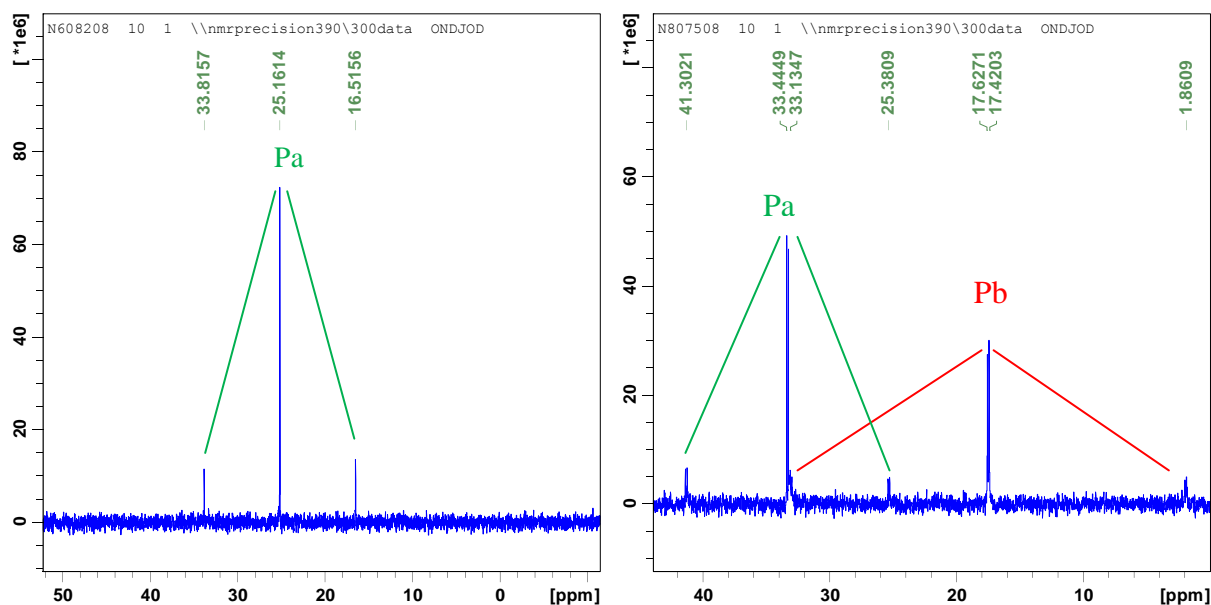


**Figure 3.43:** A comparison of the  $^{31}\text{P}\{^1\text{H}\}$  spectra data for the parent cyclometallated complexes 281-284 (left) and the triphenylphosphine substituted complexes 371-374 (right).

This *cis* coupling between the two phosphine moieties was found to be in the order of 15-16 Hz for the cyclometallated complexes which are analogous to previous work reported by this research group.<sup>6</sup> For the PNO complex, the *cis* coupling between the two phosphine moieties was found to be slightly higher at 22 Hz due to the structural differences previously discussed in **Chapter 2** in comparison to the cyclometallated complexes, **Figure 3.43**.

$^{195}\text{Pt}$   $^1\text{J}_{\text{P-Pt}}$  coupling is also observed again here as previously seen in **Chapter 2** for the parent complexes **281-285**, indicating coordination of both phosphorus moieties to the Pt (II) metal centre. The assignment of **Pa** and **Pb** is confirmed by the *trans*  $^1\text{J}_{\text{P-Pt}}$  coupling constants, which are circa. 1950 Hz for the triphenylphosphine substituted cyclometallated complexes **371-374** in contrast to 2100 Hz for the parent complexes **281-284**. This is consistent with other P-Pt-C<sub>aryl</sub> *trans*  $^1\text{J}_{\text{P-Pt}}$  coupling constants previously reported in the literature and by this research group.<sup>6,43</sup>

The second signal seen in the phosphorus NMR of the substituted complexes (**Pb**, **Figure 3.43**) arises from the newly introduced triphenylphosphine moiety *trans* to the imino-nitrogen group. The  $^1\text{J}_{\text{Pt-P}}$  coupling observed here is much greater than for **Pa** at circa 3793 Hz and again is consistent with reported P-Pt-N *trans*  $^1\text{J}_{\text{P-Pt}}$  coupling constants for analogous complexes.



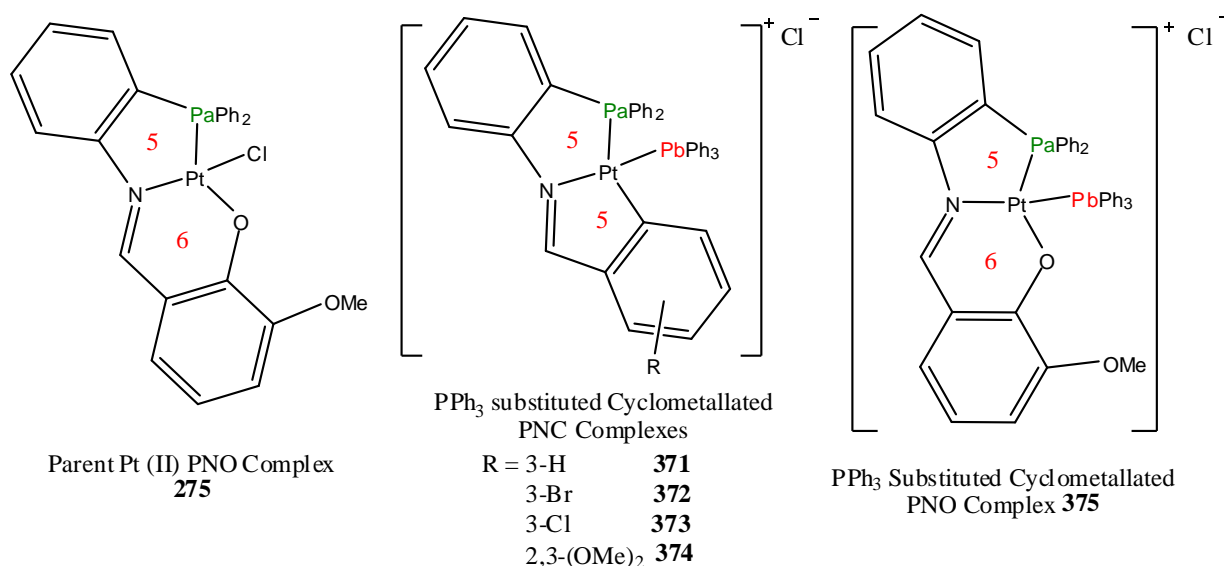


**Figure 3.44:** A structural comparison of the parent Pt (II) PNO complex (left) **275**, the substituted cyclometallated PNC complexes (middle) **371-374** and the substituted PNO complex (right) **375**.

The substituted PNO complex **375** has slightly different  $^1J_{\text{Pt-P}}$  coupling constants over the substituted cyclometallated complexes **371-374** due to the Pa phosphine being *trans* to an oxygen within the metal-fused ring system rather than a carbon, **Figure 3.44**. As previously mentioned two phosphine environments are observed here also and assigned Pa or Pb according to their coupling frequencies.

Therefore Pa is assigned as  $\delta$  19.0 ppm which is the phosphine of the tridentate ligand with P-Pt-O *trans* coupling in the order of 3606.6 3Hz, and Pb is assigned as  $\delta$  9.1 ppm, the newly introduced phosphine with coupling to the  $^{195}\text{Pt}$  *trans* to the nitrogen moiety of the ligand (P-Pt-N) in the order of 3434.43 Hz. These results are again consistent with previously studied complexes within this research group.<sup>8</sup>

### **3.8.2 NMR spectra of tridentate, cycloplatinated Pt (IV) chloro iminophosphine complexes [Pt( $\eta^3$ -PNC-L<sup>1-4</sup>)Cl<sub>3</sub>] 381-384:**

$^1\text{H}$  and  $^{31}\text{P}\{^1\text{H}\}$  NMR data for the Pt (IV) cycloplatinated species **381-384** is displayed in **Table 3.9**. As seen for all other platinum complexes reported here, the azomethine signal is again observed with  $^{195}\text{Pt}$  satellites, but this time it was found to be further upfield when compared to the parent Pt (II) complexes **281-284**.

Complex	$\delta$ ( <i>H-C=N</i> )	$\delta$ ( <i>H-Ar</i> )	$\delta$ ( <i>R=OCH<sub>3</sub></i> )	$\delta$ ( $^{31}\text{P}\{^1\text{H}\}$ )
3-H <b>381</b>	9.11 (1 H, s) $J_{\text{Pt-H}} = 81$ Hz	7.30-8.24 (18 H, m)	-	-2.1 (s) $J_{\text{Pt-P}} = 1326$ Hz
3-Br <b>382</b>	9.20 (1 H, s) $J_{\text{Pt-H}} = 83$ Hz	7.40-8.20 (17 H, m)	-	-1.7 (s) $J_{\text{Pt-P}} = 1345$ Hz
3-Cl <b>383</b>	9.21 (1 H, s) $J_{\text{Pt-H}} = 84$ Hz	6.40-8.20 (17 H, m)	-	-1.4 (s) $J_{\text{Pt-P}} = 1350$ Hz
2,3-(OMe) <sub>2</sub> <b>384</b>	9.34 (1 H, s) $J_{\text{Pt-H}} = 84$ Hz	7.23-7.90 (14 H, m) 8.07-8.16 (2 H, m)	3.91 (3H, s) 4.10 (3H, s)	-2.1 (s) $J_{\text{Pt-P}} = 1334$ Hz

1. Chemical shift values ( $\delta$ ) are expressed in ppm relative to the TMS standard for  $^1\text{H}$  and  $\text{H}_3\text{PO}_4$  for  $^{31}\text{P}$ .
2. s, singlet; d, doublet; dd, doublet of doublets; t, triplet; q, quartet; m, multiplet.
3. Coupling constants ( $J$ ) are measured in Hz

*Table 3.9: The  $^1\text{H}$  and  $^{31}\text{P}\{^1\text{H}\}$  NMR spectra<sup>1, 2, 3</sup> recorded for the chloro iminophosphine Pt (IV) complexes **381-384**. All ran in  $\text{CDCl}_3$  at 300MHz.*

As previously discussed in **Chapter 2** and for the  $\text{PPh}_3$  substituted complexes **371-374** in **Section 3.8.1**, the azomethine resonances of the parent Pt (II) species appear as singlets, which is also found here for the Pt (IV) products here. Like that seen for the parent Pt (II) complexes, changes in the electron density of the azomethine *H-C=N* bond causes a shift in the  $^1\text{H}$  NMR spectra. As discussed previously, this is due to donation of the lone pair of electrons from the imino-nitrogen donor moiety into the metal centre to stabilise the Pt-N bond.

For the  $\text{PPh}_3$  substituted Pt (II) complexes, **Section 3.7.1**, this shift was observed to be large and downfield in the  $^1\text{H}$  NMR spectra due to the introduction of another electron donating ligand trans to the imino-nitrogen donor moiety. This resulted in an increase in bond strength for the C=N bond, also noted by IR spectroscopy, since the imino-nitrogen bond is donating less electron density into the metal centre due to the presence of the new  $\text{PPh}_3$  ligand.

In the present case of the Pt (IV) complexes **381-384**, the IR spectra also noted an increase in bond strength for the C=N bond like that of the  $\text{PPh}_3$  substituted complexes. However, the azomethine *H-C=N* signal in the  $^1\text{H}$  NMR is shifted upfield in comparison to the parent Pt (II) cyclometallates **281-284** and the triphenylphosphine substituted Pt (II)

complexes **371-374**. Therefore, although the C=N bond itself has increased in strength, the effect of the newly introduced electron withdrawing chloride ligands at the axial positions of the metal centre is to pull electron density away from the metal centre, weakening the Pt-N bond. This in turn pulls electron density away from the C=N bond and conversely from the azomethine  $H-C=N$  bond as well, **Figure 3.45**. This causes electron density from the azomethine bond to be pulled into the C=N bond increasing its strength to cope with the new electron withdrawing chlorides present and is displayed as an upfield shift for the azomethine signal in the  $^1H$  NMR spectra.

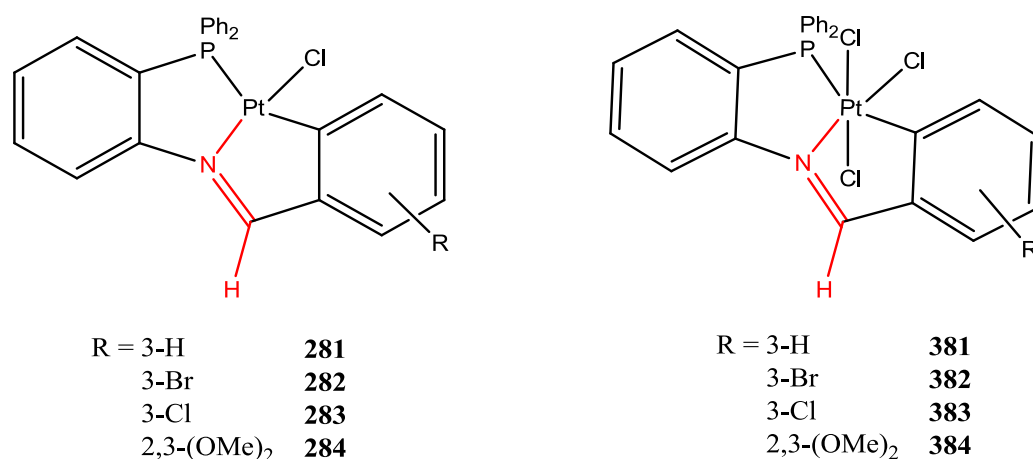


**Figure 3.45:** A comparison of the parent Pt (II) complexes **281-284** (left) with the oxidised Pt (IV) complexes **381-384** (right). Both have their azomethine  $H-C=N-Pt$  system highlighted.

**Table 3.10** contains a comparison of the azomethine signals and coupling between the Pt (II) chloro parent complexes and the newly formed Pt (IV) chloro complexes **381-384**. As discussed, the upfield shift can be directly related to the increased electrophilicity of the  $d^6$  Pt (IV) metal centre, compared to  $d^8$  Pt (II) metal centre, which influences the electronic properties of the imino-nitrogen bond of the tridentate ligand. The average upfield shift, in comparison to the Pt (II) complexes, for these complexes is ca. 0.30 ppm which is significantly less than previous reports by our research group. The largest shift was again found to be for the 2,3-(OMe)<sub>2</sub> complex **384**, due to the presence of the methoxy groups as previously discussed.

Previous reports by our research group and others on iodo Pt (IV) complexes have found upfield shifts of circa 0.7 ppm in comparison to their Pt (II) precursors.<sup>6,30</sup> This is proposed to be caused by the stronger withdrawing effect chloride possesses over iodide due to the difference in electronegativity between the two halides, as discussed in **Chapter 2**.

Pt (II) parent complexes	$\delta$ (H-C=N) ppm	Pt (IV) Oxidised complexes	$\delta$ (H-C=N) ppm	$\Delta\delta$ ppm
3-H <b>281</b>	9.40 (1 H, s) $J_{\text{H-Pt}} = 123$ Hz	<b>381</b>	9.11 (1 H, s) $J_{\text{H-Pt}} = 81$ Hz	0.29
3-Br <b>282</b>	9.40 (1 H, s) $J_{\text{H-Pt}} = 123$ Hz	<b>382</b>	9.20 (1 H, s) $J_{\text{H-Pt}} = 83$ Hz	0.20
3-Cl <b>283</b>	9.41 (1 H, s) $J_{\text{H-Pt}} = 123$ Hz	<b>383</b>	9.21 (1 H, s) $J_{\text{H-Pt}} = 84$ Hz	0.20
2,3-(OMe) <sub>2</sub> <b>284</b>	9.72 (1 H, s) $J_{\text{H-Pt}} = 126$ Hz	<b>384</b>	9.34 (1 H, s) $J_{\text{H-Pt}} = 84$ Hz	0.38

Figure 3.10: A comparison of the azomethine signal for the parent Pt (II) complexes 281-284 and the oxidised Pt (IV) complexes 381-384.

<sup>195</sup>Pt satellites were also observed for the Pt (IV) complex due to <sup>3</sup>J<sub>H-Pt</sub> coupling similar to the parent Pt (II) complexes, but the coupling constants are circa 40 Hz lower than their Pt (II) analogues **Table 3.10. Figure 3.46**. They are, however, almost identical to the Pt (IV) iodo analogous reported previously by this research group.

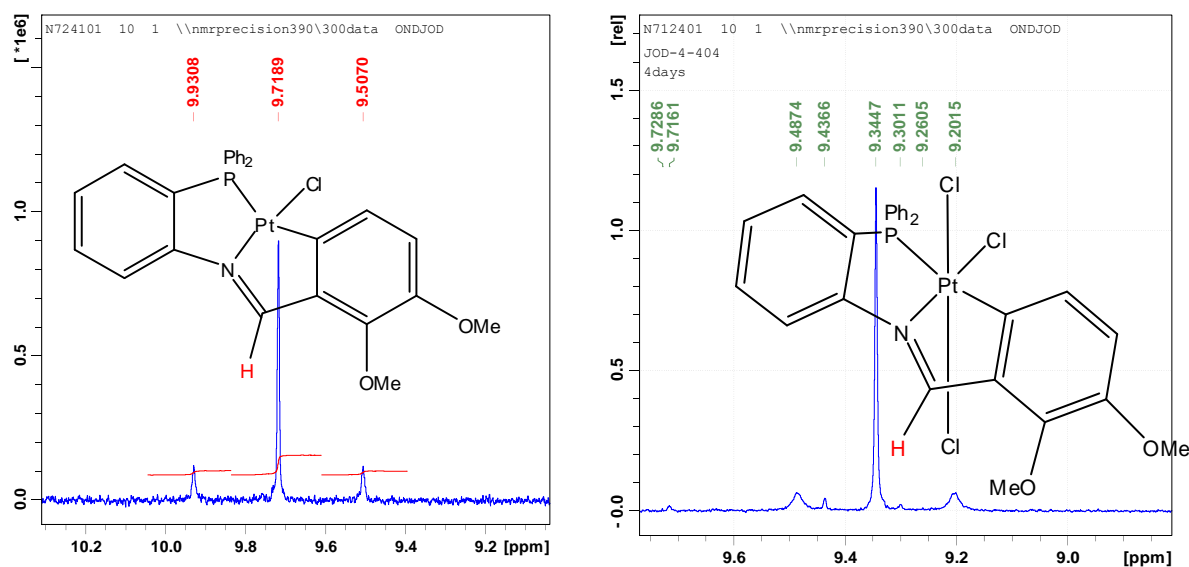


Figure 3.46: Comparison of the azomethine signal from the <sup>1</sup>H NMR spectra for the parent cyclometallated Pt (II) complex 284 (left) and the equivalent Pt (IV) complex 384 (right).

This is proposed to be as a result of the increased electrophilicity of the Pt (IV) metal centre and the resulting increased ligand-metal bond strength on comparison to the parent Pt (II) complexes. Aromatic resonances in the <sup>1</sup>H NMR Spectra were similar to those of their Pt

(II) parent complexes and appear as complex, overlapping multiplets. The aromatic ranges for each complex (and their respective integrations) are contained in **Table 3.9**.

The  $^1\text{H}$  NMR spectra of the Pt (IV) complex **384** also displayed two singlet resonances, both integrating for 3H, at  $\delta$  3.91 and  $\delta$  4.10 ppm. As expected these corresponding to the two methoxy groups present on the ligand of the complex. On comparison with the parent Pt (II) chloro complex **284**, the methoxy resonances were found to be shifted slightly upfield. This could potentially be attributed to the increased interaction of these substituents with the newly introduced axial chloride ligands, causing lengthening of the bonds due to repulsion. It's also possibly due to the increased electron withdrawing effect of the newly introduced chlorides which may pull away electron density away from the substituents.

$[\text{H}-^1\text{H}]$  COSY plots unfortunately did not allow for any significant aromatic characterisation due to the large overlapping signals caused by the shifting of the signals due to the new chloride ligands. Attempted  $[\text{C}-^{13}\text{C}]$  DEPT 45- $^1\text{H}$  HETCOR plots and other  $^{13}\text{C}$  NMR spectra were also inconclusive at this time so no further characterisation is reported due to extensive solubility issues for all the Pt (IV) complexes.

Pt (II) parent complex	$\delta$ $^{31}\text{P}\{^1\text{H}\}$ ppm	Pt (IV) Complex	$\delta$ $^{31}\text{P}\{^1\text{H}\}$ ppm	$\Delta\delta$ ppm
3-H <b>281</b>	25.3 (s) $J_{\text{Pt-P}} = 2083$ Hz	<b>381</b>	-2.3 (s) $J_{\text{Pt-P}} = 1326$ Hz	27.6
3-Br <b>282</b>	25.4 (s) $J_{\text{H-Pt}} = 2100$ Hz	<b>382</b>	-1.7 (s) $J_{\text{Pt-P}} = 1349$ Hz	27.1
3-Cl <b>283</b>	25.5 (s) $J_{\text{H-Pt}} = 2123$ Hz	<b>383</b>	-1.4 (s) $J_{\text{H-Pt}} = 1350$ Hz	26.9
2,3-(OMe) $_2$ <b>284</b>	25.2 (s) $J_{\text{H-Pt}} = 2102$ Hz	<b>384</b>	-2.1 (s) $J_{\text{H-Pt}} = 1344$ Hz	27.3

*Table 3.11: A comparison of the phosphorus signal for the parent Pt (II) complexes 281-284 and the oxidised Pt (IV) complexes 381-384.*

The  $^{31}\text{P}\{^1\text{H}\}$  NMR spectra on the other hand displayed a single resonance for each complex indicating only one phosphorus environment, like the parent Pt (II) complexes **281-284**, **Table 3.9**. A comparison of the Pt (IV) complexes **381-384** with their respective Pt (II) analogues **281-384** are contained in **Table 3.11**. There is a significant upfield shift observed

for the phosphorus donor moiety due to the introduction of the two new axial chloride ligands of circa  $\delta$  27 ppm.

Interestingly, analogous Pt (IV) iodo complexes previously reported by our research group displayed singlet resonances in the range of  $\delta$  -15.5 to  $\delta$  -16.1 ppm whereas the novel chloro Pt (IV) complexes reported here, **381-284**, give resonances in the range of  $\delta$  -1.4 to -2.3 ppm. This is a significant difference caused by the axial chloride ligands in comparison to the iodide ligands seen previously. The higher electronegativity of the chloride ligands cause a stronger electron withdrawing effect on the phosphorus donor moiety, exhibited by the further upfield shift compared to the Pt (IV) iodo complexes reported previously.<sup>6</sup>

Evidence for the continued coordination of the Pt-P bond was again provided by the presence of  $^{195}\text{Pt}$  satellites generated as a result of  $^1\text{J}_{\text{P-Pt}}$  coupling **Figure 3.47**. The coupling constants for the Pt (IV) complexes **381-384** were found to be circa 600 Hz lower than the parent Pt (II) chloro complexes **281-284**, again as a direct consequence of the increased electrophilicity of the Pt (IV) centre. These reduced coupling constants, compared to their respective Pt (II) analogues, are characteristic of Pt (IV) complexes previously identified by our research group and others.<sup>30,6</sup>

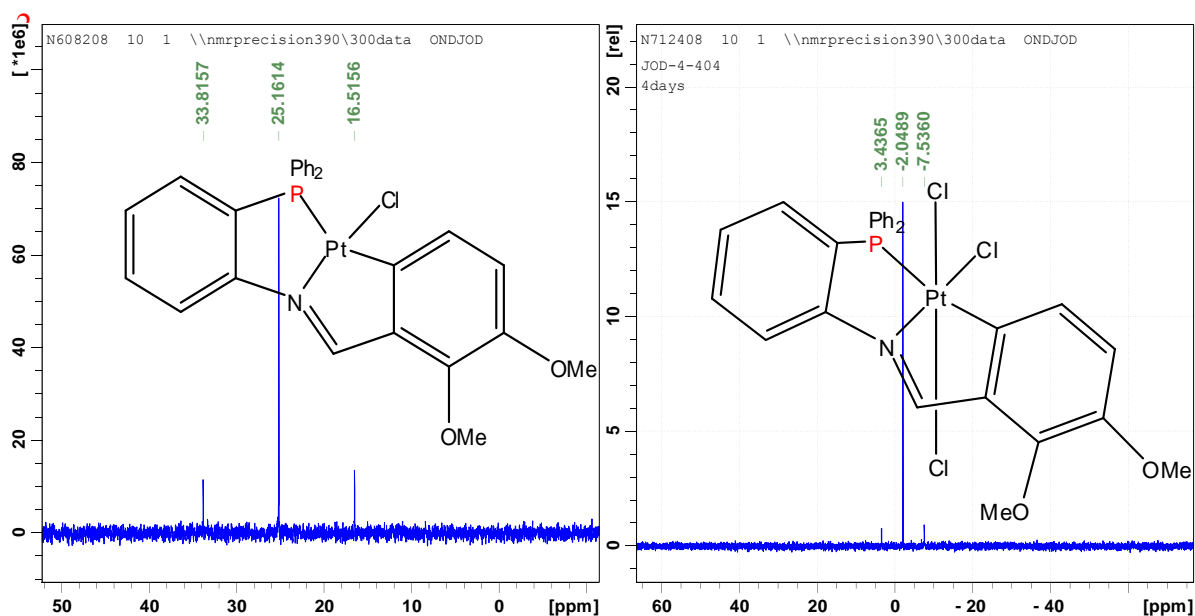


**Figure 3.47:** A comparison of the phosphorus signal from the  $^{31}\text{P}\{^1\text{H}\}$  NMR Spectra for the parent Pt (II) complexes **281-284** (left) and the oxidised Pt (IV) complexes **381-384** (right).

### 3.8.3 NMR studies of the proposed mixed axial Pt (IV) intermediates, 386 and the PNO type Pt (IV) complex 385:

$^1\text{H}$  and  $^{31}\text{P}\{^1\text{H}\}$  NMR data was also collected, where possible due to insolubility, for the mixed chloro-methoxy Pt (IV) intermediates, **386**, as described in **Figure 3.34**. As seen for all other platinum complexes reported here, the azomethine signal is again observed with  $^{195}\text{Pt}$  satellites and found to be further upfield when compared to the parent Pt (II) complexes **281-284**. However, the upfield shift observed for the mixed axial complex, **386**, is slightly less than the final Pt (IV) complexes **381-384**, and the  $^{195}\text{Pt}$  coupling frequency is only 42 Hz in comparison to 84 Hz for the final products, **Table 3.12**.

Pt (II) parent complex	$\delta$ (H-C=N) ppm	Pt (IV) products	$\delta$ (H-C=N) ppm	$\Delta\delta$ ppm
2,3-(OMe) <sub>2</sub> <b>284</b>	9.72	<b>384</b>	9.34 (1 H, s)	0.38
	$J_{\text{H-Pt}} = 126$ Hz	<b>Final Pt (IV) product</b>	$J_{\text{H-Pt}} = 84$ Hz	
2,3-(OMe) <sub>2</sub> <b>284</b>	9.72	<b>386</b>	9.38 (1 H, s)	0.34
	$J_{\text{H-Pt}} = 126$ Hz	<b>Intermediate (OMe)</b>	$J_{\text{H-Pt}} = 42$ Hz	

**Table 3.12:** A comparison of the azomethine signal for the parent Pt (II) complex **284** and the Pt (IV) methoxy-chloro mixed axial intermediate, **386**, and the final oxidised Pt (IV) complex **384**.

The  $^1\text{H}$  NMR spectra of the mixed axial ligands gave very similar azomethine signals but the reduced coupling frequencies in comparison to the final Pt (IV) complexes **381-384**, is probably due to the presence of one electron donating group at the axial position. However, there was also a slightly broad signal with  $^{195}\text{Pt}$  satellites at circa  $\delta$  2.30 ppm. This is proposed to be representing the axial methoxy ligand coordinated to the platinum metal centre and was found to have a coupling frequency of 54 Hz, **Figure 3.48**.

These values correspond very well to previous reports by Sanford *et al* who also found a methoxy signal at circa  $\delta$  2.50 ppm for Pt (IV) products completed in methanol. It is proposed that the upfield shift from the usual signal found in  $^1\text{H}$  NMR spectra for methoxy signals ( $\delta$  3.00 – 4.00 ppm) is due to the chloride ligands present.<sup>30</sup> However, unlike other reported Pt (IV) complexes these proposed Pt (IV) complexes were found to be photosensitive which caused decomposition of the complexes. The decomposition products

were insoluble in all common solvents and determination of their structure is inconclusive at this time.

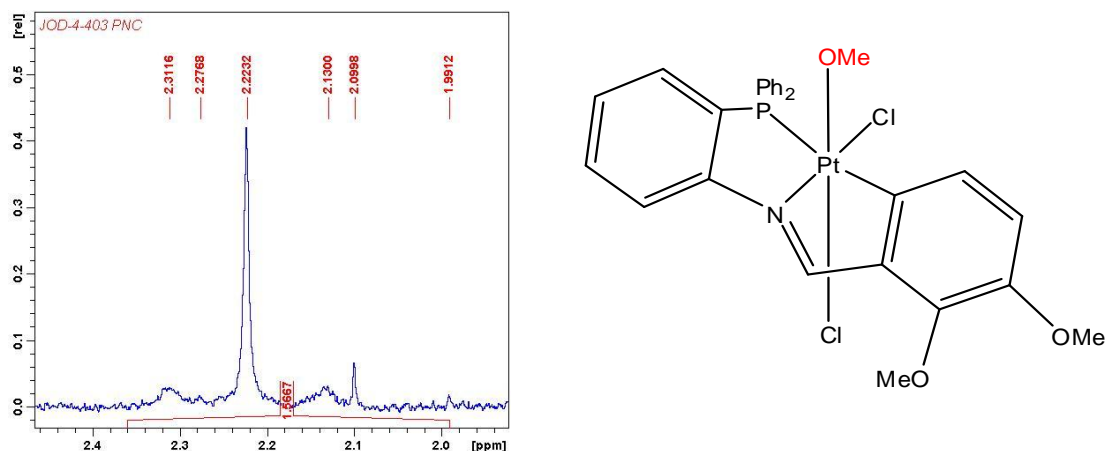


**Figure 3.48:** The slightly broad methoxy signal complete with  $^{195}\text{Pt}$  satellites found for the Pt (IV) intermediate **386**. Please note the structure may also have the axial methoxy group on the opposite side of the metal centre, but only one isomer is shown here for clarity.

The  $^{31}\text{P}\{^1\text{H}\}$  NMR spectra also gave similar results in comparison to the final chloro Pt (IV) complexes **381-384** with an upfield signal at circa  $\delta$  -2.0 ppm and  $^{195}\text{Pt}$  satellites with coupling frequencies of circa 1300 Hz.

Oxidation studies on the PNO type complex **285**, reported previously by our research group and here also in **Chapter 2**, gave inconsistent results as deduced from NMR studies.  $^1\text{H}$  and  $^{31}\text{P}\{^1\text{H}\}$  NMR data was obtained, but insolubility and varying reaction products from time to time make structural proposals tentative.

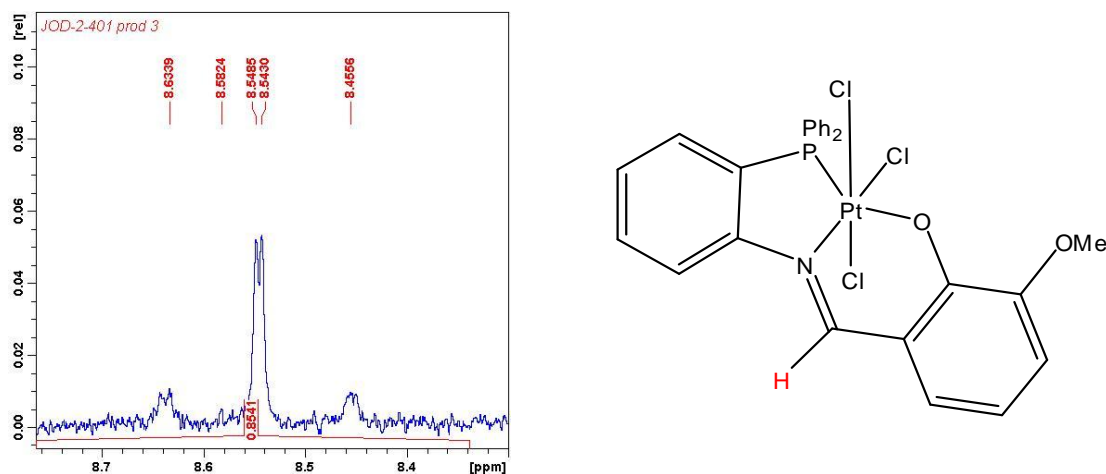


**Figure 3.49:** The azomethine signal complete with  $^{195}\text{Pt}$  satellites and proposed structure for the Pt (IV) PNO complex **385**.

An azomethine signal is observed with  $^{195}\text{Pt}$  satellites in the  $^1\text{H}$  NMR spectra and found to be further upfield when compared to the parent Pt (II) complex, **285**, **Figure 3.49**,



and represents the most upfield signal observed for all the platinum complexes reported by our research group to date

It was generally found to be present at  $\delta$  8.55 ppm and in comparison to  $\delta$  9.15 ppm for the parent Pt (II) PNO complex this represents a shift upfield of  $\delta$  0.60 ppm. The coupling frequency of the  $^{195}\text{Pt}$  satellites was calculated to be 27 Hz in comparison to 76 Hz for the parent Pt (II) PNO complex **285**. These values are generally consistent with the signals and coupling frequencies shifts observed for the cyclometallated Pt (IV) complexes **381-384** reported in **Section 3.7.2**.

The  $^{31}\text{P}\{^1\text{H}\}$  NMR spectra of the proposed PNO Pt (IV) complex **385** on the other hand gave a single phosphorus resonance with only a slight upfield shift of circa  $\delta$  1.4 ppm in comparison to the parent Pt (II) PNO complex **285**. The signal for the proposed Pt (IV) PNO complex was found to be present at  $\delta$  11.30 ppm compared to  $\delta$  13.1 ppm for the parent Pt (II) complex and  $^{195}\text{Pt}$  satellites were found to be present complete with a coupling frequency of 2343 Hz. This represents a reduction of 1474 Hz in comparison to the parent Pt (II) complex which has a coupling frequency of 3816 Hz, **Figure 3.50**.

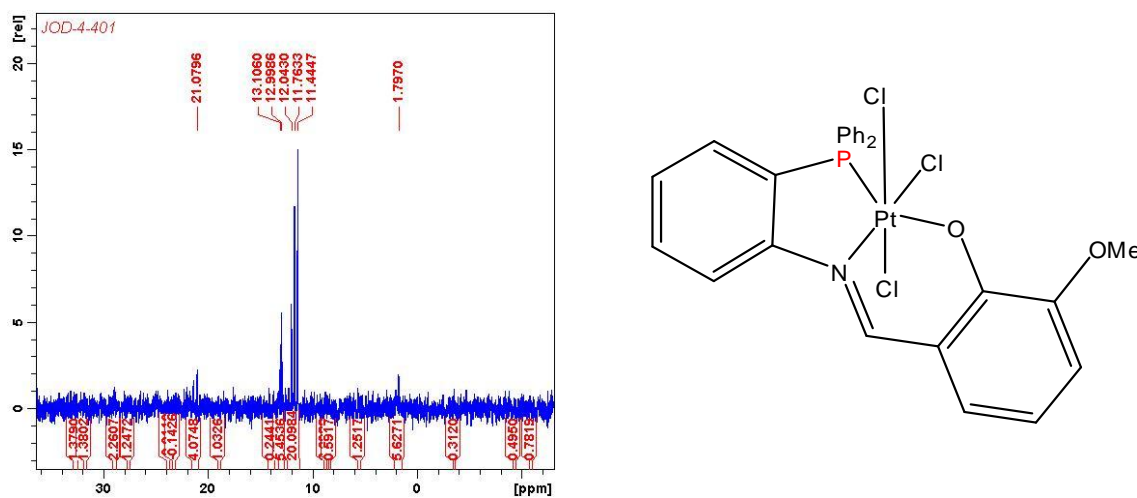


**Figure 3.50:** The signal found in the  $^{31}\text{P}\{^1\text{H}\}$  NMR spectra complete with  $^{195}\text{Pt}$  satellites and again the proposed structure for the Pt (IV) PNO complex **385**.

Again these values are consistent with those found for the other cyclometallated Pt (IV) complexes **381-384**. Unfortunately mixtures of products, that we are currently unable to separate, along with varying results found for signals and coupling frequencies, means this complex remains a proposed structure at this time with further extensive work needed to fully characterise it. Elemental analysis and IR spectra also gave varying results. The C=N stretch in the IR spectra for this complex ranged from  $1590\text{ cm}^{-1}$  to  $1602\text{ cm}^{-1}$ .

However, from the spectra recorded to date we are confident that we have successfully oxidised the Pt (II) PNO complex **285** to its Pt (IV) analogue **385** using *N*-chlorosuccinimide.

### 3.9 Chapter 3 Summary and Conclusions:

#### 3.9.1 The Triphenylphosphine Substituted Pt (II) Complexes:

The synthesis of the triphenylphosphine substituted chloro Pt (II) complexes was achieved using a novel procedure based on the success of employing chloroform in the cyclometallation reactions as discussed previously in **Chapter 2**. Previous methods used to remove a chloride from a platinum metal centre of analogous complexes, reported by our research group, involved a reaction of the parent Pt (II) complex with a one molar equivalent of silver (I) perchlorate.<sup>8</sup> The removal of the halide from the metal centre then generated a cationic, solvated intermediate and a silver (I) chloride precipitate which was filtered through celite. Addition of the appropriate monophosphine, PR<sub>3</sub> (R = Ph, *p*-tolyl, EtCN), then yielded the cationic, substituted complexes.

In this Chapter we have developed a novel one-step method for synthesis of cationic phosphine substituted Pt (II) iminophosphine complexes, without the need for silver (I) perchlorate. The one-pot synthesis of **371-375** is based on the success of employing chloroform for the reactions in **Chapter 2**. In this chapter it is used as part of a mixed solvent system similar to methods previously employed by our research group and others, with chloroform instead of acetonitrile.<sup>16,6</sup>

Substitution of the parent Pt (II) iminophosphine complexes from **Chapter 2** was achieved in a 1:1 methanol:chloroform solution and a slight excess of the appropriate monophosphine, PR<sub>3</sub> (R = Ph, EtCN), which were stirred at room temperature for 6 hours.

The yields obtained for the substituted complexes are much higher than previously obtained for analogous iodo based complexes at circa 70-90%, and so far have been successful for all the cyclometallates **281-284**. Phosphine substitution of [Pt( $\eta^3$ -PNO-L<sup>4</sup>)Cl] **275** was never successfully substituted with or without the use of the silver perchlorate salt by our research group. It has been successfully substituted here with triphenylphosphine by a new direct method for the first time yielding the cationic P,N,O complex **375** in a 70% yield.

The triphenylphosphine substitutions, previously reported by our research group, were the most difficult to achieve by both direct methods and by use of silver (I) perchlorate. This

research has found that this particular phosphine posed no difficulties primarily due to the novel solvent system employed i.e. via stabilisation of the liberated chloride anion. Despite the reduced lability of the platinum chloride bond on comparison to the platinum iodine bond reported previously, it was successfully substituted for the first time as a one-step process within this research.

All the cationic substituted complexes **371-375** were fully characterised by IR,  $^1\text{H}$  and  $^{31}\text{P}\{^1\text{H}\}$  NMR and elemental analysis. Other NMR techniques including  $[^1\text{H}-^1\text{H}]$  COSY and  $[^{13}\text{C}$  DEPT 45- $^1\text{H}]$  HETCOR plots but solubility limitations prevented full use of these methods including  $^{13}\text{C}$  NMR as previously employed in **Chapter 2**.

There is a downfield shift of the azomethine signal found in the  $^1\text{H}$  NMR spectra on coordination of the introduced phosphine moiety *trans* to the nitrogen of between 0.20 and 1.6 ppm. The azomethine signal is also now displayed as a doublet complete with  $^{195}\text{Pt}$  satellites and  $^3\text{J}_{\text{H-Pt}}$  coupling of ca. 83-86 Hz. These Pt-H coupling constants are around 40 Hz less than that of the parent Pt (II) complexes. This reduction can be attributed to the decreased electrophilicity of the Pt (II) metal centre due to the successful coordination of the electron-rich triphenylphosphine moiety.

Aromatic signals for all the complexes appear as overlapping multiplets due to the addition of three more phenyl groups in the form of triphenylphosphine. Integration of these aromatic signals, however, are as expected for each complex and  $[^1\text{H}-^1\text{H}]$  COSY plots did provide some detail but did not allow for full aromatic characterisation due to the large overlapping signals caused by the extra phenyl groups.

$^{13}\text{C}$  NMR data was particularly difficult to get for all the complexes reported in this chapter and unfortunately various attempts to collect useful  $^{13}\text{C}$ , DEPT NMR and  $[^{13}\text{C}$  DEPT 45- $^1\text{H}]$  HETCOR plots were unsuccessful at this time due to the limited solubility of the complexes. In the  $^{13}\text{C}$  NMR spectra only strong multiple overlapping signals at 128.56-135.04 ppm were found and assigned to the phosphinophenyl carbons as per the spectra obtained for the parent complexes in **Chapter 2**.

The  $^{31}\text{P}\{^1\text{H}\}$  NMR data obtained for the triphenylphosphine substituted complexes **371-375** display two sets of doublet signals. Each phosphorus signal represents one of the two phosphorus environments now present due to the two phosphines and doublet signals are observed due to *cis*  $^2\text{J}_{\text{P-P}}$  coupling. The signal at circa  $\delta$  34 ppm seen for the substituted complexes corresponds to the phosphine group of the tridentate ligand i.e. for the cyclometallated complexes this is *trans* to the  $\sigma$  Pt-C<sub>aryl</sub> bond. This represents a shift

downfield of circa  $\delta$  8 ppm in comparison to the parent Pt (II) complexes which had a phosphine signal at circa  $\delta$  25ppm.

The presence of solvent of crystallisation was also noted in the  $^1\text{H}$  NMR spectra of the complexes (dichloromethane and chloroform) and was therefore including for successful elemental analysis. This was also noted previously by our research group and others where most of the analogous iodo complexes also contained solvent of crystallisation.<sup>44,45,6,7,46</sup>

### 3.9.2 Synthesis of the Pt (IV) Complexes:

In this chapter we also describe the synthesis and characterisation of a series of novel tridentate Pt (IV) chloro cycloplatinated complexes of the general formula  $[\text{Pt}(\eta^3\text{-PNC-L}^{1-4})\text{Cl}_3]$  **381-384**. All of the Pt (IV) complexes **381-384** were synthesised by oxidising the appropriate tridentate Pt (II) complexes **281-284** reported in **Chapter 2**, with *N*-chlorosuccinimide.

Initial attempts to achieve successful oxidation of the Pt (II) complexes involved the use of hydrogen peroxide ( $\text{H}_2\text{O}_2$ ) and sodium hypochlorate ( $\text{NaOCl}$ ) as well as hydrochloric acid. All of these attempts failed. However, the reaction solution did return the parent iminophosphine Pt (II) complexes in almost quantitative yields suggest immense stability for these complexes.

The successful preparation of cyclometallated chloro-Pt (IV) iminophosphine complexes **381-384** was based on a previously reported method by *Sanford et al.*<sup>30</sup> A mixed solution of chloroform and methanol was again employed like that used for the substitution reactions for complexes **371-375**. The appropriate parent Pt (II) cyclometallated complex **281-284** was reacted with 2.1 equivalents (an excess) of *N*-chlorosuccinimide to give the Pt (IV) chloro complexes **381-384** in yields ranging from 11-36% at present with significant parent Pt (II) starting material remaining even after 48 hours stirring.

The Pt (IV) complexes **381-384** were analysed by infra-red spectroscopy which, as expected, shows an imine  $\nu(\text{C}=\text{N})$  stretching band at  $1586\text{cm}^{-1}$ . On comparison with the respective parent Pt (II) cyclometallated complex, a decrease in the imine stretching frequency was found. This indicated a weaker imine  $\text{C}=\text{N}$  bond in the Pt (IV) complexes in comparison to their parent Pt (II) complexes. This trend was also found to be evident previously in our research group for the Pt (IV) iodo complexes and are proposed to indicate successful oxidation of the Pt (II) parent complex.

$^1\text{H}$  NMR spectra of cycloplatinated Pt (IV) chloro complexes  $[\text{Pt}(\eta^3\text{-PNC-L}^{1,4})\text{Cl}_3]$  **481-384** all display singlet  $^1\text{H}$  resonances in the range  $\delta$  9.10-9.34 ppm corresponding to the azomethine signal. On comparison with the parent Pt (II) complexes resonances, we see an upfield shift of the resonance frequency for these novel complexes. Further evidence to support the evidence of successful oxidation of the Pt (II) complex comes in the form of  $^{195}\text{Pt}$  satellites which were again seen on the azomethine resonances similar to that seen for the parent Pt (II) complexes in **Chapter 2**. The coupling frequencies of the azomethine proton here however with the NMR active  $^{195}\text{Pt}$  nucleus produces coupling constants in the order of  $^3J_{\text{H-Pt}} = 81\text{-}84$  Hz, a change of circa 40 Hz in comparison to the parent Pt (II) complexes.

$^{31}\text{P}\{^1\text{H}\}$  NMR spectra for the Pt (IV) cycloplatinates **381-384** again show a single resonance identifying the single phosphorus environment of the Pt (IV) complex. However, the resonances have shifted significantly to be in the range of  $\delta$  -1.4 to -2.4ppm. This upfield shift, on comparison with the corresponding Pt (II) complex, also identifies coordination of the phosphorus to the more electrophilic Pt (IV) metal centre.  $^{195}\text{Pt}$  satellites are again present with  $^1J_{\text{P-Pt}}$  coupling in the order of 1344-1350 Hz which is also a reduction of circa 700 Hz in comparison to the Pt (II) complexes **281-284**. Interestingly, however, is the significant difference of the resonances in comparison to the previously reported Pt (IV) iodo complexes which is proposed to be due to the more electronegative chloride axial ligands in comparison to iodide.

Attempts to oxidise the phosphinoamide Pt (II) complexes reported in Chapter 2, **286-288** by all the reagents reported in this chapter has proved to be unsuccessful at this time and only decomposition was found to occur rather than a return of the parent complexes seen for the iminophosphine complexes **281-284**. Also oxidation of the iminophosphine PNO complex, **275**, proved to be unsuccessful at this time with further work required to understand the process of this particular complex. It is proposed that steric bulk around the metal centre due to the presence of an oxygen coordinated to the metal centre is hindering successful oxidation via *N*-chlorosuccinimide.

### **3.9.3 Overall Summary and Conclusion:**

The introduction of an electron rich triphenylphosphine ligand, by removing all electron-withdrawing ligands, causes the Pt (II) metal centre to decrease in electrophilicity. This is seen as a downfield shift of the ligands attached directly to the metal centre, the azomethine and phosphorus signals, in both the  $^1\text{H}$  NMR and the  $^{31}\text{P}\{^1\text{H}\}$  NMR spectra.

When the more electron withdrawing ligands (chlorides) are coordinated to the metal centre due to oxidation, we see the Pt (IV) metal centre increase in electrophilicity. This results in upfield shifts for the signals related to ligands attached directly to the platinum centre, the azomethine and phosphorus signals, in both the  $^1\text{H}$  NMR and the  $^{31}\text{P}\{^1\text{H}\}$  NMR spectra. In conclusion this chapter has explored the stability, flexibility and potential for the parent complexes reported in **Chapter 2**.

### **3.10 Chapter 3 Experimental:**

#### **3.10.1 Background:**

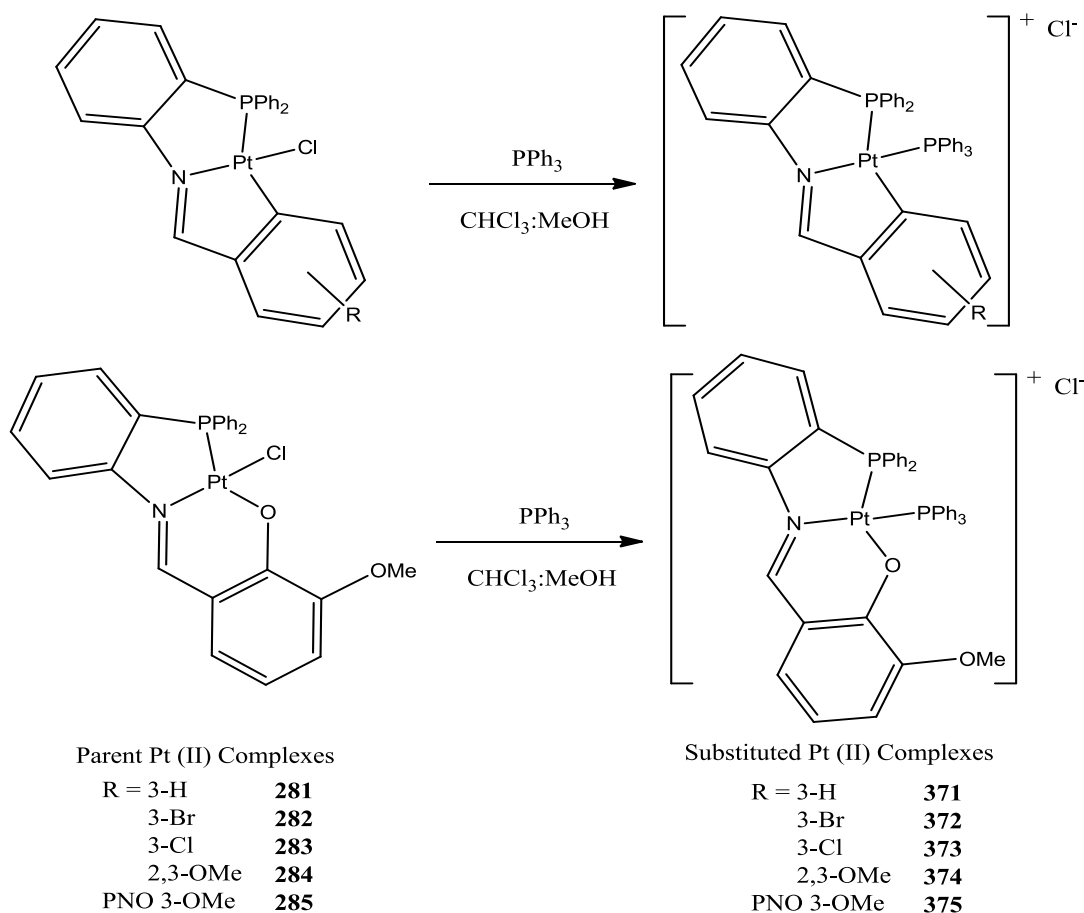
All reaction solvents were distilled prior to use, unless purchased as analytical grade (all from Sigma Aldrich Chemical Co. Ltd.). Toluene and thf were distilled directly before use from sodium-benzophenone. Methanol was distilled over magnesium/iodine according to Perrin *et al.*<sup>47</sup> and hexane was distilled over phosphorus pentoxide. *O*-diphenylphosphinoaniline was synthesized according to a variation of a method by M. K. Cooper *et al.*<sup>48</sup>

The following reagents were used as supplied; N-Chlorosuccinimide (Aldrich Chemical Co. Ltd), triphenylphosphine (Aldrich Chemical Co. Ltd); tri-*p*-tolylphosphine, triscyanoethylphosphine (both Strem chemicals),  $\text{H}_2\text{O}_2$  and NaOCl. Elemental analyses (Perkin-Elmer 2400 CHN elemental analyser) were performed by the microanalytical laboratory, University College Cork.

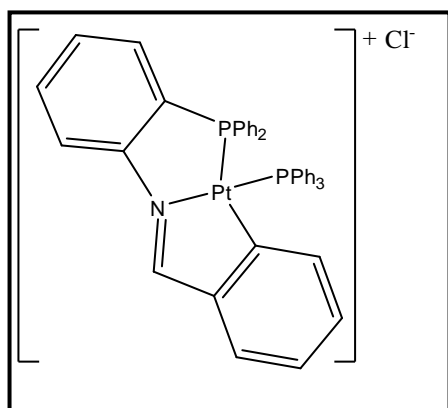
The  $^1\text{H}$  and  $^{31}\text{P}\{^1\text{H}\}$  NMR spectra were recorded on a Bruker Advance 300 MHz, 400 MHz or 600 MHz NMR spectrometer (where specified). Chemical shifts ( $\delta$ ) are expressed in parts per million (ppm) and referenced to external tetramethylsilane ( $\delta 0$ ) for  $^1\text{H}$  and 85% phosphoric acid ( $\delta 0$ ) for  $^{31}\text{P}\{^1\text{H}\}$  NMR using the high frequency positive convention.

Infrared spectra were recorded as KBr disks on a Perkin-Elmer Paragon 1000 FT spectrometer. Relative intensities are designated (s), strong; (m), medium; (w), weak; (b), broad.

### 3.10.2 Synthesis of the substituted Pt (II) complexes $[\text{Pt}^{\text{II}}(\eta^3\text{-PNC-L}^{1-4})\text{PPh}_3]\text{Cl}$ **371-375**:



A stirred solution of  $[\text{Pt}^{\text{II}}(\eta^3\text{-PNC/PNO-L}^{1-4})\text{Cl}]$  in 1:1 chloroform/methanol (10ml:10ml) was reacted with 1.1 equivalents of triphenylphosphine at room temperature for 6 hours. The resulting pale yellow solution was reduced to dryness *in vacuo* and crystallised from doubly distilled DCM-diethyl ether to yield the substituted cationic chloro complexes **371-375**. The diethyl ether removes the remaining triphenylphosphine and there are no traces of remaining Pt (II) starting material via TLC analysis of the filtrate.



**371**:  $[\text{Pt}^{\text{II}}(\eta^3\text{-PNC-L}^1)\text{Cl}]$  (0.040 g, 0.07 mmol) **281** and  $\text{PPh}_3$  (0.020 g, 0.08 mmol) gave  $[\text{Pt}(\eta^3\text{-PNC-L}^1)\text{PPh}_3]\text{Cl}$  **371** as a pale yellow metallic crystalline powder.

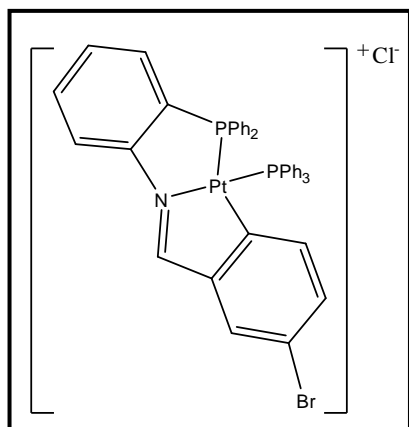
Yield: 0.050 g (88 %)

Found (required for  $\text{C}_{43}\text{H}_{34}\text{ClNP}_2\text{Pt}\cdot 0.5\text{CH}_2\text{Cl}_2$ ): C, 57.52 (57.54); H, 3.89 (3.95); N, 1.21 (1.53).

IR  $\nu_{\text{max}}$  (KBr): 3378 (b), 3048 (w), 1624 (w),

1590(m)(C=N), 1568(w), 1542(m), 1480(m), 1436(s), 1363 (w), 1303 (w), 1249 (m), 1190 (w), 1160 (w), 1097 (s), 1066 (w), 997 (m), 918 (w), 840 (w), 745 (m), 722 (w), 692 (s), 571 (m), 543 (s), 519 (s), 503 (s).

$^1\text{H}$  NMR  $\delta$  ppm: 11.02 (1 H, d) ( $J_{\text{Pt-H}} = 87$  Hz,  $J_{\text{Pt-Pb}} = 10$  Hz), 6.50-7.80 (33H, m), 5.30 ( $\text{CH}_2\text{Cl}_2$ ).  $^{31}\text{P}$  NMR  $\delta$  ppm: 33.3 (d) ( $^2J_{\text{Pa-Pb}} = 15$ ,  $J_{\text{Pt-Pa}} = 1911$  Hz), 18.4 (d) ( $^2J_{\text{Pa-Pb}} = 16$ ,  $J_{\text{Pt-Pb}} = 3794$  Hz)



**372:**  $[\text{Pt}^{\text{II}}(\eta^3\text{-PNC-L}^2)\text{Cl}]$  (0.047 g, 0.07 mmol) **282** and  $\text{PPh}_3$  (0.020 g, 0.08 mmol) gave  $[\text{Pt}(\eta^3\text{-PNC-L}^3)\text{PPh}_3]\text{Cl}$  **303** as a dark yellow metallic crystalline powder.

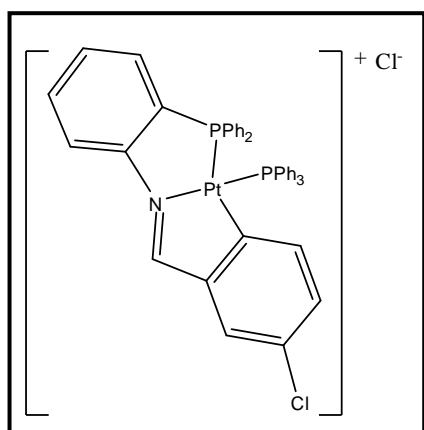
Yield: 0.024 g (35 %)

Found (required for  $\text{C}_{43}\text{H}_{33}\text{BrClNP}_2\text{Pt}\cdot 0.5\text{CH}_2\text{Cl}_2$ ): C, 53.11 (52.99); H, 3.42 (3.54); N, 1.27 (1.40).

IR  $\nu_{\text{max}}$  (KBr): 3309 (b), 2978 (w), 2863 (w), 2330 (w), 1735 (w), 1627 (w), 1591 (m)(C=N), 1568 (m), 1532 (m),

1480 (m), 1435 (s), 1347 (w), 1295 (m), 1241 (m), 1190 (m), 1168 (w), 1096 (s), 1070 (m), 1027 (w), 997 (m), 928 (w), 878 (w), 811 (m), 771 (w), 754 (m), 736 (m), 703 (m), 609 (m), 573 (m), 548 (s), 512 (s), 509 (m).

$^1\text{H}$  NMR  $\delta$  ppm: 11.36 (1 H, d) ( $J_{\text{Pt-H}} = 88$  Hz,  $J_{\text{Pt-Pb}} = 9$  Hz), 6.40-7.75 (32 H, m), 5.30 ( $\text{CH}_2\text{Cl}_2$ ).  $^{31}\text{P}$  NMR  $\delta$  ppm: 33.4 (d) ( $^2J_{\text{Pa-Pb}} = 16$ ,  $J_{\text{Pt-Pa}} = 1945$  Hz), 17.8 (d) ( $^2J_{\text{Pa-Pb}} = 16$ ,  $J_{\text{Pt-Pb}} = 3732$  Hz)



**373:**  $[\text{Pt}^{\text{II}}(\eta^3\text{-PNC-L}^3)\text{Cl}]$  (0.044 g, 0.07 mmol) **283** and  $\text{PPh}_3$  (0.020 g, 0.08 mmol) gave  $[\text{Pt}(\eta^3\text{-PNC-L}^3)\text{PPh}_3]\text{Cl}$  **373** as a dark yellow metallic crystalline powder.

Yield: 0.046 g (69 %)

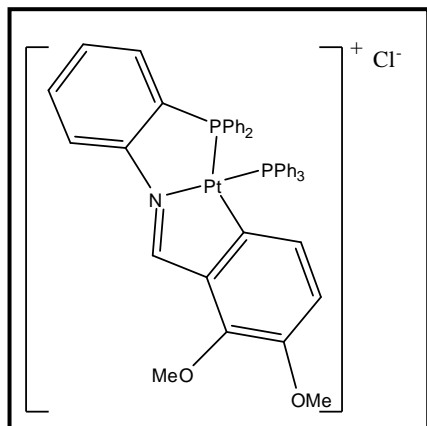
Found (required for  $\text{C}_{43}\text{H}_{33}\text{ClNP}_2\text{Pt}\cdot 2\text{CH}_2\text{Cl}_2$ ): C, 50.92 (50.92); H, 3.47 (3.51); N, 1.10 (1.32).

IR  $\nu_{\text{max}}$  (KBr): 3307 (b), 3039 (w), 2976 (w), 2863 (w), 2330 (w), 1735 (w), 1717 (w), 1627 (w), 1590 (m)(C=N),

1568 (m), 1532 (m), 1480 (m), 1435 (s), 1347 (w), 1291 (m), 1241 (m), 1190 (m), 1168 (w), 1095 (s), 1070 (m), 1027 (w), 997 (m), 928 (w), 878 (w), 810 (m), 771 (w), 757 (m), 736 (m), 703 (m), 692 (s), 611 (m), 573 (m), 543 (s), 517 (s), 506 (m), 497 (s).



$^1\text{H}$  NMR  $\delta$  ppm: 11.31 (1H, d) ( $J_{\text{Pt-H}} = 87$  Hz,  $J_{\text{Pt-Pb}} = 9$  Hz), 6.40-8.20 (32 H, m), 5.30 ( $\text{CH}_2\text{Cl}_2$ ).  $^{31}\text{P}$  NMR  $\delta$  ppm: 33.4 (d) ( $^2J_{\text{p-pa}} = 16$ ,  $J_{\text{Pt-Pa}} = 1949$  Hz), 17.9 (d) ( $^2J_{\text{p-pb}} = 16$ ,  $J_{\text{Pt-Pb}} = 3737$  Hz)



**374:**  $[\text{Pt}^{\text{II}}(\eta^3\text{-PNC-L}^4)\text{Cl}]$  (0.046 g, 0.07 mmol) **284** and  $\text{PPh}_3$  (0.020 g, 0.08 mmol) gave  $[\text{Pt}(\eta^3\text{-PNC-L}^4)\text{PPh}_3]\text{Cl}$  **374** as an orange/yellow metallic crystalline powder.

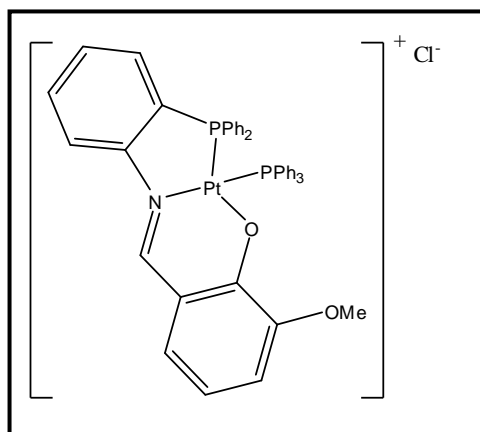
Yield: 0.062 g (89 %)

Found (required for  $\text{C}_{45}\text{H}_{38}\text{ClNO}_2\text{P}_2\text{Pt}\cdot 2\text{CH}_2\text{Cl}_2$ ): C, 51.80 (51.93); H, 4.14 (3.89); N, 1.18 (1.29).

IR  $\nu_{\text{max}}$  (KBr): 3317 (b), 3052 (w), 2932 (w), 1628 (w), 1587 (w) (C=N), 1545 (s), 1478 (s), 1437 (s), 1415 (m),

1340 (w), 1261 (s), 1207 (m), 1184 (w), 1129 (w), 1097 (s), 1025 (m), 997 (m), 955 (w), 835 (w), 809 (w), 753 (m), 729 (m), 694 (s), 581 (w), 563 (w), 544 (s), 517 (s), 507 (s).

$^1\text{H}$  NMR  $\delta$  ppm: 9.91 (1 H, d) ( $J_{\text{Pt-H}} = 86$  Hz,  $J_{\text{Pt-Pb}} = 9$  Hz), 6.17-78.27 (31 H, m), 5.30 ( $\text{CH}_2\text{Cl}_2$ ), 3.60 (3 H, s), 4.14 (3 H, s).  $^{31}\text{P}$  NMR  $\delta$  ppm: 33.4 (d) ( $^2J_{\text{Pa-Pb}} = 16$ ,  $J_{\text{Pt-Pa}} = 1956$  Hz), 17.5 (d) ( $^2J_{\text{Pa-Pb}} = 16$ ,  $J_{\text{Pt-Pb}} = 3815$  Hz)



**375:**  $[\text{Pt}^{\text{II}}(\eta^3\text{-PNO-L}^4)\text{Cl}]$  (0.045 g, 0.07 mmol) **275** and  $\text{PPh}_3$  (0.021 g, 0.08 mmol) gave  $[\text{Pt}(\eta^3\text{-PNO-L}^4)\text{PPh}_3]\text{Cl}$  **375** as an orange/yellow metallic crystalline powder.

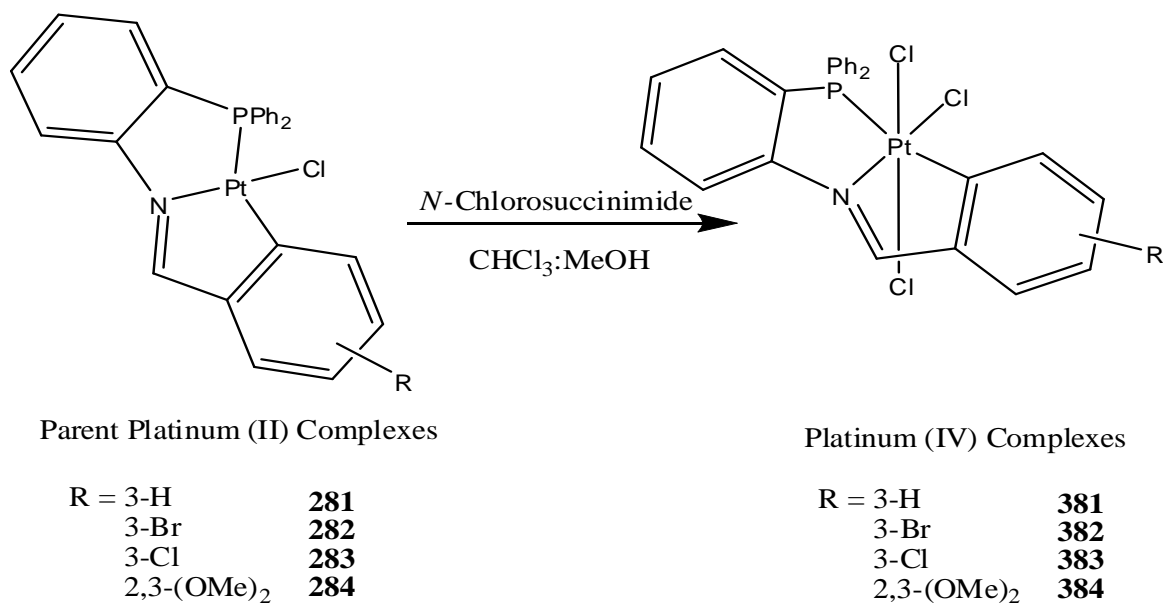
Yield: 0.048 g (69 %)

Found (required for  $\text{C}_{44}\text{H}_{38}\text{ClNO}_2\text{P}_2\text{Pt}\cdot \text{CH}_2\text{Cl}_2$ ): C, 54.53 (54.70); H, 4.06 (3.88); N, 2.41 (1.43).

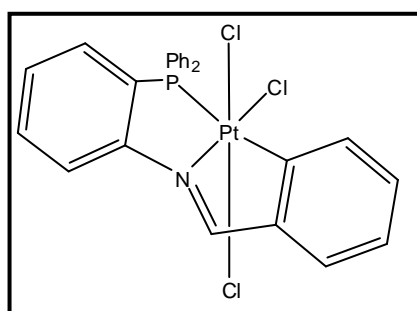
IR  $\nu_{\text{max}}$  (KBr): 3637 (w), 3572 (w), 3368 (b), 3040 (m), 3000 (m), 2346 (w), 1734 (w), 1604 (s), 1589 (s) (C=N), 1571 (s), 1541 (s), 1481 (m), 1458 (w), 1435 (s), 1396 (s), 1330 (m), 1279 (w), 1256 (s), 1230 (s), 1179 (s), 1099 (s), 1065 (m), 997 (m), 983 (m), 874 (w), 857 (w), 777 (w), 743 (s), 711 (m), 691 (s), 618 (w), 566 (m), 549 (w), 530 (s), 510 (s), 502 (s), 455 (w).

$^1\text{H}$  NMR  $\delta$  ppm: 10.06 (1 H, d) ( $J_{\text{Pt-H}} = 61$  Hz,  $J_{\text{Pt-Pb}} = 14$  Hz), 6.59-7.90 (31 H, m), 5.30 ( $\text{CH}_2\text{Cl}_2$ ), 3.20 (3 H, s).  $^{31}\text{P}$  NMR  $\delta$  ppm: 19.0 (d) ( $^2J_{\text{Pa-Pb}} = 22$ ,  $J_{\text{Pt-Pa}} = 3607$  Hz), 9.1 (d) ( $^2J_{\text{Pa-Pb}} = 22$ ,  $J_{\text{Pt-Pb}} = 3434$  Hz)

### 3.10.3 Synthesis of the Pt (IV) complexes $[\text{Pt}^{\text{IV}}(\eta^3\text{-PNC-L}^{1-4})\text{Cl}_3]$ **381-384**:



To a solution of  $[\text{Pt}^{\text{II}}(\eta^3\text{-PNC-L}^{1-4})\text{Cl}]$  **281-284** in 10 ml of a 1:1 solution of chloroform:methanol, an excess of N-chlorosuccinimide (2.1 equivalents) was added and the reaction mixture was stirred at room temperature for 16 hours. It was then reduced to dryness *in vacuo*. The residue was taken up in dichloromethane and washed with water (3x10 ml) in a separation funnel to remove the succinimide formed during the reaction. The final product mixture was then reduced to dryness *in vacuo* and re-crystallised from dichloromethane-hexane to yield compounds **281-384**.



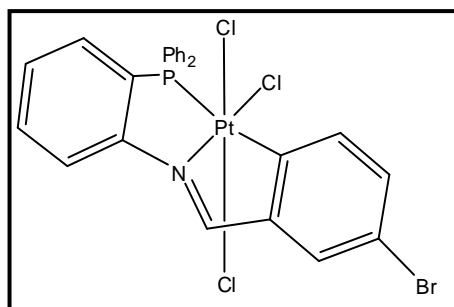
**381**:  $\text{Pt}^{\text{II}}(\eta^3\text{-PNC-L}^1)\text{Cl}]$  **281** (0.021 g, 0.035 mmol) and N-Chlorosuccinimide (0.011 g, 0.082 mmol) gave  $[\text{Pt}^{\text{IV}}(\eta^3\text{-PNC-L}^1)\text{Cl}_3]$  **381** as a dark brown, crystalline solid.

Yield: 0.007 g (30 %)

Found (required for  $\text{C}_{25}\text{H}_{21}\text{Cl}_3\text{NP}\cdot\text{CH}_2\text{Cl}_2$ ): C, 41.48 (41.59); H, 2.80 (2.82); N, 1.79 (1.87).

IR  $\nu_{\text{max}}$  (KBr): 3051 (b), 1591 (s) (C=N), 1565 (s), 1478 (s), 1434 (s), 1254 (s), 1188 (m), 1099 (s), 1068 (m), 997 (m), 970 (w), 844 (w), 767 (s), 720 (m), 693 (s), 570 (w), 528 (s), 502 (s).

$^1\text{H}$  NMR  $\delta$  ppm: 9.11 (1 H, s) ( $J_{\text{Pt-H}} = 81$  Hz), 7.30-8.24 (18 H, m), 5.30 ( $\text{CH}_2\text{Cl}_2$ ).  $^{31}\text{P}$  NMR  $\delta$  ppm: -2.1 (s) ( $J_{\text{Pt-P}} = 1326$  Hz).



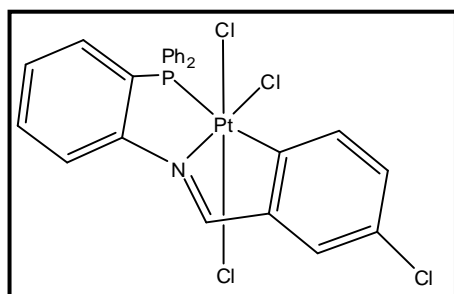
**382:**  $[\text{Pt}^{\text{II}}(\eta^3\text{-PNC-L}^2)\text{Cl}]$  **282** (0.022 g, 0.033 mmol) and N-Chlorosuccinimide (0.012 g, 0.82 mmol) gave  $[\text{Pt}^{\text{IV}}(\eta^3\text{-PNC-L}^3)\text{Cl}_3]$  **283** as a light yellow solid.

Yield: 0.003 g (11 %)

Found (required for  $\text{C}_{25}\text{H}_{18}\text{BrCl}_3\text{NPt}$ ) C, 40.12 (40.42); H, 2.40 (2.44); N, 1.78 (1.88)

IR  $\nu_{\text{max}}$  (KBr): 3317 (b), 1595 (w)(C=N), 1565 (s), 1478 (s), 1437 (s), 1415 (m), 1390 (w), 1261 (s), 1207 (m), 1189 (m), 1129 (w), 1097 (s), 1025 (m), 835 (s), 809 (w), 750 (s), 729 (m), 694 (s), 581 (w), 511 (s), 504 (s).

$^1\text{H}$  NMR  $\delta$  ppm: 9.20 (1 H, s) ( $J_{\text{Pt-H}} = 83$  Hz), 7.40-8.20 (17 H, m).  $^{31}\text{P}$  NMR  $\delta$  ppm: -1.7 (s) ( $J_{\text{Pt-P}} = 1345$  Hz).



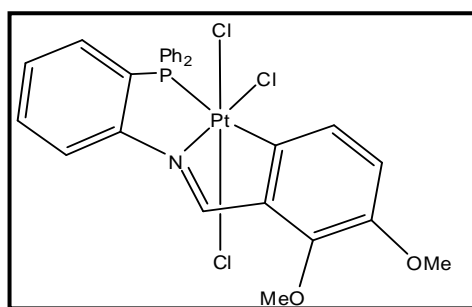
**383:**  $[\text{Pt}^{\text{II}}(\eta^3\text{-PNC-L}^3)\text{Cl}]$  **283** (0.021 g, 0.033 mmol) and N-Chlorosuccinimide (0.013 g, 0.83 mmol) gave  $[\text{Pt}^{\text{IV}}(\eta^3\text{-PNC-L}^3)\text{Cl}_3]$  **383** as a light yellow solid.

Yield: 0.006 g (25 %)

Found (required for  $\text{C}_{25}\text{H}_{21}\text{Cl}_4\text{NP}\cdot\text{CH}_2\text{Cl}_2$ ): C, 39.65 (39.77); H, 2.49 (2.57); N, 1.65 (1.78).

IR  $\nu_{\text{max}}$  (KBr): 3052(w), 1596(w)(C=N), 1541 (s), 1478 (s), 1437 (s), 1415 (m), 1340 (w), 1261 (s), 1207 (m), 1184 (w), 1129 (w), 1097 (s), 1025 (m), 997 (m), 955 (w), 835 (w), 809 (w), 753 (m), 729 (m), 694 (s), 581 (w), 563 (w), 544 (s), 517 (s), 507 (s).

$^1\text{H}$  NMR  $\delta$  ppm: 9.21 (1 H, s) ( $J_{\text{Pt-H}} = 84$  Hz), 6.40-8.20 (17 H, m).  $^{31}\text{P}$  NMR  $\delta$  ppm: -1.4 (s) ( $J_{\text{Pt-P}} = 1350$  Hz).



**384:**  $[\text{Pt}^{\text{II}}(\eta^3\text{-PNC-L}^4)\text{Cl}]$  **284** (0.025 g, 0.038 mmol) and N-Chlorosuccinimide (0.013 g, 0.084 mmol) gave  $[\text{Pt}^{\text{IV}}(\eta^3\text{-PNC-L}^4)\text{Cl}_3]$  **384** as a dark red powder.

Yield: 0.010 g (36 %)

Found (required for  $\text{C}_{27}\text{H}_{23}\text{Cl}_3\text{NO}_2\text{PPt}\cdot 0.1\text{CH}_2\text{Cl}_2$ ): C, 43.95 (44.32); H, 3.17 (3.18); N, 1.80 (1.91)

IR  $\nu_{\text{max}}$  (KBr): 3392 (w), 2932 (w), 1586 (m)(C=N), 1538 (s), 1477 (m), 1436 (m), 1410 (w), 1336 (w), 1266 (s), 1206 (w), 1134 (w), 1096 (w), 1081 (w), 1002 (m), 817 (w), 743 (m), 690 (m), 563 (w), 527 (m), 498 (m).

$^1\text{H}$  NMR  $\delta$  ppm: 9.34 (1 H, s) ( $J_{\text{Pt-H}} = 84$  Hz), 7.23-7.90 (14H, m), 8.07-8.16 (2H, m), 3.91 (3H, s), 4.10 (3H, s).  $^{31}\text{P}$  NMR  $\delta$  ppm: -2.1 (s) ( $J_{\text{Pt-P}} = 1334$  Hz).

**3.11 Bibliography:**

1. F. A. Cotton and G. Wilkinson, in *Advanced Inorganic Chemistry*, John Wiley & Son, 6th Ed., 1999, pp. 1072–1073.
2. I. Chernyaev, *Ann. Inst. Platine USSR*, 1926, **4**.
3. G. L. Miessler and D. A. Tarr, in *Inorganic Chemistry*, Pearson Education Inc., 3rd Ed., 2004, pp. 524–528.
4. J. C. Dabrowiak, in *Metals in Medicine*, John Wiley & Sons, Ltd., 1st Ed., 2009, pp. 49–72.
5. J. C. Dabrowiak, in *Metals in Medicine*, Wiley, 1st Ed., 2009, pp. 33–45.
6. T. Maguire, *PhD Thesis*, 2009, UCC, 100–153.
7. J. Lennon, *PhD Thesis*, 2005, UCC, 184–290.
8. O. M. Ni Dhubhghaill, J. Lennon, and M. G. Drew, *Dalton Transactions*, 2005, 3213–3220.
9. G. L. Miessler and D. A. Tarr, in *Inorganic Chemistry*, Pearson Education Inc., 3rd Ed., 2004, pp. 195–197.
10. A. Wong-Foy, L. M. Henling, M. Day, J. A. Labinger, and J. E. Bercaw, *Journal of Molecular Catalysis A*, 2002, **189**, 3–16.
11. A. Capapé, M. Crespo, J. Granell, M. Font-Bardía, and X. Solans, *Journal of Organometallic Chemistry*, 2005, **690**, 4309–4318.
12. M. Albrecht, P. Dani, M. Lutz, A. L. Spek, and G. van Koten, *Journal of the American Chemical Society*, 2000, **122**, 11822–11833.
13. A. Fernández, M. Lopez-Torres, A. Suárez, J. M. Ortigueira, T. Pereira, J. J. Fernández, J. M. Vila, H. Adams, and M. López-Torres, *Journal of Organometallic Chemistry*, 2000, **598**, 1–12.
14. D. Vázquez-García, A. Fernández, J. J. Fernández, M. López-Torres, A. Suárez, J. M. Ortigueira, J. M. Vila, and H. Adams, *Journal of Organometallic Chemistry*, 2000, **595**, 199–207.
15. P. M. Greensmyth, *MSc Thesis*, 2009, UCC, 56–100.
16. G. K. Anderson and G. J. Lumetta, *Inorganic Chemistry*, 1987, **26**, 1518–1524.
17. L. R. Kelland, G. Abel, M. J. McKeage, M. Jones, P. M. Goddard, M. Valenti, B. A. Murrer, and K. R. Harrap, *Cancer Research*, 1993, **53**, 2581–2586.

18. T. Soldatovic, Z. D. Bugarcic, and R. van Eldik, *Dalton Transactions*, 2009, 4526–4531.
19. N. J. Wheate, S. Walker, G. E. Craig, and R. Oun, *Dalton Transactions*, 2010, **39**, 8113–8127.
20. A. D. Ricart, J. Sarantopoulos, E. Calvo, Q. S. Chu, D. Greene, F. E. Nathan, M. E. Petrone, A. W. Tolcher, and K. P. Papadopoulos, *Clinical Cancer Research*, 2009, **15**, 3866–3871.
21. J. Cetnar, G. Wilding, D. McNeel, N. K. Loconte, T. A. McFarland, J. Eickhoff, and G. Liu, *Urologic Oncology*, 2011.
22. T. Nakai, M. Ando, Y. Okamoto, K. Ueda, and N. Kojima, *Journal of Inorganic Biochemistry*, 2011, **105**, 1–5.
23. H. Choy, C. Park, and M. Yao, *Clinical Cancer Research*, 2008, **14**, 1633–1638.
24. G. Doshi, G. Sonpavde, and C. N. Sternberg, *Expert Opinion on Drug Metabolism & Toxicology*, 2012, **8**, 103–11.
25. A. Alotaibi, *Journal of Cancer Therapy*, 2012, **03**, 78–89.
26. D. Serra, P. Cao, R. Padilla, F. Rominger, and M. Limbach, *Organometallics*, 2011, **30**, 1885–1895.
27. C. P. Newman, K. Casey-Green, G. J. Clarkson, G. W. Cave, W. Errington, and J. P. Rourke, *Dalton Transactions*, 2007, 3170–3182.
28. S. Dunham, R. D. Larsen, and E. H. Abbott, *Inorganic Chemistry*, 1993, **32**, 2049–2055.
29. C. M. Giandomenico, M. J. Abrams, B. a Murrer, J. F. Vollano, M. I. Rheinheimer, S. B. Wyer, G. E. Bossard, and J. D. Higgins, *Inorganic chemistry*, 1995, **34**, 1015–21.
30. S. R. Whitfield and M. S. Sanford, *Organometallics*, 2008, **27**, 1683–1689.
31. L. T. Ellis, H. Meng Er, and T. W. Hambley, *Australian Journal of Chemistry*, 1995, 793–806.
32. K. D. Hodges and J. V Rund, *Inorganic Chemistry*, 1975, **14**, 525–528.
33. C. E. Skinner and M. M. Jones, *Journal of the American Chemical Society*, 1969, **91**, 4405–4408.
34. J. Ruiz, J. F. J. López, V. Rodríguez, J. Pérez†, M. C. Ramírez de Arellano, and G. López, *Journal of the Chemical Society, Dalton Transactions*, 2001, 2683–2689.
35. A. Yahav, I. Goldberg, and A. Vigalok, *Organometallics*, 2005, **24**, 5654–5659.

36. L. Drougge and L. I. Elding, *Inorganic Chemistry*, 1988, **27**, 795–798.
37. F. Liu and W. Chen, *European Journal of Inorganic Chemistry*, 2006, **2006**, 1168–1173.
38. D. Monti, A. Pastorini, G. Mancini, S. Borocci, and P. Tagliatesta, *Journal of Molecular Catalysis A: Chemical*, 2002, **179**, 125–131.
39. L. A. M. Baxter, G. A. Heath, R. G. Raptis, and A. C. Willis, *Journal of the American Chemical Society*, 1992, **114**, 6944–6946.
40. J. D. Scollard, M. Day, J. A. Labinger, and J. E. Bercaw, *Helvetica Chimica Acta*, 2001, **84**, 32473268.
41. S. Lai, M. C. Chan, T. Cheung, S. Peng, and C. Che, *Inorganic Chemistry*, 1999, **38**, 4046–4055.
42. C. D. A. and E. M. Tansey, *Welcome Trust Centre*, 2007, **30**.
43. A. Fernández, P. Uría, J. J. Fernández, M. Lopez-Torres, A. Suárez, D. Vázquez-García, M. T. Pereira, J. M. Vila, and D. Vázquez-García, *Journal of Organometallic Chemistry*, 2001, **620**, 8–19.
44. E. S. Kryachko and T. Zeegers-Huyskens, *The Journal of Physical Chemistry A*, 2002, **106**, 6832–6838.
45. J. W. Slater, D. P. Lydon, N. W. Alcock, and J. P. Rourke, *Organometallics*, 2001, **20**, 4418–4423.
46. J. Mamtora, S. H. Crosby, C. P. Newman, G. J. Clarkson, and J. P. Rourke, *Organometallics*, 2008, **27**, 5559–5565.
47. W. L. F. Armarego and C. Li Lin Chai, in *Purification of Laboratory Materials*, Elsevier Inc., 6th Ed., 2009, pp. 88–444.
48. M. K. Cooper, J. M. Downes, P. A. Duckworth, M. C. Kerby, R. J. Powell, and M. D. Soucek, in *Inorganic Syntheses*, John Wiley & Sons, Inc., 1989, pp. 129–133.



**Chapter 4:**  
**Biological Activity and Photophysical Studies**



## Contents

<b>4.1 Chapter 4 Background</b> .....	255
<b>4.2 The Role of Sulphur in Platinum Anti-cancer Therapy:</b> .....	255
4.2.1 Sulphur biomolecules: .....	255
4.2.2 Sulphur biomolecules hindering the mechanism of action of Pt (II) drugs.....	256
4.2.3 Sulphur biomolecules assisting the mechanism of action of Pt (II) drugs.....	260
4.2.4 Sulphur Biomolecules Assisting Pt (IV) Pro-drugs .....	264
<b>4.3 In-Vitro Cell Testing of Cyclometallated Platinum Anti-Cancer Drugs.....</b>	<b>266</b>
4.3.1 Monofunctional Complexes.....	266
4.3.2 Tridentate Pt (II) Anti-cancer Drugs and Intercalation.....	268
<b>4.4 Photophysical Studies of Platinum Complexes and Mixed Donor Ligands .....</b>	<b>272</b>
4.4.1 Factors Influencing Luminescence of Pt (II) Complexes.....	272
4.4.2 Luminescence of Small Organic Molecules (Ligands).....	274
<b>4.5 Summary and Conclusions</b> .....	<b>277</b>
<b>4.6 Synthesis and Analysis of Cyclometallated Pt (II) Bio-Adducts.....</b>	<b>278</b>
4.6.1 Synthesis of the Pt (II) N-acetyl-L-cysteine bio-adducts of the general formula [Pt( $\eta^3$ -PNC-L <sup>1/4</sup> )N-Acetyl-L-Cys] <b>440-441</b> .....	278
4.6.2 Synthesis of the Pt (II) L-glutathione bio-adducts of the general formula [Pt( $\eta^3$ - PNC-L <sup>1/4</sup> )Glu] <b>442-443</b> .....	281
4.6.3 Other reactions involving biomolecules and platinum complexes .....	283
4.6.4 Infra-red spectroscopic studies of the platinum bio-adducts [Pt( $\eta^3$ -PNC- L <sup>1/4</sup> )Glu/NaLCys].....	284
4.6.5 NMR spectroscopic studies for the platinum bio-adducts Pt( $\eta^3$ -PNC- L <sup>1/4</sup> )Glu/NaLCys].....	286

---

<b>4.7 In-Vitro Cancer Cell Testing with Pt (II) Cyclometallates</b> .....	291
4.7.1 Background on the cell culture used.....	291
4.7.2 Propidium iodide (PI) uptake and flow cytometry.....	293
4.7.3 Analysis of morphological features.....	295
<b>4.8 Photophysical Studies of the Platinum Complexes and their Ligands</b> .....	298
4.8.1 UV-visible spectroscopy.....	298
4.8.2 Luminescence studies on platinum complexes and mixed donor ligands.....	300
<b>4.9 Chapter 4 Summary and Conclusions</b> .....	302
<b>4.10 Chapter 4 Experimental</b> .....	304
4.10.1 Background.....	304
4.10.2 Synthesis of the Pt (II) bio-adducts $[\text{Pt}(\eta^3\text{-PNC-L}^{1/4})\text{N-acetyl-L-cys/L Glu}]\text{Cl}$ <b>440-443</b> .....	305
4.10.3 <i>In-vitro</i> Cell Testing on the Pt (II) cyclometallates <b>281</b> and <b>284</b> .....	308
4.10.4 Photophysical studies on the 3-H ligand <b>261</b> and platinum complexes <b>281</b> , <b>371</b> and <b>381</b> .....	308
<b>4.11 Bibliography</b> .....	309

#### 4.1 Chapter 4 Background:

The biological role of metal ions and metal based drugs was discussed extensively in **Chapter 1**. In particular platinum based metallo-drugs were discussed in terms of their pharmacokinetics and their mechanism of action *in-vitro* and *in-vivo*. **Chapter 2** then went on to discuss the design and synthesis of a new range of Pt (II) complexes, while **Chapter 3** discussed substitution and oxidation reactions of these complexes to form cationic triphenylphosphine Pt (II) complexes and Pt (IV) complexes respectively. This chapter on the other hand aims to focus on the applications and potential biological activity of the most stable complexes reported in **Chapter 2** and **3**.

#### 4.2 The Role of Sulphur in Platinum Anti-cancer Therapy:

##### 4.2.1 Sulphur biomolecules:

Sulphur containing biomolecules such as cysteine (Cys), methionine (Met), glutathione (GSH), metallothionein (MT) and albumin play a significant role in the metabolism of platinum anti-cancer drugs due to their high affinity to the Pt (II) metal centre.<sup>1</sup>

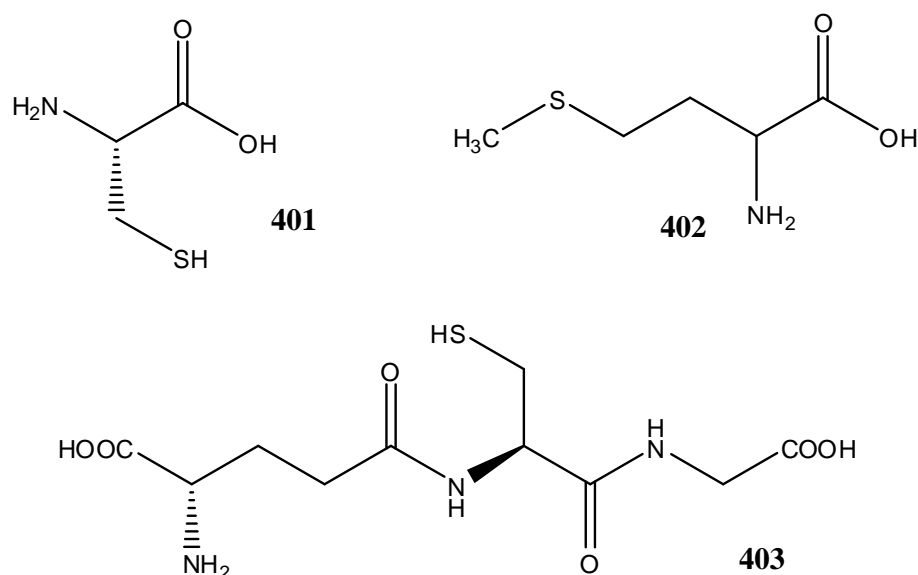


*Figure 4.1: Examples of some biomolecules involved in the metabolism of Pt (II) drugs; cysteine 401, methionine 402 and glutathione 403*

Sulphur is involved in the entire metabolic process of platinum drugs, including reactions prior to cell uptake, deactivation prior to DNA binding, and formation of DNA adducts.<sup>2</sup> Sulphur containing amino acids such as cysteine and methionine, **401** and **402**, **Figure 4.1**, play an important role in maintaining the integrity of cellular systems by influencing the cellular redox state and can detoxify unwanted compounds, free radicals and reactive oxygen species.

Sulphur containing peptides such as glutathione, **403**, **Figure 4.1**, also act as important antioxidants and play key roles in the detoxification of a variety of electrophilic compounds and peroxides. Finally, large proteins such as albumin and metallothionein are very abundant thiol rich biomolecules found in humans and have a strong affinity for certain metal ions (“soft” acids as described by the HSAB theory).<sup>2-4</sup>

However, the role of sulphur in platinum based chemotherapy has been controversial with arguments claiming that these biomolecules can hinder therapeutic efficacy as well as assist in the biological activity of platinum complexes.<sup>5-8</sup> Carboplatin for instance is much less chemically reactive than cisplatin, meaning fewer side effects, but it still has potent anti-tumour properties. This has prompted investigators to focus on ways in which it reacts with biomolecules that are normally found in the body.

Platinum-sulphur interactions are ubiquitous in the human body and many occurrences encountered during platinum chemotherapy such as uptake, excretion, resistance and toxicity are related to them. Therefore sulphur containing biomolecules play a significant role in the anti-cancer mechanism of current platinum drugs and determine the design of future analogues. Studies involving the reaction of both new platinum complexes and currently approved drugs with these biomolecules are therefore necessary to establish structure activity relationships (SAR) and determine potential anti-cancer activity.

#### **4.2.2 Sulphur biomolecules hindering the mechanism of action of Pt (II) drugs:**

Sulphur manifests its negative influence on platinum anti-cancer chemotherapy in two aspects. Firstly endogenous sulphur containing biomolecules such as cysteine, methionine and glutathione affect the metabolism of platinum drugs and exert adverse effects on the therapeutic efficacy while exogenous congeners such as amifostine and dimesna mitigate the toxic side effects of platinum drugs and serve as chemoprotectants.

It is commonly accepted that the most platinum drugs in the clinic exert their anti-cancer effect by interacting with DNA, however, these drugs will inevitably meet a variety of



oxaliplatin) (discussed in **Chapter 1**) may affect the formation and stability of platinum-DNA adducts in the presence of methionine.<sup>9,11</sup>

To further investigate this, Lippard *et al* on the solid-state (crystal) structure of the oxaliplatin-DNA adduct found hydrogen bonding between the pseudo-equatorial NH hydrogen atom of the DACH ligand, **Figure 4.3**, and the O6 atom of guanine at the site of platination. The investigators suggested that this feature of the structure shows the importance of chirality in the DACH ligand (the non-leaving group) of oxaliplatin despite any interactions with biomolecules such as methionine.<sup>12</sup>

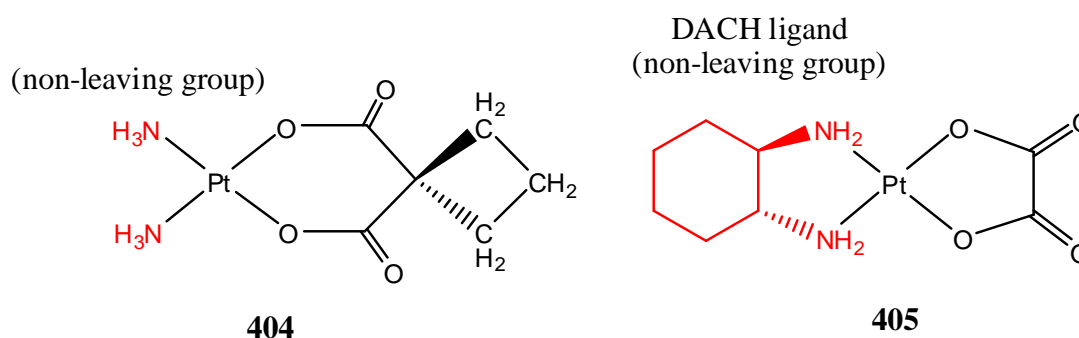


*Figure 4.3: Carboplatin 404 and Oxaliplatin 405, both of which have vastly different reactivity with biomolecules in-vivo due to the 1,2-diaminocyclohexane ligand on Oxaliplatin.*

As discussed in **Chapter 1**, cisplatin enters the cell from the blood via passive diffusion or through metal transporters, **Figure 4.2**. After hydrolysis the active species of cisplatin then enters the nuclear envelope and binds to DNA, which triggers apoptosis. However, biomolecules within the cell compete for cisplatin with DNA and have therefore been associated with increased inactivation and drug resistance (endogenous).<sup>13,14</sup>

The most important non-DNA target of cisplatin has been identified as glutathione, as it is present in cells at high concentrations. In cell cytoplasm approximately 60% of cisplatin that has entered the cell is conjugated to glutathione, leaving only a small fraction to bind with target DNA. The glutathione in cells reacts with cisplatin to form a platinum-glutathione complex that is active in the inhibition of cell-free protein synthesis and can quench DNA-platinum adducts before cross linking can occur.<sup>15</sup>

This interaction of glutathione with cisplatin reduces the amount of intracellular platinum available for interaction with DNA. Also, it has been proposed that the GS-X pump present on the cell membrane is active in the excretion of glutathione adducts from the cell due to cellular protection from “toxins”.<sup>16</sup>

As highlighted in **Chapter 1**, platinum anti-cancer drugs also cause severe toxicity such as nephro- and neurotoxicity during chemotherapy, which have also been related to their interactions with exogenous sulphur containing biomolecules such as glutathione. By forming adducts with the platinum anti-cancer complexes, protein bound thiol groups are depleted in renal cells and in respiratory enzymes particularly for cisplatin.<sup>17,18</sup>

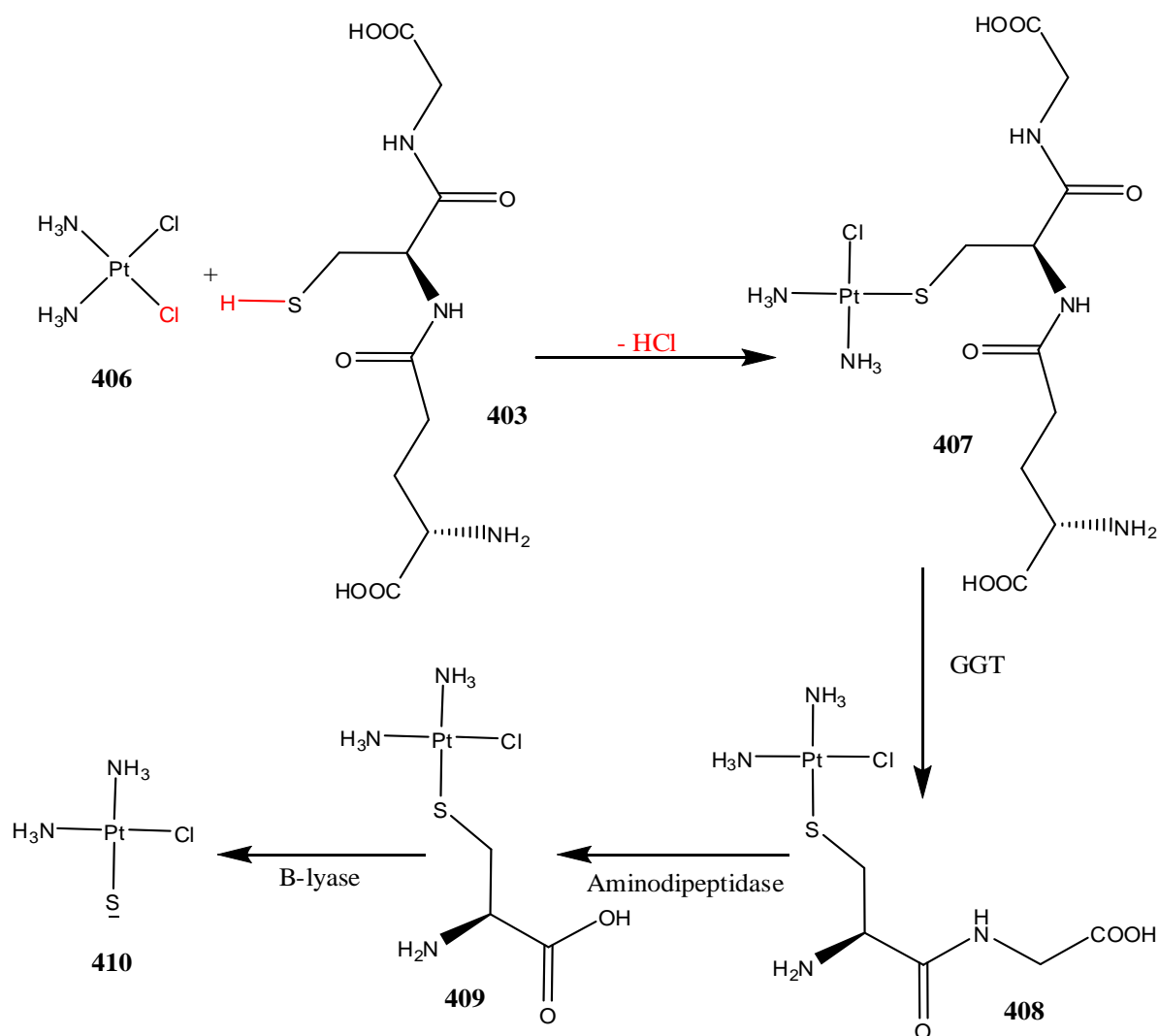


*Figure 4.4: The proposed metabolism of cisplatin 406 with glutathione 403 to form the highly reactive thiol nephrotoxin 410.<sup>19</sup>*

Nephrotoxicity is one of the major toxicities induced by platinum anti-cancer drugs and starts with the formation of a platinum-glutathione complex within the cell. After the Pt-GS adduct is transported out of the cell it undergoes cleavage into a highly reactive thiol (a nephrotoxin), **Figure 4.4**, which then binds to essential proteins.<sup>19</sup>

The enzymes involved in the cleavage and shown in **Figure 4.4** are, γ-glutamyl transpeptidase (GGT) which cleaves the Pt-GS adduct into **408**, aminodipeptidase N which

forms the adduct **409** and Cys-S-conjugate  $\beta$ -lyase which cleaves the adduct into the highly reactive thiol nephrotoxin **410**.<sup>19</sup>

#### 4.2.3 Sulphur biomolecules assisting the mechanism of action of Pt (II) drugs:

It has been proposed by a number of investigators that biomolecules can also cause opening of the 1,1-cyclobutanedicarboxylato (CBDCA) chelate ring in carboplatin, thus producing a reactive platinum fragment that could readily interact with DNA and protein targets in the cell.<sup>7,8</sup> This therefore implies that carboplatin is in fact a *prodrug*, which, although not reactive in the body as it is, is activated by some substance in the biological system to form the reactive entity, **Figure 4.4**. However, although the biomolecules can activate the drug, they can also render the same drug inactive as outlined in **Section 4.2.2**.

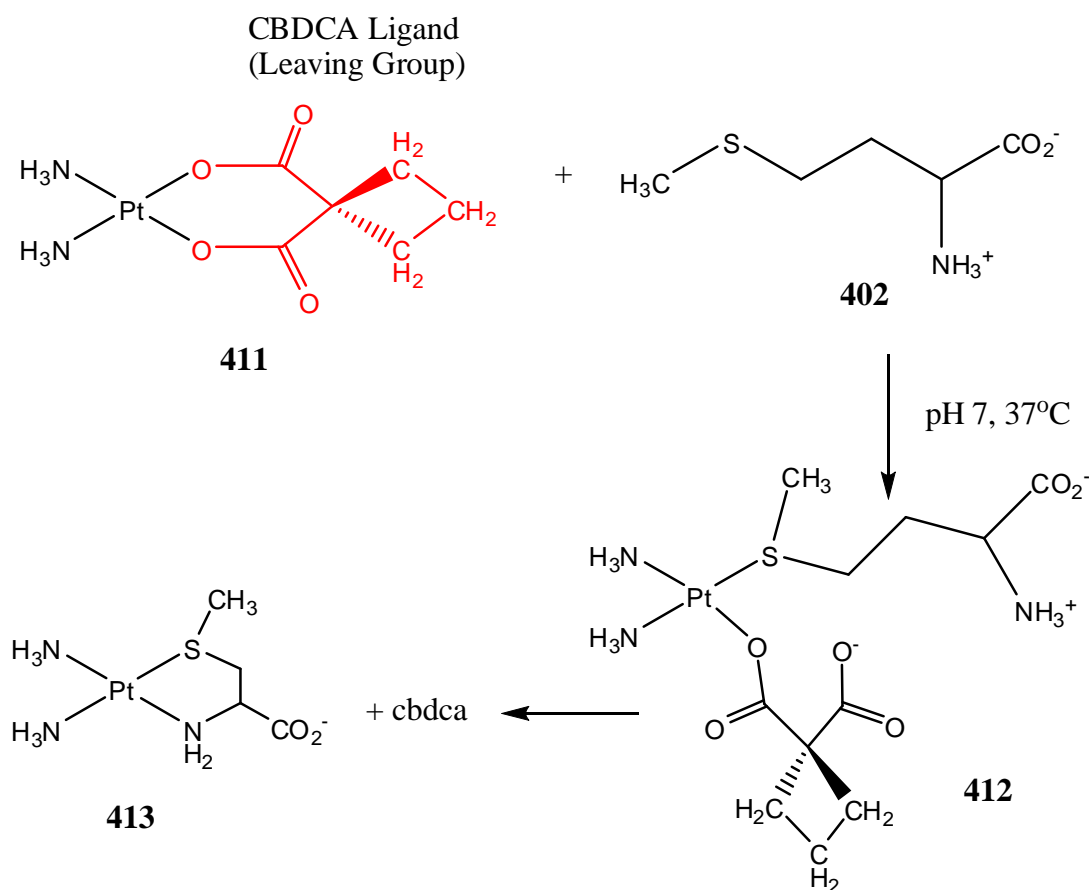


**Figure 4.4:** The reaction of carboplatin **411** with L(S)-methionine **402** in water at pH 7 to give the monomethionine adduct **412** and eventually the chelate structure **413**.<sup>7</sup>

Sadler *et al* have used various NMR studies to show that carboplatin reacts *in-vitro* with the amino acid L-Methionine (Met), which is present in blood, to produce the



monomethionine adduct, *cis*-[Pt(CBDCA-*O*)(NH<sub>3</sub>)<sub>2</sub>(L-HMet-*S*)] **412**, **Figure 4.4**. This monoadduct, was found to be quite stable toward elimination of the CBDCA ligand. It is suggested that this stability is due to intramolecular hydrogen bonding, which prevents the CBDCA ligand from being completely displaced from the platinum.<sup>7</sup>

However, eventually the CBDCA ligand is displaced to produce [Pt(L-Met-*S,N*)(NH<sub>3</sub>)<sub>2</sub>] **413**, **Figure 4.4**, which contains a methionine chelate. Due to the *trans* effect, discussed in detail in **Chapter 2** and **3**, entry of a sulphur atom into the coordination sphere of the platinum metal centre of carboplatin labilises the group that is *trans* to the sulphur i.e. ammonia. This allows the methionine chelate adduct [Pt(L-Met-*S,N*)(NH<sub>3</sub>)<sub>2</sub>] **412** to further react with nucleophiles, ultimately resulting in the loss of an ammonia molecule.<sup>7</sup>

In a comparison with cisplatin Sadler *et al* have identified the presence of the CBDCA ligand in carboplatin as core to the dramatic difference in reactivity. In reactions with other sulphur containing biomolecules, such as N-acetyl-L-cysteine and L-glutathione, they have reported low reactivity towards carboplatin for these biomolecules.<sup>7</sup> In addition to binding to amino acids and other small molecules, carboplatin also interacts with proteins in blood where some research groups have reported platinum-albumin and  $\gamma$ -globulin adducts in blood samples from carboplatin treated patients. Opening the chelate ring of carboplatin or removing it entirely results in platinum complexes that are much more toxic to cells than the intact drug.<sup>20</sup>

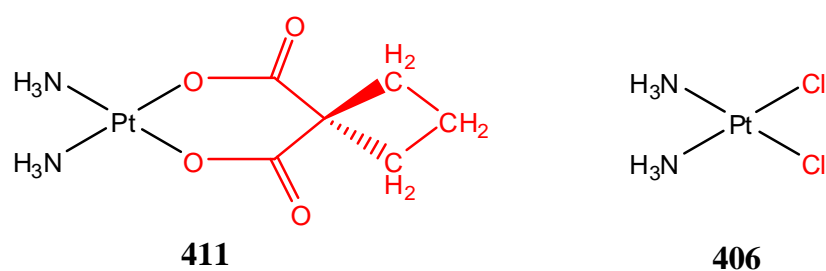


*Figure 4.5: A comparison of the leaving groups (highlighted in red) for carboplatin 411 and cisplatin 406.*

Other interesting aspects relating to the mechanism of action of carboplatin were identified by Overbeck *et al* and others who reported that carboplatin which aged in media containing chloride ions was much more toxic to *E.Coli* bacteria than freshly prepared aqueous solutions of the drug. It was found that cisplatin was present in the chloride-aged solutions of carboplatin which suggested that the antitumour effects of carboplatin could be in part due to the conversion of some of the drug to cisplatin.<sup>21-23</sup>

As seen for cisplatin, carboplatin also forms intrastrand DNA crosslinks as its primary mode of action towards cancer cells. However, various studies have found that the concentration of carboplatin required to reach a DNA-unwinding state comparable to that of cisplatin was about 100 times greater than that of cisplatin, meaning carboplatin is much less reactive towards DNA than cisplatin presumably because of the better leaving group(s) present on cisplatin, **Figure 4.5**.<sup>24,25</sup>

Interestingly though, work by Holler *et al* showed that mixing carboplatin with purified calf thymus DNA in the presence of either methionine, glutathione or thiourea cause more platinum to be bound to DNA than if these sulphur-containing molecules were not present in the reaction medium. This indicates that sulphur nucleophiles could play an important role in activating carboplatin and allow the product to react with its primary cellular target; DNA as proposed by Sadler *et al*, **Figure 4.4**.<sup>24</sup> Further work by Van Boom *et al*, in contrast to the investigations discussed in **Section 4.2.2**, has shown that the platinum adducts formed, which result in inactivation and increased toxic side-effects, due to the interactions of platinum anti-cancer drugs with sulphur based biomolecules, can in fact still coordinate to DNA, **Figure 4.6**.<sup>26</sup>

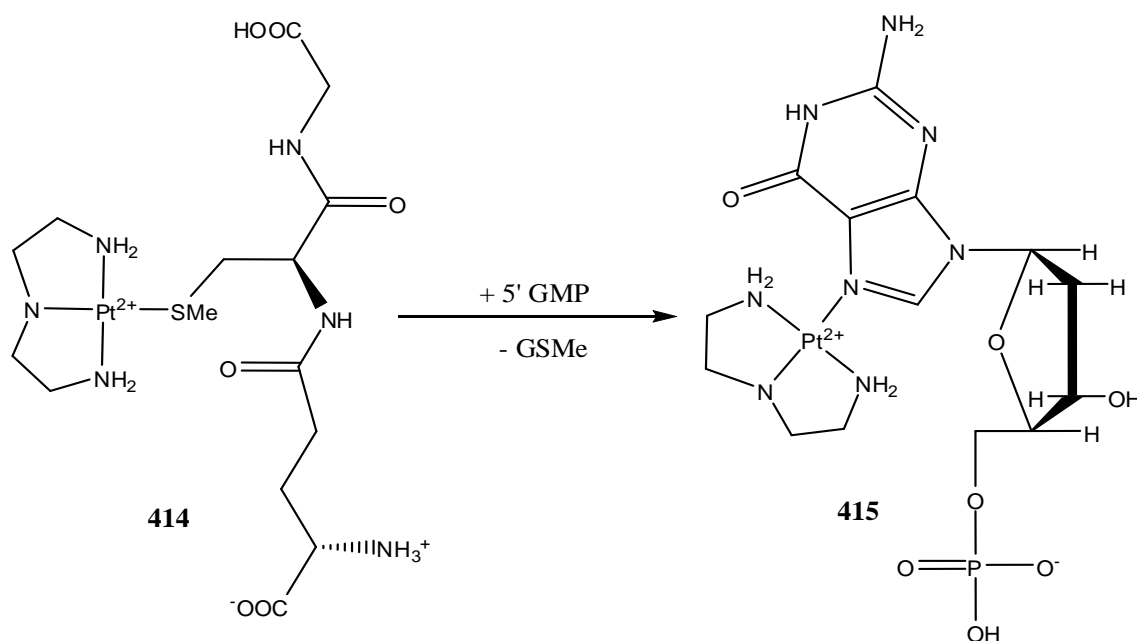


**Figure 4.6:** The reaction of 5'-GMP (through the N7 position of guanine) with a platinum biomolecule adduct (*S*-methyl-glutathione GSMe)  $[Pt(dien)(GSMe)]^{2+}$  414 demonstrating the reversible nature of some platinum-GS adducts.<sup>26</sup>

Monofunctional  $[Pt(dien)Cl]^-$  was chosen by Van Boom *et al* for their study as this species has only one leaving group, chloride, which therefore mimics the first binding step of

cisplatin to biomolecules. Also, amine release as a possible consequence of the *trans*-effect of S-donor ligands is avoided because of the stability of the dien chelate.<sup>26</sup> The  $[\text{Pt}(\text{dien})\text{Cl}]^+$  complex is also similar to the structure of the complexes described in **Chapter 2** and **3** reported here by our research group, giving a good basis for comparison with the current work. Both structures feature a single chloride leaving group and stable tridentate chelate ligand, **Figure 4.7**.

Previous work by Lempers *et al* into the reactivity of  $[\text{Pt}(\text{dien})\text{Cl}]^+$  towards glutathione and *S*-methyl-glutathione found that there was no intermolecular substitution of GSMe by 5'-GMP at room temperature.<sup>27</sup> However, ligand exchange reactions were found to occur successfully in later work by Van Boom *et al* at 37°C and pH 7, **Figure 4.6**.

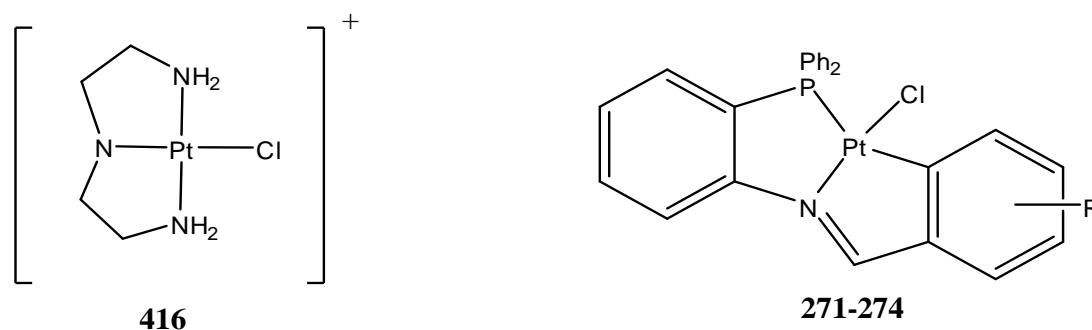


**Figure 4.7:** A comparison of the tridentate  $[\text{Pt}(\text{dien})\text{Cl}]^+$  complex **416** used by Van Boom and Lempers *et al* and the complexes described by our research group  $\text{Pt}[\eta^3\text{-PNC-L}^{1-4}]\text{Cl}$ .

Van Boom *et al* used  $^1\text{H}$  NMR spectroscopy to study the characteristic signals for N7 coordination, previously reported by Reedijk *et al*, and found that substitution by 5'-GMP in  $[\text{Pt}(\text{dien})(\text{GSMe})]^{2+}$  **414** was slow at ambient temperature but had a half-life of 31 hours at 35°C. It is proposed that this intermolecular rearrangement supports the hypothesis of a drug reservoir mechanism for platinum anti-cancer drugs, **Figure 4.8**, particularly for mono-adducts such as those described by our research group, **Figure 4.7**.

A drug reservoir mechanism is similar to that previously discussed for carboplatin in which the platinum-sulphur adducts act as an intermediate for platinum binding to DNA. *In-vivo*, such a mechanism could operate under circumstances that reduce the role of the aquation pathway usually found for cisplatin. A favourable orientation is likely to occur when proteins are located in close vicinity of, or even bind to DNA. Rearrangement is then possible where the platinum-sulphur adduct could react with the N7 position of guanine, **Figure 4.8**.<sup>28</sup>

Earlier studies also by Van Boom *et al* on the competition in platinum binding between sulphur donor atoms and reactive nucleobases using *S*-guanosyl-L-homocysteine

(SGH) as a model compound, also revealed that the N7 position of guanine can replace a sulphur donor atom in a platinum-thioether adduct as well as those studied with glutathione.<sup>29,30</sup>

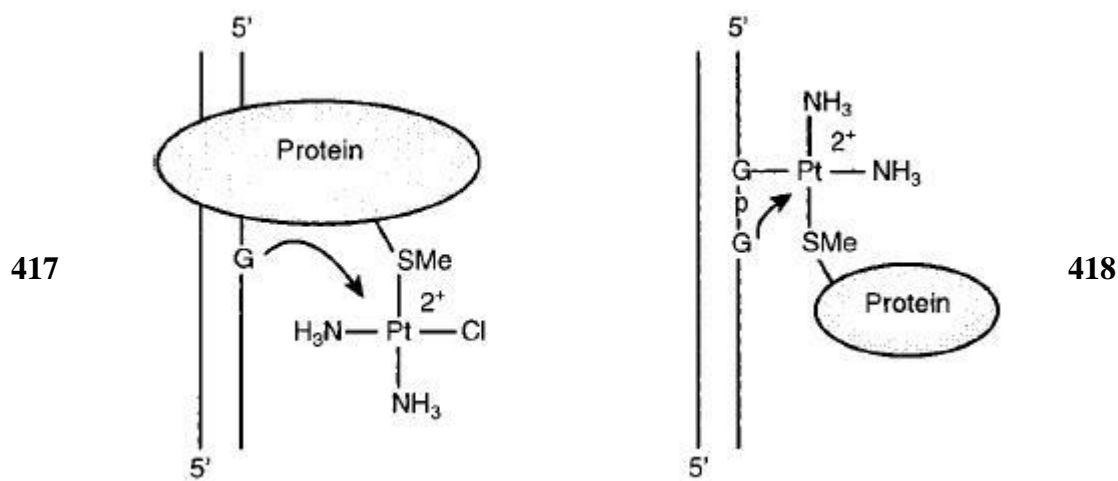


**Figure 4.8:** Possible structures with a favourable orientation of the thioether function and the N7 of guanine in (417) DNA-binding proteins and (418) the cis-platinum cross-link with DNA and a protein.<sup>26</sup>

#### 4.2.4 Sulphur Biomolecules Assisting Pt (IV) Pro-drugs:

As discussed in detail in **Chapter 1**, the new third generation of platinum anti-cancer drugs, primarily Pt (IV), are pro-drugs where *in-vivo* they are reduced to their active Pt (II) analogue. The reducing agent employed to “activate” Pt (IV) drugs has been identified most often as glutathione, which can exchange with the axial ligands forming part of the octahedral structure of the Pt (IV) pro-drug.<sup>31</sup>

The kinetic stability of the Pt (IV) axial ligand bonds in particular has been found to strongly influence the reactions and reduction potential of Pt (IV) complexes and, therefore, can be expected to exert an influence on their biological activity. The majority of Pt (IV) complexes studied as potential anti-cancer agents have either chloro or hydroxo ligands in the axial positions, with some newer drugs, such as satraplatin, having carboxylato ligands in these positions.<sup>31,32</sup>

Extensive work by Hambley *et al*, Hall *et al* and others found that in the absence of glutathione, none of the Pt (IV) complexes caused complete inhibition of cancer cell lines tested, even up to high concentrations of the drug. It was also reported that the most readily

reduced complexes bind to DNA the most, while the least readily reduced complexes binds the least. Pt (IV) complexes that were incubated with glutathione prior to reacting with DNA however showed substantially increased inhibition over the glutathione-free experiments.<sup>31,33,32,34,35</sup>

Previous work by our research group into the reduction of cyclometallated iodo Pt (II) iminophosphine complexes using sulphur based biomolecules has seen some success, **Figure 4.9**. The Pt (IV) complexes were reacted with sulphur based biomolecules (glutathione and N-acetyl-L-cysteine) at 37°C and investigated for evidence of reduction at specific time periods over 48 hours.

After 6 hours of incubation with glutathione the resulting solution contained 61 % of the Pt (II) reduced analogue, with only 9 % of the starting Pt (IV) complex remaining. Interestingly, there was also significant decomposition of the Pt (IV) complex and its ligands with a peak appearing in the aldehyde region of the <sup>1</sup>H NMR and accounting for almost 30 % of the final solution after 6 hours.

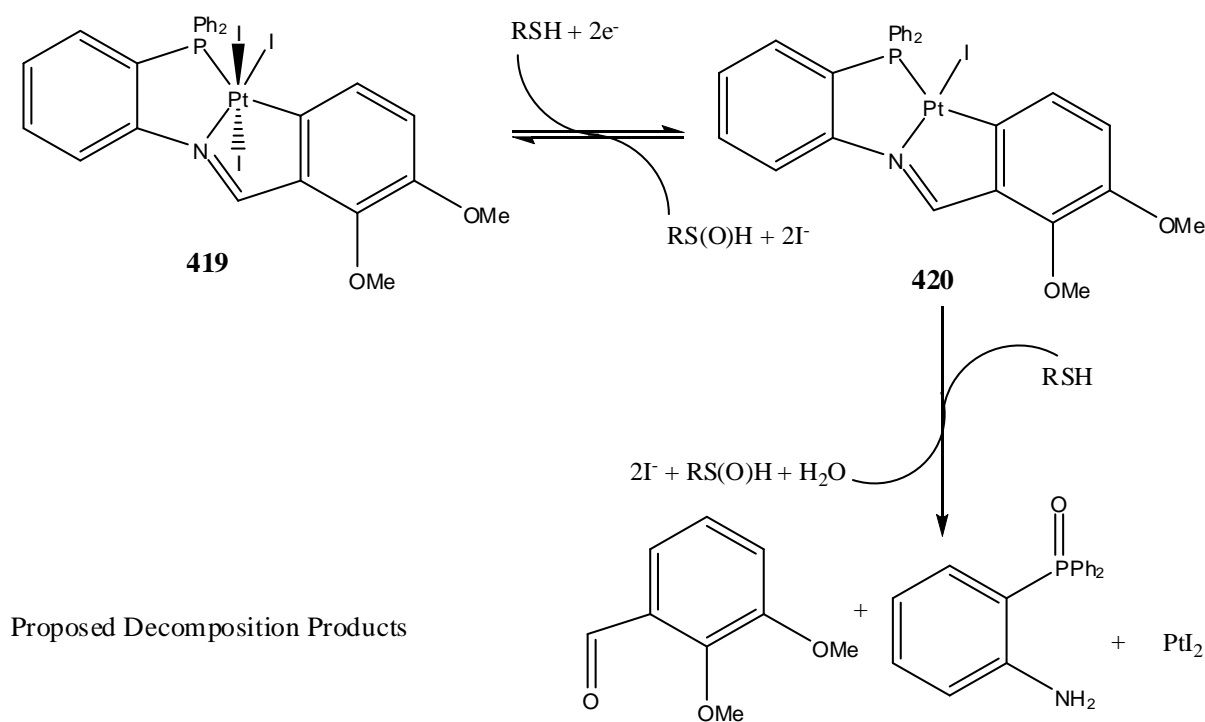


*Figure 4.9: Proposed pathway for Pt (IV) iminophosphine reduction by sulphur containing biomolecules previously reported by our research group.<sup>36</sup>*

After 48 hours the major product found in the solution was the benzaldehyde decomposition product occupying 87 % (relative NMR intensities), while the Pt (II) reduced

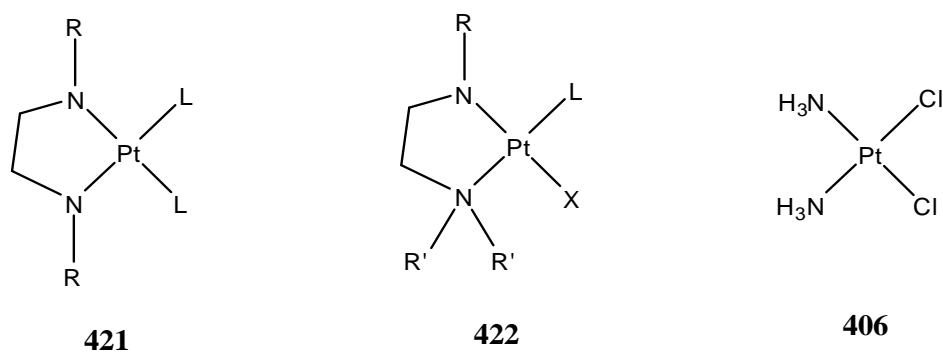
analogue, **420**, was present at 13%. There was no longer any evidence of the Pt (IV) complex, **419**, after 48 hours, indicating that it had all been reduced or suffered decomposition.<sup>36</sup>

In summary our research group has previously identified that the use of thiolates like glutathione (GSH) and N-acetyl-L-cysteine (RSH) reduce Pt (IV) iodo complexes, **419**, to their Pt (II) analogues, **420**. However, further decomposition of the reduced Pt (II) species occurs via acid catalysed hydrolysis. Products formed include an aldehyde (proposed to be similar to the starting material for the synthesis of the ligand) and the insoluble P(O)N 2-diphenylphosphinoaniline oxide, **Figure 4.9**.<sup>36</sup>

### 4.3 In-Vitro Cell Testing of Cyclometallated Platinum Anti-Cancer Drugs:

#### 4.3.1 Monofunctional Complexes:

The development of second and third generation platinum anti-cancer drugs has been driven by the attempts to broaden the spectrum of activity, overcome resistance, and obviate toxic side effects. Over the past forty years some general principles emerged as a guide to the design of new bioactive platinum based anti-cancer therapeutics, and several successful platinum anti-cancer drugs were developed as a result of this and confirmed by *in-vitro* and *in-vivo* testing as outlined in **Chapter 1**.



L = non-leaving group  
X = leaving group

*Figure 4.10: The structures of some complexes tested by Webster et al. The monofunctional complex **422** was found to be very active *in-vitro* and *in-vivo*. Cisplatin **406** is shown for comparison purposes.<sup>37</sup>*

The formation of bifunctional lesions upon the binding of cisplatin to DNA has been linked strongly to its activity and the vast majority of complexes tested to date have

bifunctional leaving groups as part of their structure. There has been much less success reported for monofunctional platinum complexes on the other hand, with many of those reported to date being charged which can cause issues with cell membrane permeability.

However, interesting exceptions have been found for some small monofunctional platinum complexes, particularly in relation to a class of organoamidoplatinum (II) complexes complete with *trans*-amine ligands reported by Webster *et al.* These complexes were found to have excellent activity across *in-vitro*, cellular, and animal studies, and comparable in size and function to that of cisplatin, **Figure 4.10**.<sup>37</sup>

Further reports by Edwards *et al* on neutral cyclometallated complexes have also seen success with their complexes acting as monofunctional DNA binding agents. The low chloride concentration of intracellular fluid leads to hydrolysis, which then forms a reactive cationic species ready to bind covalently to DNA.<sup>38</sup>

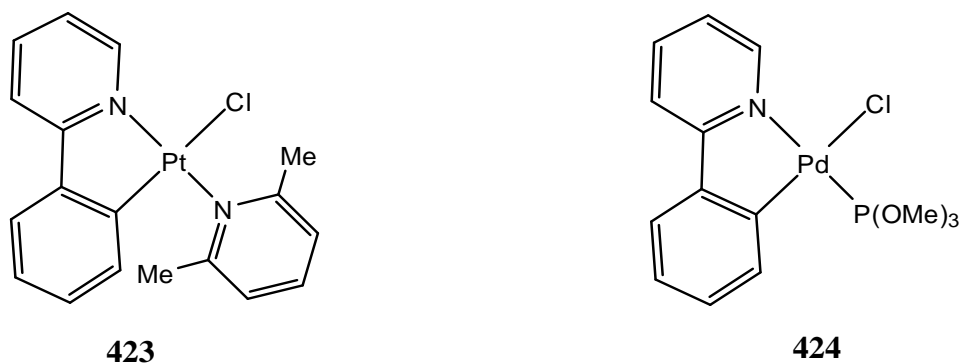


**Figure 4.11:** Neutral monofunctional cyclometallated Pt (II) **423** and palladium (II) **424** complexes reported as very active *in-vitro* with low  $IC_{50}$  values of circa  $1.1 \mu\text{mol/L}$

As the complexes reported by Edwards *et al* are neutral and therefore are insoluble in water. Therefore ethanol, ethanol-dimethyl sulfoxide, or dimethyl sulfoxide was used to prepare the stock solutions and serial dilutions required for testing. The complexes in **Figure 4.11** have an  $IC_{50}$  comparable to that of cisplatin for the same cell lines of approximately  $0.9 \mu\text{mol/L}$ . They also found that the introduction of steric crowding around the metal ion with successive  $\alpha$ -substituents on the pyridine ring, for example complex **423**, leads to greatly enhanced cytotoxicity, **423**, **Figure 4.10**.<sup>38</sup>

They also noted that the presence of unidentate phosphorus donor ligands in general also greatly inhibited cell growth at low concentrations with some complexes showing  $IC_{50}$  values approaching that of cisplatin, **424**, **Figure 4.11**. The nature of the cyclometallated ligand also appears to be crucial for activity particularly if an intercalative mode of binding is

involved in the mechanism of action for these complexes. The increased surface area of the pyrazolylphenyl ligands along with the addition of methyl groups and an extra phenyl ring resulted in enhanced activity, confirming intercalation as part of the biological function of these complexes.<sup>38</sup>

Further work by Edwards *et al* and Kodaka and co-workers into the biological activity of cyclometallated platinum complexes such as **423, Figure 4.12** have seen promising results *in-vivo* also. The platinum cyclometallates were tested against the P388 leukaemia cell line and found to have significant anti-cancer activity at relatively low doses comparable to the widely used anti-cancer agent 5-fluorouracil.<sup>38,39</sup>

In other work by Kodaka *et al* it was found that similar sterically bulky platinum anti-cancer drugs also showed activity against the cisplatin resistant mouse sarcoma 180 cell lines. This has since lead to further investigations into development of new sterically bulky platinum cyclometallated anti-cancer complexes. Interestingly, Edwards *et al* also reported that the palladium complex **424, Figure 4.11**, despite being highly active *in-vitro*, showed no antitumour activity *in-vivo* and was found to be toxic at relatively low doses.<sup>38,39</sup>

### **4.3.2 Tridentate Pt (II) Anti-cancer Drugs and Intercalation:**

Over the past decade, intercalation of Pt (II) and (IV) complexes with DNA has gained significant traction as a biologically viable function for anti-cancer activity, particularly for complexes that employ one leaving group (monofunctional). Lippard *et al* pioneered studies on DNA-metallointercalators using square-planar d<sup>8</sup> Pt (II) complexes, while Barton *et al* subsequently extended the scope to octahedral d<sup>6</sup> metal complexes with aromatic diamine ligands.<sup>40,41</sup>

Recently a number of research groups have reported various biologically active platinum complexes whose mechanism of action is proposed to be primarily intercalation into the strands of the DNA double helix structure.<sup>42–44</sup> Frassinetti *et al* have reported extensively on their complex, **425, Figure 4.12**, which has shown antiproliferative activity towards both a cisplatin-sensitive human ovarian carcinoma cell line as well as its resistant counterpart. Ligand bulkiness and hydrophobicity of the substituents on the thiourea moiety were cited as important for increased biological activity.<sup>44</sup>

As in most DNA-intercalating agents, DNA damage is promoted by the inhibition of topoisomerase II (topo II) activity, an enzyme with the role of maintaining the correct topological properties of DNA which is usually over expressed in cisplatin-resistant cells.



The concentration of  $Mg^{2+}$  ions is also an essential cofactor of topo II activity and it has been shown that decreased magnesium availability leads to the inhibition of topo II enzyme activity, resulting in cell growth arrest.<sup>45</sup>

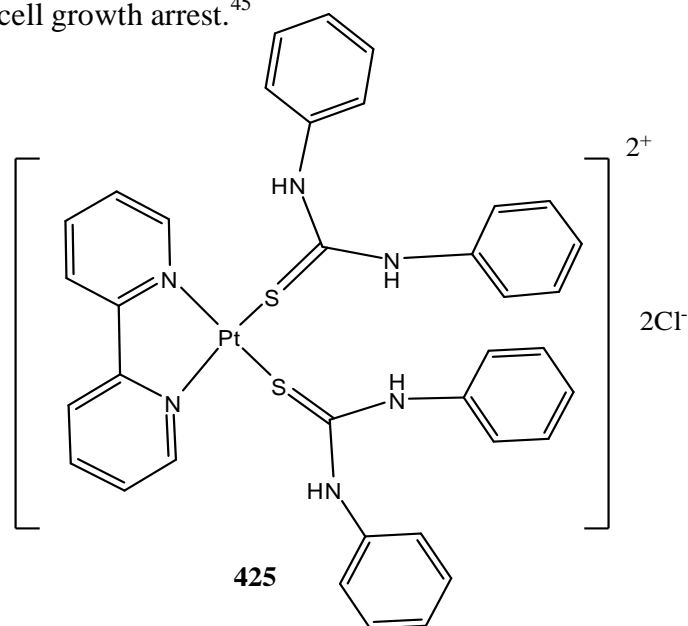
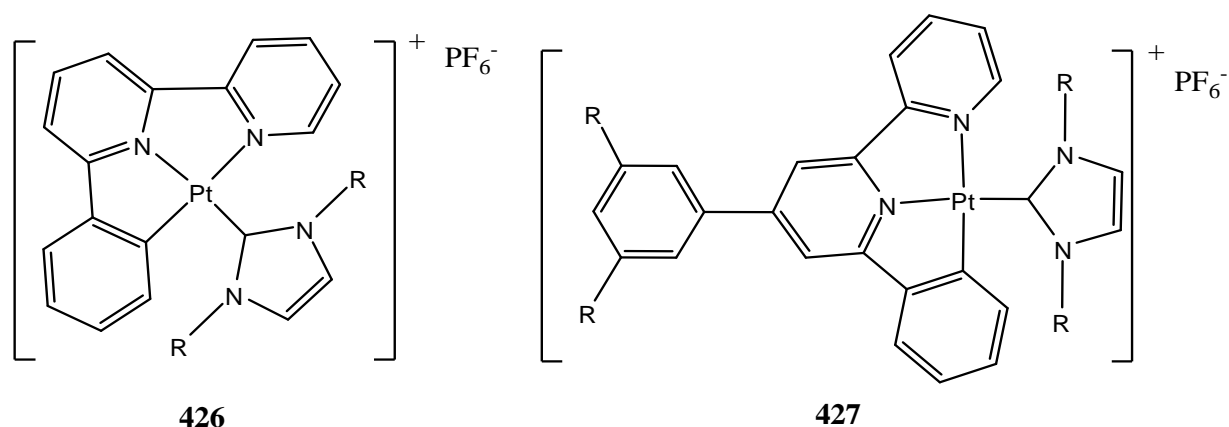


Figure 4.12: A biologically active DNA intercalating Pt (II) complex, **425**.<sup>44</sup>

Frassinetti *et al* have shown that not only does compound **425** greatly accumulate into cells and intercalate into calf thymus DNA, but it also targets topo II activity which affects DNA integrity. It forms and stabilises a ternary drug-DNA-topo II complex.

As discussed in **Chapter 2**, the presence of a strong platinum carbon bond(s) in a Pt (II) anti-cancer complex can also be beneficial for increased anti-cancer activity. It renders Pt (II) cyclometallated complexes to display enhanced stability against biological reduction and ligand exchange reactions. Tridentate chelate complexes offer further stability in the form of the chelate effect and recent work by Che *et al* on a range of bulky platinum cyclometallates has seen induced apoptosis in cancer cells through *in-vitro* and *in-vivo* testing, **Figure 4.13**.<sup>46,47</sup>

Che *et al* initially tested complex **426** with glutathione and found that ligand exchange only occurred for less than 5% of the complex, even after 72 hours. They report that the presence of bulky substituents around the metal centre prevents interaction of sulphur biomolecules with the platinum metal centre, therefore vastly reducing potential side effects of these complexes *in-vivo*.<sup>47</sup>



**Figure 4.13:** Bulky cationic monofunctional cyclometallated Pt (II) complexes reported as being very active *in-vitro* and *in-vivo* with low  $IC_{50}$  values of circa  $0.49 \mu\text{mol/L}$ .<sup>47</sup>

The *in-vitro* studies were carried out on human cancer cell lines of cervical epithelioid carcinoma (HeLa), hepatocellular carcinoma (HepG2), and nasopharyngeal carcinoma, and a normal cell derived human lung fibroblast cell line (CCD-19Lu).  $IC_{50}$  values for compound **426** in particular was found to be between  $0.057$  to  $0.77 \mu\text{M}$ , which is significantly less than the  $IC_{50}$  values for cisplatin on the same cell lines ( between  $2.4$  and  $15 \mu\text{M}$ ). Most of the complexes tested were found to be more cytotoxic than cisplatin with up to 300 fold increases in potency found for the HeLa cell line.<sup>47</sup>

Compound **426** was later carried forward for *in-vivo* testing where it was found that the drug significantly inhibited the growth of NCH-H460 non-small cell lung carcinoma cells by over 55% at  $30 \text{ mg kg}^{-1}$ . It was also noted that the mice did not die during the treatment and regular body weight measurement of the mice showed no significant weight loss.<sup>47</sup>

DNA binding studies of compound **426** with calf-thymus DNA in cell free conditions also revealed that intercalation is the primary interaction the drug has with the double stranded biomolecule. It was also found that this complex preferentially accumulates in the cytoplasmic structure of the cells instead of covalently binding to DNA. Che *et al* cite the strongly coordinating tridentate structure and platinum carbon bond as responsible for the stability of these Pt (II) complexes towards glutathione reduction/substitution within the cell.<sup>47</sup>

As well as antitumoral properties, tridentate cyclometallated platinum complexes have also shown promise as antiparasitics and antibacterial agents. Work by Smith *et al* on cycloplatinated thiosemicarbazones, **Figure 4.14**, have revealed significant antitumour activity *in-vitro* for these compounds. The complexes in **Figure 4.14** were evaluated against

the cisplatin sensitive and cisplatin resistant ovarian cell lines, A2780 and A2780cisR respectively.<sup>48</sup>

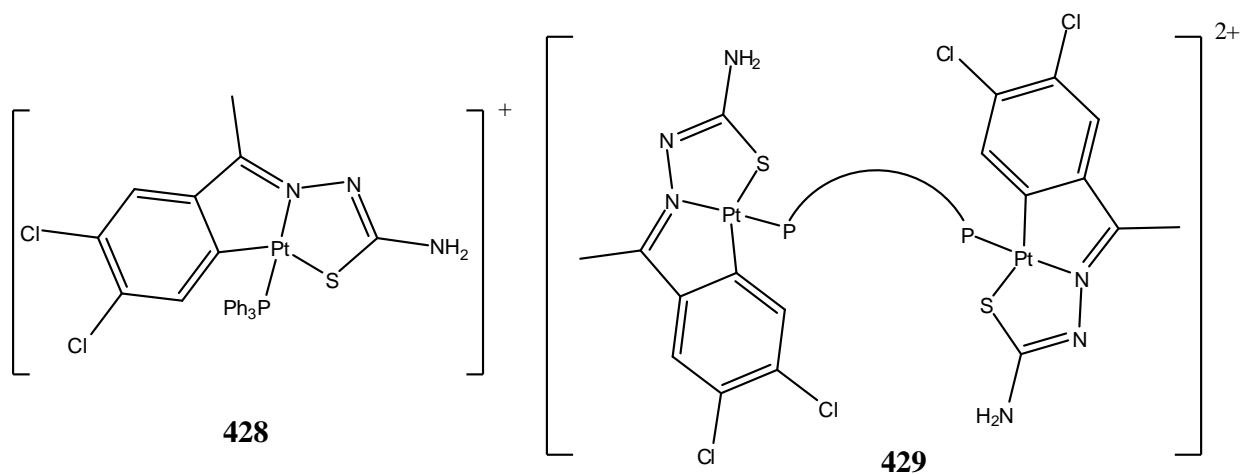


**Figure 4.14:** Tridentate cyclometallated Pt (II) complexes reported as being very active *in-vitro* for antitumour and antiparasitic activity.<sup>48</sup>

While none of the compounds tested showed activity comparable to that of cisplatin against the cisplatin sensitive cell line (A2780), they did however give markedly better results than cisplatin for the cisplatin resistant cell line (A2780cisR) suggesting perhaps that they have a different mechanism of action to cisplatin. As well as antitumour activity these complexes also show moderate antiparasitic activity *in-vitro* against *Plasmodium falciparum* strains, D10 (chloroquine sensitive), Dd2 (chloroquine-resistant), and the parasite *Trichomonas vaginalis*.<sup>48</sup>

It was found that the presence of triphenylphosphine as the ancillary ligand gave the complex better activity as an antiparasitic. Although none of the compounds tested gave activities comparable to that of chloroquine, some of the complexes showed significant percentage inhibition of up to 93%, which is very close to the current FDA approved drug; Metronidazole, which exhibits 100% inhibition at the same concentration. Furthermore it was again found that the presence of an aromatic ring enhanced the cytotoxicity of these complexes in comparison to the clinical drugs cisplatin and carboplatin.<sup>48</sup>

#### 4.4 Photophysical Studies of Platinum Complexes and Mixed Donor Ligands:

##### 4.4.1 Factors Influencing Luminescence of Pt (II) Complexes:

Around 30 years ago, much of the research into platinum coordination chemistry orientated around the unprecedented success of cisplatin and its activity towards cancer cells. However, a small number of simple Pt (II) compounds were beginning to emerge with photoluminescent properties at low temperatures or in solid state. In **Chapter 1** we discussed platinum complex luminescence in detail, as well as the background to luminescence itself. Here we are discussing some of the factors influencing luminescent platinum compounds, their applications and recent advances in the area that may be relevant to current work.

Over the past decade studies on the factors that influence the efficiencies of Pt (II) complexes have been spurred on by the potential application of triplet-emitting metal complexes as phosphors in organic light-emitting devices (OLEDs). These devices are proposed to have the ability to trap otherwise wasted triplet states, which can lead to large gains in efficiency.<sup>49</sup>

Many luminescent active Pt (II) complexes reported to date consist of bidentate diimine ligands such as bipyridine or phenanthroline and the emission depends significantly on concentration and solvent choice, **Figure 4.15**. Compound **430** for instance displays green emission in dilute dichloromethane ( $10^{-5}$  M), however, red emission becomes the dominant band at higher concentrations at the expense of the green band, but the complex retains an identical excitation spectra.<sup>50</sup>

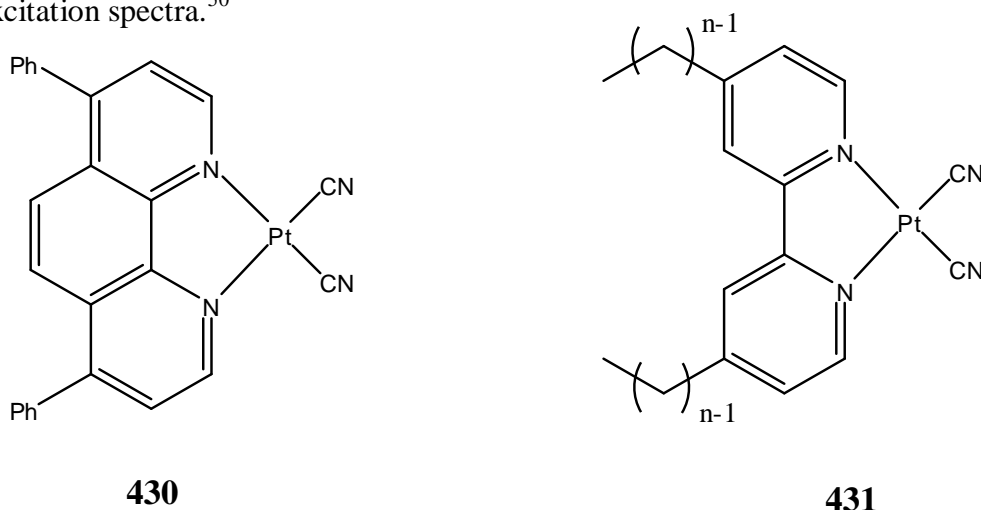


*Figure 4.15: Luminescent Pt (II) complex with the ability to switch its colour of emission in dilute dichloromethane **430**, and a complex which is solvent dependant for excimer emission **431**.<sup>50,51</sup>*



(II) complexes. Platinum carbon complexes and cyclometallated compounds (discussed in **Chapter 1**) have recently gained significant promise as variable emitters.<sup>55–58</sup>

Work by Dungey *et al* has seen the bis-mesityl complex **432**, **Figure 4.16** emit in a toluene solution at room temperature where the strongly  $\sigma$ -donating aryl groups serve to lower the energy of the excited state.<sup>53</sup> Nishida and coworkers have also found emission from a similar complex where the hydrogens on the aryl rings have been replaced by fluorine, **433**, **Figure 4.16**. Emission was however substantially shifted towards the blue region instead due to the electron withdrawing effects of the fluorine substitutions.<sup>54</sup>

Interestingly though, no emission was found to occur by Nishida *et al* for complex **434**, despite the strong emission found for its analogue **433**. The incorporation of methyl substituents at the 2 and 9 position of the dpphen ligand resulted in slightly longer Pt-N bonds due to the steric hindrance caused by the two groups.<sup>54</sup> The solid state X-ray structure also revealed that this structure is “bent” more dramatically out of the plane in comparison to its analogue **433**, resulting in reduced rigidity which is unfavourable for luminescence. Both the reduced rigidity and the increase of the Pt-N bond lengths promote unwanted non-radiative decay.<sup>54</sup>

#### 4.4.2 Luminescence of Small Organic Molecules (Ligands):

Organic LED's are of immense interest to various industries because of their mixed properties, versatility and inexpensive nature. They are generally thin, emit in the visible region, rugged and very power efficient. They generally consist of a thin sandwich of one or more specially designed organic molecules between two electrodes.

One electrode must be transparent to let the light out and a battery voltage across the electrodes generates holes and electrons in the respective layers which upon recombination emit energy in the form of light. The color (energy) of the light depends upon the choice of the organic molecule and can be tuned using well-defined organic synthetic methods.<sup>59</sup>

Usually the organic molecule used is polymeric in nature and incorporates into a single functional group such as sulphur or nitrogen. Some research groups however have found success with mixed phosphorus and nitrogen type functional groups within the polymeric structure, **Figure 4.17**, including those with imines and phosphines.<sup>59,60</sup>



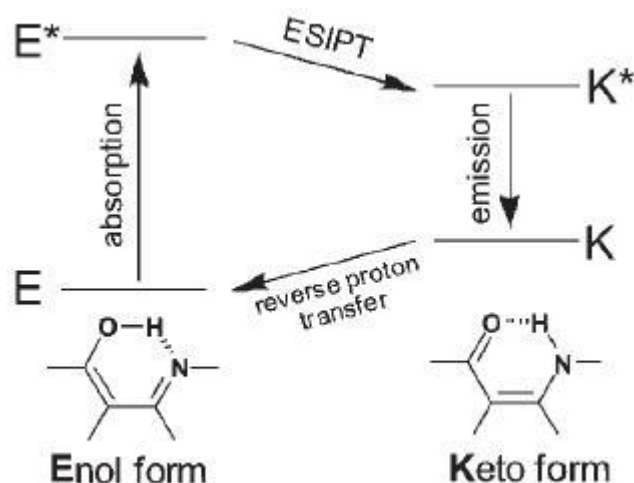


*Figure 4.19: Schematic representation of the ESIPT photocycle reported for small luminescent molecules.<sup>62</sup>*

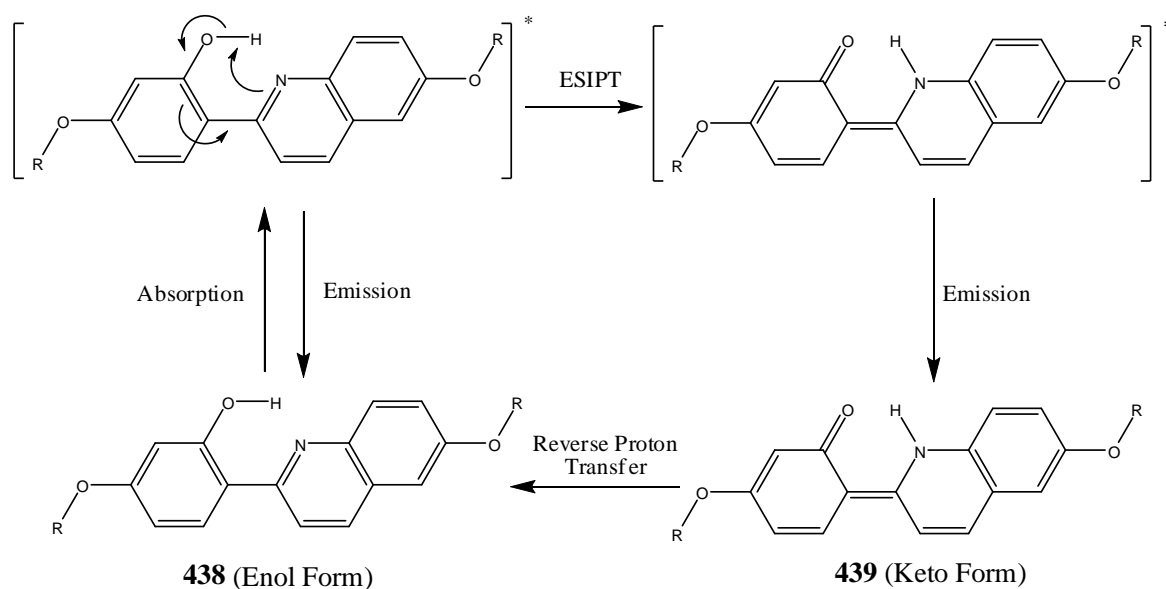


*Figure 4.20: The photophysical and photochemical processes of a phototautomerizable quinoline unit resulting in blue band emission.<sup>64</sup>*

These compounds readily form large single crystals exhibiting intense blue fluorescence at 460 nm and low-threshold amplified spontaneous emission (ASE). The steric crowding of the four phenyl groups substituted into the imidazole ring limit the excessive tight-stacking responsible for intermolecular vibrational coupling and relevant non-radiative relaxation, resulting in strong fluorescence emission in the crystal state, **Figure 4.19** and **Figure 4.20**.<sup>62</sup>



#### 4.5 Summary and Conclusions:

From the literature reviewed it is clear that sulphur based biomolecules are integral to the biological activity of Pt (II) and (IV) anti-cancer complexes. It has been found that in particular methionine and glutathione play an important role in helping the biological activity of currently approved Pt (II) drugs such as carboplatin. However, it has also been noted by a number of research groups that glutathione also deactivates Pt (II) drugs and in some cases even cause a decrease in cellular accumulation due to efflux of the platinum-glutathione adduct out of the cell.

In the case of the Pt (IV) anti-cancer complexes studied by our research group and others, glutathione was seen as essential for reduction of the complex to its active Pt (II) analogue *in-vivo*. It was found that without reduction to the Pt (II) analogue, the Pt (IV) complexes have very little or no activity towards cancer cells. Therefore it was seen that glutathione and other sulphur biomolecules are necessary for these pro-drugs to be biologically active.

Successful *in-vitro* cell testing has been reported for various Pt (II) neutral complexes even though water proved to be an unsuitable solvent for preparation of the stock solutions. Therefore, preparation and serial dilutions of a number of compounds were carried out in ethanol, ethanol-dimethyl sulfoxide, or dimethyl sulfoxide. These compounds were found to have biological functionality comparable to that of cisplatin in some cases. Successful *in-vitro* cell testing used cisplatin as the control to compare IC<sub>50</sub> values and overall activity.

The vast majority of approved platinum anti-cancer drugs are bifunctional, i.e. they have two leaving groups; which are chlorides in the case of cisplatin. However, monofunctional complexes, i.e. those that employ one leaving group, have recently also been reported capable of biological functionality via intercalation of the Pt (II) and (IV) complexes with DNA. Flat planar structures with multiple aryl rings have proven to have biological activity comparable to that of cisplatin but employ more stable molecular structures ensuring longer survival *in-vivo*.

The potential application of triplet-emitting metal complexes as phosphors in organic light-emitting devices (OLEDs) has spurred extensive research into possible Pt (II) luminescent complexes. These devices are proposed to have the ability to trap otherwise wasted triplet states, which can lead to large gains in efficiency

It has been reported that rigid platinum complexes with nitrogen donor moieties and organometallic bonds can successfully emit light across a range of light bands. However, even

slight differences in the complex structure can prevent luminescence even in analogues of very successful luminescent complexes.

Until recently, the use of ligands containing donor moieties such as nitrogen and phosphorus was dominated by research into new polymeric compounds for organic LEDs. However, in the past decade researchers have found extensive success with small organic molecules as blue-band emitters via Excited State Intramolecular Proton Transfer (ESIPT) where tautomerism from a keto form to an enol form can facilitate potential luminescence.

#### **4.6 Synthesis of Cyclometallated Pt (II) Bio-Adducts:**

All the starting materials used in this chapter are prepared as per the procedures outlined for the ligands, platinum complexes, substitution products and oxidation products in **Chapter 2** and **3**. Only the Pt (II) iminophosphine cyclometallates **281** and **284** (3-H and 2,3-(OMe)<sub>2</sub>) were used for biological studies towards sulphur containing biomolecules and *in-vitro* cell testing due to their superior yields, solubility and stability over all other compounds reported. Both complexes were purified by re-crystallisation and characterised by NMR and IR spectroscopy along with elemental analysis prior to all biological studies to ensure no impurities were present.

The ligand HL<sup>1</sup> **261** and the complexes derived from it, reported in **Chapter 2** and **3**, were also the subject of UV visible and luminescent studies to investigate their photophysical properties.

##### **4.6.1 Synthesis of the Pt (II) N-acetyl-L-cysteine bio-adducts of the general formula [Pt( $\eta^3$ -PNC-L<sup>1/4</sup>)N-Acetyl-L-Cys] 440-441:**

The synthetic method utilised for reactions with N-acetyl-L-cysteine is a variation of the procedure outlined previously in **Chapter 3** for the triphenylphosphine (PPh<sub>3</sub>) substitution reactions involving the Pt (II) cyclometallates **281-284**.<sup>65</sup> Previous reports by this research group into the reactivity of iodo Pt (II) cyclometallates with biomolecules also used a variation of this procedure (90:10 chloroform:methanol mixture).<sup>36</sup>

Non-mixed solvent systems consisting of just chloroform or just methanol proved to be unsuccessful, as did aqueous systems due to the insolubility of the platinum complexes in water and the biomolecules being insoluble in chloroform. Therefore a 1:1 mixture of dry methanol:chloroform was found to be an ideal solvent system for dissolving both the Pt (II)

complex and the biomolecule compound. A methanolic solution of N-acetyl-L-cysteine was added dropwise to a stirred solution of the iminophosphine cycloplatinated complexes **281** and **284** in a 1:1 methanol:chloroform solvent system over one hour.

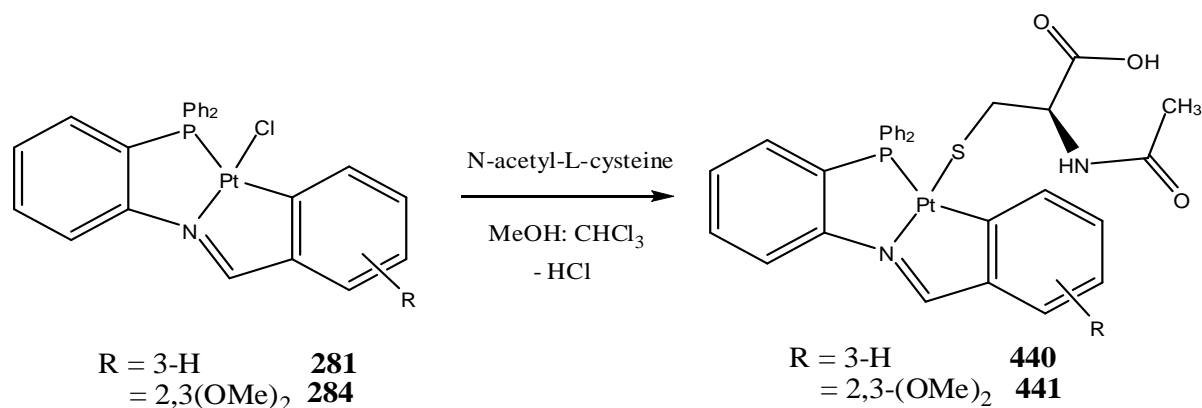


**Figure 4.21:** Formation of the Pt (II) iminophosphine biomolecule adducts with N-acetyl-L-cysteine to form **440-441**.

The solution immediately changed from orange to a dark red colour on addition of the N-acetyl-L-cysteine. After 20 hours it became a pale yellow colour and TLC analysis confirmed that the platinum (II) starting material was no longer present. The reaction mixture was then reduced to dryness *in vacuo* and then taken up in dichloromethane (where it again turned dark red) and washed once with a small portion of distilled water to remove any remaining N-acetyl-L-cysteine and HCl formed during the reaction. The organic layer was dried over MgSO<sub>4</sub>, reduced to dryness *in vacuo* again and the resulting dark red solution was crystallised from distilled methanol layered with hexane to form the neutral Pt (II) N-acetyl-L-cysteine bio-adducts **440-441**, **Figure 4.21**.

Bio-Adduct	Precursor	Physical appearance	% Yield
<b>440</b>	<b>281</b>	Dark red powder	78
<b>441</b>	<b>284</b>	Dark red powder	85

**Table 4.1:** Yields and appearances for the iminophosphine Pt (II) N-acetyl-L-cysteine bio-adducts **440** and **441**.

The reaction gave good yields, however increasing the temperature to 37°C had little or no impact on the final yield. Interestingly, however, it was found that the final platinum bio-adducts **440-441** were slightly water soluble with some of the yield being lost to the

water layer during the washing procedure to remove the remaining N-acetyl-L-cysteine. This was confirmed by TLC analysis of the water layer after the washing.

The importance of stabilisation of the displaced anion, chloride, by the solvent system, like that reported previously in **Chapter 3** for the triphenylphosphine substitutions, was again identified here. The proposed mechanism for the reaction of these platinum complexes with biomolecules therefore involves the direct displacement of the chloride moiety owing to the stronger Pt-S (soft acid-soft base) interaction formed with the newly introduced N-acetyl-L-cysteine (or L-glutathione in **Section 4.6.2**) over that of the weaker Pt-Cl (soft acid-hard base) bond, coupled with solvent assisted stabilisation of the liberated chloride as discussed in **Chapter 3**. A summary of the complexes synthesised, their yields and physical appearances, are displayed in **Table 4.1**.

These complexes were characterised and their identities confirmed by IR and NMR spectroscopy as well as elemental analysis which are all consistent with the proposed structure of these compounds and compare well with previously reported analogous complexes.<sup>66</sup> It was noted, however, that unlike previous work with PNC and PNO type complexes by our research group, both Pt (II) N-acetyl-L-cysteine bio-adducts **440-441** are air and light sensitive. The solid form decays and changes colour from dark red to yellow/orange over 16 hours in sunlight and over 48 hours without sunlight. In a solution of dimethylsulfoxide this is roughly increased to 20 hours in sunlight and 72 hours without sunlight.

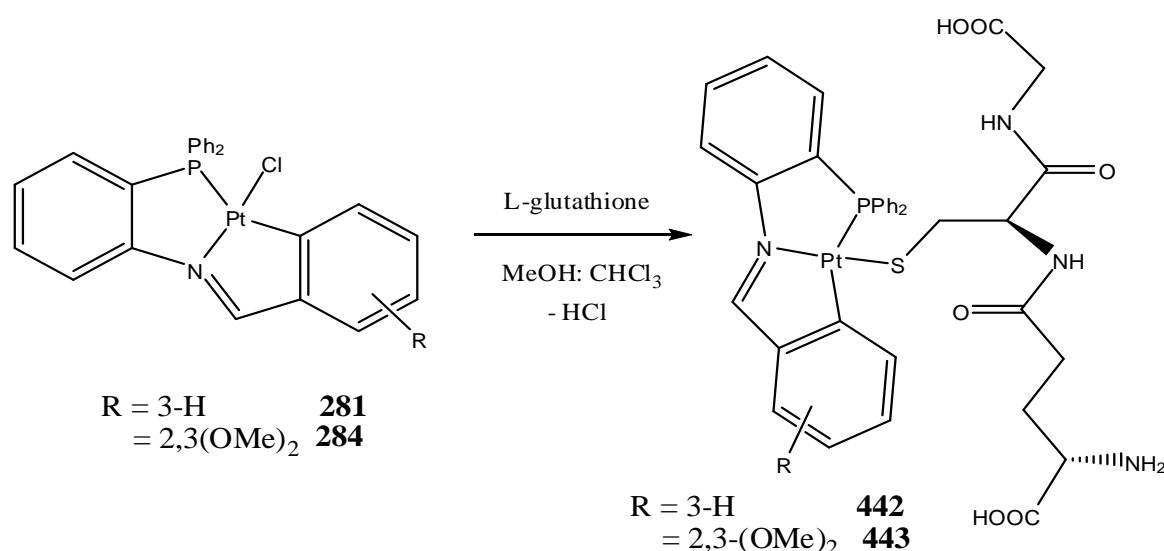
After this time there is no longer any evidence for the Pt (II) bio adduct or its Pt (II) starting material. No identifiable decomposition products, like an aldehyde peak, have been identified from these reactions, implying formation of alternative products.

Photo decomposition has been reported previously for other sulphur based Pt (II) complexes and is proposed to consist of a photo-oxidation process.<sup>67</sup> Although the resulting products are currently unidentifiable at this time for the N-acetyl-L-cysteine Pt (II) bio-adducts **440-441**, having photo sensitive properties may also have positive implications for uses in photo-dynamic therapy (PDT) if the products formed have greater cytotoxicity over the platinum bio-adducts, as discussed in **Chapter 1**. However, further research into the mechanisms employed here and products formed are required to better understand the process.

#### 4.6.2 Synthesis of the Pt (II) L-glutathione bio-adducts of the general formula [Pt( $\eta^3$ -PNC-L<sup>1/4</sup>)Glu] 442-443:

The synthetic method utilised for reactions with L-glutathione is also a variation of the procedure outlined previously in **Chapter 3** for the triphenylphosphine (PPh<sub>3</sub>) substitution reactions involving the Pt (II) cyclometallates **281-284**, and is similar to that used to that used in **Section 4.6.1** for N-acetyl-L-cysteine.<sup>65</sup>

A 1:1 mixture of dry methanol:chloroform was again found to be an ideal solvent system for dissolving both the Pt (II) complex and the biomolecule compound since an aqueous system could not be employed due to the neutral nature of the Pt (II) complexes. A methanolic solution of L-glutathione was added dropwise to a stirred solution of the iminophosphine cycloplatinated complexes **281** and **284** in a 1:1 methanol:chloroform solvent system over one hour.



*Figure 4.22: Formation of the Pt (II) iminophosphine biomolecule adducts with L-glutathione to form 442-443.*

The solution immediately changed from orange to a dark red colour on addition of the L-glutathione. After 48 hours it became a pale yellow colour and completion was confirmed by TLC analysis. The reaction mixture was then reduced to dryness *in vacuo* and taken up in dichloromethane (where it again turned dark red) and washed once with a small portion of distilled water to remove any remaining L-glutathione and HCl formed during the reaction. The organic layer was dried over MgSO<sub>4</sub>, reduced to dryness *in vacuo* again and the resulting

dark red solution was crystallised from distilled methanol layered with hexane to form the neutral Pt (II) L-glutathione bio-adducts **442-443**, **Figure 4.22**.

Like that found for the N-acetyl-L-cysteine, increasing the temperature to 37°C had little or no impact on the final yield of the reaction with L-glutathione, however, reaction time was decreased to circa 36 hours. Also it was found again here that the final platinum bio-adducts **442-443** were quite water soluble with some of the yield being lost to the water layer during the washing procedure. It was also found that these adducts were much more water soluble in comparison to the N-acetyl-L-cysteine Pt (II) adducts, **Section 4.6.1**. This was confirmed by TLC analysis of the water layer after the washing. A summary of the complexes synthesised, their yields and physical appearances, are displayed in **Table 4.2**.

Bio-Adduct	Precursor	Physical appearance	% Yield
<b>442</b>	<b>281</b>	Dark red powder	72
<b>443</b>	<b>284</b>	Dark red powder	77

*Table 4.2: Yields and appearances for the iminophosphine Pt (II) L-glutathione bio-adducts 442 and 443.*

These complexes were characterised and confirmed by IR and NMR spectroscopy as well as elemental analysis which are all consistent with the proposed structure of these compounds. It was also found that both Pt (II) L-glutathione bio-adducts are air and light sensitive, unlike previous work by our research group with chloro PNO type complexes.<sup>68</sup> Both the solid form and dimethylsulfoxide solution decay from dark red to yellow/orange over 6 hours in sunlight and over 24 hours without sunlight. This represents a shorter reaction time in comparison to the Pt (II) N-acetyl-L-cysteine bio-adducts.

After this time there is no longer evidence for the Pt (II) L-glutathione bio adduct or its Pt (II) starting material. Like that found for N-acetyl-L-cysteine no identifiable decomposition products have been identified from these reactions, although having photo sensitive properties may have positive implications for possible uses in photo-dynamic therapy (PDT) as discussed in **Chapter 1**. Of interest for this platinum bio-adduct also is its increased water solubility over the Pt (II) N-acetyl-L-cysteine bio-adduct, which is hugely beneficial for biological applications in terms of administration as an anti-cancer drug.

### 4.6.3 Other reactions involving biomolecules and platinum complexes:

Some reactions with the other cyclometallated iminophosphine Pt (II) complexes **282-283** and the Pt (II) phosphinoamides **286-288** as well as the bidentate iminophosphine complexes **271-273** were attempted. Reactions were found to occur however characterisation is currently inconclusive due to solubility issues and the formation of a complicated mixture of products.

The PNO complex **285** was also reacted with L-Glutathione but it was found that after 24 hours stirring at room temperature, the Pt (II) starting material was recovered. However, it was returned in a low yield of circa 40%, along with an unidentifiable yellow solid. However, there was no evidence of a platinum bio-adduct from IR or NMR studies and the products formed are insoluble in a variety of solvents, **Figure 4.23**.

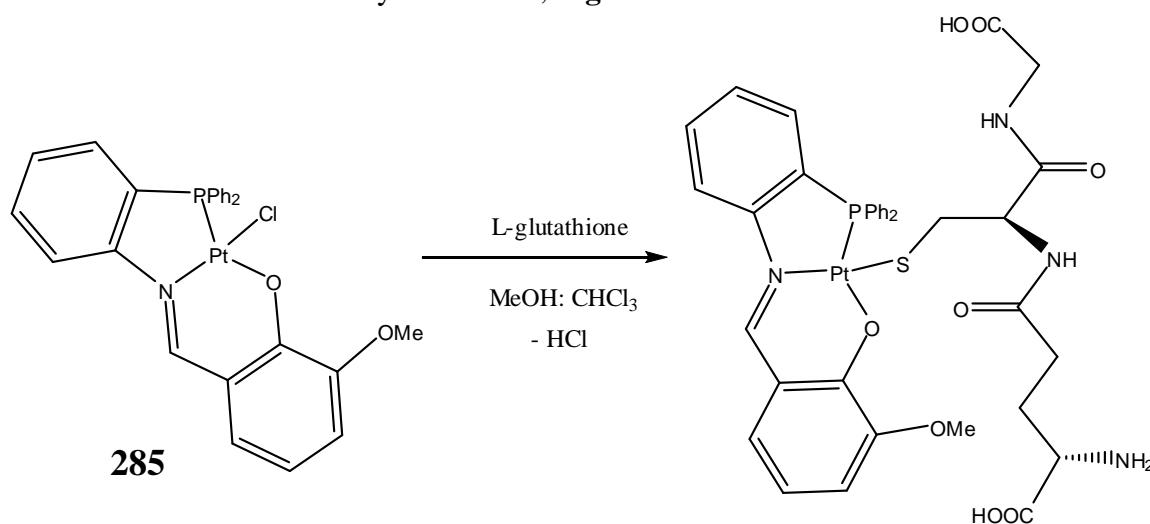


*Figure 4.23: Proposed pathway for the reaction of Pt (II) PNO iminophosphine complex with L-glutathione, which was unsuccessful.*

It is proposed that the steric crowding around the metal centre caused by the oxygen moiety of the iminophosphine ligand reduces possible interaction of the PNO complex, **285**, with L-glutathione. However, when the PNO complex was reacted with N-acetyl-L-cysteine a reaction did occur with no Pt (II) starting material remaining after 24 hours. The Pt (II) N-acetyl-L-cysteine bio-adduct could not be characterised however as the product formed was insoluble.

The iminophosphine Pt (IV) complexes **381-384** reported in **Chapter 3** were also reacted with L-glutathione with the objective of inducing biological reduction of the octahedral Pt (IV) structures to their Pt (II) square-planar analogues, **Figure 4.24**. Previously

within our research group successful reduction was observed for the analogous Pt (IV) iodo complexes where after 24 hours reduction to the Pt (II) analogue was observed.<sup>36</sup>

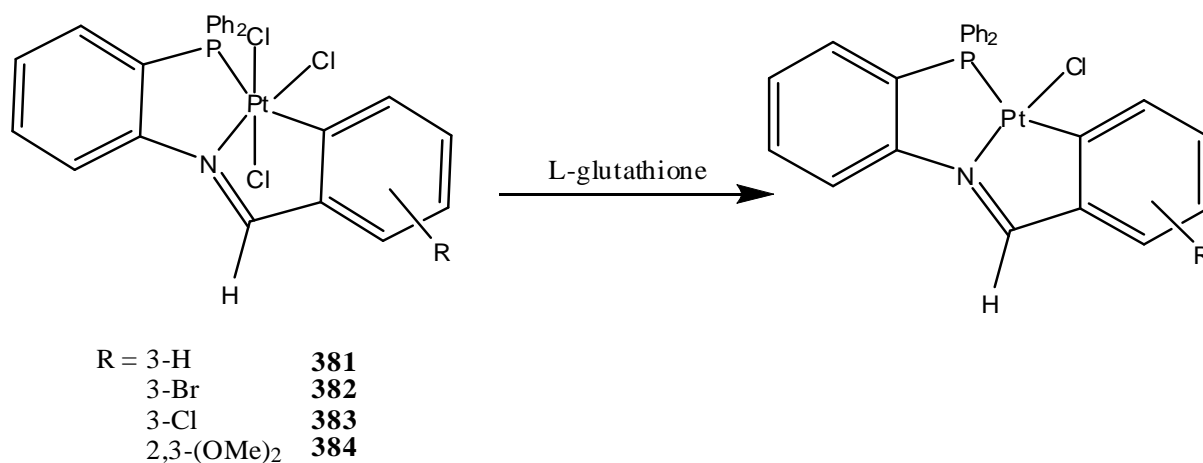


*Figure 4.24: Proposed pathway for the reaction of the Pt (IV) iminophosphine complexes 381-384 with L-glutathione, which remains inconclusive.*

The Pt (IV) complexes **381-384** were stirred with L-glutathione in a 1:1 methanol:chloroform solvent system for circa 16 hours. However, unlike previous reports by our research group, there was no evidence of reduction of the Pt (IV) complexes observed by NMR or IR. Currently, characterisation of the final products remains inconclusive with only some of the Pt (IV) starting material identified in the final products by <sup>1</sup>H NMR. Decomposition was also identified by <sup>1</sup>H NMR with the appearance of an aldehyde peak after extended reaction times of 48 hours. Further work is required for these reactions in order to better understand the mechanisms employed and obtain any potential reduction products.

#### 4.6.4 Infra-red spectroscopic studies of the platinum bio-adducts [Pt( $\eta^3$ -PNC-L<sup>1/4</sup>)Glu/NaLCys]:

Like that seen for the complexes reported in **Chapter 2** and **3**, one of the most informative peaks in the IR spectra of the platinum bio-adducts is the imine stretching band,  $\nu(\text{C}=\text{N})$  at circa  $1600\text{cm}^{-1}$ . A comparison of the stretching frequencies of the parent complexes **281** and **284** with their analogous platinum bio-adducts **441-443** are contained in **Table 4.3**, along with the stretching frequencies of the free iminophosphine ligands **HL<sup>1-4</sup>** **261-264**.



Free Ligands	$\nu(\text{C}=\text{N})$ $\text{cm}^{-1}$	Parent complex	$\nu(\text{C}=\text{N})$ $\text{cm}^{-1}$	Platinum Bio-adducts	$\nu(\text{C}=\text{N})$ $\text{cm}^{-1}$
<b>HL<sup>1</sup> 261</b>	1626	<b>281</b>	1585	<b>440</b>	1586
<b>HL<sup>4</sup> 264</b>	1615	<b>284</b>	1578	<b>441</b>	1600
<b>HL<sup>1</sup> 261</b>	1626	<b>281</b>	1585	<b>442</b>	1590
<b>HL<sup>4</sup> 264</b>	1615	<b>284</b>	1578	<b>443</b>	1602

*Table 4.3: IR data comparing the  $\nu(\text{C}=\text{N})$  of the platinum bio-adducts 440-443 with their parent complexes 281-285 and their free ligands 261-264.*

On substitution of the iminophosphine chloro complexes by N-acetyl-L-cysteine and L-glutathione, we see a slight increase observed for the  $\nu(\text{C}=\text{N})$  stretching frequency in the Pt (II) bio-adducts **440-443**. This increase is also slightly larger than that previously found for the triphenylphosphine ( $\text{PPh}_3$ ) substituted complexes reported in **Chapter 3, 371-375** by circa  $10 \text{ cm}^{-1}$ . This indicates a strengthening of, and hence shortening of, the imine  $\text{C}=\text{N}$  bond, but also weakening of the Pt-N bond due to lengthening in order to accommodate the large biomolecule *trans* to the nitrogen donor moiety. This is primarily due to the strong *trans effect*, as discussed in **Chapter 3**, exerted by the new biomolecule ligand introduced *trans* to this coordination bond.

Steric effects of the newly introduced biomolecule on the Pt (II) complex can also exert a significant influence on the bond *trans* to the Pt-S bond and therefore could also be a factor here. These trends mirror those obtained previously by our research group for the analogous iodo Pt (II) cyclometallated bio-adducts.<sup>36</sup>

Other stretching frequencies corresponding to the newly introduced biomolecule were also observed and compared to an IR spectrum obtained for N-acetyl-L-cysteine and L-glutathione prior to reaction with the platinum complexes. A shift was observed corresponding to the  $\nu(\text{C}=\text{O})$  stretching frequency in the Pt (II) N-acetyl-L-cysteine bio-adduct at  $1728 \text{ cm}^{-1}$ , which represents a slight increase from  $1717 \text{ cm}^{-1}$  observed in the free N-acetyl-L-cysteine.

This was also observed for the Pt (II) L-glutathione bio-adduct where a  $\nu(\text{C}=\text{O})$  stretching frequency was found at  $1726 \text{ cm}^{-1}$ , which is again an increase from  $1713 \text{ cm}^{-1}$  found for the free L-glutathione biomolecule. In addition to that,  $\nu(\text{O}-\text{H})$  stretching frequencies were also found for all Pt (II) bio-adducts and the free biomolecules at circa  $3415 \text{ cm}^{-1}$  as well as extra  $\nu(\text{C}=\text{C})$  stretching frequencies at circa  $1440 \text{ cm}^{-1}$ .

The most significant stretching frequency in relation to the biomolecules, however, is  $\nu(\text{S-H})$ , observed at  $2548\text{ cm}^{-1}$  for the free N-acetyl-L-cysteine biomolecule and  $2525\text{ cm}^{-1}$  for the free L-glutathione biomolecule. For the platinum bio-adducts this stretching frequency is not observed in the IR spectra, indicating successful coordination of the sulphur biomolecules to the metal centre due to the loss of the hydrogen from the sulphur group to form HCl with the chloride from the platinum complex.

#### 4.6.5 NMR spectroscopic studies for the platinum bio-adducts Pt( $\eta^3\text{-PNC-L}^{1/4}$ )Glu/NaLCys]:

Complex	$\delta$ (H-C=N)	$\delta$ (H-Ar)	$\delta$ (R=OCH <sub>3</sub> )	$\delta$ (CH <sub>3</sub> ,CH <sub>2</sub> , CH)	$\delta$ ( <sup>31</sup> P{ <sup>1</sup> H})
3-H <b>440</b>	9.68 (1H, s) <sup>3</sup> J <sub>Pt-H</sub> = 91 Hz	7.22-7.98 (18H, m)	-	1.92 (3 H, s) 2.90-3.41 (2 H, m) 4.32 (1 H, s)	31.4 (s) <sup>1</sup> J <sub>Pt-P</sub> = 2184 Hz
2,3-(OMe) <sub>2</sub> <b>441</b>	9.94 (1 H, s) <sup>3</sup> J <sub>Pt-H</sub> = 96 Hz	7.19-7.96 (16 H, m)	3.87 (3 H, s) 4.01 (3 H, s)	1.93 (3 H, s) 2.96-3.31 (2 H, m) 4.10 (1 H, s)	31.1 (s) <sup>1</sup> J <sub>Pt-P</sub> = 2195 Hz
3-H <b>442</b>	10.19 (1H, s) <sup>3</sup> J <sub>Pt-H</sub> = 84 Hz	7.37-8.24 (18H, m)	-	1.75-1.87 (2 H, m) 2.05-2.98 (6 H, m) 4.10-4.16 (2 H, m)	31.4 (s) <sup>1</sup> J <sub>Pt-P</sub> = 2188 Hz
2,3-(OMe) <sub>2</sub> <b>443</b>	10.51 (1 H, s) <sup>3</sup> J <sub>Pt-H</sub> = 86 Hz	7.41-8.27 (16 H, m)	3.98 (3 H, s) 4.05 (3 H, s)	1.25-2.18 (4 H, m) 2.20-3.58 (4 H, m) 4.63-4.67 (2 H, m)	32.2 (s) <sup>1</sup> J <sub>Pt-P</sub> = 2198 Hz

10. Chemical shift values ( $\delta$ ) are expressed in ppm relative to the TMS standard for <sup>1</sup>H and H<sub>3</sub>PO<sub>4</sub> for <sup>31</sup>P.

11. s, singlet; d, doublet; dd, doublet of doublets; t, triplet; q, quartet; m, multiplet.

12. Coupling constants (J) are measured in Hz

**Table 4.5:** The <sup>1</sup>H and <sup>31</sup>P{<sup>1</sup>H} NMR spectra<sup>1,2,3</sup> recorded for the iminophosphine Pt (II) bio-adducts **440-443**. All ran in DMSO-d<sub>6</sub> at 300 MHz for <sup>1</sup>H NMR and 121.5 Hz for <sup>31</sup>P{<sup>1</sup>H} NMR.

The <sup>1</sup>H and <sup>31</sup>P{<sup>1</sup>H} NMR data of the platinum bio-adduct complexes **440-443** are summarised in **Table 4.5**. All of the complexes display the characteristic single resonance

integrating for 1H in the azomethine region of the  $^1\text{H}$  NMR spectra, as well as extra signals for the newly introduced ligands (N-acetyl-L-cysteine and L-glutathione).

There is a downfield shift found for these azomethine resonances of between  $\delta$  0.22 and 0.79 ppm, which is a smaller shift than that found for the triphenylphosphine substituted Pt (II) complexes reported in **Chapter 3** (circa  $\delta$  1.20 ppm). Like that found for the parent Pt (II) complexes **281-285** and  $\text{PPh}_3$  substituted complexes **371-375**, on donation of the lone pair of electrons from the imino-nitrogen moiety into the metal centre, electron density is pulled towards the metal-donor coordination bond (Pt-N), weakening the  $\text{H-C=N}$  bonds.

The observed downfield shift in the NMR spectra correlates with this reduction in bond strength also seen in the IR data for these complexes, **Section 4.6.4**. The shifts for these complexes are also consistent with previously obtained results by our research group and others for analogous complexes.<sup>36</sup> These shifts indicate successful coordination of the sulphur moiety of N-acetyl-L-cysteine and L-glutathione to the metal centre. A comparison of the azomethine shifts for the Pt (II) bio-adducts **440-443** and their respective parent Pt (II) chloro complexes **281** and **284** is shown below in **Table 4.6**.

Pt (II) parent complex	$\delta(\text{H-C=N})$ ppm	Pt (II) Bio-adducts	$\delta(\text{H-C=N})$ ppm	$\Delta\delta$ ppm
3-H <b>281</b>	9.40 (1H, s) $^3J_{\text{Pt-H}} = 123$ Hz	<b>440</b>	9.68 (1H, s) $^3J_{\text{Pt-H}} = 91$ Hz	0.28
2,3-(OMe) <sub>2</sub> <b>284</b>	9.72 $^3J_{\text{Pt-H}} = 126$ Hz	<b>441</b>	9.94 (1 H, s) $^3J_{\text{Pt-H}} = 96$ Hz	0.22
3-H <b>281</b>	9.40 $^3J_{\text{Pt-H}} = 123$ Hz	<b>442</b>	10.19 (1H, s) $^3J_{\text{Pt-H}} = 84$ Hz	0.79
2,3-(OMe) <sub>2</sub> <b>284</b>	9.72 $^3J_{\text{Pt-H}} = 126$ Hz	<b>443</b>	10.51 (1 H, s) $^3J_{\text{Pt-H}} = 86$ Hz	0.78

*Table 4.6: Comparison of the  $^1\text{H}$  azomethine signals between the parent complexes **281** and **284** with that recorded for the Pt (II) bio-adducts **440-443**.*

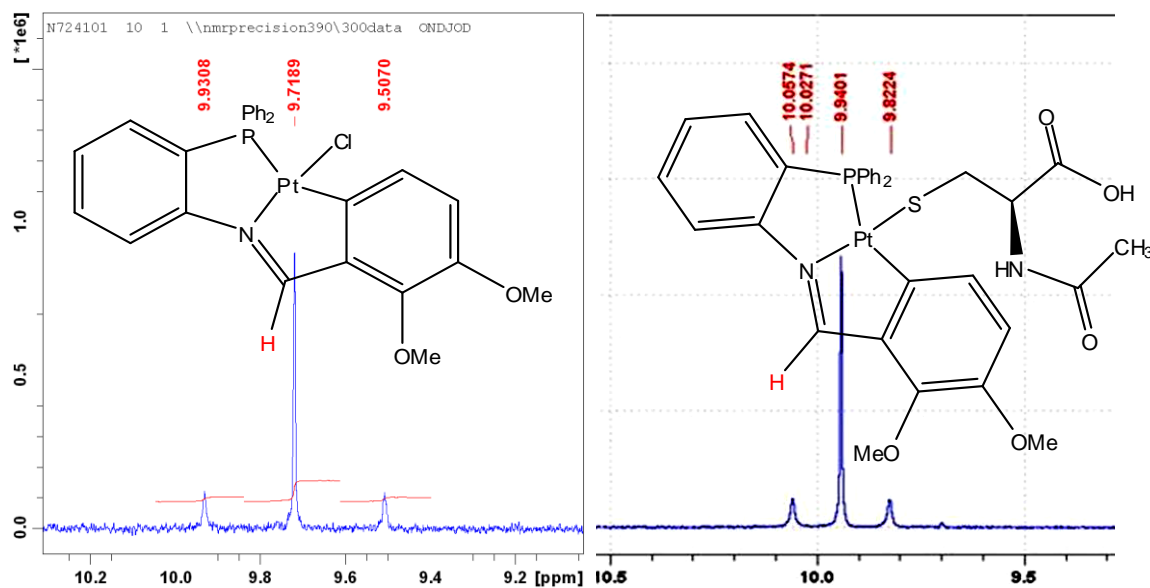


**Figure 4.25:** Comparison of the <sup>1</sup>H azomethine signal spectra for the parent cyclometallated Pt (II) complex **284** (left) and the N-acetyl-L-cysteine Pt (II) bio-adduct **441** (right).

The azomethine signals for the Pt (II) bio-adducts are displayed as a singlet resonance complete with <sup>195</sup>Pt satellites and a <sup>3</sup>J<sub>Pt-H</sub> coupling of ca. 84-96 Hz, **Figure 4.25**. Compared to the parent Pt (II) complexes there is a reduced coupling constant for <sup>3</sup>J<sub>Pt-H</sub> observed due to the strong *trans* effect and decreased electrophilicity of the Pt (II) metal centre due to successful coordination of the electron-rich sulphur biomolecule, **Table 4.6**. The coupling constants of 84-96 Hz found here are quite similar to those found for the PPh<sub>3</sub> substituted complexes reported in **Chapter 3**, which were found to be between 86 and 88 Hz.

The <sup>1</sup>H NMR spectra of the dimethoxy Pt (II) bio-adducts **441** and **443** (**Figure 4.26**) also display two singlet resonances at circa δ 3.87 and δ 4.01 ppm respectively. Like the parent Pt (II) complexes and PPh<sub>3</sub> substituted complexes these correspond to the two electron donating methoxy (-OCH<sub>3</sub>) substituents present at the C-3 and C-2 position of the lower aryl ring and integrate for 3 hydrogens each. This also represents a slight shift downfield in comparison with the parent Pt (II) complex **284** and is due to the addition of the new electron-rich sulphur biomolecule, **Table 4.5**.

Aromatic signals appear as very complex multiplets with extensive overlapping of signals in the range of δ 7.19 – 8.27 ppm, more so than that seen for the parent complexes **281-285**. However, the integration of these aromatic signals are as expected for each complex, detailed in **Table 4.5**. Limited solubility and extensive overlapping of signals unfortunately did not allow for full aromatic characterisation using [<sup>1</sup>H-<sup>1</sup>H] COSY plots and [<sup>13</sup>C DEPT 45-<sup>1</sup>H] HETCOR plots at this time.

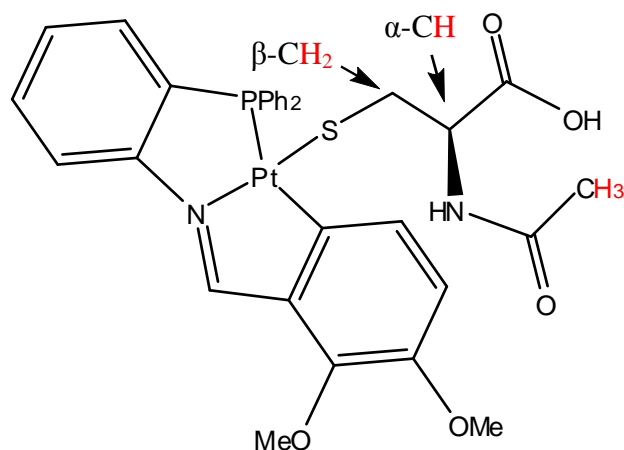


**Figure 4.26:** Illustration of the positions of the corresponding proton signals for *N*-acetyl-*L*-cysteine, as well as the  $\alpha$  and  $\beta$  positions.

Additional signals are also observed for the proton signals present in the coordinated *N*-acetyl-*L*-cysteine or *L*-glutathione confirming their presence in the Pt (II) complexes. For the *N*-acetyl-*L*-cysteine Pt (II) bio-adducts **440-441** a singlet resonance is observed integrating for three protons in the range of  $\delta$  1.92-1.93 ppm. These are characteristic for the amide methyl group, indicated in red in **Figure 4.26**. Two  $^1\text{H}$  multiplet signals are also observed in the range  $\delta$  2.90-3.41 ppm which represents the  $\beta$ - $\text{CH}_2$  group indicated in red in **Figure 4.26**. Finally a multiplet was also observed in the range  $\delta$  4.10-4.32 ppm and integrated for 1H, which corresponds to the  $\alpha$ -CH group also indicated in red in **Figure 4.26**.

The N-H resonances for these ligands are obscured by the aromatic signals present in the spectra of both Pt (II) bio-adducts **440-441**. The signals integrate for ten protons in total, which corresponds with the expected signals. The *L*-glutathione Pt (II) bio-adducts **442-443** also gave multiple signals corresponding to the proton signals on the biomolecule ligand. Unfortunately due to extensive overlapping and very broad signals obtained individual assignment is currently not possible for these complexes.

The  $^{31}\text{P}\{^1\text{H}\}$  NMR data obtained for all the Pt (II) bio-adducts **440-443** gave a single phosphorus resonance shifted downfield in comparison to the parent Pt (II) cyclometallates **281** and **284**, **Table 4.7**. The signal range of  $\delta$  31.1-32.2 ppm is similar to that observed for the iminophosphine phosphorus signal obtained for the  $\text{PPh}_3$  substituted Pt (II) complexes **371-375** which gave a range of  $\delta$  33.3-33.4 ppm. This signal represents a downfield shift of circa  $\delta$  6 ppm in comparison with the parent Pt (II) complexes which had a phosphine signal at circa  $\delta$  25 ppm, **Table 4.7**.

Pt (II) parent complex	$\delta^{31}\text{P}\{^1\text{H}\}$ ppm	Pt (II) Bio-adducts	$\delta^{31}\text{P}\{^1\text{H}\}$ ppm	$\Delta\delta$ ppm
3-H <b>281</b>	25.3 (s) $^1J_{\text{Pt-P}} = 2083$ Hz	<b>440</b>	31.4 (s) $^1J_{\text{Pt-P}} = 2184$ Hz	6.1
2,3-(OMe) <sub>2</sub> <b>284</b>	25.2 (s) $^1J_{\text{Pt-P}} = 2102$ Hz	<b>441</b>	31.1 (s) $^1J_{\text{Pt-P}} = 2195$ Hz	5.9
3-H <b>281</b>	25.3 (s) $^1J_{\text{Pt-P}} = 2083$ Hz	<b>442</b>	31.4 (s) $^1J_{\text{Pt-P}} = 2188$ Hz	6.1
2,3-(OMe) <sub>2</sub> <b>284</b>	25.2 (s) $^1J_{\text{Pt-P}} = 2102$ Hz	<b>443</b>	32.2 (s) $^1J_{\text{Pt-P}} = 2198$ Hz	7.0

Table 4.7: Comparison of the  $^{31}\text{P}\{^1\text{H}\}$  signals between the parent Pt (II) complexes **281** and **284** with the Pt (II) bio-adducts **440-443**.

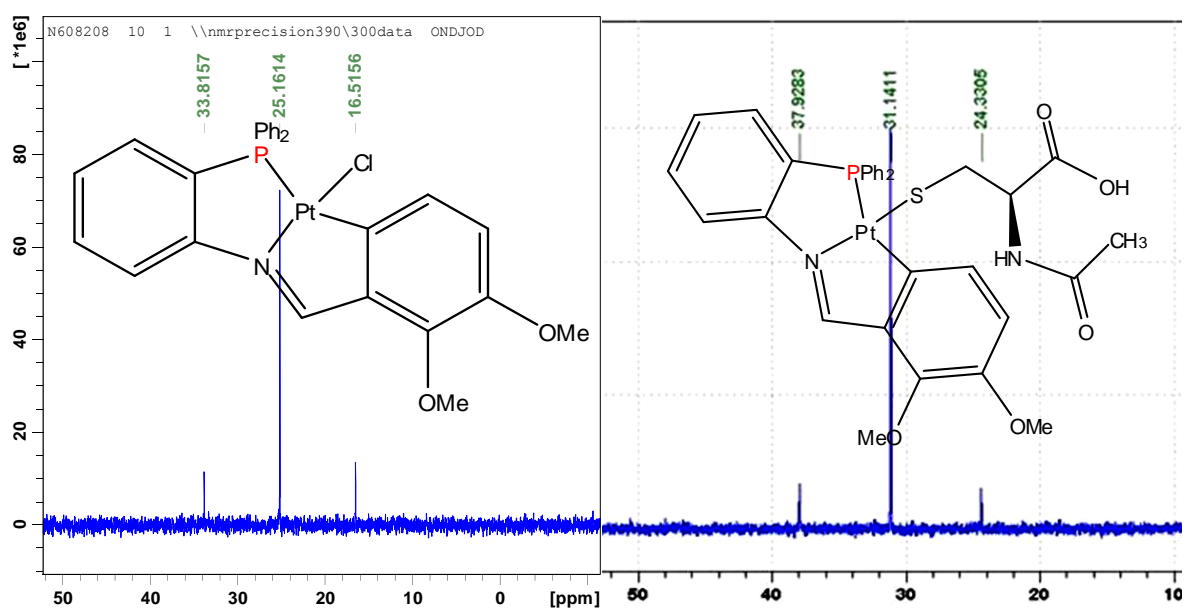


Figure 4.27: A comparison of the  $^{31}\text{P}\{^1\text{H}\}$  spectra for the parent cyclometallated complexes **281** and **284** (left) and Pt (II) bio-adducts **440-443** (right).

Evidence for the Pt-P bond was again provided by the presence of  $^{195}\text{Pt}$  satellites generated as a result of  $^1J_{\text{P-Pt}}$  coupling **Figure 4.27**. The coupling constants for all the Pt (II) bio-adducts **440-443** were found to be circa 100 Hz higher than the parent Pt (II) chloro complexes **281-284**, again as a direct consequence of the decreased electrophilicity of the metal centre due to the presence of the electron rich sulphur biomolecule. This would

identify that the sulphur moiety, even in a *cis* geometry, influences the bond strength of all the platinum-ligand group interactions.

#### 4.7 *In-Vitro* Cancer Cell Testing with Pt (II) Cyclometallates:

##### 4.7.1 Background on the cell culture used:

Due to their solubility, stability and good yield, the Pt (II) cyclometallated complexes **281** and **284** were selected for *in-vitro* cancer cell testing against squamous human esophageal cancer cells (OE21), **Figure 4.28**. Cancers of the esophagogastric region consist of highly malignant tumours with five-year survival rates of less than 16% and many research groups have shown that 88% of esophagogastric cancer patients who have received successful treatment are susceptible to the dormant cancer re-emerging as an aggressive drug-resistant metastases.<sup>69</sup>

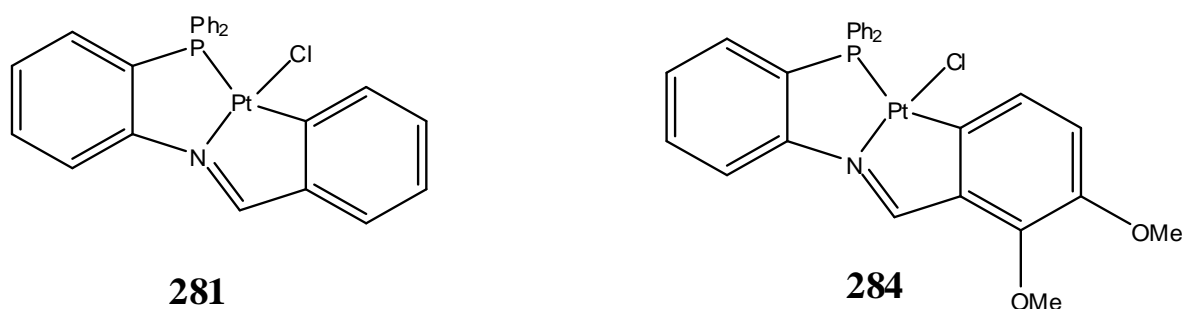


*Figure 4.28: The two Pt (II) cyclometallated iminophosphine complexes tested on human esophageal cancer cells, 281 and 284.*

Successful chemotherapeutic regimes must therefore effectively induce Programmed Cell Death (PCD) in cancer cells to overcome drug resistance and recurrence. Until recently apoptosis (**Type I PCD**) was regarded as the central mediator of PCD in response to chemotherapeutic agents and is generally characterised by loss of the nuclear membrane, fragmentation of the chromatin and cell shrinkage.<sup>70</sup>

However, other cell death programs have been identified more recently with both platinum based anti-cancer drugs and non-platinum based anti-cancer drugs.<sup>43,70</sup> **Type II** Programmed Cell Death (**PCD**) is characterised by the formation of vesicles in the cytoplasm of the cell and results in loss of the cytoplasmic structure and pyknosis of nuclear material within an intact nuclear membrane i.e. the nucleus is the only remnant of the dead cell.<sup>71</sup>

Evidence suggests that **Type II PCD** is a consequence of excessive autophagy and a number of studies have reported autophagic cell death in cultured mammalian cells. Autophagy is a cell's survival response to growth limiting conditions in which non-vital cellular components are sequestered, degraded and recycled to ensure the cell survives. Although autophagy can help cancer cells survive in response to growth-limiting conditions, the induction of excessive autophagy and **Type II PCD** may also be a major cell death mechanism that takes over when apoptosis is unavailable.<sup>72,73</sup>

Previous work by McKenna *et al* in the Cork Cancer Research Centre has concentrated on cell death programs initiated in esophageal cancer cells in response to the chemotherapeutic agents 5-fluorouracil (5-FU) and cisplatin. They have recently reported that treated cells which do not undergo apoptosis instead opt for cell death via autophagy. However, it has been shown that this can also cause some cell populations to recover when the cytotoxic drugs are withdrawn.<sup>70</sup>

As the more drug sensitive cell line, it was found that OE21 induced a predominantly apoptotic cell death morphology (**Type I PCD**) in response to 5-FU and cisplatin, with low levels of non-apoptotic cell death morphology found (**Type II PCD**). Interestingly, the more drug resistant cell lines (OE19 and KYSE450) instead displayed predominantly non-apoptotic morphology, or **Type II PCD**. The OE21 cells displayed 31 % apoptotic cell death (**Type I PCD**) and 3 % non-apoptotic cell death (**Type II PCD**) in response to cisplatin at a concentration of 40  $\mu\text{M}$ , whereas the OE19 cell line showed only 0.5 % apoptosis (**Type I PCD**) and 38 % non-apoptotic cell death (**Type II PCD**) with cisplatin.<sup>70</sup>

Based on this work by McKenna and co-workers, the OE21 cell line was chosen as an ideal candidate to compare the established biological activity of cisplatin with the potential biological activity of the cyclometallated Pt (II) complexes **281** and **284**. Propidium iodide (PI) uptake and morphological analysis were used to compare the response of human oesophageal cancer cells (OE21) to a 24 hour treatment with cisplatin, the conventional chemotherapeutic, and the two novel Pt (II) cyclometallates **281** and **284**. Each compound was made up in a solution of dimethylsulfoxide prior to treatment, as the complexes **281** and **284** were insoluble in water.



### 4.7.2 Propidium iodide (PI) uptake and flow cytometry:

Propidium iodide (PI) is used as a DNA stain for flow cytometry, to evaluate cell viability or DNA content in cell cycle analysis, and microscopy to visualise the nucleus and other DNA containing organelles. It can also be used to differentiate necrotic, apoptotic and normal cells. It is only taken up and bound by **non-viable** cells or cells that have been compromised i.e. cells that are undergoing or have undergone **Type I** or **Type II PCD**.

**Figure 4.29** shows Propidium Iodide (PI) uptake in human oesophageal cancer cells (OE21) following 24 hours treatment with cisplatin, the 3-H complex **281** or the 2,3-(OMe)<sub>2</sub> complex **284** in concentrations of 5  $\mu\text{M}$  to 30  $\mu\text{M}$  as determined by Flow Cytometric analysis. The scatter plots show the size and granularity of the cells (in the FSC-A/SSC-A panels) and PI uptake is measured on the 488 1A channel.

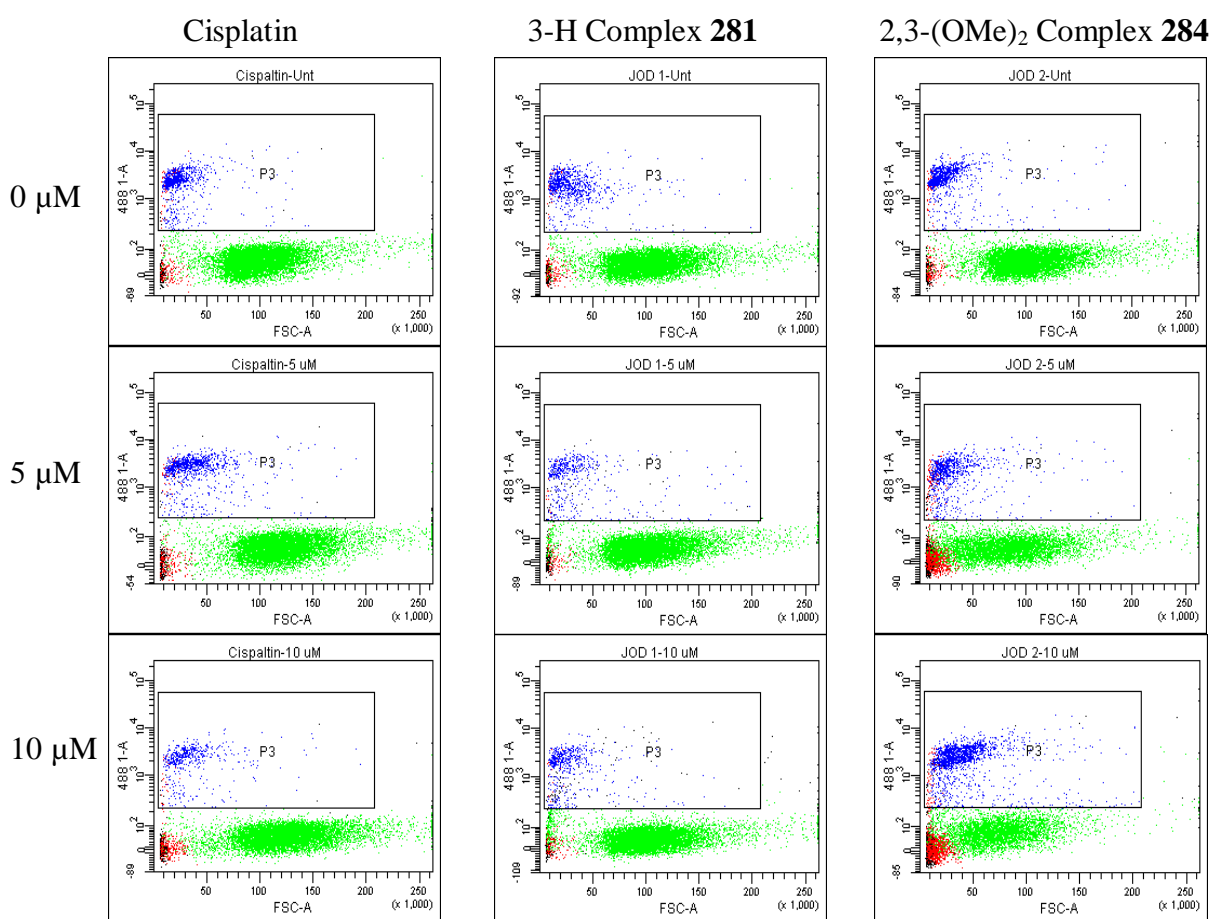


*Figure 4.29 (Part A): Propidium Iodide (PI) uptake in OE21 cancer cells after 24 hours treatment.*

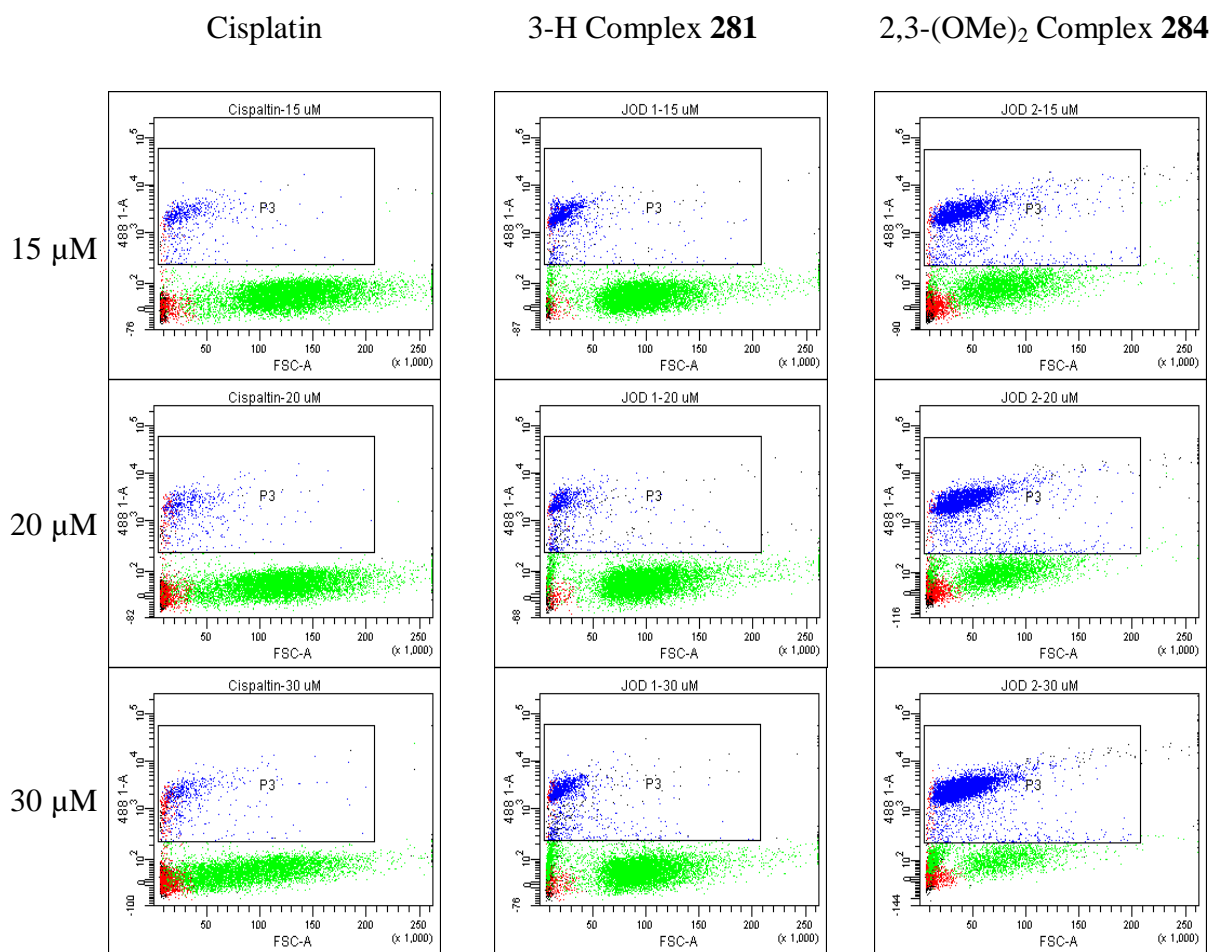


*Figure 4.29 (Part B): Propidium Iodide (PI) uptake in OE21 cancer cells after 24 hours treatment.*

Cells debris is excluded from analysis (shown in **red**), all other cells are analysed to determine whether or not they will take up PI. Cells excluding PI (**viable**) are shown in **green**, while those that take up and bind PI (PI positive, **non-viable**) are shown in the box labelled “P3” and are displayed in **blue**. A comparison of the percentage of cells taking up PI (**non-viable**, blue population) following treatment is presented in **Figure 4.30**.

From the graph in **Figure 4.30** it is clearly evident that there is a significant increase in the percentage of **non-viable** cancer cells (cells that take up PI) after 24 hours treatment found for the 2,3-(OMe)<sub>2</sub> cyclometallate **284**, in comparison to similar concentrations of cisplatin and the 3-H cyclometallate **281**. For example, at a concentration of 20 μM, cisplatin caused circa 7 % of cells to undergo cell death (take up PI) while the 2,3-(OMe)<sub>2</sub> cyclometallate **284**, at the same concentration, induced cell death in over 50% of the OE21 cells. The five bars for each test substance represent progressively higher concentrations of each compound used in this experiment.

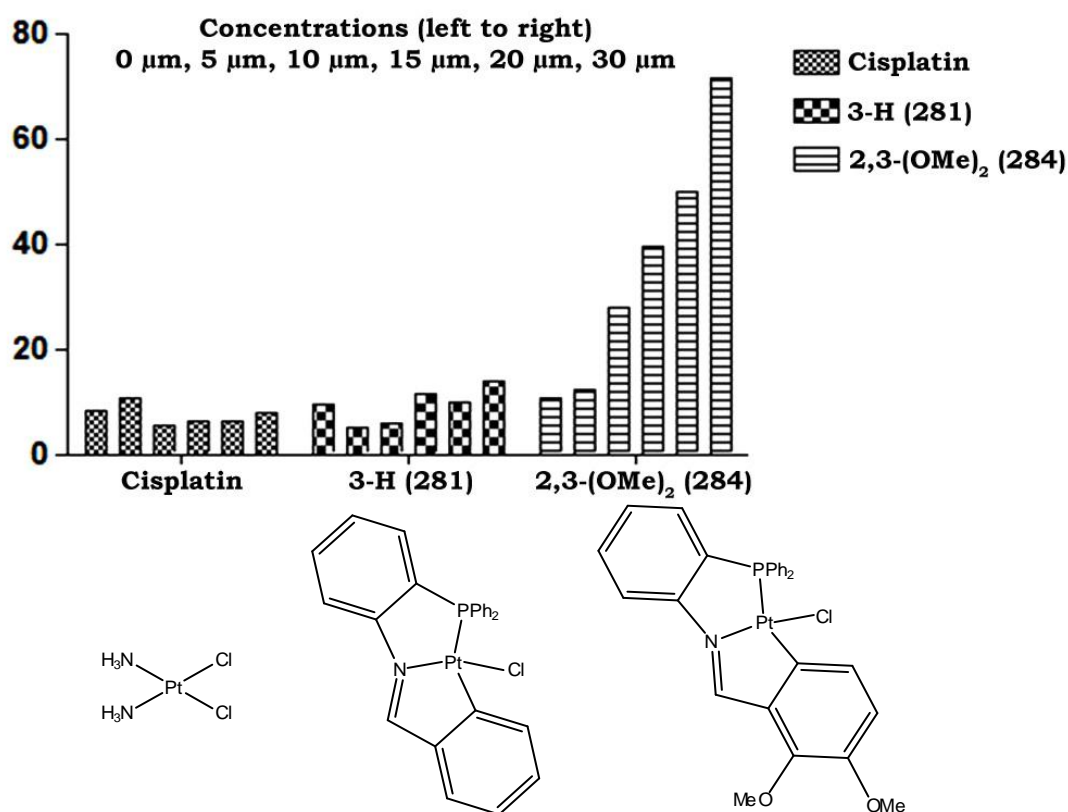


*Figure 4.30: Graphical representation of the percentage of cells taking up PI (non-viable, blue population) for each compound at each concentration after 24 hours.*

Using a linear regression model in conjunction with the percentages and concentrations obtained for the treated cell lines, gives the 2,3-(OMe)<sub>2</sub> cyclometallate **284** an IC<sub>50</sub> value of 14.3  $\mu\text{M}$ , the 3-H cyclometallate **281** an IC<sub>50</sub> value of 88.1  $\mu\text{M}$  and cisplatin an IC<sub>50</sub> value of 98.2  $\mu\text{M}$  for the OE21 squamous human esophageal cancer line.

#### 4.7.3 Analysis of morphological features:

Following treatment with cisplatin, compound **281** or compound **284**, the OE21 cancer cells were removed from the culture and cytospun onto glass slides, fixed in methanol and stained with Rapi-Diff. The morphological features of the cells following treatment were examined to determine whether **Type I PCD** or **Type II PCD** had occurred, **Figure 4.31**.

Cells that underwent apoptotic cell death (**Type I PCD**) were found to have clearly fragmented nuclei within an intact cell membrane. as expected, and are highlighted in **Figure 4.31** with **red circles**. Alternatively, cells that underwent a **Type II PCD** mechanism (through autophagy or otherwise), which is characterised by an intact nuclear membrane and

a severely compromised cytoplasm/cell membrane, are highlighted with **green circles** in **Figure 4.31**.

To determine **Type I** vs **Type II PCD**, typical markers of apoptotic cell death, such as activation of caspase-3 and mitochondrial depolarisation, were assessed. All cell images are shown at a 40X magnification. The cisplatin treated cell lines were found to undergo mainly **Type I PCD** across all concentrations, while the novel cyclometallates **281** and **284** induced **Type I PCD** at low concentrations and primarily **Type II PCD** at higher concentrations.

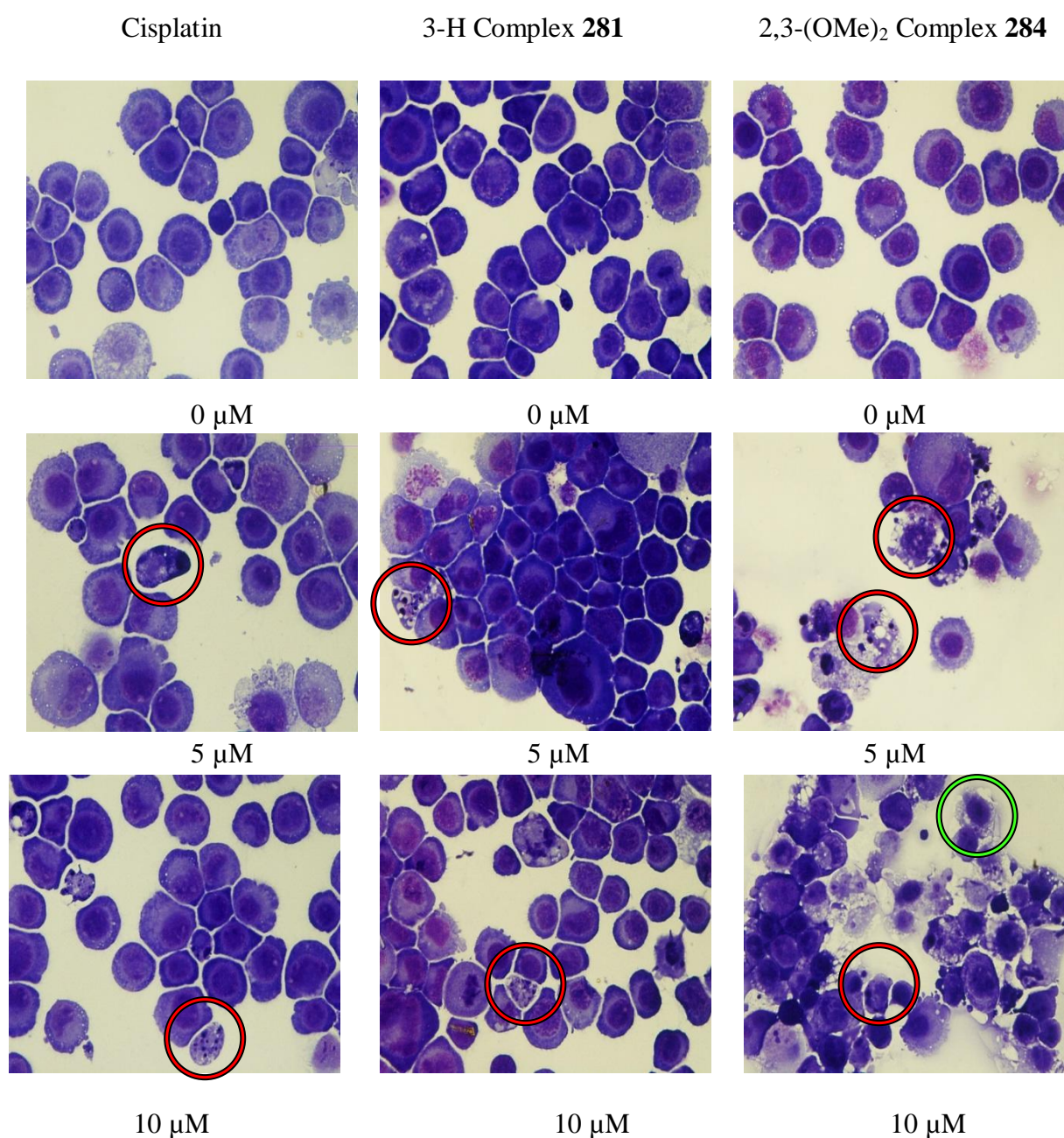


*Figure 4.31 (Part A): Analysis of the morphological features of the OE21 cancer cells after treatment, shown here at 40X magnification.*

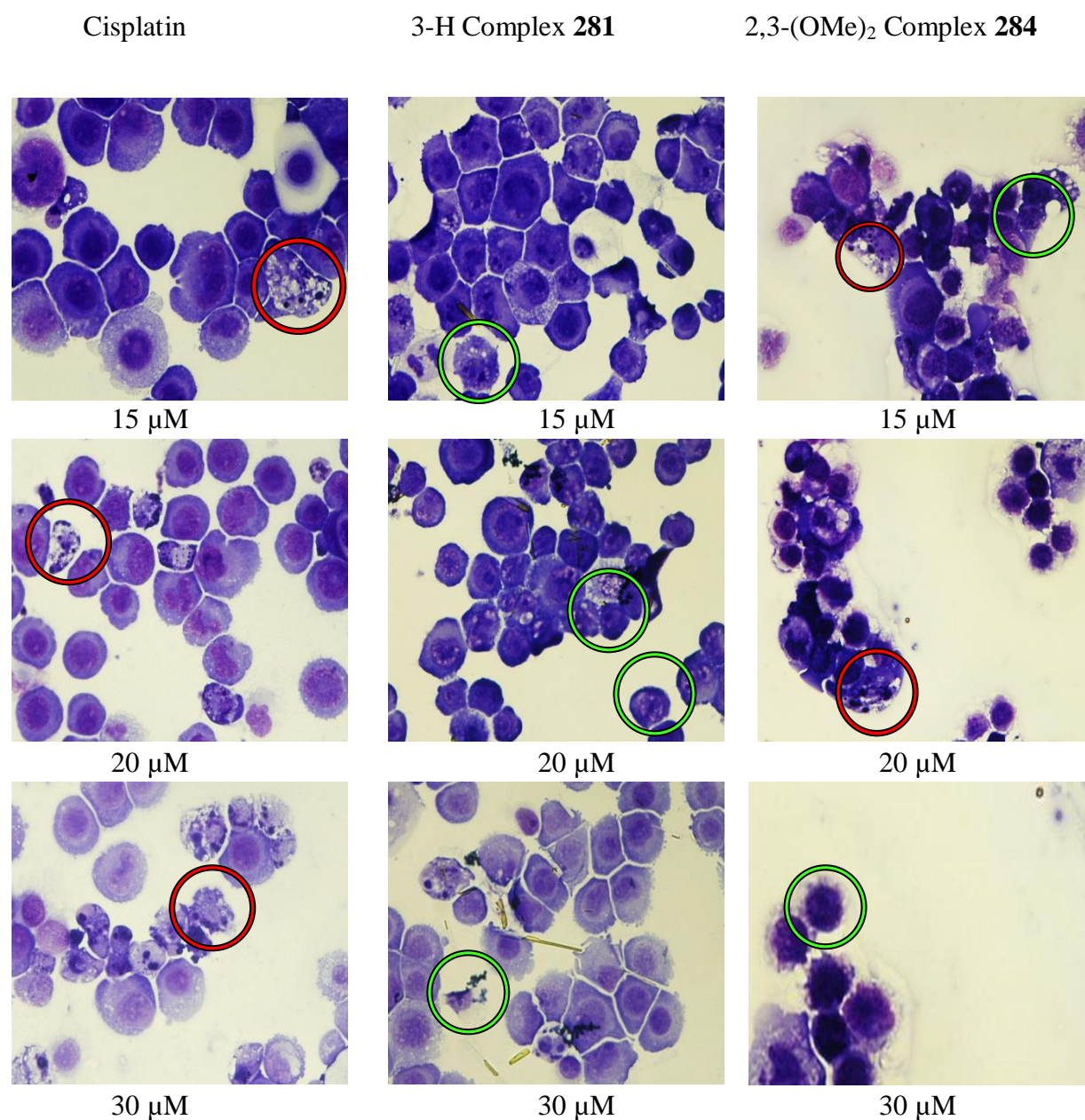


*Figure 4.31 (Part B): Analysis of the morphological features of the OE21 cancer cells after treatment, shown here at 40X magnification.*

For the 3-H cyclometallate **281** the limited solubility became a dose limiting issue at higher concentrations. This was particularly evident for the 20 μM and 30 μM solutions, where the growth of long yellow crystals in the cell culture after 24 hours was observed, **Figure 4.31**. The 2,3-(OMe)<sub>2</sub> cyclometallate **284** on the other hand was found to have much better solubility and did not form crystals. It is therefore possible that the increased biological activity of the 2,3-(OMe)<sub>2</sub> cyclometallate **284** over the 3-H cyclometallate **281** is also due to the significant difference in solubility.

For the novel cyclometallates **281** and **284**, the presence of controlled apoptosis (**Type I PCD**) as a method for biological activity which is similar to that found for cisplatin, gives further evidence for the proposed interaction of these complexes with DNA outlined in **Chapter 1** and **Section 4.3** of this chapter. We propose that these complexes bind to the N7 position of guanine monofunctionally through hydrolysis of the chloride ligand within the cell, as well as intercalate between the base pairs of DNA to induce cell apoptosis. However, these complexes also induce significantly greater **Type II PCD** in comparison to cisplatin in the OE21 cell line, implying further biological targets and mechanisms for these complexes.

If the **Type II PCD** is primarily caused by autophagy (rather than necrosis), this would imply that these complexes are inducing cell death by targeting cytoplasmic structures, forcing the cell to undergo extensive autophagy. However, further *in-vitro* studies as well as studies involving binding to nucleotide bases are required to confirm the biological mechanisms and potential cytoplasmic targets for these complexes.

#### 4.8 Photophysical Studies of the Platinum Complexes and their Ligands:

##### 4.8.1 UV-visible spectroscopy:

UV-visible (and subsequently luminescence) spectroscopy was performed on the best yielding platinum complexes and ligand, reported in **Chapter 2** and **3**, which consisted of the 3-H **261** ligand and the platinum complexes derived from it to form a “family”, **Figure 4.32**. Each compound was tested while in a solution of chloroform which was diluted to a concentration of  $10^{-5}$  M before being measured using a Carey 50 Scan, UV-visible Spectrophotometer at ambient temperature.

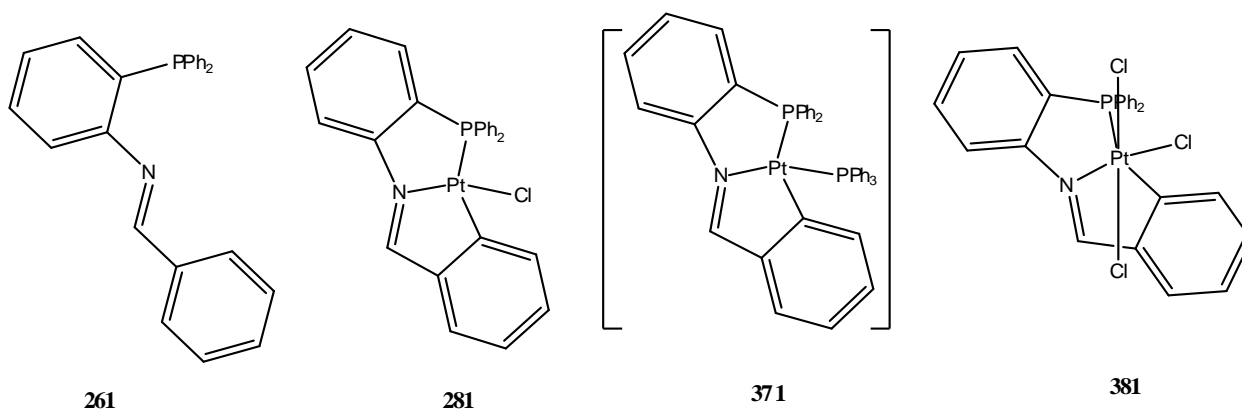


**Figure 4.32:** The  $\text{HL}^1$  ligand **264** and the platinum complexes **281**, **371** and **381** derived from it making up the “family” of compounds tested for photophysical properties.

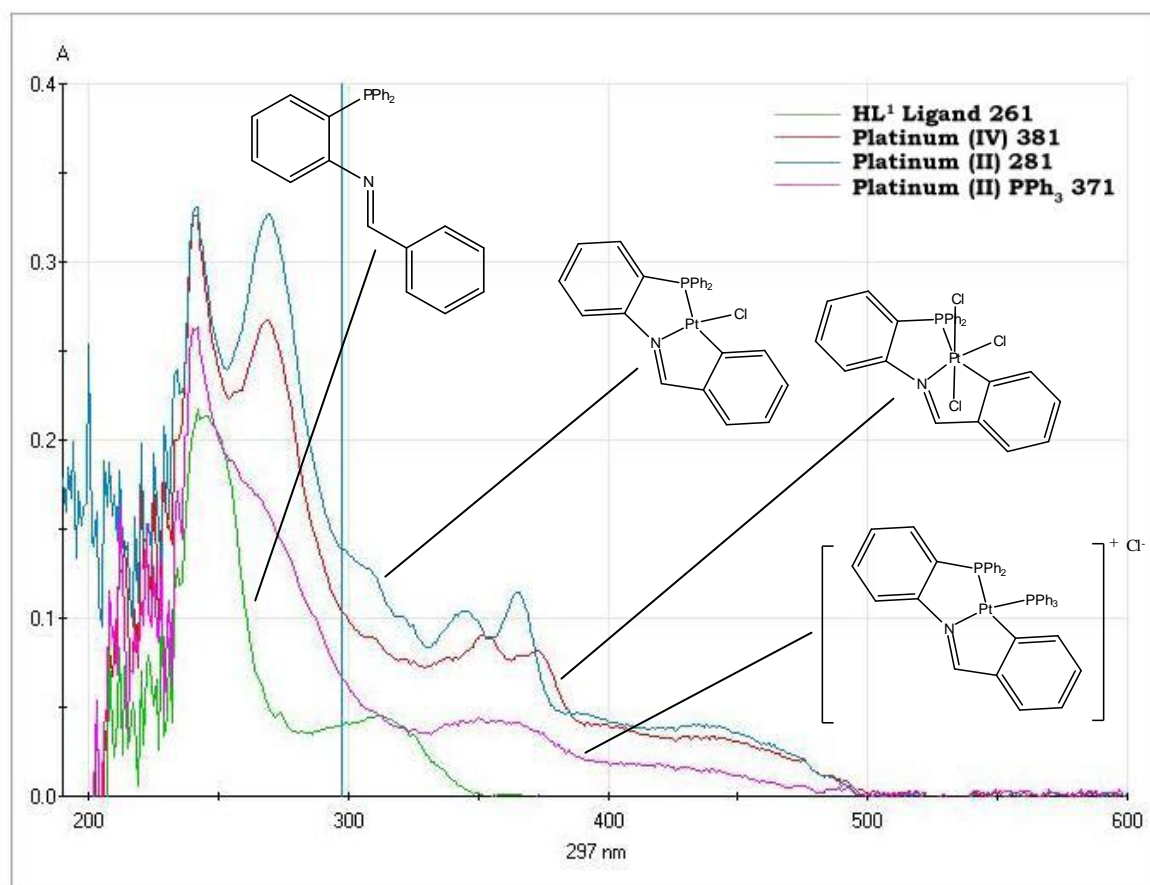


**Figure 4.33:** UV-vis spectroscopy of the 3-H  $HL^1$  ligand **261** and the derived platinum complex family **281**, **371** and **381**.

The free  $HL^1$  ligand displayed a shifted, weaker band at 320 nm. All the platinum complexes on the other hand gave a weak shoulder band at circa 450 nm, as well as a modest peak at circa 350 nm. The strong peaks observed for the Pt (II) **281**, Pt (II)  $PPh_3$  **371** and Pt (IV) **381** complexes between 320 and 350 nm are assigned to metal perturbed ligand-centred transitions ( $\pi \rightarrow \pi^*$ ) and the bands near them, observed between 370 and 380 nm, are attributed to metal-ligand charge transfer (MLCT) ( $5d(Pt) \rightarrow \pi^*(HL^1)$ ) transitions as reported previously by Fuertes *et al* and others. Finally, all the high energy intense absorption bands found below 300 nm - some of which were observed to be quite strong for the platinum complexes, **Figure 4.33** - are attributed to excitations from the singlet ground state to singlet excited states of ligand centred transitions ( $\pi \rightarrow \pi^*$ ).<sup>74-76</sup>

The maximum absorption wavelength ( $\lambda_{max}$ ) common to all the compounds tested was therefore determined to be 270 nm, which was used as the excitation wavelength for the luminescence studies outlined in **Section 4.8.2**.

There were no visible bands found higher than 350 nm for the HL<sup>1</sup> ligand **261**. However, the platinum complexes **281**, **371** and **381** were found to have absorptions in the lower energy, higher wavelength region above 350 nm. Further studies on the remaining platinum iminophosphine and phosphinoamide complexes, as well as their ligands, is required to propose further transitions and functionality.

#### 4.8.2 Luminescence studies on platinum complexes and mixed donor ligands:

None of the complexes or ligands tested were found to be photoluminescent in the solid state, despite extensive recent reports of such activity by other research groups.<sup>74,77,67</sup> This is proposed to be due to non-radiative processes concerning low-lying d-d excited states and fast decay rates.<sup>74</sup> Therefore, solutions of each compound were made up using chloroform to concentrations of 10<sup>-5</sup> M and excited at a wavelength of 270 nm as per the maximum absorption wavelength ( $\lambda_{\text{max}}$ ) obtained from the UV-vis absorption spectra in Section 4.8.1.

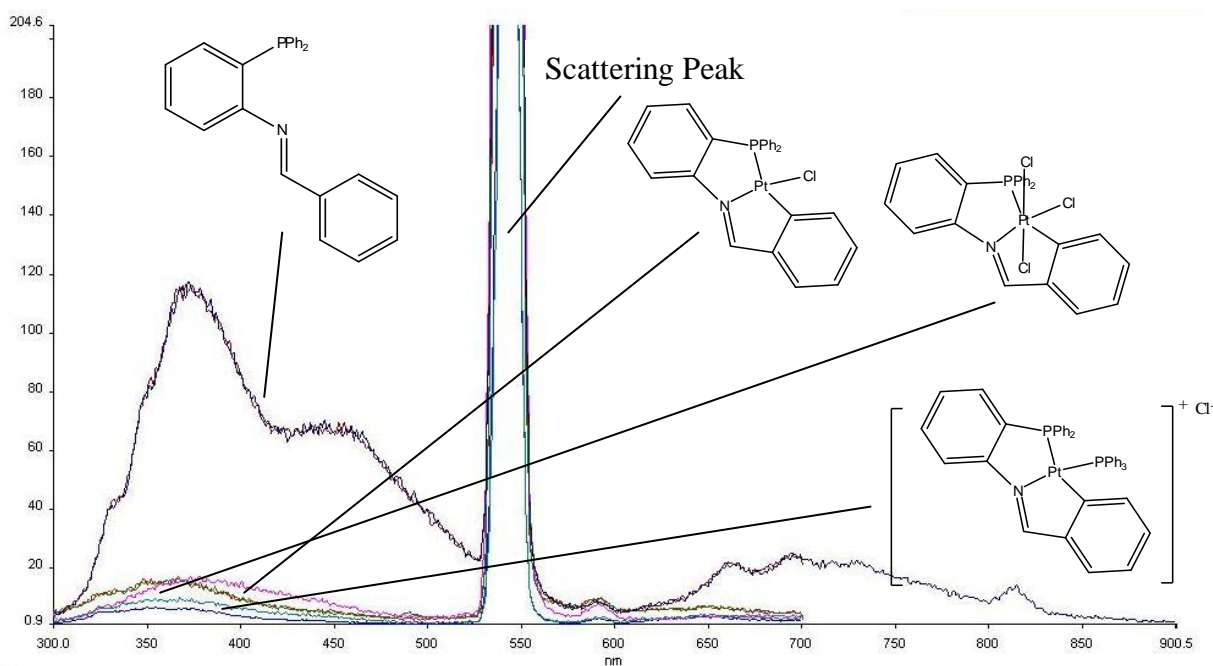


*Figure 4.34: Emission spectra for the HL<sup>1</sup> ligand **261** and Pt(II) complexes **281** and **371** along with the Pt(IV) complex **381**.*

Interestingly, the free ligand HL<sup>1</sup> **261** was found to have the highest intensity emission spectra of all the compounds tested at this time. The strongest band was found to occur in the blue region at 320 nm and represented a 6-fold increase over similar bands found



for the platinum complexes, **Figure 4.34**. An intense band was also found at 460 nm for the ligand and all the compounds displayed a band in the low energy region of 580 nm.

Also found for the ligand were bands in the very low energy (red) region of 670 nm, 700 nm and 850 nm. The ligand is proposed to undergo an Excited State Intramolecular Proton Transfer (ESIPT) process in the chloroform solution similar to previous reports by other research groups, **Figure 4.35**.<sup>62</sup>

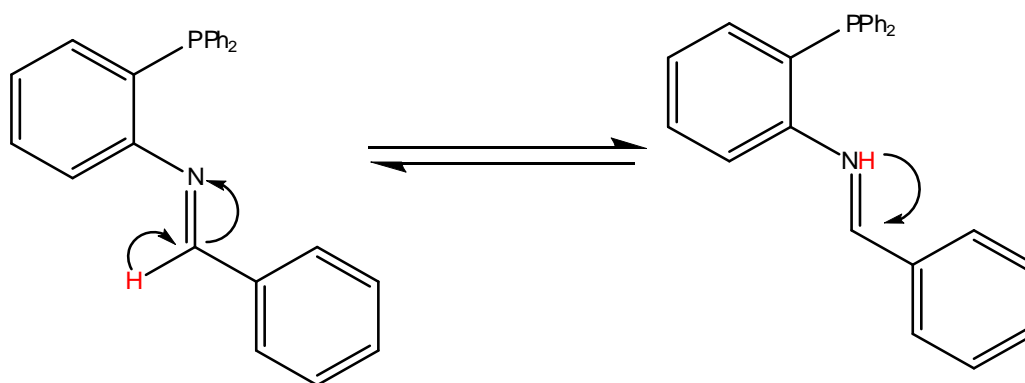


*Figure 4.35: The proposed Excited State Intramolecular Proton Transfer (ESIPT) for the HL<sup>1</sup> ligand which causes the bands found in the red region of the luminescence spectra.*

Despite having a lower emission intensity in comparison to the free ligand HL<sup>1</sup> **261**, the Pt (II) cyclometallate **281**, cationic Pt (II) PPh<sub>3</sub> substituted complex **371** and the Pt (IV) cyclometallate **381** were all found to have emission intensities greater than or equal to that reported by other research groups for similar tridentate platinum complexes, **Figure 4.36**.<sup>74,77</sup> It is proposed that the rigid square planar structures reported here, and confirmed by X-ray crystallography in **Chapter 2**, favour increased luminescent emission over less rigid structures discussed in **Chapter 1** and **Section 4.4.1** of this chapter.

Interestingly, in addition to the high energy bands observed for all the compounds between 300 nm and 500 nm, low energy bands were also found at 580 nm and circa 650 nm for all the platinum complexes tested, as well as the HL<sup>1</sup> ligand. These low energy emissions (circa 700 nm) are frequently encountered for other platinum complexes, primarily Pt (II), and are usually attributed to excimers or aggregates.<sup>74</sup>

Excimers are formed from Pt–Pt bimetallic interactions and interligand  $\pi$ – $\pi$  interactions during the formation of excimer structures. While the Pt–Pt interactions are critical for excimer formation, the interligand  $\pi$ – $\pi$  interactions also play a significant role in determining the optimal excimer geometry and the magnitude of the phosphorescence energy lowering in going from the monomer to the aggregated dimer. There have been frequent

reports by various research groups of planar platinum complexes forming dimers through the axial ligands of the metal centre and this is tentatively proposed to be occurring here also.<sup>74,78</sup>

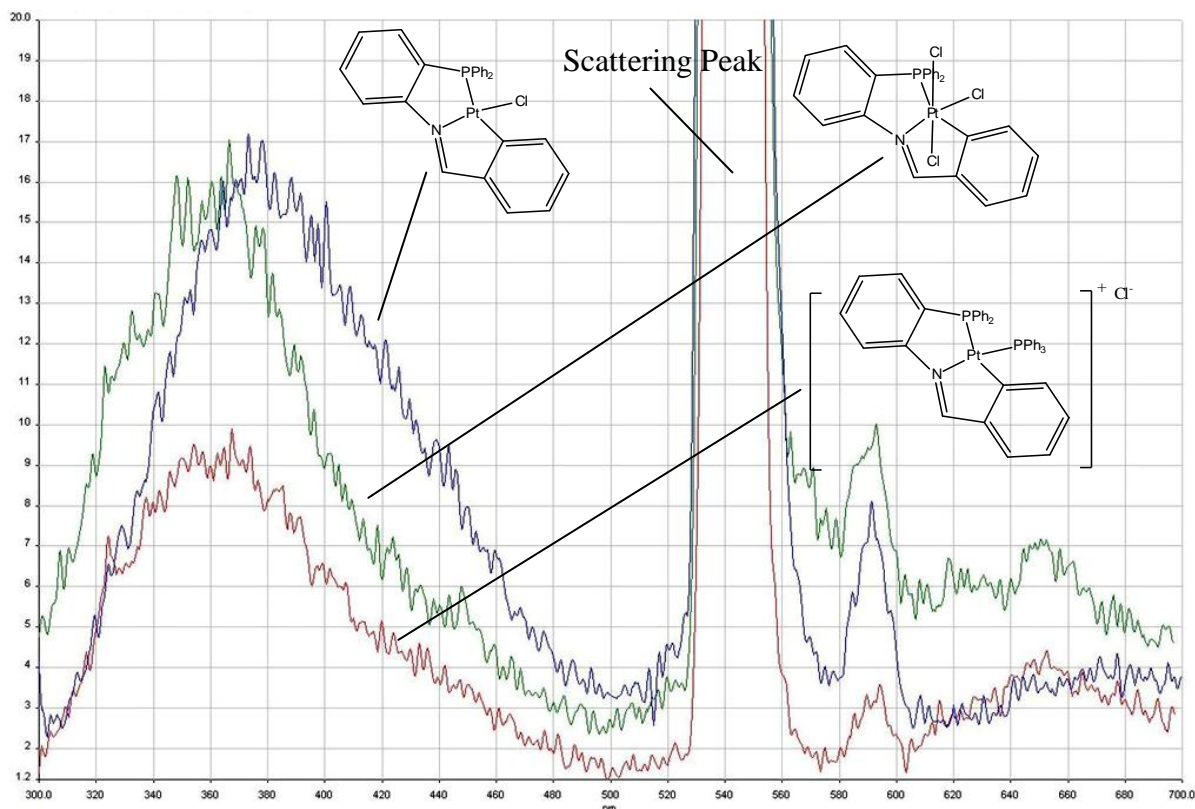


*Figure 4.36: The emission spectra obtained, using a luminescence spectrophotometer, for the 3-H Pt (II) complexes **281** and **371**, as well as the Pt (II) complex **381***

Further work involving the remaining ligands and platinum complexes reported in **Chapter 2** and **3** is required before any further proposals and structure activity relationships can be established. From the work to date it can be seen that the emission type and intensity of the free ligand HL<sup>1</sup> **261** differs significantly in comparison to the platinum complexes **281**, **371** and **381**.

#### **4.9 Chapter 4 Summary and Conclusions:**

The synthesis of the Pt (II) bio-adducts was successfully achieved using a combination of a similar procedure that was used previously by our research group and the method that was employed to achieve successful substitution of the Pt (II) cyclometallates in **Chapter 3**, with triphenylphosphine (PPh<sub>3</sub>).

Each bio-adduct synthesised from the Pt (II) cyclometallates **281** and **284** and was fully characterised by IR, <sup>1</sup>H NMR, <sup>31</sup>P{<sup>1</sup>H} NMR and elemental analysis, which together

confirmed the structure of the N-acetyl-L-cysteine and L-glutathione Pt (II) bio-adducts. Interestingly both sets of bio-adducts were found to be water soluble, but more so in the case of the L-glutathione platinum complexes. Also, all the Pt (II) bio-adducts were found to display photophysical properties and reacted to both light and air over a number of days to form unidentifiable decomposition products.

The presence of solvent of crystallisation was also noted in the  $^1\text{H}$  NMR spectra of the bio-adduct complexes (chloroform) and was therefore included for successful assignment of the elemental analysis. This was also noted previously by our research group and others where most of the analogous iodo Pt (II) complexes previously reported also contained solvent of crystallisation.<sup>79,80,36,68,81</sup>

The 3-H Pt (II) cyclometallated complex **281** and the 2,3-(OMe)<sub>2</sub> cyclometallated complex **284** were chosen as the best candidates for biological testing due to their high yield, obtained during their synthesis reported in **Chapter 2**, which allowed for further purification techniques such as re-crystallisation. It was necessary to have highly pure samples of both complexes to ensure only the platinum complex was responsible for any observed biological activity. Also, both complexes were found to have the best solubility in a wide variety of solvents needed to conduct biological studies.

*In-vitro* testing was conducted using the aggressive OE21 esophageal cancer cell line. The cancer cell line was treated for 24 hours with the 3-H Pt (II) cyclometallated complex **281**, the 2,3-(OMe)<sub>2</sub> cyclometallated complex **284** and the well established platinum anti-cancer therapeutic; cisplatin, as a comparison.

Interestingly, both novel Pt (II) cyclometallates were found to have extensive biological activity towards the OE21 esophageal cancer cell line despite having only one ligand to hydrolysis and bind to DNA. Controlled cell death in the form of apoptosis was observed for both complexes, leading to a proposed mechanism of action involving a combination of monofunctional DNA binding coupled with intercalation of the planar aryl ring structure between the nucleotide bases of DNA.

In comparison to cisplatin on the same cell line, the 3-H Pt (II) cyclometallated complex **281** was found to have a similar biological activity profile over the 24 hour period. However, the 2,3-(OMe)<sub>2</sub> cyclometallated complex **284** was found to have a 7-fold increase in activity over the well established anti-cancer drug cisplatin on this cell line which can be seen as a very positive result for Pt (II) cyclometallated anti-cancer complexes.

Both the platinum complexes and the free ligand for the 3-H **261** family of compounds were also tested for UV-vis absorption and luminescent emission. The Pt (II)

complexes **281** and **371**, as well as the Pt (IV) complex **381** were all found to have emission in the blue region.

However, the free ligand **261** was found to have a 5-fold higher emission intensity over the platinum complexes with strong bands found in the blue and green region, but also having bands in the low energy red region. These initial tests have now opened the door to future studies into the analysis of potential luminescence of all the ligands and platinum complexes reported in **Chapter 2** and **3** to establish structure activity relationships.

#### **4.10 Chapter 4 Experimental:**

##### **4.10.1 Background:**

All reaction solvents were distilled prior to use, unless purchased as analytical grade (all from Sigma Aldrich Chemical Co. Ltd.). Toluene and thf were distilled directly before use from sodium-benzophenone. Methanol was distilled over magnesium/iodine according to Perrin *et al*<sup>82</sup> and hexane was distilled over phosphorus pentoxide.

The following reagents were used as supplied; N-acetyl-L-cysteine (Sigma-Aldrich Chemical Co. Ltd), L-glutathione (Sigma-Aldrich Chemical Co. Ltd), cisplatin (Sigma-Aldrich Chemical Co. Ltd), propidium iodide (Sigma-Aldrich Chemical Co. Ltd), rapi-diff (Braidwood Laboratories). Elemental analyses (Perkin-Elmer 2400 CHN elemental analyser) were performed by the microanalytical laboratory, University College Cork.

The <sup>1</sup>H and <sup>31</sup>P{<sup>1</sup>H} NMR spectra were recorded on a Bruker Advance 300 MHz, 400 MHz or 600 MHz NMR spectrometer (where specified). Chemical shifts ( $\delta$ ) are expressed in parts per million (ppm) and referenced to external tetramethylsilane ( $\delta$ 0) for <sup>1</sup>H and 85% phosphoric acid ( $\delta$ 0) for <sup>31</sup>P{<sup>1</sup>H} NMR using the high frequency positive convention.

Infrared spectra were recorded as KBr disks on a Perkin-Elmer Paragon 1000 FT spectrometer for the Pt (II) bio-adducts. Relative intensities are designated (s), strong; (m), medium; (w), weak; (b), broad.

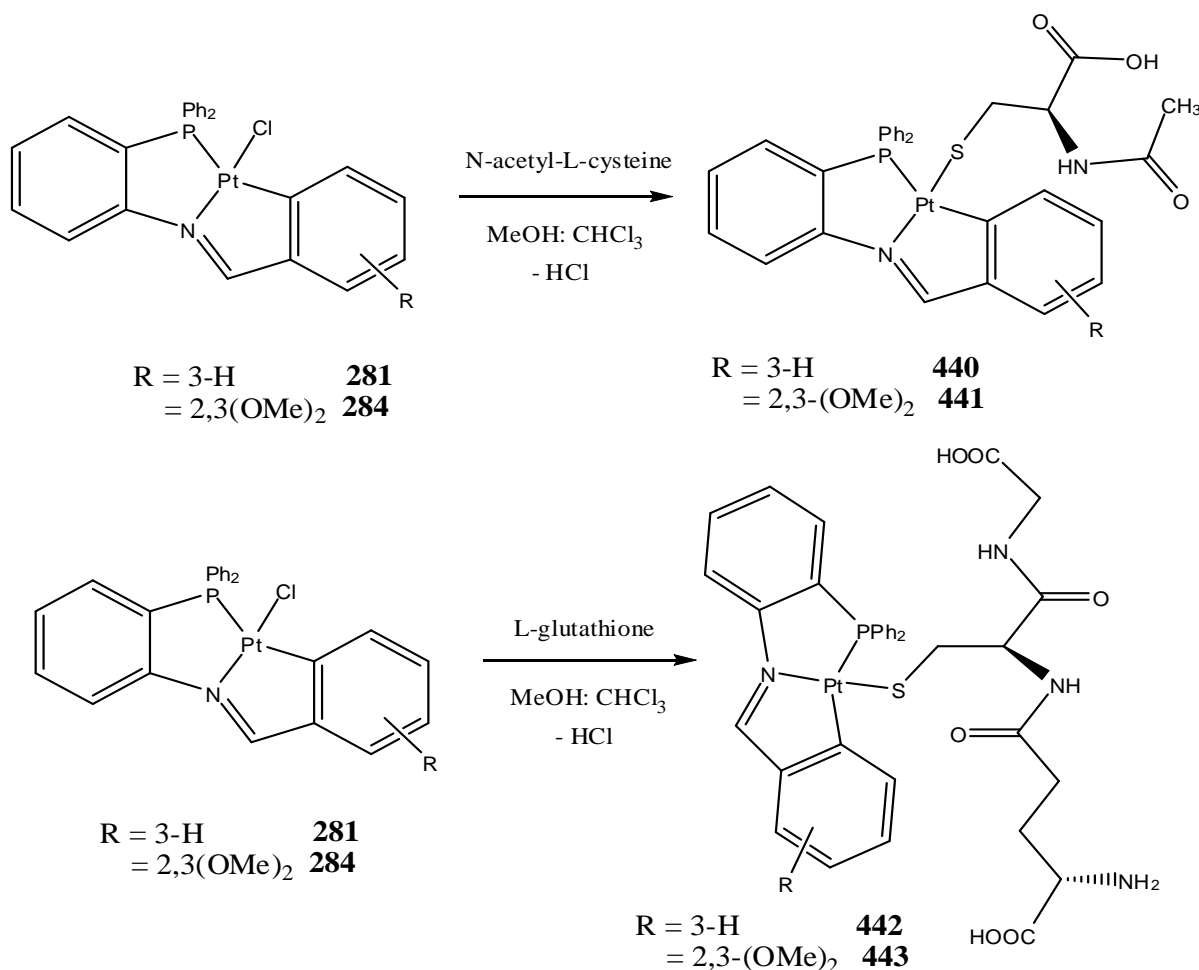
The OE21 esophageal cancer cell line was obtained from the European Collection of Cell Cultures (96062201). They were maintained in RPMI 1640 medium and supplemented with 1% penicillin/streptomycin, 10% (v/v) fetal calf serum (Gibco, 21875-034, 15070-063, 10270) at 37°C, 5% CO<sub>2</sub>.

The UV-visible absorption spectra were recorded using optical grade quartz cuvettes on a Carey 50 scan UV-visible spectrophotometer and the emission spectra were recorded on

a LS 50 B Perkin Elmer luminescence spectrophotometer using dilute chloroform solutions of the compounds.

#### 4.10.2 Synthesis of the Pt (II) bio-adducts $[\text{Pt}^{\text{II}}(\eta^3\text{-PNC-L}^{1/4})\text{N-acetyl-L-cys/L Glu}]\text{Cl}$

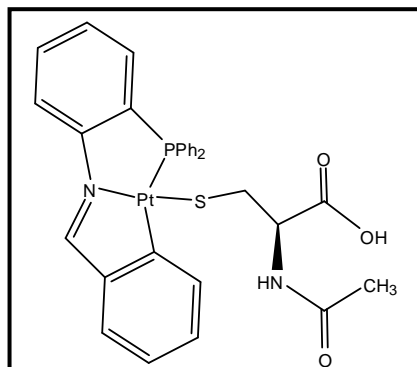
##### 440-443:



Two equivalents of the biomolecule (N-acetyl-L-cysteine or L-glutathione) in a methanolic solution was added slowly over one hour to a stirred solution of  $[\text{Pt}^{\text{II}}(\eta^3\text{-PNC-L}^{1/4})\text{Cl}]$  **281** or **284** in a 1:1 chloroform/methanol (10 ml:10 ml) solution. The solution was then stirred at ambient temperature for 24 hours in the case of N-acetyl-L-cysteine and 48 hours in the case of L-glutathione.

After 24 hours (N-acetyl-L-cysteine) or 48 hours (L-glutathione) the solution became a pale yellow colour which was then reduced to dryness *in vacuo*. It was then taken up in dichloromethane (where it again turned dark red) and washed once with a small portion of distilled water to remove any remaining N-acetyl-L-cysteine or L-glutathione and HCl formed during the reaction.

The organic layer was dried over  $\text{MgSO}_4$ , reduced to dryness *in vacuo* again and the resulting dark red solution was crystallised from distilled methanol layered with hexane to form the neutral Pt (II) bio-adducts **440-441**.



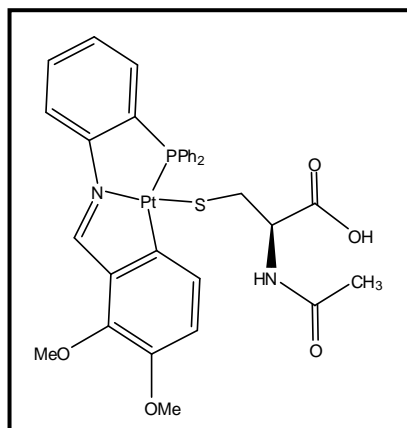
**440:**  $[\text{Pt}^{\text{II}}(\eta^3\text{-PNC-L}^1)\text{Cl}]$  (0.020 g, 0.03 mmol) **281** and N-acetyl-L-cysteine (0.011 g, 0.07 mmol) gave  $[\text{Pt}(\eta^3\text{-PNC-L}^1)\text{N-acetyl-L-cys}]$  **440** as a dark red powder.

Yield: 0.019 g (78 %)

Found (required for  $\text{C}_{30}\text{H}_{27}\text{N}_2\text{O}_3\text{PPtS}\cdot 0.3\text{CHCl}_3$ ): C, 48.10 (48.04); H, 3.91 (3.63); N, 3.79 (3.70).

IR  $\nu_{\text{max}}$  (KBr): 3415 (b), 2923 (w), 1728 (w), 1626 (m), 1586(m)(C=N), 1529 (w), 1436 (m), 1396 (w), 1240 (m), 1187 (w), 1118 (w), 911 (w), 840 (w), 745 (m), 719 (w), 692 (s), 571 (m).

$^1\text{H}$  NMR  $\delta$  ppm: 9.68 (1 H, s) ( $^3J_{\text{Pt-H}} = 91$  Hz), 7.22-7.98 (18 H, m), 1.92 (3 H, s), 2.90-3.41 (2 H, m), 4.32 (1 H, s).  $^{31}\text{P}$  NMR  $\delta$  ppm: 31.4 (s) ( $^1J_{\text{P-P}} = 2184$  Hz).



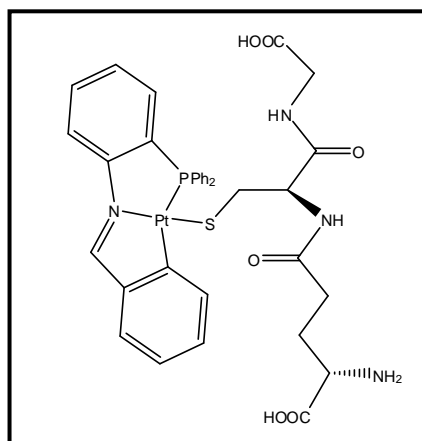
**441:**  $[\text{Pt}^{\text{II}}(\eta^3\text{-PNC-L}^4)\text{Cl}]$  (0.020 g, 0.03 mmol) **284** and N-acetyl-L-cysteine (0.011 g, 0.07 mmol) gave  $[\text{Pt}(\eta^3\text{-PNC-L}^4)\text{N-acetyl-L-cys}]$  **441** as a dark red powder.

Yield: 0.020 g (85 %)

Found (required for  $\text{C}_{32}\text{H}_{31}\text{N}_4\text{O}_5\text{PPtS}\cdot 0.3\text{CHCl}_3$ ): C, 47.29 (47.45); H, 4.16 (3.86); N, 3.31 (3.43).

IR  $\nu_{\text{max}}$  (KBr): 3366 (b), 3056 (w), 2934 (w), 2346 (w), 1718 (w), 1704 (w), 1634 (s), 1600 (m)(C=N), 1529 (m), 1477 (m), 1463 (m), 1439 (s), 1426 (w), 1409 (m), 1374 (m), 1331 (m), 1297 (w), 1267, (m), 1243 (m), 1185 (w), 1098 (s), 1084 (m), 1012 (w), 958 (m), 827 (w), 811 (m), 799 (w), 748 (m), 701 (m), 664 (m), 584 (m), 524 (s), 512 (s), 499 (m).

$^1\text{H}$  NMR  $\delta$  ppm: 9.94 (1 H, s) ( $^3J_{\text{Pt-H}} = 96$  Hz), 7.19-7.96 (16 H, m), 5.30 ( $\text{CH}_2\text{Cl}_2$ ), 3.87 (3 H, s), 4.01 (3 H, s), 1.93 (3 H, s), 2.96-3.31 (2 H, m), 4.10 (1 H, s).  $^{31}\text{P}$  NMR  $\delta$  ppm: 31.1 (s) ( $^1J_{\text{P-P}} = 2195$  Hz).



**442:** [Pt<sup>II</sup>( $\eta^3$ -PNC-L<sup>1</sup>)Cl] (0.020 g, 0.03 mmol) **281** and L-glutathione (0.021 g, 0.07 mmol) gave [Pt( $\eta^3$ -PNC-L<sup>1</sup>)L-Glu] **442** as a dark red powder.

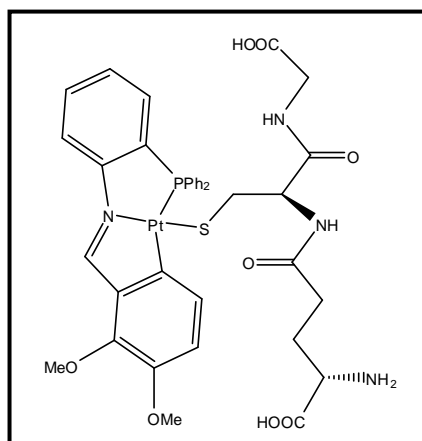
Yield: 0.021 g (72 %)

Found (required for C<sub>35</sub>H<sub>35</sub>N<sub>4</sub>O<sub>6</sub>PPtS): C, 48.20 (48.55); H, 4.40 (4.07); N, 6.05 (6.47).

IR  $\nu_{\max}$  (KBr): 3401 (b), 2922 (w), 1967 (w), 1726 (m), 1645 (w), 1590 (m)(C=N), 1527 (m), 1435 (m), 1402 (m),

1239 (m), 1187 (w), 1096 (m), 1027 (s), 912 (m), 865 (w), 762 (m), 619 (m), 567 (m), 526 (m), 419 (w).

<sup>1</sup>H NMR  $\delta$  ppm: 10.19 (1 H, s) (<sup>3</sup>J<sub>Pt-H</sub> = 84 Hz), 7.37-8.24 (18 H, m), 1.75-1.87 (2 H, m), 2.05-2.98 (6 H, m), 4.10-4.16 (2 H, m). <sup>31</sup>P NMR  $\delta$  ppm: 31.4 (s) (<sup>1</sup>J<sub>P-P</sub> = 2188 Hz).



**443:** [Pt<sup>II</sup>( $\eta^3$ -PNC-L<sup>4</sup>)Cl] (0.020 g, 0.03 mmol) **284** and L-glutathione (0.019 g, 0.07 mmol) gave [Pt( $\eta^3$ -PNC-L<sup>4</sup>)L-Glu] **443** as a dark red powder.

Yield: 0.022 g (77 %)

Found (required for C<sub>37</sub>H<sub>39</sub>N<sub>4</sub>O<sub>8</sub>PPtS): C, 48.10 (48.00); H, 4.18 (4.25); N, 6.12 (6.05).

IR  $\nu_{\max}$  (KBr): 3365 (b), 3056 (w), 2934 (w), 1718 (w), 1704 (w), 1635 (m), 1602 (w) (C=N), 1529 (s), 1477 (m),

1463 (s), 1439 (m), 1426 (w), 1374 (w), 1331 (s), 1098 (m), 1084 (w), 1012 (w), 958 (w), 827 (w), 798 (m), 748 (m), 700 (s), 667 (m), 585 (w), 565 (w), 525 (s), 509 (s), 499 (s).

<sup>1</sup>H NMR  $\delta$  ppm: 10.51 (1 H, s) (<sup>3</sup>J<sub>Pt-H</sub> = 86 Hz), 7.41-8.27 (16 H, m), 3.98 (3 H, s), 4.05 (3 H, s), 1.25-2.18 (4 H, s), 2.20-3.58 (4 H, m), 4.63 (2 H, m). <sup>31</sup>P NMR  $\delta$  ppm: 32.2 (s) (<sup>1</sup>J<sub>P-P</sub> = 2198 Hz).

#### **4.10.3 In-vitro Cell Testing on the Pt (II) cyclometallates 281 and 284:**

Cisplatin, compound **281** and **284** were all dissolved up into solutions using dimethylsulfoxide prior to treatment. Each solution was then diluted to the desired concentrations of 5  $\mu\text{M}$ , 10  $\mu\text{M}$ , 15  $\mu\text{M}$ , 20  $\mu\text{M}$  and 30  $\mu\text{M}$ . The OE21 cell cultures present in agar plates were treated with each solution and left to incubate for 24 hours.

Morphology of the cell treated with cisplatin, complex **281** and **284** were examined by light microscopy. Aliquots of vehicle control and drug treated cells were cytopun onto glass slides and stained with Rapi-Diff. The extent of apoptotic and non-apoptotic cell death was determined by counting the cells in at least three fields of view per slide, with an average of circa 100 cells per field. Apoptotic cell death was characterised by the presence of two or more of the following morphological features: cell shrinkage, chromatin condensation, DNA degradation and fragmentation into “apoptotic bodies”, within an intact membrane.

Type II programmed cell death was defined as follows: absence of a discernable plasma membrane, with a highly vesicular cytoplasm which is often associated with extensive loss of cytoplasmic material. The nucleus remains intact, with clear pyknosis (condensed regions).

#### **4.10.3 Photophysical studies on the 3-H ligand 261 and platinum complexes 281, 371 and 381:**

Each compound was made up by weighing the samples and dissolving them using chloroform to a concentration of  $10^{-3}$  M. Each solution was then subsequently diluted down to  $10^{-5}$  M for UV-vis spectroscopy and luminescent testing. Each solution was placed in a quartz cuvette, which was cleaned with chloroform between each sample test, and placed in the machine. For the luminescence spectrophotometer the samples were excited at a wavelength of 270 nm as this was the maximum absorption wavelength identified for all the compounds from the UV-visible spectra.



**4.11 Bibliography:**

1. Z. Guo and P. J. Sadler, in *Advanced Inorganic Chemistry*, Academic Press, 1999, vol. Volume 49, pp. 183–306.
2. X. Wang and Z. Guo, *Anti-Cancer Agents in Medicinal Chemistry*, 2007, **7**, 19–34.
3. V. Cepeda, M. A. Fuertes, J. Castilla, C. Alonso, C. Quevendo, and J. M. Perez, *Anti-Cancer Agents in Medicinal Chemistry*, 2007, **7**, 3–18.
4. C. D. A. and E. M. Tansey, *Welcome Trust Centre*, 2007, **30**.
5. D. Wang and S. J. Lippard, *Nature reviews. Drug discovery*, 2005, **4**, 307–320.
6. L. G. Marzilli, J. S. Saad, Z. Kuklenyik, K. Keating, and Y. Xu, *Journal of the American Chemical Society*, 2001, **123**, 2764–70.
7. K. J. Barnham, M. I. Djuran, P. D. S. Murdoch, J. D. Ranford, and P. J. Sadler, *Inorganic Chemistry*, 1996, **35**, 1065–1072.
8. R. N. Bose, L. Maurmann, R. J. Mishur, L. Yasui, S. Gupta, W. S. Grayburn, H. Hofstetter, T. Salley, and T. Milton, *Proceedings of the National Academy of Sciences of the United States of America*, 2008, **105**, 18314–9.
9. A. Küng, D. B. Strickmann, M. Galanski, and B. K. Keppler, *Journal of Inorganic Biochemistry*, 2001, **86**, 691–8.
10. O. Heudi, S. Mercier-Jobard, A. Cailleux, and P. Allain, *Biopharmaceutics & Drug Disposition*, 1999, **20**, 107–16.
11. O. Vrana and V. Brabec, *Biochemistry*, 2002, **41**, 10994–10999.
12. B. Spingler, D. A. Whittington, and S. J. Lippard, *Inorganic Chemistry*, 2001, **40**, 5596–602.
13. J. L. Nitiss, *Proceedings of the National Academy of Sciences of the United States of America*, 2002, **99**, 13963–13965.
14. E. Volckova, L. P. Dudones, and R. N. Bose, *Pharmaceutical research*, 2002, **19**, 124–31.
15. R. P. Perez, *European Journal of Cancer*, 1998, **34**.
16. T. Ishikawa, Z.-S. Li, Y.-P. Lu, and P. Rea, *Bioscience Reports*, 1997, **17**, 189–207.
17. J. Levi, C. Jacobs, S. M. Kalman, M. McTigue, and M. W. Weiner, *Journal of Pharmacology and Experimental Therapeutics*, 1980, **213**, 545–550.

18. M. Kruidering, B. Van de Water, E. de Heer, G. J. Mulder, and J. F. Nagelkerke, *The Journal of Pharmacology and Experimental Therapeutics*, 1997, **280**, 638–49.
19. D. M. Townsend, *Journal of the American Society of Nephrology*, 2003, **14**, 1–10.
20. R. Xie, W. Johnson, L. Rodriguez, M. Gounder, G. S. Hall, and B. Buckley, *Analytical and Bioanalytical Chemistry*, 2007, **387**, 2815–22.
21. A. J. Di Pasqua, C. R. Centerwall, D. J. Kerwood, and J. C. Dabrowiak, *Inorganic Chemistry*, 2009, **48**, 1192–7.
22. A. J. Di Pasqua, J. Goodisman, D. J. Kerwood, B. B. Toms, R. L. Dubowy, and J. C. Dabrowiak, *Chemical Research in Toxicology*, 2007, **20**, 896–904.
23. T. Overbeck, J. Knight, and D. Beck, *Mutation Research/DNA Repair*, 1996, **362**, 249–259.
24. G. Natarajan, R. Malathi, and E. Holler, *Biochemical Pharmacology*, 1999, **58**, 1625–1629.
25. F. a Blommaert, H. C. van Dijk-Knijnenburg, F. J. Dijt, L. den Engelse, R. a Baan, F. Berends, and a M. Fichtinger-Schepman, *Biochemistry*, 1995, **34**, 8474–80.
26. S. S. G. E. Van Boom, B. W. Chen, J. M. Teuben, and J. Reedijk, *Inorganic Chemistry*, 1999, **38**, 1450–1455.
27. E. L. M. Lempers and J. Reedijk, *Inorganic Chemistry*, 1990, 217.
28. Z. M. Banjar, L. S. Hnilica, R. C. Briggs, J. Stein, and G. Stein, *Biochemistry*, 1984, **23**, 1921–6.
29. S. S. G. E. van Boom and J. Reedijk, *Journal of the Chemical Society, Chemical Communications*, 1993, 1397.
30. J. Teuben, S. S. G. E. Van Boom, and J. Reedijk, *Journal of the Chemical Society, Dalton Transactions*, 1997, 3979–3980.
31. L. T. Ellis, H. Meng Er, and T. W. Hambley, *Australian Journal of Chemistry*, 1995, 793–806.
32. M. D. Hall, R. A. Alderden, M. Zhang, P. J. Beale, Z. Cai, B. Lai, A. P. Stampfl, and T. W. Hambley, *Journal of Structural Biology*, 2006, **155**, 38–44.
33. M. D. Hall, R. Dolman, and T. W. Hambley, *Centre for Heavy Metals Research*, 2006, 297–323.
34. M. D. Hall, S. Amjadi, M. Zhang, P. J. Beale, and T. W. Hambley, *Journal of Inorganic Biochemistry*, 2004, **98**, 1614–1624.

35. T. W. Hambley, A. R. Battle, G. B. Deacon, E. T. Lawrenz, G. D. Fallon, B. M. Gatehouse, L. K. Webster, and S. Rainone, *Journal of Inorganic Biochemistry*, 1999, **77**, 3–12.
36. T. Maguire, *PhD Thesis*, 2009, UCC, 100–153.
37. T. Talarico, D. R. Phillips, G. B. Deacon, S. Rainone, and L. K. Webster, *Investigational New Drugs*, 1999, **17**, 1–15.
38. G. L. Edwards, D. S. C. Black, G. B. Deacon, and L. P. G. Wakelin, *Canadian Journal of Chemistry*, 2005, **83**, 980–989.
39. I. M. El-Mehasseb, M. Kodaka, T. Okada, T. Tomohiro, K. Okamoto, and H. Okuno, *Journal of Inorganic Biochemistry*, 2001, **84**, 157–158.
40. K. E. Erkkila, D. T. Odom, and J. K. Barton, *Chemical Reviews*, 1999, **99**, 2777–96.
41. E. R. Jamieson and S. J. Lippard, *Chemical reviews*, 1999, **99**, 2467–98.
42. M. Cusumano, M. L. Di Pietro, A. Giannetto, and P. A. Vainiglia, *Journal of Inorganic Biochemistry*, 2005, **99**, 560–5.
43. P. Wang, C. H. Leung, D. L. Ma, R. W. Sun, S. C. Yan, Q. S. Chen, and C. M. Che, *Angewandte Chemie (International Ed. in English)*, 2011, **50**, 2554–2558.
44. G. Marverti, A. Ligabue, M. Montanari, D. Guerrieri, M. Cusumano, M. L. Di Pietro, L. Troiano, E. Di Vono, S. Iotti, G. Farruggia, F. Wolf, M. G. Monti, and C. Frassinetti, *Investigational New Drugs*, 2011, **29**, 73–86.
45. G. Pratesi, G. Capranico, M. Binaschi, P. De Isabella, S. Pilotti, R. Supino, and F. Zunino, *International Journal of Cancer*, 1990, **46**, 669–674.
46. D.-L. Ma and C.-M. Che, *Chemistry (Weinheim an der Bergstrasse, Germany)*, 2003, **9**, 6133–44.
47. R. Wai-Yin Sun, A. Lok-Fung Chow, X.-H. Li, J. J. Yan, S. Sin-Yin Chui, and C.-M. Che, *Chemical Science*, 2011, **2**, 728.
48. P. Chellan, K. M. Land, A. Shokar, A. Au, S. H. An, C. M. Clavel, P. J. Dyson, C. De Kock, P. J. Smith, K. Chibale, and G. S. Smith, *Organometallics*, 2012, **31**, 5791–5799.
49. L. Murphy and J. A. G. Williams, *Top Organometallic Chemistry*, 2009, **28**, 75–111.
50. H. Kunkely and A. Vogler, *Journal of the American Chemical Society*, 1990, **112**, 5625–5627.
51. M. Kato, Y. Shishido, Y. Ishida, and S. Kishi, *Chemistry Letters*, 2008, **37**, 16–17.

52. K. J. Laidler, J. H. Meiser, and B. C. Sanctuary, *Physical Chemistry*, Houghton Mifflin Company, 4th Ed., 2003.
53. K. E. Dungey, B. D. Thompson, N. a. P. Kane-Maguire, and L. L. Wright, *Inorganic Chemistry*, 2000, **39**, 5192–5196.
54. J. Nishida, A. Maruyama, T. Iwata, and Y. Yamashita, *Chemistry Letters*, 2005, **34**, 592–593.
55. D. M. Jenkins and S. Bernhard, *Inorganic chemistry*, 2010, **49**, 11297–308.
56. Z. Yang, G. Zhang, J. Feng, and A. Ren, *Science China Chemistry*, 2012, **55**, 1405–1412.
57. S. P. Jiang, K. J. Luo, Y. H. Wang, X. Wang, Y. Jiang, and Y. Y. Wei, *Chinese Chemical Letters*, 2011, **22**, 1005–1008.
58. D. N. Kozhevnikov, V. N. Kozhevnikov, M. Z. Shafikov, A. M. Prokhorov, D. W. Bruce, and J. A. G. Williams, *Inorganic Chemistry*, 2011, **50**, 3804–15.
59. T. Baumgartner and R. Réau, *Chemical Reviews*, 2006, **106**, 4681–727.
60. Y. Park, B. Kim, K.-H. Lee, J.-H. Lee, S.-Y. Oh, and J. Park, *Journal of Nanoscience and Nanotechnology*, 2012, **12**, 4325–4329.
61. M.-Y. Lai, C.-H. Chen, W.-S. Huang, J. T. Lin, T.-H. Ke, L.-Y. Chen, M.-H. Tsai, and C.-C. Wu, *Angewandte Chemie*, 2008, **120**, 591–595.
62. S. Park, J. Seo, S. H. Kim, and S. Y. Park, *Advanced Functional Materials*, 2008, **18**, 726–731.
63. M. C. R. Rodriguez, J. C. Penedo, R. J. Willemse, M. Mosquera, and F. Rodriguez-Prieto, *Journal of Physical Chemistry A*, 1999, **103**, 7236–7243.
64. S. Kim, D. W. Chang, and S. Y. Park, *Macromolecules*, 2002, **35**, 6064–6066.
65. S. Lai, M. C. Chan, T. Cheung, S. Peng, and C. Che, *Inorganic Chemistry*, 1999, **38**, 4046–4055.
66. O. M. Ni Dhubhghaill, J. Lennon, and M. G. Drew, *Dalton Transactions*, 2005, 3213–3220.
67. F. Juliá, P. G. Jones, and P. González-Herrero, *Inorganic chemistry*, 2012, **51**, 5037–49.
68. J. Lennon, *PhD Thesis*, 2005, UCC, 184–290.
69. M. Sant, T. Aareleid, F. Berrino, B. M. Lasota, P. M. Carlie, and J. Faivre, *Annals of Oncology*, 2003, **14**, 61–118.

70. T. R. O'Donovan, O. Gerald, and S. L. McKenna, *Autophagy*, 2011, 509–524.
71. P. G. H. Clarke, *Anatomy and Embryology*, 1990, **181**, 195–213.
72. F. Scarlatti, R. Granata, A. J. Meijer, and P. Codogno, *Cell death and Differentiation*, 2009, **16**, 12–20.
73. J. Debnath, E. H. Baehrecke, and G. Kroemer, *Autophagy*, 2005, 66–74.
74. S. Fuertes, S. Brayshaw, and P. Raithby, *Organometallics*, 2012, **31**, 105–119.
75. W. Lu, M. W. C. Chan, K. Cheung, and C. Che, *Organometallics*, 2001, 2477–2486.
76. C. Anionic, C. C. P. Complexes, R. Berenguer, E. Lalinde, J. Torroba, and L. Rioja, *Inorganic Chemistry*, 2007, **46**, 9919–9930.
77. D. N. Kozhevnikov, V. N. Kozhevnikov, M. M. Ustinova, A. Santoro, D. W. Bruce, B. Koenig, R. Czerwieniec, T. Fischer, M. Zabel, and H. Yersin, *Inorganic Chemistry*, 2009, **48**, 4179–89.
78. D. Kim and J.-L. Brédas, *Journal of the American Chemical Society*, 2009, **131**, 11371–80.
79. E. S. Kryachko and T. Zeegers-Huyskens, *The Journal of Physical Chemistry A*, 2002, **106**, 6832–6838.
80. J. W. Slater, D. P. Lydon, N. W. Alcock, and J. P. Rourke, *Organometallics*, 2001, **20**, 4418–4423.
81. J. Mamtora, S. H. Crosby, C. P. Newman, G. J. Clarkson, and J. P. Rourke, *Organometallics*, 2008, **27**, 5559–5565.
82. W. L. F. Armarego and C. Li Lin Chai, in *Purification of Laboratory Materials*, Elsevier Inc., 6th Ed., 2009, pp. 88–444.

**Chapter 5:**  
**Final Conclusions and Future Work**

## Contents

<b>5.1 Final Conclusions and Summary</b> .....	316
5.1.1 Aims of the project.....	316
5.1.2 Synthesis of the platinum (II) cyclometallated complexes.....	317
5.1.3 Substitution of the Platinum (II) Complexes <b>281-284</b> [Pt( $\eta^3$ -PNC-L <sup>1-4</sup> )Cl]...	319
5.1.4 Oxidation of the Platinum (II) Complexes <b>281-284</b> [Pt( $\eta^3$ -PNC-L <sup>1-4</sup> )Cl].....	320
5.1.5 Platinum bio-adducts with N-acetyl-L-cysteine and L-glutathione .....	322
5.1.6 <i>In-vitro</i> cancer cell testing.....	323
5.1.7 Photophysical studies.....	324
<b>5.2 Future Work</b> .....	325
5.2.1 Novel Synthetic Routes .....	325
5.2.2 <i>In-vitro</i> cell testing and photophysical studies.....	327
<b>5.3 Bibliography</b> .....	328

## 5.1 Final Conclusions and Summary:

### 5.1.1 Aims of the Project:

This work began with the aim of producing a series of novel chloro analogues of the iodo platinum complexes reported previously by our research group, **501**, **Figure 5.1**. Previously, the ONiD group reported some success for chloro based PNO type platinum (II) complexes for example **Figure 5.1**, but all previous attempts to synthesis and isolate chloro based platinum cyclometallates were unsuccessful.

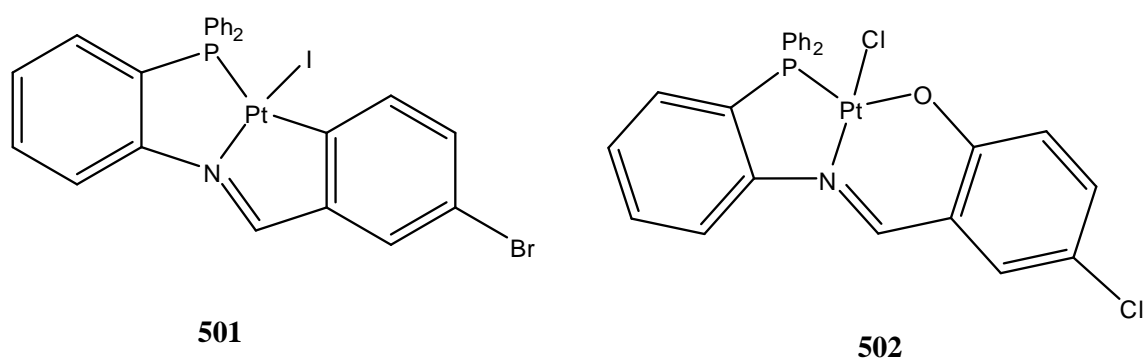


*Figure 5.1: Iodo-PNC type platinum (II) cyclometallates 501 and chloro-PNO type platinum (II) cyclometallates 502 previously reported by our research group.*

From the literature reviewed in **Chapter 1**, chloro based platinum complexes have been identified as having greater potential for anti-cancer activity over complexes with iodide or bromide as the leaving group. This is due to the natural concentration of chloride ions in the blood and within cells. Also, cisplatin's established mode of action involves hydrolysis of the chloride ligands within the cell in order for it to bind to DNA and induce cell apoptosis.<sup>1</sup> Therefore, the presence of the Pt-chloride bond is seen as very important to the biological activity of platinum complexes.

Also found in the literature was the interesting feature of double-stranded DNA in that flat planar molecules (usually containing aromatic groups) that are hydrophobic, can insert themselves between the base pairs of DNA through a process known as intercalation. This acceptance of an intercalating molecule increases the length of the DNA helix, which affects the template function of DNA in terms of replicating.<sup>2,3</sup>

Therefore, aside from simply binding a metal centre to a donor atom on a DNA strand, certain metal complexes that contain flat aromatic residues can also bind to DNA by



intercalation. Therefore a further aim of this work was to synthesis novel planar chloro platinum complexes capable of binding monofunctionally with DNA, as well as having intercalating properties due to the planar structure of aromatic rings. Forming tridentate complexes was therefore seen as desirable to increase stability through the chelate effect as well as ensuring the complex remains planar in order to achieve intercalation.

### 5.1.2 Synthesis of Chloro Platinum (II) Cyclometallated Complexes:

Initial work was centred on the synthesis of the iminophosphine ligands HL<sup>1-4</sup> **261-264** which required that the 2-diphenylphosphinoaniline (2-DPPA) starting material be synthesised. To store the 2-diphenylphosphinoaniline for long periods of time, it was stored in a freezer which prevented the previously reported photophysical interactions as well as ensuring a fresh batch was readily available at all times.<sup>4</sup>

Coordination studies with the iminophosphine ligands were initially undertaken with PtCl<sub>2</sub> as a starting material as this was used previously within our research group to successfully produce the chloro platinum (II) PNO complexes. However, the reactions of PtCl<sub>2</sub> with the iminophosphine ligands gave insoluble bidentate platinum (II) complexes **271-273** which were characterised by IR spectroscopy and elemental analysis. All attempts to further react these insoluble bidentate complexes with external bases such as NaOAc, in order to achieve cyclometallation, proved unsuccessful.

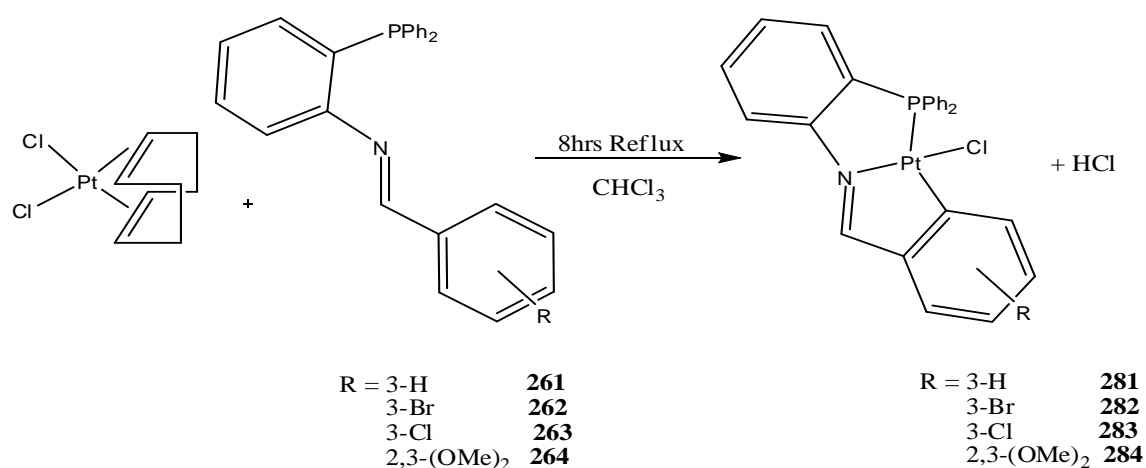


*Figure 5.2: Synthesis of the novel platinum (II) tridentate iminophosphine complexes **281-284** via direct thermal and solvent assisted cyclometallation.*

However, changing the starting material from  $\text{PtCl}_2$  to  $\text{PtCl}_2(\text{cod})$  and reacting it with the appropriate iminophosphine ligand  $\text{HL}^{1-4}$  **261-264** in dichloromethane afforded a series of soluble products. Evidence of a shifted imine signal in the  $^1\text{H}$  NMR spectra complete with  $^{195}\text{Pt}$  satellites gave the first evidence of successful coordination.

Subsequent “fine-tuning” of the reaction conditions including; changing the solvent from dichloromethane to chloroform to help thermal cyclometallation, adding the ligand slowly over a long period of time to allow time for coordination and dilution of the solution to prevent dimerisation of the bidentate intermediates, gave good reproducible yields of circa 60% for most of the complexes, **Figure 5.2**. Also formed from the reaction of  $\text{PtCl}_2(\text{cod})$  and the  $\text{HL}^4$  ligand **264** was the previously reported PNO tridentate complex **285** as a minor product due to the interesting reactivity of the platinum metal centre towards on of the methoxy groups.

Once the series of platinum (II) iminophosphine cyclometallates were isolated and fully characterised **281-284**, attention was then directed to the phosphinoamide ligands **265-267** and their potential complexes, **Figure 5.3**. The ligands were synthesised from a novel method in good yields of circa 60% and for the first time, extensive NMR analysis revealed two isomers were present in solution. The phosphinoamide ligands were found to tautomerise in solution to form two iminol isomers with the *E*-isomer being the major of the two.

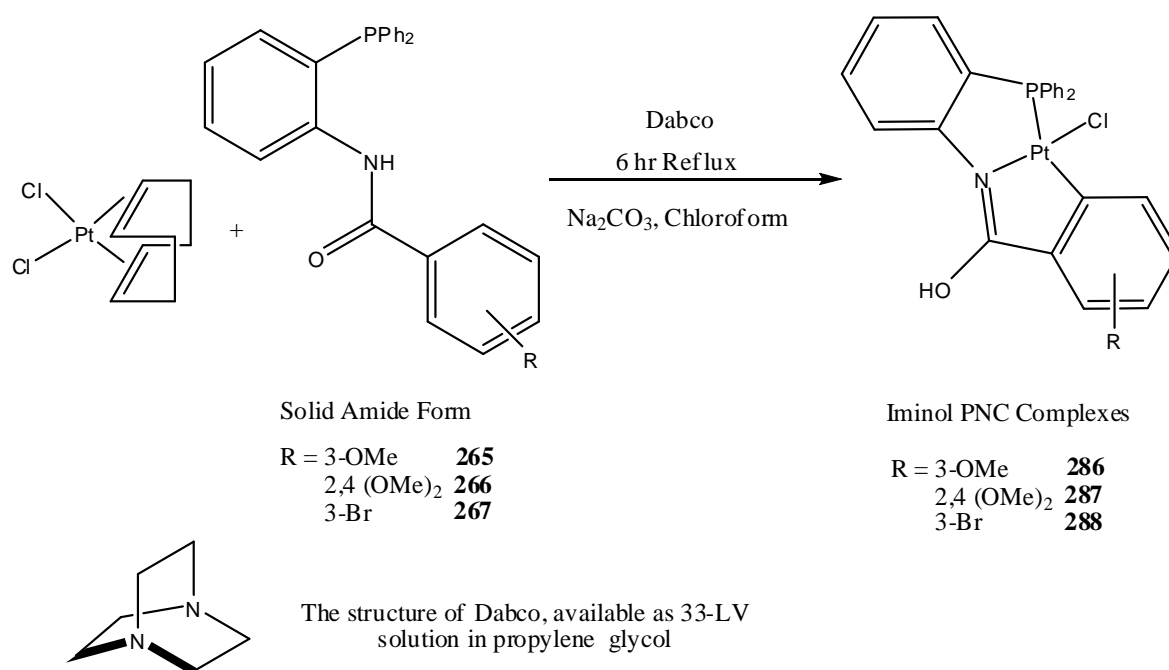


**Figure 5.3:** Synthesis of the novel platinum (II) tridentate phosphinoiminol complexes **286-288** via direct thermal and solvent assisted cyclometallation.

Initial attempts to produce an identifiable product from the reaction of the phosphinoamide ligands with  $\text{PtCl}_2(\text{cod})$  proved to be very difficult with solubility issues, multiple products formed and decomposition identified by NMR spectroscopy. However, by using a bulky external base called Dabco resulted in the removal of the HCl formed during the cyclometallation which reduced decomposition of the ligand prior to coordination to the  $\text{PtCl}_2(\text{cod})$ .

Novel platinum (II) phosphinoiminol complexes **286-288** were therefore successfully isolated and characterised by NMR and IR spectroscopy as well as elemental analysis. Due to the tautomerism of the ligands in solution, the yields of these complexes were found to be very low, **Figure 5.3**. As well as cyclometallated complexes, a novel tridentate PNO phosphinoiminol complex **289** was also identified from the reaction of  $\text{PtCl}_2(\text{cod})$  with the HL<sup>6</sup> ligand **266**. This is formed in a similar way to the iminophosphine PNO complex discussed earlier, however, it was found to be too unstable for full characterisation and isolation.

As well as the PNO complex **289**, the cyclometallates formed, **286-288**, were also found to be significantly less stable than their iminophosphine counterparts **281-284**. Therefore, these complexes were deemed suitable for further studies and applications, in particular for oxidation and substitution reactions where all initial reactions with them proved to be unsuccessful.

### **5.1.3 Substitution of the Platinum (II) Complexes 281-284 [Pt( $\eta^3$ -PNC-L<sup>1-4</sup>)Cl]:**

One of the most important influences on the biological function required of platinum anticancer compounds is the lability of the leaving group(s), in this case the Pt-Cl bond. To investigate this for the platinum (II) cyclometallates **281-284**, substitution of the chloride ligand with a bulky phosphine (triphenylphosphine -  $\text{PPh}_3$ ) was attempted. In **Chapter 2** it was found that solvents can stabilise chloride ions, which can assist in the cyclometallation reactions.

Here similar solvent systems are used to stabilise the chloride ion in solution, which allows for novel one-step phosphine substitution of chloro iminophosphine complexes. The iminophosphine platinum (II) complexes **281-284** were reacted with triphenylphosphine to successfully form the novel cationic platinum (II) substituted  $\text{PPh}_3$  tridentate PNC and PNO complexes which were isolated and characterised by IR and NMR spectroscopy along with elemental analysis, **Figure 5.4**.

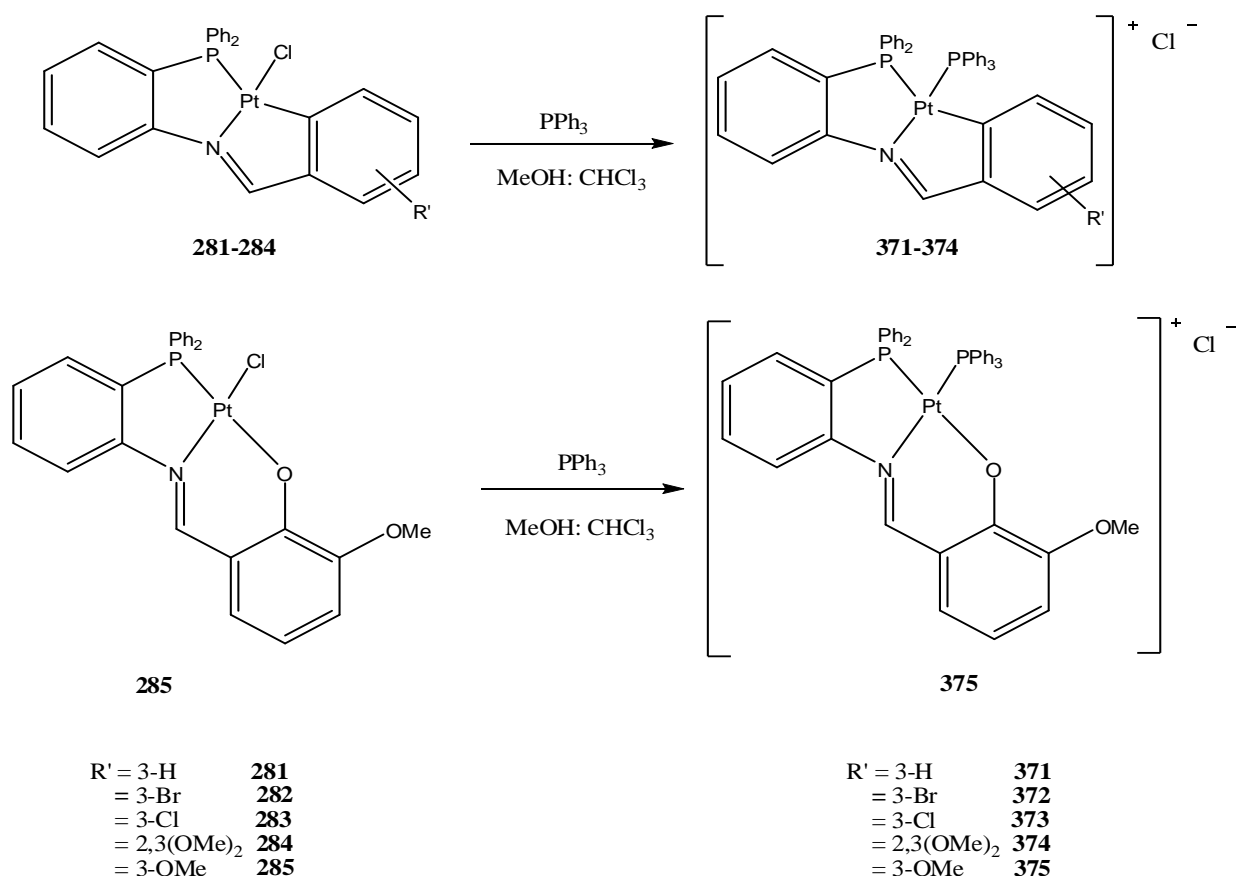


**Figure 5.4:** Direct substitution of the platinum (II) iminophosphine complexes, **281-285**, with triphenylphosphine ( $\text{PPh}_3$ ).

Achieving one-step phosphine substitution in short reaction times is a significant improvement on previous work by our research group and others. These relied on halide scavengers to initially remove the chloride ligand prior to the addition of the new phosphine ligand.<sup>5</sup>

#### 5.1.4 Oxidation of the Platinum (II) Complexes 281-284 [Pt( $\eta^3\text{-PNC-L}^{1-4}$ )Cl]:

The ongoing success of the platinum (IV) complex Satraplatin, as well as the limited past success of Tetraplatin, has increased research interest into novel platinum (IV) complexes. As an oral based drug, Satraplatin has convenient dosing and so far has not been associated with the same level of toxicity as the currently approved platinum based anti-cancer compounds. At the time of writing, it remains in clinical trials in the United States but given the lack of an overall survival benefit, satraplatin has not received approval by any regulatory authority.<sup>6</sup>

After the success of the substitution reactions, **Section 5.1.3**, oxidations were attempted on the platinum (II) cyclometallates **281-284** in the hope of forming stable chloro

platinum (IV) complexes for biological applications. However, all initial attempts of oxidising the platinum (II) cyclometallates **281-284** using methods previously found successful for our research group and others, proved to be unsuccessful. Interestingly, even at excessive concentrations of hydrogen peroxide, the platinum (II) iminophosphine complexes **281-284** were returned from the reaction quantitatively with no signs of decomposition.

After an extensive literature search, a select number of papers identified the use of N-chlorosuccinimide (NCS) as a successful reagent for oxidising platinum complexes via the addition of chloride ligands at the axial positions. In these papers, the researchers reported fast reaction time, good yields and stable platinum (IV) complexes formed from NCS.<sup>7</sup>

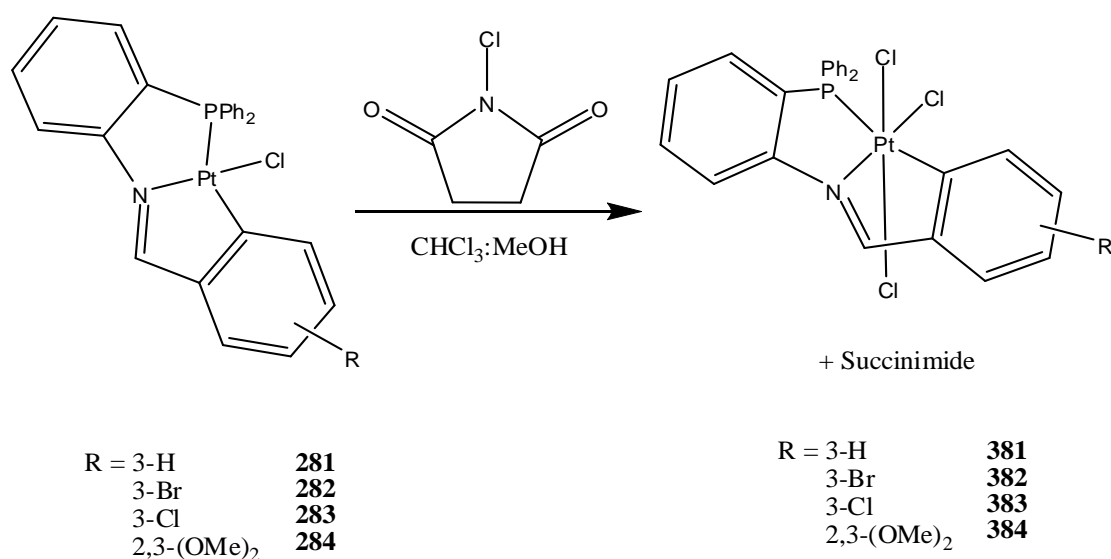


*Figure 5.5: Successful oxidative addition of two equivalents of chlorine to the iminophosphine platinum (II) complexes, **281-284** using N-chlorosuccinimide to form the novel platinum (IV) complexes **381-384**.*

These methods and reagents were successfully applied to the platinum (II) cyclometallated complexes **281-284**, but the novel series of platinum (IV) complexes formed, **381-384**, proved to be significantly less stable than their parent platinum (II) analogues. Sensitivity to acids, bases and light were noted in varying amounts while trying to remove the excess N-chlorosuccinimide from the reaction solution. Nonetheless, low yields of the octahedral platinum (IV) complexes were isolated and characterised by IR and NMR spectroscopy as well as elemental analysis, **Figure 5.5**.

Oxidation reactions were also attempted with the platinum (II) phosphinoiminol complexes **286-288**, however the products formed were insoluble in all common solvents and evidence of decomposition was noted in the NMR spectra.

### 5.1.5 Platinum Bio-adducts with N-acetyl-L-cysteine and L-glutathione:

From the literature reviewed it was identified that sulphur based biomolecules can have both a detrimental and beneficial effect on the biological activity of platinum complexes, so reactions involving biomolecules was a necessary step in the evaluation of the potential biological activity of these novel complexes.

It was determined that the most stable complexes formed in this work, which also had the highest yields of all the platinum (II) complexes reported, were the unsubstituted 3-H platinum (II) iminophosphine **281** and the 2,3-(OMe)<sub>2</sub> platinum (II) iminophosphine **284** complexes. It was therefore decided that these two complexes would be ideal candidates for extensive biological testing. The platinum (II) cyclometallates **281** and **284** were reacted with N-acetyl-L-cysteine and L-glutathione to form novel platinum bio-adduct complexes, **Figure 5.6**.

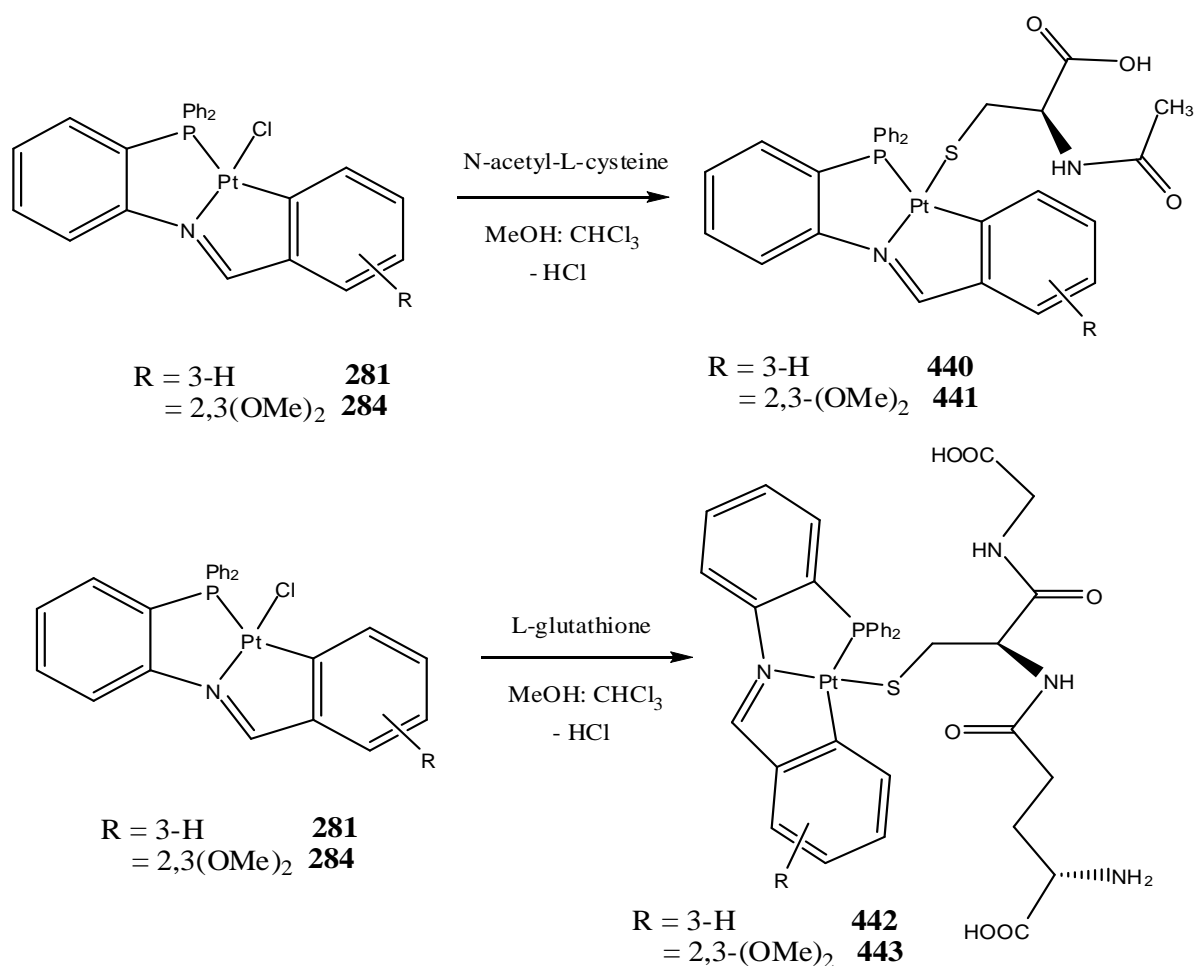


*Figure 5.6: Formation of the platinum (II) iminophosphine biomolecule adducts with N-acetyl-L-cysteine and L-glutathione to form 440-441.*

Both platinum (II) cyclometallates tested were found to react quite readily with N-acetyl-L-cysteine and formed slightly water soluble platinum (II) bio-adducts. More interestingly however was that they also reacted very readily with the large sulphur based biomolecule; L-glutathione, which produced water soluble platinum (II) bio-adduct complexes with greater water solubility in comparison to the N-acetyl-L-cysteine bio-adduct complexes, **Figure 5.6**.

All the bio-adducts were isolated in good yields and characterised by IR and NMR spectroscopy as well as elemental analysis, but further investigation into the reactivity of these platinum complexes with other biomolecules is required to successfully established a full biological reactivity profile.

#### **5.1.6 In-vitro cancer cell testing:**

To fully investigate the biological activity of the platinum complexes, *in-vitro* cancer cell testing was required. Through Dr. Sharon McKenna, the Cork Cancer Research Centre was contacted to facilitate the testing; which is an independent foundation whose research activity is based in the Leslie C. Quick Jnr. Laboratory in the BioSciences Institute, UCC.

After extensive discussions the best candidate platinum complexes were chosen to be those which gave the best yield in order to provide a sufficient supply for the tests as well as having the best solubility in a medium that could be utilised with cells. The platinum (II) complexes **281** and **284** were chosen as having the greatest potential to display biological activity from the 24 novel complexes reported in this project.

Under the supervision of professional cancer cell biologists and biochemists, the solutions of each complex, as well as cisplatin, were made up in dimethylsulfoxide and each cell line was treated for 24 hours with one of the three platinum (II) complexes. It is also worth noting that the cell cultures were kept away from light during the incubation period to prevent any possible photophysical effects for this test.

Interestingly the 2,3-(OMe)<sub>2</sub> platinum (II) cyclometallated complex **284** was found to be significantly more active than both the unsubstituted platinum (II) cyclometallate **281** and the well established anticancer therapeutic, cisplatin. These results are a testament to the ongoing research into the biological potential of cyclometallated platinum complexes where both Type I and Type II programmed cell death (PCD) was observed, **Figure 5.7**.

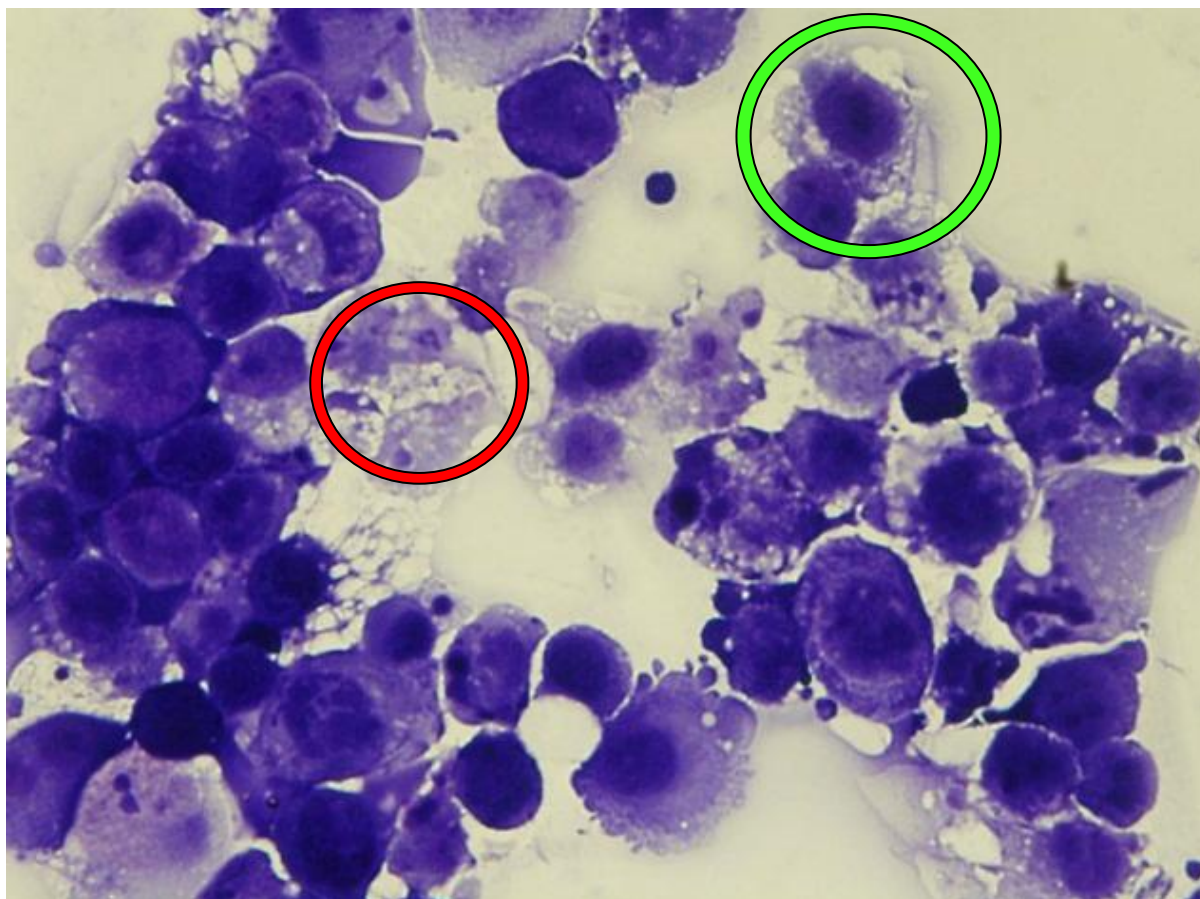


*Figure 5.7: OE21 Cancer cells after treatment with the novel platinum (II) complex 284 over 24 hours, which induced Type I PCD (red circle) and Type II PCD (green circle).*

### **5.1.7 Photophysical Studies:**

Throughout this project, photophysical effects were observed for nearly every type of complex and ligand reported. When left in direct sunlight, all the ligands were found to have undergone oxidation processes with a signal appearing at circa  $\delta$  30 ppm in the  $^{31}\text{P}\{^1\text{H}\}$  NMR spectra corresponding to the oxidised phosphine group. This was particularly evident in chlorinated solutions and usually took a number of days where the solution would gradually turn from yellow to orange. Also, the initial coordination studies attempted with the  $\text{PtCl}_2$  and iminophosphine ligands uncovered some very unusual colour changes with samples left in NMR tubes changing to bright pink, red and even green after a number of days. However, NMR spectra only identified decomposition products such as aldehyde peaks.

After a literature investigation it was found that a number of rigid, stable tridentate platinum (II) complexes with mixed donor ligands have been reported over the past decade



with luminescent properties. These types of complexes in particular have found applications in OLEDs alongside traditional purely organic molecules.

Initial studies on the luminescence properties of the iminophosphine ligands and complexes proved to be unsuccessful due to low concentrations, solvent choice and issues with the luminescent spectrophotometer. After consulting colleagues in the Centre for Research into Atmospheric Conditions (CRAC), also based in UCC, a study was undertaken with UV-visible spectroscopy to identify the ideal solvent, concentration ( $10^{-5}$ M) and ideal wavelength for excitation to investigate any possible luminescence for the compounds in this project.

The highest yielding ligand and complexes were chosen for the study i.e. the 3-H ligand HL<sup>1</sup> **261** and the platinum complexes derived from it. Emission spectra were found for all tridentate platinum complexes tested **281**, **371** and **381**, where significant luminescence was observed. However, the 3-H ligand **261** was found to have over five times greater emission intensity in comparison to the platinum complexes. This work has opened the door to the possibilities of using iminophosphine, and possibly phosphinoamide, ligands as organic molecules for organic LED applications as well as spurring further investigations into luminescence of cyclometallated platinum complexes.

## 5.2 Future Work:

### 5.2.1 Novel Synthetic Methods:

To date all reactions completed have been achieved using solvents, in particular chloroform. Initial work in this project for the coordination of PtCl<sub>2</sub> to the iminophosphine ligands **261-264** in **Chapter 2**, involved some solid state reactions. Solid state reactions are desirable for green chemistry synthetic routes to novel products as it reduces the current reliance on solvents which are harmful to the environment and saves money on purchase of solvents.

As identified in **Chapter 2**, the reaction between PtCl<sub>2</sub> and the iminophosphine ligands HL<sup>1-4</sup> initially form platinum (II) bidentate complexes **271-273**. These complexes then undergo an intramolecular reaction (cyclometallation) which occurs via thermal means. Therefore the bidentate complexes were heated as a solid for a number of hours to induce cyclometallation with the hope of forming the cyclometallated platinum (II) complexes **281-284** using a solid state reaction mechanism.

During the course of the reaction, using pH paper and a pH meter, HCl gas was identified from the solid, which implied successful cyclometallation since HCl is the expected by-product of the cyclometallation reaction. However, despite several attempts, only barely detectable amounts of the cyclometallated complexes **281-284** were identified by NMR spectroscopy. Unfortunately, thermal decomposition was also found to occur with a black solid forming after 2-3 hours, which we propose is metallic platinum.

The observation of HCl and some NMR results pointed to some successful cyclometallation which gives this method some promise. Further work into fine-tuning of these solid state reactions may lead to increased yields, with the added bonus of reducing solvent usage for a novel green chemistry route to platinum (II) cyclometallates. Some research groups have already identified solid state thermal cyclometallation of platinum complexes, which gives this proposed method even more potential.<sup>8,9</sup>

The formation of the platinum (IV) complexes via the reaction of the platinum (II) cyclometallates with N-chlorosuccinimide, although successful, gave very low yields. One possible solution to this would be the use of chlorine gas generated *in-situ* to oxidise the platinum (II) cyclometallates (and also maybe the PNO type complexes) by bubbling the halogen through a solution of the platinum (II) complex. This method has been cited by a number of research groups as being a primary method for platinum (II) oxidation and a test reaction within this project using *in-situ* generation of chlorine gas also proved to be successful, **Figure 5.8**.<sup>7,10</sup>

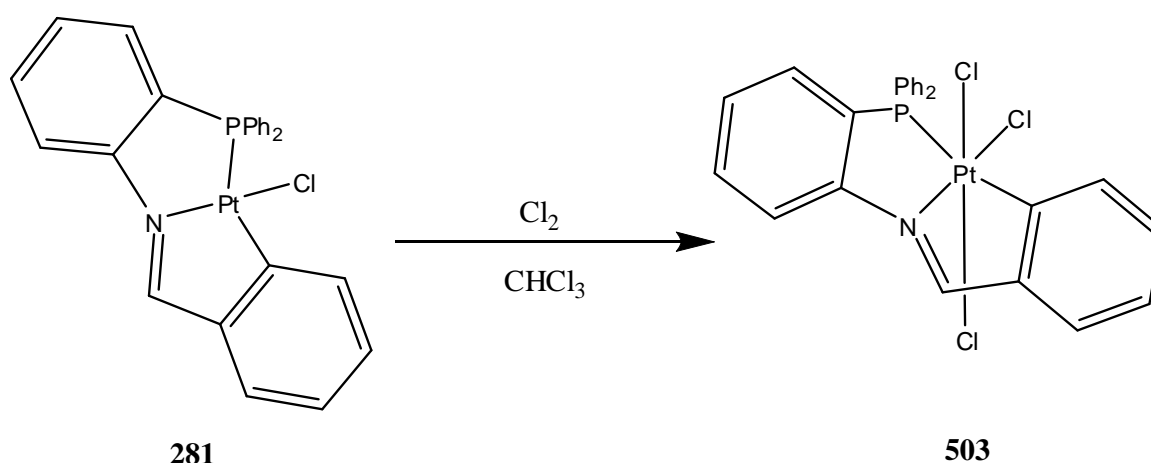


**Figure 5.8:** A test reaction using this method proved to be successful, possibly providing a method to increase the yield of the platinum (IV) complexes allowing for reactivity studies

The test method involved the slow addition of dilute hydrochloric acid onto solid N-chlorosuccinimide, which produced the green chlorine gas in a sealed vessel. This sealed vessel was fed through to another vessel where it was bubbled through a solution of the platinum (II) cyclometallate **281**, which itself was kept under a continuous flow of N<sub>2</sub>. After an hour, the solution turned pale yellow and evidence was found in the NMR spectra for the platinum (IV) complex previously reported in **Chapter 3, 381**. However, other unidentifiable products were also found so further work on this method is required.

Further work could also be completed on the platinum (II) interactions with sulphur based biomolecules, reported in **Chapter 4**. The reactivity of the rest of the platinum (II) complexes reported in this work could be established, which would then give a basis for structure activity relationships. Also the reactivity of the platinum (IV) complexes towards biomolecules could be investigated further to see if they can be reduced by other biomolecules such as L-methionine or if they are active in their Pt (IV) form.

### **5.2.2 In-vitro cell testing and photophysical studies:**

The success of the 2,3-(OMe)<sub>2</sub> platinum (II) cyclometallate towards the OE21 cancer cell line gives significant weight to justifying further testing of the platinum complexes reported in this work. Also, of particular interest is the potential reactivity of the platinum bio-adduct complexes towards cancer cells, in order to investigate whether the complexes are still active as bio-adducts or whether the addition of the biomolecule prevents biological activity. The water solubility of the platinum bio-adducts may also provide further test methods currently unavailable to the platinum (II) and platinum (IV) cyclometallates.

Also, other cisplatin sensitive and cisplatin resistant cell lines could be tested in order to compare activity profiles and types of cell death induced in cancer cells by these complexes. The impact of light on the activity of the complexes undergoing *in-vitro* testing, in particular the platinum (II) bi-adducts, could also be of significant interest in terms of potential Photo-Dynamic Therapy (PDT).

Finally, in terms of photophysical studies, the remaining “families” of platinum complexes and ligands, of which there are 7 in total from this work, could yield extensive structure activity relationships for all the complexes. The high intensity emission observed for the ligands in particular should be investigated further with all the ligands reported in this project, as well as ligands previously reported within our research group which may also have high intensity emission spectra.<sup>5</sup>

### 5.3 **Bibliography:**

1. M. D. Hall, R. A. Alderden, M. Zhang, P. J. Beale, Z. Cai, B. Lai, A. P. Stampfl, and T. W. Hambley, *Journal of Structural Biology*, 2006, **155**, 38–44.
2. J. C. Dabrowiak, in *Metals in Medicine*, John Wiley & Sons, Ltd., 1st Ed., 2009, pp. 49–72.
3. J. K. Barton and S. J. Lippard, *Metal Ions in Biology*, 1980, **1**, 31–113.
4. M. K. Cooper, J. M. Downes, P. A. Duckworth, M. C. Kerby, R. J. Powell, and M. D. Soucek, in *Inorganic Syntheses*, John Wiley & Sons, Inc., 1989, pp. 129–133.
5. O. M. Ni Dhubghaill, J. Lennon, and M. G. Drew, *Dalton Transactions*, 2005, 3213–3220.
6. G. Doshi, G. Sonpavde, and C. N. Sternberg, *Expert Opinion on Drug Metabolism & Toxicology*, 2012, **8**, 103–11.
7. S. R. Whitfield and M. S. Sanford, *Organometallics*, 2008, **27**, 1683–1689.
8. Y. Scaffidi-Domianello, A. . Nazarov, M. Haukka, M. Galanski, B. K. Keppler, J. Schneider, P. Du, R. Eisenberg, and V. Y. Kukushkin, *Inorganic Chemistry*, 2007, **46**, 4469–4482.
9. M.-H. Thibault, B. E. G. Lucier, R. W. Schurko, and F.-G. Fontaine, *Dalton Transactions*, 2009, 7701–16.
10. J. Mamtora, S. H. Crosby, C. P. Newman, G. J. Clarkson, and J. P. Rourke, *Organometallics*, 2008, **27**, 5559–5565.



# Appendices



